

Dilute Solution Properties of a Polyurethane.

I. Linear Polymers*

HAROLD C. BEACHELL and JEAN C. PETERSON,† *Department of Chemistry, University of Delaware, Newark, Delaware 19711*

Synopsis

A linear polyurethane of high molecular weight was prepared in solution by the polyaddition of equimolar amounts of ethylene glycol and methylene bis(4-phenyl isocyanate). The polymer was fractionated by using a direct sequential extraction procedure, with a solvent-nonsolvent system consisting of *N,N'*-dimethylformamide (DMF) and acetone (A). The resulting fractions were characterized by viscosity and light-scattering measurements. The relationship between the intrinsic viscosity and molecular weight was found in DMF at 25°C. to be $[\eta] = 3.64 \times 10^{-4} M^{0.71}$. The unperturbed polymer chain dimensions were determined from intrinsic viscosity measurements carried out under experimentally determined theta conditions.

INTRODUCTION

A number of synthetic routes are available for the preparation of homopolyurethanes.¹ The most important synthetic route is of the addition type and involves the reaction of a diisocyanate and glycol to give a polyurethane.

The polyaddition reaction is preferred over other methods, since the reaction yields no by-products, and side reactions that could lead to branched and crosslinked products can be eliminated, or at least minimized, by choosing optimum reaction conditions.²

In this study a homopolyurethane was prepared, in solution, by the polyaddition of equimolar amounts of methylene bis(4-phenyl isocyanate) and ethylene glycol. The reaction was carried out under anhydrous conditions, at low temperature and in the absence of catalyst.

This paper describes the solution properties of the linear homopolyurethane, poly[ethylene methylene bis(4-phenyl carbamate)].

EXPERIMENTAL

Polymer Preparation

The linear polyurethane was prepared² by the polyaddition of equimolar amounts of methylene bis(4-phenyl isocyanate) (MDI) and ethylene glycol

* Presented at 153rd National American Chemical Society Meeting, Polymer Division, Miami Beach, April, 1967.

† Present address: Rohm and Haas Co., Research Laboratories, Spring House, Pennsylvania 19477.

(EG). The reaction was carried out under anhydrous conditions in a three-neck flask fitted with a stirrer, condenser, dropping funnel and nitrogen-gas inlet. The entire system was flamed-out under nitrogen prior to reaction and was protected from atmospheric moisture with drying tubes.

The MDI (0.1 mole, 25.02 g) was added to the reaction flask as a suspension in 40 ml of 4-methyl-2-pentanone. The ethylene glycol (0.1 mole, 6.20 g, 5.56 ml) in 40 ml of dimethyl sulfoxide (DMSO), was added dropwise to the rapidly stirred MDI suspension. The reaction mixture was slowly stirred and heated at 115°C for 1½-2 hr.

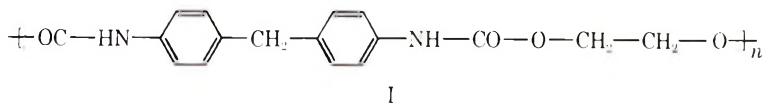
The resulting polyurethane was isolated from the reaction mixture by pouring the clear, viscous solution into distilled water. The precipitation was carried out by adding small amounts of the reaction mixture from a dropping funnel, directly into an excess of distilled water, contained in a Waring Blender.

The precipitated polyurethane was collected in a fritted-glass funnel of medium porosity, under water aspiration. The polymer was washed extensively with additional portions of distilled water and dried in a vacuum oven, at room temperature, for several days.

Prior to further usage or analysis, the polyurethane was purified by redissolution in *N,N'*-dimethylformamide (DMF), followed by treatment with discoloring charcoal, filtered and reprecipitated in distilled water as before. The resulting white polymer was collected and dried extensively, ground to facilitate further drying, and given a final drying over P₂O₅.

The average polymer yield was 95-100% prior to purification. The average polymer softening temperature was about 240°C. The polyurethane product was extremely tough and fibrous in nature and a good film former when evaporated from DMF solution.

The repeating unit of poly[ethylene methylene bis(4-phenyl carbamate)] has the structure I and will be designated PU throughout this paper.



A purified portion of the homopolymer was sent for elemental analysis.

ANAL. Calcd for (C₁₇H₁₆N₂O₄)_n: C, 65.40%; H, 5.12%; N, 8.98%. Found: C, 65.20%; H, 5.31%; N, 8.93%.

Polymer Fractionation

A direct sequential extraction procedure gave satisfactory fractionation of the poly[ethylene methylene bis(4-phenyl carbamate)]. This procedure involved the extraction of a 12-g sample of PU with a solvent system having progressively increasing solvent power for the polymer. The solvent-nonsolvent system used was composed of *N,N'*-dimethylformamide (DMF) and acetone (A). The viscosity measurements and molecular weights of the resulting fractions are listed in Table I.

TABLE I
Experimental Results of Viscosity Measurements of a Series of Fractions and Whole Polymer Samples of Poly[ethylene methylene bis(4-phenyl carbamate)].

Polymer sample	$\bar{M}_w \times 10^{-3}$	State of polymer ^a	$[\eta]$, dl/g (DMF, 25 $\pm 0.1^\circ\text{C}$)	b^b	k'^b
PU	24	U	0.46	0.090	0.425
PU1 ^c	3.3	F	0.11 ₅	0.005 ₇	0.430
PU2	8.7 ^c	F	0.22 ₈	0.005	0.096 ₂
PU3					
PU4	10	F	0.25 ₂	0.028	0.449
PU5	12	F	0.29 ₂	0.009	0.106
PU7	16.5	F	0.35 ₈	0.019	0.148
PU7A	24	F	0.46 ₄	0.094	0.437
PU7B	33	F	0.59	0.134	0.385
PU8	35.5	F	0.62	0.160	0.417
PU9	42	F	0.69 ₅	0.143	0.295

^a F = fractionated, U = unfractionated.

^b Determined from the graphical representation of the Huggins equation: $\eta_{sp}/c = [\eta] + k'[\eta]^2c$, where b is the measured slope and k' is $b/[\eta]^2$.

^c Fractions 2 and 3 were combined to afford enough sample for analysis.

Viscosity Measurements

Viscosities were measured in a Cannon-Ubbelohde dilution viscometer at a temperature of $25 \pm 0.02^\circ\text{C}$. All solvents and solutions were filtered, prior to measurement, through fine fritted-glass or solvent-resistant Millipore filters. The initial polymer concentrations were determined by evaporating to dryness an aliquot of the filtered polymer solution. In each determination, five dilutions were usually made and three to four readings were usually taken for each single dilution to obtain flow times within 0.2 sec of one another; these times were then averaged. The measurements were made under conditions of free fall. No kinetic energy corrections were applied.

The intrinsic viscosity, $[\eta]$, was obtained as usual, according to the Huggins equation (1) and the Kraemer equation (2):

$$\eta_{sp}/c = [\eta] + k' [\eta]^2c \quad (1)$$

$$\eta_{rel}/c = [\eta] - k'' [\eta]^2c \quad (2)$$

where η_{sp} is the specific viscosity;³ c , the concentration of the polymer in grams/100 ml; k' , the Huggins constant; η_{rel} , the relative viscosity; and k'' , the Kraemer constant. The data obtained were represented satisfactorily by these two equations, and the intrinsic viscosity values were therefore obtained by extrapolation of both η_{sp}/c and η_{rel}/c versus concentration to infinite dilutions. The two plots were made on the one graph so as to provide a cross-check, the common ordinate intercept being used as

the intrinsic viscosity value. The Huggins constants k' were obtained from the slope measurements of the Huggins plots of the whole and fractionated polymer samples. The results of the Huggins constant measurements are given in Table I.

Molecular Weight Determination

By use of the light-scattering-intrinsic viscosity data given by Lyman² with the intrinsic viscosities determined in this study, the molecular weights of the whole and fractionated polyurethanes were determined. The intrinsic viscosity and molecular weight data are given in Table I.

From the data collected, the constants K and a in the Mark-Houwink equation (3):

$$[\eta] = KM^a \quad (3)$$

were determined. This was done by plotting the logarithm of $[\eta]$ of each fraction against the logarithm of its corresponding \bar{M}_w . The slope of the resulting line yields the constant a and the ordinate intercept, the constant K . The resulting Mark-Houwink equation (4) in DMF at 25°C. is:

$$[\eta] = 3.64 \times 10^{-4} M^{0.71} \quad (4)$$

The constants in the Mark-Houwink equation were determined for various solvent-nonsolvent mixtures, also at 25°C; these values are given in Table II.

TABLE II
Constants in the Mark-Houwink Equation at $25 \pm 0.02^\circ\text{C}^a$

Solvent system ^b	$K \times 10^4$	a
100 DMF	3.64	0.71
95 DMF/5 Acetone	6.29	0.65
90 DMF/10 Acetone	7.19	0.63
85 DMF/15 Acetone	10.02	0.59
79 DMF/21 Acetone	14.19	0.56
71 DMF/29 Acetone (Θ)	30.00	0.50

^a In determining the slope a and the ordinate intercept K from experimental data, linear least-squares analyses on the logarithms of these values were carried out on a LOCI-2, desk-top computer, by using a program No. S106.

^b In mixed solvent systems, the volume ratio of the polymer solvent (DMF) is given first and the volume ratio of the polymer nonsolvent (acetone) is given second.

Estimation of Unperturbed Polymer Dimension from Viscosity Measurements

The intrinsic viscosity of a linear polymer in a theta solvent and in a nontheta solvent can be expressed by eqs. (5) and (6) respectively:

$$[\eta]_{\Theta} = K_{\Theta} M^{1/2} \quad (5)$$

$$[\eta] = KM^{1/2} \alpha^3 \quad (6)$$

where K is a constant for one given polymer, and is independent of the solvent and the molecular weight M . The constant K_θ can be related to the root-mean-square end-to-end distance of the polymer chain, $\langle R^2 \rangle_0^{1/2}$, in an ideal or theta solvent by eq. (7):

$$K_\theta = \Phi_0 A^3 = \Phi_0 [\langle R^2 \rangle_0 / M]^{3/2} \quad (7)$$

since

$$A^2 = \langle R^2 \rangle_0 / M$$

In equation (7), Φ_0 is the universal viscosity or hydrodynamic constant equal to 2.87×10^{21} dl/mole-cc.

In order to determine the unperturbed chain dimensions, $\langle R^2 \rangle_0$, of a polymer, one has to determine the intrinsic viscosity of the polymer under theta conditions, calculate the value of the constant K_θ by using eq. (5), and then in turn determine $\langle R^2 \rangle_0$ from the relationship given in equation (7). In addition, by measuring the intrinsic viscosity of a polymer in a theta solvent and in a nontheta solvent, as described by eqs. (5) and (6), the expansion parameter α , can be evaluated. The factor α is defined as the viscosity expansion parameter and is actually a measure of the effect a solvent has on the polymer configuration, in terms of molecular expansion. We can write an expression for the expansion parameter:

$$\alpha = \{[\eta]/[\eta]_\theta\}^{1/3} \quad (8)$$

The quantity $\{[\eta]/[\eta]_\theta\}^{1/3}$ can be written as $\alpha[\langle R^2 \rangle_0 / M]^{1/2}$, where

$$\alpha = \{\langle R^2 \rangle / \langle R^2 \rangle_0\}^{1/2} \quad (8')$$

Like eq. (8), eq. (8') provides a measure of the expansion or perturbation of the polymer coil relative to the unperturbed dimensions, $\langle R^2 \rangle_0^{1/2}$, as a result of long-range interactions.

Polymer Dimensions From Viscosity Measurements under Theta Conditions

One single solvent, or a mixture of solvents in a definite proportion, may have a unique theta temperature for the particular polymer system. However, in many cases, the resulting theta temperatures can be quite awkward to work with. To get around this, one can assign a convenient working temperature as the theta temperature, and then adjust the proportions of the polymer nonsolvent and solvent needed to achieve the desired theta conditions.

In our work, we chose the latter route and assigned a working temperature of 25°C as the theta temperature. The composition corresponding to the theta solvent was then determined by following a method described by Bianchi et al.⁴ Following their procedure, we measured the intrinsic viscosities for the polyurethane samples of known molecular weight, in a DMF-acetone, polymer solvent-nonsolvent system. The volume ratio of acetone to DMF was gradually increased from zero acetone concentration

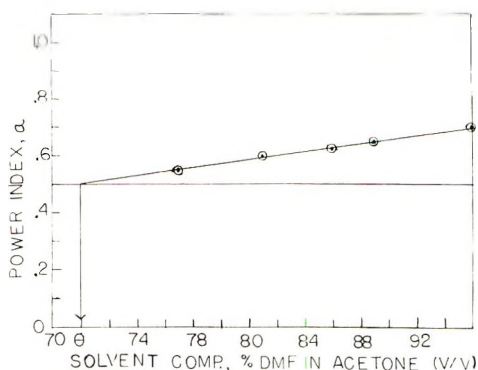


Fig. 1. Power index α of the Mark-Houwink equation as a function of the solvent composition. Nonsolvent, acetone; solvent, DMF.

to acetone/DMF = 21/79 (by volume). The logarithms of the resulting intrinsic viscosities for each DMF-acetone system used were plotted against the logarithms of their corresponding molecular weights according to the Mark-Houwink equation, eq. (3). The resulting slope values, which correspond to the exponential α in eq. (3), and the ordinate intercepts K were determined from the experimental data through linear least-square analyses carried out on the LOCI-2, desk-top computer, program No. S106. (Wang Laboratories, Inc., Tewksbury, Mass.).

The resulting slope values α , which are given in Table II, were then plotted against their corresponding DMF-acetone compositions as illustrated in Figure 1. The resulting line was produced to intersect with the line drawn at the value of $\alpha = 0.5$. The abscissa of the point of intersection was taken as the composition of the theta solvent.

A 71 DMF/29 acetone (v/v) mixture was determined to be the theta-solvent composition at 25°C. It then follows, that all intrinsic viscosities measured in this same solvent-nonsolvent mixture at 25°C are intrinsic viscosities determined under theta conditions and thus obey eq. (5). The

TABLE III
Perturbed Chain Dimensions Calculated for PU in DMF-Acetone System at 25°C

Solvent system	$[\eta]$, dl/g	$[\eta]_0^a$	α^b	$[\langle R^2 \rangle_0 / M]^{1/2} \times 10^{9c}$	$[\langle R^2 \rangle / M]^{1/2} \times 10^{9d}$
100 DMF	0.46	0.28 _n	1.18	8.60	10.11
95 DMF/5 A	0.47		1.19		10.19
90 DMF/10 A	0.48		1.19		10.25
85 DMF/15 A	0.45		1.17		10.04
79 DMF/21 A	0.44		1.16		9.97

^a Calculated from eq. (5).

^b Calculated from eq. (8).

^c Calculated from average K_0 determined by Stockmayer-Fixman relationship.

^d Calculated from eq. (8').

value of the constant K_{θ} can then be determined according to eq. (5) and the unperturbed dimensions subsequently from eq. (7).

The values of the constant K_{θ} , and the corresponding unperturbed dimension, $[\langle R^2 \rangle_0/M]^{1/2}$, estimated by the method described above, are given in Table III.

DISCUSSION OF RESULTS

Estimation of Theta Conditions

A temperature of 25°C was assigned to our polymer investigations as the experimental theta temperature. Following the procedure of Bianchi et al. as described above, the theta solvent-nonsolvent system was found to be a solution composed of a 79 to 21 volume ratio of DMF to acetone.

$[\eta]$ - \bar{M}_w Relationship

At the theta point, $[\eta]_{\theta}$ is directly proportional to the square root of the molecular weight, as expressed by eq. (5).⁶

Once the molecular weights of the various fractions of the polyurethane are known, then examination of the $[\eta]$ - \bar{M}_w relationship can be carried out. The resulting relationship for poly[ethylene methylene bis(4-phenyl carbamate)] in DMF at 25°C, is represented by eq. (4) above, $[\eta] = 3.64 \times 10^{-4} M^{0.71}$.

The same relationship for poly[ethylene methylene bis(4-phenyl carbamate)] in the theta solvent mixture, 71 DMF/29 acetone, at 25°C is given in eq. (11).

$$[\eta]_{\theta} = 3.0 \times 10^{-3} M^{1/2} \quad (11)$$

Estimation of Constant K_{θ}

The value for K_{θ} reported in eq. (11) is 3.0×10^{-3} . The value of K_{θ} corresponds, of course, to the ordinate intercept obtained upon plotting the double logarithmic plot of the Mark-Houwink equation of intrinsic viscosity measurements determined in the theta-solvent mixture at 25°C. According to eq. (7), K_{θ} should be directly proportional to $[\langle R^2 \rangle_0/M]^{3/2}$ and is dependent on the chain bond dimensions and free-rotation about them. The value of K_{θ} should therefore be independent of solvent composition in the unperturbed state.

In the work reported here, the K_{θ} was derived from the intrinsic viscosities of the polyurethane samples measured in the theta mixed solvent, the composition of which was determined as described above. When the Stockmayer-Fixman theory is applied to the same data, approximately the same K_{θ} value is obtained regardless of the amount of polymer nonsolvent added. Kurata and Stockmayer⁵ point out, however, that there is no absolute basis for believing the unperturbed dimensions to be independent of solvent. A number of cases have been reported where the variations of K_{θ} with solvent are quite noticeable; see, for example, the summaries by

Kurata and Stockmayer,⁵ Bianchi,⁷ Ciferri,⁸ and a paper by Crescenzi and Flory.⁹ From the data compiled by these workers, one would expect such variations to be most noticeable in polar polymer systems. Indeed our polyurethane does contain polar groups in its chain, and although the procedures used here do not give one unique value for the constant K_{θ} , the values are of the same magnitude and the difference could be attributed to polymer-solvent interaction.

Estimation of Unperturbed Chain Dimensions

Once the value of K_{θ} has been determined, the unperturbed dimensions, $[\langle R^2 \rangle_0/M]^{1/2}$, may be calculated from the relationship given in eq. (7). Throughout our calculations, we have used the best accepted numerical value of Φ_0 ,⁶ i.e., 2.87×10^{21} dl/mole-cc. The value of unperturbed dimension, $[\langle R^2 \rangle_0/M]^{1/2}$, is 8.60×10^{-9} . Once this value is estimated, then the perturbed dimensions $[\langle R^2 \rangle/M]^{1/2}$ and the molecular expansion parameters can be calculated.

The expansion parameter α and the unperturbed root-mean-square end-to-end distance for the fractions of PU, definitely increase with molecular weight, as one would expect. The variation of the root-mean-square unperturbed end-to-end distance $[\langle R^2 \rangle_0^{1/2}]$ with molecular weight is illustrated in Figure 2.

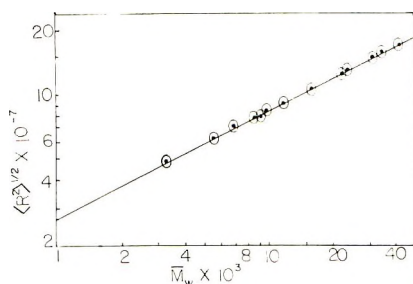


Fig. 2. Unperturbed root-mean-square end-to-end distance of PU as a function of molecular weight; in DMF at 25°C.

The variation of the perturbed chain dimensions with solvent composition is given in Table III. The general trend is a decrease in the chain dimensions approaching the theta conditions, however, the differences are rather subtle. The polymer analyzed here was a heterogeneous, unfractionated sample.

We are presently extending our investigations to include the solution properties of a number of carbamate-nitrogen substituted poly[ethylene methylene bis(4-phenyl carbamate)] samples. The pendent groups will be substituted in varying amounts and will be both polar and nonpolar in nature. It will be interesting to see how the same characterized backbone

conformation will be changed by the nature and extent of the various substitutions.

This paper is taken in part from the Ph.D. dissertation of Jean Coberg Peterson, University of Delaware, October 1967.

References

1. D. J. Lyman, *Rev. Macromol. Chem.*, **1**, 191 (1966).
2. D. J. Lyman, *J. Polym. Sci.*, **45**, 49 (1960).
3. L. H. Cragg, *J. Colloid Sci.*, **1**, 261 (1946).
4. U. Bianchi, V. Magnasco, and C. Rossi, *Ric. Sci.*, **28**, 1412 (1958).
5. M. Kurata and W. H. Stockmayer, *Fortschr. Hochpolym. Forsch.*, **3**, 196 (1963).
6. P. J. Flory, *Principles of Polymer Chemistry*, Cornell University Press, Ithaca, N. Y., 1953, Chap. 14.
7. U. Bianchi, *J. Polym. Sci. A*, **2**, 3083 (1964).
8. A. Ciferri, *J. Polym. Sci. A*, **2**, 3089 (1964).
9. V. Crescenzi and P. J. Flory, *J. Amer. Chem. Soc.*, **86**, 141 (1964).

Received July 23, 1968

Revised July 23, 1968

Determination of Penetrant Solubility from Transient Permeation Measurements

D. R. PAUL, *Department of Chemical Engineering, The University of Texas, Austin, Texas 78712*

Synopsis

The permeability coefficient for the transport of a gas, vapor, or liquid through a polymer film is the product of the penetrant solubility and a diffusion coefficient. A transient permeation experiment known as the time-lag technique can be used to separate this product, provided the diffusion coefficient is independent of penetrant concentration. In this well-known experiment the polymer is initially free of penetrant. A new transient permeation experiment where the polymer is initially saturated with penetrant is suggested here. A general mathematical proof is given to show that by using the results from these two transient experiments which have different initial conditions one can determine the penetrant solubility no matter how the diffusion coefficient depends on penetrant concentration. Also one can determine two different concentration averaged diffusion coefficients from the results.

The transport rate of gases, vapors, and liquids through polymer films is of considerable interest for a variety of reasons, and a great deal of effort has been directed towards understanding this process.¹ Aside from the geometry of the film, i.e., area and thickness, the steady-state transport rate is determined by a permeability coefficient which is a property of the penetrant and the film. This coefficient is the product of the solubility of the penetrant in the polymer and the diffusion coefficient for the penetrant in the polymer. To analyze the transport process fundamentally, it is necessary to separate this product; however, this cannot be done by steady-state permeation measurements. In principle, one can measure the solubility by an independent method, but in practice this may be very difficult or impractical. In simple cases, this difficulty may be overcome by transient permeation measurements or the time-lag technique² which makes a separation possible. Unfortunately, in many important cases this approach is not applicable, since the diffusion coefficient is dependent on the penetrant concentration. Here the steady-state permeability coefficient is the product of the solubility and an integrated average diffusion coefficient. Frisch³ has developed a rigorous approach to this more complex case, but in most situations an impractical number of conditions must be studied to effect this analysis. Frisch's work is extended here to show that the solubility can be obtained by two transient permeation experiments even when the diffusion coefficient depends on concentration.

The situation of interest is a film of thickness l with diffusion along the x axis only. Initially the concentration of the penetrant is c_0 throughout the sample. At time $t = 0$, the surface at $x = 0$ is exposed to a gas, vapor, or liquid which immediately establishes an equilibrium concentration of penetrant, c_2 , within the film at $x = 0$. At the same time, conditions on the other side of the film are so adjusted that the penetrant concentration at $x = l$ is c_1 , which is set equal to zero here since this is the common experimental practice.

To illustrate the technique suggested here, the case where the diffusion coefficient D is independent of concentration will be considered first, then the more general case will be developed. For this simple situation Fick's second law can be solved rigorously to give Q_t , the amount of penetrant which has left unit area of the film after a time t . This result is well known.⁴

$$\frac{Q_t}{lc_2} = \frac{Dt}{l^2} - \frac{1}{6} - \frac{2}{\pi^2} \sum_{n=1}^{\infty} \frac{(-1)^n}{n^2} e^{-Dn^2\pi^2 t/l^2} + \frac{1}{2} \frac{c_0}{c_2} \left[1 - \frac{8}{\pi^2} \sum_{m=0}^{\infty} \frac{1}{(2m+1)^2} e^{-D(2m+1)^2\pi^2 t/l^2} \right] \quad (1)$$

In the usual time-lag approach, the film is initially freed of penetrant, i.e., $c_0 = 0$, so the group of terms in brackets in eq. (1) does not appear. The lower curve in Figure 1 illustrates this familiar response on a plot which

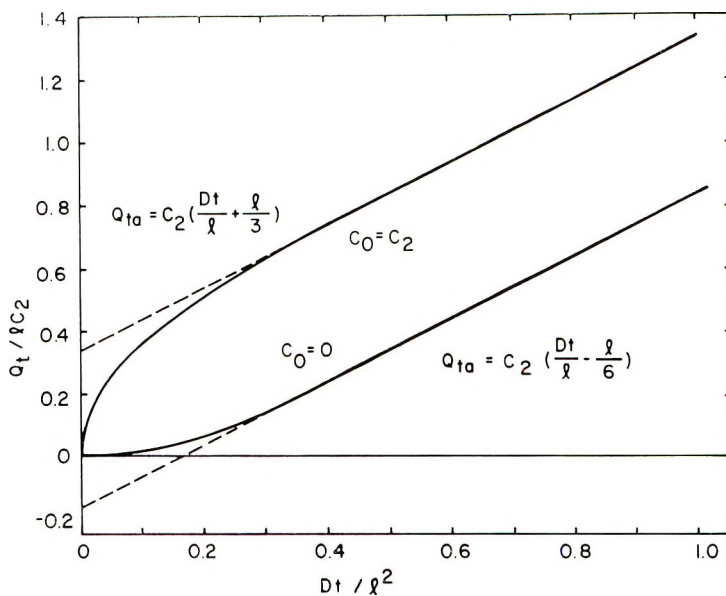


Fig. 1. Illustration of transient permeation with two different initial conditions within the film: saturated with penetrant, $c_0 = c_2$, and free of penetrant, $c_0 = 0$. The curves are drawn for a constant D .

employs the dimensionless coordinates suggested by eq. (1). It is worthwhile to note the intercepts an extrapolation of the steady-state part of this solution makes on the horizontal and vertical axes. Another initial condition that can be realized experimentally is $c_0 = c_2$: that is, the film is initially saturated throughout with penetrant. The upper curve in Figure 1 shows the response for this initial condition. This latter case seems to have never been studied before; although, in principle it should be possible to make measurements of this type. It is important to note that the algebraic difference between the intercepts on the $t = 0$ axis for these two experiments with different initial conditions is $c_2l/2$ when the results are plotted on Q_t versus t coordinates.

The results obtained with $c_0 = c_2$ can be represented in another informative way by plotting Q_t against the square root of time. Figure 2 illustrates this type of representation. The dimensionless groups suggested by eq. (1) are also used here. Initially, there is a linear relationship as one would expect since this part of the permeation is equivalent to a desorption experiment.

This additional experiment produces no new information when D is independent of c , but it will now be shown that the difference in the intercepts on the $t = 0$ axis is still $c_2l/2$ even when D does depend on c , which is a new and useful result. This demonstration utilized methods outlined earlier by Frisch.³

For a concentration dependent diffusion coefficient Fick's second law is

$$\frac{\partial c}{\partial t} = \frac{\partial}{\partial x} \left[D(c) \frac{\partial c}{\partial x} \right] \tag{2}$$

This equation, when integrated over x from an arbitrary value of $x = z$ to $x = l$, gives

$$\int_z^l (\partial c / \partial t) dx = [D(c) (\partial c / \partial x)]_{x=l} - [D(c) (\partial c / \partial x)]_{x=z} \tag{3}$$

Next eq. (3) is integrated over time from $t = 0$ to an arbitrary time t to get

$$\int_0^t \int_z^l \frac{\partial c(x, \tau)}{\partial \tau} dx d\tau = \int_0^t \left[D(c) \frac{\partial c(x, \tau)}{\partial x} \right]_{x=l} d\tau - \int_0^t \left[D(c) \frac{\partial c(x, \tau)}{\partial x} \right]_{x=z} d\tau \tag{4}$$

The double integral on the left side of eq. (4) is equal to

$$\int_z^l c(x, t) dx - c_0(l - z)$$

while the first term on the right is equal to $-Q_t$. With these identifications, eq. (4) becomes

$$Q_t = c_0(l - z) - \int_z^l c(x,t)dx - \int_0^t \left[D(c) \frac{\partial c(x,\tau)}{\partial x} \right]_{x=z} d\tau \quad (5)$$

A final integration over z from 0 to l is performed on eq. (5) to give

$$Q_t = \frac{c_0 l}{2} - \frac{1}{l} \int_0^l \int_z^l c(x,t)dx dz - \frac{1}{l} \int_0^l \int_0^t \left[D(c) \frac{\partial c(x,\tau)}{\partial x} \right]_{x=z} d\tau dz \quad (6)$$

The last double integral on the right in eq. (6) can be evaluated as follows

$$\begin{aligned} \int_0^l \int_0^t \left[D(c) \frac{\partial c(x,\tau)}{\partial x} \right]_{x=z} d\tau dz &= \int_0^t \int_0^l \left[D(c) \frac{\partial c(x,\tau)}{\partial x} \right]_{x=z} dz d\tau \\ &= - \int_0^t \int_0^{c_2} D(c) dc d\tau = - t \int_0^{c_2} D(c) dc \quad (7) \end{aligned}$$

As steady state is approached, $c(x,t)$ ceases to be a function of time, so the other double integral in eq. (6) becomes constant. Thus the steady-state asymptote of eq. 6 is

$$Q_{\infty} = \frac{c_0 l}{2} - \int_0^l \int_z^l c(x)dx dz + \frac{t}{l} \int_0^{c_2} D(c)dc \quad (8)$$

The double integral in eq. (8) can be reduced to a single integral by integration by parts. Substitution of this simplification yields

$$Q_{\infty} = \frac{c_0 l}{2} - \frac{1}{l} \int_0^l zc(z)dz + \frac{t}{l} \int_0^{c_2} D(c)dc \quad (9)$$

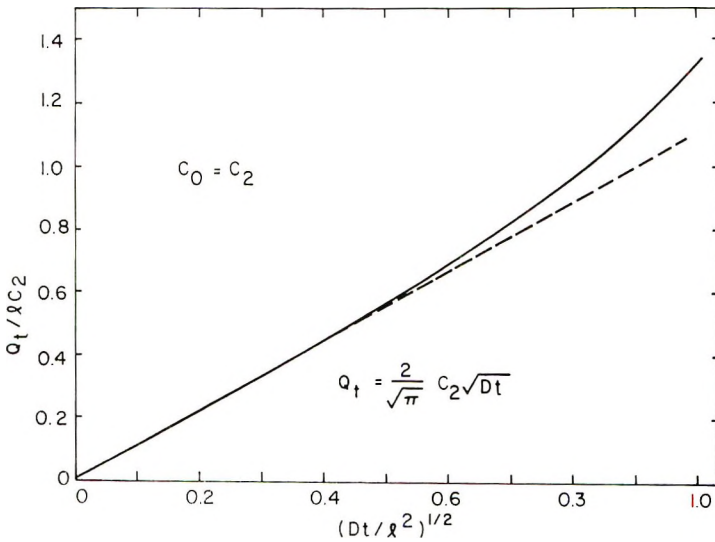


Fig. 2. Transient portion of the permeation for the initially saturated film, $c_0 = c_2$. The curve is drawn for constant D .

This equation gives the steady-state asymptotes for all cases where c_0 is any constant and D is any function of c . For the special case when D is independent of c , the steady-state concentration profile is $c(x) = c_2[1 - (x/l)]$. Substitution of this profile into either eq. (8) or (9) yields the lower equation in Figure 1 when c_0 is set equal to zero and the upper equation in Figure 1 when c_0 is set equal to c_2 .

If D depends on c , then the double integral in eq. (8) or the single integral over z in eq. (9) cannot be evaluated without explicit knowledge of how D depends on c , which of course is unknown. However, it is very interesting to note that the last two terms in eqs. (8) and (9) are independent of c_0 . This means that the steady-state plots of Q_t versus t for $c_0 = 0$ and $c_0 = c_2$ differ by the constant value $c_2l/2$. Consequently the algebraic differences between the intercepts of the steady-state extrapolations to the $t = 0$ axis for these two experiments is still $c_2l/2$ even though D depends on c .

In summary, eq. (9) [or (8)] gives the steady-state asymptotes for both the normal time-lag experiment where $c_0 = 0$ and the new experiment suggested where $c_0 = c_2$. If one performs either of these two experiments alone, the solubility c_2 cannot be deduced from the results due to the unknown double integral in eq. (8) or its equivalent in eq. (9), but by using both experiments the unknown integral can be eliminated and the desired quantity c_2 can be deduced.

It is interesting to see what other information can be obtained from these results. The steady-state slope from both experiments leads to an integrated diffusion coefficient, i.e., $\int_0^{c_2} D(c)dc$. The transient portion of the experiment with $c_0 = c_2$ can be analyzed in a fashion similar to that shown in Figure 2. The slope of this plot will give an average diffusion coefficient equal to that obtained from a desorption experiment but different from the average coefficient calculated from the slope of the steady-state data.

The new technique proposed here should prove useful in situations where the diffusion coefficient is concentration dependent and the penetrant solubility is small or adequate techniques are not available to determine it independently. Further, it may provide an informative way to study water permeation where apparently clustering leads to anomalous results.

This work was supported in part by a grant from the National Science Foundation.

References

1. J. Crank and G. S. Park, Eds., *Diffusion in Polymers*, Academic Press, New York, 1968.
2. H. Daynes, *Proc. Roy. Soc. (London)*, **A97**, 286 (1920).
3. H. L. Frisch, *J. Phys. Chem.*, **61**, 93 (1957).
4. J. Crank, *Mathematics of Diffusion*, Oxford Univ. Press, London, 1956, p. 47.

Received June 19, 1968

Revised July 26, 1968

Poly-2,5-distyrylpyrazine and Its Properties

SHOEI FUJISHIGE* and MASAKI HASEGAWA, *The Textile Research Institute of Japanese Government, Kanagawa, Yokohama, Japan*

Synopsis

Four possible structural models with novel steric character are proposed for poly-2,5-distyrylpyrazine: two of them are extended chains and the others are kinked coils. In order to prove the molecular characteristic of the new polymer, a procedure to solubilize the polymer into some organic solvents was developed. It was recognized by viscometry that no significant degradation of the polymer does occur during the preparation. The lack of the shear rate dependence of the dilute solution viscosities would seem to indicate that the polymer molecule in solution can be regarded as a chain, not extended linearly, but kinked randomly. The crystallization of the polymer proceeds only in the presence of a sufficient amount of the solvent which enables the polymer chains to move and crystallize. These imply that the possible structure of the polymer is constructed of 1,2- or 1,3-*cis* type cyclobutane linkages with restricted rotation.

Introduction

In the preceding papers¹⁻³ it has been reported that a new type of crystalline polymer having a cyclobutane ring in its repeating unit was obtained from *trans*, *trans*-2,5-distyrylpyrazine through a solid-state polymerization reaction induced by the action of ultraviolet light or sunlight.

The novel characteristic of the poly-2,5-distyrylpyrazine in comparison with many of the other natural and synthetic polymers is its molecular structure with closely restricted free rotation around the cyclobutane unit in the main chain. It was anticipated that the effects of such important steric hindrance might be demonstrated either in the dilute solution properties or in the solid-state behavior. As already reported, however, the polymer is highly crystalline and insoluble in most conventional organic solvents except for some strong acids, such as concentrated sulfuric, dichloroacetic, or trifluoroacetic acid, so that the molecular characteristic of the new polymer has not yet been proved experimentally.

In order to characterize the polymer, a procedure for preparing soluble poly-2,5-distyrylpyrazine was developed. It was found that the polymer becomes soluble into some organic solvents such as *m*-cresol or *o*-chlorophenol at room temperatures after being subjected to a pretreatment for regeneration of the crystalline solid polymer.

* Present address: c/o Prof. Dr. H.-G. Elias, Technisch-Chemisches Laboratorium, Swiss Federal Institute of Technology, CH-8006 Zurich 6, Universitatstrasse 6, Schweiz.

In this paper, preparation of soluble poly-2,5-distyrylpyrazine, and some examples of the characteristic behavior of the polymer thus prepared are described.

Molecular Structure

Although the steric configuration has not yet been established, it is tentatively proposed^{1,2} on the basis of the infrared and NMR spectra that the molecular structure for the poly-2,5-distyrylpyrazine is, as shown schematically in Figure 1, i.e., 1,2- or 1,3-diphenyl cyclobutane derivative.

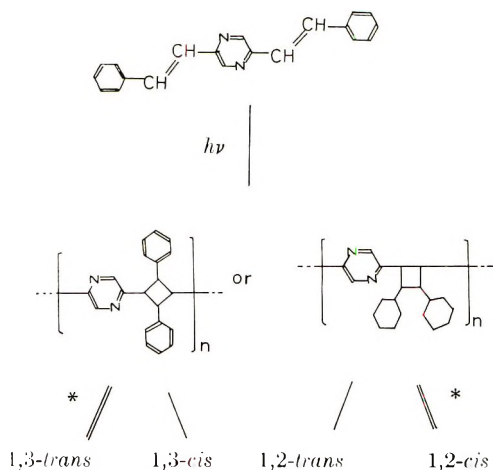
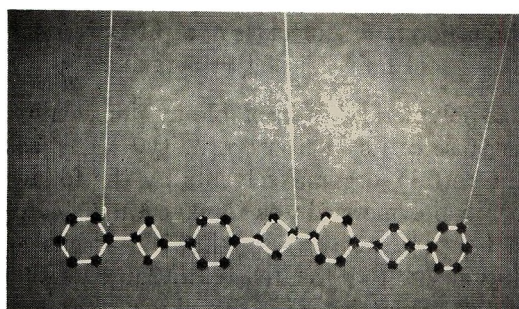


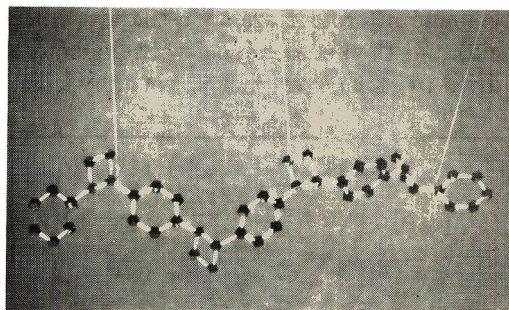
Fig. 1. Polymerization of *trans,trans*-2,5-distyrylpyrazine and the proposed structural unit of the polymer thus obtained. The asterisk (*) indicates the stronger probability.

Both the structures, moreover, have *trans* and *cis* steric isomers. Molecular models for each of the skeletal structures of the polymer are shown in Figure 2. It is seen that the steric characters are distinctly reflected on the chain configurations. If the structure is assumed to be that of the 1,3-*trans* derivative, on one hand, the overall shape of the polymer molecule isolated in dilute solution is a rodlike, linearly extended chain as given in Figure 2*a*. If the structure is of the 1,2-*trans* type, as shown in Figure 2*b*, the effects of the steric hindrance on the chain configuration are slightly decreased compared to the 1,3-*trans* type structure. On the other hand, if the structure is composed of 1,2- or 1,3-*cis* type, the polymer is a randomly kinked coil as shown in Figures 2*c* and 2*d*.

In consequence it is anticipated that these configurational characteristics, either rodlike or kinked coil, would reflect directly on the hydrodynamic behavior, e.g., non-Newtonian flow behavior of the dilute solutions and also on the crystallization behavior.



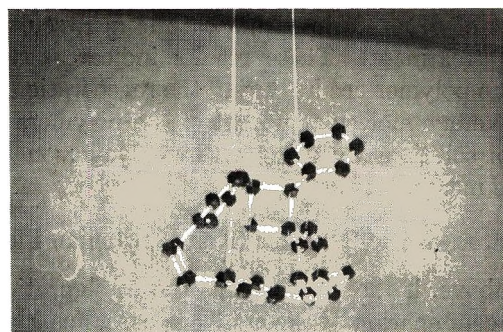
(a)



(b)



(c)



(d)

Fig. 2. Molecular models for possible skeletal structures of poly-2,5-distyrylpyrazine: (a) 1,3-*trans* type; (b) 1,2-*trans* type; (c) 1,3-*cis* type; (d) 1,2-*cis* type.

Solubilization and Molecular Weight Determination of Poly-2,5-distyrylpyrazine

The polymer as-polymerized is insoluble in almost all conventional organic solvents because of its high crystallinity.¹ This solid material becomes soluble in certain organic solvents by the following treatments. First, the polymer as-polymerized was dissolved in dichloroacetic acid with stirring at room temperatures and a yellowish viscous solution was prepared. The solution was then poured into a large amount of water containing sufficient triethylamine and the precipitates were collected by filtration. The polymer thus obtained was washed repeatedly with aqueous dilute triethylamine in order to remove the last traces of the solvent (dichloroacetic acid) and then successively with aqueous acetone and acetone and finally dried *in vacuo* over phosphoric anhydride.

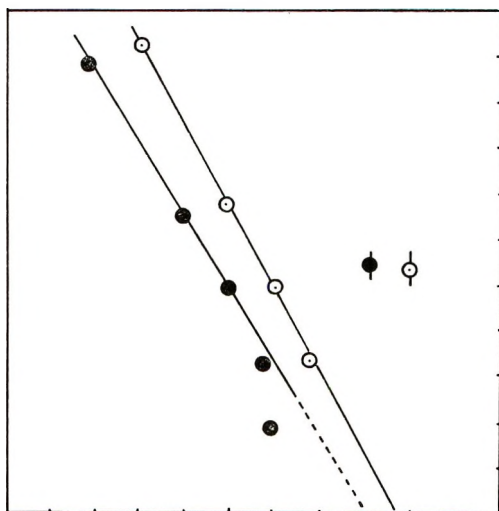


Fig. 3. Viscosity-concentration relationships of a poly-2,5-distyrylpyrazine ($M_n = 6 \times 10^4$) in dichloroacetic acid solutions: (●) before and (○) after the regeneration.

Figure 3 shows the viscosity-concentration relationship of polymer of molecular weight of 6×10^4 in dichloroacetic acid solutions before and after the above treatment. These results indicate that no significant degradation of the polymer occurs during the regeneration process.

The number-average molecular weight of the polymers was determined in *o*-chlorophenol solutions by using a Zimm-Mayerson type osmometer with gel cellulose membranes at 25°C.

Hydrodynamic Behavior (Non-Newtonian Flow)

As described above, if the polymer has the configuration of either 1,3- or 1,2-*trans* type combination, the overall shape is a linearly extended chain or wormlike extended chain, respectively, as shown in Figures 2*a* and 2*b*,

and a noticeable non-Newtonian flow behavior is naturally anticipated to be observed on the dilute solution viscosities. The effects of rate of shear on the solution viscosities were investigated by using modified Ubbelohde capillary viscometers⁴ up to about 1200 sec^{-1} for a polymer of molecular weight of 6×10^4 and up to about 240 sec^{-1} for a polymer of molecular weight of 6×10^5 at 25°C .

Contrary to our expectation, no significant indication of the shear rate dependence of the viscosities to demonstrate the shape effects of the extended chain molecules was observed either with *m*-cresol solutions or with *o*-chlorophenol solutions.

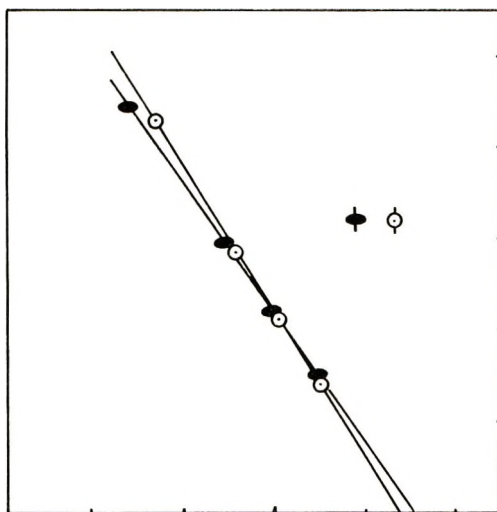


Fig. 4. Viscosity-concentration relationships for *m*-cresol solutions and *o*-chlorophenol solutions of a poly-2,5-distyrylpyrazine ($M_n = 6 \times 10^5$) at 25°C .

The lack of the shear rate dependence of the dilute solution viscosities would seem to indicate that the polymer molecule in solution can be regarded as a chain not extended linearly but kinked randomly (i.e., 1,2- or 1,3-*cis* type), with closely restricted steric rotation around the cyclobutane linkages.

The viscosity-concentration relationships for *m*-cresol solutions and *o*-chlorophenol solutions of a polymer of molecular weight of 6×10^5 are shown in Figure 4. It is seen that the two linear relationships are very close to each other in spite of the fact that the viscosity of *m*-cresol is ten times that of *o*-chlorophenol. This fact may be attributed mainly to the situations due to a possible free-draining effect of the solvent molecules throughout the kinked coil following the Kirkwood-Risemann model⁵ or a possible thermodynamic solvent-solute interaction which gives rise to the same order of effective volume of the polymer molecules in both the dilute solutions, irrespective of the solvent used.

Crystallization Behavior

Another representative feature of poly-2,5-distyrylpyrazine was observed during the course of its crystallization. Owing to the novel steric character and the thermal properties (e.g., the melting point at 321°C and the decomposition temperature at 339°C)⁶ crystallization of the polymer does not proceed from its melt but occurs in the presence of a sufficient amount of solvent to permit the molecular motion and the intermolecular interaction of the polymers.

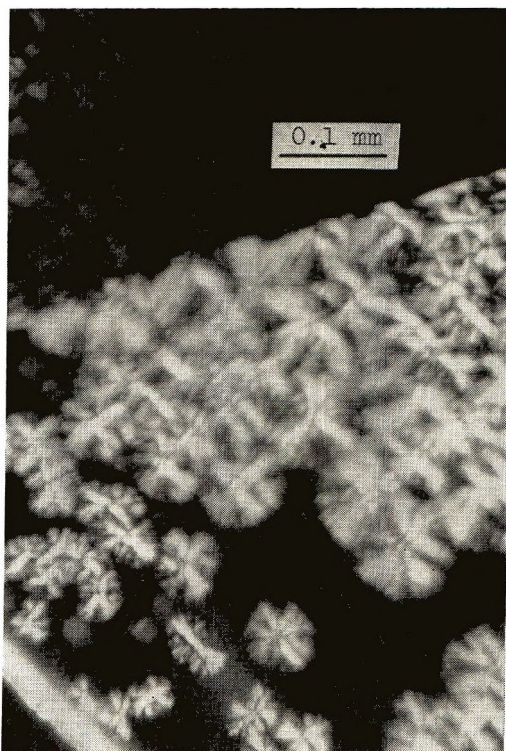


Fig. 5. Partially crystallized polymer film observed by polarization microscopy.

If the solvent is evacuated rapidly from the polymer-solvent system, the remaining polymer chains are no longer able to form the crystallized texture due mainly to the restricted molecular motion, so that the crystallization process is interrupted and only amorphous polymer film results.

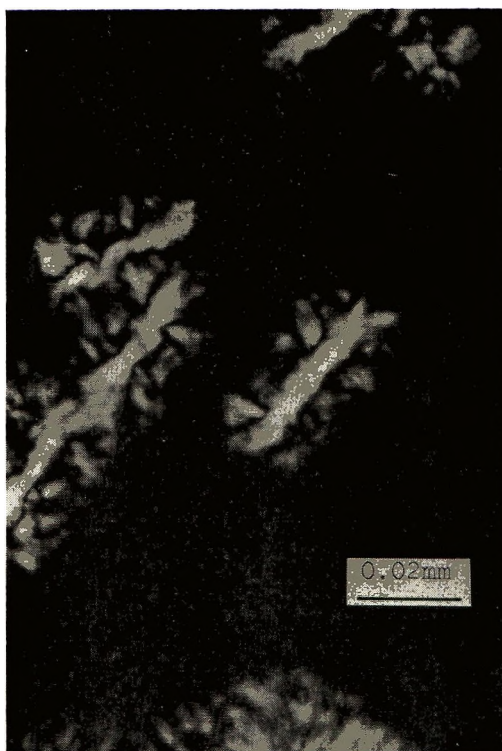
Figure 5 shows such behavior as observed by polarization microscopy on a partially crystallized polymer film cast from 1% polymer-*o*-chlorophenol solution by slow evaporation of the solvent for 2-4 weeks at room temperature. Figure 6 shows this behavior also in a series of pictures taken from a different part of the same specimen shown in Figure 5 by using a new orthomat microscope camera attachment (E. Leitz, Welzer) attached to

TABLE I
Spacing Parameters Calculated from the X-Ray Diffraction Patterns of Figure 7

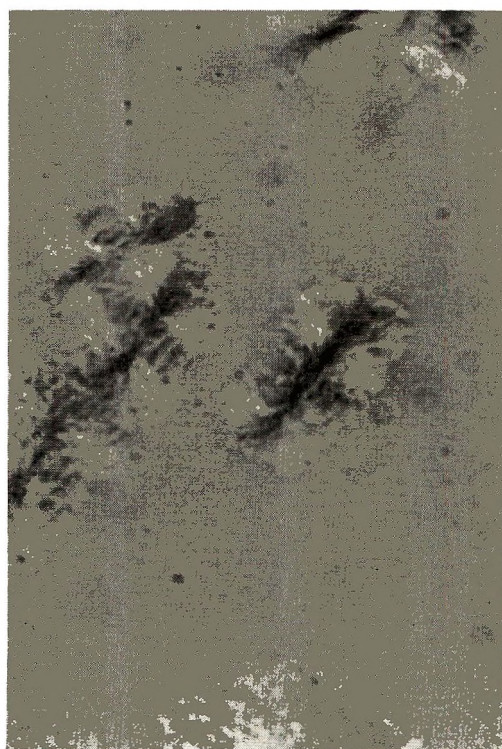
As-polymerized			Thin film			Thick film			Stretched film		
cm (intensity)	2θ	\AA	cm(intensity)	2θ	\AA	cm(intensity)	2θ	\AA	cm(intensity)	2θ	\AA
6.31(w) ^a	30.5 ₈	2.9	—	—	—	6.7(vw)	32.1	2.8	—	—	—
5.90(s)	28.8 ₈	3.1	—	—	—	5.9(vw)	28.9	3.1	6.0(vw)	29.3	3.0
5.46(w) ^a	27.0 ₈	3.3	—	—	—	—	—	—	—	—	—
5.12(m) ^a	25.15	3.5	5.2(s) ^b	25.9	3.4	5.2(s) ^b	25.9	3.4	5.2(s) ^b	25.9	3.4
4.80(vs)	24.1 ₆	3.7	—	—	—	4.8(vw)	24.2	3.7	4.8(vw)	24.2	3.7
4.38(s) ^a	22.3 ₁	4.0	—	—	—	4.5(s)	22.8	3.8	—	—	—
4.00(vs) ^a	20.5 ₄	4.3	4.15(s) ^b	21.3	4.2	4.15(s) ^b	21.3	4.2	4.15(s) ^b	21.3	4.2
3.62(vs) ^a	18.7 ₀	4.8	—	—	—	—	—	—	—	—	—
3.10(vs) ^a	16.1 ₇	5.4	3.15(vs) ^b	16.1	5.3	3.6(s)	18.6	4.8	3.15(vs) ^b	16.1	5.3
2.86(s) ^a	14.9 ₇	5.9	—	—	—	3.15(vs) ^b	16.1	5.3	—	—	—
2.38(m)	12.5 ₈	7.1	2.38(m)	12.6	7.1	2.38(m)	12.6	7.1	2.38(m)	12.6	7.1
1.80(m)	9.5 ₆	9.3	1.7(m)	9.0	9.8	1.8(w)	9.5	9.3	—	—	—

^a Characteristic patterns detected with the as-polymerized sample.

^b Characteristic patterns detected with the recrystallized specimens.



(a)

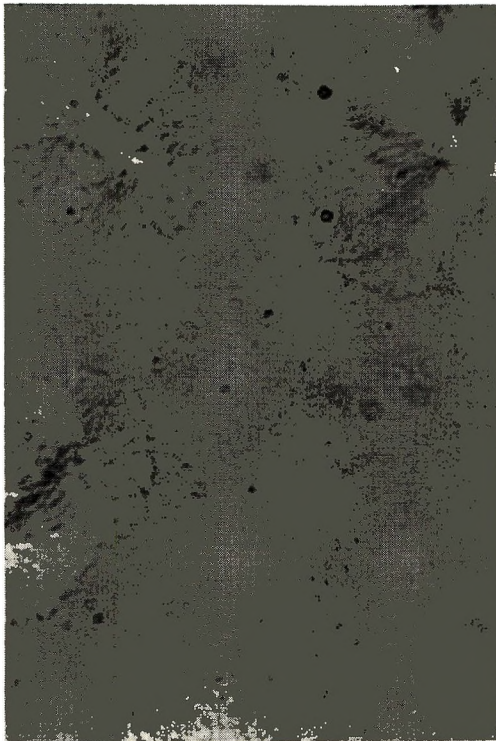


(b)

Fig. 6. Several stages of spherulite formation gradually developing from the crystallized, sheaflike textures; a series of the pictures are taken from different parts of the same specimen as shown in Figure 5. Each pair shows results by the crossed-polarizer method (a) and also by the phase-contrast method (b).



(c)



(d)

Fig. 6 (continued)

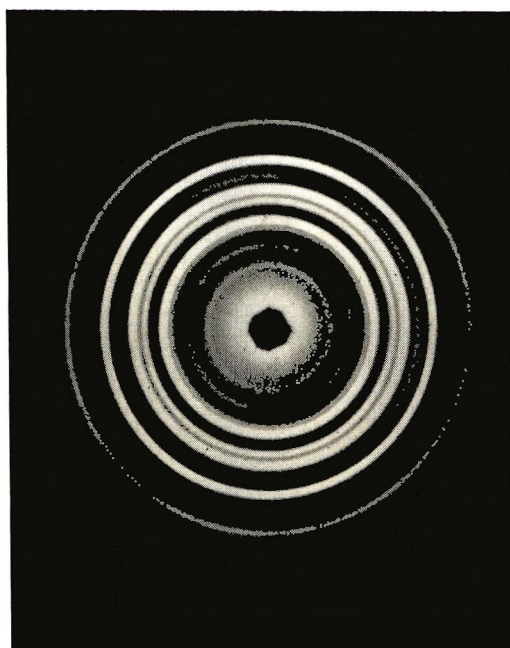


(e)



(f)

Fig. 6 (continued)



(a)



(b)

Fig. 7. X-Ray diffraction patterns of (a) the as-polymerized crystalline powder of poly-2, 5-distyrylpyrazine as compared to those of recrystallized specimens prepared (b) by slow evacuation of the solvent from its *o*-chlorophenol solution (thin film) or (c) by conditioning the amorphous polymer film in a mixture of solvent-nonsolvent (thick film) or (d) by stretching an amorphous polymer film followed by conditioning in the mixture of the same composition. (cf. Table I.)

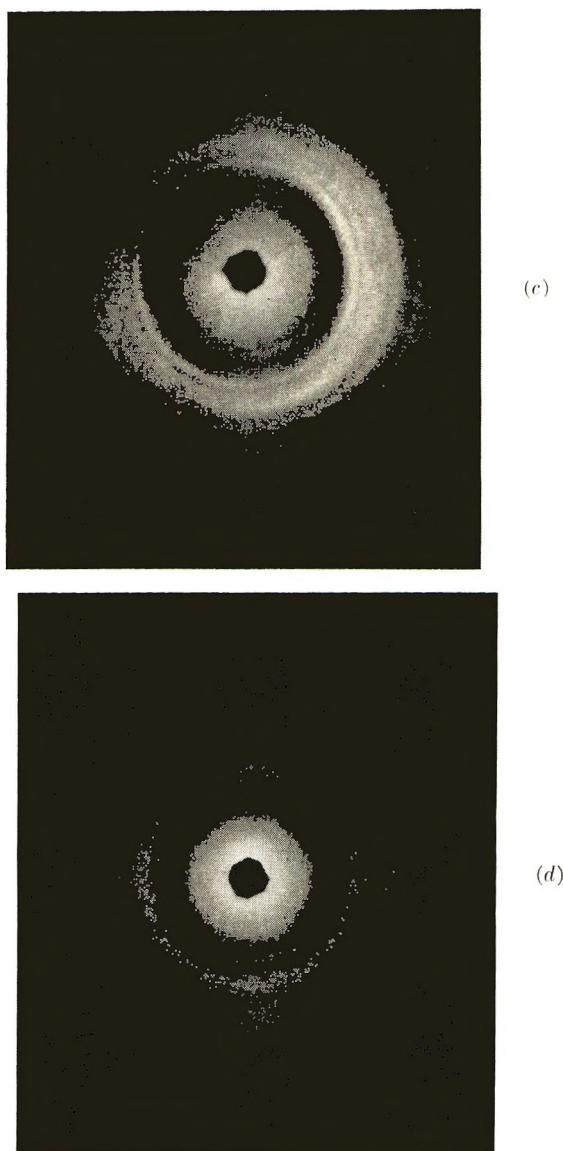


Fig. 7 (continued)

a polarization microscope. Several stages of the spherulite formation gradually developing from the crystallized, sheaflike textures are shown.

The crystalline structures of the spherulite textures of the poly-2,5-distyrylpyrazine were also examined by wide-angle x-ray diffraction and the results obtained are compared in Figure 7 with those of the as-polymerized material.

Crystallized specimens for x-ray examination were prepared by either slow evaporation of the solvent from its *o*-chlorophenol solutions as de-

scribed above or by conditioning an amorphous polymer film in a solvent-nonsolvent mixture for over two weeks. The fiber diagram was also examined on a stretched film conditioned in the mixture of the same composition. Spacing parameters calculated from the x-ray diffraction patterns of the samples shown in Figure 7 are compared with those of the as-polymerized material in Table I. It is seen that some of the characteristic patterns are not identical, i.e., patterns corresponding to 2.9, 3.3, 4.0, 4.3, 4.8, 5.4, and 5.9 Å were detected in the as-polymerized sample compared with 3.4, 4.2, and 5.3 Å in the recrystallized specimens.

From this we may infer that an irreversible transition of the crystal structure of the poly-2,5-distyrylpyrazine does occur from the quasi-stable state in the as-polymerized material to the stable state in the recrystallized textures during the course of the above treatments.

Conclusion

The most important features to be anticipated from the viewpoint of the novel molecular structure of poly-2,5-distyrylpyrazine are reflected in both the hydrodynamic behavior of the dilute solutions and the crystallization behaviors.

Contrary to our expectations, no indication of the shear rate dependence of the viscosities of the dilute polymer solutions has been proved.

In consequence, it was suggested that the poly-2,5-distyrylpyrazine molecule in solution can be regarded as a randomly kinked rather than a linearly extended chain. This implies that the possible structure of the polymer is constructed of 1,2- or 1,3-*cis* type cyclobutane linkages with restricted free rotation.

In crystallization of the polymer, it was found that the crystallization proceeds only in the presence of a sufficient amount of the solvent which enables the polymer molecules to move and crystallize.

Although quantitative verification has not yet been fully demonstrated, these several observations are amenable to interpretation from this point of view.

References

1. M. Hasegawa and Y. Suzuki, *J. Polym. Sci. B*, **5**, 813 (1967).
2. M. Iguchi, H. Nakanishi, and M. Hasegawa, *J. Polym. Sci. A-1*, **6**, 1955 (1968).
3. H. Nakanishi and M. Hasegawa, *J. Polym. Sci.*, in press.
4. S. Fujishige, J. Kuwana, and M. Shibatama, *J. Polym. Sci. B*, **1**, 355 (1963).
5. J. G. Kirkwood and J. Riseman, *J. Chem. Phys.*, **16**, 565 (1948).
6. H. Kanetsuna, unpublished data.

Received January 15, 1968

Revised September 27, 1968

Metal Coordination Polymers. II. Molecular Weight Studies of Beryllium Phosphinate Polymers in Toluene

P. J. SLOTA, C. M. GRIEVE, N. R. FETTER, and A. J. BILBO, *Naval Weapons Center, Corona Laboratories, Corona, California 91720*

Synopsis

The number-average molecular weights of beryllium 4-biphenyl(phenyl)phosphinate, di-*n*-pentylphosphinate, di-*n*-heptylphosphinate, and trifluoromethyl(phenyl)phosphinate are degraded by the presence of water in toluene. It is proposed that easily hydrolyzable P—O—P bonds contribute, in part, to the bonding of these polymers.

INTRODUCTION

The recently published observation by Ripamonti et al.¹ that zinc dialkylphosphinate polymers undergo reversible degradation in noncoordinating solvents led us to examine several of our beryllium phosphinates by means of membrane osmometry. We had observed that the number-average molecular weight \bar{M}_n of beryllium 4-biphenyl(phenyl)phosphinate in toluene appeared to decrease over a period of several days from approximately 170 000 to 30 000. This paper describes the results of systematic measurements of \bar{M}_n versus time of several beryllium phosphinate polymers. Determination of molecular weights in both ordinary reagent-grade toluene and dry toluene have led to the conclusion that solutions of these materials are readily degraded by moisture.

EXPERIMENTAL

All molecular weights were measured on a Hewlett-Packard Model 502 membrane osmometer operating at 37°C with the use of S & S 0-8 deacetylated acetyl cellulose nonaqueous membranes.

Sample solutions were prepared in 10 ml volumetric flasks and concentrations ranged from 0.5 to 2.5 mg/ml. All samples were dissolved at room temperature with the aid of magnetic stirring bars.

Reagent-grade toluene was used without treatment. Dry toluene was obtained by distilling reagent-grade toluene from LiAlH₄. The solvent was stored over molecular sieve (Type 4A) in a dry box.

Dry sample solutions were prepared by weighing the polymer in oven-dried flasks, transferring them into the dry box, and dissolving the samples

under the dry atmosphere. The flasks were stored over Drierite in a desiccator when measurements were not being made. When determinations were being made, there was no control over absorption of atmospheric moisture, but each measurement required no more than 5 min.

The beryllium phosphinates, with the exception of beryllium trifluoromethyl(phenyl)phosphinate, were prepared by the reaction of beryllium acetylacetonate with the appropriate phosphinic acid.² Beryllium trifluoromethyl(phenyl)phosphinate was prepared by adding a stoichiometric amount of diethylberyllium in 50 ml of toluene to a toluene solution (100 ml) of trifluoromethyl(phenyl)phosphinic acid. The diethylberyllium was added dropwise to the acid solution which was magnetically stirred and maintained at 25°C. After the addition was complete, the solution was heated to 70°C for 20 hr. The toluene was distilled until 15 ml of solution remained. The remaining solvent was removed under high vacuum for 4 hr at 140°C. Approximately 5 g of glassy, white polymer was obtained.

RESULTS AND DISCUSSION

The selection of beryllium phosphinate polymers was limited to those which were soluble in a nonpolar organic solvent and had number-average molecular weights \bar{M}_n large enough for one to observe changes with time. The candidates selected were beryllium 4-biphenyl(phenyl)phosphinate, beryllium di-*n*-pentylphosphinate, beryllium di-*n*-heptylphosphinate, and beryllium trifluoromethyl(phenyl)phosphinate. Other polymers which were soluble in toluene had low molecular weights which did not vary with time. These were beryllium di-*n*-butylphosphinate ($M_n = 15\,000$), beryllium methyl(phenyl)phosphinate ($M_n = 6\,000$), and beryllium 2-biphenyl(phenyl)phosphinate ($M_n = 15\,000$).

The results for beryllium 4-biphenyl(phenyl)phosphinate, the first of this group to be studied, are shown in Figure 1. In undried toluene, the extrapolated zero-time number-average molecular weight (\bar{M}_n) of 170 000 decayed rapidly at first, but gradually decreased to an almost constant value of 33 000.

The molecular weight of this polymer in dry toluene remained constant at $300\,000 \pm 10\,000$ for six days. However, there was evidence of microgel formation in the solutions, making this M_n value questionable. When a microdrop of water (~ 0.01 ml) was added to each 10 ml solution, the molecular weight decreased to 100 000 after 8 hr, and after 24 hr had decreased to 35 000, where it remained stable.

To assure that the addition of a microdrop of water to the sample solution did not, by itself, affect the value of \bar{M}_n , drops of water were added to dry toluene solutions of ArRo C-300-4 ($M_n = 97\,200$) molecular weight standard. Before water was added, M_n was 89 000, and after, M_n was 100 000.

To test the suggestion by Ripamonti et al.³ that beryllium phosphinate polymers dissolved in nonpolar solvents were equilibrium mixtures whose

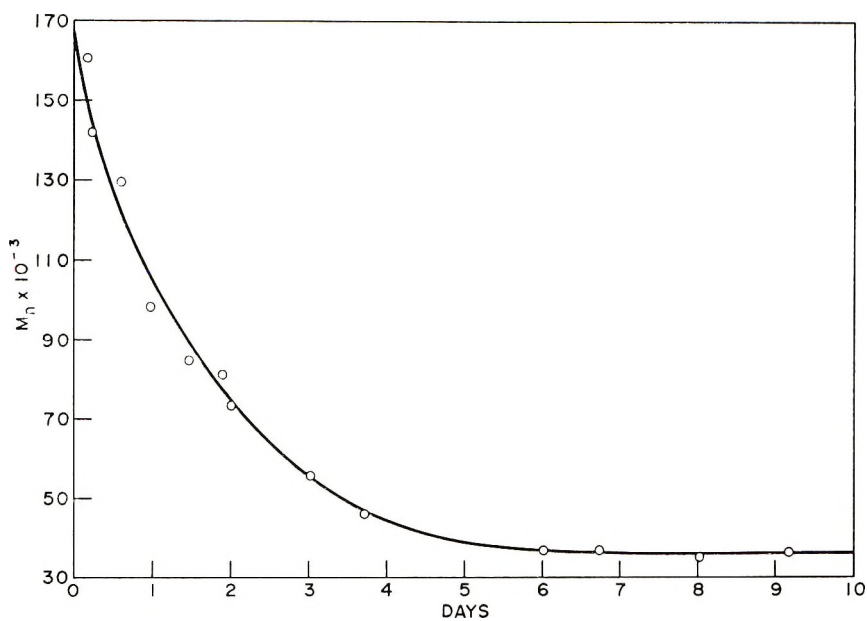


Fig. 1. Number-average molecular weights of beryllium 4-biphenyl(phenyl)phosphinate in undried toluene.

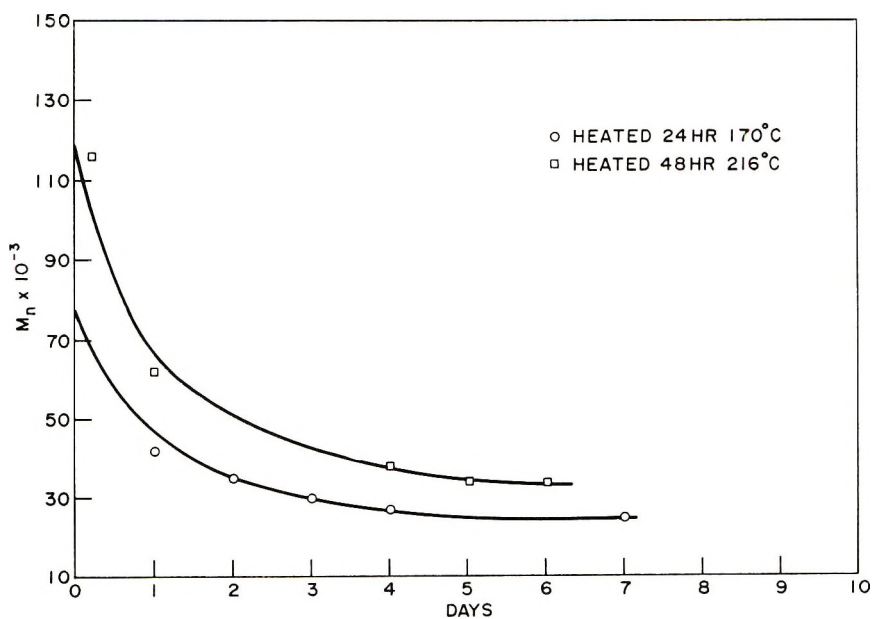


Fig. 2. Number-average molecular weights of regenerated beryllium 4-biphenyl(phenyl)phosphinate in undried toluene.

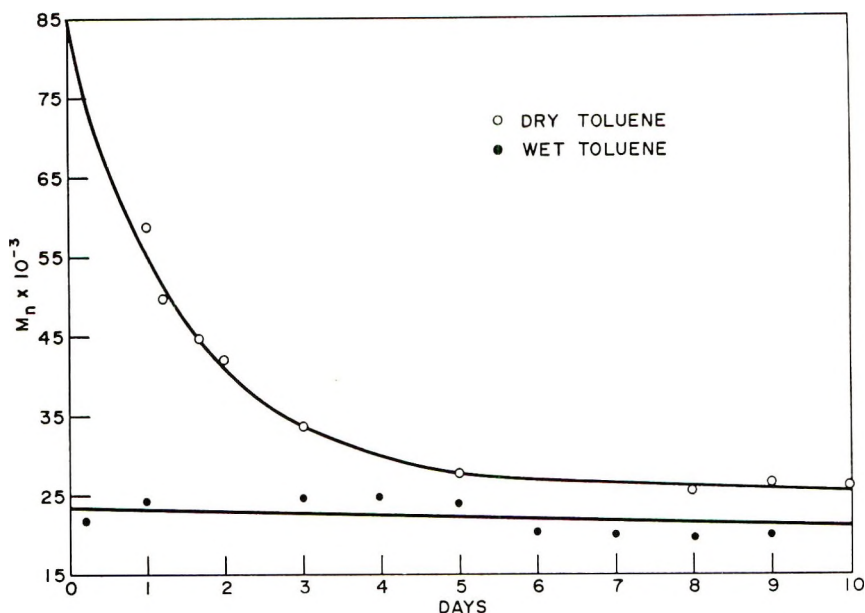


Fig. 3. Number-average molecular weights of beryllium di-*n*-pentylphosphinate in toluene.

molecular weight was a function of concentration, an attempt was made to regenerate a sample of beryllium 4-biphenyl(phenyl)phosphinate ($\bar{M}_n = 29\,000$) which had been dissolved in undried toluene for 10 days. The solvent was slowly removed from the sample by vacuum transfer at 50°C for 24 hr; \bar{M}_n found was 39 000.

The molecular weight of this sample could be restored close to the initial value of 140 000 by heating under high vacuum at 215°C for 48 hr. A -196°C trap attached to the vacuum system collected a few milligrams of water. The molecular weight of this material in undried toluene was 117 000. The molecular weights of this sample and another which was heated at 170°C for 24 hr degrade with time, as shown in Figure 2.

It is apparent from the results obtained with beryllium 4-biphenyl(phenyl)phosphinate that toluene solutions of polymer with traces of water in reagent grade toluene resulted in decrease of the number-average molecular weight. This change apparently is not reversible in solution, vigorous heating under high vacuum being required to remove the water which has reacted with the polymer.

Unfortunately, Ripamonti and his co-workers^{1,3} do not discuss the treatment of the solvents used for molecular weight determinations; but, unless solutions were kept scrupulously dry, there may be some doubt cast upon the validity of their molecular weight and viscosity measurements.

We also observed similar behavior in samples of two berylliumdialkyl phosphinates; namely, the di-*n*-pentyl and di-*n*-heptyl derivatives. The materials appear to be even more moisture-sensitive than beryllium 4-bi-

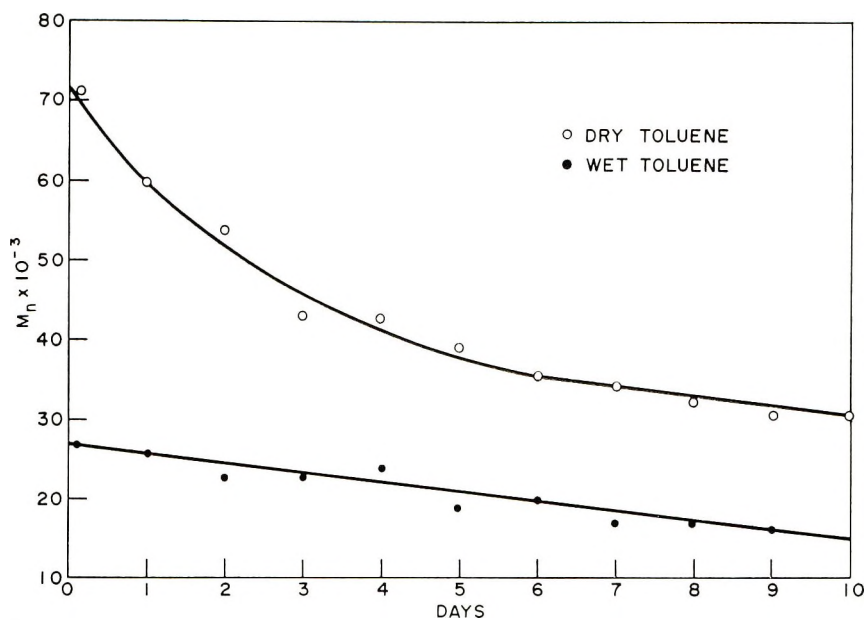


Fig. 4. Number-average molecular weights of beryllium di-*n*-heptylphosphinate in toluene.

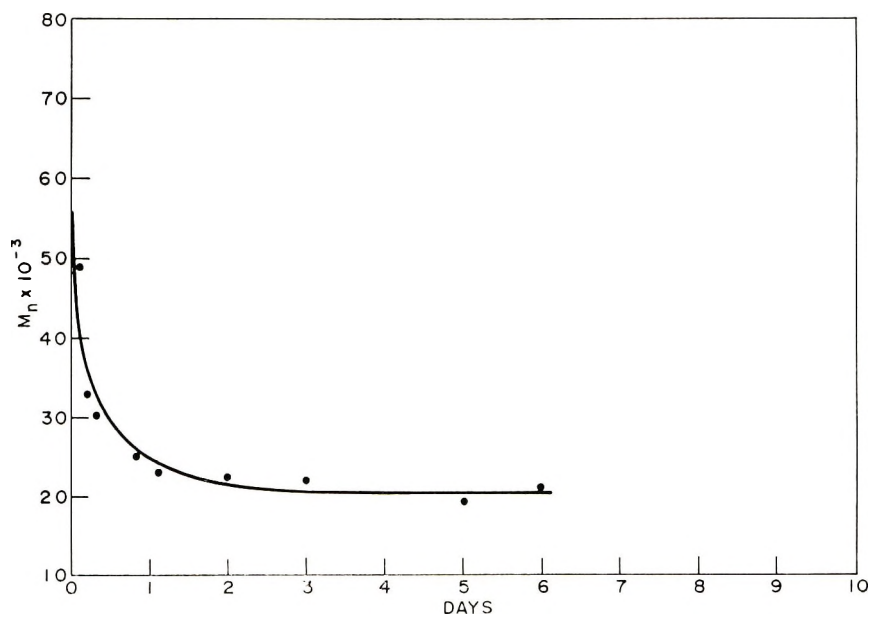


Fig. 5. Number-average molecular weights of beryllium trifluoromethyl(phenyl)phosphinate in undried toluene.

phenyl(phenyl)phosphinate. The decay curves shown in Figures 3 and 4 were obtained in dry toluene. In undried toluene, molecular weights were low and remained nearly constant through a 10-day period. In dry toluene, beryllium di-*n*-pentylphosphinate had an extrapolated zero-time M_n of approximately 90 000. This value decreased rapidly to 28 000 in 5 days with slow degradation to 25 000 in 10 days. In undried toluene, the initial M_n was 23 000 and decayed slowly to 21 000 over a 10-day period. The addition of a microdrop of water to each solution of a series which had been dissolved in dry toluene, resulted in a decrease from $M_n = 70 000$ to $M_n = 32 000$ in 30 min.

This very rapid decay in the presence of added water indicates that the gradual decrease of molecular weight in dry toluene is the result of traces of water absorbed during the handling of solutions outside the storage desiccators.

The behavior of beryllium di-*n*-heptylphosphinate in dry toluene is similar, with the extrapolated zero-time $M_n = 72 000$ and a more gradual decay to 30 000 over a 10-day period. The initial M_n in undried toluene was 27 000 with a gradual decay to 15 000 after 10 days.

TABLE I
Molecular Weights of Beryllium Phosphinates

Compound	Condition of toluene	Initial M_n	Mer	Final M_n	Mer
Beryllium 4-biphenyl (phenyl)phosphinate	Dry	300 000	500	300 000	500
	Wet	170 000	286	33 000	55
Beryllium di- <i>n</i> -pentyl phosphinate	Dry	90 000	215	25 000	60
	Wet	23 000	55	21 000	50
Beryllium di- <i>n</i> -heptyl phosphinate	Dry	72 000	140	30 000	57
	Wet	27 000	51	15 000	28
Beryllium trifluoromethyl (phenyl)phosphinate	Dry	87 000	200	Not measured	
	Wet	50 000	157	20 000	47

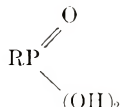
The only beryllium phosphinate of intermediate constitution which had both an aryl and an aliphatic group attached to phosphorus and which had a high enough molecular weight to exhibit decrease with time was beryllium trifluoromethyl(phenyl)phosphinate.

The molecular weight of this material in undried toluene decayed very rapidly from approximately 50 000 to 20 000 in 3 days, where it remained constant until the measurements were stopped at 6 days as shown in Figure 5. In dry toluene, the polymer dissolved slowly, and concentrations greater than 1.32 g/l. yielded some undissolved material. One determination made 20 hr after the addition of solvent showed $M_n = 87 000$.

Listed in Table I are the molecular weights at the beginning and end of each of the experiments shown in the Figures 1-5. Also listed are the number of monomer units (mer) which correspond to these M_n values.

The data in Table I show that, for beryllium 4-biphenyl(phenyl)phosphinate and beryllium trifluoromethyl(phenyl)phosphinate in undried toluene and beryllium di-*n*-pentylphosphinate and beryllium di-*n*-heptylphosphinate in dry toluene, the number-average molecular weight reaches an approximately constant value near 50 units, regardless of the initial molecular weight.

This observation suggests that these polymers may have at least two kinds of bonds, one of which is water-sensitive and the other relatively insensitive. The waterproof bonds appear to give polymer chains of approximately 50 units, and the water sensitive bonds may increase the length to as much as 500 units. This latter type may be P—O—P crosslinking bonds, formed from the interaction of occasional phosphonic acid molecules in the phosphonic acid reagent. Phosphonic acids, with the general formula



may be incorporated in the polymer chain with an active OH group. Under the temperatures required for complete reaction (200°C), two phosphonic acids on adjacent chains could react to form a P—O—P bond with the elimination of water. Such bonds are easily hydrolyzed.

The authors wish to acknowledge valuable discussions with Drs. A. Adicoff and A. Neilson of the Naval Weapons Center, China Lake, California, and financial support from Air Systems Command, U. S. Navy Department.

References

1. V. Giancotti, F. Giordano, and A. Ripamonti, *J. Chem. Soc. (A)*, **1968**, 757.
2. P. J. Slota, Jr., L. P. Freeman, and N. R. Fetter, *J. Polym. Sci. A-1*, **6**, 1975 (1968).
3. F. Gemitì, V. Giancotti, and A. Ripamonti, *J. Chem. Soc. (A)*, **1968**, 763.

Received October 15, 1968

Polymerization of Coordinated Monomers. II. Stereoregulation in the Free-Radical Polymerization of Methacrylonitrile-Zinc Chloride or Methacrylonitrile-Stannic Chloride Complexes

HIDEFUMI HIRAI, TADASHI IKEGAMI, and SHOJI MAKISHIMA,
*Department of Industrial Chemistry, Faculty of Engineering, University of
Tokyo, Bunkyo-ku, Tokyo, Japan*

Synopsis

The effect of complex formation on stereoregulation in free-radical polymerization was studied. Complexes of methacrylonitrile with $ZnCl_2$ and $SnCl_4$ were prepared and their properties and structures examined. The complexes were polymerized by initiation of α, α' -azobisisobutyronitrile or by irradiation with γ -rays from a ^{60}Co source or ultraviolet rays either in solution or in bulk at various temperatures ranging from -78 to $100^\circ C$. The triad tacticities of the resulting polymethacrylonitrile were determined by converting it to poly(methyl methacrylate) for NMR spectroscopy. The radicals in complexed forms were studied by ESR spectroscopy with the polymerization system in toluene irradiated with ultraviolet rays at $-120^\circ C$. The tacticities of the resulting polymers and their dependencies on the polymerization temperature were found to be characteristic of the complex species, i.e., the kind of metal chloride and the stoichiometry, being different from the tacticities and the dependencies, respectively, of the polymer obtained with pure methacrylonitrile. The 2:1 and the 1:1 complexes with $SnCl_4$ were found to give an eleven-line and a nine-line spectrum, respectively. On the basis of the results of both the tacticities and the ESR spectra, it was estimated that the proportion of the intracomplex reaction was 40%, and that the probabilities of isotactic diad addition of intra- and intercomplex reaction were 0.70 and 0.48, respectively.

INTRODUCTION

There exists a considerable literature on the polymerization of the complexes of polar vinyl monomers with metal salts.¹⁻⁶ There have been only a few reports, however, on stereoregulation in the polymerization of the complexes.⁷⁻⁹ In our previous paper,⁷ the tacticities of the resulting polymers were found to be independent of the polymerization temperature when the complex of methyl methacrylate with $ZnCl_2$ or $SnCl_4$ was used, and the effects of complex formation on the stability of the complex, the effect of solid state, the bulkiness of side group, the aggregation of the complex and the intracomplex reaction and on the tacticities were discussed. In conclusion, the specific tacticity of the resulting polymers was attributed to either the aggregation of the complex or the intracomplex reaction.

In the present study, our attention is focused on the intracomplex reaction. The weak coordination bond in complexes such as the complex of methyl methacrylate with $ZnCl_2$, however, makes it difficult to obtain the polymer in a complexed form with the same coordination state as the monomer complex, like a polymer of divinylxydimethylsilane¹⁰ or vinylphosphine complex,⁵ since the coordination bond is easily broken by the addition reaction on polymerization or by treatment after polymerization. Consequently, it is very difficult to ascertain whether or not an intracomplex reaction contributes to the tacticity from examination only of the polymers resulting from a monomer complex which has two or more than two monomers as ligands in a complex molecule. Vinyl nitriles are known to form more stable complexes with metal salts than does methyl methacrylate.¹¹ The triad tacticities of polyacrylonitrile are difficult to determine, whereas those of polymethacrylonitrile are readily determined by NMR spectroscopy after its conversion to poly(methyl methacrylate.)¹² In free-radical polymerization, the growing end of the polymer, i.e., the growing radical, can be studied by ESR spectroscopy, which is expected to give some information on the conformation of the growing end. We have previously succeeded in observing the ESR spectra of growing radicals with hyperfine structure in the polymerization of the complexes.⁹

In this investigation, complexes of methacrylonitrile were prepared with $ZnCl_2$ or $SnCl_4$, and polymerized by use of α, α' -azobisisobutyronitrile or by irradiation with γ -rays from ^{60}Co or ultraviolet rays. The tacticities of the resulting polymers were determined by NMR spectroscopy and the radical species in the polymerization system were examined by ESR spectroscopy. On the basis of these results, a mechanism for polymerization was discussed especially with reference to the intracomplex reaction. The probability of the intracomplex reaction was estimated from ESR spectra to calculate the probability of isotactic diad addition with either intra- or intercomplex reaction.

EXPERIMENTAL

Materials

Methacrylonitrile (MAN) was obtained by the dehydration of acetone cyanhydrine with phosphorus pentoxide and distilled under reduced pressure. Solvents were purified by the accepted procedure. Zinc chloride and stannic chloride were purified by sublimation and distillation, respectively.

Preparation of Complexes

A weighed amount of metal chloride was placed in an ampoule, into which an excess of monomer was distilled *in vacuo*. The mixture was heated to 50°C and shaken to make a transparent solution, which was cooled to precipitate the crystalline complex. The excess monomer was removed by

distillation *in vacuo* at room temperature to isolate the crystalline needles. After the stoichiometry and the solubility of the complex had been determined, the preparation could be also carried out by adding metal chloride to a solution of monomer in a solvent at a predetermined molar ratio of monomer to metal chloride and, if necessary, by removing the solvent by distillation under reduced pressure in nitrogen. The compositions of the complexes were determined by a gravimetric method which measured the increment of weight to a predetermined amount of the chloride, by titration of the metal with ethylenediaminetetraacetic acid (EDTA) and by elemental analysis.

Polymerization of Complexes

The polymerization of complex either in bulk or in solution was carried out by use of α, α' -azobisisobutyronitrile (AIBN) as an initiator or by γ -radiation from a ^{60}Co source in sealed ampoules at various temperatures. The free-radical polymerization below 0°C with AIBN was performed under irradiation from a high-pressure mercury lamp (Rikosha Model PHI-Tc, 500 W). The resulting polymers were purified by use of a solvent-precipitant system (acetone-methanol containing hydrochloric acid). The metal chloride incorporated in the polymer was thoroughly removed by repeated precipitation. The purified polymer was dried at 60°C *in vacuo*.

Degree of Polymerization

The intrinsic viscosity of polymethacrylonitrile (PMAN) was determined from viscosity measurements in dilute *N,N*-dimethylformamide solution at $29.2 \pm 0.1^\circ\text{C}$. The viscosity-average degree of polymerization was calculated from the equation derived by Overberger:¹³

$$[\eta] = 2.53 \times 10^{-3} P_v^{0.503}$$

Conversion of Polymethacrylonitrile to Poly(methylmethacrylate)

PMAN was converted to poly(methacrylic acid) (PMAA) by hydrolysis and then to PMMA by esterification of the PMAA. The hydrolysis was carried out as follows. A 30% aqueous potassium hydroxide solution containing PMAN was heated to 90°C for 72 hr and then refluxed for 100 hr. The polymer solution was acidified with hydrochloric acid to precipitate PMAA. The resulting PMAA was washed to remove any remaining potassium chloride and dried under reduced pressure at room temperature. The PMAA was esterified with diazomethane according to the method of Katchalsky and Eisenberg.¹⁴ The derived anhydride and remaining cyano group were examined by infrared spectroscopy. The degree of hydrolysis of PMAN was determined by elemental analysis.

Determination of Tacticities of Polymers

NMR spectra were obtained from 5–10% (w/v) chloroform solution of polymer at 50°C . Proportions of the isotactic (*I*), heterotactic (*H*), and

syndiotactic (*S*) triads were calculated from relative areas of the respective α -methyl proton signals according to the method of Bovey and Tiers.¹⁵

Spectral Measurement

Infrared spectra were recorded on a Japan Spectroscopic Model 102 or 103 infrared spectrometer. For measurements in the range of 200–600 cm^{-1} , KRS-5 windows were used. NMR spectra were run at 22.5 and 50°C on a Japan Electron Optics Laboratory Model C-60 or 3H-60 high resolution spectrometer at 60 Mc. ESR spectra of the system were re-recorded on a Japan Electron Optics Laboratory Model JES-3BSX spectrometer at -120°C either under ultraviolet irradiation or after irradiation at 15°C by the use of a Ushio Denki Model HB500/B high-pressure mercury lamp.

RESULTS

Properties of Complexes

Table I shows the properties of MAN–metal chloride complexes. Complexes with ZnCl_2 and SnCl_4 were colorless, crystalline needles except for the 1:1 MAN– ZnCl_2 complex, which was a white, amorphous, sticky solid. All the complexes were hygroscopic.

TABLE I
Properties of MAN–Metal Chloride Complexes

Complex	Composi- tion ^a	State at room temperature	Solvent ^b
$\text{ZnCl}_2(\text{MAN})$	1.08	Amorphous sticky solid	Bz, Tol
$\text{ZnCl}_2(\text{MAN})_2$	1.99	White needles, mp 40°C	Bz, Tol
$\text{SnCl}_4(\text{MAN})$	1.05	White needles, mp $\sim 40^\circ\text{C}$	Bz, Tol, Hex
$\text{SnCl}_4(\text{MAN})_2$	2.01	White needles, mp $\sim 40^\circ\text{C}$	Bz, Tol, Hex

^a Mole ratio of MAN to metal chloride.

^b Bz, benzene; Tol, toluene; Hex, *n*-hexane.

Data on infrared and NMR spectra of the complexes are summarized in Table II. The $\text{C}\equiv\text{N}$ stretching frequency at 2230 cm^{-1} was shifted by $20\text{--}30\text{ cm}^{-1}$ to higher frequencies on complex formation. A slight shift of the $\text{C}=\text{C}$ stretching band (1623 cm^{-1}) towards lower frequencies ($\Delta\nu < 5\text{ cm}^{-1}$) was noticed.

The NMR spectra were measured at different concentrations (14–50 mole-%), since the solubility of complexes in benzene varied with their species. The chemical shifts of MAN in the complexes were observed in lower magnetic fields than those of pure MAN.

The complexes were stable in benzene or in toluene because the infrared spectra of the complexes in these solvents had no cyano group absorption band due to free monomer at 2230 cm^{-1} . The 2:1 MAN– ZnCl_2 complex revealed an unusual behavior when dissolved in aromatic solvents; for

TABLE II
Changes in Infrared Frequency and Proton Chemical Shifts
of MAN on Complex Formation

Complex	Shift of infrared band, cm^{-1a}		Change in proton chemical shift, ppm ^b		
	$\Delta\nu(\text{C}\equiv\text{N})$	(C=C)	$\Delta\tau(\alpha\text{-CH}_3)$	$\Delta\tau(\text{H}_c)^c$	$\Delta\tau(\text{H}_t)^c$
$\text{ZnCl}_2(\text{MAN})$	+40	-5	-0.05	-0.40	-0.38
$\text{ZnCl}_2(\text{MAN})_2$	+40	-5	-0.05	-0.33	-0.38
$\text{SnCl}_4(\text{MAN})$	+25	-5	-0.25	-0.05	-0.10
$\text{SnCl}_4(\text{MAN})_2$	+35	-5	-0.23	-0.05	-0.10

^a For pure MAN, $\nu(\text{C}\equiv\text{N})$ at 2230 cm^{-1} and $\nu(\text{C}=\text{C})$ at 1623 cm^{-1} .

^b Chemical shift (τ) is expressed in ppm as referred to tetramethylsilane ($\tau = 10.00$) at 60 Mc: for pure MAN, $\tau(\alpha\text{-CH}_3)$ at 8.00 ppm, $\tau(\text{H}_c)$ at 4.18 ppm and $\tau(\text{H}_t)$ at 4.29 ppm.

^c H_c and H_t denote the vinyl protons in *cis* and *trans* position relative to the nitrile group, respectively.

example, the complex dissolved in benzene to form homogeneous solution when the molar ratio of benzene to MAN in the complex was approximately unity, while the solution separated into two liquid layers at molar ratios larger than unity.

The infrared spectra of the SnCl_4 complexes in the range of $250\text{--}450\text{ cm}^{-1}$ are shown in Figure 1. The 2:1 MAN- SnCl_4 complex, as a crystalline solid or in toluene or MAN solution, had three absorption bands (356,

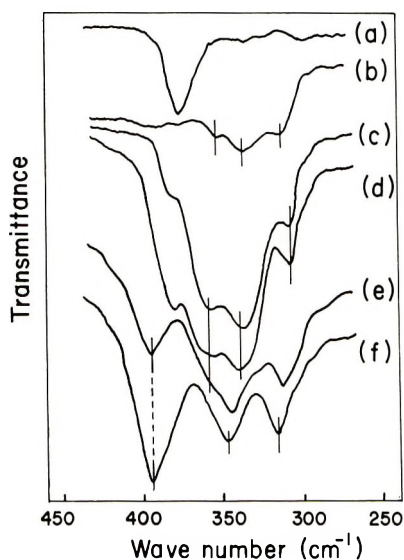


Fig. 1. Infrared spectra of complexes of MAN with SnCl_4 in the range of $250\text{--}450\text{ cm}^{-1}$: (a) pure MAN, (b) $\text{SnCl}_4(\text{MAN})_2$ in solid state; (c) $\text{SnCl}_4(\text{MAN})_2$ in MAN; (d) $\text{SnCl}_4(\text{MAN})_4$ in toluene (14 mole-%); (e) $\text{SnCl}_4(\text{MAN})_2$ in toluene (7 mole-%); (f) $\text{SnCl}_4(\text{MAN})$ in toluene.

TABLE III
 Polymerization of MAN-ZnCl₂ Complexes

Initiator (γ -ray) dose rate, 10 ⁴ r/hr	Solvent ^a	Temp, °C	Time, hr	Conver- sion, %	\bar{P}_n	Tacticity			$P(I)^b$	ρ^c
						$I, \%$	$H, \%$	$S, \%$		
1:1 MAN-ZnCl ₂ complex										
4.4	Bz	0	15	49.5	—	26	57	17	0.54	0.87
7.6	Bz	30	3	59.3	—	27	56	17	0.55	0.88
7.6	Bz	60	3	90.8	8500	28	52	20	0.54	0.95
7.6	Bz	100	1.5	77.0	—	—	—	—	—	—
2:1 MAN-ZnCl ₂ complex										
7.6	—	80	1.5	32.2	12000	29	53	18	0.56	0.93
1.3	—	60	2	6.0	—	—	—	—	—	—
7.6	Bz	0	17	75.5	—	28	52	20	0.54	0.95
7.6	Bz	30	2	23.2	—	30	51	19	0.56	0.96
7.6	Bz	60	15	84.5	—	34	47	19	0.58	1.03
7.6	Bz	80	1.5	27.8	14000	37	46	17	0.60	1.04
7.6	Tol	0	17	67.3	1600	—	—	—	—	—
7.6	Tol	30	2	17.3	—	29	51	20	0.54	0.97
7.6	THF	30	2	6.3	—	—	—	—	—	—
d	Bz	30	3	8.0	—	28	53	19	0.55	0.93

^a Solvent/MAN = 1/1 (mole ratio); Bz, benzene; Tol, toluene; THF, tetrahydrofuran.

^b $P(I)$, probability of the isotactic diad addition, calculated from the equation: $P(I) = (I + H/2)/100$.

^c ρ , persistence ratio introduced by Coleman and Fox.¹⁶

^d AIBN, 4.0 mole-% based on monomer.

TABLE IV
 Polymerization of MAN-SnCl₄ Complexes

Initiator (AIBN), mole-% on monomer	Mole ratio solvent (toluene); MAN	Temp, °C	Time, hr	Conver- sion, %	Tacticity			$P(I)$	ρ
					$I, \%$	$H, \%$	$S, \%$		
1:1 MAN-SnCl ₄ complex									
4.1 ^a	2	0	53	1.7	21	53	26	0.47	0.94
4.1	2	30	110	29.6	23	49	28	0.48	1.02
4.1	2	60	24	12.3	25	49	26	0.49	1.02
4.1	2	80	2	2.6	23	48	29	0.47	1.03
2:1 MAN-SnCl ₄ complex									
5.1 ^a	3	-5	65	10.6	31	47	22	0.54	1.05
5.1 ^a	3	0	52	7.8	32	48	20	0.56	1.03
5.1	3	30	48	11.0	30	46	24	0.53	1.08
5.1	3	60	6	12.3	28	49	23	0.52	1.02
5.1	3	80	4	4.8	29	51	20	0.55	0.97
b	—	60	2	1.8	21	56	23	0.49	0.89

^a Under irradiation with a high-pressure mercury lamp.^b γ -ray, dose rate 1.3×10^4 r/hr.

338, and 307 cm^{-1}). The 1:1 MAN-SnCl₄ had a strong band at 395 cm^{-1} in toluene as well as other bands at 340 and 318 cm^{-1} . At a concentration of 7 mole-% in toluene, the spectrum of the 2:1 complex became very similar to that of the 1:1 complex.

Polymerization of Complexes

The results are summarized in Tables III-V for the MAN complexes, and in Table VI for pure MAN. The reactivity of MAN greatly increased on complex formation. The polymerization rate of the 2:1 MAN-ZnCl₂ complex was about 300 times that of pure MAN. The complex, however, was hardly polymerized thermally. The reactivity of the complex was not affected by nonpolar solvents, such as benzene or toluene, while it decreased in polar solvents, e.g., tetrahydrofuran, owing to the dissociation of the complex, as indicated in the infrared spectra.

TABLE V
Polymerization of MAN Complexes in the Solid State

Initiator (γ -ray) dose rate, 10^4 r/hr	Temp, $^{\circ}\text{C}$	Time, hr	Conver- sion, %	Tacticity			$P(I)$	ρ
				I , %	H , %	S , %		
2:1 MAN-ZnCl ₂ complex								
5.8	-78	290	2.6	35	47	18	0.58	1.03
10	15	15	14.2	33	50	17	0.58	0.98
10	15	46	36.5	—	—	—	—	—
10	15	89	72.5	30	47	23	0.49	1.06
2:1 MAN-SnCl ₄ complex								
5.8	-78	290	2.4	23	51	26	0.49	0.98
10	15	15	9.1	25	48	27	0.49	1.04
10	15	46	71.3	25	49	26	0.50	1.02
10	15	89	80.4	—	—	—	—	—

TABLE VI
Bulk Polymerization of Pure MAN

Initiator (AIBN) mole-% based on monomer	Temp, $^{\circ}\text{C}$	Time, hr	Conver- sion, %	\bar{P}_n	Tacticity			$P(I)$	ρ
					I , %	H , %	S , %		
4.4	30	117	4.5	430	34	48	18	0.58	1.02
3.0	45	65	11.5	—	33	49	18	0.57	1.00
2.8	60	42	44.0	—	30	48	22	0.54	1.03
3.9	80	24	26.5	410	27	47	26	0.51	1.06
2.5	100	29	15.5	—	28	48	24	0.52	1.04
a	60	15	3.0	—	—	—	—	—	—
a	80	1.5	0.1	—	—	—	—	—	—

^a γ -ray initiation, dose rate 7.6×10^4 r/hr.

The 1:1 MAN-SnCl₄ complex in benzene solution was less reactive at 80°C than at 60°C. At the former temperature, the polymerization mixture turned reddish brown. The reactivity of the complex was found to decrease according to the following order: ZnCl₂(MAN) > ZnCl₂(MAN)₂ > SnCl₄(MAN)₂ > SnCl₄(MAN).

Hydrolysis and Esterification

The degree of hydrolysis of PMAN to PMAA was about 90–94% based on monomer, as determined by the nitrogen content of polymer. A small amount of nitrogen seemed to remain in the resulting polymer as amide group derived from nitrile group after hydrolysis, because the infrared spectra showed no absorption band due to C≡N stretching. The esterification is known to be effected quantitatively with diazomethane. The total conversion of PMAN to PMMA was about 60–80%, since a portion of PMAA was lost during purification. Almost no decrease in molecular weight of polymer was found on hydrolysis.

Tacticity of Resulting Polymer

The tacticity of PMMA derived from PMAN is shown in Tables III–VI. The tacticities are plotted against the polymerization temperature in Figures 2 and 3. The contours of the three α -methyl group peaks were drawn and the area of each peak was estimated according to the procedure of Kato and Nishioka.¹⁷ The standard deviation of the estimated values was found to be 1.5% for each peak. The ratios of intensities of α -CH₃, OCH₃, and CH₂ were found to be in the correct range of 1:1:0.67 \pm 0.02. The isotacticity of PMAN which was obtained by free-radical polymerization of pure MAN decreased with increasing temperature. The triad contents were found to decrease in the sequence: *H* > *I* > *S*. This tendency is similar to that for polyacrylonitriles reported by Murano and

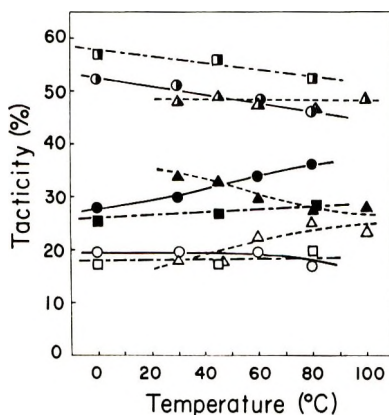


Fig. 2. Temperature dependence of the tacticities (■, ●, ▲) *I*, (□, ○, △) *H*, and (□, ○, △) *S* in the polymerization of MAN-ZnCl₂ complexes: (■, □) ZnCl₂(MAN); (●, ○) ZnCl₂(MAN)₂; (▲, △) pure MAN.

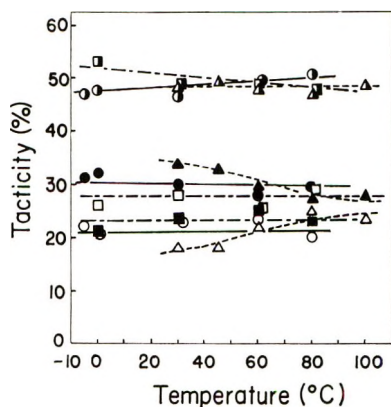


Fig. 3. Temperature dependence of the tacticities (■, ●, ▲) *I*, (▣, ○, △) *H*, and (□, ○, △) *S* in the polymerization of MAN-SnCl₄ complexes: (■, ▣, □) SnCl₄(MAN); (●, ○, ○) SnCl₄(MAN)₂; (▲, △, △) pure MAN.

Yamadera.¹⁸ The polymers obtained from the complexes with ZnCl₂ at lower temperature had higher heterotacticity than those from pure MAN. In the solution polymerization of the 2:1 MAN-ZnCl₂ complex

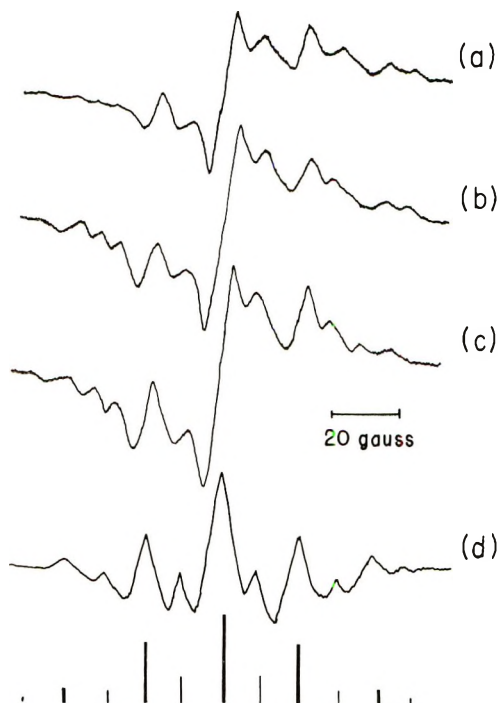


Fig. 4. ESR spectra observed at -120°C of the 2:1 MAN-SnCl₄ complex in toluene (14 mole %) irradiated with ultraviolet rays at 15°C : (a) after irradiation for 1 hr; (b) after irradiation for 1.5 hr; (c) after irradiation for 3 hr; (d) the second derivative of the spectrum of (c).

in benzene or toluene, the isotacticity increased and the heterotacticity decreased with the increasing temperature, while the syndiotacticity remained constant. When the complexes with SnCl_4 were polymerized in toluene solution, the tacticities did not change with polymerization temperature. The triad contents for both the 2:1 and the 1:1 MAN-ZnCl_2 complex decreased in the sequence; $H > I > S$. The sequence of triad contents for the 2:1 MAN-SnCl_4 complex was $H > I > S$, whereas that for 1:1 MAN-SnCl_4 complex changed to $H > S > I$. In the solid-state polymerization of the 2:1 complex, the order of triad tacticities was $H > I = S$, that is, the tacticities were intermediate between those for the 2:1 and the 1:1 complexes in solution polymerization.

ESR Spectra of Irradiated Stannic Chloride Complexes

The ESR spectra of the complexes irradiated with high-pressure mercury lamp are shown in Figures 4 and 5. The spectra were found to be characteristic of the 2:1 and the 1:1 complex, respectively. The irradiated 2:1 MAN-SnCl_4 complex gave a symmetrical eleven-line spectrum, superposing a singlet due to the radical from the solvent, i.e., toluene, on the central line. The spectrum was composed of two sets of lines. One was an intense quintet and the other was a sextet. From the second derivative of the spectrum the hyperfine splittings of each set were found to be 22.4

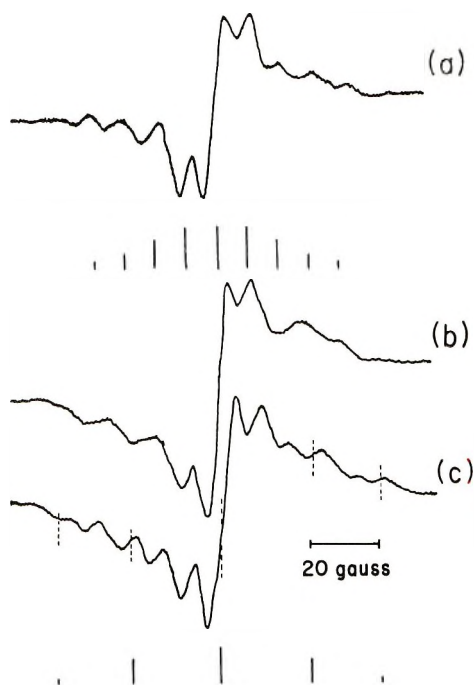


Fig. 5. ESR spectra observed at -120°C of the 1:1 MAN-SnCl_4 complex in toluene on ultraviolet irradiation at 15°C : (a) after irradiation for 1 hr; (b) after irradiation for 1.5 hr; (c) after irradiation for 2.5 hr.

gauss. The relative intensities of the quintet and the sextet were estimated to be 1:4:6:4:1 and 1:5:10:10:5:1, respectively. No change was observed in the shape of the spectra with time, although the intensity decreased slightly. On the other hand, the irradiated 1:1 complex showed a nine-line spectrum with a spacing of 9.0 gauss at an early stage of irradiation. This spectrum changed with increasing irradiation time to a nine-line plus a five-line signal. These characteristic spectra of both the 1:1 and the 2:1 complex were obtained with good reproducibility. After irradiation at 15°C, the complexes gave the same spectra as those obtained

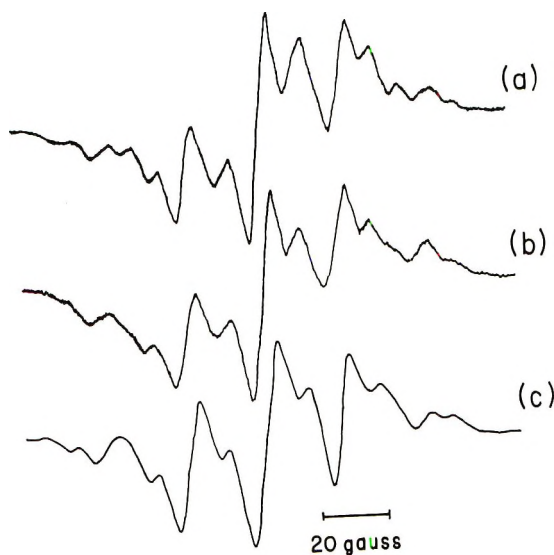


Fig. 6. Effect of concentration on the ESR spectra of the 2:1 MAN-SnCl₄ complex: (a) 14 mole-% solution in toluene irradiated with ultraviolet rays at -120°C in the presence of benzoyl peroxide, observed at -120°C; (b) 25 mole-% solution in toluene; (c) irradiation in solid state with γ -rays at -196°C, observed at -60°C.

after irradiation at -120°C. The relative ratio of the peak height of sextet to that of quintet was found to be independent of the reaction temperatures, being 0.42 at -120°C, 0.38 at -100°C, and 0.40 at 15°C.

The effect of the concentration of complex on the spectra is given in Figure 6. The spectra were measured at -120°C in the presence of benzoyl peroxide as a sensitizer, since the intensity of the signal due to the solvent radical became negligible at -120°C. The sextet became weaker with increasing concentration of the complex. This indicates that two species of radicals exist in the polymerization system of the 2:1 MAN-SnCl₄ complex. The spectrum observed in the solid-state polymerization of the 2:1 MAN-SnCl₄ complex consisted of both a strong quintet and a weak sextet, but the sextet was much weaker than that in solution.

DISCUSSION

Structure of Complexes

The shifts of the $C\equiv N$ stretching band to higher frequencies on complex formation indicate coordination to the metal atom via the lone pair electrons on the nitrogen atom of monomer molecule. This implies that all the complexes are of the sigma type.⁹ Changes in the chemical shifts of protons to lower magnetic fields are considered to be due to electron withdrawal by the coordinated metal atom through sigma bonding. The 2:1 MAN-SnCl₄ complex may have a six-coordinated octahedral structure, on the basis of the results of both stoichiometry and infrared spectra. In general, the infrared active vibration bands of the Sn-Cl bond in various complexes of SnCl₄ have been observed in the range of 250-400 cm⁻¹. For the octahedral complexes of the 2:1 MAN-SnCl₄, two isomers with a *trans* and a *cis* configuration would exist (Fig. 7).

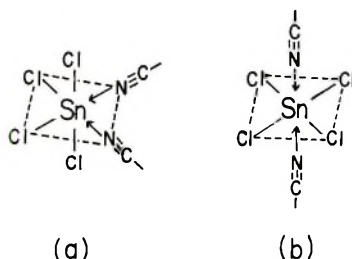


Fig. 7. Structure of the 2:1 MAN-SnCl₄ complex; (a) *cis* configuration; (b) *trans* configuration.

Theoretically, the *cis* isomer has three infrared active vibration bands, whereas the *trans* isomer has only one.^{19,20} As described previously, the 2:1 MAN-SnCl₄ complex was found to have three absorption bands both in solution and solid state. This suggests that the complex has a *cis* configuration. The same structure was proposed by Beattie for the 2:1 acetonitrile-SnCl₄ complex.¹⁹ The 1:1 MAN-SnCl₄ complex might have a five-coordinated trigonal bipyramidal structure, on the basis of the infrared spectra, as other 1:1 complexes with SnCl₄.²¹

The structure of the 2:1 MAN-ZnCl₂ complex may be tetrahedral with four ligands and the 1:1 MAN-ZnCl₂ complex has probably a dimer structure bridged by the two chlorine atoms, as described in the previous paper.⁷

The benzene solution of the complexes with ZnCl₂ showed no absorption band due to free monomer as described before. The 2:1 MAN-SnCl₄ complex was stable at a concentration of 14 mole-% in toluene, which was applied to the polymerization condition in solution, while the dissociation of the 2:1 complex into the 1:1 one was found to occur at a concentration of 7 mole-% as indicated by the appearance of the absorption band at 395 cm⁻¹, which is characteristic of the 1:1 complex.

Structure of Growing End of Polymer

An ESR spectrum with a hyperfine structure has not yet been reported in the usual polymerization in solution, except in rapid-flowing systems.²²

The ESR spectra of the complexes with SnCl_4 obtained by the irradiation at -120°C were probably attributable to the radicals of the growing ends of polymer for the following reasons: first, these spectra were identical with those obtained by the irradiation at 15°C , where the initiated radicals could not exist in any appreciable amount; secondly, the shapes of the spectra were kept unchanged with the extension of irradiation time.

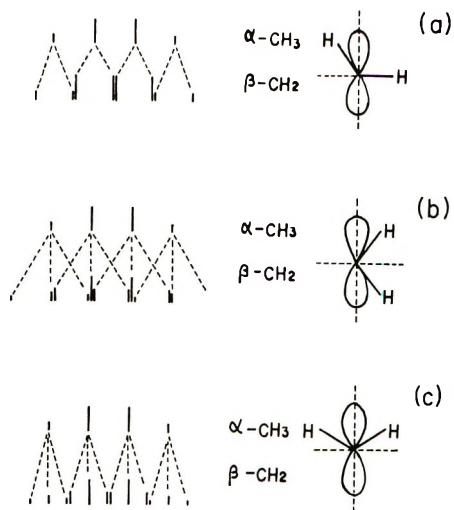


Fig. 8. Conformation of β -methylene protons of the radicals of growing ends and expected hyperfine splittings of their ESR spectra: (a) quintet; (b) sextet; (c) nine-line spectrum.

In the polymerization system of the 2:1 complex with SnCl_4 two species of radicals are expected to exist; one is associated with the quintet and the other is done with the sextet. The quintet was very similar to that with a hyperfine constant of 24 gauss obtained by Marx and Bensasson²³ with pure MAN on irradiation with x-rays. The quintet, however, is not considered to be due to the radical from pure MAN, because no dissociation of the complex was found by infrared spectroscopy at a concentration of 14 mole-% of the complex in toluene and the reactivity of the complex, moreover, is much higher than that of pure MAN. The probable structures of the growing end of polymer proposed are shown in Figure 8.

The quintet is attributed to the radical with a conformation shown in Figure 8a, in which three protons of the α -methyl group and one of two β -methylene protons interact effectively with the unpaired electron, as explained in the case of pure MMA by Ingram et al.²⁴ The sextet can be reasonably ascribed to the radical in which three protons of α -methyl and two

protons of β -methylene couple equally with the unpaired spin, as depicted in Figure 8*b*.

The hyperfine splitting constant allows us to estimate the spin density on the α -carbon; the spin density for the complex is lower by 17% than that for pure MAN. The reason for the decrease in the density is that the conjugation system composed of the C=C and C \equiv N bonds in MAN extends to the tin atom on complex formation. In the case of the 1:1 complex, the nine-line spectrum can be explained by assuming the radical conformation shown in Figure 8*c*. A similar conformation was proposed by Sohma and Komatsu²⁵ with respect to the radical from poly(methyl methacrylate). The five-line spectrum superposed on the nine-line one may be ascribed to the same conformation as Figure 8*a*.

Polymerization Mechanism

Polymethacrylonitrile obtained from pure MAN by free-radical polymerization was found to be specific in both the tacticity and its dependency on the polymerization temperature. In spite of the presence of the strong polar group, -C \equiv N, the polymer has a higher isotactic content than syndiotactic one, and the effect of the temperature on the tacticity is small, compared with other polar vinyl monomer such as vinyl chloride and MMA.²⁶ In bulkiness, a methyl group is larger than a nitrile group, while in polarity the latter is stronger. It is probable that in the polymerization of MAN the nitrile group tends to be arranged in the same direction in a certain conformation of the propagating chain, while the methyl groups turn away from each other due to steric hindrance, and that these two effects, polarity and bulkiness, compete with each other to result in the specific tacticity of polymer obtained.

In the polymerization of the 2:1 MAN-SnCl₄ complex with *cis* configuration, alternate addition of intra and intercomplex can participate, since the complex is expected to behave like a divinyl monomer such as methacrylic anhydride. The probability of stereoregular addition is probably different for intra- and intercomplex addition, in consideration of the difference between the tacticities for the 2:1 and for the 1:1 complex. The presence of intracomplex addition in the polymerization of the 2:1 complex is supported by the ESR spectra. In the spectra of the irradiated 2:1 complex, the signal of the radical formed by the cyclic intracomplex addition is considered to be superposed on that formed by the intercomplex addition. The spectra can be best explained by assuming that the strong quintet corresponds to the radical formed by intercomplex addition and the weaker sextet corresponds to that formed by intracomplex addition. The basis for this is first, that the signal of intracomplex addition is expected to be weaker than that of intercomplex addition, since the proportion of the intracomplex addition to total addition reaction is at most 0.5; secondly, the probability of intracomplex addition decreases with increasing concentration of the complex, since the increase in the concentration is favorable for the intercomplex addition. The ratio of the intracomplex addition to the intercomplex

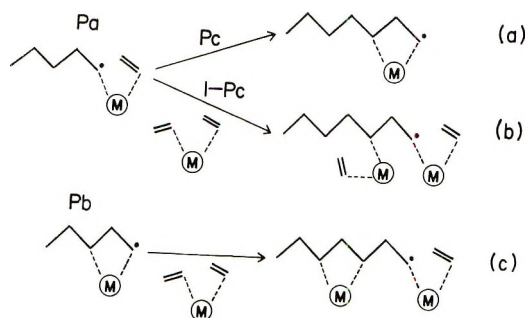


Fig. 9. Scheme for the polymerization of the 2:1 MAN-SnCl₄ complex; (a) inter-intra (b) inter-inter, and (c) intra-intercomplex addition reaction.

addition can be estimated by the peak heights of the quintet and the sextet on the second derivative curve of spectrum of 2:1 complex, provided that the reaction rate of intercomplex addition is approximately equal to that of intracomplex one.

In the intercomplex addition, one of two β -methylene protons probably can interact effectively with the radical of the growing end (see Fig. 8a). On the other hand, two of those protons should interact equally with the unpaired electron in the intracomplex addition, owing to the steric configuration of the β -methylene protons twisted by the ring formation. In this configuration, the cyano groups can be arranged in a plane with the β -methylene bonding.

If the intracomplex addition occurs in probability of P_c and the probability of the presence of growing end formed by intercomplex addition is P_a and that formed by intracomplex addition is P_b (see Fig. 9), eqs. (1) and (2) hold true in the propagation step;

$$P_a + P_b = 1 \quad (1)$$

$$P_a P_c = P_b \quad (2)$$

Consequently,

$$P_a = 1/(1 + P_c) \quad (3)$$

$$P_b = P_c/(1 + P_c) \quad (4)$$

$$P_c = P_b/P_a \quad (5)$$

P_c can be estimated by the ratio of the peak height of sextet to that of quintet. The ratio was almost independent of the reaction temperatures in the range from -120 to 15°C as described before and is supposed to be unchanged up to 80°C in consideration of the fact that the tacticities of polymers were independent of temperatures in the range from 0 – 80°C . Consequently, the P_c value at 15°C (0.40) was reasonably applied to the values at the temperatures ranging from -120 to 80°C . Triad tacticity can be calculated as shown in eqs. (6)–(8):

$$I = 100 \{ P_a [P_c \sigma_2 \sigma_1 + (1 - P_c) \sigma_2^2] + P_b \sigma_1 \sigma_2 \} \\ = 100 / (1 + P_c) [(1 - P_c) \sigma_2^2 + 2P_c \sigma_1 \sigma_2] \quad (6)$$

$$H = 200 / (1 + P_c) [(1 - P_c) (1 - \sigma_2) \sigma_2 \\ + P_c (1 - \sigma_1) \sigma_2 + P_c (1 - \sigma_2) \sigma_1] \quad (7)$$

$$S = 100 / (1 + P_c) [(1 - P_c) (1 - \sigma_2)^2 + 2P_c (1 - \sigma_1) (1 - \sigma_2)] \quad (8)$$

Here σ_1 and σ_2 are probabilities of isotactic diad additions of intra- and intercomplex reaction, respectively. The value of σ_2 is estimated to be equal to the probability of isotactic diad addition for the 1:1 complex, and σ_1 can be calculated by eq. (9).

$$\sigma_1 = (1/P_c) \left\{ \frac{(2I + H)(1 + P_c)}{200} - \sigma_2 \right\} \quad (9)$$

These values are listed in Table VII. The values for other complexes including MMA complexes and methacrylic anhydride were calculated with an assumption of $P_c = 1.0$. In the polymerization of the 2:1 MAN-SnCl₄ complex, σ_1 was found to be greater than σ_2 ; the isotactic diad addition is favored in the intracomplex reaction over in the intercomplex one.

TABLE VII
Estimation of the Probability of Intracomplex Isotactic Diad Addition
in the Polymerization of the 2:1 Monomer-Metal Chloride Complexes

Complex	Solvent	Temp, °C	$P(I)^a$	σ_2^b	σ_1^c
2:1 MAN-SnCl ₄	Tol	0	0.56	0.47	0.79
	Tol	30	0.53	0.48	0.66
	Tol	60	0.52	0.50	0.61
	Tol	80	0.55	0.47	0.73
2:1 MAN-ZnCl ₂	Bz	0	0.54	0.54	0.54
	Bz	30	0.56	0.55	0.57
	Bz	60	0.58	0.54	0.57
2:1 MMA-SnCl ₄ ^d	—	-78	0.19	0.13	0.31
	—	-18	0.29	0.13	0.38
	—	15	0.20	0.14	0.36
2:1 MMA-ZnCl ₂ ^d	—	-78	0.25	0.32	0.21
	—	-20	0.23	0.33	0.13
	—	15	0.22	0.27	0.18
Methacrylic anhydride ^e	Tol	-50	0.33	0.13	0.87
	Bz	20	0.56	0.21	0.79
	Bz	60	0.66	0.24	0.92

^a The probability of isotactic diad addition in polymerization of the 2:1 complex.

^b σ_2 = the value of $P(I)$ for the corresponding 1:1 complex.

^c σ_1 = The probability of intracomplex isotactic diad addition, calculated from the equation; $\sigma_1 = (1/P_c) \{ [(2I + H)(1 + P_c)/200] - \sigma_2 \}$.

^d The values were calculated from the data reported in our previous paper.⁷

^e The values were calculated from the results of the intra-inter cyclic polymerization of methacrylic anhydride, reported by Miller et al.²⁷

This behavior is similar to that of methacrylic anhydride in the intra-intermolecular cyclic polymerization, in which the syndiotactic sequence, i.e., $\dots ddddlll \dots$ was predominant at low temperature.^{27, 28}

The fact that the value of σ_2 is lower than that of free MAN, $P(I)$, can be explained by assuming that bulkiness of the side group of the 1:1 complex makes the syndiotacticity preferable to the isotacticity.

The tetrahedral 2:1 MAN-ZnCl₂ complex can undergo intracomplex addition. The complexes with ZnCl₂, however, had a tendency to aggregate, which leads to the preorientation of the monomer in the complex, as described in the previous paper.⁷ Moreover, the concentrations of the solutions of these complexes in benzene or toluene were high enough because of their specific solubilities in these solvents. It is plausible that the probability of the intracomplex addition is low under these conditions. In addition, the 1:1 complex in dimeric structure can be polymerized in a kind of intracomplex reaction. Consequently, it is reasonable that the tacticities are not very different for the 2:1 complex and the 1:1 one.

The persistence ratio (ρ) of the resulting polymers were calculated according to the equation of Fox and Coleman¹⁶ and are listed in the last columns of Tables III-VI. The deviation of this value from unity means that the polymerization system does not obey to Bernoullian statistics, i.e., the penultimate effect exists in the polymerization. The values of ρ were in the range of 1.02-1.04 for the polymerization of pure MAN; those for the polymerization of the 1:1 MAN-ZnCl₂ and the 2:1 MAN-ZnCl₂ complex were smaller than unity and especially at lower temperatures in the range, where they were 0.87-0.88 and 0.95-0.97, respectively. The 2:1 MAN-SnCl₄ complex gave the values of ρ of 1.05-1.08, which is slightly larger than those for pure MAN. A significant difference was not obtained between the values for the 1:1 MAN-SnCl₄ and those for pure MAN. The deviation of the values of ρ for the complex with ZnCl₂ was also observed for the 1:1 MMA-ZnCl₂ complex,⁷ which is plausibly due to the aggregation of the complex, and its dimeric structure. The penultimate effect was reported in the alternate intra-intermolecular polymerization of methacrylic anhydride by Fox and Reinmøller.²⁹ It seems reasonable to consider that intermolecular addition subsequent to the intramolecular addition exhibits a remarkable penultimate effect at low temperatures. The probability of intracomplex addition in the polymerization of the 2:1 MAN-SnCl₄ complex, however, may be so low that it may not make an appreciable contribution to the deviation of the value of ρ .

References

1. M. Imoto, T. Otsu, and Y. Harada, *Makromol. Chem.*, **65**, 180 (1963).
2. M. Imoto, T. Otsu, and M. Nakabayashi, *ibid.*, **65**, 194 (1963).
3. A. Takeda, J. Furukawa, T. Tsuruta, and T. Amari, *Kogyo Kagaku Zasshi*, **66**, 1233 (1963).
4. H. Sumitomo, K. Kobayashi, and Y. Yahama, *ibid.*, **67**, 1658 (1964).
5. F. J. Welch and H. I. Paxton, *J. Polym. Sci. A*, **3**, 3427 (1965).
6. S. Tazuke and S. Okamura, *J. Polym. Sci. A-1*, **5**, 1083 (1967).

7. S. Okuzawa, H. Hirai, and S. Makishima, *J. Polym. Sci. A-1*, **7**, 1039 (1969).
8. T. Otsu, B. Yamada, and M. Imoto, *J. Macromol. Chem.*, **1**, 61 (1966).
9. H. Hirai, S. Okuzawa, T. Ikegami, and S. Makishima, *J. Fac. Eng. Univ. Tokyo, B*, **29**, 115 (1967).
10. S. Murahashi, S. Nozakura, M. Sumi, and M. Furue, Preprints of Internat. Symp. Macromol. Chem. Tokyo, Kyoto, I-136 (1966).
11. R. J. Kern, *J. Inorg. Nucl. Chem.*, **25**, 5 (1963).
12. H. Sobue, T. Uryu, and K. Matsuzaki, *J. Polym. Sci. A-2*, **61** (1964).
13. C. G. Overberger, *J. Polym. Sci.*, **34**, 109 (1959).
14. A. Katchalsky and E. Eisenberg, *J. Polym. Sci.*, **6**, 145 (1951).
15. F. A. Bovey and G. V. D. Tiers, *J. Polym. Sci.*, **44**, 173 (1960).
16. R. K. Coleman and T. G. Fox, *J. Polym. Sci. A-1*, 3183 (1963).
17. Y. Kato and A. Nishioka, *Bull. Chem. Soc. Japan*, **37**, 1614 (1964).
18. R. Yamadera and M. Murano, *J. Polym. Sci. A-1*, 1059 (1967).
19. J. R. Beattie, *J. Chem. Soc.*, **38**, 1514 (1963).
20. I. Nakagawa and T. Shimanouchi, *Spectrochem. Acta*, **23A**, 2099 (1967).
21. R. A. Walton, *Quart. Rev.*, **19**, 126 (1965).
22. C. Corvaja, H. Fisher, and G. Giacometti, *Z. Physik. Chem. Neue Folge*, **45**, 1 (1965).
23. R. Marx and M. R. Bensasson, *J. Chim. Phys.*, **57**, 674 (1960).
24. D. J. Ingram, M. C. R. Symons, and M. G. Townsend, *Trans. Faraday Soc.*, **54**, 409 (1958).
25. J. Sohma and T. Komatsu, *J. Polym. Sci. A-3*, 287 (1965).
26. J. W. L. Fordham, P. H. Burleigh and C. L. Sturn, *J. Polym. Sci.*, **41**, 73 (1959).
27. W. L. Miller, W. S. Brey, and C. B. Butler, *J. Polym. Sci.*, **54**, 329 (1961).
28. J. C. H. Hwa, W. A. Fleming, and W. L. Miller, *ibid.*, *A-2*, 2385 (1964).
29. M. Reinmüller and T. G. Fox, *Polymer Division Preprints, Am. Chem. Soc.*, **7**, 1005 (1966).

Received November 4, 1968

Grafting Acrylic Acid Monomer to Poly-(vinyl Alcohol) and Methyl Cellulose by Ceric Ion

SAILES MUKHOPADHYAY, BHAIKAB CHANDRA MITRA, and SANTI R. PALIT, *Department of Physical Chemistry, Indian Association for the Cultivation of Science, Jadavpur, Calcutta-32, India*

Synopsis

A graft copolymer of acrylic acid on poly(vinyl alcohol) was prepared by use of the ceric ion-polyol redox system in aqueous medium. The graft copolymer obtained was water-soluble under the specified experimental conditions. The efficiency of grafting was determined by measuring carboxyl group content (as expected from acrylic acid unit) in the copolymer by applying the newly developed reverse dye-partition technique. The graft copolymer was also characterized by viscosity and solubility measurements. The effect of varying concentration of catalyst, monomer, and grafting time has also been determined.

INTRODUCTION

In recent years, interest has developed in the field of graft and block copolymers since new synthetic methods¹ have become available and modern analytical techniques²⁻⁴ have been developed. Also of interest is the unique properties of the copolymers, which are very different from both the constituent polymers and their mixtures. Scanty reports are available in the literature about preparation of water-soluble⁵ graft copolymers. The present communication reports two such copolymers, i.e., acrylic acid monomer grafted onto poly(vinyl alcohol) and methyl cellulose, and the characterization of the graft copolymers. The widely applied ceric ion-polyol redox system⁵⁻⁹ was used for this purpose. This technique yields essentially pure graft copolymer, since the free radicals are formed exclusively on the backbone. Determination of the weight of the monomer present in copolymer as grafted was made by applying the newly developed dye-partition technique.¹⁰

EXPERIMENTAL

Materials

Poly(vinyl alcohol) (PVOH, $[\eta] = 0.75$), methyl cellulose (B.D.H), ceric ammonium sulfate (CAS) (E. Merck), and Disulfine blue VN 150 (I.C.I. Ltd.) were used without further purification. Acrylic acid (AA) was purified by distillation at reduced pressure¹¹ and acrylamide (AM) was

purified by recrystallization from chloroform. The distilled water (pH 5.5–6.0) was obtained by distilling from an alkaline permanganate solution.

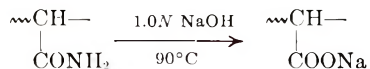
Grafting Procedure

P(VOH–AA). A typical grafting of acrylic acid monomer (AA) to poly(vinyl alcohol) was carried out in a thermostatted two-necked flask. A 3.0-g portion of PVOH was dissolved in 90 ml of water at 80–90°C and then cooled down to the requisite temperature. The required amount of acrylic acid and 10 ml of an acidified CAS solution freed from oxygen were added. The polymerization was carried out in an atmosphere of nitrogen.

When polymerization was over, after a definite time, the solution was poured into an excess of acetone to precipitate the gross polymer. Poly(acrylic acid) is not precipitated by acetone, and so the precipitate is graft copolymer along with PVOH homopolymer.¹² The polymer mixture was filtered and dried completely under vacuum and then weighed. The difference between this weight and the weight of PVOH taken gives the weight of PAA as grafted on the backbone. The graft copolymer was then converted to its corresponding sodium salt by treating the copolymer solution with an excess of sodium hydroxide solution in the presence of phenolphthalein indicator. Both the indicator and the excess sodium hydroxide were then removed by precipitating the copolymer with a mixture of 50% methanol–50% acetone. This was repeated twice, and the polymer was then finally precipitated with acetone and dried under vacuum.

P(VOH–AM). Acrylamide was grafted on PVOH in a similar manner. The mixture of graft copolymer and homopolymer PVOH was precipitated with excess acetone, dried, and weighed. The weight of PAM grafted on PVOH was calculated.

The amide units were converted into carboxylate by hydrolyzing the polymer in 1.0*N* sodium hydroxide solution at 90°C for 5 hr.



The excess alkali was removed by several precipitations of the polymer with a mixture of methanol–acetone and finally with acetone.

Methyl cellulose–PAA. The grafting of acrylic acid onto methyl cellulose was carried out in a very similar manner. Since the aqueous solution of methyl cellulose is very viscous, only 0.5 g of methyl cellulose was dissolved in 40 ml at 25°C. A 10-ml portion of acidic CAS solution was added, and polymerization was carried out in nitrogen atmosphere. The copolymer and homopolymer were precipitated by raising the temperature of the solution to 60°C. The polymer was filtered through glass wool and repeatedly washed with boiling water. Thus the polymer was completely free from the initiator and poly(acrylic acid). The grafted poly(acrylic acid) was converted into its salt as discussed in the previous method

and the excess sodium hydroxide and the indicator were removed by reprecipitation.

Characterization of the Graft Copolymers

The graft copolymers are expected to have physical and chemical properties different from those of the parent pure polymers. The changes of solubility and viscosity have been used to characterize the graft copolymers.

On grafting of acrylic acid onto nonionic polymers, the polymer chains become less coiled due to the repulsion of the neighboring charged acrylic acid units, and thus the solubility of graft copolymer is less than that of the parent polymer.

The viscosity of both the grafted copolymers of poly(vinyl alcohol) and methyl cellulose was studied in water at 25°C. η_{sp}/c was plotted against the different concentrations c of the copolymers in Figure 1. In Curves II and III represent the data for two different samples of graft copolymer of poly(vinyl alcohol)-acrylic acid in Figure 1 *a* and methyl cellulose-acrylic acid in Figure 1 *b*, while curves Ia and Ib show the behavior of samples of ungrafted polymers. Curves II and III display a unique dependence on concentration. They undergo a marked increase with dilutions which are many times the intrinsic viscosity (curves I) which would be expected for the polymer in the absence of charge.

A viscosity study of P(VOH-AA) in 0.1M NaCl solution shows that the addition of salt has a negligible effect on viscosity (curves IV and V). This is quite reasonable in the sense that the sequence of charged units may be repeated by uncharged units in graft copolymers.

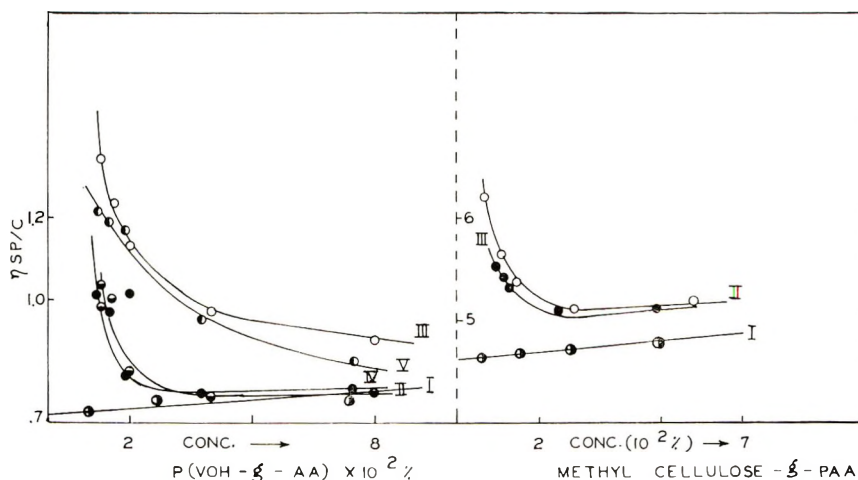


Fig. 1. Viscosity of graft copolymers of acrylic acid on (a) poly(vinyl alcohol) and (b) on methyl cellulose: (Ia) poly(vinyl alcohol); (IIa), and (IIIa) PVOH-AA graft copolymers (in water); (IVa), (Va) same graft copolymers in 0.1M NaCl solution; (Ib) methyl cellulose; (IIb) and (IIIb) AA-methyl cellulose graft copolymers.

Reverse Dye-Partition Technique

In the normal dye-partition technique the dye in aqueous solution is partitioned with the dye-reacting polymer in benzene or chloroform; the amount of dye passing into the organic layer is a measure of the particular endgroup present in the polymer. In the reverse dye-partition technique (RDP technique) the disulfine blue dye bound to a known polymer [poly-(methyl methacrylate) with amine endgroups] dissolved in chloroform is partitioned with an aqueous solution of unknown polymer containing acidic functional groups.¹⁰ From the amount of dye passing to the aqueous medium (as determined by spectrophotometry of the chloroform layer) the amount of active groups present in the aqueous layer is calculated. Every partition test is performed against a blank using water only. But, since methyl cellulose may contain a few carboxyl groups, a dilute solution of methyl cellulose (1×10^{-2} g/l.) has been used as blank.

To determine the composition of the resulting graft copolymers they were subjected to the RDP test. For this purpose solutions were prepared in such a manner that the carboxyl concentrations were in the range 1×10^{-5} – $5 \times 10^{-5}M$. All the copolymer solutions including the distilled water used for the blank were maintained at a constant value of pH. The optical density (OD) data presented in Tables I and II represent the difference between the OD values of the blank and that of the polymer solution.

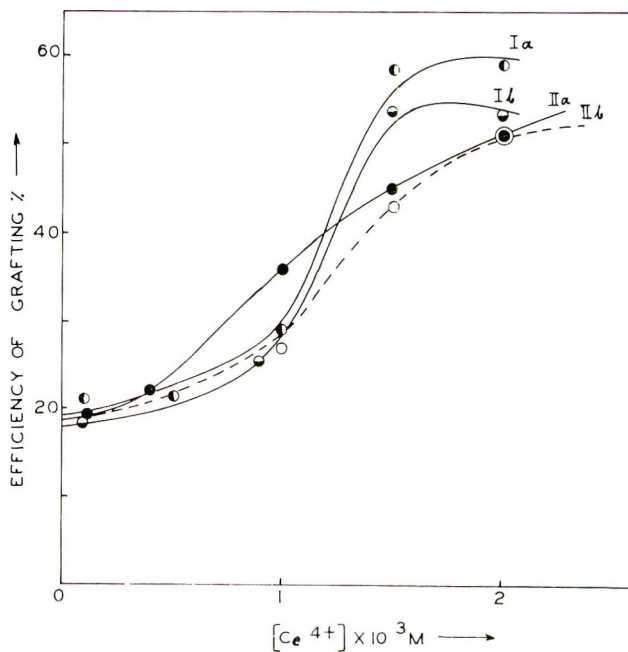


Fig. 2. Comparative studies of the results of the efficiencies of grafting obtained by (a) the RDP technique and (b) the gravimetric method: (I) P(VOH-AM); (II) P(VOH-AA).

This RDP technique has been suitably employed to detect the number of carboxyl groups and hence the number of acrylic acid units grafted onto poly(vinyl alcohol) or methyl cellulose. One can calculate easily the average weight of a segment of the graft copolymer carrying one carboxyl group by applying the reverse dye-partition technique¹⁰ from which the percentage of monomeric unit present in the graft copolymer can be determined. The efficiency of grafting is thus obtained according to the following definition:

$$\text{Efficiency} = \frac{\text{Weight of monomer grafted in copolymer}}{\text{Weight of monomer added in the polymerization system}} \times 100$$

It has been observed from the nature of the curves shown in Figure 2, that the grafting efficiency obtained from the dye-partition technique (Ia and IIa) is almost similar to that obtained by the gravimetric method (Ib and IIb). While in the gravimetric method the complete isolation of the graft copolymer is essential for correct results, the dye-partition technique does not require such a rigorous precipitation, since only an adequate portion of the purified graft copolymer will serve the purpose for the determination grafting efficiency.

RESULTS AND DISCUSSION

The variables affecting the ceric ion-induced grafting of acrylic acid to poly(vinyl alcohol) and methyl cellulose were studied.

Effect of Concentration of Catalyst

The effect of the concentration of CAS on the grafting is shown in Figure 3. The sulfuric acid concentration was $1.0 \times 10^{-2} N$ and monomer used was 20% of the polymer. The curve I which embodies the results of the grafting reaction of acrylic acid on poly(vinyl alcohol) at 35°C, shows that grafting efficiency increases more or less linearly with the increase of $[Ce^{4+}]$. The same phenomenon is observed in the case of grafting of acrylic acid onto methyl cellulose (curve II, Fig. 3), but the increase is less prominent. The results of reverse dye partition test are presented in Tables I and II.

TABLE I
Grafting of AA on PVOH at 35°C

Concn of Ce^{4+} , M	Concn of polymer solution, g/l. $\times 10^2$	OD at 630 $m\mu$	Corresponding NaLS $\times 10^5$, M	AA in the grafted chain, wt-%	Efficiency, %
2.0×10^{-3}	1.32	0.374	1.70	10.3	51.5
1.5×10^{-3}	2.05	0.520	2.35	9.0	45.0
1.0×10^{-3}	1.90	0.442	2.00	7.2	36.0
1.0×10^{-4}	2.30	0.242	1.10	3.8	19.0

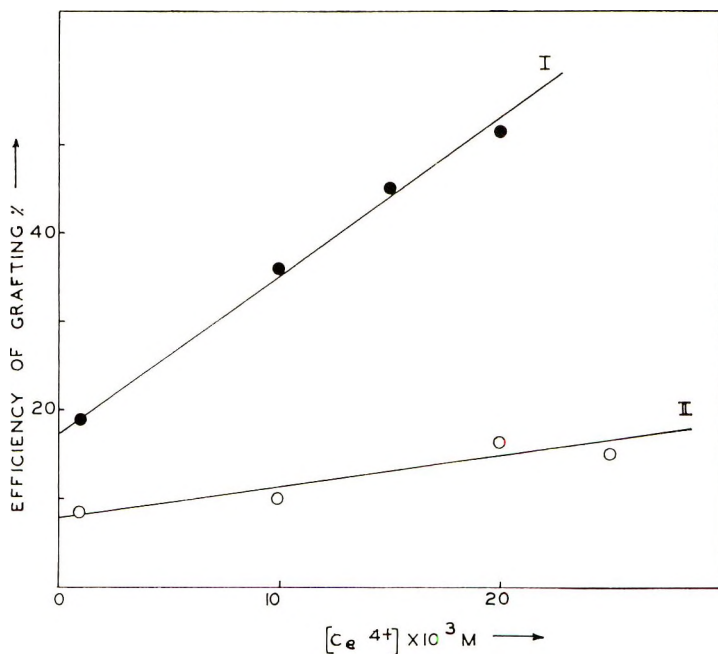


Fig. 3. Effect of catalyst concentration on grafting efficiency: (I) P(VOH-AA); (II) methyl cellulose-PAA.

TABLE II
Grafting of AA on Methyl Cellulose at 20°C

Concn of Ce^{4+} , M	Concn of polymer solution, g./l. $\times 10^3$	OD at 630 $m\mu$	Corresponding NaIs $\times 10^5$, M	AA in the grafted chain, wt-%	Efficiency, %
2.5×10^{-3}	9.4	0.798	3.50	3.0	15.0
2.0×10^{-3}	4.97	0.490	2.20	3.3	16.5
1.0×10^{-3}	6.94	0.430	1.90	2.0	10.0
1.0×10^{-4}	14.1	0.739	3.30	1.7	8.5

Time of Maximum Grafting

The grafting of AA as a function of time is shown in Figure 4. It can be seen that this is an S-shaped curve; the extent of grafting increases with time, attains a steady state, and finally falls off. The maximum grafting value was achieved within 50–60 min with $1.0 \times 10^{-3} M$ CAS and within 60–70 min with $1.5 \times 10^{-3} M$ CAS. In both the polymerization AA was 20% of the PVOH (by weight).

Effect of Monomer Concentration

The effect of monomer concentration on the grafting of AA was evaluated in a series of polymerization in which the concentration of the monomer was

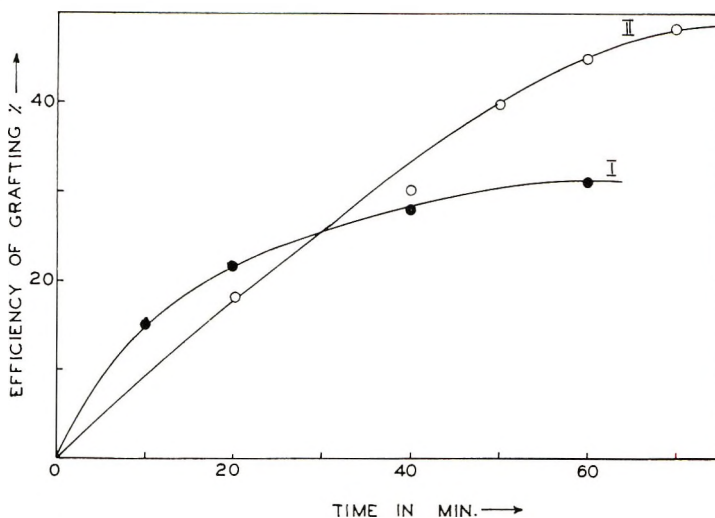


Fig. 4. Efficiency of grafting as a function of time: (I) $[Ce^{4+}] = 1.0 \times 10^{-3} M$; (II) $[Ce^{4+}] = 1.5 \times 10^{-3} M$.

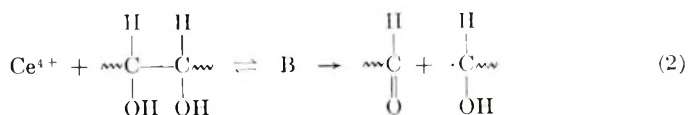
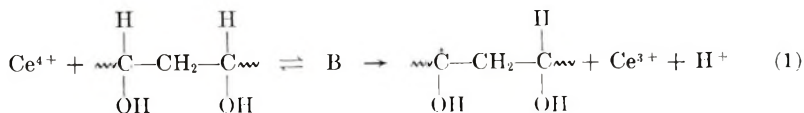
varied from 10 to 30% of the polymer used. Polymerization was carried out at two concentrations of CAS, 1.0×10^{-3} and $2.0 \times 10^{-3} M$. A slight increase of grafting efficiency was observed when monomer concentration was in the range 25–30%.

Mechanism

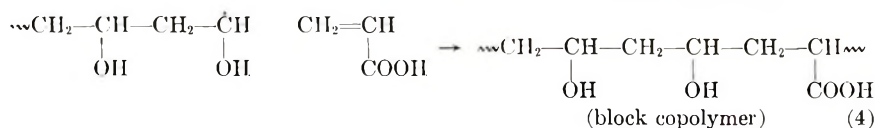
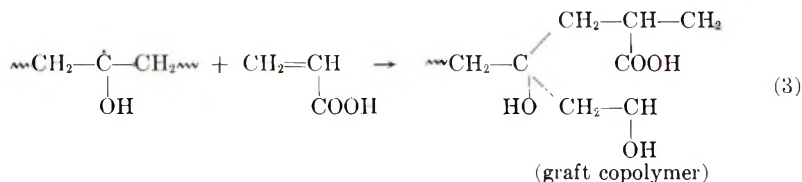
A large number of papers⁵⁻⁹ are available on the synthesis of graft copolymer in redox systems in which a Ce^{4+} salt functions as the oxidizing agent, reduced by the polymer itself.

In our systems of polymerization, the same mechanisms are followed. In the PVOH chain either the extraction of a hydrogen atom forms an active point to produce a graft polymer, or breaking up of the chain at the 1:2 glycol unit gives rise to a block copolymer. The proposed mechanism is given in eqs. (1)–(4).

Formation of macroradicals:



Propagation:



Regarding the structure of the graft copolymer of methyl cellulose and AA the limitation of our present method is that it cannot differentiate the formation of a mixture of graft and block copolymer, although Iwakura et al.¹⁶ have shown in the case of grafting on cellulose with the same initiator that the structure of graft copolymer consists of a mixture of block and graft type.

Thanks are due to National Bureau of Standards (U.S.A.) for financial assistance to the authors B. C. M. and S. M.

References

1. G. Smets and R. Hart, *Advan. Polym. Sci.*, **2**, 173 (1960).
2. V. E. Shashona and K. E. Holde, *J. Polym. Sci.*, **28**, 395 (1958).
3. E. Schonfeld and I. Waltcher, *J. Polym. Sci.*, **35**, 536 (1959).
4. Z. Reyes, C. E. Rist, and C. R. Russel, *J. Polym. Sci. A-1*, **4**, 1031 (1966).
5. G. Mino and S. Kaizerman, *J. Polym. Sci.*, **31**, 243 (1958).
6. G. Mino, S. Kaizerman, and E. Rasmussen, *J. Polym. Sci.*, **38**, 393 (1958).
7. G. Mino, S. Kaizerman, and E. Rasmussen, *J. Polym. Sci.*, **39**, 523 (1959).
8. G. Mino, S. Kaizerman, and E. Rasmussen, *J. Amer. Chem. Soc.*, **81**, 1494 (1959).
9. A. A. Katai, V. K. Kulshrestha, and R. H. Marchessault, in *Fourth Cellulose Conference (J. Polym. Sci. C, 2)*, R. H. Marchessault, Ed., Interscience, New York, 1963, p. 403.
10. S. Mukhopadhyay, B. C. Mitra, and S. R. Palit, unpublished results.
11. S. R. Palit and P. Ghosh, *J. Polym. Sci.*, **58**, 225 (1962).
12. S. P. Papkov, S. G. Yefimova, N. V. Mikhailov, and L. F. Byrkova, *Polymer Sci. USSR*, **8**, 72 (1966).
13. J. Moens and G. Smets, *J. Polym. Sci.*, **23**, 931 (1957).
14. S. R. Palit, *Makromol. Chem.*, **36**, 89 (1959); *ibid.*, **38**, 96 (1960).
15. M. K. Saha, P. Ghosh, and S. R. Palit, *J. Polym. Sci. A*, **2**, 1365 (1964).
16. Y. Iwakura, T. Kurosaki, and Y. Imai, *J. Polym. Sci. A*, **3**, 1185 (1965).

Received November 22, 1968

Combination of Cellulosic Materials and Metallic Ions

YOSHITAKA OGIWARA and HITOSHI KUBOTA, *Faculty of Engineering, Gunma University, Kiryu, Japan*

Synopsis

Cellulosic materials (DP, SCP) and PVA fibers were treated with four kinds of metallic ions (Ca^{2+} , Fe^{2+} , Fe^{3+} , Ce^{4+}), and the adsorption behavior was studied to elucidate the manner in which the celluloses and the metallic ions were combined. The effects of treatment temperature, time, and concentration upon the amount of the metallic ions adsorbed were examined. With Ca^{2+} and Fe^{2+} , the effects of such factors on the adsorption were slight, while with Fe^{3+} and Ce^{4+} the effects of time, temperature, and ion concentration were pronounced. Also, it was evident that the amount (molar) of equilibrium adsorption of Ca^{2+} or Fe^{2+} was approximately the same as the content of carboxyl groups in the cellulose sample, and the amount of equilibrium adsorption of Fe^{3+} or Ce^{4+} was approximately the same as that of total carbonyl group content. When the samples which had adsorbed these metallic ions were treated with 0.1*N* hydrochloric acid, the Ca^{2+} and Fe^{2+} were completely desorbed while about 80% of the adsorbed Fe^{3+} and Ce^{4+} remained. These results indicate that there are two types of combinations of cellulosic materials and metallic ions involved: one is thought to be an ionic bond, while the other is considered to be a chelate bond.

INTRODUCTION

In studies of the reactivity of cellulosic materials, it was found that ceric ions and ferric ions were adsorbed in great amounts on the cellulosic materials.¹⁻³ Previously it had been thought that the combination of a cellulosic material and metallic ions involves mainly an ionic bond with acidic groups in the substance, and that the amount of the carboxyl group contained is important.⁴ Recently the adsorptive reaction of several metallic ions towards silk, wool, and poly(vinyl alcohol) was reported by Hojo et al.,⁵⁻⁷ and it was recognized that a chelate bond is formed. There was also a report⁸ which indicated the possibility of chemical combination from a study of the rates of adsorption of zinc and cobalt onto cellulose. Hartley⁹ reports that wool binds aluminum ions by means of ionic and van der Waals forces. Generally speaking, it is known that metallic ions easily undergo coordinate chelation with carbonyl oxygen in an organic compound and are able to form complexes. It is thought, therefore, that the behavior of metallic ions towards cellulosic materials may result in the formation of complexes, but no studies have been carried out to explore this.

In the present study two kinds of pulp samples having different compositions and one kind of poly(vinyl alcohol) fiber were acted upon by four

kinds of metallic ions, and the mechanism of combination was investigated from the examination of their adsorptive behaviors.

EXPERIMENTAL

Materials and Reagents

Commercial dissolving pulp (DP) from softwoods and commercial bleached semichemical pulp (SCP) from hardwoods were used as cellulose samples. The air-dried pulp was tumbled in a mixer, the portions passing through a net of 40-mesh screen were removed, and the remaining parts were used. Commercial poly(vinyl alcohol) fibers (PVA fibers) were cut into about 1-cm lengths, boiled several times in water in order to desize them thoroughly, and air-dried. The carboxyl content in the samples was determined as described in the previous report¹⁰ from the calcium ion concentration in the filtrate obtained by treating the sample with an aqueous solution of calcium acetate. The total carbonyl group content was determined by the hydroxylamine method.¹⁰

In order to examine four kinds of metallic ions, the purity of the following commercial metallic salts used were determined: $\text{Ce}(\text{NO}_3)_4 \cdot 2\text{NH}_4\text{NO}_3$, $\text{FeCl}_2 \cdot 6\text{H}_2\text{O}$, $\text{FeSO}_4 \cdot 7\text{H}_2\text{O}$, and $\text{CaCl}_2 \cdot 2\text{H}_2\text{O}$.

Adsorption of Metallic Ions on Samples

A cellulose sample (0.50 g) and 40 ml of an aqueous solution of known concentration of metallic salt were placed in a 100-ml flask maintained at a constant temperature. After a given time the samples were filtered on a glass filter and washed three times with about 100 ml of distilled water.

Determination of Adsorbed Metallic Ions

The amount of ceric ions adsorbed on cellulose samples was determined by adding a given amount of ferrous sulfate and back-titrating with ceric sulfate with *o*-phenanthroline as indicator.

The amount of adsorbed ferric ions was determined as follows: a 5-ml portion of concentrated hydrochloric acid was added to a sample on which ferric ions were adsorbed and placed in a 300-ml flask. Then 10 ml of an aqueous solution of 20% potassium iodide was added to the mixture, and the flask was sealed. After standing for 20 min, the new mixture was diluted to 200 ml with water. Then, the liberated iodine was titrated with 0.1*N* sodium thiosulfate.

The amount of adsorbed ferrous ions was determined as follows. A sample was dispersed in water and was titrated with an aqueous solution of ceric sulfate of a known concentration, *o*-phenanthroline being used as indicator.

The sample on which calcium ions were adsorbed was maintained in a dispersion in water, and the determination of adsorbed calcium ions was

carried out by titration with EDTA at a fixed pH with Eriochrome Black T as indicator.

RESULTS AND DISCUSSION

Figure 1 shows the relationship between the adsorption of calcium ions on DP and SCP, and the time of treatment at 45°C. The amounts of adsorption on the two kinds of cellulose samples reached equilibrium values in several minutes of reaction at a 10 mmole/l. concentration of calcium ions. The amounts of equilibrium adsorption on DP and SCP were 1.2 and 3.1 mmole/100 g of cellulose, respectively. The amounts of adsorption at a treatment temperature of 3°C were approximately the same. It became clear, therefore, that the temperature had little effect upon the amount of calcium ions adsorbed on the cellulose.

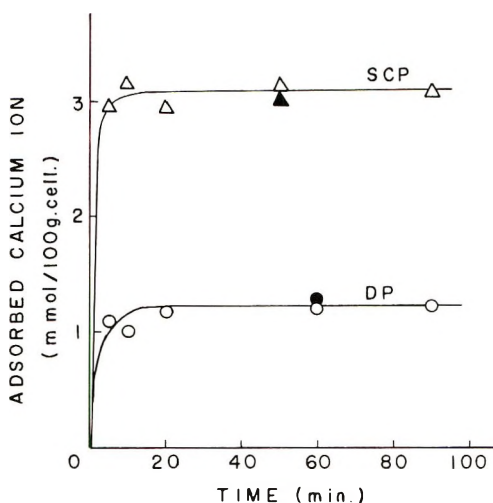


Fig. 1. Changes of the adsorbed calcium ions with treatment time: (○) DP, treatment temperature, 45°C; (△) SCP, 45°C; (●) DP, 3°C; (▲) SCP, 3°C. Concentration of calcium ions used, 10 mmole/l.

Figure 2 shows the relationship between the amount of calcium ions adsorbed and the concentration. The amounts adsorbed on these samples reached constant values at a concentration of calcium ions of about 5 mmole/l. which were practically the same as the equilibrium values in Figure 1.

Figures 3 and 4 show the same relation for ferrous ions as Figures 1 and 2 for calcium ions. It is clear from Figure 3 that the amount of adsorbed ferrous ions reached equilibrium values within a few minutes after treatment, and there was only a slight difference in the equilibrium values in the $[\text{Fe}^{+2}]$ range of 1–10 mmole/l. As Figure 4 shows, the adsorption became practically constant when the concentration of ferrous ions was 3 mmole/l. or over. Adsorption on DP and SCP, respectively, was 0.4 and 1.1

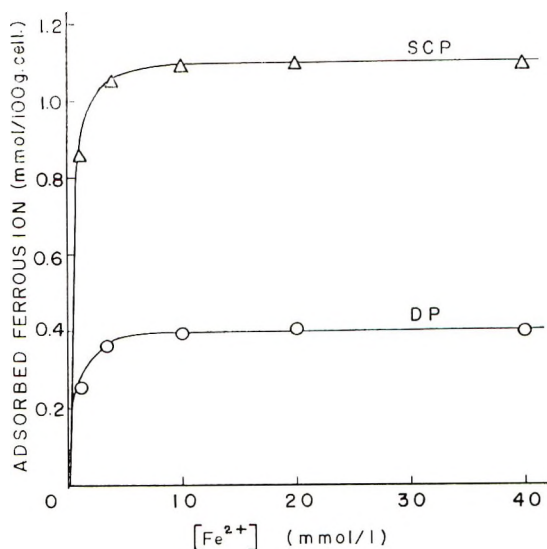


Fig. 2. Effect of the concentration of calcium ions on amount of adsorbed calcium ions. Treatment temperature, 45°C; time, 60 min.

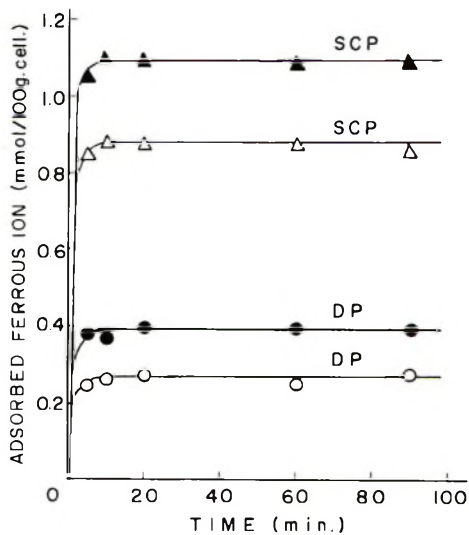


Fig. 3. Changes of the adsorbed ferrous ions with treatment time at various concentrations of ferrous ions: (○) DP, 1 mmole/l.; (●) DP, 10 mmole/l.; (△) SCP, 1 mmole/l.; (▲) SCP, 10 mmole/l. Treatment temperature, 45°C.

mmole/100 g of cellulose; these values were about one-third of the amounts of equilibrium adsorption of calcium ions.

These results indicate that the amount of adsorption of divalent ions, such as calcium ions or ferrous ions, on the samples reaches its equilibrium value in a few minutes, and that although this value is little affected by the

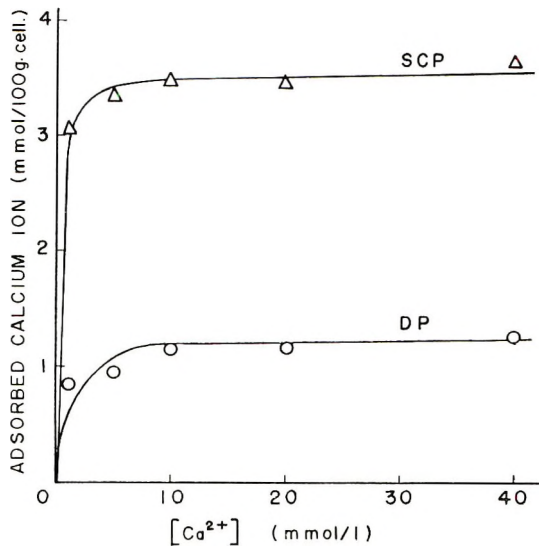


Fig. 4. Effect of the concentration of ferrous ions on amount of adsorbed ferrous ions. Treatment temperature, 45°C; time, 60 min.

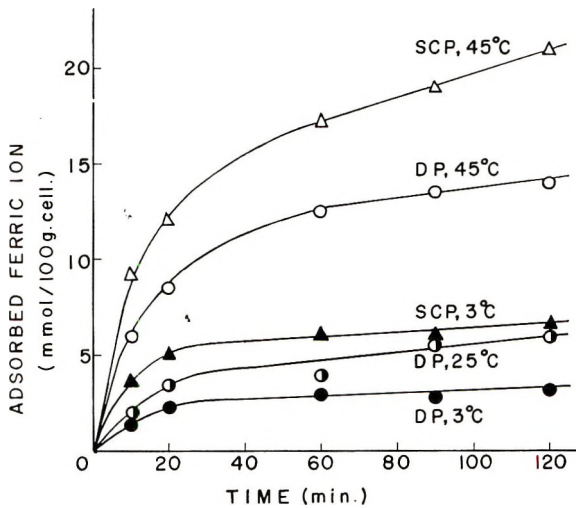


Fig. 5. Changes of the adsorbed ferric ions with treating time. Concentration of ferric ions used, DP, 5 mmole/l.; SCP, 10 mmole/l.

treating temperature or the concentration of ions, it varies with the kinds of cellulose. As it was thought that the adsorptive properties of metallic ions had much to do with the electrical charge of ions, the same investigations were carried out with ions having a higher electrical charge, i.e., ferric ions and ceric ions.

Figure 5 shows the relationship between the amount of adsorbed ferric ions and the treating time. It is clear from Figure 5 that the amount of

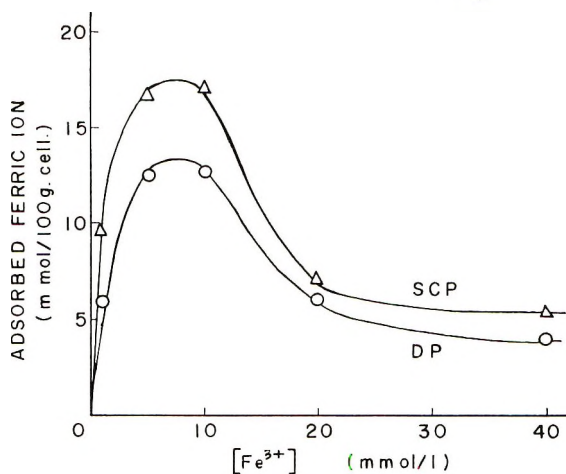


Fig. 6. Effect of the concentration of ferric ions on amount of adsorbed ferric ions. Treatment temperature, 45°C; time, 60 min.

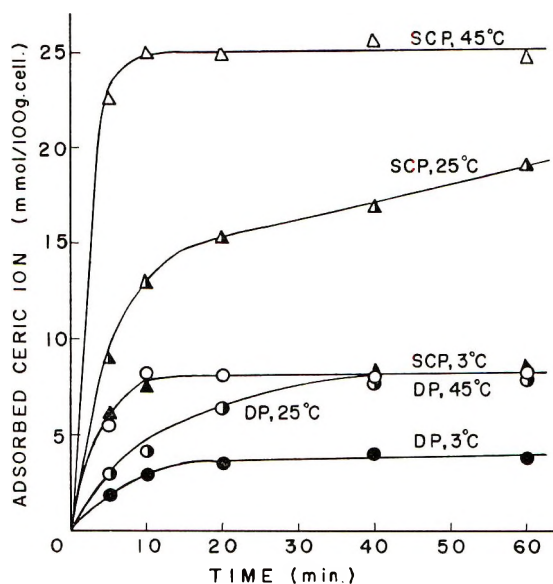


Fig. 7. Changes of the adsorbed ceric ions with treatment time. Concentration of ceric ions used, 10 mmole/l.

adsorbed ferric ions varied not only with the kind of cellulose, i.e., DP or SCP, but also with the treating time. Also, it was evident that the amount adsorbed was greater, the higher the temperature. In particular, it was found that there was a marked difference in the adsorption rate at an early stage of reaction and that the amount of adsorption did not easily reach its equilibrium value in about 100 min.

Figure 6 shows the amount of ferric ions adsorbed at 45°C for 60 min at various Fe³⁺ concentrations. At ferric ion concentrations of 8–9 mmole/l.,

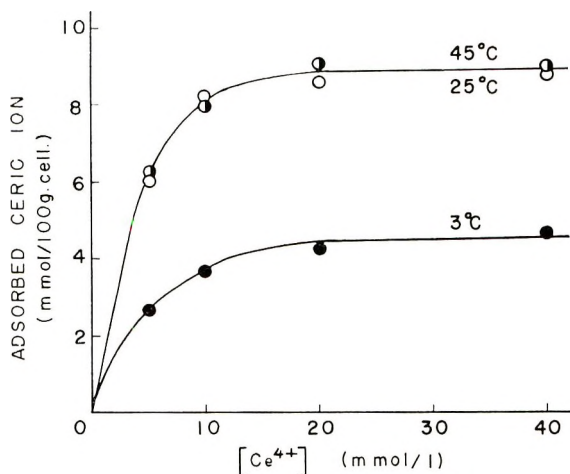


Fig. 8. Effect of the concentration of ceric ions on amount of ceric ions adsorbed on DP. Treatment time, 60 min.

the amounts of adsorption on the two samples were greatest. The amounts of adsorption were decreased sharply beyond the concentrations showing the maximum amount. However, we believe that the adsorption curve changes considerably for longer treatment times. That is, it is known that when DP and SCP were treated with a 40 mmole/l. concentration of ferric ions at 45°C for 7 hr, the amounts of adsorbed ferric ions were 32.3 and 34.8 mmole/100 g cellulose. It is thus clear that the amount of adsorbed ferric ions varies with the ion concentration, treatment temperature, and time, as well as with the kind of cellulose.

Figure 7 shows behavior of ceric ions. As in the case of ferric ions, the amount of adsorption varied widely with the different temperatures of treatment. In some cases more than 60 min was required for the adsorption to reach an equilibrium value. The amounts of ceric ions adsorbed on DP and SCP, respectively, were 8.2 and 25.0 mmole/100 g of cellulose. These values were considerably greater than the amounts of adsorbed calcium ions and ferrous ions. Our previous report¹ showed a good linear relation between the amount of equilibrium adsorption of ceric ions and the total carbonyl group content in various cellulose and oxidized cellulose samples. The present study showed the amount of equilibrium adsorption to be about the same number of moles as the total carbonyl group content in the samples.

Figure 8 shows the relationship between the adsorption of ceric ions on DP and the concentration of ceric ions. The adsorption after treatment for 60 min at 45°C was about the same as that at 25°C, but the value at 3°C was about half the above amount. This shows that the temperature of treatment has considerable bearing on the amount of the adsorption.

The adsorptive behavior of ferric and ceric ions on cellulosic materials are clearly quite different from those of calcium ions and ferrous ions; the

amount of adsorption of Fe^{3+} and Ce^{4+} is influenced by the treating time, temperature, and concentration, and the amounts of equilibrium adsorptions were several times as great as those of calcium ions and ferrous ions.

In our previous report,¹ we indicated that ceric ions adsorbed on a cellulose sample were very stable to dilute acid and that the combination was very strong and not simply ionic. The stability of the combination of ferric ions and a cellulose sample was therefore examined; the results are shown in Table I.

TABLE I
Stability of Ferric Ions Adsorbed on Cellulose

Concentration of HCl, <i>N</i>	DP		SCP	
	Adsorbed ferric ion, mmole/100 g cellulose	Adsorbed ferric ion, mmole/100 g cellulose	Adsorbed ferric ion, mmole/100 g cellulose	Adsorbed ferric ion, mmole/100 g cellulose
0	6.6 ^a	12.6 ^a	7.3 ^a	17.1 ^a
0.1	4.9	9.4	5.5	12.6
0.5	3.3	6.8	3.2	10.8
1.0	2.9	5.9	2.4	7.5
2.0	1.2	2.8	1.4	4.2
5.0	0	0	0	0

^a The different amounts of adsorption in each sample are due to the difference in the conditions of adsorption.

TABLE II
Amount of Various Metallic Ions Adsorbed onto Cellulosic Materials and PVA Fibers^a

Type	Fiber		Ion	Ion adsorbed, mmole/100 g cellulose	
	COOH content, mmole/100 g cellulose	Total C=O content, mmole/100 g cellulose		No HCl treatment	After HCl treatment ^b
DP	2.2	9.4	Ca^{2+}	1.2	0
			Fe^{2+}	0.4	0
			Fe^{3+}	12.6	9.4
			Ce^{4+}	8.2	6.1
			Ca^{2+}	3.1	0
SCP	6.4	21.5	Fe^{2+}	1.1	0
			Fe^{3+}	17.1	12.6
			Ce^{4+}	23.7	17.8
			Ca^{2+}	0	0
			Fe^{2+}	0	0
PVA	0	5.1	Fe^{3+}	3.2	2.4
			Ce^{4+}	4.3	3.2

^a Treatment temperature, 45°C; treatment time, 60 min; concentration of metallic ions used, 10 mmole/l.

^b After treatment with 0.1*N* hydrochloric acid.

The amount of adsorption was obtained as follows: 0.50 g of a cellulose sample on which ferric ions were adsorbed was dipped in 100 ml of hydrochloric acid of various concentrations at room temperature and then washed with water. The ferric ions remaining in the sample were then determined. When the sample was treated with 0.1*N* hydrochloric acid, about 20% of the originally adsorbed ions were desorbed. If it was treated with 2*N* hydrochloric acid, a small amount of Fe⁺³ still remained, and the sample had to be treated with 5*N* hydrochloric acid to obtain complete desorption. Table II shows the amounts of adsorption of several metallic ions (45°C, 60 min, approximately equilibrium adsorption) on cellulose samples and PVA fibers, and the amounts of ions remaining after these samples were treated with 0.1*N* hydrochloric acid. Table II also shows the analytical values of the total carbonyl group and carboxyl group in the cellulose samples and PVA fibers.

The amount of calcium or ferrous ions adsorbed on DP and SCP was about the same as the content of carboxyl group in the samples; adsorption of these metallic ions on PVA fibers, which contain no carboxyl groups, was very slight. It was also clear that those adsorbed ions were easily desorbed by dilute hydrochloric acid. Consequently, we believe that these ions combined ionically with the carboxyl group in the cellulose. On the other hand, with ferric or ceric ions, the amount of ions adsorbed on a cellulose sample was much influenced by the treating temperature, time, and concentration, and these ions are believed to combine with the carbonyl group as chelates in the cellulose. In other words, the amount of adsorption of these metallic ions is about the same as the (molar) carbonyl group content in each sample, and the association was so strong as not to be reversed easily by dilute hydrochloric acid. This strong combination was clearly distinct from an ionic bond. Thus, it is thought that there are two kinds of combination of metallic ions and celluloses: ionic bonding, which can be observed with calcium ions and ferrous ions, and chelate bonding, which can be recognized with ferric ions and ceric ions.

The authors wish to acknowledge the contributions of Mrs. Yukie Ogiwara and Mr. Kazuyuki Kobayashi in the experimental work.

References

1. Y. Ogiwara, Y. Ogiwara, and H. Kubota, *J. Polym. Sci. A-1*, **6**, 1489 (1968).
2. Y. Ogiwara, H. Kubota, and Y. Ogiwara, *J. Polym. Sci. A-1*, **6**, 3119 (1968).
3. Y. Ogiwara, Y. Ogiwara, and H. Kubota, *J. Appl. Polym. Sci.*, **12**, 2575 (1968).
4. S. A. Rydholm, *Pulping Processes*, Interscience, New York, 1965, pp. 1050, 1115.
5. N. Hojo, *Sen-i Gakkaishi*, **13**, 102 (1957).
6. N. Hojo and H. Hojo, *Sen-i Gakkaishi*, **14**, 675 (1958).
7. N. Hojo, H. Shirai, and N. Arakawa, in paper presented at 15th High Polymer Chemistry Conference (Japan), Nagoya, 1966; *Abstracts*, p. 130.
8. A. A. Muzzarelli, G. Marcotrigiano, Ch. S. Liu, and A. Freche, *Anal. Chem.*, **39**, 1762 (1967).
9. F. R. Hartley, *Austral. J. Chem.*, **21**, 1013 (1968).
10. Y. Ogiwara, Y. Ogiwara, and H. Kubota, *J. Polym. Sci. A-1*, **5**, 2791 (1967).

Received December 3, 1968

Application of Preparative Gel-Permeation Chromatography to Studies of Low Molecular Weight Carboxy-Polybutadienes

RONALD D. LAW, *Thiokol Chemical Corporation, Wasatch Division,
Brigham City, Utah 84302*

Synopsis

Low molecular weight carboxy-polybutadiene liquid polymers are used as the binder-fuel fraction in solid composite propellants. Analytical GPC determinations of low molecular weight materials (100 through 500 molecular weight range) were previously found to correlate significantly with final propellant properties. These low molecular weight materials are being characterized, and studies of their role in determining propellant physical properties are being conducted. Sufficient quantities of material in the 100-500 molecular weight range have been isolated by using preparative scale GPC to establish the chemical nature of these materials. Infrared and chemical analysis of fractions collected by using preparative GPC also has permitted the construction of functional group distribution profiles. In addition, narrow fractions isolated over the molecular weight range of the whole polymer were analyzed for average molecular weight by vapor pressure osmometry and have been used as calibration standards for analytical GPC.

INTRODUCTION

Final mechanical properties of solid propellant in which HB liquid polymer (polybutadiene-acrylic acid-acrylonitrile) is used as the binder are affected to a major degree by the low molecular weight materials, particularly acids, in the polymer. The primary cure reaction in HB propellant systems involves a reaction between the carboxyl groups in the HB polymer chain and epoxy groups in the curing agent.

Good correlations have been established between low molecular weight acid content (determined by solvent extraction or molecular distillation) and final propellant mechanical properties.¹ Gas chromatographic analysis (GLC) of the volatile fraction obtained by molecular distillation of HB showed that the low molecular weight material contained 4-carboxycyclohexene, 4-cyanocyclohexene, 4-vinylcyclohexene, and several additional unidentified materials.² These cyclohexene derivatives presumably are formed through Diels-Alder addition of butadiene to acrylic acid, to acrylonitrile, and to itself during the emulsion polymerization process used in preparation of HB.

As previously reported,³ the low molecular weight portion was further

characterized, with special emphasis on the 100–500 molecular weight range, to investigate the role played by these materials in governing solid propellant mechanical properties. GPC was selected because of its applicability to estimation of the amount and distribution of low molecular weight materials and to their separation from the bulk of the polymer. Low molecular weight materials in the 100–500 molecular weight range, as determined by GPC, correlated significantly with all propellant properties

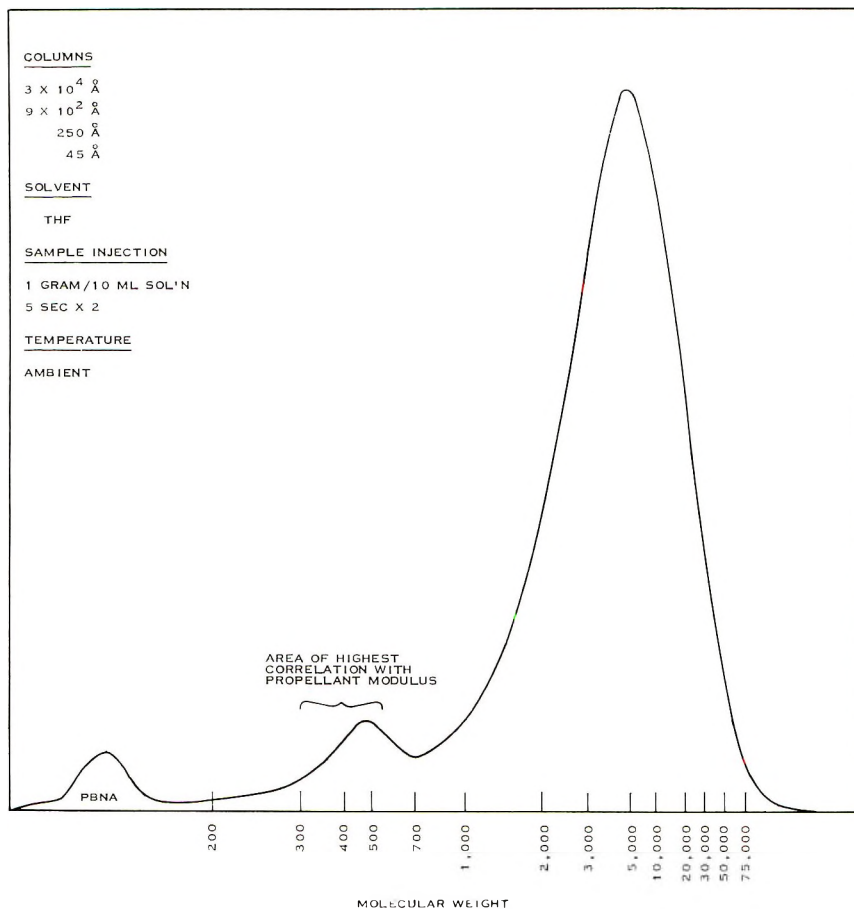


Fig. 1. Raw GPC scan of HB polymer.

(Fig. 1). As a result of GPC analysis, it is apparent that the chemical species in this low molecular weight portion of the polymer influence propellant mechanical properties profoundly, either directly or by interaction with other propellant ingredients. The final stages of these HB polymer studies, described in this paper, have centered on two main areas.

(1) Preparative scale GPC and other separation techniques were used to isolate and firmly identify as many as possible of the low molecular weight

chemical species in the 100–500 molecular weight range fraction of the polymer.

(2) Calibration studies were conducted in which preparative GPC was employed to isolate narrow HB fractions which were then used as analytical molecular weight standards.

EXPERIMENTAL METHOD

Preparative GPC Apparatus

A preparative-scale gel-permeation chromatograph was assembled from commercially available components (Figs. 2 and 3). The column, measuring 4 ft in length and 2 in. diameter, was packed on special order by Waters Associates, Inc. with gels of two different porosities. The first 2-ft section was packed with gel having a nominal porosity of 1000 Å, the remaining 2 ft with gel having a nominal porosity of 250 Å. At least two gel porosities were

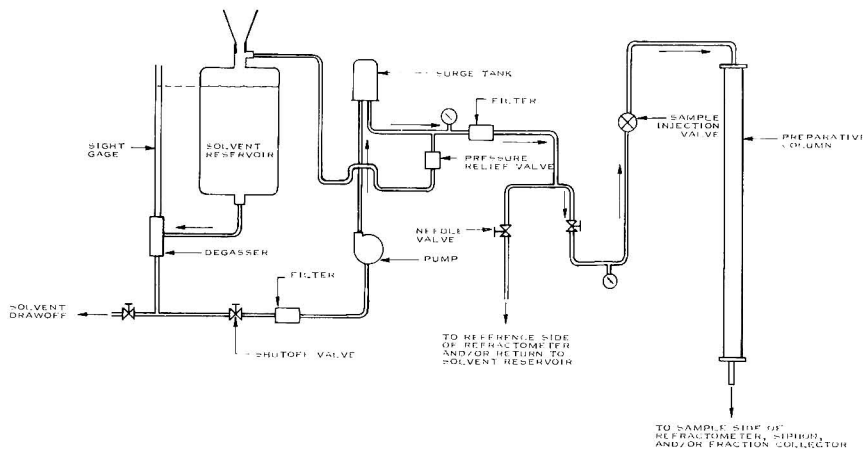


Fig. 2. Flow diagram for preparative GPC.

required to fractionate in the range of molecular weights found in HB polymer. The mixed gel preparative column had a resolution of 1,520 plates/ft at a flow rate of 10 ml/min with the use of dodecane as standard. All preparative GPC work employed: chloroform as solvent; flow rates of 10–12 ml/min; ambient temperature; and sample sizes of 0.8–1.0 g/run. The samples were injected as a 20% solution in chloroform with a 5-ml loop in the injection valve. The material which eluted from the preparative column was fed into the refractometer-recorder system of a Waters Model 100 GPC and fractions were collected as they dumped from a 24 ml siphon.

Calibration Studies

A major problem area in GPC work with carboxy-butadienes has been that elution of standards of known molecular weight and size differs from

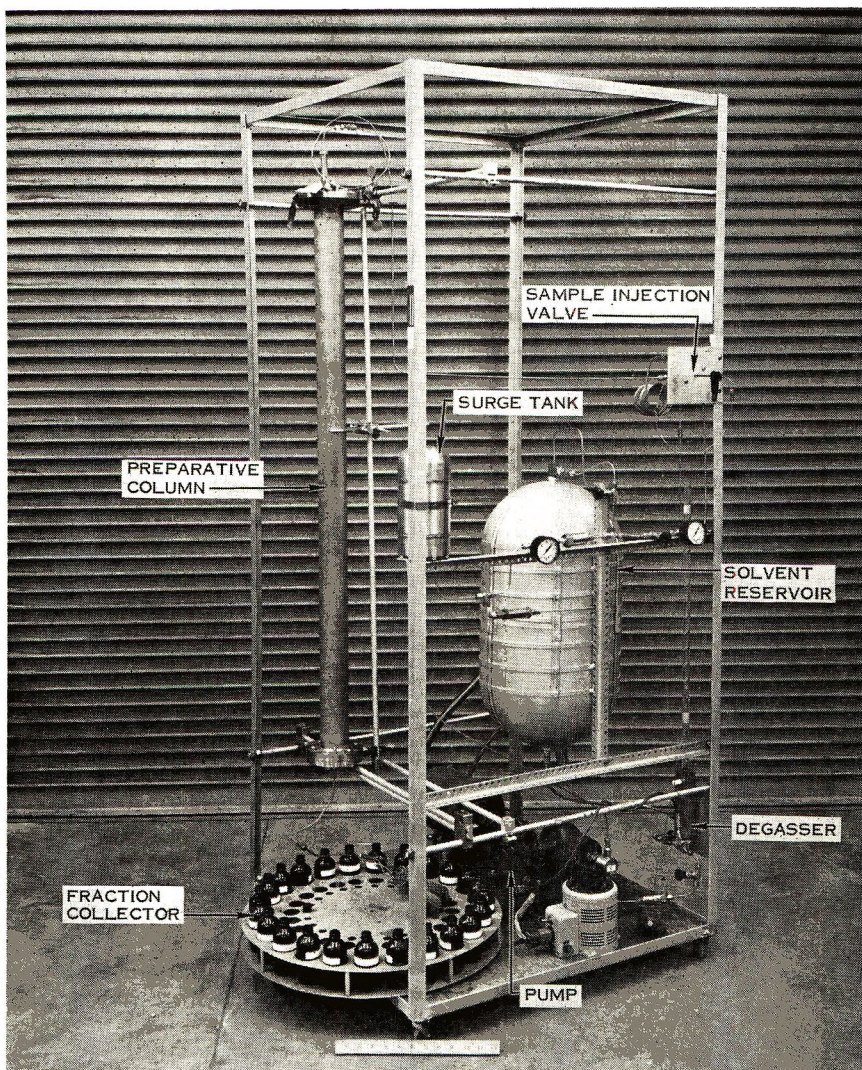


Fig. 3. Preparative GPC apparatus.

that of the sample being run if sample and standard differ in chemical structure. At present, no standards chemically similar to HB polymer are commercially available. Available polystyrene, polyglycol, and straight-chain hydrocarbon molecular weight standards have been used for calibration work at Thiokol-Wasatch; however, any error in molecular weight distribution data for HB polymer calculated using these standards was unknown. This portion of the study was undertaken to determine extent of the error by preparing standards as narrow cuts separated from HB itself. A sample of whole HB was first split into four rough fractions, one rich in high molecular weight material, one rich in low molecular weight material, the other two falling between these. Fractionation was accomplished by

TABLE I
 Analytical Data for HB Standard Fractions

Fraction	GPC peak count	Cor- rected \bar{M}_w/\bar{M}_n	Calcu- lated peak MW	$[\eta]$, dl/g	\bar{M}_n by VPO	Calcu- lated \bar{M}_w	Peak MW \times $[\eta]$
95A	21.41	2.66	37400	0.2280	19250	51200	8527
95B	21.75	2.53	27300	0.1832	14200	35900	5001
95C	21.90	2.28	22200	0.1800	12600	28700	3996
95F	22.60	1.96	7470	0.1115	4800	9400	833
95J	23.45	1.19	2760	0.0847	2500	3000	234
95L	24.50	1.15	1736	0.0671	1600	1900	116
95N	26.00	1.28	792	0.0480	690	880	38

 TABLE II
 Analytical Data for Commercial Standards

Standard	GPC peak count	\bar{M}_w/\bar{M}_n	Certified peak MW	$[\eta]$, dl/g	\bar{M}_n	\bar{M}_w	Peak MW \times $[\eta]$
PS-50,000	21.00	1.06	50000	0.3070	49000	51000	15350
PS-19,800	21.72	1.06	19800	0.1687	19000	20200	3340
P-4,000	22.80	1.01	3950	0.0804	3900	4000	318
P-750	25.82	1.01	794	0.0295	790	798	23
Octacosane	27.22	1.00	395	0.0288	395	395	11
Stearic acid	28.32	1.00	284	0.0342	284	284	10
Decanoic acid	29.77	1.00	172	0.0180	172	172	3
Dodecane	30.40	1.00	172	0.0055	172	172	1

selective precipitation from chloroform through addition of ethanol-water. The high and low rough fractions then were further fractionated by using the preparative GPC apparatus, and 20 fractions were collected. Of these, seven fractions were selected for further study and eventual use as calibration standards. Using preliminary analytical GPC results, these fractions were estimated to cover the range of 700 through 30 000 molecular weight; quantities ranged from 0.3 g for the extreme high and low fractions to 3.0 g in the middle region. The number-average molecular weight (\bar{M}_n) of these fractions was determined by vapor pressure osmometry in chloroform at 25°C with the use of a Mechrolab Model 301A instrument. The instrument was calibrated against certified polystyrenes, polyglycols, fatty acids, and straight-chain hydrocarbons, and both fractions and commercial standards were checked by VPO at four concentration levels to permit extrapolation to zero concentration. The fractions and standards also were analyzed with a Waters Model 100 GPC containing tetrahydrofuran solvent and using four columns having porosities of 3×10^4 , 900, 250, and 45 Å. The GPC analyses were performed at ambient temperature and at a flow rate of 1 ml/min. In addition, intrinsic viscosity of all fractions and com-

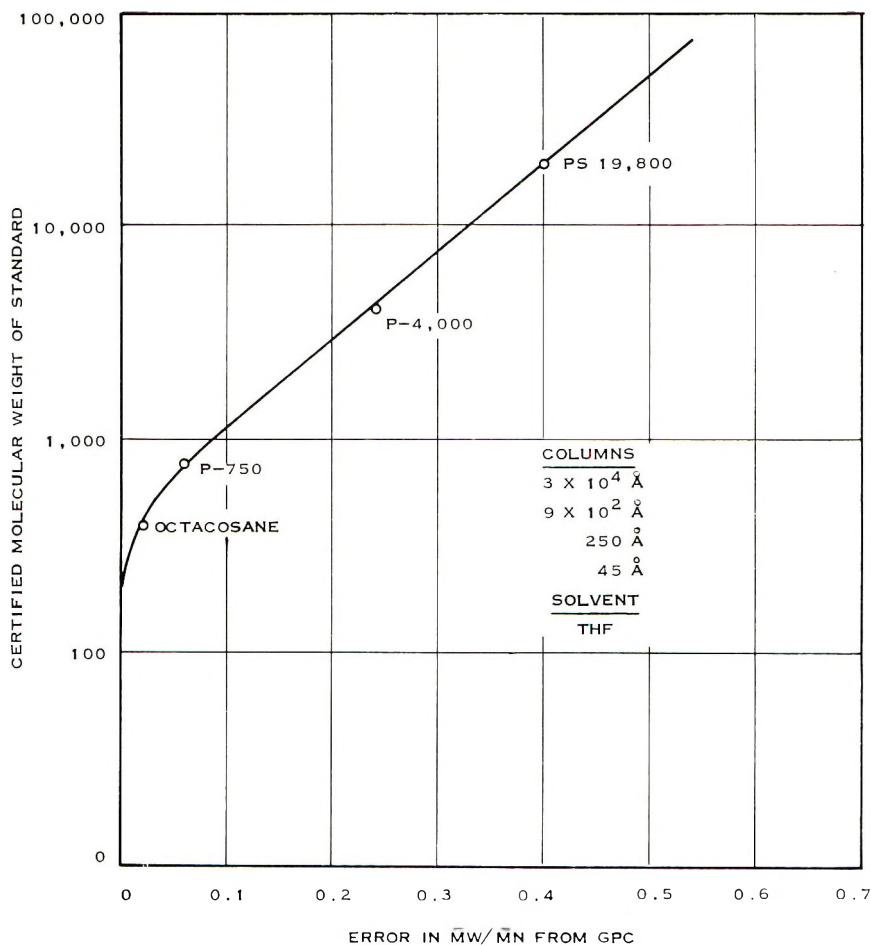


Fig. 4. Error in \bar{M}_w/\bar{M}_n vs. molecular weight.

mercial standards in benzene was measured by using a Cannon-Ubbelohde viscometer. These data are presented in Tables I and II.

In harmony with results reported by others in the field,⁴ the error in \bar{M}_w/\bar{M}_n calculated from raw GPC data for known standards was found to be directly proportional to the peak molecular weight of the standard (Fig. 4). This error arises from dispersion effects during passage through the chromatograph. By using this empirical relationship, the true \bar{M}_w/\bar{M}_n for HB fractions may be estimated, and \bar{M}_w then may be calculated, since \bar{M}_n has been determined independently. For narrow fractions whose elution curves are gaussian in shape, the peak molecular weight is very closely approximated by the root mean square of \bar{M}_n and \bar{M}_w . These data also are presented in Table I, and a plot of peak molecular weight vs GPC elution volume for both HB fractions and the commercial standards is illustrated in Figure 5. A fair agreement was obtained but, as the figure shows,

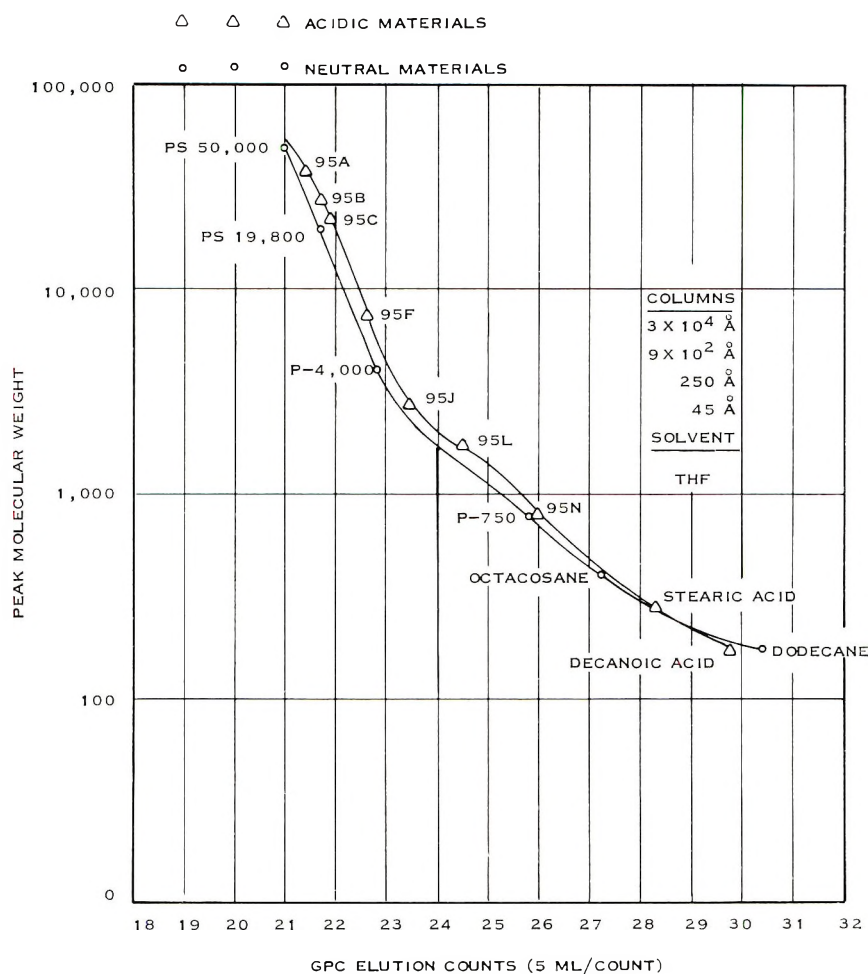


Fig. 5. GPC calibration curves.

there apparently is a real difference in elution behavior between neutral and acidic materials.

Experiments reported by several workers in the field⁵⁻⁸ have strongly supported the theory that GPC separation is based on molecular hydrodynamic volume. Since intrinsic viscosity is (for most polymer molecules) a function of hydrodynamic volume, the log of the product of intrinsic viscosity and molecular weight vs GPC elution volume has been recommended as a "universal" calibration curve regardless of polymer type. Application of this approach is illustrated in Figure 6. Disappointingly, when an intrinsic viscosity correction factor is used there is poorer agreement between the HB polymer fractions and the commercial standards. The reason for this disparity is not known, but it appears likely that the polarity of the carboxyl and nitrile groups affects the intrinsic viscosity

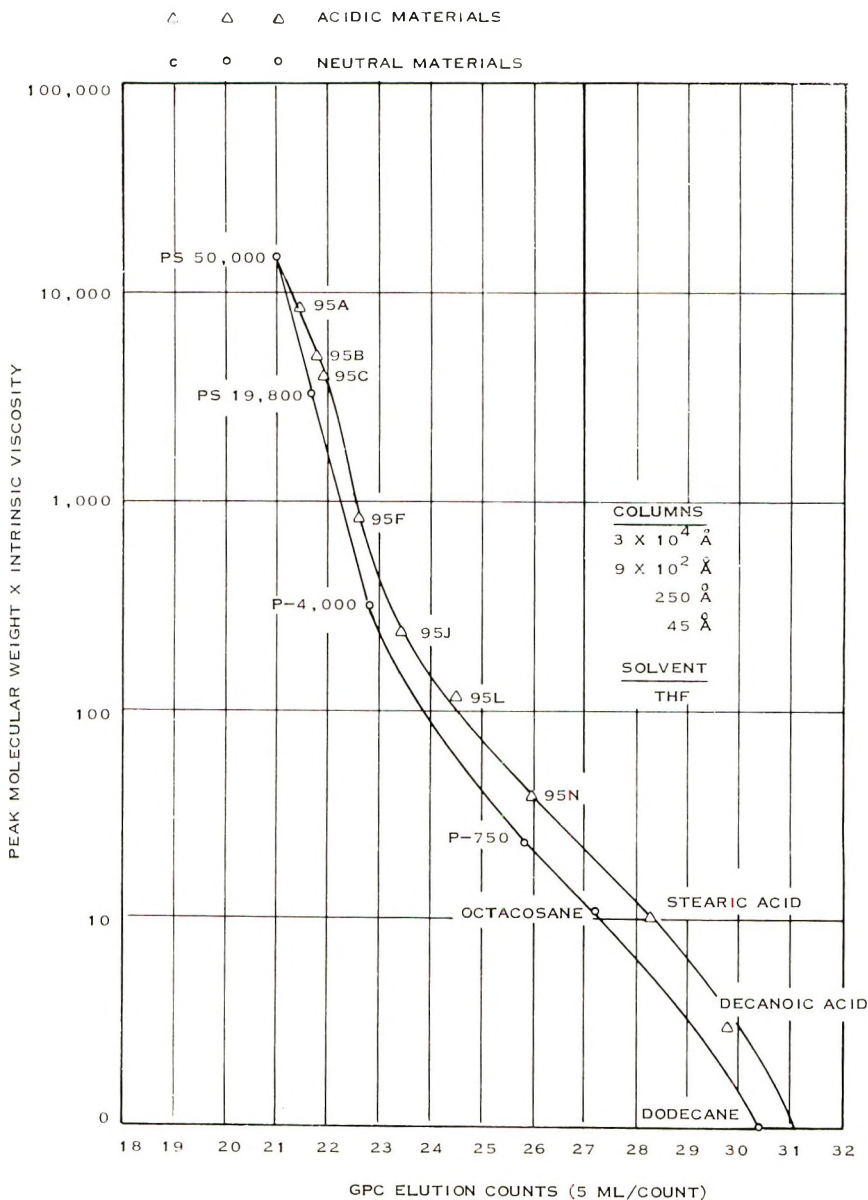


Fig. 6. GPC calibration curves obtained with the use of intrinsic viscosity factor.

and/or GPC data for these low molecular weight standards, thus invalidating application of the type of relationship noted for higher molecular weight polystyrenes, polyethylenes, polybutadienes, etc. As a double-check on the intrinsic viscosity and \bar{M}_n measurements, the Mark-Houwink relationship was plotted (Fig. 7) and an excellent fit was obtained. An additional source of error which must be considered when attempting to calculate the

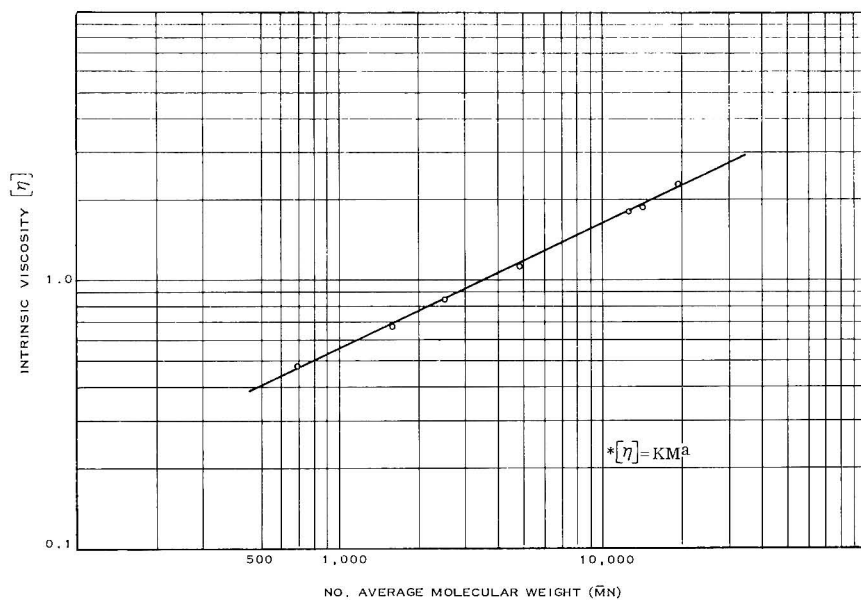


Fig. 7. Mark-Houwink intrinsic viscosity-molecular weight relationship for HB fractions.

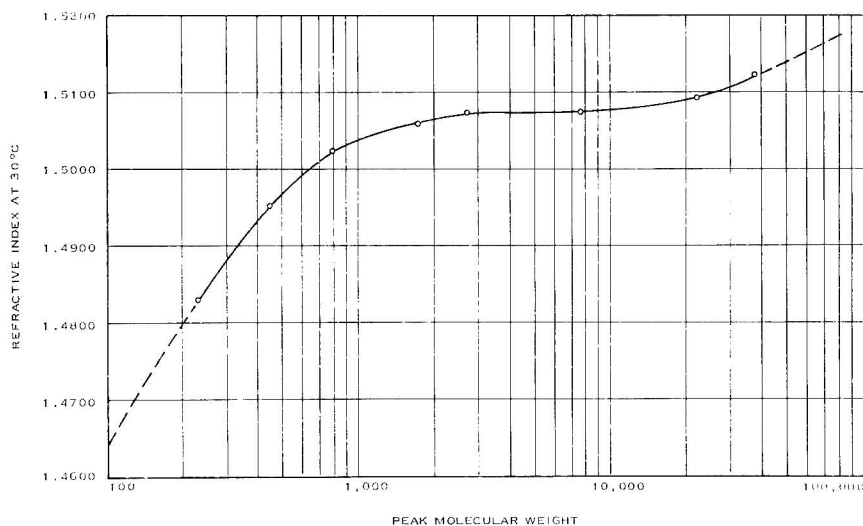


Fig. 8. Refractive index vs. molecular weight for HB polymer fractions.

true molecular weight distribution of HB polymer from raw GPC data is the fact that the refractive index of HB increases with increasing molecular weight. This problem was evaluated by determining the refractive index of the fractions prepared during this study, and resulting data and correction factors are summarized in Table III and Figure 8. Comparison of a raw GPC curve with the molecular weight distribution of HB corrected

TABLE III
Refractive Index Versus Molecular Weight for HB Polymer and Fractions

Sample	Peak MW	Refractive Index at 30°C (n)	Δn^a	Correction factor ^b
95A	37400	1.5120	0.1070	0.951
95C	22200	1.5087	0.1030	0.988
95F	7420	1.5072	0.1022	0.996
95J	2760	1.5072	0.1022	0.996
95L	1736	1.5060	0.1010	1.008
95N	792	1.5022	0.0972	1.047
101D-8	420	1.4952	0.0902	1.129
101D-11	230	1.4830	0.0780	1.305
THF	—	1.4050	—	—
Whole polymer ^c	8000	1.5068	0.1018	—

^a Refractive index of fractions minus refractive index of THF solvent.

^b Refractive index of whole polymer/refractive index of fractions.

^c After removal of PBNA antioxidant.

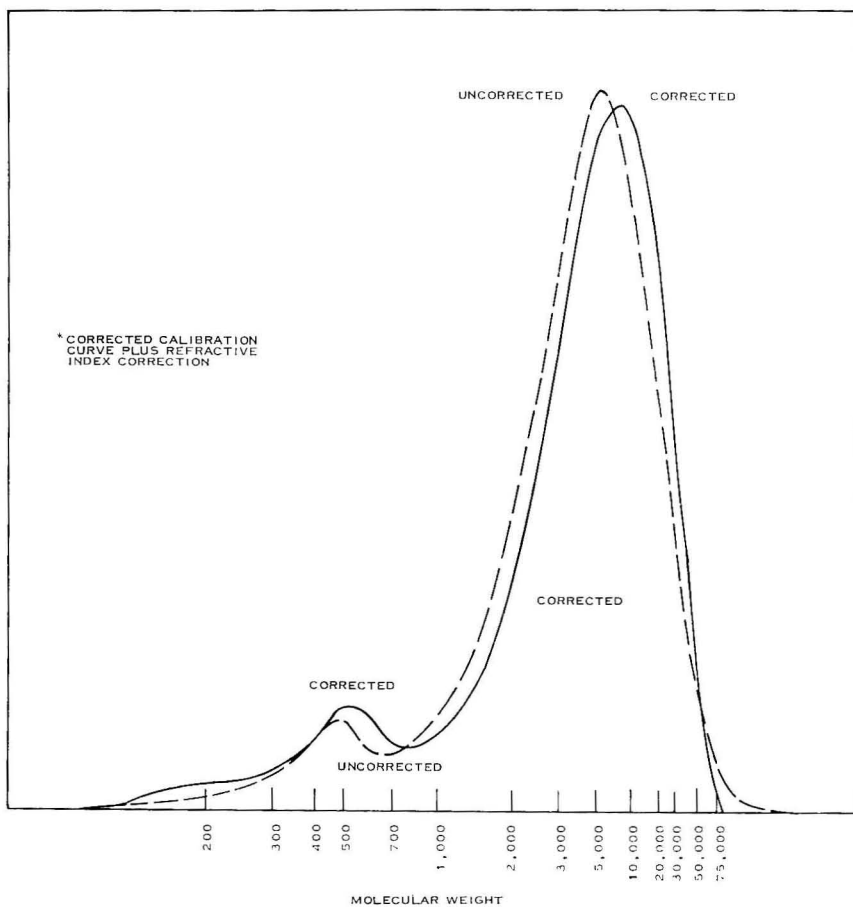


Fig. 9. Corrected molecular weight distribution of HB vs. uncorrected GPC data.

TABLE IV
Molecular Weight Distribution of HB via GPC
(Corrected vs. Uncorrected)

Molecular weight	Uncorrected, %	Corrected, %
50000	4.5	6.1
30000	10.1	14.7
20000	14.8	18.1
10000	20.5	18.5
5000	18.9	15.4
3000	13.5	10.9
2000	7.3	5.3
1000	2.6	2.1
700	1.6	2.0
500	2.8	2.9
400	2.1	2.0
300	0.9	1.1
200	0.4	0.9
\bar{M}_n	2 798	2 878
\bar{M}_w	11 834	14 037

for the disagreement in the calibration curve between HB fractions and the commercial standards, and for refractive index variation, is presented in Figure 9 and Table IV.

It should also be noted that comparison of \bar{M}_n determined by VPO and GPC for HB polymer is now available over the molecular weight range covered by the HB fractions prepared in this study (Table V).

Isolation and Identification of Low Molecular Weight Species

Before any preparative GPC runs were conducted, the polymer sample was subjected to several operations which simplified subsequent isolation and identification of chemical species. Since only the 100–500 molecular weight range was of interest during this portion of the study, a fraction rich in these low molecular weight materials was isolated from 1000 g of polymer by solvent–nonsolvent extraction of 100-g portions. A 100-g portion of polymer was dissolved in 500 ml of CHCl_3 , and 420 ml of ethanol–water (85:15) was added slowly, yielding two phases. Material in the upper phase was isolated by using a Rinco evaporator, then dissolved in ethyl ether and washed with H_2O to remove Ammonyx G (cetyldimethylbenzylammonium chloride) residual soap from emulsion polymerization. After removal of the solvent and drying on a Rinco evaporator, a total of 47.5 g was obtained. Chemical analysis yielded the comparison with the original polymer shown in Table VI.

The acids whose sodium salts are soluble in water were then separated by dissolving the extract in ether and washing twice with 5% NaOH. After neutralization of the caustic solution with dilute HCl, 9.1 g of acids was obtained by washing with ether. This material was very fluid, bright orange-red in color, and contained at least three components, according to

TABLE V
Comparison of \bar{M}_n Results from VPO and GPC

Sample	\bar{M}_n from VPO	Corrected \bar{M}_n from GPC
95A	19250	19677
95B	14200	13580
95C	12600	11831
95F	4800	5110
95J	2500	2839
95L	1600	1474
95N	690	780

TABLE VI

	Polymer	Extract
Acid no., equiv/100 g	0.064	0.170
Iodine no., gI ₂ /100 g	352	232
Sulfur, %	1.05	2.19
Nitrile, as acrylonitrile, %	11.0	5.2

TABLE VII

	Acid fraction (9 g)	Neutral residue (35 g)
Acid no., equiv/100 g	0.761	0.038
Sulfur, %	0.06	3.16

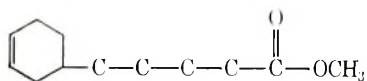
its GPC chromatogram, the principal component being 4-carboxycyclohexene. Gas chromatographic analysis gave only one peak, corresponding to 4-carboxycyclohexene. This indicates that the other acids were not sufficiently volatile to respond to GLC, or that they decompose before vaporizing. Chemical analysis yielded the results shown in Table VII.

All of the acid fraction was quantitatively converted to mixed methyl esters by reacting with an excess of freshly prepared diazomethane in ether. Vacuum distillation at 0.5 mm Hg with the use of a 3.5-in. glass bead column gave three cuts.

Cut 1. At 24–26°C, 70 wt-% of the ester fraction distilled. This boiling point corresponds to the methyl ester of 4-carboxycyclohexene. GPC, GLC, infrared analysis, and iodine number (167) confirmed this conclusion. This ester is water white.

Cut 2. Approximately 20 wt-% of the ester fraction distilled at 72–75°C. GPC analysis showed a molecular weight of approximately 200 and the presence of small amounts of lower and higher molecular weight materials. This molecular weight strongly suggests a reaction product of two moles of butadiene with one of acrylic acid, as also indicated from previous work.³ The iodine number (125) corresponding to one double bond per

mole, molecular weight (200), and infrared spectrum of this ester are consistent with only one structure (I):



I

The acid from which the ester was formed, recognized as a homolog of 4-carboxycyclohexene, probably is formed by reaction of vinyl cyclohexene and acrylic acid, and may be named ω -(cyclohexenyl-3)-pentanoic acid. The impure ester has a yellow-orange color.

Cut 3. Approximately 10% of the ester fraction remained as still bottoms. This material was dark red in color and contained 28% polymeric material (500–4000), a peak at MW 340 (15%), a peak at MW 240 (8%), and a peak at MW 138, according to GPC analysis. In view of the very small quantities of these materials in the polymer (less than 0.02% for any individual acid), the question of their exact structure is academic, and no attempts were made to further identify them.

The neutral fraction had high sulfur content, as expected from previous work which indicated the presence of sulfides.³ The sulfur and nonsulfur components were separated by oxidation of a 13-g portion at 0°C with H₂O₂ in methyl ethyl ketone (MEK) to convert the sulfides to mixed sulfoxides and sulfones, followed by separation on an activated silica gel column. Nonfunctional nonsulfur material was isolated by eluting first with chloroform. The mixed sulfoxides and sulfones were isolated by washing next with ether–chloroform (2:1). Washing with ether and then acetone removed higher molecular weight acidic materials. Chemical analysis yielded the results shown in Table VIII.

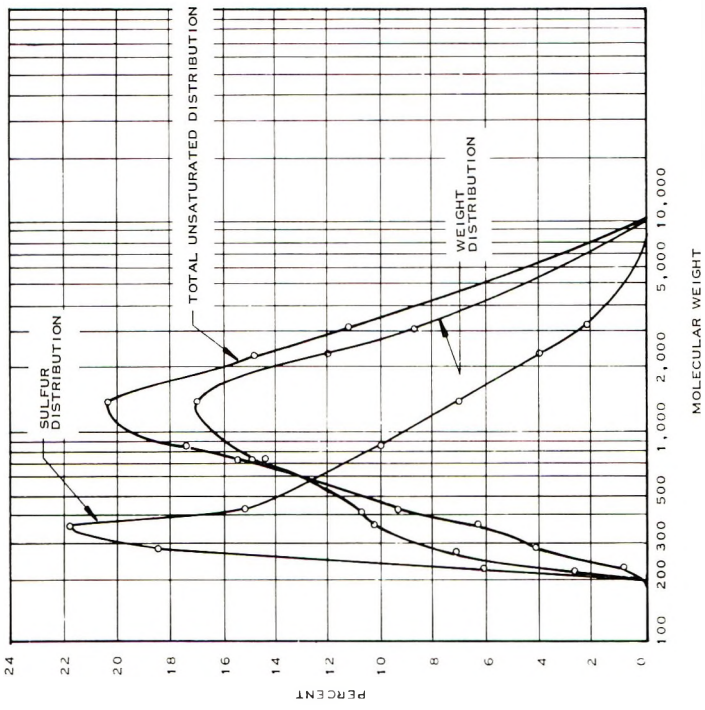
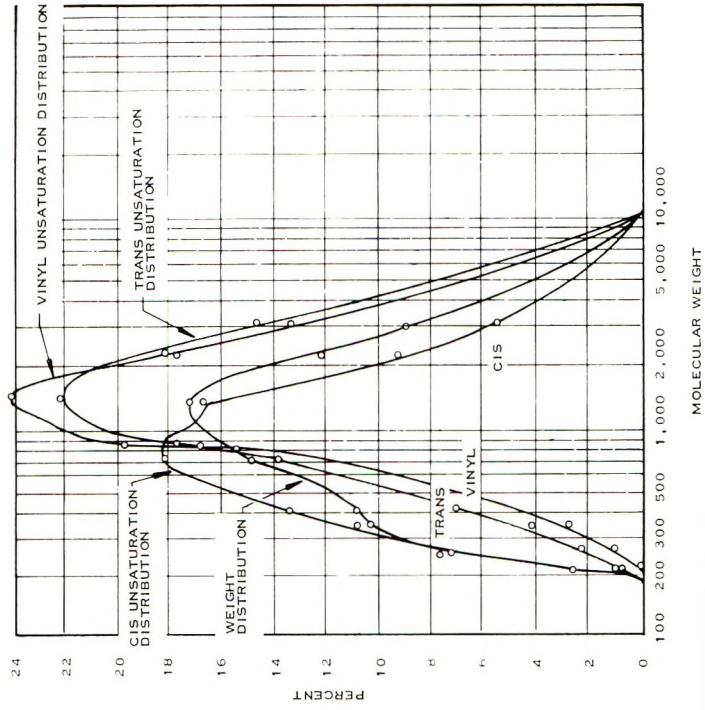
TABLE VIII

	Nonfunctional fraction (1.3 g)	Mixed sulfoxide- sulfone fraction (7.4 g)
Iodine no., g I ₂ /100 g	86	193
Sulfur, %	0	5.0

TABLE IX
Analytical Data for Nonsulfur Neutral Fractions

Fraction	MW range	Iodine no., g I ₂ /100 g	<i>Trans</i> , % ^a	<i>Cis</i> , % ^a	Vinyl, % ^a
2	400–1500	130	55	35	10
3	300–500	49	24	76	0
4	200–500	38	22	74	5
5	200–400	43	4	95	1
6	200–300	40	4	95	1

^a Per cent of total unsaturation.



NOTE: ALL DATA NORMALIZED TO PERCENT FOR COMPARATIVE PURPOSES, I.E., THE AREA UNDER EACH CURVE IS IDENTICAL.

Fig. 10. Functional group distribution of high sulfur neutral fraction.

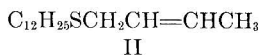
Each of these fractions was further fractionated using the preparative GPC and the fractions were analyzed for per cent sulfur, iodine number, infrared spectrum, and molecular weight. The resulting data are presented in Tables IX and X and Figure 10. The three lowest molecular weight fractions from the high sulfur material were purified by refractionation on the preparative GPC. The two lowest molecular weight fractions

TABLE X
Analytical Data for Neutral Fractions High in Sulfur

Fraction no.	Peak MW	Weight, g	Sulfur, %	Iodine no., g I ₂ /100 g	<i>Trans</i> , % ^a	<i>Cis</i> , % ^a	Vinyl, % ^a
3	3100	0.343	1.0	249	72	17	11
4	2200	0.472	1.3	240	67	22	11
5	1360	0.685	1.6	227	60	29	11
6	850	0.612	2.5	218	56	34	10
7	710	0.590	3.8	198	50	42	8
8	420	0.418	5.7	172	41	51	8
9	350	0.410	8.2	119	36	60	4
10	270	0.284	10.0	109	32	65	3
11	230	0.105	8.9	61	25	72	3

^a Per cent of total unsaturation.

were the mixed sulfoxide-sulfones of the following compounds II and III in nearly pure form (as judged from the very narrow GPC scans), except that both *cis* and *trans* forms appear to be present (judged from infrared spectra):



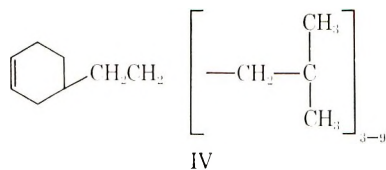
II



III

These compounds must result from direct reaction of dodecyl mercaptan (used as a chain transfer agent in HB polymer preparation) and butadiene. The sulfur content, iodine number, and infrared spectra indicate that the higher fractions are mixtures of the higher homologs of these compounds.

The fractions from the nonfunctional material did not yield pure chemical species, but mixtures of polyisobutylenes (containing one double bond per mole), rather than polybutadienes as had been originally supposed. The formation of polyisobutylenes can only be accounted for by the presence of isobutylene as an impurity in the butadiene used in the manufacture of HB polymer. Industrial grade butadiene frequently contains as much as 1% isobutylene. The infrared spectra of these fractions indicate that the unsaturation is predominantly present in the cyclohexenyl form, and since iodine numbers are consistent with only one double bond, compounds such as IV are suggested.



Materials of this type would presumably arise by reaction of vinylcyclohexene (butadiene dimer) and a growing isobutylene chain.

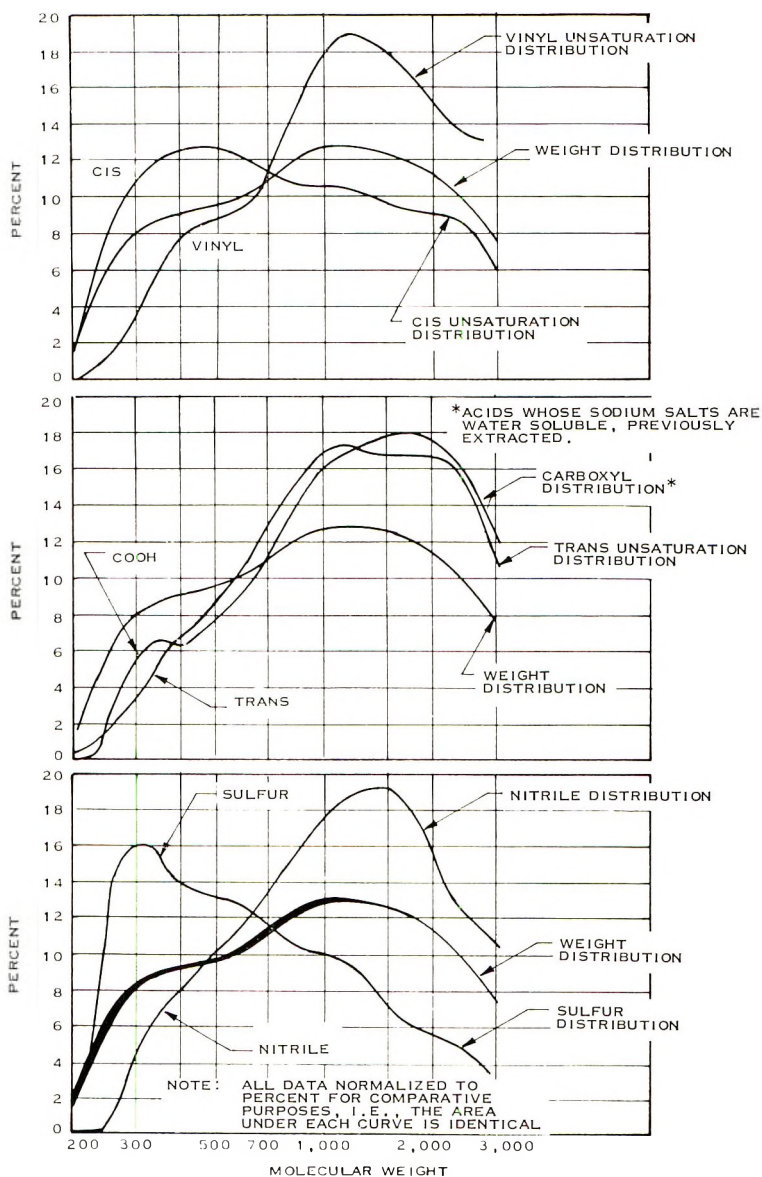


Fig. 11. Functional group distribution of low molecular weight portion of IIB polymer.

A portion of the neutral fraction also was fractionated directly with the preparative GPC column prior to oxidation and silica gel separation, yielding 16 cuts, which were analyzed by infrared for carboxyl and nitrile content (matched 0.2-mm cells) and the *cis*, *trans*, vinyl interrelationship. The sulfur content, iodine number, and molecular weight also were determined. After correction for iodine consumption by nitrile groups, the iodine number is a measure of total unsaturation, which permits quantitative calculation of *cis*, *trans*, vinyl content. To permit meaningful comparisons, the data were normalized to percentages, and the per cent at each molecular weight was plotted versus molecular weight (Fig. 11). The figures can be superimposed, since the scale is identical; however, the data are presented in three parts to avoid confusion. The percentage scale refers to percent in the extract, not in the whole polymer. Caution should be exercised in drawing conclusions from the carboxyl distribution curve, since the lowest acids had been removed prior to this fractionation. However, the distribution of nitrile, sulfur, *trans*, *cis*, and vinyl should be indicative of the nature of the lower molecular weight portion of HB polymer.

RESULTS

Calibration Studies

Calibration standards were prepared from HB polymer, and a true calibration curve was obtained (Fig. 5), and the effect of a varying refractive index on GPC readout was determined. Calculation of the molecular weight distribution of HB polymer using the true calibration curve, and application of suitable correction factors for refractive index errors, results in a moderate shift toward higher molecular weights and reveals an increased quantity of material in the lower end, compared to the uncorrected result calculated using chemically dissimilar standards. The effect on number-average molecular weight is quite small, since the two correction factors tend to cancel each other in calculating \bar{M}_n , but an overall rise in \bar{M}_n of 2000 to 3000 is noted. Error in calculating molecular weight distribution from GPC data caused by peak spreading due to dispersion arising from factors other than true fractionation in the gel was not evaluated in this study.

Functional group distribution curves obtained during these calibration studies reveal that the lower molecular weight portion of HB is deficient in carboxyl, nitrile, and vinyl groups in comparison with the major portion of the polymer, and that this lower portion is comparatively rich in sulfur (dodecyl mercaptan chain transfer products) and *cis* unsaturation, which are in turn associated with nonfunctional materials. In the major higher molecular weight portion of the polymer (1 000 to 50 000) the nitrile, carboxyl, unsaturation, and weight distribution curves were similar in shape.

A comparison of \bar{M}_n calculated from corrected GPC data and \bar{M}_n determined by VPO indicates that the two methods are comparable within

normal experimental error when applied to narrow molecular weight distribution materials.

Isolation and Identification of Chemical Species

The eight chemical species listed in Table XI with an estimate of their relative concentration in the whole polymer, have been isolated from the low molecular weight portion of HB polymer in sufficient quantities to permit identification.

Polyisobutylene-butadiene materials in the 200–500 molecular weight range also were isolated, but not in sufficient purity or quantity to permit exact identification. Higher molecular weight homologs or near homologs of the eight listed species almost certainly are present, judging from infrared and chemical analyses of numerous fractions prepared during these studies. Also present are: PBNA antioxidant (phenyl β -naphthylamine), at the 1.0–1.2% level; and a residual soap (cetyldimethylbenzylammonium chloride) at the 4–6% level. The approximate composition of the 100 to 500 molecular weight portion of HB polymer is as shown in Table XII (trace materials not included).

This breakdown indicates that on the average, only about 90% of HB is actually functional polymer, the remainder being either inert or capable of consuming epoxy curing agent without contributing to the mechanical strength of the cured propellant.

It is apparent that 90% of all acids in the 100–500 molecular weight range can be accounted for by the combination of cyclohexene carboxylic acid and the cyclohexenyl pentanoic acid. In view of the known correlation between the 250–500 molecular weight materials as determined by GPC and pro-

TABLE XI

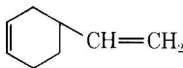
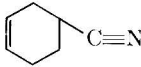
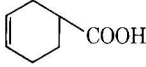
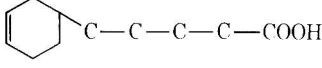
Compound	Estimated level in HB, %	Molecular weight
$\text{H}_2\text{C}=\text{CHCOOH}$	Trace	72.1
	Trace	108.2
	Trace	107.2
	0.5–1.0	126.2
	0.2–0.3	182.3
$\text{C}_{12}\text{H}_{25}-\text{SH}$	Trace	202.4
$\text{C}_{12}\text{H}_{25}-\text{SCH}_2\text{CH}=\text{CHCH}_3$	0.1–0.2	256.5
$\text{C}_{12}\text{H}_{25}\text{SCH}_2\text{CH}=\text{CH}-\text{CH}_2-\text{CH}_2\text{CH}=\text{CH}-\text{CH}_3$	0.2–0.4	310.6

TABLE XII

Primary area of concentration (MW)	Type of material (100-500 MW)	Content in whole polymer, %
100-200	Carboxylic acids, primarily cyclohexene derivatives	0.8-1.5
250-500	Straight chain sulfides, derived from DDM and BD	1.5-3.0
150-500	Polyisobutylene-butadienes of low unsaturation	0.2-0.5
^a	Residual soap	4.0-6.0
^b	PBNA antioxidant	1.0-1.2
	Total	7.5-12.2

^a Does not appear as a detectable peak on the GPC scan due primarily to a low refractive index compared to IIB.

^b Elutes last from GPC as a separate distinct peak, due apparently to sorption on the gel. PBNA's high refractive index renders this peak abnormally prominent.

pellant mechanical properties, and the small amount of acids in this region, it appears likely that the sulfides influence propellant properties even more than had been suspected previously.

The portion of highest GPC correlation with propellant mechanical properties is extremely rich in sulfur, suggesting again that the sulfides formed by reaction of dodecyl mercaptan and butadiene may be largely responsible for the high GPC correlations.

The portion of highest GPC correlation with propellant mechanical properties also is rich in cis unsaturation and low in vinyl and trans unsaturation, indicating that the polyisobutylene materials which contain primarily cis unsaturation also play a role in the GPC correlation. This area also is very low in nitrile content, reconfirming earlier studies.

CONCLUSIONS

Preparative-scale GPC greatly facilitated the isolation of low molecular weight materials in sufficient quantity to permit identification. Preparation of standard materials from HB polymer itself has made possible the construction of a true calibration curve applicable to carboxy-butadienes in the 1000-50000 molecular weight range. Application of an intrinsic viscosity correction factor failed to yield a universal calibration curve. Three major types of chemical species were identified in the low molecular weight range of HB polymer, i.e., reaction products of one mole of acrylic acid with two or more moles of butadiene, reaction products of one mole of dodecyl mercaptan with one or more moles of butadiene, and reaction products of one or two moles of butadiene with three or more moles of isobutylene impurity. The acids were concentrated in the lower portion of the 100-500 molecular weight range, with the mercaptan products (sulfides) and the polyisobutylenes concentrated in the 250-500 range.

The effect of acidic materials on propellant mechanical properties is known to be caused by consumption of epoxy curing agent. The sulfides and polyisobutylenes have no reactive cure site, but would be capable of plasticizing effects. These nonfunctional materials predominate in the area of highest GPC correlation and are presumed to be responsible for this correlation. An increase in the 100–500 \bar{M}_w material is invariably accompanied by a decrease in modulus, again indicating plasticizing action.

The composition and distribution of chemical species in the lowest molecular weight portion of HB polymer is significantly different from that of the bulk of the polymer. This low region, which is largely responsible for variations in propellant mechanical properties, is rich in sulfides and other nonreactive materials and deficient in nitrile, vinyl, and carboxyl functionality.

References

1. R. D. Law and H. G. Pulsipher, *The Development of Laboratory Tests for the Prediction of HB/ECA Ratio in TP-H1011 Propellant*, Technical Report MQA 16-64, Thiokol Chemical Corp., Wasatch Div., Brigham City, Utah, 1964.
2. J. E. Poelman, R. R. Hendricksen, C. K. Schaab, S. J. Bennett, and J. H. Stoker, *Low Molecular Weight Materials in HB Polymer*, Technical Report PDSR 4-65, Thiokol Chemical Corp., Wasatch Div., Brigham City, Utah, 1966.
3. R. D. Law, *J. Polym. Sci. C*, **21**, 225 (1968).
4. H. W. Osterhoudt and L. N. Ray, *J. Polym. Sci. C*, **21**, 5 (1968).
5. H. Benoit, Z. Grubisic, P. Rempp, D. Decker, and J. Zilliox, paper presented at 3rd International Symposium on GPC, Geneva, Switzerland, May 19–20, 1966.
6. Z. Grubisic, P. Rempp, and H. Benoit, *J. Polym. Sci. B*, **5**, 753 (1967).
7. K. Boni, F. Sliemers, and P. Stickney, "Universal Calibration of GPC for Polymer Characterization," Fourth International Seminar on Gel Permeation Chromatography, May 22–24, 1967.
8. E. Drott, "Effect of Branching on Calibration Curves for Low Density Polyethylene," Fourth International Seminar on Gel Permeation Chromatography, May 22–24, 1967.

Received December 10, 1968

Investigation of the Epoxide-Carboxylic Acid Reaction in Model Compound and Polymerization Reactions

FRANCIS B. ALVEY, *Celanese Coatings Company, Louisville, Kentucky* 40202*

Synopsis

The reaction of epoxide and acid has been studied in the model reaction of bisphenol-A diglycidyl ether and acetic acid with several base catalysts at 60, 95, and 115°C. The results suggest that no greater than 5% side reactions occur. A series of polyhydroxyl-ester polymers were prepared from bisphenol-A diglycidyl ether and adipic acid. The polymers gel rapidly upon heating at 200°C. Terpolymers of bisphenol-A diglycidyl ether, bisphenol-A, and azelaic acid were prepared. These also gel at 200°C when 50 mole-% of the active hydrogen reactant is azelaic acid.

The oxirane ring of epoxide compounds reacts with carboxylic acids to form hydroxylalkyl esters. The functional groups present in this reaction can participate in several competing side reactions which include etherification, esterification, transesterification, hydrolysis, and hydration.¹ The polymerization of diepoxides and dicarboxylic acids to yield essentially linear polyhydroxylalkyl esters will be successful only if these side reactions can be controlled or desirably eliminated.

It has been generally reported that monocarboxylic acids react with glycidyl ethers under base catalysis to yield hydroxylalkyl esters with little side reaction.¹⁻³ However, side reactions occur in the reaction of fatty acids and ethylene oxide.⁴ Also, it has been reported that bisphenol-A diglycidyl ether (BDG) reacts with dicarboxylic acids to produce insoluble, infusible polymers because of concomitant etherification.⁵

We have investigated the model reaction of acetic acid and BDG with several base catalysts to find reaction conditions which promote chiefly the epoxide-acid reaction. These conditions were then used to prepare fusible, soluble polyhydroxylalkyl ester (PHAE) polymers by the bulk polymerization of dicarboxylic acids and BDG. The products from the acetic acid-BDG model reactions were analyzed for epoxide and acid content. As a working hypothesis and on the basis of the literature, we assumed that only etherification and esterification would be important side reactions. Thus, model reaction conditions affecting equal degrees of acid and epoxide reaction would also yield linear polymers in the BDG-dicarboxylic acid reactions.

* Present address: Department of Pharmacology, University of Louisville Medical School, Louisville, Kentucky 40202.

Our model studies and polymerizations were carried out without solvents to eliminate side reactions with solvent. The catalysts employed were *N,N*-dimethylacetamide (DMA), triisopropanolamine (TIA), tri-*n*-butylamine (TNB), and KOH. We have reported before that DMA and TIA are useful catalysts for the epoxide-phenol reaction.^{6,7}

EXPERIMENTAL

Reactants

Catalysts were obtained as follows: DMA, duPont, technical grade; TNB, Eastman, Eastman grade; TIA, Union Carbide, technical grade; KOH, Baker, reagent grade. The catalysts were used as received. Reactants were obtained as follows: acetic acid, Baker, reagent grade; adipic acid, duPont; azelaic acid, Emery, 3577-R; bisphenol-A, Monsanto: BDG, Celanese Resins, Epi-Rez 510 (model reactions) and Epi-Rez 509 (polymerizations). One quantity of BDG was employed in each series of reactions. The epoxide equivalent weight of BDG was determined by the pyridine-HCl method⁸ and the equivalent weight of the acids by titration with 0.1*N* KOH (ethanol-water, 1:1) with phenolphthalein indicator.

Model Reactions

BDG, acetic acid, and catalyst were stirred for 10 hr at 65°C, 5 hr at 90°C, or 2 hr at 115°C. The reaction mixtures were cooled to room temperature and analyzed for acid and epoxide. Acid titrations were carried out as for the starting acids. Epoxide analyses were made by the methyl ketone procedure⁹ and were corrected for acid.

Polymerization Reactions

Polymerizations were conducted in two stages. Stage I was carried out with stirring in glass flasks to dissipate reaction exotherm. The reactants were rapidly heated to reaction temperature, 125°C ± 2°C, and stirred until the viscosity increase becomes too great. The reaction mixture was transferred to aluminum reaction vessels and cooled to room temperature. A small sample of the intermediate product was heated in a 125°C ± 1°C oven until gelation to determine gel time. Then in stage II, the intermediate product was oven-aged at 125 ± 1°C to a condition just short of gelation as indicated by the predetermined gel times. The bulk polymer was cooled to room temperature and pulverized.

Samples were taken during both reaction stages for analyses of acid and epoxide. The terpolymerizations of BDG, bisphenol-A, and azelaic acid were conducted similarly. The azelaic acid was added in stage I after BDG and bisphenol-A had been allowed to react for 1 hr.

Gel times at 200°C were determined by probing small samples in aluminum pans on a 200°C constant-temperature cure plate. Loss of fluidity at 200°C and insolubility at room temperature was taken as indication of gela-

tion. The melting range of the polymers was determined on a Fischer hot-stage melting point apparatus.

RESULTS AND DISCUSSION

Model Reactions

Tables I and II give results of the model reactions. The difference in per cent reaction of epoxide and acid extrapolated to 100% reaction of epoxide

TABLE I
Reaction of Bisphenol-A Diglycidyl Ether (0.250 mole)
and Acetic Acid (0.500 mole) with Several Catalysts (5.00×10^{-3} mole)
at 65, 90, and 115°C

Catalyst	Reaction temperature, °C	Reaction hr	Reaction of epoxide, %	Reaction of acid, %	Difference in % reaction ^a
None	65	10	11.7	9.9	16
DMA	65	10	63.7	19.4	70
TNB	65	10	60.3	35.3	42
TIA	65	10	45.9	39.9	13
KOH	65	10	57.8	38.0	34
None	90	5	22.0	18.2	17
DMA	90	5	63.7	48.0	25
TNB	90	5	63.7	60.1	5.6
TIA	90	5	64.4	60.6	6.1
KOH	90	5	59.3	41.7	30
None	115	2	46.3	23.4	50
DMA	115	2	76.9	68.2	11
TNB	115	2	85.3	80.7	5.3
TIA	115	2	74.6	69.6	6.8
KOH	115	2	67.7	63.4	6.3

^a Extrapolated to 100% reaction of epoxide.

TABLE II
Reaction of Bisphenol-A Diglycidyl Ether (0.250 mole) and Acetic Acid
(0.500 mole) with Several Catalysts (1.00×10^{-2} mole) at 90 and 115°C

Catalyst	Reaction temperature, °C	Reaction time, hr	Reaction of epoxide, %	Reaction of acid, %	Difference in % reaction ^a
DMA	90	5	68.0	61.6	9.4
TNB	90	5	82.4	77.8	5.6
TIA	90	5	79.7	77.0	3.4
KOH	90	5	68.4	63.8	6.7
DMA	115	2	94.9	85.7	9.7
TNB	115	2	98.7	92.3	6.5
TIA	115	2	86.1	81.7	5.1
KOH	115	2	84.1	77.1	8.3

^a Extrapolated to 100% reaction of epoxide.

TABLE III
Bulk Polymerization of Bisphenol-A Diglycidyl Ether and Adipic Acid at 125°C

Polymer	Catalyst	BDG, mole	Adipic acid, mole	Catalyst × 10 ² , mole	Reaction Time Hr		Weight epoxide, g ^b	Weight acid, g ^b	Gel time at 200°C, hr	Melting range, °C
					Stage I ^a	Stage II ^a				
P-1	TIA	1.000	1.000	2.000	3.0	3.0	4 580	2 880	—	—
P-2	DMA	1.000	1.000	2.000	2.3	0.5	7 870	3 497	0.25	85-95
P-3	TNB	1.000	1.000	2.000	1.3	3.5	α	12 900	0.23	80-90
P-4	TIA	1.000	0.9500	2.000	1.5	3.0	6 806	10 705	0.06	100-110
P-5	TIA	0.9500	1.000	2.000	1.5	5.5	α	2 800	0.16	70-80
P-6	TNB	1.000	1.000	4.000	0.58	9.5	α	17 080	0.50	85-95
P-7 ^e	TNB	1.000	1.000	2.000	1.3	6.0	α	14 030	0.15	90-100
P-8 ^d	TNB	1.000	1.000	2.000	0.5	22.5	—	—	0.36	80-90
P-9 ^e	TNB	1.000	1.000	2.000	1.5	32.0	—	—	1.3	110-120
P-10	TNB	1.000	0.5000	2.000	0.5	f	702	α	0.45	—
P-11	TNB	0.5000	1.000	2.000	2.0	13.0	—	—	0.66	—

^a See experimental section for stage I and stage II conditions.

^b Based on end group titrations for epoxide and acid.

^c Also contains 0.0100 mole benzoic acid.

^d Also contains 0.0500 mole benzoic acid.

^e Also contains 0.100 mole benzoic acid.

^f Too reactive for second stage.

was used as a measure of the contribution of side reactions to the overall process. From these data it appeared that BDG and dicarboxylic acids could be polymerized to yield PHAE polymers with about 95% linear reaction with TNB or TIA catalysts at 90–115°C. In the model reactions, the conversion of epoxide was consistently greater than that of acid. This indicated that the chief side reaction is epoxide with the hydroxyl group of the hydroxylalkyl ester.

Table III gives data concerning bulk polymerizations of BDG and adipic acid carried out at 125°C with several catalysts, catalyst concentrations, and monomer mole ratios. We used a slightly higher temperature in the polymerizations to facilitate stirring in the stage I reaction. The relative consistency in the differences in conversion for TNB and TIA catalysts at 90°C and 115°C seemed to warrant the change to the higher temperature.

Under the conditions of our two-stage polymerization procedure, the total reaction time for stage I and stage II given in Table III approximates gel time for the particular polymerization. It is therefore possible to analyze these reactions for the effect of changes in reaction parameters on gel time. Excess BDG shortens gel time. This was readily apparent in P-10 (in comparison to P-3), where the mole ratio of BDG to adipic acid was 2:1. Gel time is increased by use of excess adipic acid as seen in P-11 (in comparison to P-3), where the mole ratio of adipic acid to BDG was 2:1. These effects of excess reactants on gel time suggest that the chief side reaction is etherification. This agrees with the consistently greater conversion of epoxide observed in the model studies.

Benzoic acid was added to polymers P-7, P-8, P-9, as a chain terminator. The gelation tendency was significantly reduced by the benzoic acid. In the case of P-9, the use of 0.05 mole benzoic acid increased the gel time to greater than 33 hr. This also indicates that the gel-producing functional group is terminal epoxide.

The PHAE polymers have melting ranges from 80 to 120°C. Endgroup analyses for weight per epoxide and weight per acid values show that the equimolar polymers have molecular weights between 5×10^3 and 2×10^4 . TNB catalysis yields product of higher molecular weights than TIA and DMA (compared P-1, P-2, P-3). Also, increasing the concentration of TNB appears to yield product of higher molecular weight (compare P-6 to P-3).

Tables IV–VI give analytical data on aliquots from P-1, P-2, and P-3. The difference in per cent reaction of epoxide and acid is less in these polymerization aliquots than was observed in the model reactions. TNB gives better reaction balance than TIA and DMA. This is in agreement with the higher molecular weight obtained without gelation with TNB catalyst. It is of interest to note that the difference values are relatively constant at all degrees of conversion for each catalyst.

All of the PHAE polymers of Table III and intermediates of Tables IV, V, and VI undergo rapid gelation at 200°C. Gel times are about 30 min in most cases. Even the polymers containing benzoic acid terminator show

this effect. This gelation at 200°C can be attributed to the occurrence of esterification and transesterification reactions which would be expected at this temperature with the PHAE polymers.

Bulk polymerization of BDG and bisphenol-A under conditions similar to

TABLE IV
Bulk Polymerization of Bisphenol-A Diglycidyl Ether
(1.000 mole) and Adipic Acid (1.000 mole) at 125°C with
Tri-*n*-butylamine Catalyst (0.02000 mole)^a

Sample	Reaction time, hr	% reaction ^b			Gel time at 200°C, hr
		Epoxyde	Acid	Difference	
1	0.33	68.1	65.6	2.5	0.76
2	0.66	88.0	85.3	2.7	0.66
3	1.00	93.6	90.8	2.8	0.53
4	1.33	94.9	92.1	2.8	0.46
5	2.50	100	97.2	2.8	0.43
6	4.66	100	98.0	2.0	0.23

^a Polymerization P-3 of Table III.

^b Based on endgroup analysis for epoxyde and acid.

TABLE V
Bulk Polymerization of Bisphenol-A Diglycidyl Ether (1.000 mole)
and Adipic Acid (1.000 mole) at 125°C with Triisopropanolamine
Catalyst (0.02000 mole)^a

Sample	Reaction time, hr	% reaction ^b			Gel time at 200°C, hr
		Epoxyde	Acid	Difference	
1	0.50	66.6	62.8	3.8	1.5
2	1.00	78.5	74.6	3.9	0.87
3	1.50	85.0	81.3	3.7	0.72
4	3.00	94.2	90.1	4.1	0.50

^a Polymerization P-1 of Table III.

^b Based on endgroup analysis for epoxyde and acid.

TABLE VI
Bulk Polymerization of Bisphenol-A Diglycidyl Ether
(1.000 mole) and Adipic Acid (1.000 mole) at 125°C
with *N,N*-Dimethylacetamide Catalyst (0.02000 mole)^a

Sample	Reaction time, hr	% reaction ^b			Gel time at 200°C, hr
		Epoxyde	Acid	Difference	
1	0.50	61.9	57.1	4.8	1.0
2	1.0	79.3	73.9	5.4	0.62
3	1.5	92.5	86.7	5.8	0.33
4	2.5	96.4	92.1	4.3	0.30
5	3.0	96.7	92.5	4.2	0.25

^a Polymerization P-2 of Table III.

^b Based on endgroup analysis for epoxyde and acid.

TABLE VII
Bulk Polymerizations of Bisphenol-A Diglycidyl Ether (1.000 mole), Bisphenol-A [X] and Azelaic Acid [1-X] at 125°C with Triisopropanolamine Catalyst (0.02000 mole)

Polymer	X Bisphenol-A, mole	1-X Azelaic acid, mole	Reaction time, hr ^a	Gel time, hr		Weight epoxide g ^c	Weight acid, g ^c
				125°C ^b	200°C		
P-12	1.000	—	48	>72	>2	4496	—
P-13	0.9700	0.03000	48	>72	>2	3267	α
P-14	0.9500	0.05000	48	>72	>2	3784	α
P-15	0.9000	0.1000	48	>72	>2	4419	α
P-16	0.8500	0.1500	49	>72	>2	3643	α
P-17	0.7500	0.2500	46	>72	1.7	8012	α
P-18	0.5000	0.5000	4	8	1.5	3524	4446
P-19	0.2500	0.7500	9	11	1.1	10664	16020
P-20	0.05000	0.9500	8	9.5	0.5	11858	6561
P-21	—	1.000	4	6.0	0.5	8356	2999

^a Total for stage I and stage II.

^b Based on intermediate sample from stage I (see experimental section).

^c Determined by endgroup analysis for epoxide and acid.

those of this study do not gel.⁶ Furthermore, the polymers produced do not support the facile 200°C gelation. We prepared a series of terpolymers of BDC, bisphenol-A, and azelaic acid to determine what concentration of dicarboxylic acid in the monomer mixture produces gelation properties in the polymer. The total moles of active hydrogen were equivalent to epoxide moles in these polymers. Azelaic acid was used instead of adipic acid to reduce reaction medium viscosity. Table VII shows that the gelation tendency becomes apparent when 50 mole-% of the active hydrogen monomer is dicarboxylic acid.

References

1. H. Kakiuchi and Y. Tanaka, *J. Org. Chem.*, **31**, 1559 (1966).
2. L. Shechter and J. Wyustra, *Ind. Eng. Chem.*, **48**, No. 1, 86 (1956).
3. W. Hofmann and W. Fisch, *F.A.T.I.P.E.C.*, 6th Wiesbaden, 243 (1962); *Chem. Abstr.*, **58**, 7038d (1963).
4. J. D. Malkemus and J. D. Swan, *J. Amer. Oil Chemists' Soc.*, **34**, 342 (1957).
5. Y. Iwakura and K. Matsuzaki, *Kobunshi Kagaku*, **17**, 703 (1960).
6. F. B. Alvey, U. S. Pat. 3,336,257 (1967).
7. F. B. Alvey, U. S. Pat. 3,350,353.
8. H. Lee and K. Neville, *Handbook of Epoxy Resins*, McGraw-Hill, New York, 1967, p. 4-17.
9. V. G. Jung and W. Kleeberg, *Kunststoffe*, **51**, 714 (1961).

Received December 10, 1968

Formation of Free Radicals during Machining and Fracture of Polymers

D. K. BACKMAN and K. L. DEVRIES, *Mechanical Engineering Department, University of Utah, Salt Lake City, Utah 84112*

Synopsis

Electron paramagnetic resonance measurements of the number of free radicals formed during cutting and grinding of polymers are described. It was found in the semicrystalline polymers studied that below the glassy transition temperature that the number of free radicals formed is about $2 \times 10^{13}/\text{cm}^2$ of surface formed. It is proposed that this number results from the crack progressing selectively through the glassy regions about more ordered regions in the polymers.

INTRODUCTION

Recently Eckert presented evidence that free radicals are formed during machining of polymers.¹ Electron paramagnetic resonance (EPR) measurements in our laboratory not only substantiate this observation but provide a quantitative measure of the number of free radicals present and information about their identities.

EPR is a type of absorption spectroscopy that detects the presence of unpaired electrons resulting from ruptured covalent bonds such as those in polymer chains. The Varian E-3 used in these studies has a sensitivity of approximately 10^{11} – 10^{12} unpaired electrons under ideal conditions. This equipment has a TE₁₀₂ (rectangular) microwave cavity (2.29 cm height, 1.02 cm width, and 2.54 cm depth).

The sensitivity of this equipment is enhanced at low temperature approximately as the inverse of the absolute temperature. Also, free radicals, once formed, become very stable at liquid nitrogen temperature. Therefore, all spectra were recorded at low temperatures even though the sample material was ground at various temperatures (room temperature $\pm 50^\circ\text{C}$) before quenching to liquid nitrogen temperature for storage and observation.

One might expect that machining, cutting, grinding, or other fracturing of many polymers should result in bond ruptures. For a random array of molecular chains with the density and molecular structure of nylon 66, one would expect a plane passing through the cross section of a sample to "cut" somewhat more than 2×10^{14} chains/cm². A discussion of such calculations has been given by Peterlin.²

A comparison of the carbon-carbon bond energy (83 kcal/mole), giving rise to the tensile strength of the chain, with the secondary bond energy

(3–6 kcal/mole), resulting in an interchain viscoelastic force, would lead one to expect chain segments of embedded material over about 100 carbon units in crystallites to rupture before “pulling out.”³ Hence under proper conditions it should be possible to accumulate sufficient free radicals for detection by EPR techniques.

EXPERIMENTAL

As previously noted, a Varian Model E-3 EPR spectrometer was used in the present work. This equipment operates in the 8.8–9.6 GHz range and uses a field modulation of 100 kHz. Temperature control of the sample while the absorption spectrum was recorded was accomplished by a Varian E-4557/E-9540 variable temperature accessory. This accessory normally provides a sample space 4 mm diameter by 24 mm long. It was modified by the authors to provide a space 10 mm diameter by 24 mm long. This adaptation did result in a slight deterioration of the temperature-maintaining capability of the accessory and an increase in temperature gradients. These were not, however, considered significant for the present studies and the modification allowed much more sample material to be present in the cavity thus generating much stronger signals.

The samples were prepared by slicing the end of strips of sample material in a specially prepared device. The resulting shavings were of the approximate dimensions of $1.1 \times 0.15 \times 0.07$ cm. Approximately 50 such slices could be placed in the cavity. The slicing device consisted of a plane driven by a small dc electric motor as shown in Figure 1. A jet of dry pure nitrogen carried the newly formed slice through a tube where it was quenched in

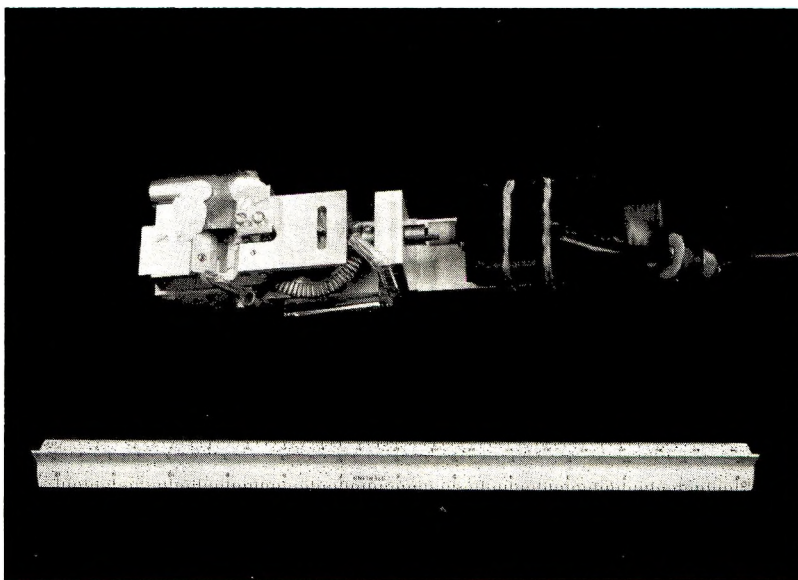


Fig. 1. Photograph of apparatus used in preparation of the samples of sliced polymers.

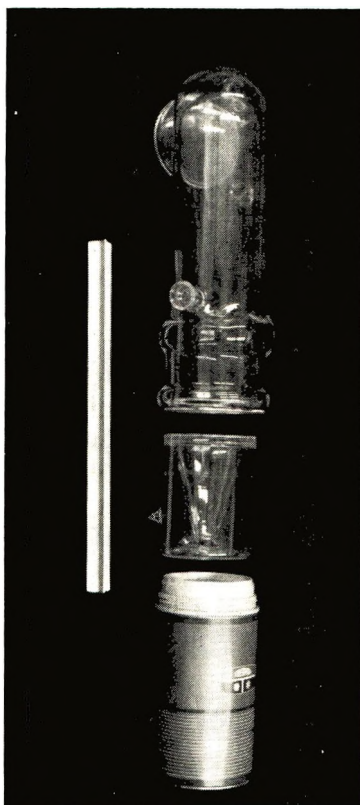


Fig. 2. Environmental chamber for the slicing apparatus.

liquid nitrogen within $1/2$ sec of slicing. It was found that the sample material once quenched could be kept at least a week at these temperatures with no detectable decrease in concentration of free radicals. The temperature and atmosphere at which the slices were formed was controlled by placing the entire slicing device in a double-walled glass container (Fig. 2). The space between the walls was evacuated, thus minimizing heat losses. The present studies were made in a dry nitrogen atmosphere because oxygen exposure results in the development of peroxy signals and rapid decay of the concentration of free radicals.⁴ In these studies the temperature was varied from -30°C to $+110^{\circ}\text{C}$.

Sample materials included commercial grades of nylon 66, polyethylene, and polypropylene, all in sheet form. Hot melt extrusion was used to form the sheets. The sheets were purchased in 0.050 in. thicknesses and cut to size for the slicing apparatus. The nylon was DuPont Zytel 101 and the extrusion of the sample materials was by the Polymer Corporation, Polypenco Division. A series of tests on desiccated nylon (in silica gel) were made to see what if any effect moisture content might have.

Nylon 66 was also ground with a small rotary file while submerged in liquid nitrogen. The grindings were studied under 50 power magnification

on a metallograph. They were highly irregular in shape but typically had dimensions of the order of 10^{-3} – 10^{-1} mm. The surface area was measured on a Perkin-Elmer-Shell sorptometer and found to be 3 000–7 000 cm^2/g . It should be noted that the sorptometer is most accurate in the range of surface areas of 100 000 cm^2 or more, resulting in this large variation.

There are two possible sources of error that are worthy of comment. The first is the reaction of new free radicals with oxygen or other species in the working atmosphere. Pure nitrogen was used but it is extremely difficult to keep it completely free of contamination. One source of contamination, for example, was the liquid nitrogen used as a quench. Inevitably it contained some oxygen which had been absorbed from the air during transportation and storage; some of it is likely to find its way into the slicing system. A second possible error relates to the type of reaction which might take place between free radicals and the metal they slide over for the short time after formation. There was a slight charge build-up on the metal. However, after establishing equilibrium, conservation of charge should restrict any further electron transfer. To date the authors have been unable to develop ways of quantitatively evaluating these sources of error. However, indirect evidence such as the consistency and reasonableness of the results indicate that the error from these sources is not extremely large.

One other possible source of error is perhaps worthy of a few comments. Could it be that free radicals are formed in much larger concentrations than observed but part of them (for example, those right at the surface) have a lifetime much too short for observation by these techniques? A number of tests were conducted in an attempt to determine whether this occurred. The most definitive of these was careful and slow grinding of polymers at liquid nitrogen temperature. Studies of the signal strength immediately after grinding and after warming did not seem to indicate the presence of any such reactions. Such studies are not completely conclusive but gave us some confidence that the numbers measured probably do quite accurately represent the actual values.

RESULTS

Free radicals were observed in the sliced polymers. The nylon spectrum observed was very similar to the spectrum observed for the free radicals resulting from irradiation, grinding, and tensile loading.⁴⁻⁷ Its characteristic shape is attributed to the free radical being situated at the site $-\text{CO}-\text{NH}-\dot{\text{C}}\text{H}-(\text{CH}_2)_n-$, where n alternates between 3 and 5. A typical spectrum for nylon sliced at 24°C is shown in Figure 3. Polypropylene and polyethylene are very susceptible to combining of their free radicals with oxygen and forming the peroxy radical. Consequently, the spectrum taken for these two were peroxy in nature. This must be attributed to the presence of traces of oxygen in the liquid nitrogen, evaporating into the system and causing a slight partial pressure of oxygen. For polyethylene the peroxy spectrum has been attributed to the free radical.⁶



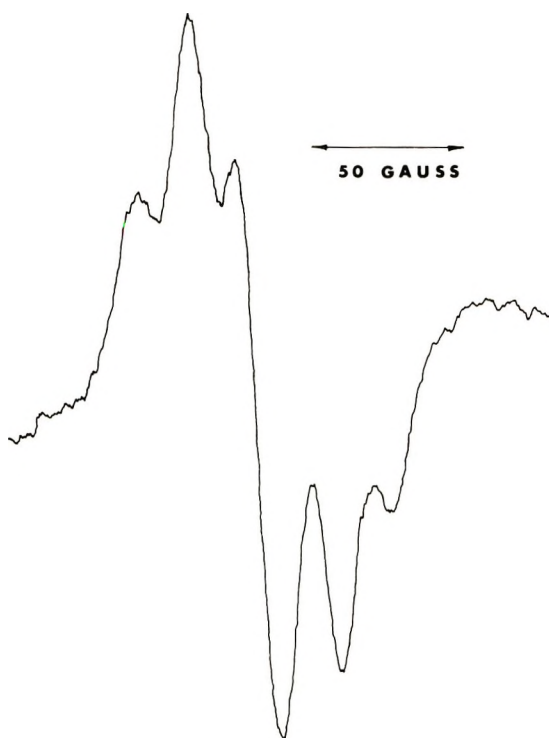


Fig. 3. Typical EPR spectrum of sliced nylon 66.

It is relatively unimportant that a peroxy radical has formed, since the number can still be determined. Our studies indicate that at the oxygen concentrations involved here, the number of radicals before and after peroxy formation are the same within experimental error. However, it is desirable to keep the concentration of oxygen in the slicing atmosphere small in order to reduce the rate of radical decay.⁸

The radicals observed by the spectrometer are in most cases not those formed directly by the rupture processes but rather secondary radicals formed from the original radicals by proton migration along the chain. More careful studies at very low temperature have isolated free radicals directly attributed to chain scission.⁶

By computer double integration of the recorded spectrum and a comparison of the resulting value with suitable standards the total number of "spins" could be determined.⁹ The total sliced surface area in the cavity was determined by counting the slices since all had the same dimensions. Free-radical concentration based on the sliced or cut area was of the order of 10^{13} spins/cm². A very marked dependence on the temperature of the polymer during cutting was noted (Figs. 4-6). For nylon, the free-radical density begins to decrease rapidly between 40 and 50°C, which is close to the glass transition temperature of approximately 50°C.¹⁰ Polypropylene, on the other hand, shows a decrease in the surface density at about 0-10°C

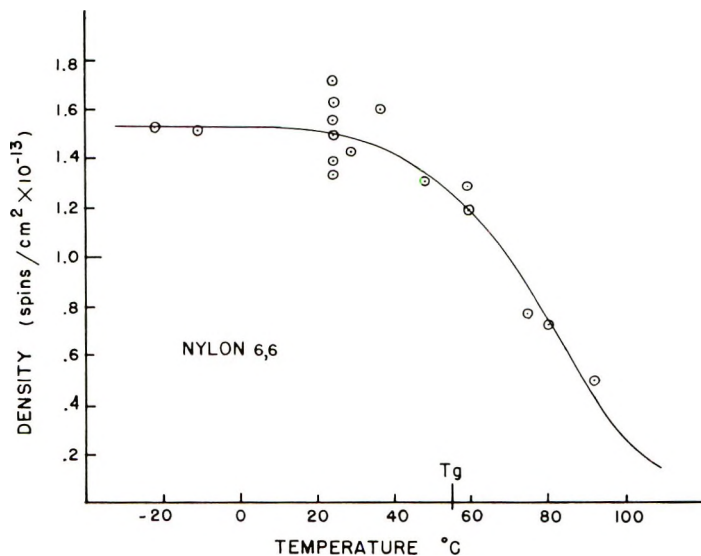


Fig. 4. Dependence of free-radical surface density on fracture temperature of nylon 66.

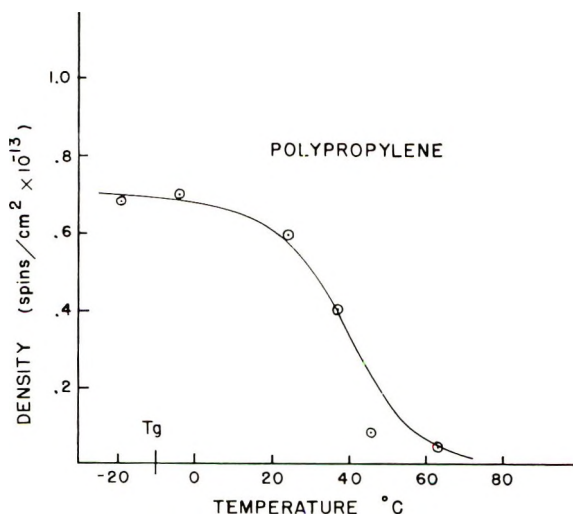


Fig. 5. Dependence of free-radical surface density on fracture temperature of polypropylene.

and a reported glass transition of -10°C .¹⁰ For polyethylene the temperature at which the free-radical surface density begins to drop appears to be out of the temperature limits of the slicing apparatus. Polyethylene has a glass transition temperature reported¹⁰ to be about -125°C . It would appear that in each of the polymers tested the free-radical surface density depends highly on the glass transition temperature of the polymer. Tests on desiccated nylon indicate that small amounts of water absorbed into

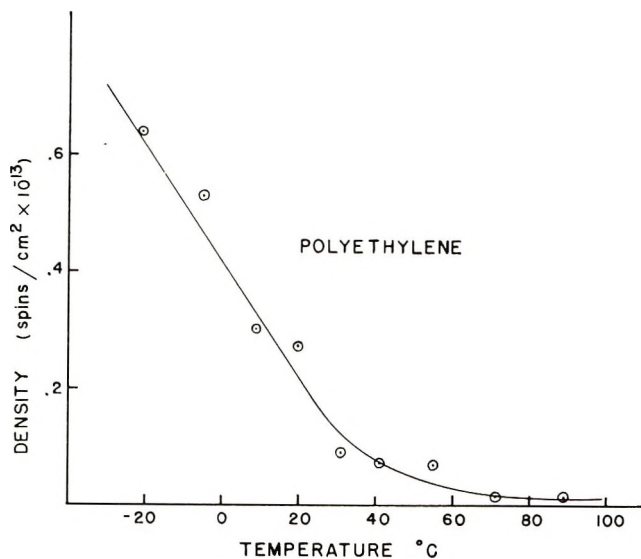


Fig. 6. Dependence of free-radical surface density on fracture temperature of polyethylene.

polymer structures have little if any effect on the surface spin concentration. The sample material formed by grinding in liquid nitrogen is difficult to collect in large quantities; therefore, the surface area determination is relatively unprecise. The values obtained correspond to 7×10^{12} to 2×10^{14} spins for each square centimeter of new surface formed by the grinding.

Part of the pronounced decrease in free-radical concentration above the glass transition temperature might be attributed to more rapid decay of free radicals at these temperatures. More studies of the kinetics of this decay at these temperatures must be made before exact figures can be given for this, but in light of the present studies it would appear that even at the highest temperatures studied, free-radical decay is not too significant in the short time between slicing and quenching.

DISCUSSION

A number of interesting conclusions can be drawn from the above experimental results. A significant number of bonds are broken during cutting fracture in all the polymers studied. However, the number of bonds broken is considerably less than one might at first expect from the earlier arguments where it was stated that a plane passing through a cross-section would cut more than 10^{14} bonds/cm². The actual number measured was one order of magnitude less than this. It would appear from these results that of the total surface energy required to form a new surface (determined by a crack or tear growth study to be of the order of 10^3 ergs/cm² or more) the amount that can be attributed to primary bond rupture is only approximately 43 ergs/cm² or a small fraction of the total.

We are of the opinion that the supposed discrepancies can be resolved in not too difficult a manner. The materials studied fall in the class of semicrystalline polymers and are often portrayed as shown in Figure 7 with alternating regions of amorphous and crystalline material.¹¹ A spherulite in nylon, for example, might be viewed as a sheaf or polycrystalline cluster consisting of a great many tiny single crystallites with intervening and interconnecting amorphous materials. Our studies would indicate that the crack surface then selectively chooses a path through this maze where less bonds need be ruptured than should it follow a plane. In the case of inter-

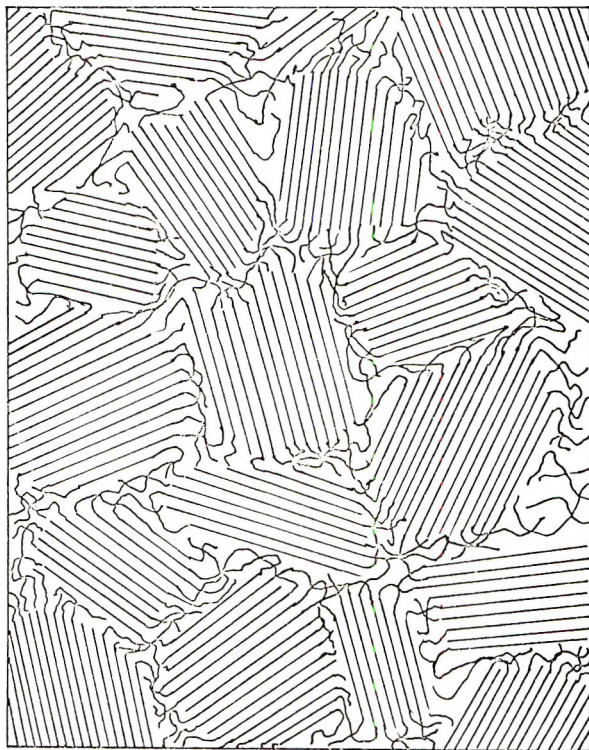


Fig. 7. Fringed micelle model of semicrystalline polymers after Flory.¹¹

est here it is apparently able to follow paths requiring less than one-tenth as many scissions as would be expected by a "cutting plane." A possible behavior for the Flory fringed micelle model is shown in Figure 8. While this particular model is perhaps rather outdated, it does, in common with most more recent models of the morphology of semicrystalline polymers, portray the basic concept of regions of high crystallinity being surrounded by more amorphous regions.

The energy required to form a new surface during rupture must, as a consequence of the small amount that apparently goes into rupturing primary bonds, be largely that required to rupture secondary bonds and

include plastic or viscoelastic deformation, somewhat analogous to the work of plastic deformation in front of a crack in metals.

It should perhaps be noted that based on different types of studies Peterlin et al. have arrived at similar conclusions.¹²⁻¹⁴ Based on these observations we hypothesize that the fracture character and some other properties of semicrystalline polymers are strongly related to the regions between microcrystals and the number and character of the "tie chains" connecting these. These regions are drastically altered by drawing ratio, drawing temperature, etc.¹²⁻¹⁴ The large effect of drawing on strength



Fig. 8. Flory's fringed micelle model of a semicrystalline polymer showing a selective fracture path.

(increases in tensile strength by an order of magnitude are common) is very likely largely dependent on these changes.

It would be of interest to know how the free radicals formed during rupture are distributed. Are all of the free radicals located at or very near the fracture surface, or are they more or less uniformly distributed throughout the volume, i.e., how localized is the damage? Since oxygen readily reacts with free radicals, studies of the kinetics of diffusion and reaction of oxygen on the cut or fractured sample should provide pertinent information about the depth at which bonds are broken. Our results in this respect are as yet

still very preliminary but would indicate that for the slicings more than 90% of the broken bonds lie within a couple of microns or so of the surface.

While the studies reported here relate to surfaces resulting from cutting and grinding operations, the conclusions might be much more general in their implications and should also apply to cases such as rupture during tensile fracture. Indeed one might expect that in the case of tensile fracture the crack might be even less restricted in following an "easy" fracture path with perhaps a further reduction in the number of broken bonds per square centimeter of crack. In the cutting operations the large stresses are restricted to a very localized region with the result that the crack might not always be able to progress along the easiest path. Other work in this laboratory⁶ as well as the work of Zhurkov and others¹⁵ have shown that EPR can indeed be used to study bond rupture during other types of mechanical rupture such as tensile fracture.

The authors would like to acknowledge the assistance of M. L. Williams in preparation of this paper. Portions of this work were supported by the National Science Foundation and National Aeronautics and Space Administration.

References

1. R. E. Eckert and T. R. Maykantz, *Polym. Letters*, **6**, 213 (1968).
2. A. Peterlin and D. Campbell, *Polym. Letters*, **6**, 481 (1968).
3. F. W. Billmeyer, *Textbook of Polymer Science*, Interscience, N. Y., 1966.
4. M. L. Williams and K. L. DeVries, *An EPR Investigation of Newly-formed Fracture Surfaces*, Presented at 14th Sagamore Army Materials Research Conference, Raquette Lake, New York, August 23, 1967.
5. C. T. Graves and M. G. Ormerod, *Polym.*, **4**, 81 (1963).
6. D. K. Roylance, *An EPR Investigation of Polymer Fracture*, Ph.D. Dissertation, University of Utah, 1968.
7. D. Ballantine and Y. Shinohara, *J. Chem. Phys.*, **36**, 3042 (1962).
8. S. E. Bresler, E. I. Kazheksov, V. H. Fornichev, F. Sech, and P. Smeitek, *Soviet Phys.—Solid State*, **5**, 1402 (1963).
9. M. Bersohn and J. C. Baird, *An Introduction to Electron Paramagnetic Resonance*, W. A. Benjamin, N. Y., 1966.
10. J. Brandrup and E. H. Immergut, *Polym. Handbook*, Interscience, N. Y., 1966.
11. P. J. Flory, *Principles of Polymer Chemistry*, Cornell University Press, Ithaca, New York, 1953.
12. A. Peterlin, personal communication.
13. A. Peterlin and R. Corneliussen, *J. Polym. Sci. A-2*, **6**, 1273 (1968).
14. G. Meinel and A. Peterlin, *Polym. Letters*, **5**, 197 (1967).
15. S. N. Zhurkov, *Intern. J. Fracture Mechanics*, Vol. 1, No. 4, 1965, p. 311.

Received December 27, 1968

Polymers from 12 α -Hydroxymethylabiet-7,8-enoic Acid and Vinyl 12 α -Hydroxymethylabiet-7,8-enoate

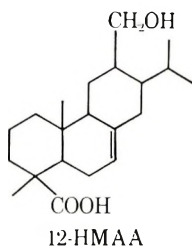
MOTOO SAGA and C. S. MARVEL, *Department of Chemistry, The University of Arizona, Tucson, Arizona 85721*

Synopsis

12 α -Hydroxymethylabiet-7,8-enoic acid has been homopolymerized by melt condensation, and a partially crystalline polyester has been obtained. Vinyl 12 α -hydroxymethylabiet-7,8-enoate has been prepared from 12 α -hydroxymethylabiet-7,8-enoic acid by vinyl interchange with vinyl acetate and has been homopolymerized, copolymerized with vinyl chloride, vinyl acetate, butadiene, and acrylonitrile, and terpolymerized with styrene and acrylonitrile. Polymers thus obtained have been characterized.

In a continuation of the studies on the preparation of polymers containing abietic acid derivatives,¹⁻⁵ 12- α -hydroxymethylabiet-7,8-enoic acid (12-HMAA) has been investigated. The preparation and some reactions of 12-HMAA have been investigated by Black and Hedrick.⁶ This present paper deals with polymerization studies of 12 HMAA and also of its vinyl ester.

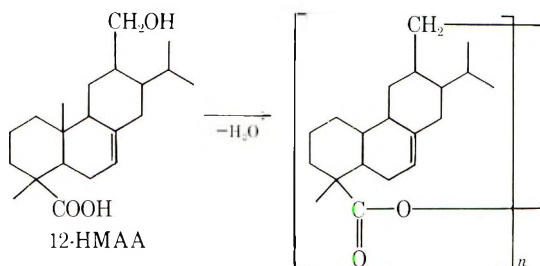
12-HMAA was provided by the Naval Stores Research Laboratory, Olustee, Florida, one of the laboratories in the Southern Utilization Research and Development Division of U.S.D.A. The compound as received was a mixture of the dihydro- and tetrahydro- compounds. Pure 12- α -hydroxymethylabiet-7,8-enoic acid (12-HMAA) was obtained by recrystallization of the crude acid from 65% aqueous ethanol. The pure compound is a colorless crystalline substance having a melting point of 192°C. The elemental analysis and infrared spectrum of this compound was the same as has been reported.⁶



Vinyl 12- α -hydroxymethylabiet-7,8-enoate (VHMA) has been prepared from 12-HMAA by vinyl interchange with vinyl acetate in the presence of mercuric acetate and sulfuric acid. 12-HMAA has both hydroxy and

carboxyl groups in the same molecule. There is a possibility for several undesirable side reactions with vinyl acetate as was reported for 12-hydroxystearic acid.⁷ At room temperature, a colorless viscous liquid which solidified on standing a few days was obtained. The infrared spectrum of this compound showed characteristic vinyl ester absorption band at 1740 cm^{-1} , $\text{—C}=\text{C}$ stretching frequency at 1645 cm^{-1} , and OH stretching frequency at 3440 cm^{-1} .

In spite of low solubility of the acid, in vinyl acetate, VHMA was obtained in fairly good yields (85.9%). The ester was too soluble in common organic solvents to be recrystallized, but the product had a melting point of $63\text{--}68^\circ\text{C}$, and analysis indicated it was quite pure.



The self-condensation of 12-HMAA has been conducted by melt polymerization methods with the use of a small amount of antimony trioxide⁸ or no catalyst at all. The experimental data are given in Table I. All these polymers were obtained as pale yellow to pale brown clear glassy materials which gave white powders on reprecipitation from a THF solution

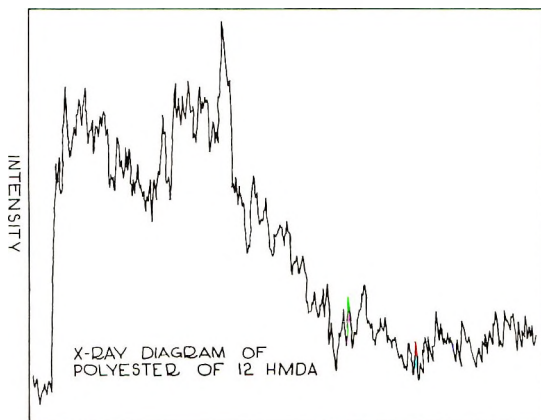


Fig. 1. X-ray diagram of polyester of 12-HMAA.

by pouring into methanol. The polymers have a high melting point and the x-ray diffraction pattern of the powdered polymer (Table I, run I-2) is shown in Figure 1. The x-ray diffraction pattern was obtained by a Phillips x-ray diffractometer with a Cu target. The major machine settings

TABLE I
 Self-Condensation of 12-HMAA^a

Run no.	Catalyst	Temp. °C	Time, hr	Conversion, %	Mp, °C	η_{inh}^b
I-1	—	200	2	72.4	185–190	0.124
		220	3			
		250	3			
I-2	—	200	2	73.8	187–192	0.130
		220	3			
		250	6			
I-3	—	200	2	79.0	215–220	0.10 ^c
		250	3			
		270	10			
I-4	Sb ₂ O ₃	200	2	74.6	220–222	0.188
		220	3			
		250	5			
I-5	Sb ₂ O ₃	200	2	76.9	220–223	0.175
		220	3			
		250	8			
I-6 ^d	—	200	2	80.2	186–189	0.186
		240	6			

^a All of the self condensations were conducted in a Pyrex test tube using 4 g (0.025 mole) of monomer.

^b Determined on the solution of 0.18–0.27 g/100 ml of THF at 30°C.

^c The sample was not completely soluble in THF. This figure was obtained on solution of 0.25/100 ml of H₂SO₄ at 30°C.

^d The monomer was dissolved in excess anhydrous methanol and refluxed for 5 hr. before polymerization.

 TABLE II
 Homopolymerization of VHMA^a

Run no.	System	Catalyst		Time, hr	Conversion, %		Softening range, °C	Found ^d	
		Type ^{a,b}	Amt, %		η_{inh}^c	C, %		H, %	
II-1	Emulsion ^e	K ₂ S ₂ O ₈	5	20	9.3	0.041	207–211		
II-2	“	“	5	40	10.7	0.053	210–213	75.46	9.83
II-3	“	“	5	60	9.6	0.055	210–213		
II-4	“	“	5	40	8.5	0.038	208–211	75.53	8.90
II-5	Solution	DEABIB	5	24	22.4	0.055	213–215	75.53	9.76
II-6	“	“	5	48	36.7	0.107	213–218	75.56	9.89
II-7	“	AIBN	5	24	26.3	0.052	213–217	75.39	9.72
II-8	“	“	5	48	42.3	0.134	215–230	75.48	9.67

^a All of the polymerizations were conducted at 60 ± 2°C. by tumbling in the water bath.

^b DEABIB = diethyl azobisisobutyrate; AIBN = azobisisobutyronitrile

^c Determined on the solution of 0.31 — 0.38 g/100 ml of THF at 30°C.

^d Calculated for (C₂₃H₃₇O₃)_n: C, 76.66%, H, 10.00%.

^e Siponate DS-10 was used as emulsifier.

TABLE III
 Copolymerization of VHMA and VCl (in Emulsion)^a

Run no.	Charged Composition		Wt initiator (K ₂ S ₂ O ₈), g	Con- version, %	Found			Copolymer composition ^c	
	VCl, g	VHMA g			Wt-%	C, %	H, %	Cl, %	VCl, %
III-1	4.5	0.5	0.1	79.0	42.23	5.31	51.64	89.87	10.13
III-2	4.0	1.0	0.1	70.3	43.88	5.66	46.79	85.50	14.50
III-3	3.5	1.5	0.1	57.8	47.09	6.07	42.66	71.10	22.90

^a All of the polymerizations were conducted at $60 \pm 2^\circ\text{C}$ by tumbling the tubes end over end for 24 hr and with the use of Siponate DS-10 as emulsifier.

^b Determined on solutions of 0.33–0.41 g/100 ml of THF.

^c Based on analyses for C, H, and Cl in the copolymer.

TABLE IV
 Copolymerization of VHMA and VAc (in emulsion)^a

Run no.	Charged composition		Initiator	Conversion, %	η_{inh}^b	Found		Copolymer composition ^c	
	VAc wt-%	VH-MA wt-%				C, %	H, %	VAc, %	VHMA, %
IV-1	90	10	K ₂ S ₂ O ₈	69.4	0.31	57.57	7.54	91.2	8.8
IV-2	80	20	"	62.8	0.22	60.06	7.87	78.9	21.1
IV-3	70	30	"	49.2	0.12	63.49	8.11	62.2	37.8
IV-4	60	40	"	46.0	0.10	66.28	8.53	48.6	51.4
IV-5	90	10	AIBN	79.4	0.32	57.83	7.57	89.9	10.1
IV-6	80	20	"	63.0	0.21	60.53	7.79	76.7	23.3
IV-7	70	30	"	53.0	0.14	63.80	8.28	60.7	39.3
IV-8	60	40	"	45.8	0.11	67.05	8.64	44.8	55.2

^a All of the polymerizations were conducted at $60 \pm 2^\circ\text{C}$ by tumbling the tubes end over end for 24 hr and with the use of Siponate DS-10 as emulsifier.

^b Determined on solution of 0.31–0.39 g/100 ml of THF.

^c Based on analyses for C and H in the copolymer.

were: 40 Kv, 20 Ma, with a N: filter. Some peaks are observed in the pattern, which indicate some crystallinity of the polymer.

The infrared spectrum of polyester showed ester carbonyl absorption band at 1725 cm^{-1} , whereas the starting material, 12-HMAA, showed acid carbonyl absorption band at 1700 cm^{-1} . 12-HMAA exhibits a very strong —OH stretching frequency at 3440 cm^{-1} , but no hydroxy bands were indicated in the polyester.

Free-radical homopolymerization of VHMA has been conducted in emulsion and in solution. The experimental data are given in Table II.

The polymers were obtained as white powders soluble in tetrahydrofuran and having rather high softening points, but the conversion and inherent viscosity were not high. The results were slightly different according to the method and catalyst used. The infrared spectrum of homopolymer exhibited a clear —OH stretching frequency at 3420 cm^{-1} and no —C=C— stretching frequency at approximately 1645 cm^{-1} which is characteristic band for VHMA.

Copolymers of VHMA and vinyl chloride have been prepared with different charging compositions by means of a free-radical initiator. The experimental data are given in Table III. The per cent of VHMA incorporated was calculated from the content of carbon, hydrogen, and chlorine in the copolymer. Copolymers were obtained as white or pale tan powders. All were soluble in tetrahydrofuran and could be molded into transparent films.

Four different vinyl acetate copolymers have been prepared by using potassium persulfate and AIBN as initiators. The experimental data are given in Table IV. All of these copolymers were obtained as pale yellow to pale brown powders according to the charged composition, and were

soluble in tetrahydrofuran. The copolymers could be molded into water-clear but brittle films. These results indicated that VHMA could be incorporated into the polymer composition up to 55.2%. The intensity of infrared absorption bands characteristic for VHMA, 1740 cm^{-1} and 3440 cm^{-1} , were consistent with the amount of VHMA incorporated in copolymer.

A series of four different VHMA-butadiene copolymers has been made. The experimental data are given in Table V. The copolymers were obtained as light tan rubbery crumbs and were not completely soluble in tetrahydrofuran or other organic solvents. Soluble and insoluble parts are divided by using hot tetrahydrofuran solution. The infrared spectrum of both parts showed that the compositions contained both components. On the basis of infrared spectra of the copolymers and literature,^{9,10} the polybutadiene segments incorporated into copolymer appeared to contain a high 1,4-*trans* structure.

TABLE V
Copolymerization of VHMA and BD^a

Run no.	Charged composition		Conversion, %	Soluble part, % ^b	VHMA, % ^c	η_{inh}^d
	VHMA, wt-%	BD, wt-%				
V-1	10	90	86	12	8.4	0.26
V-2	20	80	78	17	22.3	0.33
V-3	30	70	66	15	27.4	0.28
V-4	40	60	62	25	34.3	0.39

^a All of the polymerizations were conducted at $60 \pm 2^\circ\text{C}$ by tumbling the tubes end over end for 48 hr and with the use of 5.0 g of total monomers, of Siponate DS-10 (0.1 g) as emulsifier, $\text{K}_2\text{S}_2\text{O}_8$ (0.1 g) as initiator, and 15 ml of buffered water (pH 7.00).

^b % by weight, soluble in hot THF.

^c % by weight, based on analysis for C and H in the polymer.

^d Determined on solutions of ca. 0.2–0.3 g/100 ml. THF of soluble part, 30°C .

Although unfavorable reactivity relationship for the monomers was expected between VHMA and acrylonitrile, it was of interest to see what kind of a polymer could be obtained. A series of VHMA and acrylonitrile copolymers were prepared by using potassium persulfate as initiator. Emulsion copolymerization of VHMA and acrylonitrile was conducted in three compositions at 50 and 60°C , respectively. Experimental data are given in Table VI. All of the copolymers were obtained as white powders which were insoluble in hot dimethylformamide (DMF) and did not dissolve in other common organic solvents. The infrared spectra of copolymers appeared to have characteristic bands for both monomers, namely, they exhibit strong absorption at frequencies of 3430, 2250, and 1725 cm^{-1} . These correspond to hydroxy, nitrile, and ester carbonyl groups, respectively. No further investigation of these polymers was conducted because of their insolubility.

TABLE VI
 Copolymerization of VHMA and AN^a

Run no.	Charged composition		Temp, °C	Time, hr	Conversion, %	Solubility ^b
	VHMA, %	AN, %				
VI-1	10	90	60	24	96	Insoluble
VI-2	20	80	60	24	90	Swollen
VI-3	30	70	60	24	86	"
VI-4	10	90	50	12	92	"
VI-5	20	80	50	12	92	"
VI-6	30	70	50	12	82	"

^a All of the copolymerizations were conducted by tumbling the tubes end over end and with the use of 5.0 g of total monomers Siponate DS-10 (0.1 g) as emulsifier, K₂S₂O₈ (0.1 g) as initiator and 15 ml of air-free distilled water.

^b Solubilities of polymers were examined in hot DMF.

Another combination of monomers which was hoped might give some useful polymer is VHMA, acrylonitrile, and styrene. Three different terpolymers of varying composition were prepared. The experimental data are given in Table VII. It was found that VHMA could be incorporated into acrylonitrile/styrene composition up to 15 wt-%. In every case, about one half the charged VHMA was incorporated into the copolymer. All of the terpolymers obtained were white powders which were soluble in organic solvents such as dimethylformamide, dimethylacetamide, and dimethylsulfoxide and then could be molded into clear tough films.

 TABLE VII
 Terpolymerization of VHMA, St, and AN^a

Run no.	Charged composition			Conversion, %	Elemental analyses			Incorporated ratio ^b			η_{inh}^c
	VH-MA, wt-%	St, wt-%	AN, wt-%		C, %	H, %	N, %	VHMA, %	St, %	AN, %	
	%	%	%		%	%	%	%	%	%	
VII-1	10	60	30	92	83.60	7.18	8.29	5.0	62.1	31.9	2.19
VII-2	20	50	30	89	82.22	7.21	9.36	9.0	55.6	35.4	3.27
VII-3	30	40	30	90	81.00	7.14	9.63	15.0	48.5	36.5	4.03

^a All of the terpolymerizations were conducted at $60 \pm 2^\circ\text{C}$ by tumbling the tubes end over end for 48 hr with the use of 5.0 g of total monomers, Siponate DS-10 (0.1 g) as emulsifier, K₂S₂O₈ (0.1 g) as initiator, and 15 ml of air-free distilled water.

^b % by weight, based on analysis for C, H and N in the polymers.

^c Determined on solutions containing 0.25–0.30 g/100 ml of DMF at 30°C.

EXPERIMENTAL

Preparation of VHMA

To a one-liter, three-necked round-bottomed flask equipped with a stirrer and a condenser protected with a drying tube, 30 g (0.087 mole)

of 12-HMAA, 3 g of mercuric acetate, 0.2 g of copper resinate and 700 ml of freshly distilled vinyl acetate were added. The mixture was stirred vigorously, then 0.5 ml of sulfuric acid was added. The reaction was allowed to continue for 72 hr at room temperature (25–30°C). The pale green reaction mixture was heterogeneous for the first part of the reaction. But, as the reaction proceeded, the mixture became homogeneous, and at last the mixture turned to a clear pale brown solution. At the end of this period, 2.0 g of sodium acetate was added to stop the reaction. At room temperature, the excess vinyl acetate was distilled off under reduced pressure. The light yellow, oily liquid thus obtained was dissolved in 300 ml of anhydrous ether and 100 g of acid washed activated alumina (Merck and Co., Inc.) was added. After stirring for 10 hr, the filtrate was dried over anhydrous sodium sulfate. The solvent was removed under reduced pressure. The yield was 27.5 g (85.9%) of a solid, mp 66–68°C.

Anal. Calcd for $C_{23}H_{36}O_3$: C, 76.25%; H, 9.89%; O, 13.85%. Found: C, 76.66%; H, 9.99%; O, 13.33%.

Self-Condensation of 12-HMAA

Melt polymerization of 12-HMAA. 12-HMAA (4 g, 0.012 mole) was placed in a Pyrex test tube and heated in an oil bath under reduced pressure (<0.1 mm Hg). The 12-HMAA melted at 190–200°C. After 2 hr the bath temperature was raised to 220°C for 3 hr then to 250°C for another 3 hr. During the reaction, the evolution of water was noted. At the end of reaction, the polymer was allowed to cool to form a brittle glassy substance. The crude polyester was dissolved in 50 ml of tetrahydrofuran and poured into excess methanol. The yield was 2.73 g (72.4%) of vacuum oven-dried material (60°C/48 hr) which was a white powder. (Run I-1 in Table I).

Melt Polymerization of 12-HMAA with Sb_2O_3 as Catalyst. 12-HMAA (4 g, 0.012 mole) and 0.01 g of antimony trioxide were placed in a Pyrex test tube and heated at 200°C for 2 hr under reduced pressure. After this period, the bath temperature was raised to 220°C for 3 hr and then to 250°C for 5 hr. On termination of the reaction, the product was dissolved in tetrahydrofuran and reprecipitated in methanol, washed with water and acetone, and dried *in vacuo* to give a product which had the expected infrared spectrum. The yield was 2.9 g (76.9%) (run I-5 in Table I).

Homopolymerization of VHMA

Emulsion Polymerization. VHMA (1.0 g), $K_2S_2O_8$ (0.05 g), Siponate DS-10 (0.02 g) and air-free distilled water (4 ml) were charged in a 2-oz pressure tube, cooled to Dry Ice–acetone temperature, and evacuated under 0.1 mm Hg pressure and flushed with nitrogen three times. The mixture was emulsified at room temperature and polymerized at $60 \pm 2^\circ\text{C}$ for 40 hr. The emulsion was poured into 50 ml of methanol, and 2 ml of saturated

sodium chloride solution was added. The isolated material was dissolved in 5 ml of THF and poured into 50 ml of methanol. The mixture was allowed to stand for a day before filtering. The yield was 0.167 g (10.7%) of vacuum oven-dried (50°C/48 hr) white powder (run II-2 in Table II).

The procedure for the other free-radical polymerizations in emulsion was similar to the one described.

Solution Polymerization. VHMA (4 g) was diluted with *n*-heptane to 20 ml in a volumetric flask and dried over sodium metal.

The VHMA solution prepared (5 ml containing 1 g of VHMA) was charged into the test tube and DEABIB (48 mg) was added to the solution. The mixture was cooled to Dry Ice-acetone temperature, evacuated under 0.1 mm Hg pressure, and flushed with nitrogen three times, and then the vessel was sealed under reduced pressure. Polymerization was carried out at $60 \pm 2^\circ\text{C}$ for 24 hr. The reaction mixture was poured into 60 ml of methanol. The isolated material was dissolved in 10 ml of THF and poured into 100 ml of methanol. The mixture was allowed to stand for a day before filtration. The yield was 0.224 g (22.4%) of vacuum oven-dried (50°C/48 hr) white powder (run II-5 in Table II).

The procedures for the other free-radical polymerizations in solution were similar to the one described.

Copolymerization of VHMA

Copolymerization of VHMA and VCl. VHMA (0.5 g), $\text{K}_2\text{S}_2\text{O}_8$ (0.1 g), Siponate DS-10 (0.1 g), and air-free distilled water (15 ml) were charged under nitrogen in a pressure tube (1 × 7 in.) cooled to Dry Ice-acetone temperature, and then evacuated under 0.1 mm Hg pressure and flushed with nitrogen three times.

Then VCl was charged in excess and allowed to boil down to 4.5 g. The mixture was emulsified at room temperature and polymerized at $60 \pm 2^\circ\text{C}$ for 48 hr. The reaction mixture was poured into the methanol. 2 ml of sodium chloride aqueous solution was added to settle the emulsion, and the mixture allowed to stand overnight.

The isolated polymer was dissolved in 50 ml of THF and reprecipitated in 250 ml of methanol. The mixture was allowed to stand for 2 days before filtering. The isolated polymer was washed with methanol sufficiently, then dried in a vacuum oven at 50°C for 2 days. The yield was 3.95 g (79%) (run III-1 in Table III).

The procedures for other experiments shown in Table III were similar to the one described.

Copolymerization of VHMA and VAc. VHMA (0.5 g), VAc (4.5 g), AIBN (0.2 g), Siponate DS-10 (0.1 g), and air-free distilled water (15 ml) were charged in a pressure tube (1 × 7 in.), cooled to Dry Ice-acetone temperature, then evacuated to 0.1 mm Hg pressure and flushed three times with nitrogen.

The comonomer was charged in excess and allowed to boil down to 4.5 g. The mixture was emulsified at room temperature. Heating at $60 \pm 2^\circ\text{C}$

for 48 hr. yielded a good emulsion containing sticky material which was poured into a methanol-water mixture (200 ml/200 ml). A 20-ml portion of saturated sodium chloride and 3 ml of 18% hydrochloric acid were added to the mixture. The polymer precipitated with difficulty. The mixture was allowed to stand for overnight before filtration. The isolated material was dissolved in 50 ml of THF and poured into 400 ml of water. The mixture was allowed to stand for 3 days before filtering. The yield was 3.97 g (79.4%) of vacuum oven-dried (50°C/48 hr) pale yellow powder (run IV-5 in Table IV).

The procedure for other experiments given in Table IV was similar to the one described.

Copolymerization of VHMA and BD. VHMA (0.5 g), $K_2S_2O_8$ (0.1 g), Siponate DS-10 (0.1 g), air-free distilled water (7.5 ml), and Beckman pH 7.00 buffer solution (7.5 ml) were charged under nitrogen in a pressure tube (1 × 7 in.).

The tube was cooled to Dry Ice-acetone temperature, evacuated to 0.1 mm Hg, and flushed with dry nitrogen. This was repeated three times before BD was added. The excess of BD was allowed to boil down to 4.5 g before capping. The mixture was emulsified at room temperature and polymerized at $60 \pm 2^\circ C$ for 48 hr. The latex formed was poured into 200 ml of methanol, and 10 ml of 18% HCl solution was added. The isolated material was washed with methanol and suspended in a hot THF solution. Then the suspended mixture was poured into an excess of methanol. The yield was 4.3 g (86%) of vacuum oven-dried (50°C/24 hr) light tan-colored rubbery crumbs (run V-1 of Table V). The procedure of experiments for the other compositions shown in Table V was similar to the one described.

Copolymerization of VHMA and AN. VHMA (0.5 g), AN (4.5 g, freshly distilled), $K_2S_2O_8$ (0.1 g), Siponate DS-10 (0.1 g), and air-free distilled water (15 ml) were charged into a pressure tube (1 × 7 in.) which was cooled to Dry Ice-acetone temperature, evacuated, and flushed with nitrogen three times before capping. The mixture was emulsified at $60 \pm 2^\circ C$ by tumbling end over end for 24 hr. The reaction mixture was poured into 300 ml of methanol. The isolated material was washed with water and methanol and suspended in a hot DMF solution. Then the mixture was poured into an excess of methanol. The yield was 4.8 g (96%) of vacuum oven-dried (50°C/24 hr) material (run VI-1 of Table VI). The procedure for the other compositions was similar to the one described above.

Terpolymerization of VHMA

Terpolymerization of VHMA, St, and AN. VHMA (0.5 g), styrene (3.0 g), acrylonitrile (1.5 g), $K_2S_2O_8$ (0.1 g), Siponate DS-10 (0.1 g), and air-free distilled water (15 ml) were charged into a pressure tube (1 × 7 in.), which was cooled to Dry Ice-acetone temperature, evacuated, and flushed with nitrogen three times before capping. The mixture was emulsified at room temperature and polymerized at $60 \pm 2^\circ C$ by tumbling end over end for 24 hr. The latex obtained was poured into a water-methanol mixture

(100 ml/200 ml), and 10 ml of sodium chloride solution (5%) was added. The isolated material was dissolved in hot DMF and poured into methanol. The reprecipitated material weighed 4.6 g (92%) of vacuum-oven dried (50°C/24 hr) white powder, (run VII-1 in Table VII).

The procedure for the other compositions was similar to the one described above.

This is a partial report of work done under contract with the Western and Southern Utilization Research and Development Divisions, Agricultural Research Service, U. S. Department of Agriculture, and authorized by the Research and Marketing Act. The contract is supervised by Dr. Glenn Fuller of the Western Division. We are indebted to Dr. Glen W. Hedrick of the Naval Stores Research Laboratory of Southern Utilization Research and Development Division of the Agricultural Research Service, U. S. D. A., Olustee, Florida, for furnishing the 12- α -hydroxymethyl-8(14)-abietenoic acid.

We are indebted to Professor Quintus Fernando for the x-ray pattern of the polyester.

References

1. J. R. Sowa and C. S. Marvel, *J. Polym. Sci. B*, **4**, 431 (1966).
2. R. Liepins and C. S. Marvel, *J. Polym. Sci. A-1*, **4**, 2003 (1966).
3. W. Fukuda and C. S. Marvel, *J. Polym. Sci. A-1*, **6**, 1050 (1968).
4. W. Fukuda and C. S. Marvel, *J. Polym. Sci. A-1*, **6**, 1281 (1968).
5. W. Fukuda, M. Saga, and C. S. Marvel, *J. Polym. Sci. A-1*, **6**, 1523 (1968).
6. D. K. Black and G. W. Hedrick, *J. Org. Chem.*, **32**, 3758 (1967).
7. T. Shono and C. S. Marvel, *J. Polym. Sci. A*, **1**, 2067 (1963).
8. N. A. Higgins, U. S. Pat. 2,676,945 (April 27, 1954).
9. R. Zbinden, *Infrared Spectroscopy of High Polymers*, Academic Press, New York-London, 1964, p. 25.
10. J. L. Binder, *J. Polym. Sci. A*, **1**, 47 (1963).

Received December 30, 1968

A Contribution to the Theory of the Structural Glass Transition

G. M. BARTENEV, I. V. RAZUMOVSKAYA, D. S. SANDITOV, and I. A. LUKYANOV, *Laboratory of Physicochemical Mechanics of Inorganic Materials, Lenin Teachers' Training University, Moscow, U.S.S.R.*

Synopsis

The equations characterizing the temperature dependence of the mobility of molecules in the glass transition region are compared and analysed. A relationship between the parameters of the relaxation theory of the glass transition and the concept of free volume is established. The Williams-Landel-Ferry equation is treated in terms of the relaxation theory of glass transition.

INTRODUCTION

The term "glassy state" has different meanings, depending on whether mechanical properties or the structure of the amorphous substance is being considered. In connection with this it was proposed to make distinctions between the structural and mechanical glass transition.¹ Kobeko² was the first to formulate clearly the essence of the structural glass transition as a relaxation process, which is dependent on the "freezing" of the structure. In works by Debye, Fuoss, Kirkwood, Alexandrov, Lazurkin and others³⁻⁶ a process similar to the structural glass-transition, i.e., the transition of fluids and polymers from the liquid or highly elastic state to the viscosolid state under variable mechanical and electric loads, was investigated. But this process ("mechanical glass transition") is not the proper glass transition process, though it is called so in the literature.¹⁻⁶ The mechanical glass transition does not depend on the "freezing" of the structure and always is observed above the temperature of the structural glass-transition temperature.

Taking as a basis the considerations² of the relaxational nature of the glass transition, Vol'kenstein and Ptitsyn⁷ developed a molecular-kinetic theory of the glass transition for a simple fluid model, which qualitatively reflects the nature of the given phenomenon. Gibbs and DiMarzio⁸ proposed, with reference to polymeric systems, a statistical theory of glass transition, which differs essentially from the former. In interpreting the glass-transition process many investigators⁹⁻¹² also make extensive use of the theory of free volume. It naturally is expected that these different approaches to the same phenomenon i.e., the structural glass transition,

must be interrelated. Recently Eisenberg and Saito¹³ showed that the theory proposed by Gibbs and DiMarzio and the theory of free volume are practically equivalent within the limit of experimental error. In this work an attempt is made to establish a relationship between the relaxation theory of the glass transition and the theory of free volume.

The natural laws governing changes of the relevant properties in the glass-transition range are the same for all amorphous substances, though the latter include substances consisting of molecules of very different structure, and their glass transition temperatures T_g differ by more than one order of magnitude. Evidently, near T_g , in the first approximation, an integrated mechanism of the temperature effect on molecular-kinetic processes in glasses differing in nature and chemical composition is the same. Williams, Landel, and Ferry¹² have shown that the behavior of all perfectly investigated glasses near T_g can be described by a universal semi-empirical equation which is called Williams-Landel-Ferry equation (WLF). The authors associate the temperature dependence of the mobility of the molecules or their parts (in the case of polymer) with the temperature dependence of the free volume. As was pointed out by Fox and Flory,⁹ with decreasing temperature and closer approach to the glass transition temperature, the relative free volume decreases sharply, which is the main factor leading to an increase of the viscosity. Worthy of interest is the interpretation of the WLF equation in terms of the molecular kinetic theory of glass transition, which would allow a relationship to be established between the free volume and the relaxation theory parameters.

Because of the dependence of the glass transition temperature on the rate of cooling,^{14,15} a "standard" glass transition temperature T_g^{st} at which the relaxation time τ is 10^2 sec, was introduced, the cooling rate of about 1–3 °C/min, which usually is used in dilatometric measurements in many countries, corresponding to this reference glass transition temperature. Therefore, much literature data (including that given in this paper) relate to the reference glass transition temperature.

BASIC EQUATION OF GLASS TRANSITION

The relation between the rate of molecular rearrangement and the rate of cooling is of great importance when the glass-transition process is considered. For common reasons, one of the authors^{1,14} proposed an equation

$$q\tau_g = C \quad (1)$$

relating the absolute value of the cooling rate $q = |\partial T/\partial t|$ and the molecular relaxation time τ at $T = T_g$ (basic equation of glass transition);* C is a certain constant. The meaning and value of the constant C and its relation to the constants from the universal WLF equation are defined below. According to the relaxation theory, T_g satisfies the conditions:⁷

$$(d\tau/dT)_{T_g} = -1/q \quad (2)$$

* In this case T_g is the glass transition temperature (not "standard") corresponding to the arbitrary rate of cooling.

If it is assumed that near T_g the known equation of the molecular relaxation time¹⁶ is justified:

$$\tau = \tau_0 \exp(\mathbf{u}/kT) \quad (3)$$

(where, according to theory,^{1,16} τ_0 has the order of frequency heat vibrations in solids $\tau_0 \cong 10^{-12}$ sec, U is the activation energy of particles rearranging, and k is the Boltzman constant), then from eq. (2), considering eq. (3) and assuming $U = U_g = \text{constant}$, one obtains

$$q\tau_g = kT_g^2/U_g \quad (4)$$

from which the physical sense of C in eq. (1) is clear cut:

$$C = kT_g^2/U_g \quad (5)$$

From numerical calculations, by using eq. (3) it can be shown^{1,15} that for all amorphous substances

$$U_g/kT_g^{\text{st}} \simeq 3q \quad (6)$$

Actually, putting into eq. (3) $\tau_0 = 10^{-12}$ sec and $\tau_g = 10^2$ sec, we shall obtain relation (6). Consequently, the constant C is approximately 20°C for inorganic glasses $T_g = T_g^{\text{st}} \sim 600^\circ\text{K}$ and 10°C for organic glasses $T_g = T_g^{\text{st}} \sim 300^\circ\text{K}$. On the other hand, according to the basic equation, eq. (1), at $q = 1\text{--}3^\circ\text{C}/\text{min}$ and $\tau_g = 10^2$ sec, the constant C is 1.5–5°C. Thus, the value of C from eq. (5) is somewhat overrated, which probably depends on the deviation from eq. (3) in the glass-transition range.

It is known, as a matter of fact, that eq. (3) is justified, if the motion of the given particle can be considered regardless of the motion of its neighbors. In the range of the glass transition this supposition is not fulfilled.^{1,12,17,18} In order to take into account (change of the structure with temperature) the cooperative effect near T_g , the activation barrier in eq. (3) can be considered as a function of temperature $U = \mathbf{u}(T)$. Then, we shall obtain from eq. (2):

$$q\tau_g = \kappa kT_g^2/U_g \quad (7)$$

where

$$\kappa = [1 - (T_g/U_g) (\partial U/\partial T)_{T_g}]^{-1} \quad (8)$$

At $U = \text{constant}$, it is natural that $\kappa = 1$ and eq. (7) becomes eq. (4). Since, in fact, the energy of the molecular interaction increases with decreasing temperature,¹ i.e. $\partial U/\partial T < 0$, then $\kappa < 1$ and the value of the constant from eq. (5) must be made $\kappa^{-1} > 1$ times higher. Unfortunately, the dependence $U(T)$ near T_g now is not known exactly. However, the semiempirical equations of $\tau(T)$ can be used to evaluate κ and C .

The experimental data obtained for a great number of supercooling fluids and polymers, shows that in the range of the glass transition (T_g , $T_g + 100^\circ\text{C}$) the dependence $\tau(T)$ is well described by WLF equation:^{12,18}

$$\ln(\tau/\tau_g) = -A[(T - T_g)/(T - T_g + B)] \quad (9)$$

TABLE I
 Characteristics of the Structural Glass Transition
 of Several Organic and Inorganic Glasses

Material	T_g , °K	B , °C	C , °C	T_0 , °K	α	U_∞ , kcal/- mole	
Organic glasses ^a							
Polyisobutylene	202	38.1	104.4	2.8	97.6	1.9	7.9
Poly(vinyl acetate)	305	35.9	46.8	1.2	258.2	6.4	3.4
Natural rubber	300	38.5	53.6	1.4	246.4	5.6	4.1
Polyurethane	238	35.6	32.6	1.0	205.4	7.3	2.3
Inorganic glasses ^b							
Na—Ca—Si NI	783	36.1	284	7.8	499	0.36	20.5
Na—Ca—Si N IO	828	36.8	320	8.7	508	0.38	23.5
Na—Ca—Si	788	30.0	260	8.6	528	0.33	15.6
Na—Pb—Si	713	32.2	280	8.7	433	0.39	18
Boron anhydride B ₂ O ₃	533	42.6	246	5.7	288	0.46	20.9

^a Data of Kargin and Slonimskii.⁶

^b Data of Doolittle and Doolittle.¹⁰

Here, A and B are empirical constants (Table I) that can be given a reasonable physical interpretation:^{12,17}

$$A = \frac{1}{f_g}$$

$$B = f_g/\alpha \quad (10)$$

where f_g is a part of the free volume f at $T = T_g$, α is the difference between thermal expansion coefficients f above and below T_g . For all glasses the value of A varies near $A \cong 35$ (Table I), i.e., the constant A practically is universal, and B varies from system to system. It is readily seen that eq. (9) corresponds to eq. (3), if it is assumed in the latter that

$$\tau_0 = \tau_0 e^{-A} \quad (11)$$

$$U = \frac{kAB}{1 - [(T_g - B)/T]} = \frac{U_\infty}{1 - (T_0/T)} \quad (12)$$

where

$$U_\infty = kAB$$

$$T_0 = T_g - B$$

Let us note that at $\tau_g \cong 10^2$ sec and $A \cong 35$, we shall have $\tau_0 \cong 10^2 e^{-35} \cong 10^{-12}$ sec, which is in agreement with literature data for τ_0 . By putting $\tau(T)$ from eq. (3) and considering eqs. (11) and (12), into eqs. (7) and (8) we shall find a simple relation of the constant C with constants from the WLF equation:

$$q\tau_g = B/A \quad (13)$$

$$C = B/A = f_g^2/\alpha \quad (14)$$

Thus, the constant C appears to be related to the thermal expansion coefficient and the free volume share of the system at T_g . Using experimental data^{12,18} for A and B we calculated the value of C (Table I). As was expected, for many organic and inorganic glasses it was found to be about 1.5 and 8°C, respectively. If, in order to calculate C , we use, in the same way, an empirical equation by Shishkin¹⁹ for $\tau(T)$ we also shall obtain considerably smaller values of C , than from eq. (5) (about 0.6 and 8°C for organic and inorganic glasses, respectively).*

Let us note that, considering the universality of A , the basic equation for the glass transition can be rewritten in the form (dividing both parts by B):

$$q^* \tau_g = C^* \quad (15)$$

where $C^* = 1/A \cong 0.03$, as being distinct from C , is a universal constant; $q^* = q/B$ is a certain reduced rate of cooling. In this case q^* means the rate with which the value of f related to f_g , a free volume share, changes at the glass transition temperature. Really, since $B = f_g/\alpha$, but $\alpha = df/dt$ and $q = dT/dt$ (certainly, near T_g), then $q^* = (1/f_g)(df/dt)$.

RELATIONSHIP BETWEEN CONSTANTS OF WILLIAMS-LANDEL-FERRY EQUATION AND EQUATION FOR THE DEPENDENCE OF THE GLASS TRANSITION TEMPERATURE ON COOLING RATE

Proceeding from the basic equation of glass transition, eqs. (1), and eq. (3), the following dependence of the glass-transition temperature on the rate of cooling was proposed (Bartenev equation):^{1,14}

$$(1/T_g) = C_1 - C_2 \ln q \quad (16)$$

where $C_1 = C_2 \ln(C/\tau_0)$ and $C_2 = k/Ug$. Equation (16) was proved correct on a great set of silicate glasses and polymers.^{15,20} In this case the relation of C_1 and C_2 was found to be practically a universal value for all glasses (Table I). If q is expressed in degrees per second, $C' = C_1/C_2 \cong 33$. From eq. (16) it is readily seen

$$C' = \frac{U_g}{kT_g} + \ln q \quad (17)$$

Since, as a rule $U_g/kT_g \gg \ln q$ (e.g., in the case $T = T_g^{sl}$), eq. (17) can be rewritten in the form:

$$C' \cong U_g/kT_g \quad (18)$$

The presence of practically universal constants $C' \cong U_g/kT_g$ and $A = 1/f_g$ in the Bartenev and WLF equations and the satisfactory coincidence of their numerical values (~ 33) which obviously is not accidental, draws

* Near T_g , the WLF equation proves to be more exact than Shishkin's equation. The latter works well above T_g .

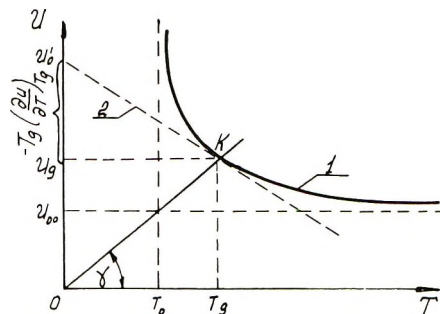


Fig. 1. Temperature dependence of the activation energy in the glass-transition range (curve 1) according to eq. (12). The tangential line to point K (line 2) corresponds to eq. (21). For all glasses the angle γ is constant, because $U_0/T_0 = \text{constant}$.

one's attention. The activation barrier of molecules rearranging and their heat agitation must be related to the free volume: the lower the mean energy of the heat agitation and the higher the barrier, the smaller the free volume and the more limited the molecular motion. It will be shown below that, in fact, these constants coincide ($C' \equiv A$). Let us note that the latter conclusion also follows from the comparison of eq. (3) at $T = T_0$ and eq. (11), which can be rewritten in the form $\tau_0 = \tau_0 e^A$ and $\tau_0 = \tau_0 e^{u_0/kT_0}$. In connection with this it is of interest to express each constant of the WLF equation separately through the relaxation theory parameters. By comparing eq. (7) and (13) it is seen that

$$B/A = \kappa(kT_0^2/U_0) \quad (19)$$

from which, according to the previous considerations, it follows that

$$A = U_0/kT_0$$

$$B = \kappa T_0 = [1 - (T_0/U_0)(\partial U/\partial T)_{T_0}]^{-1} T_0 \quad (20)$$

A schematic representation of the temperature dependence of the activation energy near T_0 according to eq. (12) is given in Figure 1. In a narrow range of cooling rates (approximately two orders),¹ a section of the activation energy curve (curve 1) may be approximated by a section of the tangent (curve 2) which is expressed by

$$U = U_0' - (\partial U/\partial T)_{T_0} T \quad (21)$$

where U_0' is a section on the ordinate axis which is cut off by the tangent. The magnitude U_0' has no definite physical meaning; however it can be considered approximately constant in a limited range of cooling rates. After substituting $(\partial U/\partial T)_{T_0} T_0$ from the latter equation at $T = T_0$ into eq. (8), we arrive at the following expression (geometric meaning) for κ :

$$\frac{1}{\kappa} = 2 - (U_0'/U_0)$$

Thus, at $U_0' = 2U_g$ the value κ and the constant $B = \kappa T_g$, respectively, become infinitely great. Further, at sufficiently high rates of cooling, i.e., where function $U(T)$ is steeply increasing, the value κ can attain negative meanings, which means $T_0 > T_g$ and limits the slope $U(T)$. Evidently, the values κ , B , and T_0 in Table I practically relate to the reference rate of cooling $q \simeq 1\text{--}3^\circ\text{C}/\text{min}$.

INTERPRETATION OF WILLIAMS-LANDEL-FERRY EQUATION IN TERMS OF THE RELAXATION THEORY OF GLASS TRANSITION

It is easy to verify that the WLF equation cannot be derived from the common equation of the molecular relaxation time (3), if it has $U = \text{constant}$. The consideration of the known^{1,15,16,19} dependences $U(T)$ also does not lead to eq. (9). As was pointed out above, it can be shown that the WLF equation is formally derived from the temperature dependence of the activation energy of the form (12), where T_0 is the extrapolated temperature below which $U = \infty$, U_∞ is the value of U at $T \gg T_0$. The introduction of a temperature of the T_0 type proved to be necessary when the viscosity and dielectric dispersion of supercooled fluids and polymers were considered.²¹⁻²³ By putting $T = T_g$ into eq. (12) we obtain the following relationship between T_0 and T_g :

$$T_0 = T_g - (U_\infty/U_g)T_g \quad (22)$$

When eqs. (12) and (22) are taken into account, eq. (3) for $\tau(T)$ near T_g takes the form

$$\tau = \tau_0 \exp \left\{ \frac{U_\infty}{k[T - T_g + (U_\infty/U_g)T_g]} \right\} \quad (23)$$

from which we obtain, for $\ln(\tau/\tau_0)$, an expression identical with the WLF equation, eq. (9):

$$\ln \frac{\tau}{\tau_0} = - \left(\frac{U_g}{kT_g} \right) \frac{T - T_g}{[T - T_g + (U_\infty/U_g)T_g]} \quad (24)$$

Thus, according to the relaxation theory of glass transition the constant A in the WLF equation practically coincides with the constant C' in eq. (18) or with the constant $1/C^*$:

$$A \equiv C' = U_g/kT_g = 1/q^*\tau_0 \quad (25)$$

and the constant B is equal to

$$B = (U_\infty/U_g)T_g = U_\infty/kA \quad (26)$$

The values of C' given in Table II were determined^{1,15,20} at the constant rate $q = 3^\circ\text{C}/\text{min}$. Various literature data^{12,18} were used to determine A , therefore it is possible that $q \neq \text{constant}$ and this explains the relatively wide scatter of the values of A (Table I). As distinct from A , the constant B depends largely on the substance (structure and forces of interaction).

TABLE II
Values of Constants in the Equation for the Dependence of the Glass
Transition Temperature on the Rate of Cooling

Material	$C_1 \times 10^3,$ °C ⁻¹ degrees	$C_2 \times 10^5,$ °C ⁻¹ degrees	$C' = C_1/C_2$
Rosin	3.08	9.3	33.3
Polystyrene	2.78	9.0	31.2
Poly(methyl methacrylate)	2.75	8.9	31.2
Boron anhydride	1.31	5.6	32.2
Lead silicate glass	1.34	4.28	31.2
Alkali silicate glass	1.19	3.6	33.3
Alumina silicate glass	0.94	2.67	34.4

as B , according to eqs. (20) and (26), depends on the change of molecular interaction ($\partial U/\partial T$). As it would be expected, values $U_\infty = kAB$ for inorganic glasses appear to be greater than for organic glasses (Table I). Thus for sodium-calcium silicate glass $U_\infty \cong 17$ kcal/mole, for natural rubber $U_\infty \cong 4$ kcal/mole. It is worthy of note that the values of U_∞ given in Table I agree satisfactorily with the available data for the activation energy at elevated temperatures.^{23,24} As is seen from eqs. (25) and (26), T_g is included in the constants of the WLF equation; consequently, in principle, they must depend on the rate of cooling. Probably, the data^{12,18} refer to the reference glass transition temperature.

RELATIONSHIP BETWEEN THE ACTIVATION ENERGY AND THE FREE VOLUME

From comparison of eq. (10) and (25) for the constant A it follows that

$$U_g/kT_g = 1/f_g \quad (27)$$

The relationship between U , kT , and f of the type (27) in the common case can be found from comparison of equations^{10,16} of viscosity η (as $\eta \sim \tau$): $\eta \cong \exp \{U/kT\}$ and $\eta \sim \exp \{D/f\}$, where, according to Doolittle and Doolittle¹⁰ D is a constant approximately equal to unity. Note in this connection that the dependence $U(T)$ of the form (12) might be obtained from the relation between U and f of the type (27), if, as was done by many investigators,^{9,12,17} in the glass transition range f is represented as

$$f = \alpha(T - T_0') \quad (28)$$

where T_0' is the extrapolated temperature below which $f = 0$. Naturally, the "absence" of the free volume share ($f = 0$) required to move a kinetic particle is equivalent to an "infinitely" high barrier for molecules rearranging ($U = \infty$). Consequently, interpretations of WLF equation in terms of the free volume theory and in terms of the relaxation theory lead to similar results. Specifically, our supposition (12) concerning the activa-

tion energy is equivalent to an assumption of the linear dependence of the free volume share on temperature eq. (28).

Attempts to define what the structural and physical properties required of have materials easily undergoing the glass transition have been made recently.^{25,26} Qualitatively, it is clear that the reduction of the mobility of particles due the intensification of molecular interaction and to the reduction of the free volume is an indispensable condition of the glass transition. The constancy of the constants C' and A means that, regardless of the structural peculiarities, the transition of the fluid to the glass occurs only when the mean energy of the heat agitation of a particle kT_θ is about $1/33 \cong 3\%$ of the barrier U_θ [eq. (6)] and when the free volume share of the system decreases to 3% [eq. (27)]. Turnbull and Cohen²⁵ propose a quantitative criterion for evaluating the glass transition properties, in the form of the reduced temperature of crystallization $\theta_s = kT_s/Q$, where T_s is the thermodynamic temperature of recrystallization and Q is the heat of evaporation referred to a kinetic unit. The less θ_s , the more distinctly the glass-transition properties are evident. However, the reduced glass transition temperature θ_g is practically unchanged, and its value almost coincides with the universal constant C^* or $1/A$ and $1/C$:

$$\theta_g = \frac{kT_\theta}{Q} \simeq 0.025-0.03$$

In this connection it is worthy of note that practically universal constants, which numerically coincide with C^* , also are encountered in other works considering the mobility and packing of particles. So, for instance, the radial distribution function of Prins²⁷ includes a parameter equal for different substances to

$$\frac{kT}{a^3/\beta} \cong 0.03$$

where a^3 is the volume per particle and β is the modulus of compressibility. Further, according to Bueche,¹⁷

$$f_c/n \cong 0.025-0.03$$

where f_c is the minimum share of the free volume required to move a group of n kinetic units. A similar parameter $1/\lambda^* \simeq 0.03$ associated with the probability of the existence of the critical free-volume share in the system of interacting spheres is encountered in work by Kirkwood.²⁸

POSSIBLE RELATIONSHIP BETWEEN THE RELAXATION AND STATISTICAL THEORIES OF GLASS TRANSITION

Unlike the statistical theory, the relaxation theory considers the glass-transition as a kinetic process which in principle differs from phase changes. In connection with this it is worthy of noting that Moacanin and Simha²⁹ recently have shown that at certain ratios between the parameters E and

ϵ , which characterize molecular interaction and the flexibility of the chains, respectively, the Gibbs and DiMarzio theory (GD) predicts no gap for the thermal expansion coefficient at $T = T_g$, i.e., the glass transition is not the second-order transition, as it had been supposed previously. From experimental data Eisenberg and Saito¹³ found that the parameters E and ϵ are dependent linearly on T_g . Note that according to^{1,15,20} for all amorphous substances activation energy is a typical parameter of the relaxation theory, which characterizes molecular interaction, and also depends linearly on T_g . Since, according to the GD theory the relations E/kT_g and ϵ/kT_g depend only on the free volume share f_g , this means the constancy of f_g at $T = T_g$. The calculated value¹³ $f_g \simeq 0.03$ coincides with the data given above.

Since, as is shown above, there is relationship between the relaxation theory of glass transition and the theory of free volume, and the latter, according to Eisenberg and Saito,¹³ is equivalent to the Gibbs and DiMarzio theory, so the relaxation and statistical theories of glass transition must necessarily be interrelated, though their basic principles and ultimate formulae are different.³⁰

CONCLUSIONS

The equations characterizing the temperature dependence of the molecular mobility in the glass-transition range are compared and analyzed. The meaning and the value of the constant of the basic equation of glass transition are specified, and a relationship between certain parameters of the relaxation theory of glass transition and the theory of free volume is established. It is shown that the universal constants in Williams-Landel-Ferry equation and in the Bartenev equation for the dependence of the glass transition temperature on the rate of cooling coincide; their physical meaning is discussed.

References

1. G. M. Bartenev, *Structure and Mechanical Properties of Inorganic Glasses*, Publishing House on Construction, Moscow, 1966; *Dokl. Akad. Nauk SSSR*, **110**, 805 (1956); *Glassy State*, Academy of Sciences, USSR, Moscow, 1960, pp. 147-153.
2. P. P. Kobeko, *Amorphous Substances*, Academy of Sciences, USSR, Moscow-Leningrad, 1952.
3. P. Debye, *Polar Molecules*, SSEPH (State Science Engineering Publishing House), Moscow, 1931.
4. J. Y. Kirkwood and R. M. Fuoss, *J. Phys. Chem.*, **9**, 329 (1941).
5. A. P. Alexandrov, Lazurkin, Yu. S., *Zh. Tekh. Fiz.*, **9**, 1949 (1939).
6. V. A. Kargin and G. L. Slonimskii, *Survey on Physical Chemistry of Polymers*, Moscow Univ., 1960.
7. M. V. Vol'kenstein and O. B. Ptitsyn, *Dokl. Akad. Nauk SSSR*, **103**, 795 (1955); *Zh. Tekh. Fiz.*, **26**, 2204 (1956).
8. J. H. Gibbs and E. A. DiMarzio, *J. Chem. Phys.*, **28**, 375 (1958).
9. T. G. Fox and P. J. Flory, *J. Appl. Phys.*, **21**, 581 (1950).
10. A. K. Doolittle and D. B. Doolittle, *J. Appl. Phys.*, **28**, 901 (1957).
11. A. J. Kovacs, *Rheol. Acta*, **5**, 262 (1966).
12. W. L. Williams, R. F. Landel, and J. D. Ferry, *J. Amer. Chem. Soc.*, **77**, 3701 (1955).

13. A. Eisenberg and S. Saito, *J. Chem. Phys.*, **45**, 1673 (1966).
14. G. M. Bartenev, *Dokl. Akad. Nauk SSSR*, **76**, 227 (1951).
15. G. M. Bartenev and I. A. Lukyaanov, *Zh. Fiz. Khim.*, **29**, 1486 (1955).
16. Ya. I. Frenkel, *Kinetic Theory of Fluids*, Academy of Sciences, USSR, Moscow-Leningrad, 1941.
17. F. Bueche, *J. Appl. Phys.*, **24**, 418 (1956).
18. B. A. Bestul, *Glastech. Ber.*, **32K**, 59 (1959).
19. N. I. Shishkin, *Zh. Tekh. Fiz.*, **26**, 1461 (1956).
20. G. M. Bartenev and Yu. A. Gorbatkina, *Vysokomol. Soedin.*, **1**, 769 (1959).
21. G. Tamman, *Der Glaszustand* (Leipzig, 1932).
22. G. S. Fulcher, *J. Amer. Ceram. Soc.*, **8**, 339 (1925).
23. P. Caillon and E. Groubert, *C. R. Acad. Sci. (Paris)*, **248**, 2093 (1959).
24. R. L. Müller, *J. Appl. Chem.*, **28**, 363, 1077 (1955).
25. D. Turnbull and M. Cohen, *J. Chem. Phys.*, **31**, 1164 (1959).
26. W. Weyl and E. Marboe, *J. Soc. Glass Tech.*, **43**, 417 (1959).
27. J. A. Prins and H. Peterson, *Physica*, **3**, 147 (1936).
28. J. Kirkwood, *J. Chem. Phys.*, **7**, 919 (1939).
29. J. Moacanin and R. Simha, *J. Chem. Phys.*, **45**, 964 (1966).
30. A. J. Staverman, *Rheol. Acta*, **5**, 283 (1966).

Received June 29, 1968 ¹

Revised December 30, 1968

Solvent and Salt Effects on Reaction of Na Amalgam with Acrylonitrile and Methacrylonitrile

Y. ARAD, M. LEVY, H. ROSEN, and D. VOFSI, *Plastics Research Laboratory, The Weizmann Institute of Science, Rehovot, Israel*

Synopsis

The reaction of acrylonitrile (AN) and methacrylonitrile (MeAN) with Na amalgam was studied in diglyme solution. It was shown that addition of dimethyl sulfoxide (DMSO) increases only the rate of hydrodimerization of AN to adiponitrile, while addition of water increases only the rate of hydrogenation of AN to propionitrile. The proposed mechanism assumes two separate intermediates for these two simultaneous reactions. The reaction of MeAN with Na amalgam was found to be 100 times slower than that of AN. DMSO increases the rate of both the hydrodimerization and hydrogenation reactions via the same intermediate. Addition of quaternary ammonium salts to AN in diglyme has an effect similar to that of DMSO. The salts, however, react at very low concentrations due to accumulation of the cations on the charged amalgam surface. The effect of the size and structure of the quaternary cations was studied and is discussed.

INTRODUCTION

The study of organic electrochemical reactions has gained renewed interest in the last few years and many experimental and theoretical contributions have been published on the subject. Amalgam reductions, on the other hand, have been used for many years as a synthetic tool but very little quantitative work is available in the literature. Amalgam reactions are basically indirect electrochemical reductions on a mercury cathode, with the difference that both an electron and an alkali metal ion have to be transferred from the mercury to the solution. In fact, amalgams when dissolved in a medium where their reactivity towards water or other proton donors is low due to hydrogen overvoltage are a very convenient source of alkali metals. The advantage of amalgam over direct electrochemical reactions is in that electrolytes are not necessary, and therefore reactions can be carried out in any solvent. The present work is an attempt to treat the subject of amalgam reactions in a quantitative form, to study the mechanism of the reactions involved, and to derive some kinetic data about the elementary steps of electron transfer and radical ion reactions.

The work was started as a study of the hydrodimerization of acrylonitrile (AN) to adiponitrile (ADN). It was found that there exists a specific solvent effect which determines the path of the reaction to either the hydrodimer or the hydrogenated monomer, propionitrile (PN). The study was

then extended to methylacrylonitrile (MeAN), and to anthracene in order to show the analogy. Finally, as it was found by Baizer,¹⁻⁵ Matsuda,⁶ and also reported by us,⁷ quaternary ammonium salts have a strong effect on the hydrodimerization reaction. We have, therefore, carried out experiments with these salts and drawn some analogies between the solvent and the salt effects.

EXPERIMENTAL

In a heterogeneous system, such as the one in question, the reaction takes place on the interface. The reaction rate will depend on the rate of stirring when all other factors are kept constant. We have checked this dependence and found that at the beginning the reaction rate increases linearly with the stirring rate but above 2000 rpm the increase is much slower and is almost at a plateau (Fig. 1). We have chosen to work at this level of stirring where the system is not so sensitive to small variations in speed.

The reaction vessel used was a round-bottomed flask with four baffles and an exit tube at the bottom. It was equipped with a stirrer connected to an rpm counter and an electric stop watch actuated by a common switch. The flask was kept in a constant temperature bath at 0°C. The volume of the amalgam was always constant, and a large excess of it was used in each experiment. The volume of the organic layer was also kept constant for a given series of experiments. Blank experiments carried out with all the manipulations but without stirring, showed negligible degree of conversion.

The procedure was as follows. The amalgam was introduced into the reaction and allowed to cool to the reaction temperature. In another flask the reactants were weighed and cooled to the same temperature. They

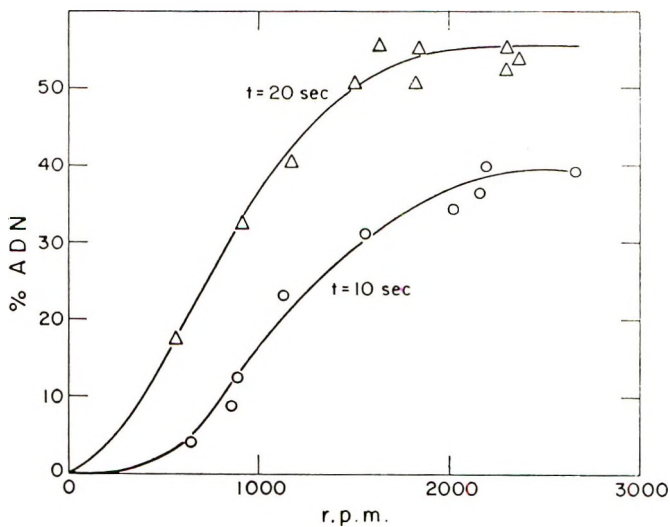


Fig. 1. Dependence of conversion to adiponitrile on rate of stirring: (O) 10 sec reaction; (Δ) 20 sec reaction.

were then transferred to the reaction flask, stirred for the required period at the specified stirring rate, and then the amalgam was withdrawn through the exit tube at the bottom. The reaction mixture was then collected, and the products were extracted with methylene chloride and analyzed by gas chromatography (polyester LAC 446 on Chromosorb w). The results were reproducible to within 10%.

The AN and MeAN were distilled prior to use. Anthracene was spectroscopic grade. DMSO was dried over molecular sieves, and diglyme was dried over CaH_2 . Both were distilled *in vacuo*. The quaternary ammonium salts were commercial-grade aqueous solutions. The amalgam was prepared by electrolysis of NaOH solution, and its Na content was determined by titration before and after reaction.

RESULTS AND DISCUSSION

Solvent Effect

Acrylonitrile. Reaction of Na amalgam with AN in solvents of low dielectric constant, such as ether, dioxane, acetonitrile, or diglyme, with water as proton donor, results essentially in hydrogenation to PN. When, however, a dipolar aprotic solvent, such as dimethyl sulfoxide (DMSO) or dimethylformamide is used, hydrodimerization to ADN takes place, and a pronounced acceleration of the reaction rate is observed. Using the standard technique described in the experimental part, we first measured the rate of the reaction as a function of the Na concentration in the amalgam. In all cases the amalgam was in very large excess, so that the concentration could be assumed constant in a given run. The results presented in Figure 2 show a first-order dependence with respect to Na for a reaction carried out in diglyme. The same dependence was also shown for the reaction in the presence of up to 15% DMSO; the order with respect to AN is seen from Tables I and II for diglyme and diglyme-DMSO mixtures, re-

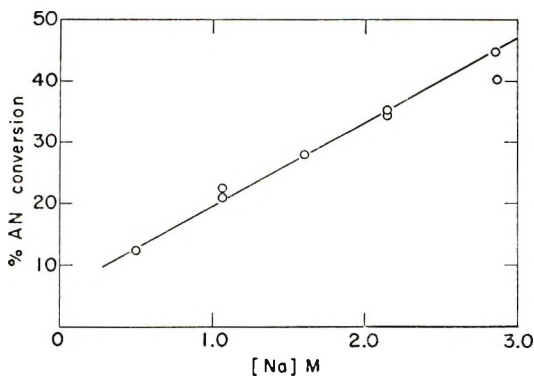


Fig. 2. Dependence of rate on the concentration of Na in the amalgam. Solvent, diglyme; 20 cc solution; 40 cc Na amalgam; $[\text{AN}] = 0.19M$; $(\text{H}_2\text{O}) = 2.1M$; $t = 10$ sec, stirring speed = 2200 rpm.

TABLE I
Dependence of Rate on AN Concentration in Diglyme Solution^a

[AN] ₀ , M	PN, %	ADN, %
0.047	8.5	2.5
0.10	10.3	3.6
0.14	7.7	4.1
0.188	6.9	4.0
0.235	7.7	4.9
0.288	5.0	4.4
0.38	6.0	4.3
0.48	4.8	3.6
0.57	5.7	3.7

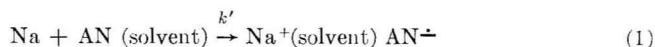
^a [H₂O] = 1.4M; [Na] = 1.1M; *t* = 5 sec; stirring speed = 2200 rpm.

TABLE II
Dependence of Rate on AN Concentration in Diglyme-DMSO Solution^a

[AN] ₀ , M	PN, %	ADN, %
0.012	—	35.0
0.023	4.4	43.5
0.05	3.0	47.0
0.10	2.0	47.5
0.16	1.5	53.5
0.23	1.1	50.0
0.28	1.8	46.5
0.33	2.0	55
0.38	2.1	41
0.49	2.2	32
0.57	2.0	29

^a [H₂O] = 1.4M; [DMSO] = 1.9M; [Na] = 1.1M; *t* = 5 sec; stirring speed = 2200 rpm.

spectively. It can be seen that the reaction is first-order in AN for both PN and ADN formation. This was checked over a wide range of concentrations and was also confirmed for a variety of mixtures of water and DMSO in diglyme. The rate-determining step is, therefore, the primary reaction shown in eq. (1).



We can calculate an apparent first-order rate constant for this reaction under the specified conditions, normalized for a 1M concentration of Na in the amalgam. As both, the reaction leading to PN and the one leading to ADN are first-order with respect to AN, we can obtain apparent rate constants for PN and ADN separately by eq. (2).

$$-d[\text{AN}]/dt = d[\text{PN}]/dt + d[\text{ADN}]/dt = (k'_{\text{PN}} + 2k'_{\text{ADN}}) [\text{AN}] \quad (2)$$

(The factor 2 is necessary, since for every electron transferred in the primary process, two AN molecules are consumed to form one molecule of ADN and the amount of ADN in our data is expressed in moles of AN and is therefore

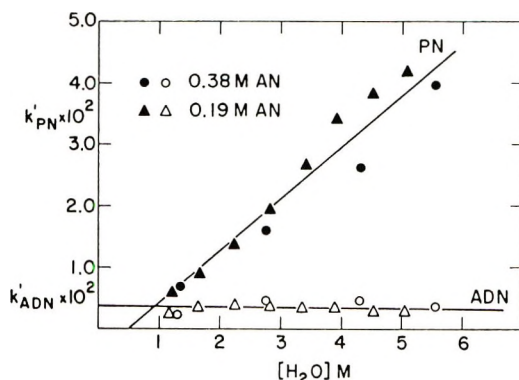


Fig. 3. Effect of water on the apparent rate constants of PN and ADM formation in diglyme solution: (●, ○) 0.38*M* AN; (▲, △) 0.19*M* AN. 20 cc solution; 40 cc amalgam; [Na] = 2.1*M*; *t* = 10 sec, stirring speed = 2400 rpm.

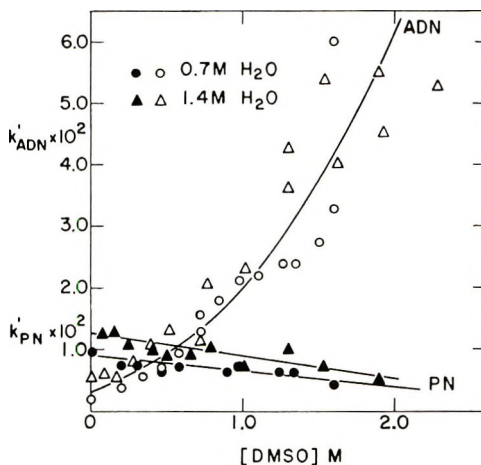


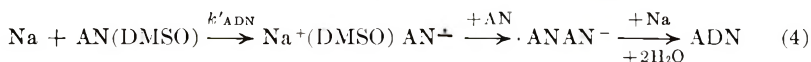
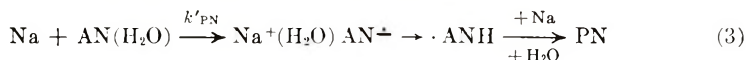
Fig. 4. Effect of DMSO on the apparent rate constants of PN and ADM formation in diglyme solution: (●, ○) 0.7*M* H₂O; (▲, △) 1.4*M* H₂O. 20 cc solution; [AN] = 0.19*M*; 40 cc Na amalgam; [Na] = 2.1*M*; *t* = 5 sec, stirring speed = 2400 rpm.

always double the molar value.) We thus obtain from the total AN consumed the value of $(k'_{PN} + 2k'_{ADN})$, and from the relative amounts of PN and ADN we can calculate the individual values. We can now study the effect of water and DMSO on the apparent rate constants. Water is the terminating agent and is therefore an integral part of the reaction. It has an effect of increasing the overall rate of the reaction in diglyme solution as can be seen from Figure 3. One can see that while k'_{ADN} remains constant k'_{PN} increases almost linearly with concentration of water. The reverse effect is observed upon addition of DMSO; while k'_{ADN} increases very rapidly, k'_{PN} remains almost constant (see Fig. 4).

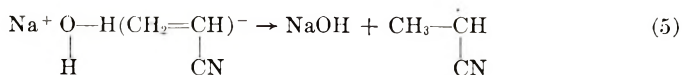
We can conclude that the rate-determining step is the primary reaction which is heterogeneous in character and consists of a transfer of an elec-

tron to AN and simultaneous transfer of Na^+ to the solution. This reaction was found to be first-order with respect to Na and AN, and therefore we have to assume that all other reactions following this must be very fast and not rate-controlling. However, the primary reaction itself is accelerated by both water and DMSO, the latter being more efficient than the former. For example, with a 2M water concentration in diglyme only $k'_{\text{PN}} = 1.3 \times 10^{-2}$ l./mole-sec while for 2M DMSO $k'_{\text{ADN}} = 5.5 \times 10^{-2}$ l./mole-sec per mole of water present. The most important point is, that the hydrogenation and the hydrodimerization reactions are independent of each other, and it is possible to accelerate one without changing the other by using the proper solvent composition. This, of course, is true only when both water and DMSO are present in relatively low concentrations in a large excess of a nonpolar solvent. When higher concentrations of either solvent are used, the reactions become competitive and are no longer independent.

In order to account for all the experimental facts we propose that two reactions are taking place independently at the interface:



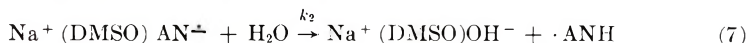
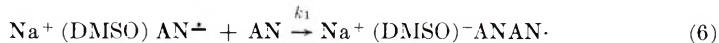
The electron transfer to AN from the amalgam must be followed by transfer of Na^+ , and therefore the rate will be determined by the energy level of the solvent-separated ion pair which is, apparently, higher in the case of diglyme than with either water or DMSO as solvating species. This is so, because diglyme solvates only the Na^+ . It is not possible to measure the rate in complete absence of water as polymerization will take place, but by extrapolation to anhydrous conditions one can see from Figure 3 that diglyme leads mainly to ADN with an apparent rate constant $k'_{\text{ADN}} = 0.3 \times 10^{-2}$ l./mole-sec. This does not change on addition of water within the range of concentrations studied where the medium consists mainly of diglyme. The rate of PN formation, however, increases with the water concentration. This is due to the additional gain in solvation energy by hydrogen bonding of water to the radical ion. The water solvated intermediate has a very short life, since the free energy gained by the reaction with water is very appreciable, as both the hydroxyl and the proton of the water react simultaneously [eq. (5)].



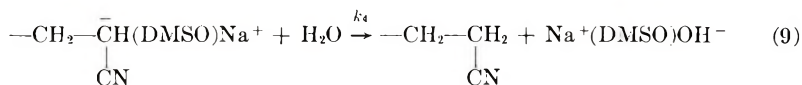
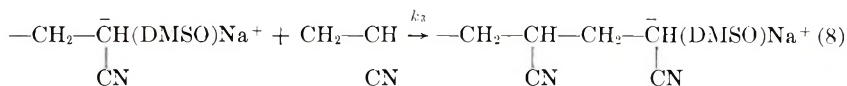
The free radical formed has a much lower reduction potential and it will interact immediately with another Na atom to yield the ion, which upon protonation will give PN.

DMSO reacts in a way analogous to water probably by solvating both the cation and the anion, thus accelerating the primary reaction. This

solvated species, however, has a longer life and can either react with another AN molecule or with water. The reactions (6) and (7) of the DMSO-solvated ion pair have to be considered:



Reaction (7) is much slower than reaction (5), because in the former case the Na^+ and AN^- are separated by the DMSO molecule and not by water. DMSO also binds water and reduces its activity and this would further slow the reaction with water. On the other hand, it facilitates the addition of another molecule of AN to give the dimeric anion radical. This in turn will immediately react with a second Na atom from the amalgam to give the dimeric dianion. The question now remains of the relative rate of polymerization as compared to termination of the carbanion end.



Equations (8) and (9) describe the conventional propagation and termination of anionic polymerization. It is well known that $k_4 \gg k_3$, and this is why water is an inhibitor of anionic polymerization. We thus have to assume that the behavior of the dimeric anion is considerably different from that of the primary AN radical ion. While in the former the reaction with water is faster, $k_4 > k_3$, in the latter case the reaction with AN is faster, $k_1 > k_2$. This is an apparent inconsistency and can only be explained by the notion that in the free-radical ion the charge is delocalized over the whole conjugated system and the reaction with water is therefore slower than with AN. In the carbonion, the charge is more localized on the α -carbon atom, and consequently it will react faster with water. Further confirmation of these assumptions is obtained from the study of MeAN and anthracene.

Methacrylonitrile. The same reaction can also be carried out with MeAN, the difference being that the reduction potential of MeAN is 0.2 V higher than that of AN. One would therefore expect a much lower rate of electron transfer. This is really the case. In diglyme solution up to 15M in H_2O the rate of hydrogenation to isobutyronitrile (IBN) is very slow. At higher water contents, however, the rate increases considerably (Fig. 5). If we restrict ourselves to water concentrations not higher than 15M we can calculate an apparent rate constant for the primary reaction for MeAN and compare it under the same conditions to that of AN. It turns out that $k'_{\text{PN}}/k'_{\text{IBN}}$ is higher than 100. DMSO increases the rate of the MeAN reaction just as in the case of AN and yields the hydrodimer, 2,5-dimethyl adiponitrile (diMeADN). We have compared the rate of reaction of AN

TABLE III
Effect of DMSO on the Rate of MeAN Reaction^a

<i>t</i> , sec	DMSO, <i>M</i>	IBN, %	diMeADN, %	$(k_1/k_2)_{\text{MeAN}}$
30	0	5.3	0	0
	1.9	3.3	0.4	9.0
	3.0	2.5	0.4	11.8
	6.3	13.0	2.4	13.6
	7.1	23.0	6.5	21.5
	7.5	24.5	8.1	24.5
	9.1	47.6	19.6	31.0
	11.0	33.0	24.0	52.5
10	0	3.8	0	0
	2.9	1.0	0	0
	4.0	1.8	0.3	11.8
	7.0	5.1	1.3	17.5
	9.0	9.5	3.2	23.0
	11.4	13.3	9.1	48.0

^a [MeAN] = 0.15*M*; [H₂O] = 1.1*M*; [Na] = 1.1*M*; stirring speed = 2200 rpm.

and MeAN in DMSO with 1.1*M* H₂O and found that while AN yielded 12% ADN in 10 sec and 25% in 20 sec, MeAN yielded only 1.3% diMeADN in 120 sec and 4.3% in 300 sec under otherwise identical conditions. From this we can calculate $k'_{\text{ADN}}/k'_{\text{diMeADN}} = 120$ in the presence of DMSO. This seems to indicate that DMSO increases the rate of electron transfer to both monomers by about the same factor, so that the ratios of the rate constants in diglyme and DMSO are about the same.

The effect of DMSO can be investigated by the gradual increase of its concentration in diglyme. In this case, if we work at a water concentration of about 11*M*, the reaction corresponding to reaction (3) is relatively unimportant and we can neglect it; but because of the high water content, the reaction analogous to reaction (7) competes with that analogous to reaction

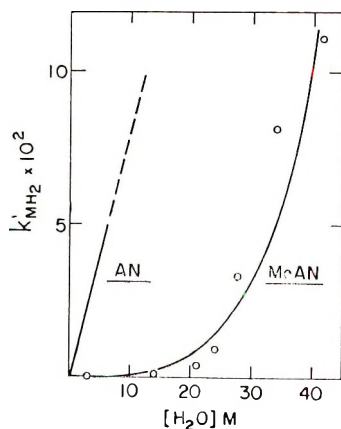


Fig. 5. Effect of water on the apparent rate constant of IBN and PN formation from MeAM and AN, respectively, in diglyme solution.

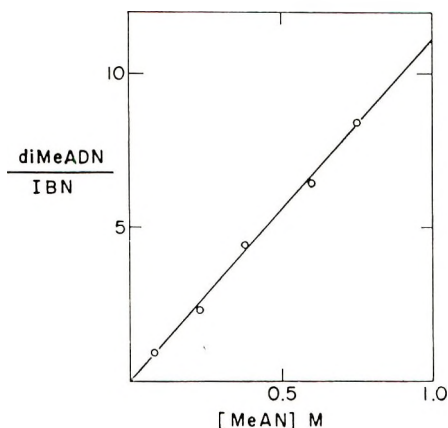


Fig. 6. Ratio of hydrodimer to reduced monomer as a function of the increase in MeAN concentration in diglyme-DMSO solution. $[\text{H}_2\text{O}] = 5.55M$; $[\text{DMSO}] = 6.6M$; $t = 30$ sec; stirring speed = 2100 rpm.

(6). This can be seen from the data of Table III. One can thus calculate $(k_1/k_2)_{\text{MeAN}}$ from the ratios of both products as seen in the last column Table III. This ratio increases with the DMSO concentration as expected, because solvation of the ion pair and binding of the water by DMSO will tend to favor reaction (6) over reaction (7). The ratio $(k_1/k_2)_{\text{MeAN}}$ increases up to an asymptotic value of about 250 at a ratio of $\text{DMSO}/\text{H}_2\text{O} = 4.5$.

From the results at hand it clearly appears that, unlike the case of AN, in the case of MeAN, IBN and diMeADN are formed from a common intermediate, namely $\text{Na}^+(\text{DMSO})\text{MeAN}^{\ddagger}$. This can also be shown by studying the effect of the initial concentration of MeAN in a given solvent composition of H_2O and DMSO. As the dimerization reaction involves a second molecule of MeAN it should be favored by an increase in its concentration. That this is so can be seen from Table IV and from the linear plot of diMeADN/IBN versus MeAN in Figure 6. Table IV also shows that the rate-determining step of the overall reaction still remains the electron transfer to MeAN; consequently, the per cent $(\text{IBN} + \frac{1}{2} \text{diMeADN})$

TABLE IV
Dependence of Rate on the MeAN Concentration in Diglyme-DMSO Solution^a

$(\text{MeAN})_0$, <i>M</i>	IBN, %	diMeADN %	$(\text{IBN} + \frac{1}{2}$ diMeADN), %	diMeADN/ IBN
0.08	18.3	17.0	26.8	0.93
0.23	11.6	26.8	25.0	2.3
0.38	6.3	27.0	18.3	4.4
0.60	5.2	32.2	21.3	6.4
0.75	4.1	34.4	21.3	8.4

^a $[\text{H}_2\text{O}] = 5.6M$; $[\text{DMSO}] = 6.6M$; $[\text{Na}] = 1.1M$; $t = 30$ sec; stirring speed = 2100 rpm.

formed, per unit time, which is a measure of the electron transfer, remains constant and independent of the initial MeAN concentration, at a given DMSO content. When the DMSO concentration is increased the overall rate of the reaction also increases (Table III).

The value of (k_1/k_2) for AN could not be measured due to the much higher rate of the direct reaction with water. In order to measure this value one has to work at much lower concentrations of water which would lead to AN polymerization. From the present data, and the fact that we do not have any increase in PN formation even at 5.5M H₂O, we can conclude that in a medium containing DMSO, the ratio $(k_1/k_2)_{AN}$ is at least as high as $(k_1/k_2)_{MeAN}$, namely, above 250. This explains why one gets in this solvent the hydrodimer rather than the hydrogenated monomer.

The proposed mechanism is in general agreement with that suggested by M. Figgeys et al.,^{8,9} who have applied the molecular orbital theory to the study of electrolytic hydrodimerization. In the hydrodimerization of MeAN we did not detect any dimer 2,2,4-trimethylglutaronitrile as reported by Jones and Ledford,¹⁰ but we do not exclude the possibility that the latter dimer is present in very small amounts.

Anthracene. In an attempt to confirm the mechanism assumed above for AN and MeAN we have carried out a few experiments with anthracene (A). The reduction potential of anthracene is close to that of AN (−1.94 V). It has the advantage that the anion is colored and no polymerization can take place, so that the reduction process can be followed more easily. Anthracene dissolved in THF or diglyme gives the blue mono- and dinegative anions when interacting with a Na mirror. However, when it is stirred with Na amalgam, no color can be noticed and the anthracene remains intact. This is probably due to the lower reactivity of Na in the amalgam. Apparently the free-energy gain from solvation of Na⁺ by diglyme is not sufficient to shift the equilibrium in favor of the solvated ion pair. When water is added to the reaction mixture, again no color is formed, but reaction does take place, and in 10 min stirring 32% of the 9,10 dihydroanthracene (AH₂) is produced. This is equivalent to reaction (3) and suggests, that whenever an anthracene molecule is on the amalgam surface (and a water molecule is within interaction distance) a Na atom is transferred to produce the intermediate Na⁺(H₂O)A[−], which is almost instantaneously protonated to the free radical HA·. This, in turn, will immediately acquire another electron and react with a water molecule to yield the reduced anthracene.

When DMSO is added gradually to a solution of anthracene in diglyme in contact with a Na amalgam, a blue color of the anthracene anion appears at about 20% DMSO content. The blue color is stable and does not seem to fade with time. This is a very clear indication that the DMSO can shift the equilibrium probably by virtue of solvation of the ion pair. This



is also indicated from a decrease in the half-wave potential of anthracene

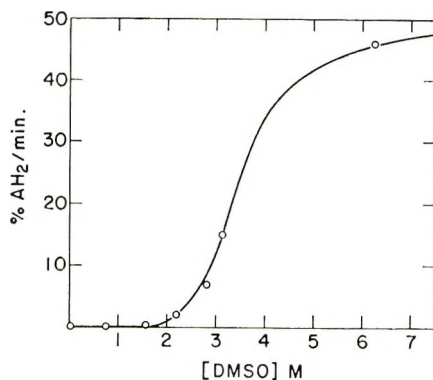


Fig. 7. Rate of reduction of anthracene to 9,10-dihydroanthracene (AH₂) in diglyme solution as a function of the DMSO concentration. [Anthracene] = 0.025*M*; [H₂O] = 7*M*; *t* = 1 min; shaking by hand.

upon addition of DMSO, as compared to dimethoxyethane, reported by Peover.¹¹ The A⁻ formed can react with water to yield the reduced anthracene. This reaction, however, is slower than the electron transfer. For example, if a solution containing anthracene and 5% water in DMSO is stirred with Na amalgam the whole organic layer becomes strongly colored. When the stirring is interrupted, the color disappears gradually. In this case it is possible to measure both, the equilibrium constant and the rate of termination.

In order to get an idea about the overall effect of DMSO we have measured the rate of reduction of anthracene as a function of increasing concentration of DMSO in diglyme containing 12% H₂O. The results are plotted in Figure 7, which shows that DMSO increases the rate of electron transfer to anthracene just as in the case of AN and MeAN. Here, however, no dimerization can take place and, therefore, the slow reaction with water determines the outcome of the overall reaction. One can also show that the reaction of Na⁺(DMSO)A⁻ with AN or MeAN is much faster than with water. On adding a solution of A⁻ in DMSO-diglyme to a solution of AN or MeAN in the same solvent, the blue color disappears in a fraction of a second. However, if a solution of A⁻ is added to a solution of water in DMSO, the color disappears slowly during a period of about 2 min. It is clear from this observation that for the reaction of A⁻ corresponding to eqs. (6) and (7), respectively, we have $k_1 \gg k_2$ just as for the reaction of AN⁻. This was also confirmed by measurements of the competitive reaction of A⁻ and HA⁻ with water, butyl bromide, and other reactants.¹²

Salt Effect

As was shown in the previous section, when the reduction of AN by sodium amalgam was carried out in an ether such as tetrahydrofuran, dioxane, or diglyme, and in the presence of water as proton donor, the main product was PN, and only a minor quantity of ADN was formed. How-

ever, when a salt such as tetraethylammonium tosylate or trimethylbenzylammonium tosylate was added to the solution, only hydrodimerization was observed, with little or no PN formation. The amounts of salt needed were catalytic, and as little as 0.1% was enough to affect the reaction path.

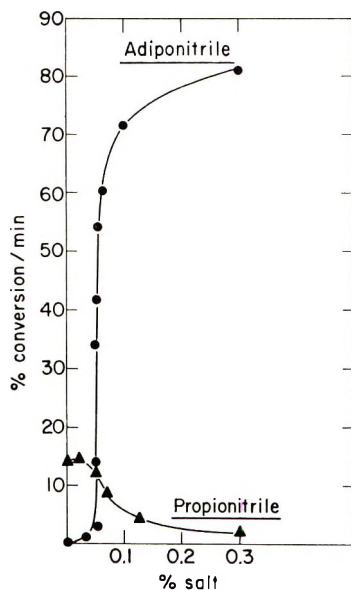


Fig. 8. Rate of ADN and PN formation in a solution containing 5% AN and 10% H₂O in diglyme, as a function of the concentration of trimethylbenzylammonium tosylate.

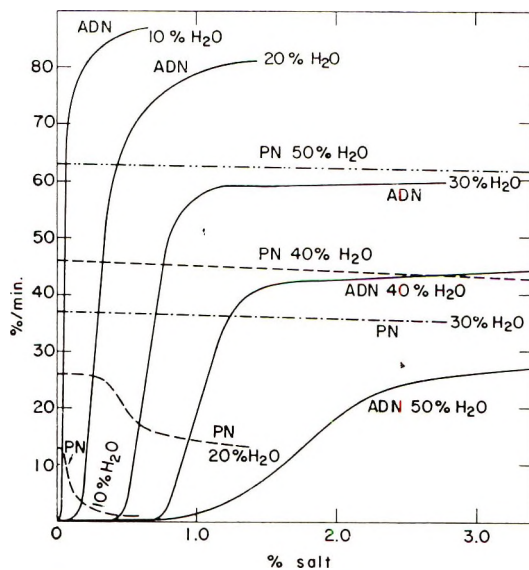


Fig. 9. Rate of ADN and PN formation in solution containing 5% AN and 10–50% water in diglyme, as a function of the concentration of trimethylbenzylammonium tosylate.

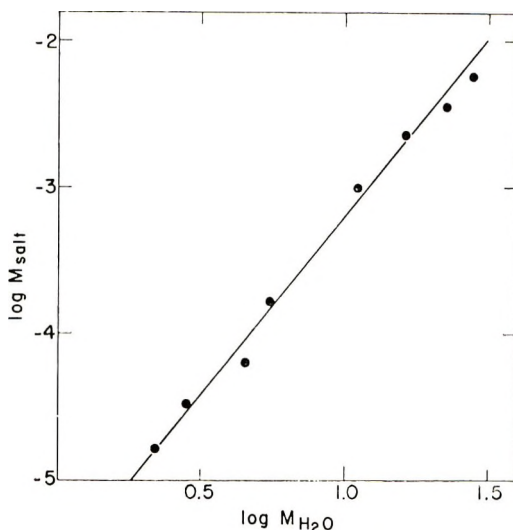


Fig. 10. Logarithmic plot of the salt concentration at the inflection point vs. water concentration of the solution.

This is an indication that in an organic medium the salt is strongly adsorbed on the amalgam surface and can therefore be effective in very low concentrations. Indeed, one can completely cancel the effect of the quaternary ammonium salt by adding a large excess of an inactive salt such as LiBr. About a 30-fold excess of LiBr is needed, presumably to cover the amalgam surface completely and thus exclude any quaternary salt from the active site. It was also found that the anion does not play any role, and even the free base can be used. Indeed, as the reaction is carried out without any pH control and NaOH is formed by the decomposition of the amalgam, one is always working in a strongly alkaline medium. It was also found that the quaternary salts increase considerably the overall rate of the reaction, and consequently, an analogy with the solvent effect seems reasonable.

We have carried out some experiments with quaternary ammonium salts. A typical set of data is shown in Figure 8. In these experiments the AN concentration in diglyme was 5%, and the water concentration was 10%. One can see that in the absence of salt the amount of ADN was very low, while conversion to PN amounted to 15%/min. When trimethylbenzylammonium tosylate was added, the rate of ADN formation increased slowly, but at about 0.05% salt there was a sharp jump in rate to 60%/min while the rate of PN formation went down from 15% to 12%/min. Addition of further quantities of salt increased the ADN rate to a smaller extent and much larger amounts produced mainly ADN with only minor quantities of PN. The inflection point in the curve is probably an indication of a cumulative effect that may be the result of a critical coverage of the amalgam surface by the salt. This critical concentration is a function of the water concentration in the reaction medium, the higher the water concentra-

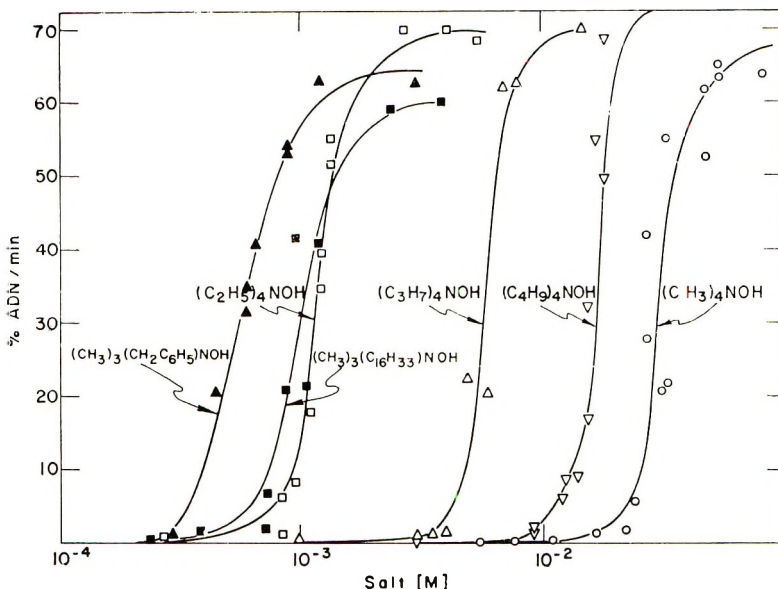
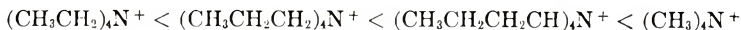


Fig. 11. Effect of cation size and structure on the rate of ADN formation in a diglyme solution containing 5% AN and 10% H₂O.

tion the higher the salt concentration required to obtain the inflection point (Fig. 9). It is interesting to note that there is a linear relationship between the logarithm of the critical salt concentration (as measured at the inflection point) and the logarithm of the water concentration (Fig. 10). This is an indication that the chemical potential of the salt of the amalgam surface is a function of the chemical potential of the water on that surface. The exact interpretation of the relationship is undoubtedly connected to the adsorption characteristics of these cations.

A better insight into these phenomena could be gained by comparing the effect of cations of different size. The effect of tetramethyl-, ethyl-, propyl- and butylammonium hydroxides was investigated under identical conditions. In every case the solution consisted of 5% AN and 10% H₂O in diglyme. The results are presented in Figure 11. In all cases a sharp change in reaction rate at a certain critical concentration was observed. However, this concentration is not regular function of the cross section of the cations but shows the following order:



The tetramethylammonium cation seems to be out of place. A possible interpretation can be found in the work of Wen and Saito.¹³ From their measurements of partial molar volumes of a homologous series of the salts they found that these salts have two opposing effects: the hydrophobic and the charge effect. In Me₄N⁺ the charge effect is considerable because the cation is relatively small and the water molecules are under the influence of the charge; but the hydrophobic effect that increases the solva-

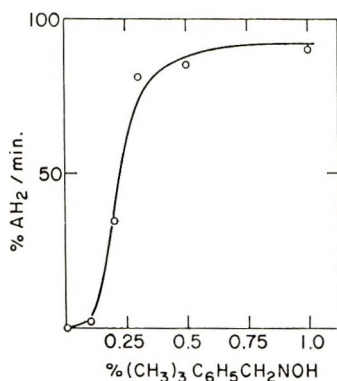


Fig. 12. Rate of reduction of anthracene to 9,10-dihydroanthracene (AH₂) in diglyme solution as a function of trimethylbenzylammonium hydroxide concentration. [Anthracene] = 0.025*M*; [H₂O] = 7*M*; *t* = 1 min; shaking by hand.

tion of AN is limited. Et₄N⁺ seems to be optimal, having a small charge effect and a large enough hydrophobic one. In Pr₄N⁺ and Bu₄N⁺ the charge effect decrease causes a decrease in the activity. When one cancels the hydrophobic effect by using tetraethanolammonium hydroxide, only PN is formed with minor amounts of ADN even at very high salt concentrations. On the other hand, one can combine the charge and hydrophobic effects in the same cation by attaching a large substitute to a trimethylammonium cation. We have tried trimethylbenzyl- and trimethylcetyl-ammonium hydroxides, and they both proved to be more effective than tetraethylammonium hydroxide (Fig. 11).

It is interesting to note that quaternary ammonium salts have also an effect on the reduction of anthracene. On addition of trimethylbenzylammonium hydroxide to a solution of anthracene in diglyme, a blue color appears on the solution-amalgam interface but disappears upon diffusion into the bulk of the solution. The effect of the salt concentration on the rate of the reduction can be seen from Figure 12 for a solution 7*M* in water and 0.015*M* in anthracene. The analogy with the DMSO effect seems to be quite general (cf. Fig. 7).

The mechanism of the reaction of the quaternary ammonium ions is not clear. It was suggested that quaternary ammonium amalgam may be formed. However, the equilibrium proposed by Littlehailes and Woodhall¹⁴ will not be favored, as the quaternary salts are in catalytic amounts. Moreover, the quaternary amalgam is unstable and would easily decompose to side products. At this stage we can only point out the analogy between the quaternary ammonium cations and DMSO. Their high reactivity is due to the fact that, being positively charged, their concentration at the negatively charged amalgam surface is high; they are thus strongly adsorbed on the mercury surface and can solvate the AN molecule. They probably form an ion pair with an AN radical ion. This accelerates the addition of another AN molecule while simultaneously excluding the water and thus

slowing down the reaction with it. A proper balance has to be found between the hydrophobic effect, which is responsible for excluding the water from the surface and solvating the AN molecule, on the one hand, and the charge effect, which determines the concentration of cations on the surface and strength of the ion pairing with AN^+ on the other. Therefore, an optimal structure of the cation is required for maximal reactivity. Admittedly this description is only qualitative and any further discussion will await a more quantitative study of this complex problem.

In conclusion, we have shown that dipolar aprotic solvents and quaternary ammonium salts have a similar effect favoring the hydrodimerization reaction rather than hydrogenation. We have gained some insight into the elementary reactions involving intermediate radical ions. These reactions have not been studied previously and are important for understanding of anionic reductions and polymerizations.

This paper is taken in part from the Ph.D. thesis of H. Rosen, to be presented to the Scientific Council of the Weizmann Institute of Science.

The authors are indebted to U.C.B. (Union Chimique-Chemische Bedrijven) S. A. Brussels, Belgium, for financial support of this work.

References

1. M. M. Baizer, *J. Electrochem. Soc.*, **111**, 215 (1964).
2. M. M. Baizer and J. D. Anderson, *ibid.*, **111**, 223 (1964).
3. M. M. Baizer, *J. Org. Chem.*, **29**, 1670 (1964).
4. M. M. Baizer and J. D. Anderson, *ibid.*, **30**, 1348 (1965).
5. J. P. Petrovich, J. D. Anderson, and M. M. Baizer, *J. Org. Chem.*, **31** (1966).
6. Fujito Matsuda, *Tetrahedron Letters*, **49**, 6193 (1966).
7. Y. Arad, M. Levy, I. R. Miller, and D. Vofsi, *J. Electrochem. Soc.*, **114**, 889 (1967).
8. M. Figeys and H. P. Figeys, *Tetrahedron*, **24**, 1097 (1968).
9. M. Figeys, *Tetrahedron Letters*, **24**, 2237 (1967).
10. G. C. Jones and T. H. Ledford, *Tetrahedron Letters*, **24**, 615 (1967).
11. M. E. Peover, *Electroanalytical Chemistry*, Edited by Bard, Vol. 2, Chapter 1, p. 12.
12. I. Walcher and M. Levy, in preparation.
13. W. Y. Wen and S. Saito, *J. Phys. Chem.*, **68**, 2639 (1964).
14. J. D. Littlehales and B. J. Woodhall, *Chem. Comm.*, No. 14, p. 665 (1967).

Received December 31, 1968

Radical Polymerization Behavior of Hydroxystyrenes

MASAO KATO, *The Textile Research Institute of the Japanese Government, Yokohama, Japan*

Synopsis

Homopolymerizations of *m*- and *p*-hydroxystyrene and their copolymerizations with styrene and methyl methacrylate by use of azobisisobutyronitrile as initiator were investigated, and the results were compared with those obtained previously *o*-hydroxystyrene. Intrinsic viscosities of *m*- and *p*-hydroxystyrene polymers obtained by bulk and solution polymerizations were ca. 2 to 3 times larger than those of *o*-hydroxystyrene polymers obtained by the similar conditions. The structures of the polymers thus produced were investigated by infrared and ultraviolet spectroscopy. These studies suggested that all of the homopolymers consisted mainly of structures of normal vinyl type polymer. R_p was proportional to $[I]^{0.52}$ for *m*-hydroxystyrene and to $[I]^{0.50}$ for *p*-hydroxystyrene, for *o*-hydroxystyrene R_p was proportional to $[I]^{0.72}$. A reasonable chain transfer mechanism for these monomers was postulated. The apparent activation energies of polymerization for *m*- and *p*-hydroxystyrene were found to be 20.1, and 18.0 kcal/mole, respectively, compared to the value of 21.5 kcal/mole for *o*-hydroxystyrene. Monomer reactivity ratios and $Q - e$ values for *m*- and *p*-hydroxystyrene were determined, and the results were also compared with the case of *o*-hydroxystyrene. Copolymerization generally gave a polymer with relatively high intrinsic viscosity, even in the case of *o*-hydroxystyrene.

INTRODUCTION

Polymerization behavior of hydroxystyrenes has been studied by other groups.¹⁻⁴ The results however, are rather fragmentary and inconsistent for different authors. The lack of agreement might be attributable to the instability of the monomers or variations in polymerization behavior caused by differences in polymerization procedure.

Up to this time, we have investigated⁵⁻⁷ the polymerization of *o*-hydroxystyrene and its copolymerization with other vinyl monomers in some detail. In this paper, radical polymerizations of *m*- and *p*-hydroxystyrene and their copolymerizations were examined, and the results thus obtained are compared with those for *o*-hydroxystyrene.

EXPERIMENTAL

Materials

p-Hydroxystyrene (PHS) was synthesized by the procedure of Coroson et al.⁸ In this work, *p*-hydroxyacetophenone was used as starting material. From 25.0 g of *p*-acetoxy styrene there was obtained 16.5 g (89%) of crude

crystals of PHS. The crude product was recrystallized by dissolving it in warm (30–35°C) petroleum ether and cooling it below –20°C; the product had mp 69–70°C (lit.⁹ mp, 71–72°C).

m-Hydroxystyrene (MHS) was prepared from *m*-hydroxyacetophenone by a procedure similar to the one used for the preparation of PHS. From 40.0 g of *m*-acetoxystyrene (bp 73°C/0.7 mm; lit.¹⁰ bp, 65°C/0.4 mm) there was obtained 24.0 g (81%) of colorless oil, bp after redistillation, 75–77°C/1 mm (lit.¹¹ bp 114–116°C/16 mm).

These monomers were carefully purified just before use.

Styrene and methyl methacrylate used as comonomers were commercially available materials purified by distillation just before use.

Azobisisobutyronitrile (AIBN) used as initiator was purified by recrystallization from methanol.

Tetrahydrofuran as solvent for polymerization was refluxed with sodium for several hours, and then distilled over lithium aluminum hydride.

Polymerizations

Homopolymerizations and copolymerizations were carried out according to almost the same procedure described in the previous paper.⁶

Preparation of MHS and PHS Model Polymers

The *m*- and *p*-acetoxystyrene obtained in the process of preparation of MHS and PHS were polymerized with AIBN (1% based on monomer) at 60°C in absence of oxygen. The reaction mixture was dissolved in benzene, and the solution was poured into vigorously stirred methanol to precipitate the polymer. The isolated fluffy polymer, poly-*m*-acetoxystyrene, $[\eta] = 0.485$ dl/g; poly-*p*-acetoxystyrene, $[\eta] = 0.652$ dl/g was dispersed in aqueous 1*N* sodium hydroxide–dioxane mixture and stirred for 4 hr at 80–90°C under nitrogen. The brown and transparent solutions thus produced was cooled, an excess of hydrochloric acid solution added dropwise into the solution with stirring to isolate the polymer, which was then filtered and rinsed with water. Purification of the polymer was done by dissolving the polymer into methanol and precipitating it from water. This operation was repeated twice, after which the purified polymer was filtered, rinsed with water, and then dried *in vacuo* at 50°C.

Characterization of Polymer

The intrinsic viscosity of polymer was measured in tetrahydrofuran solution in an Ubbelohde-type viscometer in $30 \pm 0.05^\circ\text{C}$.

Infrared and ultraviolet absorption spectra were taken with Hitachi Recording spectrophotometers, Models EP-S2 and EPS-3T, respectively.

RESULTS AND DISCUSSION

Homopolymerization

Table I shows polymerization conditions and results of polymerization for MHS and PHS. From these results, it can be seen that both of the

TABLE I
Radical Homopolymerizations of *m*- and *p*-Hydroxystyrene

Monomer	Monom. concn, % ^a	AIBN, % based on monomer	Temp, °C	Time, hr	Con- version, %	[η], dl/g
MHS	100	0.5	70	45	46	0.295
MHS	100	0.5	60	43	52	0.322
MHS	66.7	1.0	50	20	49	0.237
MHS	66.7	1.0	70	20	50	0.165
PHS	55.6	1.0	70	20	66	0.176
PHS	50.0	1.0	50	48	44	0.281
PHS	50.0	0.5	50	48	32	0.245

^a Tetrahydrofuran was used as solvent.

monomers polymerized through an almost normal free-radical mechanism; generally, intrinsic viscosity increased with decreasing temperature and initiator concentration. A similar tendency has been found in the case of *o*-hydroxystyrene (OHS).⁵ However, the intrinsic viscosity of OHS polymer obtained by polymerization under similar conditions to these cases, ranges from 0.090 to 0.133 dl/g (MW below 10000) and is significantly lower than that of MHS and PHS polymers.

There was perfect correspondence between the infrared pattern of the polymer and the corresponding model polymer in each case, as seen in the case of OHS polymer prepared with AIBN.⁵ Accordingly, it is suggested that MHS and PHS polymers obtained by the radical polymerization with AIBN consist mainly of structures formed through a normal vinyl polymerization mechanism.

The ultraviolet spectra of OHS, MHS, and PHS polymer in absolute ethanol were also compared with those of the corresponding model polymers. For the purpose of interpreting the spectra of the polymers, the ultraviolet spectra of some phenol derivatives in ethanol were investigated.⁷ The results obtained are shown in Table II. It can be found that the absorption maxima of the monosubstituted phenols show essentially the same values regardless of the substituent (methyl or the α -phenyl ethyl) if the substituted position is the same. It is also known¹³ that methyl-, ethyl- and cyclohexyl-phenols reveal the same absorption maxima if the substituted position is the same. In the case of disubstituted phenol, the absorption maximum is also considered to be shifted toward higher wavelength when a substituted group (such as shown in Table II) is located in the *para* position with respect to the hydroxyl group of phenol than when no *p*-substituent is present. These data may be helpful in interpreting the polymer structures, especially for OHS and PHS polymers. If a hydroxystyrene polymer contains some element of structure due to the reaction between the vinyl group and the phenol nucleus, the shape of the ultraviolet absorption curve and the absorption maximum of polymer are expected to differ from that of the corresponding model polymer.

TABLE II
Absorption Maxima of Ultraviolet Spectra for Phenol
Derivatives in Absolute Ethanol

Compound	λ_{max} , m μ
<i>o</i> -Cresol	275
<i>m</i> -Cresol	275
<i>p</i> -Cresol	280
<i>o</i> -(α -Phenylethyl)phenol ^a	275
<i>p</i> -(α -Phenylethyl)phenol ^a	279
2,6-Dimethyl phenol	273
2,4-Dimethyl phenol	281

^a Synthesized according to the method of Frisch.¹²

It was of interest that the absorption maxima of OHS, MHS, and PHS model polymer were at 275, 274, and 279 m μ , respectively, which agreed with those of *o*-, *m*-, and *p*-cresols (275, 275, and 280 m μ , respectively). Moreover, the shapes of the absorption curves of the model polymers were very similar to those of the corresponding cresols. The spectrum of the polymer obtained by the polymerization with AIBN showed a perfect agreement with that of the corresponding model polymer. This suggests that all of the polymers formed by the radical polymerization consist mainly of the structures of vinyl type polymer. A different spectrum was observed in the case of polymerization with cationic catalyst, as described in the following paper.¹⁴

Kinetics of Polymerization

The rates of homopolymerization of MHS and PHS, as dependent on initiator concentration and temperature, are given in Table III. In each case the monomer concentration was fixed at 2.081 mole/l. No inhibition effect (induction period) was observed in these polymerizations. In the case of OHS, the earlier study⁶ indicated that, when the polymerization was conducted on monomer which had been stored 1 week at 0°C after distillation, a significant inhibitory effect below 70°C was induced.

Logarithmic plots of the rate R_p against initiator concentration [I] for MHS and PHS are shown in Figure 1. The plots are reasonably linear, having slopes of 0.52 and 0.50, for MHS and PHS, respectively. Even though there are certain limitations in the experimental accuracy, these relationships suggest that most of the growing chain was being stopped by mutual termination and that only OHS (having a slope of 0.72)⁶ exhibits somewhat anomalous behavior.

The relationship between the rate of polymerization and monomer concentration for MHS and PHS at 70°C was examined. Logarithmic plots of the rate against monomer concentration [M] are given in Figure 2. Both plots were linear with a slope of 1.0, which is the same value as for OHS.

Arrhenius plots for the polymerizations of MHS and PHS are given in

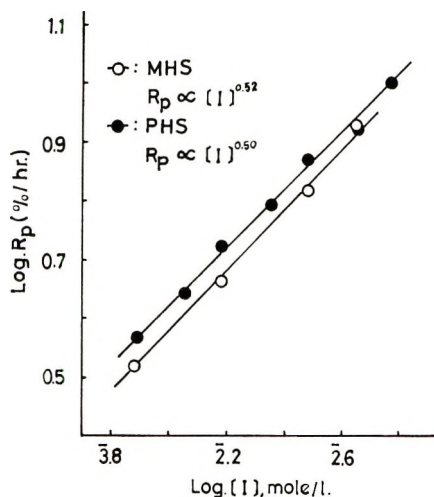


Fig. 1. Log-log plots of initial polymerization rates R_p of MHS and PHS in tetrahydrofuran against initiator (AIBN) concentration at 70°C; (○) MHS; (●) PHS. Monomer concentration constant (2.081 mole/l.).

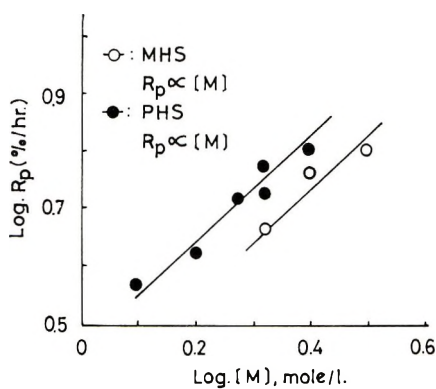


Fig. 2. Log-log plots of initial polymerization rates R_p of MHS and PHS in tetrahydrofuran against monomer concentration at 70°C: (○) MHS; (●) PHS. AIBN concentration constant (1.522×10^{-2} mole/l.).

Figure 3. From the plots, the apparent activation energies of polymerization for MHS and PHS were calculated to be 20.1, and 18.0 Kcal/mole, respectively.

The experimental results thus obtained are summarized in Table IV, together with the result of OHS. As mentioned above, comparison of the rate equations suggests that only OHS shows anomalous polymerization behavior; i.e., the fact that R_p is proportional to $[I]^{0.72}$ implies that the growing chain radicals are terminated not only by the mutual termination but also to a considerable extent by a chain-transfer mechanism. Therefore, the polymerization mechanism which was previously illustrated⁶ should be revised.

TABLE III
 Polymerizations of *m*- and *p*-Hydroxystyrene in
 Tetrahydrofuran; Dependence on Initiator
 (AIBN) Concentration and Temperature^a

Monomer ^a	Temp., °C	[I] × 10 ² , mole/l.	R _p , %/hr
MHS	60	1.522	1.8
	70	0.761	3.3
	70	1.522	4.6
	70	3.044	6.6
	70	4.566	8.6
	75	1.522	7.9
PHS	80	1.522	10.5
	60	1.522	2.2
	65	1.522	3.3
	70	0.761	3.7
	70	1.142	4.4
	70	1.522	5.3
	70	2.284	6.1
	70	3.052	7.4
	70	4.567	8.3
	70	6.103	10.1
	75	1.522	6.8
	80	1.522	12.3

^a Monomer concentration = 2.081 mole/l.

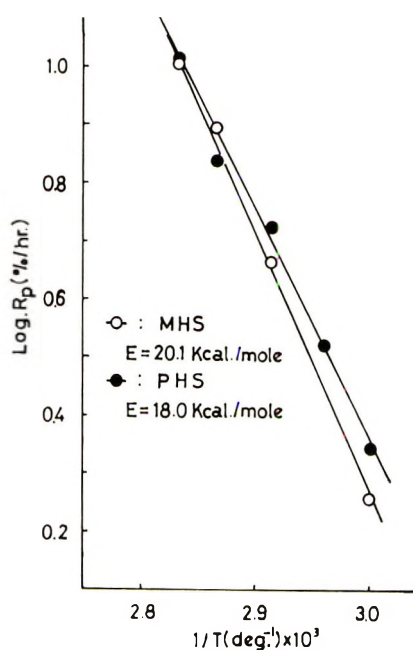
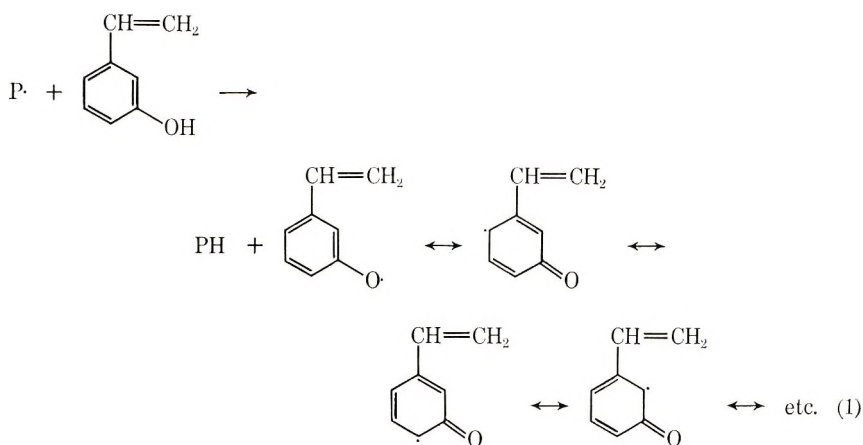


Fig. 3. Arrhenius plots for polymerizations of MHS and PHS with the use of AIBN as initiator: (○) MHS; (●) PHS.

TABLE IV
 Experimental Equations of the Rate of Polymerization
 and Apparent Activation Energies of Polymerization for
o-, *m*-, and *p*-Hydroxystyrene

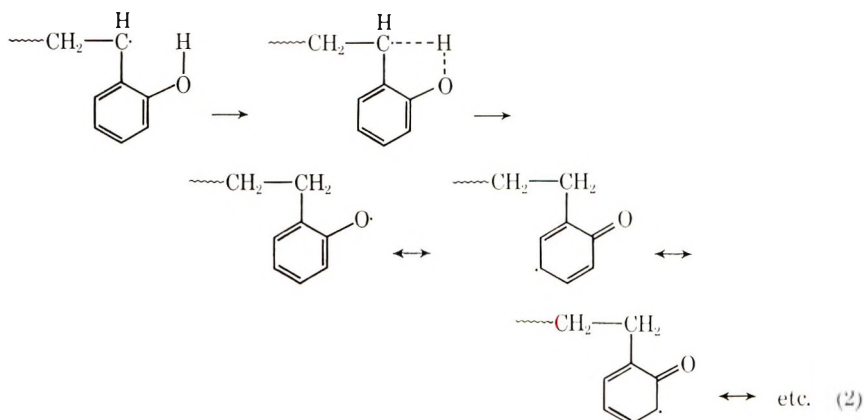
Monomer	Rate of polymerization R_p , mole/l. sec	Apparent activation energy, kcal/mole
OHS	$K_o[M][I]^{0.72}$	21.5
MHS	$K_m[M][I]^{0.62}$	20.1
PHS	$K_p[M][I]^{0.50}$	18.0

The reactions of initiation and propagation might follow the usual free-radical mechanism in each case. However, the termination reactions are very complicated. It is possible to give some explanations for the reactions. Minoura et al.¹⁵ have shown that phenol and cresols act as weak chain-transfer agents in polymerization of styrene under oxygen-free conditions. Similar transfer reactions are considered to occur in these monomers as illustrated in eq. (1).



The growing radical $P\cdot$ attacks the hydroxyl group of the monomer molecule to terminate by hydrogen abstraction. Of course, chain transfer to polymer seems to occur, but is quite limited at the initial reaction step because of low polymer concentration. The contribution of such termination reactions as attack of $P\cdot$ on the phenol nucleus might be present to a very small extent.

If the transfer reaction proceeds through a mechanism of the type shown in eq. (1), transfer should take place very frequently only in the case of OHS, and whereas to a limited extent with MHS and PHS. However, there is no plausible reason why OHS shows such a peculiarity. Accordingly, other mechanisms may be concerned in addition to the mechanism as shown in eq. (1). One of them may be of the type shown in eq. (2).



Here the growing radical abstracts a hydrogen atom from the adjacent hydroxyl group located in the same nucleus to deactivate the radical. This intramolecular self-deactivating reaction, therefore, can be regarded as an *ortho* effect.

Owing to resonance, the radicals formed in eqs. (1) and (2) should be relatively stable and not likely to regenerate active chain radicals by adding monomers. If such radicals are incapable of carrying on the polymerization chains, they eventually disappear through combination with other growing free radicals or with each other. Accordingly, polymer formed through the free-radical mechanism contain linkages due to the substitution of the phenol nucleus and the etherification of the hydroxyl group, although these must be in the minority.

Copolymerization

Relationships between monomer and initial copolymer compositions are illustrated in Figures 4 and 5. The copolymer composition was determined by elementary analysis for carbon and hydrogen.

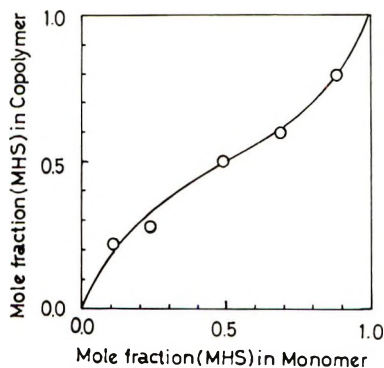


Fig. 4. Initial copolymer composition in relation to monomer composition for the MHS-methyl methacrylate system.

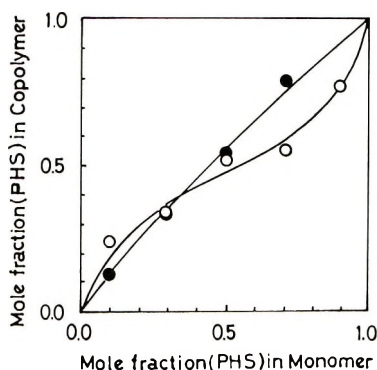


Fig. 5. Initial copolymer composition in relation to monomer composition: (O) PHS-methyl methacrylate; (●) PHS-styrene.

The monomer reactivity ratio was determined graphically¹⁶ for each pair. The results are listed in Table V, together with $Q-e$ values calculated by the equation of Alfrey and Price.¹⁷ Data for the MHS-styrene system in Table V were derived from the results of Bonsoll *et al.*³ The alternating tendency in each case is greater in methyl methacrylate than in styrene. Values of Q_1 and e_1 for each hydroxystyrene monomer with methyl methacrylate and with styrene differ somewhat between pairs; the Q_1 and e_1 values are lower in methyl methacrylate than in styrene. Although different $Q-e$ values were obtained, OHS and PHS can be considered to be monomers having similar negative polarities, the negativities being larger than that for MHS. This result agrees with the interpretation derived from the resonance theory.

Complex formations of OHS and PHS with maleic anhydride were investigated by Kumano-tani *et al.*⁴

The results for the copolymerizations of OHS, MHS, and PHS with methyl methacrylate or styrene (1:1 molar ratio) with the use of AIBN

TABLE V
Monomer Reactivity Ratios r_1, r_2 and $Q-e$ Values for *o*-, *m*-, and *p*-Hydroxystyrene at 60°C

Co-Monomer		r_1	r_2	$r_1 r_2$	Q_1	e_1
(M ₁)	(M ₂) ^a					
OHS ^b	St	1.32 ± 0.25	0.72 ± 0.10	0.950	1.66	-1.03
OHS ^b	MMA	0.21 ± 0.06	0.33 ± 0.08	0.069	1.15	-1.23
MHS ^c	St	1.21	0.91	1.10	1.10	-0.80
MHS	MMA	0.40 ± 0.02	0.43 ± 0.06	0.172	1.02	-0.93
PHS	St	1.20 ± 0.13	0.79 ± 0.08	0.948	1.52	-1.03
PHS	MMA	0.25 ± 0.04	0.34 ± 0.06	0.085	1.14	-1.16

^a St = Styrene, MMA = methyl methacrylate.

^b These data were reported in the previous paper.⁶

^c Data given for the MHS-St system are derived from the results of Bonsoll *et al.*³

TABLE VI
Copolymerizations of *o*-, *m*-, and *p*-Hydroxystyrene with
Methyl Methacrylate and Styrene

Monomer molar ratio	Monomer concn, % ^a	AIBN, % based on monomer	Temp, °C	Time, hr	Con- version, %	[η], dl/g
OHS/St = 1	75.0	1.0	65	45	97	0.321
OHS/MMA = 1	75.0	1.0	65	39	100	0.432
MHS/MMA = 1	50.0	1.0	70	24	89	0.341
PHS/MMA = 1	50.0	1.0	60	45	100	0.438

^a Tetrahydrofuran was used as solvent.

are shown in Table VI. A relatively higher intrinsic viscosity was obtained in each case. In the case of OHS, the mechanism of eq. (2) seems to be reduced significantly by exchanging some portion of OHS with these comonomers.

The author is deeply indebted to Prof. S. Okajima of Tokyo Metropolitan University, and Dr. H. Kamogawa and Dr. M. Hasegawa of our laboratory for many helpful suggestions and discussions relating to this work.

References

1. C. S. Marvel and N. S. Rao, *J. Polym. Sci.*, **4**, 703 (1949).
2. T. Tanaka, T. Yamashita, and T. Yokoyama, *Kogyo Kagaku Zasshi*, **60**, 1595 (1967).
3. E. P. Bonsoll, L. Vallentine, and H. W. Melville, *Trans. Faraday Soc.*, **48**, 763 (1952).
4. J. Kumanotani *et al.*, paper presented at meeting of (1) the Society of Polymer Science, Japan, June, 1964 and June, 1966; (2) the Chemical Society of Japan, April, 1968.
5. M. Kato and H. Kamogawa, *J. Polym. Sci. A-1*, **4**, 1773 (1966).
6. *Ibid.*, **4**, 2271 (1966).
7. M. Kato and H. Kamogawa, *Kogyo Kagaku Zasshi*, **71**, 587 (1968).
8. B. B. Coroson, W. J. Heintzelman, L. H. Schwartzman, H. E. Tiefenthal, R. J. Lokken, J. E. Nickels, G. R. Atwood, and F. J. Pavlik, *J. Org. Chem.*, **23**, 544 (1958).
9. W. J. Dale and H. E. Hennis, *J. Am. Chem. Soc.*, **80**, 3645 (1958).
10. P. Ferruti, *Chimica Ind. Milan*, **74**, 496 (1965); through *C. A.*, **63**, 5734 (1958).
11. B. J. F. Hudson and R. Robinson, *J. Chem. Soc.*, **1945**, 715.
12. K. C. Frisch, *J. Org. Chem.*, **15**, 587 (1950).
13. R. A. Friedel and M. Orchin, "Ultraviolet Spectra of Aromatic Compounds," John Wiley, New York, N. Y. (1951).
14. M. Kato, *J. Polym. Sci. A-1*, in press.
15. Y. Minoura, N. Yasumoto, and T. Ishii, *Makromol. Chem.*, **71**, 159 (1964).
16. F. R. Mayo and F. M. Lewis, *J. Am. Chem. Soc.*, **66**, 1594 (1944).
17. T. Alfrey and C. C. Price, *J. Polym. Sci.*, **2**, 101 (1947).

Received November 15, 1968

Revised January 20, 1969

Polyaryleneimides of *meso*- and *dl*- 1,2,3,4-Butanetetracarboxylic Acid Dianhydrides

D. F. LONCRINI* and J. M. WITZEL,
*Insulating Materials Department, General Electric Company,
Schenectady, New York 12305*

Synopsis

High molecular weight polyarylene amic acids have been prepared by reacting aromatic diamines with equimolar amounts of either *meso*- or *dl*-1,2,3,4-butanetetracarboxylic acid dianhydride (TCBA) in organic polar solvents. Heat converted these soluble precursors to insoluble polyimides having good high-temperature physical properties.

INTRODUCTION

In the search for polymers that retain good mechanical properties at elevated temperatures, the polyimides are one type which have received considerable attention. Early work on all-aliphatic systems showed that these polymers exhibited poor thermal properties, were low-melting and thermoplastic.¹⁻³ Somewhat improved thermal properties were obtained with systems based on aromatic dianhydrides and aliphatic diamines,^{4,5} however, such polymer systems were found to have low glass transition temperatures. Outstanding thermal and oxidative properties have been reported for polyimides derived from all-aromatic precursors.⁶⁻⁸ These polymers, unlike their aliphatic counterparts, show either no second-order transition state or one above 250°C., are nonmelting, and are completely resistant to organic solvents. Similar properties have been observed in all-aromatic polyimides containing ester⁹ or amide¹⁰ linkages.

It has now been observed that polyimides prepared from an aliphatic dianhydride and aromatic diamines possess unique properties unlike those prepared from aromatic dianhydrides and aliphatic diamines. This paper describes the preparation and properties of a series of linear polyimides from the reaction of aromatic diamines with *meso*- and *dl*-1,2,3,4-butanetetracarboxylic acid dianhydride (TCBA).†

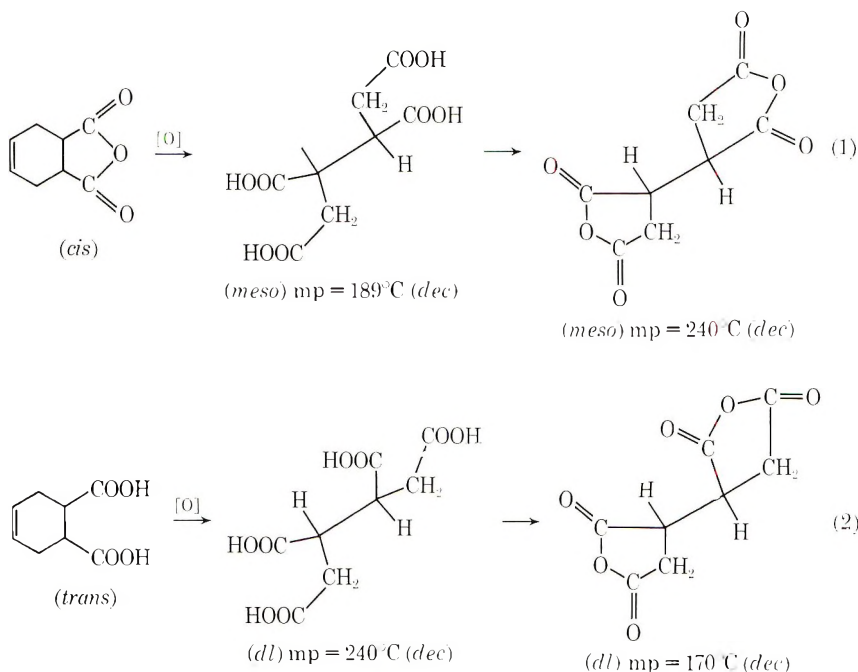
* Present address: P. D. George Company, St. Louis, Missouri 63147.

† Polyaryleneimides of *meso*-1,2,3,4-butanetetracarboxylic acid dianhydride have recently been reported by V. V. Kudryavtsev et al.¹¹

RESULTS AND DISCUSSION

Synthesis of 1,2,3,4-Butanetetracarboxylic Acid Dianhydrides

The *meso*- and *dl*- forms of the butanetetracarboxylic acids were obtained in high yields by the nitric acid oxidation of *cis*- and *trans*- Δ^4 -1,2-tetrahydrophthalic acids following the procedure described by Lynn and Roberts.¹² These acids were converted to the corresponding stereoisomeric dianhydrides by refluxing with acetic anhydride [eqs. (1) and (2)].



Preparation of the Polyimides

Both the *meso*- and *dl*-forms of the butane dianhydrides reacted readily with aromatic diamines in polar solvents to give high molecular weight linear polyamic acids. Cyclization to the polyimides was carried out by heating cast films to 300°C . The reaction sequence for the *meso*-form is shown in eq. (3) (where Ar is an aromatic nucleus).

The conversion of the polyamic acid to the polyimide was confirmed spectroscopically. The disappearance of the amide I band at 1650 cm^{-1} and the appearance of new bands at 1780 and 718 cm^{-1} during heating are consistent with the interpretation that the amic acids converted to the cyclic imides.

The polymers shown in Table I were all prepared in *N*-methyl-2-pyrrolidone (NMP) as the solvent. Intrinsic viscosities were determined in NMP by using an extrapolation of reduced viscosities determined at four different concentrations. All polymers in Table I showed film-forming

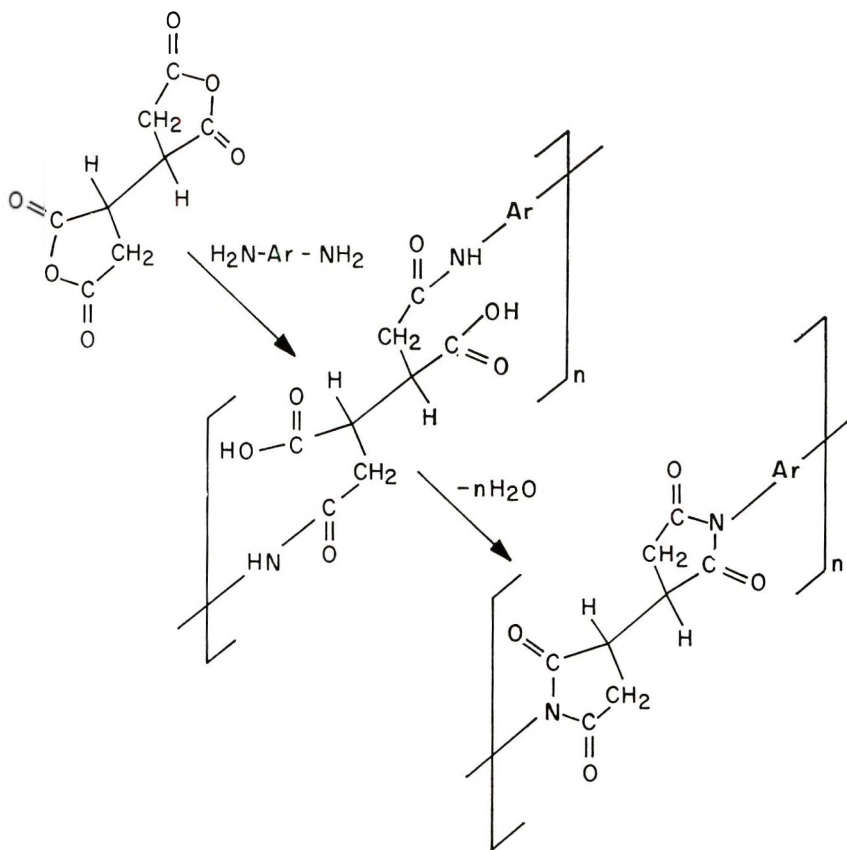


TABLE I
Properties of Polyaryleneimides

Dianhydride	Diamine	Intrinsic viscosity	Properties of cured films ^a	Polymer melt temperature, °C
<i>meso</i> -TCBA	4,4'-Diaminodiphenyl methane	0.62	Flexible	>400
<i>meso</i> -TCBA	4,4'-Diaminodiphenyl ether	0.65	Flexible	"
<i>meso</i> -TCBA	<i>m</i> -Phenylenediamine	0.59	Flexible	"
<i>meso</i> -TCBA	<i>p</i> -Phenylenediamine	0.62	Flexible	"
<i>meso</i> -TCBA	Benzidine	0.46	Flexible	"
<i>meso</i> -TCBA	3,5-Diaminobenzoic Acid	0.23	Flexible	"
<i>meso</i> -TCBA	<i>o</i> -Dianisidine	0.26	Flexible	"
<i>dl</i> -TCBA	4,4'-Diaminodiphenyl methane	0.63	Flexible	"
<i>dl</i> -TCBA	4,4'-Diaminodiphenyl ether	0.73	Flexible	"
<i>dl</i> -TCBA	<i>m</i> -Phenylenediamine	0.35	Flexible	"
<i>dl</i> -TCBA	Benzidine	0.48	Flexible	"
<i>dl</i> -TCBA	{ 50% Benzidine 50% 4,4'-Diaminophenyl ether	0.57	Flexible	"

^a The film was judged to be flexible if it would take a full 180° bend without cracking.

properties, even those having low intrinsic viscosities. Although there is no apparent explanation for this behavior, similar observations have been reported in polyhydrazide systems.¹³

PROPERTIES

Physical

Some typical properties of several polyimide films prepared from the butane dianhydrides and aromatic diamines are shown in Table II. The tensile properties were determined on films which were removed from an aluminum substrate. It is of interest to note that at 200°C these polymers retain approximately 50% of their room temperature tensile strengths. All of the films were flexible and would not crack with a fingernail crease.

Electrical

The electrical properties of these polyimides are excellent and are summarized for two typical polymers in Table III.

Thermal-Oxidative Stability

The thermal-oxidative stability of the polymers prepared with 4,4'-diaminodiphenyl ether (ODA) was examined by heating free films in an air circulating oven for 100 hr at each of the following temperatures: 200, 220, 240, and 260°C. The weight losses of the films after each heating cycle are recorded in Table IV. The films were still flexible to a fingernail

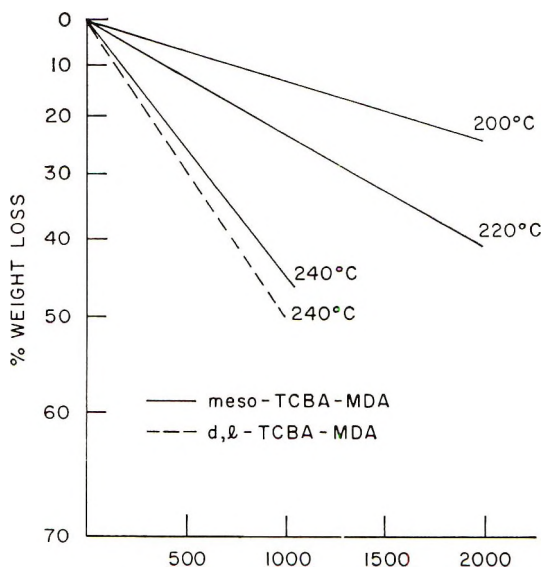


Fig. 1. Isothermal weight loss of polyimides from *meso* and *dl*-TCBA and MDA in air.

TABLE II
Tensile Properties of Polyaryleneimide Films

TCBA dihydride	Diamine	Room temperature			200°C		
		Tensile strength, psi × 10 ^{3a}	Tensile modulus, psi × 10 ³	Elongation, %	Tensile strength, psi × 10 ^{3a}	Tensile modulus, psi × 10 ³	Elongation, %
<i>meso</i>	4,4'-Diaminodiphenylmethane	14.2	445	11.2	7.94	245	7.2
<i>meso</i>	4,4'-Diaminodiphenyl ether	13.2	482	11.0	8.18	228	8.1
<i>meso</i>	<i>m</i> -Phenylene-diamine	8.2	94.7	2.1	5.2	64.1	3.2
<i>meso</i>	Benzidine + 4,4'-diaminodiphenyl ether ^b	13.5	107	8.7	7.0	101	7.6
<i>dl</i>	4,4'-Diaminodiphenylmethane	14.4	152	10.2	7.5	107	7.4
<i>dl</i>	4,4'-Diaminodiphenyl ether	13.3	87.7	9.1	6.8	31.1	6.1
<i>dl</i>	<i>m</i> -Phenylene-diamine	7.8	218	2.0	—	—	—

^a ASTM D-638.

^b 50/50 equivalent mixture of the two diamines.

TABLE III
Electrical Properties of Films (1-2 mil)

Polymer ^a	Dielectric strength, V/mil	Dissipation factor, % (60 cycles)	
		125°C	200°C
<i>meso</i> -TCBA-MDA	4 000-7 000	0.79	3.83
<i>meso</i> -TCBA-ODA	4 000-7 000	0.57	2.89

^a MDA = 4,4'-diaminodiphenylmethane; ODA = 4,4'-diaminodiphenyl ether.

TABLE IV
Weight Loss of Polymers Heated at Various Temperatures in Air

Dianhydride	Diamine	Wt loss during 100 hr of heating, wt-%				Total wt loss, wt-%
		200°C	220°C	240°C	260°C	
<i>meso</i> -TCBA	ODA	0.47	1.15	2.06	48.4	52.1
<i>dl</i> -TCBA	ODA	0.82	1.23	1.45	53.5	56.9

crease after the 100-hr treatment at 240°C. Very rapid decomposition occurred at 260°C, at which point the films became brittle.

The thermal-oxidative stability of the polymer prepared from 4,4'-diaminodiphenyl methane (MDA) was studied by using an isothermal weight loss method. Free films (1-1.5 mils) were placed in an air circulat-

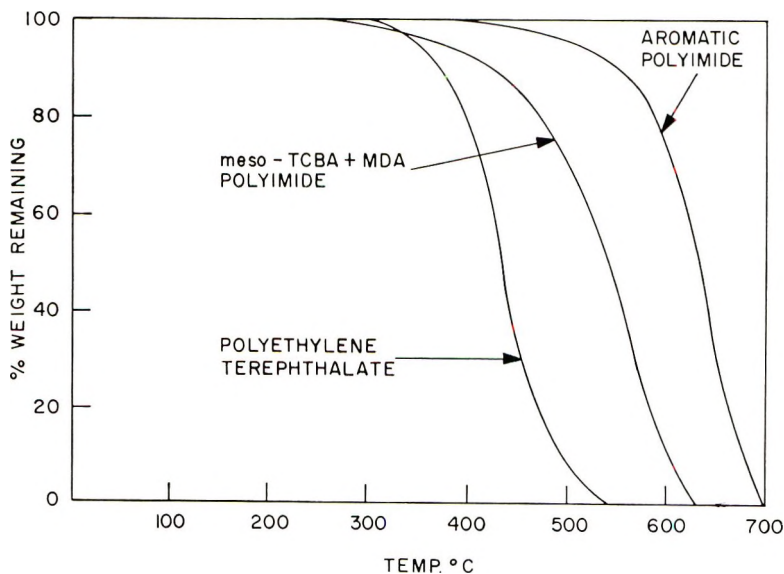


Fig. 2. TGA thermograms of poly(ethylene terephthalate), a polyimide from *meso*-TCBA and MDA, and an aromatic polyimide from pyromellitic dianhydride and 4,4'-diaminodiphenyl ether in air.

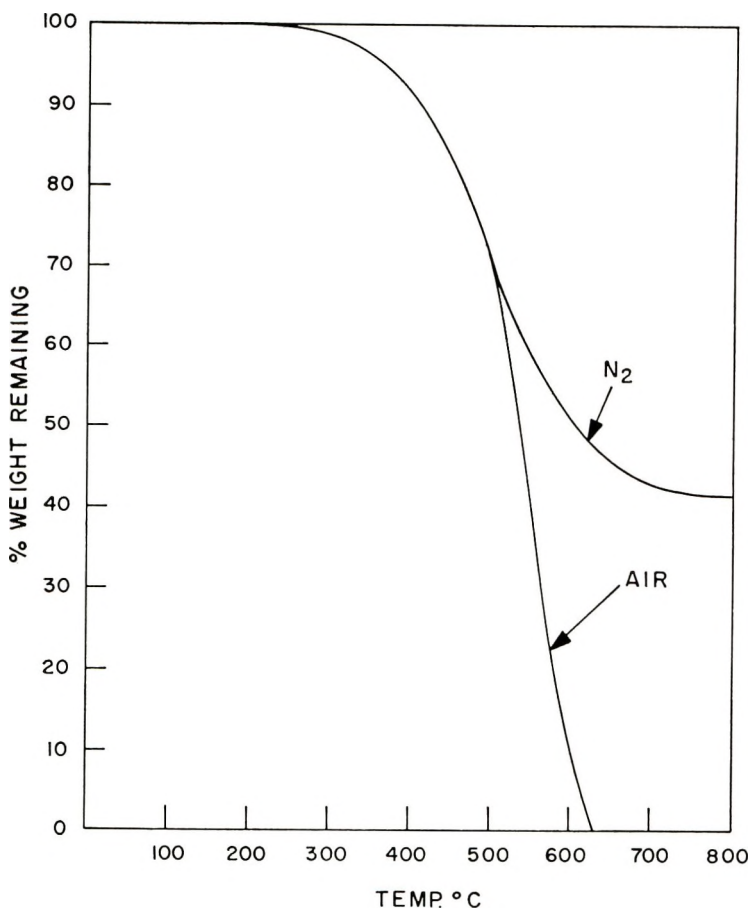


Fig. 3. TGA thermograms of polyimide from *meso*-TCBA and 4,4'-diaminodiphenyl ether in air and in nitrogen.

ing oven at 200, 220, and 240°C. The films were checked regularly for per cent weight loss and flexibility. The weight loss data are summarized in Figure 1. These polymers are not as stable as the well known aromatic polyimides. The films remained flexible (no cracking on wrapping around $\frac{1}{8}$ -in. mandrel) until more than 30% weight loss had occurred.

The thermogravimetric curves, as shown in Figure 2, give a comparison of the thermal-oxidative stability of these polymers versus poly(ethylene terephthalate) and an aromatic polyimide prepared from 4,4'-diaminodiphenyl ether and pyromellitic dianhydride. The thermograms were determined in an air atmosphere at a heating rate of 4.5°C/min.

The degradation process is enhanced in the presence of oxygen as can be seen from the thermogram in Figure 3. The polymer under study in this diagram was based on *meso*-butanetetracarboxylic acid dianhydride and 4,4'-diaminodiphenyl ether. The thermogravimetric curve shows that in the absence of oxygen, approximately 40% of the polymer remains after the

initial pyrolytic decomposition. This is a very close approximation to the aromatic carbon content of the polymer (39.7%) and suggests that the initial pyrolysis is closely associated with the aliphatic portion of the polymer.

EXPERIMENTAL

Preparation of *meso*- and *dl*-1,2,3,4-Butanetetracarboxylic Acid

By the procedure described by Lynn and Roberts,¹² the nitric acid oxidation of tetrahydrophthalic anhydride gave an 80% yield of the *meso*-acid, mp = 189°C, while the nitric acid oxidation of *trans* Δ^4 -1,2-tetrahydrophthalic acid afforded a 42% yield of the *dl*-acid, mp = 240°C (dec).

Preparation of *meso* and 1,2,3,4-*dl*-Butanetetracarboxylic Acid Dianhydrides

A 2:1 weight mixture of acetic anhydride and the tetraacid was refluxed for 30 min, and after cooling to room temperature and filtering, afforded a 60% yield of *meso*-dianhydride, mp = 248°C (dec) and a 34% yield of the *dl*-dianhydride, mp = 170°C (dec).

Preparation of Polyarylene Amic Acids

To an equivalent mixture of the diamine and the dianhydride was added enough organic solvent to make a 20–30% solids concentration; the mixture was stirred vigorously under a nitrogen atmosphere. The intrinsic viscosities were determined after allowing the polymer solutions to stand overnight at room temperature.

Film Preparation

The viscous polymer solutions obtained from the reaction were filtered, deaerated and cast onto aluminum (20 mil) with a doctor knife having a 15–20 mil opening. The panels were heated in an air circulating oven for 1 hr each at 100, 200, and 240°C, and finally for 30 min at 300°C. The free films were obtained by dissolving the aluminum in a large excess of dilute hydrochloric acid, washed well with water and dried at 100°C for a period of 30 minutes.

The authors gratefully acknowledge the help of Mr. R. B. Hughes in some of the polymer preparations.

References

1. British Patent 470, 858 (1945).
2. C. J. Frosch, U.S. Patent 2,421,024 (1947).
3. J. Lincoln and J. G. Drewitt, U.S. Patent 2,502,576 (1949).
4. W. F. Gresham and M. A. Nayler, U.S. Patents, 2,731,447 (1956) and 2,712,543 (1955).
5. W. M. Edwards and I. M. Robinson, U.S. Patent 2,900,369 (1959).

6. C. E. Stoog, A. L. Endrey, S. V. Abramo, C. E. Berr, W. M. Edwards, and K. L. Oliver, *J. Polym. Sci. A*, **3**, 1373 (1965).
7. G. M. Bower and L. W. Frost, *J. Polym. Sci. A*, **1**, 3135 (1963).
8. S. D. Bruck, *Polymer*, **6**, (1), 49 (1965).
9. D. F. Loncrini, *J. Polym. Sci. A 1*, **4**, 1531 (1966).
10. J. H. Freeman, L. W. Frost, G. M. Bower, and E. J. Traynor, SPE Transactions, April, page 75 (1965).
11. V. V. Kudryavtsev, A. P. Rudakov, and M. M. Koton, *Vysokomol. Soedin. A*, **9**, 1985 (1967).
12. J. W. Lynn and R. L. Roberts, *J. Org. Chem.*, **26**, 4303 (1961).
13. A. H. Frazer and F. T. Wallenberger, *J. Polym. Sci. A*, **2**, 1137 (1964).

Received December 30, 1968

Revised January 20, 1969

Influence of Structure of 1,1,3-Trimethyl-5-carboxy-3-(*p*-carboxyphenyl)indan upon Polyamide Properties

JAMES S. RIDGWAY, *Textiles Division, Monsanto Company, Pensacola, Florida 32502*

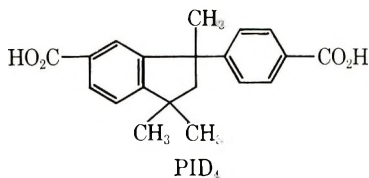
Synopsis

Copolyamides of nylon 66 and 1,1,3-trimethyl-5-carboxy-3-(*p*-carboxyphenyl)indan (PIDA) were prepared by melt polycondensation of nylon 66 salt with PIDA in combination with hexamethylenediamine, *trans*-1,4-cyclohexanebis(methylamine), and *m*-xylylenediamine. In addition, hexamethylenediamine-PIDA was incorporated into the copolymer system of nylon 66-poly(hexamethylene terephthalamide). The effect of PIDA upon the intrinsic viscosity, crystallinity, density, melting point, moisture regain, tenacity, initial modulus, and the boiling-water shrinkage of such polyamides was determined. Particular emphasis was placed upon the influence of PIDA on the glass transition temperature of the polyamides. The effect of moisture on the glass transition temperature was also discussed. The physical properties of PIDA copolymers indicate that crystallinity virtually disappears above 20 mole-% PIDA concentration; however, the glass transition temperature measured at 0 and 30% RH increases sharply with increased PIDA concentration.

INTRODUCTION

The glass transition temperature of a polymer can be readily changed by structural modification of the polymer. The incorporation of stiff segments, such as aromatic or alicyclic rings, into the polymer chain will produce an increase in T_g . Similar effects result from the introduction of bulky side groups, or from an increase in the steric hindrance of backbone groupings.

An unusual condensation intermediate, 1,1,3-trimethyl-5-carboxy-3-(*p*-carboxyphenyl)indan—often referred to as phenylindane dicarboxylic acid—(PIDA) has a structure with such features.



Evidence that PIDA does form increased T_g copolyamides¹ and polyesters² has appeared, but data on the fiber properties of such polymers are rather limited. Accordingly, several series of nylon 66 copolyamides are de-

scribed in some detail regarding the influence of PIDA upon polymer and fiber properties. The compositions selected for study were: nylon 66 with PIDA and hexamethylenediamine; nylon 66 with PIDA and *trans*-1,4-cyclohexanebis(methylamine); nylon 66 with PIDA and *m*-xylylenediamine; and nylon 66 with PIDA, terephthalic acid, and hexamethylenediamine. The selection of these compositions allows the effect of PIDA to be determined in combination with aliphatic, alicyclic, and aromatic polyamide segments of varying ability to form isomorphous copolyamides.

EXPERIMENTAL

Materials

All chemicals were obtained from commercial sources. The polyamide salts were generally prepared by a slow addition of a 75% aqueous solution of the diamine to a 50–75% aqueous solution, or slurry, of the diacid in a 1:1 molar ratio. The mixture was warmed until solution was attained, then it was treated with activated carbon, Celite filter aid, and filtered. An excess of ethanol was added, and the solution was cooled at 0–5°C for 24 hr. The precipitated polyamide salt was filtered, washed with ethanol, and dried under vacuum at 65°C. Yields of 85–95% were generally obtained by this method.

The adipic acid salt of *trans*-1,4-cyclohexanebis(methylamine) was obtained by this procedure from a 60% *trans*–40% *cis* isomer mixture. The *trans* isomer precipitated leaving in solution the *cis* form. One recrystallization from water–ethanol was sufficient to remove any trace quantities of *cis* isomer remaining in the salt.

The nylon salts and the corresponding polymers are designated by the following code: the first number shows the number of carbon atoms in the diamine, the second shows the number of carbon atoms in the diacid; terephthalic acid is denoted by TA, *m*-xylylene diamine by MXD, and *trans*-1,4-cyclohexanebis(methylamine) by t-CBMA. For example, 6-PIDA is the hexamethylenediamine salt or polymer of 1,1,3-trimethyl-5-carboxy-3-(*p*-carboxyphenyl)indan and MXD-6 is the *m*-xylylenediamine salt or polymer of adipic acid.

Methods

Polymerization. The polyamides were prepared from combinations of the various nylon salts. 66/t-CBMA–PIDA was prepared from a mixture of the salts of nylon 66 with t-CBMA-6 and 6-PIDA in quantities such that the net effect was a copolymer of 66/t-CBMA–PIDA. The MXD–PIDA copolyamides were similarly prepared. The mixed salts were combined with sufficient water to form a 75% aqueous slurry. This slurry was added to a stainless steel, high pressure autoclave which was purged of air by the use of purified nitrogen. The temperature and pressure were slowly raised to 220°C and 250 psig. Then the temperature was further increased

to 243°C, while the pressure was maintained at 250 psig, during which time there was the continuous removal of steam condensate. At this point the pressure was gradually reduced to atmospheric over a 25-min period. The polymer melt was allowed to equilibrate for 30 min at about 15°C above the melting point. This finished polymer was melt spun directly from the autoclave through a single hole spinneret into a quench water bath, and then taken up on a bobbin with a Universal Winder.

This fiber was drawn four to five times its original length over a 60–90°C hot pin.

Polymer Melting Point. The melting point was determined by observing the junction point of intersecting filaments of drawn fiber between crossed nicol polarizers on an electrically heated hot-stage microscope. The melting point T_m was taken as the temperature at which the last trace of birefringent crystallinity disappeared. In several cases, such a melting point could not be obtained because of a lack of fiber birefringence, so the temperature at which the polymer began to flow was taken.

Intrinsic Viscosity. The polyamides were dissolved in *m*-cresol at 21°C for 1 hr on a shaker assembly. Solutions of 0.4% concentration at 21°C were used for viscosity measurement by the method of Burke and Orofino.³

Density. The densities of the polyamides were measured at 25°C in a density-gradient tube prepared with toluene and carbon tetrachloride. The polymer samples used in the measurement were undrawn fibers spun from the melt, unless otherwise indicated.

Moisture Regain. Moisture regain was determined on unoriented fiber which was dried at 60°C in a vacuum oven at about 10 mm Hg for 4 hr, then exposed to 25°C air having a relative humidity of 65% for 48 hr. The fiber was weighed, and then desiccated completely in a vacuum oven at 60°C for 24 hr and weighed again. The difference in weight is the amount of moisture in the fiber at 65% RH. This value can then be converted to a percentage of moisture in the fiber.

Boiling Water Shrinkage. The boiling water shrinkage was determined on fibers which had been drawn approximately five times. These fibers were immersed in boiling water for 5 min. A comparison of the original and final length gives the boiling water shrinkage, which is expressed as a percentage of original length.

Denier. Fiber deniers were determined with a vibrascope.

Tenacity, Elongation, and Modulus. The tenacity, elongation, and modulus values of the drawn fibers were determined on an Instron tester at a rate of extension of 100%/min with the use of a 1-in. gauge length, a head speed of 1 in./min, and a chart speed varied according to the particular sample measured. Young's modulus of elasticity was calculated from the initial slope of the stress-strain curve. All measurements were made at 65% RH, 21°C.

Sonic Modulus. The dynamic tensile modulus (E_s), in grams per denier, was measured at 15000 cps as a function of temperature over the range 30–150°C at 0.03 g/den stress level at 0 and 30% RH. Drawn samples

were preconditioned at constant length at 150°C in nitrogen for 15 min before measurements were made.

Glass Transition Temperature. The glass transition temperatures were determined on the Vibron instrument (Toyo Instrument Company, Tokyo, Japan), a direct-reading dynamic viscoelastometer. The glass transition temperature was taken as the maximum in the $\tan \delta$ peak. The $\tan \delta$ curve was obtained from the plot of the loss modulus (E'') divided by the dynamic modulus (E') as a function of temperature ($\tan \delta = E''/E'$). Measurements were made at 11 cps at 0.03 g/den load on drawn samples which had been preconditioned relaxed at 150°C for 15 min.

RESULTS AND DISCUSSION

Changes in Crystallinity

Copolyamides. The three series of nylon 66 copolyamides with PIDA and hexamethylenediamine, *trans*-1,4-cyclohexanebis(methylamine), and *m*-xylylenediamine were prepared at varying concentrations of diamine-PIDA. The intrinsic viscosities in *m*-cresol ranged from 1.10 to 0.76. The homopolyamide of 6-PIDA had a somewhat lower viscosity of 0.57. These data show that sufficiently high molecular weights were obtained for polymer-fiber formation.

The copolyamides of 66/6-PIDA become translucent beginning at 5 mole-% 6-PIDA substitution. These polymers are completely transparent at 15 mole-% substitution levels, whereas the copolyamides of MXD and t-CBMA are transparent at only 10 mole-% substitution. Birefringence disappears with 30 mole-% or more PIDA substitution.

The x-ray diffraction patterns of the 6-PIDA copolyamides indicated that crystallinity decreased with increased PIDA content. At 30 mole-% substitution crystallinity and orientation virtually disappeared. No difference in the basic crystal cell with increasing PIDA content of the fiber was apparent until crystallinity was destroyed.

From the x-ray data the lateral order index was determined, which is a relative measure of the amount of order of the planes of the crystals in the polymer in a direction perpendicular to the *c* axis of the crystals. The index indicates low crystallinity compared to nylon 66 prepared and drawn

TABLE I
X-Ray Diffraction Measurements^a

Sample	Lateral order index, % ^b	$\beta^{1/2}$ Width	
		100	110 + 010
Nylon 66	53	15.5°	14.5°
66-10 mole-% 6-PIDA	22	28.2°	26.1°
66-15 mole-% 6-PIDA	20	23.7°	21.3°

^a Measurements made on fiber samples drawn about 5.0x.

^b Calculated by a modification of the formula used by Ingersoll¹ for cellulose.

under similar conditions. Highly crystalline nylon 66 may have a lateral order index as high as 85%. The orientation angles for the Miller indices show that the drawn fibers are fairly oriented, as unoriented nylon 66 has a theoretical 90° orientation. Data for the 10 and 15 mole-% 6-PIDA copolymers are given in Table I.

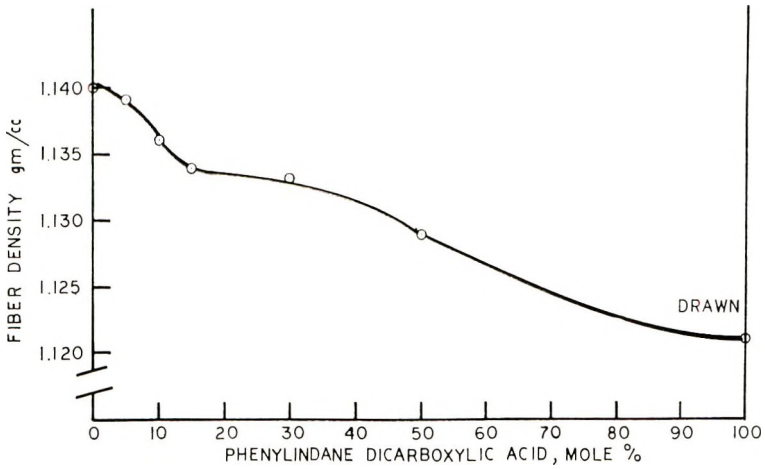


Fig. 1. Influence of PIDA substitution upon the fiber density of nylon 66.

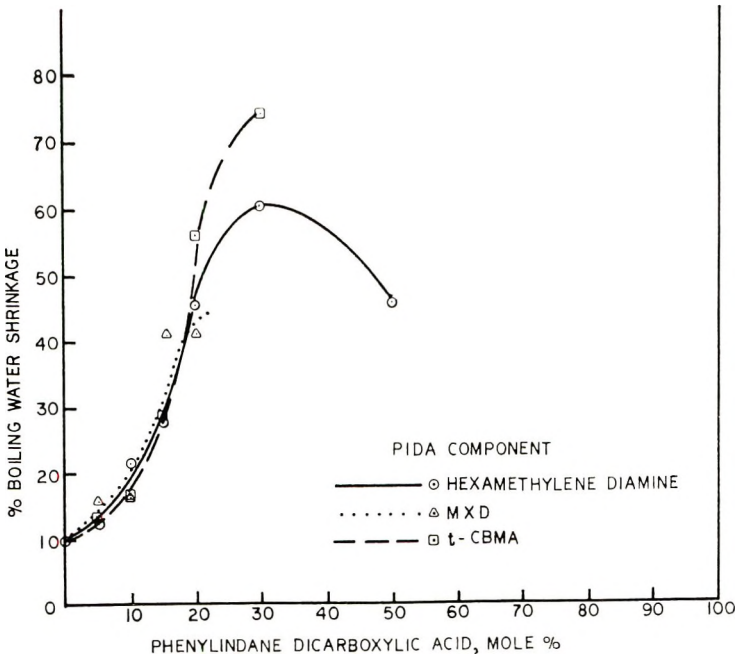


Fig. 2. Effect of PIDA in combination with various diamines upon the boiling water shrinkage of nylon 66.

The disruption of polymer crystallinity is also reflected in some of the physical properties of the PIDA copolymers. The plots of composition versus density, percentage boiling water shrinkage, and moisture regain, (Figs. 1-3) confirm the loss of crystallinity above 20 mole-% substitution of the 6-PIDA copolyamides.

The greatest change in density occurs over the narrow 0-15 mole-% region, after which the rate of loss with concentration is more gradual, indicating that considerable loss of crystallinity has occurred. This result confirms that of Steitz and Knobloch,² although the change in density of the copolyamide between 0 and 100% substitution is only 1.7%, compared to 16.0% for substitution of PIDA for terephthalic acid in poly(ethylene terephthalate). The actual degree of change is probably somewhat greater

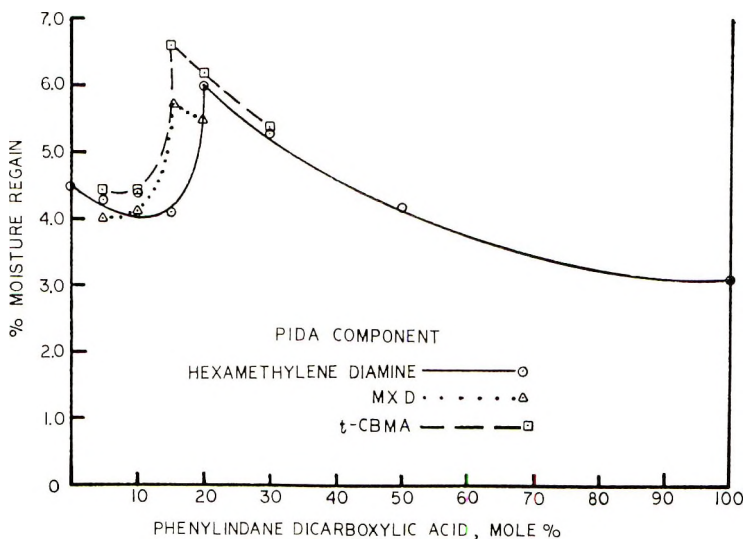


Fig. 3. Effect of PIDA in combination with various diamines upon the percentage moisture regain at 65% RH of nylon 66.

than 1.7% because the 6-PIDA homopolymer sample was drawn, which would be expected to increase the density slightly. However, one would expect less change in polyamides, due to the chemical and structural differences between PET and nylon 66.

Likewise, the greatest changes in boiling water shrinkage occur up to 20 M% PIDA substitution. This again reflects that crystallinity has virtually disappeared because the chain-bonding crystalline forces have been disrupted, thus allowing the polymer chains to return to the lower energy state.

Moisture regain reaches a maximum at 20% because openings in the polymer chains allow increased moisture uptake. The resultant decrease in regain at concentrations above 20% is due simply to the presence of fewer amide linkages in the polymer.

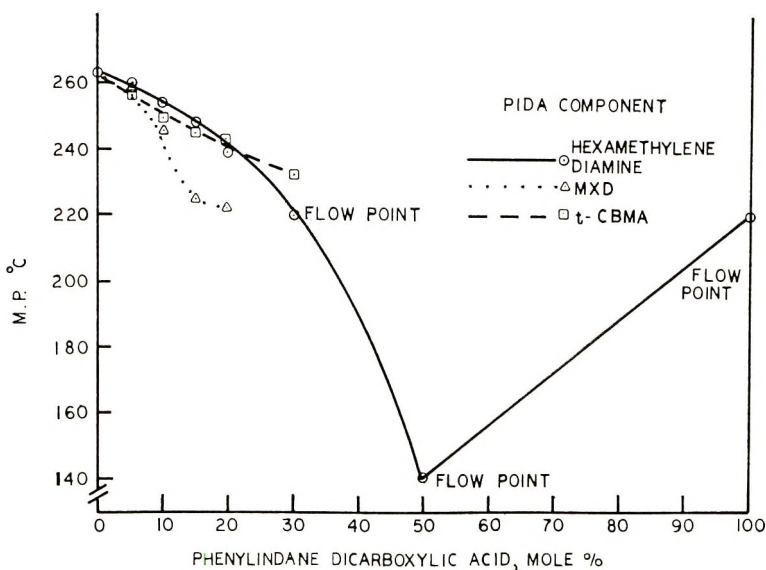


Fig. 4. Melting point vs. composition curves of nylon 66-PIDA copolyamides.

The boiling water shrinkage and moisture regain-composition curves for the CBMA-PIDA and MXD-PIDA show similar changes (Figs. 2 and 3). These curves indicate that the disruptive effect upon polymer crystallinity is heightened by MXD and t-CBMA. However, the MXD copolymers do not appear to open the polymer chains as much.

TABLE II
Tensile Properties of PIDA Copolyamides

Composition	Tenacity, g/den	Elongation, %	Modulus, g/den
66	7.10	18	33
66-5 mole-% 6-PIDA	6.03	18	32
66-10 mole-% 6-PIDA	5.11	20	31
66-15 mole-% 6-PIDA	5.62	15	32
66-20 mole-% 6-PIDA	4.54	43	27
66-30 mole-% 6-PIDA	1.34	56	26
66-50 mole-% 6-PIDA	1.48	43	27
6-PIDA	0.167	53	4
66-5 mole-% t-CBMA-PIDA	3.94	22	27
66-10 mole-% t-CBMA-PIDA	4.54	14	31
66-15 mole-% t-CBMA-PIDA	3.36	10	31
66-20 mole-% t-CBMA-PIDA	3.96	16	27
66-30 mole-% t-CBMA-PIDA	2.43	16	29
66-5 mole-% MXD-PIDA	5.72	16	29
66-10 mole-% MXD-PIDA	4.86	10	46
66-15 mole-% MXD-PIDA	3.18	16	59
66-20 mole-% MXD-PIDA	1.68	35	37

TABLE III
Physical Properties of PIDA Terpolyamides with Terephthalic Acid

Composition			T_m , °C	Moisture regain, %	Boiling water shrinkage, %	Tenacity, g/den	Elongation, %	Modulus, g/den
66, mole-%	6-TA mole-%	6-PIDA mole-%						
85	10	5	257	4.3	12.0	6.6	18	30
80	15	5	258	4.3	—	7.7	15	29
80	10	10	250	4.2	—	6.0	18	30
70	20	10	254	4.6	17.8	5.3	8	49
70	15	15	247	6.2	33.3	4.4	8	49
60	30	10	269	6.5	34.0	4.9	16	31
50	30	20	220 ^a	5.3	Disintegrated	1.2	4	35
40	30	30	228 ^a	4.8	Disintegrated	2.0	15	40
100	0	0	262	4.5	10.0	7.1	18	33
70	30	0	283	4.2	13.0	7.0	18	52

^a Flow point.

The melting point–composition curves for the PIDA copolymers are shown in Figure 4. As would be expected, the crystalline melting point is depressed by increased PIDA content. In the 66/6-PIDA copolymers, melting points could not be determined at 30 mole-% substitution or above because of the lack of sample birefringence, so flow points were obtained instead.

Tenacity, elongation, and modulus values for the copolymers are listed in Table II. These properties further reflect the loss of crystallinity and orientation in that tenacity falls with increased PIDA substitution. Once again, the greatest change in physical property occurs near 20 mole-% substitution. However, no particular trend is observed in initial modulus among the copolymers.

In general, the useful property range for textile fibers appears limited to copolymers containing 20 mole-% PIDA or less.

Terpolyamides. The influence of PIDA upon the fiber properties of the nearly isomorphous copolyamide of nylon 66–poly(hexamethylene terephthalamide) (6-TA) is illustrated in Table III.

As with PIDA copolyamides, reasonable fiber-forming molecular weights were achieved. The intrinsic viscosities ranged from 1.22 to 0.82. The physical properties of the terpolyamides show the conflicting effects of 6-TA vs. 6-PIDA substitution. In general, the introduction of TA into nylon 66 does not greatly change the basic crystallinity of the polymer system. The 30% 6-TA copolymer is opaque, higher melting, and has suffered little change in tenacity, moisture regain, and boiling water shrinkage compared to nylon 66. In addition, the stiffening effect of the benzene ring produces increased modulus. The use of PIDA, however, gives opposite results, as observed from the copolymer data. Therefore, PIDA would be expected to produce similar changes in crystallinity and physical properties in the nearly isomorphous 66–6-TA copolymer system, as it did with nylon 66 alone. Such results were obtained. Transparency occurred at 10 mole-% 6-PIDA substitution. Higher levels (10–20 mole-%) of 6-PIDA again give the greatest change in properties. Shrinkage and moisture regain are increased, while tenacity and melting point decrease. These effects are seen most clearly at levels of high total substitution (>30 mole-%) of TA and PIDA.

A judicious combination of structures, therefore, could produce a polymer of high T_g , but with the added advantages of increased melting point and modulus over those possible with the copolyamides alone.

Effects upon the Glass Transition Temperature

An indirect measurement of the glass transition temperature T_g may be obtained from the sonic modulus versus temperature plot. Such a method is useful because direct determination of T_g is difficult. The usual means of T_g measurement such as penetration modulus, differential thermal analysis, various dynamic mechanical methods, and the host of determinations based upon changes in the temperature coefficients of various thermodynamic

functions (specific volume, heat content, etc.) are time-consuming. Often these techniques do not correlate well with each other. In addition, moisture greatly affects T_g in many polyamides,⁵ which requires that great care be taken to control humidity during the course of the measurement. The physical state of the polymer also exerts an influence on T_g . Orientation and, to a small extent, crystallinity⁶ produce changes in T_g , which means that all samples must be in the same state during measurement. Since the emphasis in this paper is principally on the properties of polyamide fibers, the determination of the T_g of fiber samples becomes more meaningful.

Therefore, the measurement of the fiber's sonic modulus versus temperature was chosen because this method is rapid, allows a number of samples to be studied simultaneously, and permits good humidity control during measurement. The principal disadvantage of this method is that the T_g itself cannot easily be measured because of the difficulty of determining exactly at which temperature the modulus begins to change most rapidly.

The sonic modulus-temperature curves for nylon 66 at 0 and 30% RH are illustrated in Figure 5.

An increase in T_g results in a shift of the curve along the axis to the right. Similarly, a decrease in T_g produces a shift to the left. For convenience, approximate differences among high T_g polymers can be expressed by the per cent retention of modulus at a particular temperature, T . This value is obtained from the modulus at temperature T divided by the modulus at 30°C multiplied by 100. If the retention of modulus of a polymer at a particular temperature is higher than that of the control sample at the same temperature, then the polymer is said to have a higher T_g than the control. Such a measurement is useful in establishing the relative differences in T_g among fibers. While the actual value of sonic modulus varies from sample to sample, such changes do not affect the T_g comparisons made in this paper.

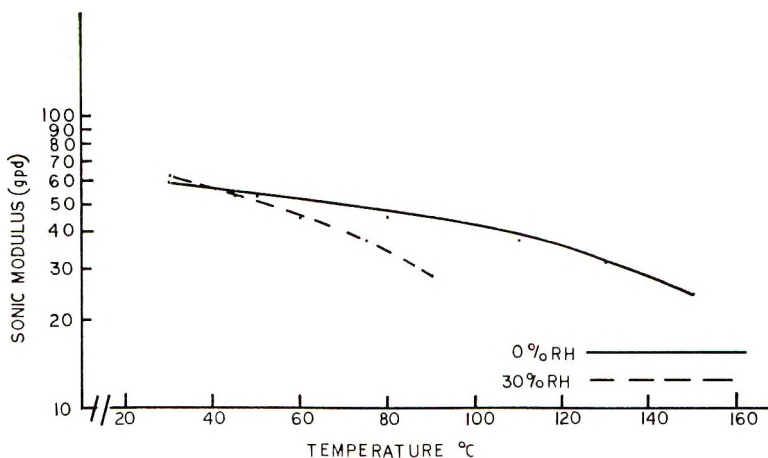


Fig. 5. Relationship of sonic modulus of nylon 66 to temperature and humidity.

TABLE IV
Influence of PIDA Copolyamides upon the Glass Transition
Temperature of Nylon 66

Composition	E_s retained, %		T_g , °C		tan δ_{max}	
	0% RH, 130°C	30% RH, 90°C	0% RH	30% RH	0% RH	30% RH
	66-0 mole-% 6-PIDA	55	54	110	90	0.093
66-5 mole-% 6-PIDA	61	57	125	100	0.080	0.088
66-10 mole-% 6-PIDA	64	64	126	110	0.115	0.115
66-15 mole-% 6-PIDA	75	70	145	>120	0.146	>0.106
66-20 mole-% 6-PIDA	—	—	140	130	0.232	0.200
66-5 mole-% t-CBMA-PIDA	74	66	130	100	0.090	0.094
66-10 mole-% t-CBMA-PIDA	74	68	140	110	0.127	0.104
66-15 mole-% t-CBMA-PIDA	79	75	—	—	—	—
66-20 mole-% t-CBMA-PIDA	84	77	160	130	0.265	0.200
66-5 mole-% MXD-PIDA	63	61	—	—	—	—
66-10 mole-% MXD-PIDA	64	63	—	—	—	—
66-15 mole-% MXD-PIDA	67	67	—	—	—	—
66-20 mole-% MXD-PIDA	66	71	—	—	—	—

Sonic modulus-temperature measurements were made at both 0 and 30% RH in order to determine differences in the moisture sensitivity of T_g , as well as to establish relative differences in transition temperatures. The figure of 90°C at 30% RH was selected because humidity control in the instrument is quite difficult above this temperature.

Verification of the sonic modulus response was then obtained by direct T_g measurement via low frequency dynamic mechanical (Vibron) property techniques. However, both dynamic techniques sometimes show some variation in data due to sample-to-sample differences in crystallinity, orientation, and draw ratio. While these differences are small, they will cause some data scatter in fiber-fiber comparisons.

Copolyamides. The retention of sonic modulus (E_s) at 0 and 30% RH for the copolymers (Table IV) indicate that PIDA does greatly increase the T_g of nylon 66. As expected, the copolymers with CBMA possess the

TABLE V
Influence of PIDA-TA Terpolyamides upon the Glass Temperatures of Nylon 66

66, mole-%	Composition		E_s retained, %		T_g , °C		tan δ_{max}	
	6-TA, mole-%	6-PIDA, mole-%	0% RH,	30% RH,	0% RH	30% RH	0% RH	30% RH
			130°C	90°C				
100	0	0	55	54	110	90	0.093	0.084
85	10	5	70	60				
80	15	5	71	60	130	110	0.100	0.083
80	10	10	71	67				
70	20	10	74	70	140	120	0.138	0.130
70	15	15	74	72				
60	30	10	71	72				
95	5	0	57	48	152	122	0.180	0.150
90	10	0	57	59	110	100	0.074	0.088
80	20	0	69	62	120	102	0.086	0.095
70	30	0	74	63	130	110	0.087	0.086
							0.098	0.097

greatest modulus stability. This effect is undoubtedly due to the stiff, compact, symmetrical cyclohexane ring. Surprisingly, the copolymers which incorporate MXD are inferior to the hexamethylene diamine polymers. The lack of symmetry in the *m*-substituted aromatic ring, coupled with the bulky PIDA ring, has obscured the stiffening influence of the aromatic ring, which is shown in polymers such as MXD-6.⁷

The t-CBMA-PIDA copolyamides have higher T_g values at 0% RH than those of 6-PIDA, but are identical at 30% RH (Table IV). Such results indicate that the polymers of t-CBMA-PIDA are more susceptible to the plasticizing action of water.

The low-frequency dynamic measurements also offer additional evidence concerning the loss of crystallinity of PIDA copolyamides of nylon 66. The $\tan \delta_{\max}$ height increases with increased PIDA substitution. Takayanagi⁸ attributes increased $\tan \delta_{\max}$ height to decreased polymer crystallinity. As can be seen from the data, the copolyamides of t-CBMA-PIDA are less crystalline than those of 6-PIDA.

Terpolyamides. The sonic modulus retention at 0 and 30% RH for the terpolyamides of 66/6-TA-/6PIDA shows that PIDA substitution allows a further increase in T_g over that possible with 66/6-TA. Higher retentions of modulus are obtained at lower levels of substitution of both PIDA and TA. The data are given in Table V.

Similar results are obtained at low frequency, in that the T_g of selected samples follows the sonic modulus trends. However, an increase in the amorphous character of the terpolyamides over the PIDA copolyamides is indicated by higher $\tan \delta$ values.

The author gratefully acknowledges the technical assistance of Mr. J. A. Shaver in the preparation of some of the polymers described in this paper. Assistance was also obtained from Mr. W. H. Howard and Mr. T. Murayama for dynamic mechanical data, and from Mr. B. B. Bowles for x-ray data. The author is also indebted to Mr. G. C. Stow for his suggestions and criticisms.

References

1. J. S. Ridgway, U. S. 3,376,270, April 2, 1968.
2. A. Steitz, Jr., and J. O. Knobloch, paper presented to Organic Coatings and Plastics Division, 155th American Chemical Society National Meeting, San Francisco, California, March 1968; *Abstracts of Papers* **28**, No. 1, 638 (1968).
3. J. J. Burke and T. A. Orofino, *J. Polym. Sci. A-2*, in press.
4. H. B. Ingersoll, *J. Appl. Phys.*, **17**, 924 (1946).
5. G. M. Bryant and A. T. Walter, *Text. Res. J.*, **29**, 211 (1959).
6. L. E. Nielsen, *Mechanical Properties of Polymers*, Reinhold, New York, 1962, p. 248.
7. E. I. duPont de Nemours and Company, Brit. Pat. 918,637 (February 13, 1963).
8. M. Takayanagi, *Mem. Fac. Eng. Kyushu Univ.*, **23**, No. 1, 2 (1963).

Received January 29, 1969

Copolymerization of Acrylonitrile. I. Copolymerization with Styrene Derivatives Containing Nitrile Groups in the Side Chain

SAMUEL H. RONEI and DAVID H. KOHN, *Department of
Chemistry, Technion—Israel Institute of Technology, Haifa, Israel*

Synopsis

Acrylonitrile was copolymerized in bulk with cinnamionitrile (I), ethyl benzylidencyanoacetate (II), and benzylidenemalononitrile (III) by radical initiation up to low conversions. The conventional scheme of copolymerization fitted all the three copolymer pairs.

INTRODUCTION

Polyacrylonitrile, unlike most other industrial thermoplastic polymers, is actually insoluble in almost all organic solvents and also incompatible with the conventional plasticizers. It is only soluble in very polar solvents such as dimethyl sulfoxide, dimethylformamide, or in concentrated aqueous solution of certain salts. Polyacrylonitrile is stable up to 150–200°C, turning yellow at higher temperature.¹ On ignition it burns only slowly and it has a comparatively good stability in sunlight.

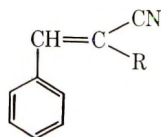
This exceptional high stability of polyacrylonitrile against heat and sunlight and its restricted solubility in highly polar solvents only is due to the structure of the polymer, dominated by the strong dipole–dipole interaction between the nitrile groups.^{2,3}

Although these properties of polyacrylonitrile are very advantageous for certain applications, it is just due to this stability and the consequent lack of flow that processing of the homopolymer of acrylonitrile by the conventional molding methods for thermoplastic polymers is very difficult.

In order to overcome these drawbacks, copolymers of acrylonitrile which could be processed by conventional methods, but which had a lower temperature and solvent stability than the homopolymer, were prepared industrially.

It was the object of this investigation to copolymerize acrylonitrile with such polar comonomers, which owing to their bulkiness could act as internal plasticizers without decreasing the stability of the copolymers in comparison to polyacrylonitrile.

The comonomers used have the general formula:



where R is H(I), $-\text{COOC}_2\text{H}_5$ (II), or $-\text{CN}$ (III). These comonomers have been previously investigated together with styrene⁴⁻⁶ and were found to result in improved temperature stability in comparison to homopoly-styrene.

EXPERIMENTAL

Materials and Preparation of Monomers

Acrylonitrile. Commercial Eastman product was dried over calcium chloride and distilled before use under nitrogen at 77°C .

Comonomers. Cinnamionitrile, ethyl benzylideneacrylate, and benzylidenemalononitrile were prepared as described previously.⁴

Benzoyl Peroxide. Eastman pure grade was used after recrystallization from methanol.

Dimethyl Sulfoxide (DMSO). Fluka product (purum) was distilled at 95°C at 25 mm Hg and kept under nitrogen.

Copolymerization

The parameters of copolymerization were determined by bulk copolymerization with the use of free radicals for initiation. Polymerizations were carried out in Pyrex tubes with a bulb at the lower end and a constriction near the upper end. After flushing with nitrogen, the monomers (10–15 g) and the initiator (benzoyl peroxide: 0.1% by weight) were introduced and frozen immediately in a Dry Ice–acetone mixture. The tubes were flushed three times with nitrogen, evacuated down to 0.3 mm, sealed at the constriction, and kept in the Dry Ice–acetone mixture until the start of polymerization.

The copolymerizations were carried out in a temperature-controlled bath fitted with shaking device in order to keep the reaction mixtures well mixed. At the fixed polymerization temperature (70°C), the starting reaction mixture was a homogeneous solution. The proper time of copolymerization, i.e., the time necessary to polymerize not more than 10% of the mixture, was found by trial and error. After the polymerization, the reaction tubes were cooled to room temperature, opened, and the reaction mixture was poured into methanol. The products were washed with methanol and repeatedly precipitated by methanol from a solution in dimethyl sulfoxide. The purified copolymers were dried at 80°C under reduced pressure for 24 hr.

Analyses of Products

All the copolymers were obtained as yellowish powders. The composition of the copolymers was determined by microanalyses for C, H, N, and O. In all cases, residues (2.5–5%) were obtained after combustion, and the compositions of the copolymers were calculated accordingly.

Melting Ranges

Attempts to determine the melting range of the various copolymers in capillaries under air and under nitrogen were unsuccessful. All the copolymers showed a color change to brown and then to black and were carbonized above 300°C.

Solubility

All copolymers are soluble in dimethyl sulfoxide.

RESULTS AND DISCUSSION

The conditions and results of the various copolymerizations are summarized in Tables I–III.

TABLE I
Acrylonitrile (M_1) and Cinnamionitrile I (M_2)

Experiment no.	M_2 , mole fraction of monomer 2	Time of polymerization, min	Conversion, %	Nitrogen content of copolymer, %	m_2 , mole fraction in copolymer
69/2	0.8	1210	0.9	16.2	0.45
69/3	0.7	505	2.4	18.9	0.28
69/4	0.54	155	1.8	22.0	0.15
69/6	0.4	140	2.5	23.5	0.09
69/7	0.3	63	2.1	23.45	0.09
69/8	0.2	50	2.2	25.4	0.03
69/9	0.1	30	3.2	23.35	0.09

The calculation of the reactivity ratios for the various copolymers were based on the elementary analyses of the products. It was therefore of greatest importance to free the copolymers from any residual monomer. In order to prevent the inclusion of any monomer in the copolymers during purification, precipitation of the copolymers was carried out in a Waring Blender.

A further problem was the complete removal of the solvent, dimethyl sulfoxide, which tends to be bound to the polar groups of the polymer. Only by heating the copolymer at 80°C under reduced pressure (0.5 mm Hg) for at least 10 hr could the last traces of the solvent be removed.

Infrared spectra were obtained after purification of the polymers.

TABLE II
Acrylonitrile (M_1) and Ethyl Benzyldenecyanoacetate II (M_2)

Experiment no.	M_2 , mole fraction of monomer 2	Time of polymerization, min	Conversion, %	Nitrogen content of copolymer, %	m_2 , mole fraction in copolymer
63/1	0.9	690	2.8	21.7	0.077
63/2	0.8	690	3.8	21.7	0.077
63/3	0.7	120	1.05	23.6	0.0435
63/4	0.6	72	1.7	23.25	0.048
63/5	0.5	40	0.9	24.0	0.035
63/6	0.4	50	3.0	24.0	0.035
63/7	0.3	40	1.85	24.6	0.025
63/8	0.2	40	7.0	24.15	0.032
63/9	0.1	7	1.02	25.2	0.015

TABLE III
Acrylonitrile (M_1) and Benzyldenemalononitrile III (M_2)

Experiment no.	M_2 , mole fraction of monomer 2	Time of polymerization, min	Conversion, %	Nitrogen content of copolymer, %	m_2 , mole fraction in copolymer
66/3	0.7	600	3.8	24.4	0.100
66/4	0.6	465	1.8	25.5	0.035
66/6	0.4	255	5.2	25.8	0.025
66/7	0.3	120	8.5	25.7	0.03
66/8	0.2	60	3.9	25.4	0.045
66/9	0.1	30	3.0	25.75	0.028

The reactivity ratios r_1 and r_2 were determined by the graphical method⁷ (Figs. 1-3) by using the equation (1):

$$r_2 = (M_1/M_2) \{ (m_2/m_1) [1 + (M_1/M_2)r_1] - 1 \} \quad (1)$$

which is the linear form of

$$m_1/m_2 = (M_1/M_2) [(r_1 M_1 + M_2)/(r_2 M_2 + M_1)] \quad (2)$$

The negative values obtained for r_2 are due to some inaccuracies in the elementary analyses and in the graphical method. Actually $r_2 = 0$ for all three comonomers was reported previously,⁴ and no homopolymers were obtained by radical initiation.

As there exists a penultimate effect for all three comonomers in copolymerization with styrene, the possibility of such an effect was also examined for copolymerization with acrylonitrile by use of the scheme of Merz⁸ and Barb's notation:⁹

$$r_1 = [(n-1)/x^2] (1/r_1') + (n-2)/x \quad (3)$$

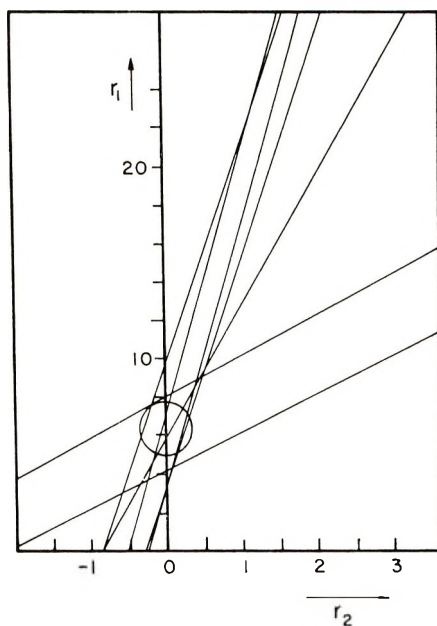


Fig. 1. Copolymerization of acrylonitrile (M_1) with cinnamionitrile (M_2). Determination of r_1 and r_2 by using eq. (1). $r_1 = 6.4 \pm 1$; $r_2 = 0 \pm 0.5$.

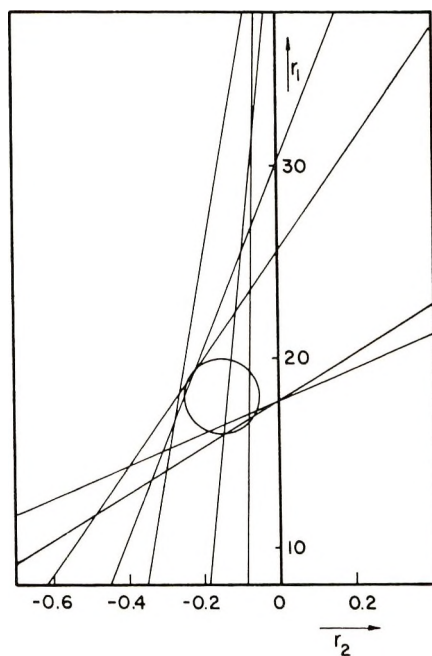


Fig. 2. Copolymerization of acrylonitrile (M_1) with ethyl benzylideneacrylate (M_2). Determination of r_1 and r_2 by using eq. (1). $r_1 = 18 \pm 2$; $r_2 = -0.15 \pm 0.1$.

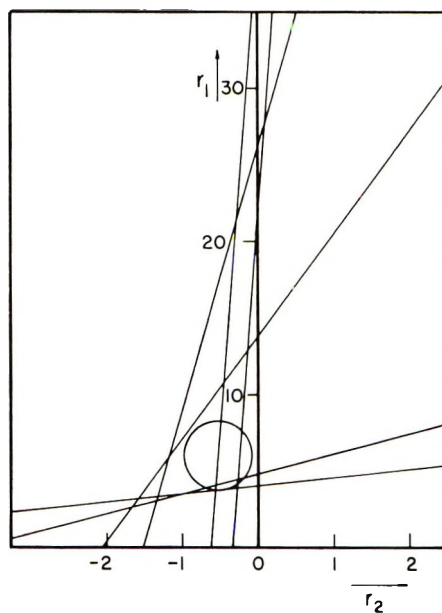


Fig. 3. Copolymerization of acrylonitrile (M_1) with benzylidenemalononitrile (M_2). Determination of r_1 and r_2 by using eq. (1). $r_1 = 6.2 \pm 1.8$; $r_2 = -0.5 \pm 0.4$.

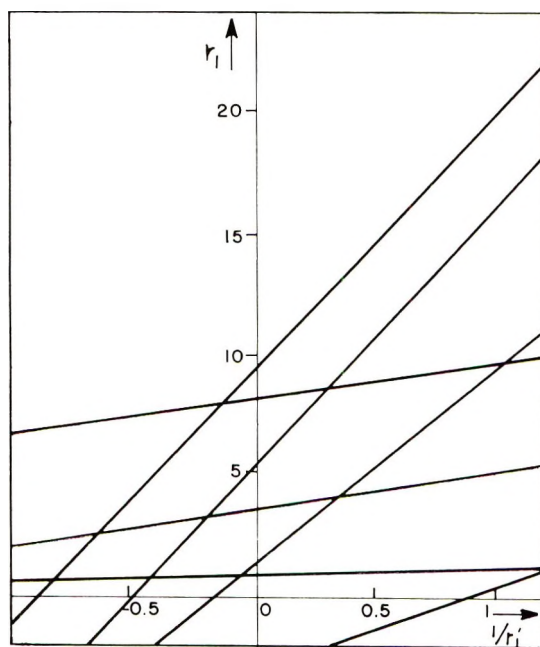


Fig. 4. Copolymerization of acrylonitrile (M_1) with cinnamonnitrile (M_2). Attempted determination of r_1 and r_1' by using the enlarged scheme.

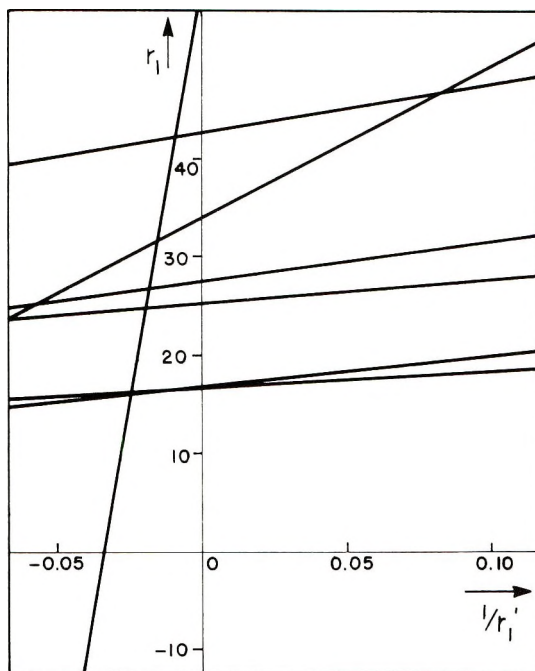


Fig. 5. Copolymerization of acrylonitrile (M_1) with ethyl benzylidenecyanoacetate (M_2). Attempted determination of r_1 and r_1' by using the enlarged scheme.

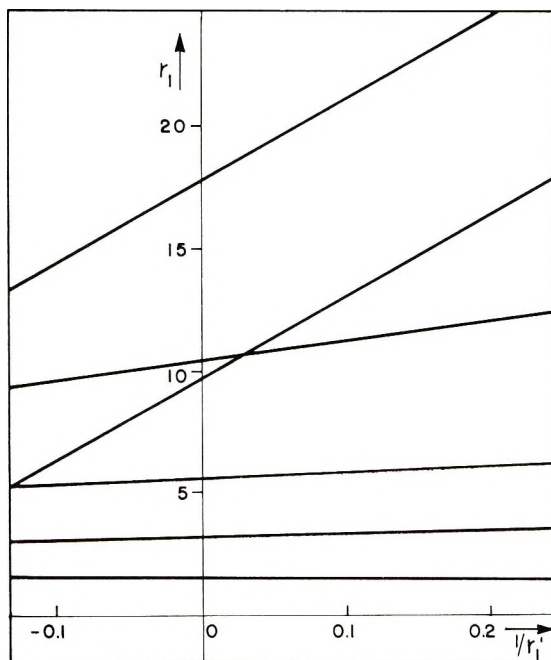


Fig. 6. Copolymerization of acrylonitrile (M_1) with benzylidenemalononitrile (M_2). Attempted determination of r_1 and r_1' by using the enlarged scheme.

where $x = M_1/M_2$ and $n = m_1/m_2$. Graphs for r_1 against $1/r_1'$ yielded widely scattered lines, and thus there seems to be no penultimate effect for these copolymers (Figs. 4-6). Thus this effect exists for the copolymerizations of the three comonomers with styrene (a nonpolar monomer⁴) but not, as expected, for their copolymerization with acrylonitrile, when the whole copolymer chain consists of monomers of similar polarity.

The Alfrey-Price Q_2 and e_2 values¹⁰ (Table IV) were calculated according the equation

$$r_1 = (Q_1/Q_2) \exp\{-e_1(e_1 - e_2)\} \quad (4)$$

The r_1 values used, were obtained from the copolymerization of the three comonomers with acrylonitrile (present paper) and from their copolymerization with styrene either according the improved scheme⁴ or according the simple kinetic scheme.* It was assumed that $Q_1 = 1.0$ and $e_1 = -0.8$ for styrene and $Q_1 = 0.60$ and $e_1 = 1.20$ for acrylonitrile.

TABLE IV
 Q and e Values

Monomer	Q_2	e_2	Reference
Cinnamionitrile (I)	0.11	1.21	This paper ^a
	0.11	1.19	This paper ^b
	0.32	0.75	10
Ethyl benzylidenecyanoacetate (II)	0.13	2.70	This paper ^a
	0.14	2.44	This paper ^b
	1.24	0.87	10
Benzylidenemalononitrile (III)	0.52	2.60	This paper ^a
	0.38	2.35	This paper ^b
Acrylonitrile (AN)	0.60	1.20	10
Crotononitrile (CN)	0.009	1.13	11
Methyl α -cyanoacrylate (MCA)	17	2.48	12
Vinylidene cyanide (VC)	20.13	2.58	10
Ethyl cinnamate (EC)	0.18	0.46	13
Methyl atropate (MA)	6.1	1.3	14
Ethyl atropate (EA)	4.28	1.41	13
Diethyl chloromaleate (DCM)	0.056	1.65	10

^a r_1 from copolymerization with styrene according to improved scheme.

^b r_1 from copolymerization with styrene according to simple kinetic scheme.

In addition, Q_2 and e_2 for comonomers I and II as reported by Ham¹⁰ are given in Table IV. Our Q_2 and e_2 values differ from those reported by Ham, yet his results were obtained from one set of data only.

For comparison, Q_2 and e_2 of several monomers, having chemical structures similar to those of our three comonomers, are given.

One can see, that the Q_2 of the 1,2-disubstituted vinyl (cinnamionitrile, I) is quite low and similar to the Q_2 values of EC, and the same applies to

* The values of r_1 for the copolymerization of the comonomers I, II, and III with styrene, calculated by the simple kinetic scheme are: St-I, $r_1 = 2.3$; St-II, $r_1 = 0.51$; St-III, $r_1 = 0.25$.

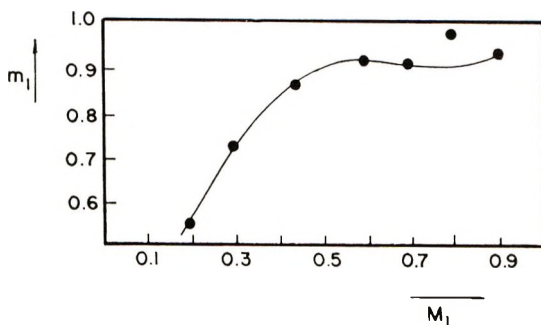


Fig. 7. Copolymerization of acrylonitrile (M_1) with cinnamionitrile (M_2). Initial copolymer composition vs. composition of monomer feed.

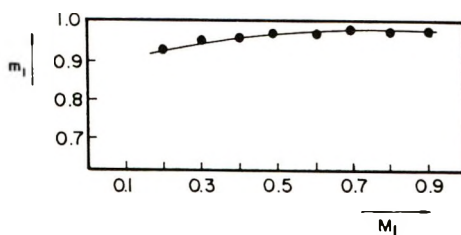


Fig. 8. Copolymerization of acrylonitrile (M_1) with ethyl benzylidenecyanoacetate (M_2). Initial copolymer composition vs. composition of monomer feed.

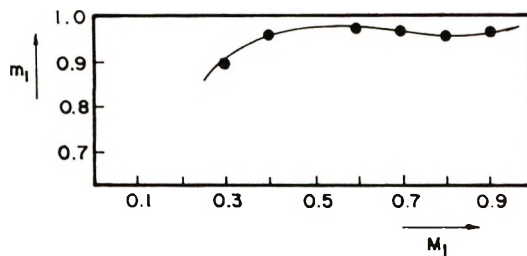


Fig. 9. Copolymerization of acrylonitrile (M_1) with benzylidenemalononitrile (M_2). Initial copolymer composition vs. composition of monomer feed.

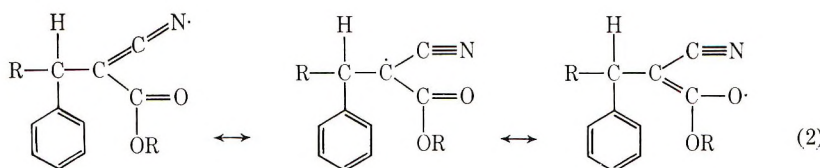
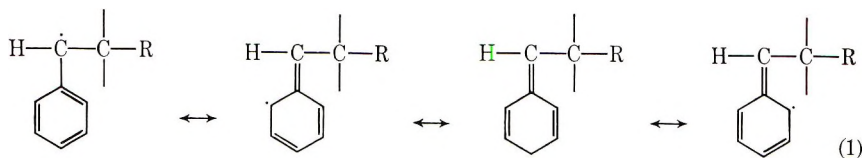
1,1,2-trisubstituted monomers (II, III, DCM). On the other hand, unsymmetrical 1,1-disubstituted monomers with a $\text{CH}_2=\text{C}$ group (VC, MCA, MA, EA) have a rather high Q_2 . Regarding e_2 , characterizing the polarity, the values for AN, I, and CN are nearly equal, and the same applies to the corresponding pairs II-MCA and III-VC.

The dependence of the composition of the copolymers m_1 on the composition of the monomer mixture M_1 is given in Figures 7-9. In all three cases, the copolymers show a much higher content of acrylonitrile than the monomer mixtures. As the three comonomers do not homopolymerize under the conditions given above, one can assume that the monomer sequence in the three copolymers consists of larger blocks of acrylonitrile

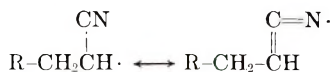
units, interrupted by single comonomer molecules. The dependence of the rates of copolymerization can be summarized for all three pairs as follows. The rates of copolymerization decrease with increasing comonomer content. This rate decrease is about three times up to 30% comonomer content, but becomes much stronger with a comonomer content of up to 80%. However, as the rate of polymerization of acrylonitrile is very high indeed, the addition of small quantities of these comonomers would be even useful for control of the polymerization reaction itself, provided that the copolymers obtained excel the homopolymer regarding certain properties.

The rate of polymerization depends on the polarities of the monomers, on steric factors, and on the resonance stabilization of the radicals. Due to the α and β substitution of the double bond, there exists a strong steric factor for all three comonomers in comparison to acrylonitrile. Thus at about equal polarity but due to the steric factor, the acrylonitrile radical seems to react preferably with another acrylonitrile molecule than with one of the comonomers.

Due to the presence of a phenyl group, one or two nitrile groups, or an ester group, all three comonomers have a conjugated system. By the attack of free radicals on the α,β -substituted double bond, resonance-stabilized radicals are produced:



The resonance stabilization according to (1) is of course greater, yet both possibilities affect a decrease of the reactivity of the comonomer radicals. The acrylonitrile radical is rather weakly stabilized,



and consequently the composition of the resulting copolymer is determined mainly by the relatively high rate of self-addition of acrylonitrile. Further, the faster diffusion of the acrylonitrile in comparison with the bulky comonomers may have to be considered. In the copolymerization with styrene, where all the monomers are rather bulky and all are highly stabilized, an increase of the rate of polymerization seems to be mainly due to the polarity of the comonomers.

The reluctance of the three comonomers (I, II, and III) to copolymerize with acrylonitrile in comparison to their readiness to copolymerize with styrene is also consistent with their $Q-e$ values.

This paper is taken in part from a thesis submitted by Samuel H. Ronel to the Department of Chemistry, Technion—Israel Institute of Technology, Haifa, in partial fulfillment of the degree of M.Sc.

References

1. S. L. Madorsky, *Thermal Degradation of Organic Polymers*, Interscience Publishers, Inc., New York, 1964.
2. R. D. Andrews and R. M. Kimmel, *J. Polym. Sci. B*, **3**, 167 (1965).
3. P. H. Lindenmayer and R. Hoseman, *J. Appl. Phys.*, **34**, 42 (1963).
4. M. Kreisel, U. Garbatski, and D. H. Kohn, *J. Polym. Sci. A*, **2**, 105 (1964).
5. M. Narkis and D. H. Kohn, *J. Polym. Sci. A-1*, **5**, 1033 (1967).
6. M. Narkis and D. H. Kohn, *J. Polym. Sci. A-1*, **5**, 1049 (1967).
7. T. Alfrey, Jr., J. J. Bohrer, and H. Mark, *Copolymerization*, Interscience Publishers, New York, 1952.
8. E. Merz, T. Alfrey, and G. Goldfinger, *J. Polym. Sci.*, **1**, 75 (1946).
9. W. G. Barb, *J. Polymer Sci.*, **11**, 117 (1953).
10. G. E. Ham, *Copolymerization*, Interscience Publishers, Inc., New York, 1964.
11. Y. Minoura, T. Tadokoro, and Y. Suzuki, *J. Polym. Sci. A-1*, **5**, 2641 (1967).
12. T. Otsu and B. Yamada, *Makromol. Chem.*, **110**, 297 (1967).
13. T. Otsu, B. Yamada, and T. Nozaki, *Kogyo Kagaku Zasshi*, **70**, 1941 (1967).
14. K. Chikanishi and T. Tsuruta, *Makromol. Chem.*, **73**, 231 (1964).

Received January 23, 1969

Copolymerization of Acrylonitrile. II. Physical and Mechanical Properties of Copolymers with Styrene Derivatives Containing Nitrile Groups in the Side Chain

SAMUEL H. RONEL and DAVID H. KOHN, *Department of Chemistry, Technion—Israel Institute of Technology, Haifa, Israel*

Synopsis

Copolymers of acrylonitrile with cinnamionitrile (I), ethyl benzylidenecyanoacetate (II), and benzylidenemalononitrile (III) were prepared in suspension up to high conversions. Films and molded specimens were made from the copolymers and their basic physical and mechanical properties, such as solubility, viscosity, glass transition temperature, and tensile and compressive strength were determined. Further, treatment by heat and ultraviolet light, the permeability of water vapors, and the behavior of films in a weathering tester were studied.

INTRODUCTION

In the preceding paper,¹ the copolymerization in bulk of acrylonitrile together with cinnamionitrile (I), ethyl benzylidenecyanoacetate (II), and benzylidenemalononitrile (III) and the determination of their copolymerization parameters, were reported. The conversion curves show, that the comonomer content m_2 of the copolymers of acrylonitrile with comonomers I, II, and III is 4-8 mole-%, regardless of the composition of the monomer mixture.

It was the object of the work reported in the present paper to develop a suitable polymerization method for these new copolymers and further to study, in comparison with homopolyacrylonitrile, the basic physical and mechanical properties of films and molded specimens made from these copolymers.

EXPERIMENTAL

Preparation of Copolymers

Suspension Polymerization. The reactions were carried out in a resin flask, fitted with a Teflon stirrer, reflux condenser, gas-inlet tube and a buret. The flask was placed in a thermocontrolled waterbath ($\pm 1^\circ\text{C}$). Most of the experiments were carried out with freshly precipitated calcium phosphate as suspending agent.²

TABLE I
Copolymerization of Acrylonitrile with Comonomers I, II, and III in Suspension

Experi- ment no.	Water, ml.	Suspending agent	Acrylonitrile		Comonomer		Initiator, g	Tem- pera- ture, °C	Time, hr	Yield		Acrylo- nitrile content, %	[η], dl/g
			g	mole	Type	g				mole	g		
122.1	260	Ca phosphate	106	2	—	—	0.70	68	4	90	85	100	9.45 ^a
98.1	75	"	26.5	0.5	I	7.05	0.17	60	15	15	45.5	91	3.35
101.1	200	"	79.5	1.5	II	20.1	0.35	70	4	63	64	95	3.20
125.1	400	"	160	3	III	12	1.2	64	3	110	65	86	3.15

^a The intrinsic viscosity [η] in dimethylformamide at 35°C was 7.1.³

The monomer mixture, containing the initiator azodiisobutyronitrile, was added dropwise at the reaction temperature to the aqueous suspension of the phosphate under constant stirring (about 450 rpm) and in a nitrogen atmosphere. The copolymer precipitated in the form of small pearls, which were washed first with hydrochloric acid (about 15%) and then with water, methanol, and diethyl ether. Details on the reaction conditions and results are summarized in Table I.

The preparation of the comonomers and purification of acrylonitrile and the initiators are given in the preceding paper.¹

Purification of Polymers. For molding of specimens and preparations of films, the polymers were ground to a fine powder, extracted with methanol in a Soxhlet apparatus for 24 hr, and dried at 80°C under reduced pressure.

For chemical analyses, viscosity, infrared and thermogravimetric analyses, the polymers were further purified by dissolving them in dimethyl sulfoxide, followed by precipitation with methanol and drying for 24 hr at 70°C at 0.5 mm Hg.

Preparation of Films. Films of 10-120 μ thickness, were prepared from solutions of the polymers in dimethyl sulfoxide (1-3%) by evaporation of the solvent at 60°C under reduced pressure (about 4 mm Hg). The disappearance of the solvent was examined by infrared analysis. The films were transparent and colourless.

The solutions should not be left in the open, because they absorb water and then produce opaque films on evaporation.

Preparation of Molded Specimens. Cylindrical specimens (diameter 10 mm) of various heights and rectangular specimens (length 70 mm, width 10 mm, height 1-2 mm) were prepared by compression molding. The optimal molding conditions were experimentally determined for each polymer. All the molded specimens were transparent but yellowish.

Physical and Mechanical Test Methods

Viscosity. For determination of the intrinsic viscosity, the copolymers were dissolved in dimethyl sulfoxide and measurements were carried out in a Ubbelohde viscometer at $25 \pm 0.01^\circ\text{C}$. Dimethyl sulfoxide is hygroscopic, and therefore in order to exclude humidity from the air the preparations of the solutions and the viscosity measurements were carried out under nitrogen. The values of the intrinsic viscosity of the polymers under investigation are given in Table I.

Infrared Spectra. Infrared analyses of polymer films with a thickness of about 30 μ were determined (Figs. 1-4) on a Perkin-Elmer 237 spectrophotometer. The films were prepared from dimethyl sulfoxide solution, and dried for 3 days at 70°C under reduced pressure. Absorption in the region 3500-3650 cm^{-1} appeared in films kept under normal atmospheric conditions for some time but was not visible when measured shortly after drying.

The strong absorptions at 2220 and 1440 cm^{-1} correspond to the nitrile group; for the copolymer with II, there is also the absorption band of the ester group (1730 cm^{-1}). The absorption bands for the phenyl group at about 1600 cm^{-1} appear in all three copolymers.

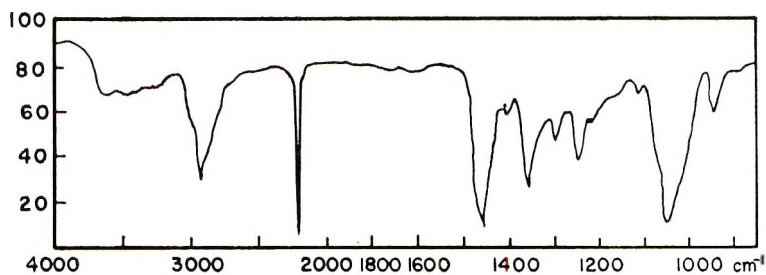


Fig. 1. Infrared spectrum of polyacrylonitrile.

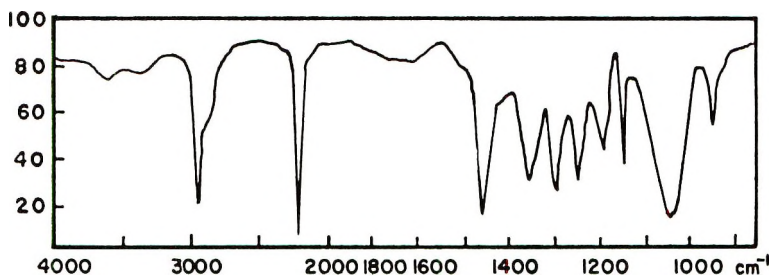


Fig. 2. Infrared spectrum of acrylonitrile-cinnamitrile copolymer.

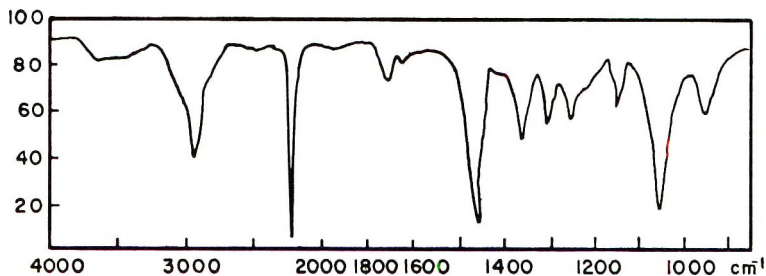


Fig. 3. Infrared spectrum of acrylonitrile-ethyl benzylidenecyanoacetate copolymer.

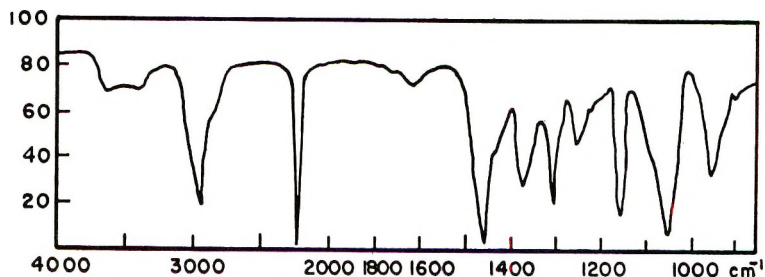


Fig. 4. Infrared spectrum of acrylonitrile-benzylidenemalononitrile copolymer.

Glass Transition Temperature. The glass transition temperature was determined according to the method of Edgar and Ellery⁴ on specimens either molded at the optimum molding conditions or pressed at room temperature at a pressure of about 6000 kg/cm².⁵ According to this method, a

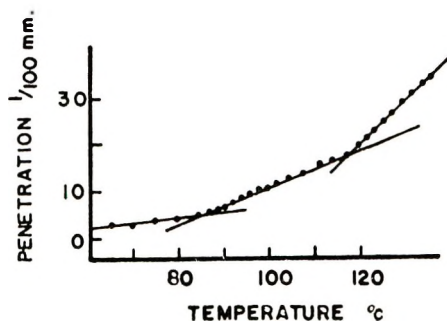


Fig. 5. Determination of the glass transition temperature of polyacrylonitrile.

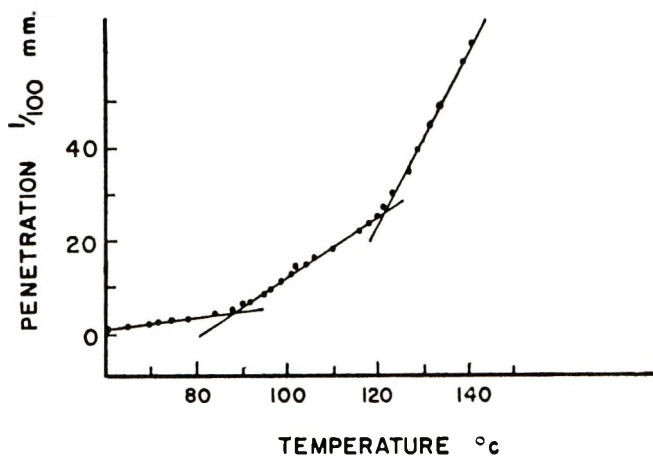


Fig. 6. Determination of the glass transition temperature of acrylonitrile-cinnamionitrile copolymer.

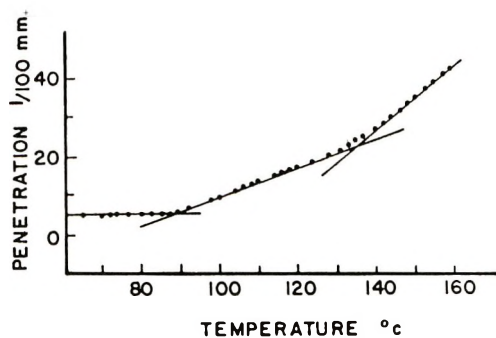


Fig. 7. Determination of the glass transition temperature of acrylonitrile-ethyl benzylidene cyanoacetate copolymer.

TABLE II
 Glass Transition Temperature

Experiment no.	Polymer type ^a	Hot molded		Fig. no.	Cold pressed; first transition, °C
		First transition, °C	Second transition, °C		
122.1	PAN	87	136.5	5	76
98.1	AN-I	88.5	121.5	6	77
101.1	AN-II	85.5	118	7	84.5
125.1	AN-III	88.5	123.5	8	91

^a PAN = polyacrylonitrile; AN-I = acrylonitrile-cinnamionitrile; AN-II = acrylonitrile-ethyl benzylidenecyanoacetate; AN-III = acrylonitrile-benzylidenemalononitrile.

needle having a circular cross section of 1 mm² and carrying a weight of 1-4 kg presses on the specimen, which is placed in a silicon-oil-bath. The temperature is raised uniformly at a rate of 1°C/min, and the penetration of the needle into the specimen is recorded. On plotting the penetration against the temperature, first a nearly straight line is obtained, but on reaching the glass transition point, a steep increase of the penetration occurs (Figs. 5-8). The results are summarized in Table II.

Thermogravimetric Measurements. The thermal behavior of the polymers was examined with a Stanton Thermobalance in nitrogen atmosphere.

Ultraviolet Irradiation. The films were irradiated by ultraviolet lamps (125 and 1000W) and their behavior followed by changes in the infrared spectra.

Tensile Strength. The films, 10 cm long and 1 cm wide, were tested on an Instron apparatus at 20°C and 48% RH. Before the test, the films were kept in a desiccator.

The tensile strength of molded rectangular specimens was tested on an apparatus made by Tensometer Ltd., Croydon, England.

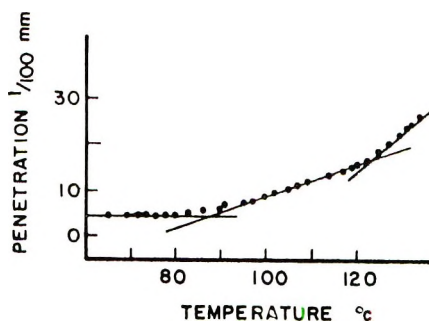


Fig. 8. Determination of the glass transition temperature of acrylonitrile-benzylidenemalononitrile copolymer.

Compressive Strength. The compressive strength of molded cylindrical specimens was tested on an apparatus made by Tensometer Ltd.

Weathering Test. The behavior of the films (strips 10 cm long and 1 cm wide) was examined in a Xenotest apparatus for 100 hr at 24–28°C and 90% RH.

After the test, the infrared spectra and the tensile strength of the specimens were determined and compared with those of untreated specimens.

Permeability to Water Vapor. The permeability of films of the various polymers for water vapor was determined gravimetrically,⁶ and the permeability coefficient P was calculated according to eq. (1):

$$P = Ql/\Delta pAt \quad (1)$$

where Q is the quantity of water vapor which passed during time t through a polymer film of a thickness l and an area A at a pressure drop Δp .

RESULTS AND DISCUSSION

Methods of Polymerization

When the copolymers were prepared either by the emulsion method with the use of sodium lauryl sulfate as emulsifier and the redox pair potassium persulfate–sodium metabisulfite as initiator⁷ or by the slurry method with the same redox initiator,⁷ yields were rather low.

Due to the presence of electron-attracting substituents, anionic initiation by sodium methylate⁸ or butyllithium⁹ seemed most promising. Although copolymerization occurred with yields up to about 50%, all the products were yellow and they could neither be molded nor had they any film-forming properties.

The copolymers were obtained in good yield by the suspension method with freshly precipitated calcium phosphate as suspending agent and with a radical producing initiator. The copolymers were obtained in the form of small white particles, which could easily be dispersed to a white powder and actually contained no residual monomers. These copolymers were used for study of their main physical properties in comparison with homopolyacrylonitrile prepared under identical conditions.

Properties of Copolymers

Solubility. Contrary to the increased solubility of the copolymer of acrylonitrile with vinyl acetate, in comparison with polyacrylonitrile, the copolymers of acrylonitrile with I, II, and III, like the homopolymer, are insoluble in conventional solvents, e.g., alcohols, chlorinated hydrocarbons, aromatics, nitrobenzene, phenol, tetrahydrofuran, pyridine, etc., and also in acids and bases. They do, however, dissolve in warm dimethyl sulfoxide, dimethylformamide, and dimethylacetamide or in certain hot aqueous salt solutions such as in an aqueous solution of $ZnCl_2$.¹⁰

Glass Transition Temperatures. Like polyacrylonitrile,¹¹ the acrylonitrile copolymers with I, II, and III show two transition points. As can

be seen in Table II, the first transition is nearly equal for the homo- and copolymers, whereas the second transition is definitely lower for the copolymers.

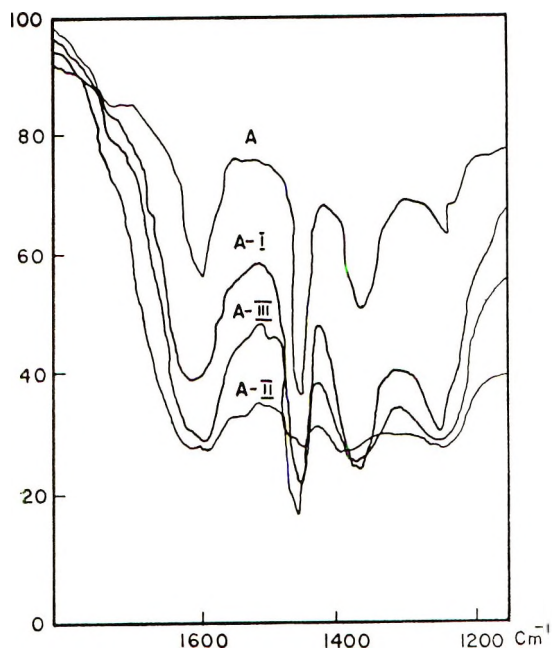


Fig. 9. Infrared spectra of polymer films after heating at 200–205°C for 3 hr. (A) polyacrylonitrile; (A-I) acrylonitrile-cinnamionitrile copolymer; (A-II) acrylonitrile-ethyl benzylidenecyanoacetate copolymer; (A-III) acrylonitrile-benzylidenemalononitrile copolymer.

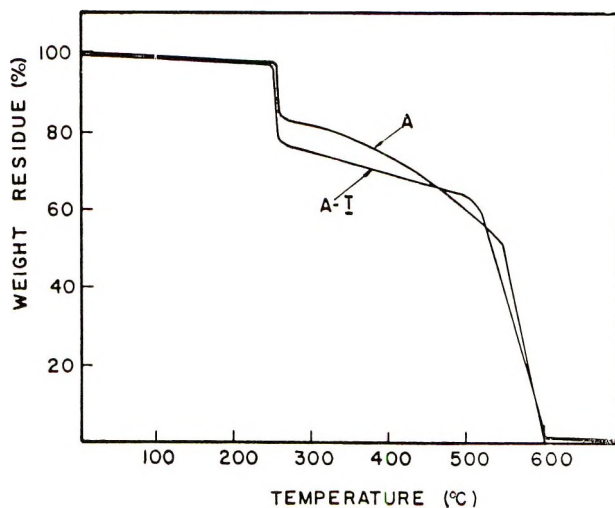


Fig. 10. Thermogravimetric analysis: (A) polyacrylonitrile; (A-I) acrylonitrile-cinnamionitrile copolymer.

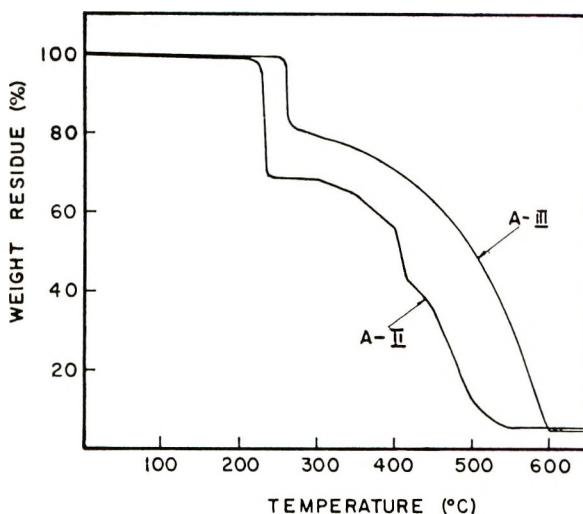


Fig. 11. Thermogravimetric analysis: (A-II) acrylonitrile-ethyl benzylidenecyanoacetate copolymer; (A-III) acrylonitrile-benzylidenemalononitrile copolymer.

This marked difference of the second transition could be due to the bulkiness of the substituents of the comonomers. Kimmel and Andrews,¹¹ by studying the birefringence effects, explained the two transitions of polyacrylonitrile by the presence of two secondary intermolecular forces: the weaker van der Waals forces, which dissociate at about 90°C, and the stronger dipole-dipole forces between nitrile groups, which still exist at this temperature and thus prevent rubbery-type flow. These dipoles dissociate at about 140°C. The bulkiness of the comonomers in the copolymer chain reduces the possibility of dipole bond formation and thus the second transition point correspondingly. Consequently, copolymer A-II, containing the most bulky comonomer, shows the greatest reduction of the second transition point.

For specimens molded at about 200°C, only one definite transition at about 150°C was found, and their infrared spectra showed absorption at 1600–1700 cm^{-1} , corresponding to the $-\text{C}=\text{N}-$ band.

In order to prevent any crosslinking or ring formation by heat molding, cold-pressed specimens were tested for comparison.⁵ The first transition only could be observed with good agreement for AN-II and AN-III. The values for AN-I and PAN differ from those for the heat-molded specimens by up to 10°C. This was attributed to the too-large particle size of the resins. It was not possible to determine the second transition of the cold-pressed copolymers by the penetrometer method.

Thermal Behavior. The behavior of the copolymers with increasing temperature was followed by changes of the infrared spectra of the heated polymer films and by thermogravimetric analysis.

Film strips were heated in an oven first at 130°C for 3 hr, when no visible changes and no changes in the infrared spectra occurred. After heating at

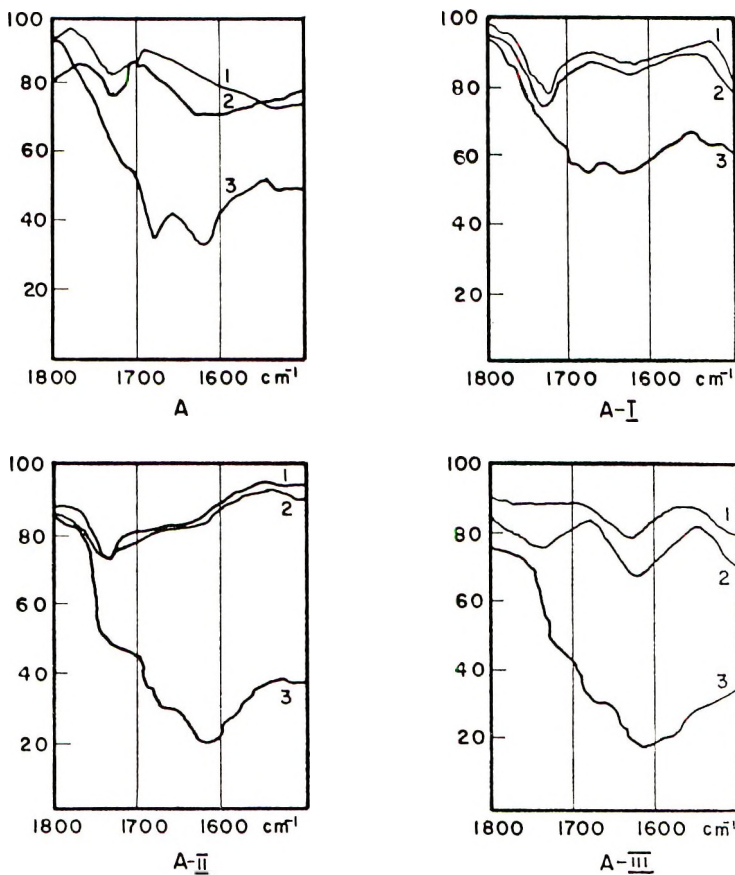


Fig. 12. Infrared spectra of polymer films after ultraviolet irradiation: (1) 2 hr, 125-W lamp; (2) 12 hr, 125-W lamp; (3) 5 hr, 1000-W lamp.

200–205°C for 3 hr, the films became yellow, more breakable, and the infrared spectra indicated definite changes in their chemical structure, a great increase in the 1600–1700 cm^{-1} region (Fig. 9) for the conjugated $-\text{C}=\text{N}-$ group¹² being observed.

In the thermogravimetric graphs (Figs. 10 and 11), the first major decompositions for the three copolymers occur at about 250°C, just as with polyacrylonitrile, with weight losses of about 33% for copolymer AN-II and of about 25% for AN-I and AN-III, compared to 17% for polyacrylonitrile. For AN-II, decomposition starts at about 230°C. At 500°C the weight losses for AN-I, AN-II, and AN-III were 50, 90, and 44%, respectively, compared to 40% for homopolyacrylonitrile.

Thus ethyl benzylideneacrylate causes a marked decrease in the temperature stability.

Irradiation by Ultraviolet Light. Films strips (2 cm long; 1 cm wide) were irradiated either by a 125-W lamp for 2 or 12 hr or by a 1000-W lamp for 5 hr. The behavior of the films was followed by infrared spectroscopy.

TABLE III
Tensile Properties of Films^a

Experiment no.	Polymer type	Thickness, μ	Yield strength, kg/cm ²	Elongation at yield point, %	Tensile strength, kg/cm ²	Elongation at break, %	Modulus of elasticity $\times 10^{-4}$, kg/cm ²
122.1	PAN ^b	18	765	6.8	755	8.5	5
98.1	AN-I	17	650	4.9	635	5.6	2.6
101.1	AN-II	18	640	4.6	610	10.2	2.8
125.1	AN-III	80	540	7.0	470	15.5	2.0
	Mylar	—	—	—	1300	—	3.8
	Polyethylene	—	—	—	170	—	0.2
	Cellulose acetate	—	—	—	600	—	2.3

^a See footnote Table II.

^b All values are the average from at least five specimens.

As can be seen from the graphs (Fig. 12), the copolymers are quite stable to ultraviolet light of lower intensity, but become yellow and brittle at higher intensity with the appearance of a strong absorption band in the 1600–1700 cm^{-1} region.¹²

Tensile Properties of Films. Of the mechanical properties of the films, only the tensile strength was examined. As can be seen in Table III, the tensile properties of the films of the copolymers are similar to those of polyacrylonitrile. Compared with commercial polymer films, the values for the copolymers are similar to those of cellulose acetate, inferior to those of poly(ethylene terephthalate) (Mylar), but superior to those of polyethylene.¹³

Weathering Test. After the Xenotest, the specimens showed no visible change, and an additional band appeared in the infrared spectra for the hydroxy group due to absorption of water. The tensile strengths of the treated copolymers were of the same order of magnitude as those of the untreated ones.

Permeability to Water Vapor. As can be seen from Table IV, the values of the permeability coefficient for water vapor for the polymers under investigation are quite low, and they are in the range of polypropylene and poly(vinyl chloride). It seems that this low permeability is due to strong bonding of water molecules to the polar groups of the polymer by hydrogen bonds.

Mechanical Tests on Molded Specimens. No visible deformation occurred on the molded specimens during tests for their tensile and compressive strength. Therefore only the values as obtained and the molding conditions are summarized in Tables V and VI, respectively.

The copolymers could be molded in a broader temperature range than polyacrylonitrile. Although the specimens were tough, hard, and clear, some yellowing appeared during molding. This could be prevented by reducing the molding cycle with an efficient injection press. Further, one has to consider, that no stabilizers were added to the copolymers. At lower molding pressures, the specimens were opaque and too brittle for

TABLE IV
Permeability to Water Vapor

Experiment no.	Polymer	$P \times 10^9$, g-cm/cm Hg $\text{cm}^2\text{-sec}$
122.1	PAN	5.2
98.1	AN-I	6.8
101.1	AN-II	15.9
125.1	AN-III	13.2
	Poly(vinylidene chloride)	0.1–1.0
	Polypropylene	5
	Poly(vinyl chloride)	15
	Polystyrene	150
	Polycarbonate	140

TABLE V
Tensile Strength of Copolymers

Experiment no.	Polymer type	Molding conditions			Tensile strength, kg/cm ²
		Pressure, kg/cm ²	Temperature, °C	Time, min	
122.1	PAN	6000	170	6	270
111.1	AN-I	6000	175	30	170
111.1	AN-I	6000	180	20	175
111.1	AN-I	6000	200	15	260
101.1	AN-II	7000	175	8	210
124.2	AN-III	7000	170	3	170

TABLE VI
Compressive Strength of Copolymers

Experiment no.	Polymer type	Molding conditions			Compressive strength, kg/cm ²
		Pressure, kg/cm ²	Temperature, °C	Time, min	
122.1	PAN	6000	135	4	1240
98.1	AN-I	6000	145	10	1440
101.1	AN-II	2000	155	5	1080
125.1	AN-III	4000	215	3	1260

testing, whereas at higher temperature, the specimens became dark and their infrared absorption showed an increase at 1600–1700 cm⁻¹ and a decrease at 2230 cm⁻¹, which indicates crosslinking.

In comparison to other thermoplastic polymers, the tensile strength of the copolymers is rather near the values of the lower-strength polymers, yet the values of the compressive strength are similar to those of polystyrene, poly(methyl methacrylate), etc. The molded specimens were rather brittle, and no visible deformation appeared during testing. Similar results were obtained by Jordan et al.¹⁴ for copolymers of acrylonitrile with various *N-n*-alkylacrylamides.

The more promising application of the copolymers seems to be as films. Conditions for formation of fibers and their basic properties are still to be investigated.

This paper is taken in part from a thesis submitted by Samuel H. Ronel to the Department of Chemistry, Technion-Israel Institute of Technology, Haifa, in partial fulfillment of the degree of M.Sc.

References

1. S. H. Ronel and D. H. Kohn, *J. Polymer Sci. A-1*, in press.
2. S. H. Pinner, *A Practical Course in Polymer Chemistry*, Pergamon Press, Oxford, 1961.
3. H. Kobayashi, *J. Polym. Sci.*, **39**, 369 (1959).
4. O. B. Edgar and E. Ellery, *J. Chem. Soc.*, **1952**, 2633.
5. B. Y. Teitelbaum, V. G. Gizatullena, and T. A. Yagfarov, *Polymer Sci. USSR*, **6**, 324 (1964).

6. ASTM designation: E 96-53T.
7. W. R. Sorensen and T. W. Campbell, *Preparative Methods of Polymer Chemistry*, Interscience, New York, 1961.
8. A. Zilkha and B. A. Feit, *J. Appl. Polym. Sci.*, **5**, 251 (1961).
9. B. A. Feit, D. Mirelman, and A. Zilkha, *J. Appl. Polymer Sci.*, **9**, 2459, 2475 (1965).
10. J. Brandrup and E. H. Immergut, *Polymer Handbook*, Interscience, New York, 1966.
11. R. M. Kimmel and R. D. Andrews, *J. Appl. Phys.*, **36**, 3063 (1965).
12. N. Grassie and J. N. Hay, *J. Polym. Sci.*, **56**, 189 (1962).
13. R. E. Kirk and D. F. Othmer, *Encyclopedia of Chemical Technology*, 1st Suppl. Vol., Interscience, New York, 1957, p. 692.
14. E. F. Jordan, Jr., G. R. Riser, W. E. Parker, and A. N. Wringley, *J. Polym. Sci. A-2*, **4**, 975 (1966).

Received January 23, 1969

Water Flow through Polymeric and Nonaqueous Liquid Membranes

N. LAKSHMINARAYANAIAM and M. S. WHITE, *Department of Pharmacology, University of Pennsylvania, Philadelphia, Pennsylvania 19104*

Synopsis

Osmotic and isotopic water flows through polymeric and nonaqueous liquid membranes have been measured. The polymeric membranes were of the polyethylene-styrene graft copolymer type containing sulfonic acid groups. The nonaqueous liquid membranes were water-saturated 1-butanol and benzene. Osmotic water flux through both types of membranes was larger than isotopic (THO) water flux. Using these data, values for the equivalent pore radius for these membranes have been derived. The significance of such values has been briefly discussed.

INTRODUCTION

Solid membranes made from polymeric materials and containing different quantities of water have been used as models to understand the behavior of physiological membranes.¹ The space occupied by water in the rigid model membranes has been equated to the pore volume² which is quite fixed at any given external environment. This concept of pore losses its meaning when applied to a biological membrane which is considered to exist in a semirigid, semifluid state³ possessing a lability characteristic of a liquid in which the molecules are subject to thermal, attractive, and dispersive intramolecular forces. The space between molecules in motion or "hole" will be dynamic, and water passage through a structure or barrier physically resembling a lipid-like liquid will be governed by the solubility of water in that structure; the greater the solubility, greater will be the flow of water through such a barrier provided there are no special bonding forces operating. Whether or not this flow is all diffusional or is made up of other components is not known, *a priori*.

Mauro^{4,5} has presented a thermodynamic analysis of the nature of water flow through a semipermeable membrane subject to a pressure gradient. According to this, any barrier that has the property of semipermeability would give rise to a flow composed of both diffusional and nondiffusional components, the relative magnitudes of which are a function of the tightness of the membrane, i.e., water content. There are few measurements of water flow through nonaqueous membranes. Recently Rosano et al.^{6,7} have reported osmotic flow measurements through water-saturated 1-butanol. Whether this flow was all diffusional or was made up of other com-

ponents was not investigated. This paper presents the results of such an investigation.

EXPERIMENTAL

Solid Membranes

Solid cation-exchange membranes (AMF C-103, AMF C-104) were supplied by the American Machine and Foundry Company. They were converted to the hydrogen form by conditioning in 1.0 *M* HCl solution followed by repeated washing with deionized water. The osmotic and diffusional fluxes were determined by methods similar to those described elsewhere.⁸ In this work, measurements were made only with AMF C-104 membranes. Data for AMF C-103 were taken from the work of Lakshminarayanaiah.⁸ The driving force for the bulk flow through AMF C-104 membrane was achieved by an osmotic gradient with the use of sucrose solutions. Little sucrose escaped through the membrane.

Liquid Membranes

Fischer certified 1-butanol and benzene were used after distillation. Deionized water and the nonaqueous components were saturated with each

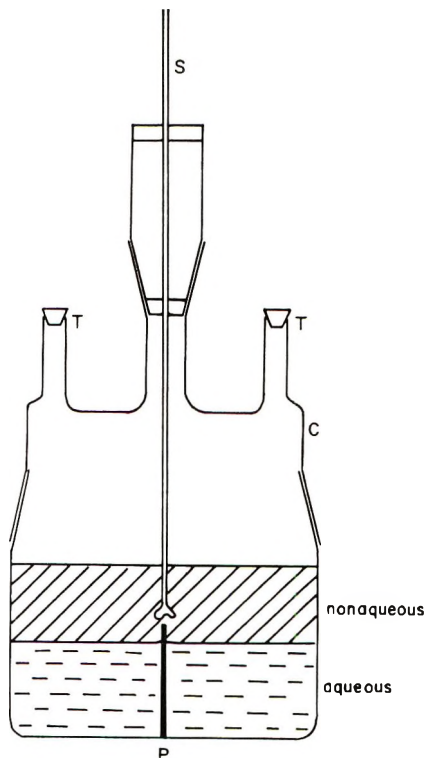


Fig. 1. All-glass transport cell for use with liquid membranes: (P) the glass partition bisecting the cell; (S) stirrer; (C) ground-glass cover for the cell.

other and used in a cell of the type shown in Figure 1. P was an impermeable barrier (glass) bisecting the all glass transport cell, the mouth of which was sealed from the atmosphere by the ground glass cap C. On one side 1.0M KCl (25 ml) previously saturated with the nonaqueous component was placed, while on the other side solvent saturated deionized water (25 ml) was used; then 25 ml of water-saturated organic phase was pipetted out on top of the aqueous layers. The upper phase was stirred at a rate sufficient to cause agitation of the two interfaces (500 rpm) by a stirrer S, which entered the cell through a series of Teflon bushings. The transport cell was kept in a water thermostat maintained at the desired temperature to within 0.02°C. The increase on the KCl side or decrease on the water side of the level of the interface was followed on a cathetometer with time. When the reading was taken on the cathetometer, the stirring was stopped to have a stationary interface. As the area of the interface was known by an independent measurement, the rate of volume flow was thus determined.

The flux of tritiated water (THO) was followed by keeping THO-labeled water on one side (25 ml) and deionized water (25 ml) on the other side, the increase in activity of which was followed by taking an 0.05 ml aliquot for counting at known intervals of time. Aliquots were removed from the cell via the opening T and transferred into polyethylene vials (capacity about 25 ml) into which 12.5 ml of Bray's solution⁹ were added. Samples were counted in a Packard Tri-Carb liquid scintillation counter.

RESULTS

Solid Membranes

Membrane parameters and calculated data are presented in Table I together with the corresponding quantities taken from the work of Lakshminarayanaiah for AMF C-103 membrane.⁸ The diffusional flow of THO was evaluated in the manner described elsewhere.^{4,8,10} From the counting rate ($D_w A_w/d$) was evaluated and for $\Delta P = 1$ dyne/cm² from eq. (1), the flux of THO, i.e. (dn/dt) , was evaluated,

$$(dn/dt)_{\text{THO}} = (D_w A_w/d)(\Delta P/RT) \quad (1)$$

where D_w is the diffusion coefficient of THO in water, A_w is the total pore area, d is the equivalent pore length. The osmotic permeability coefficient L_p was evaluated from the volume flow according to the equation

$$J_v = L_p \Delta P \quad (2)$$

The water flow rate as a function of sucrose concentration is plotted in Figure 2 and diffusional flux is shown in Figure 3. From the two sets of experiments the equivalent pore radius r can be derived² from the equation

$$r = \sqrt{8\eta_w L_p / (A_w/d)} \quad (3)$$

where η_w is the viscosity of water. The magnitude of the quantity (A_w/d) depends on the value of D_w chosen. Ideally, the actual value of D_w will

approach the value for the self-diffusion coefficient of water when the nature of flow is all diffusional and free from the frictional influences resulting from flow through the membrane. To realize an absolute value for D_w in these systems is not possible, and so it is assumed to be the same as the self-diffusion of THO in water.¹¹ Therefore the value of D_w (2.63×10^{-5} at 25°C and 3.47×10^{-5} at 35°C) was obtained by interpolation from the data of Wang.¹² Using this value, (A_w/d) was estimated.

TABLE I
Water Permeability through Membranes

Property	Membrane				
	AMF C-103	AMF C-104	1-Bu- tanol	Benzene, 25°C	Benzene, 35°C
Membrane area, cm^2	2.85	2.85	9.73	9.733	9.73
Membrane thickness, μ	152 ^a	145 ^b	—	—	—
Water content, g/g	0.21 ^a	0.16 ^b	0.20 ^c	0.00072 ^c	0.0010 ^c
Osmotic permeability coefficient L_p , $\text{cm}^3 \text{sec}^{-1}/\text{dyne cm}^{-2} \times 10^{12}$	0.59 ^a	0.26	6.44	0.044	0.083
$D_w A_w/d$, $\text{cm}^3/\text{sec} \times 10^5$	10.3 ^a	7.78	106	1.035	1.829
Volume (osmotic) flow, mole $\text{sec}^{-1}/\text{dyne cm}^{-2} \times 10^{15}$	32.8 ^a	14.39	360	2.43	4.62
Diffusional flow $(dn/dt)_{\text{THO}}$, mole $\text{sec}^{-1}/\text{dyne cm}^{-2} \times 10^{15}$	4.2 ^a	3.14	42.8	0.42	0.71
Flux ratio (diffusional/total)	1/7.8	1/4.6	1/8.4	1/5.8	1/6.5
A_w/d , cm	3.92	2.96	40.3	0.39	0.53
Equivalent pore radius r , Å	10.4	7.91	10.7	8.9	9.6
Total pore area, cm^2	0.098	0.074	2.22	0.007	
Fractional pore area	0.034	0.026	0.228	0.0007	

^a Data taken from Lakshminarayanaiah.⁸

^b Data obtained from Lakshminarayanaiah and Moulik.¹⁵

^c Values obtained from solubility data.¹⁶

A definite value for the equivalent pore length d also cannot be assigned. It can only be estimated in the following manner. The geometrical thickness of the membrane ($\sim 150 \mu$ for each membrane) together with a tortuosity factor which for these membranes is assumed to be 0.75 gives a total pore length of 200μ . The unstirred liquid adjacent to each side of the membrane surface must also be taken into account. The thickness of these layers (δ) is dependent on the rate of stirring of the solution. Ginzburg and Katchalsky,¹³ using an experimental setup similar to ours and employing stirring rates greater than ~ 200 rpm, found values for δ to lie between 12 – 47.5μ . Peterson and Gregor¹⁴ found that the thickness of the unstirred film at the surface of a solid ion exchange membrane increased from 1 to 30μ as the speed of the stirring decreased from 1200 to 200 rpm. In the present work, the rate of stirring was constant at ~ 500 rpm, and so a value of 25μ was assumed for δ . This gives a total value for d of 250μ . The pore area A_w was calculated with the use of this value and is given in Table I.

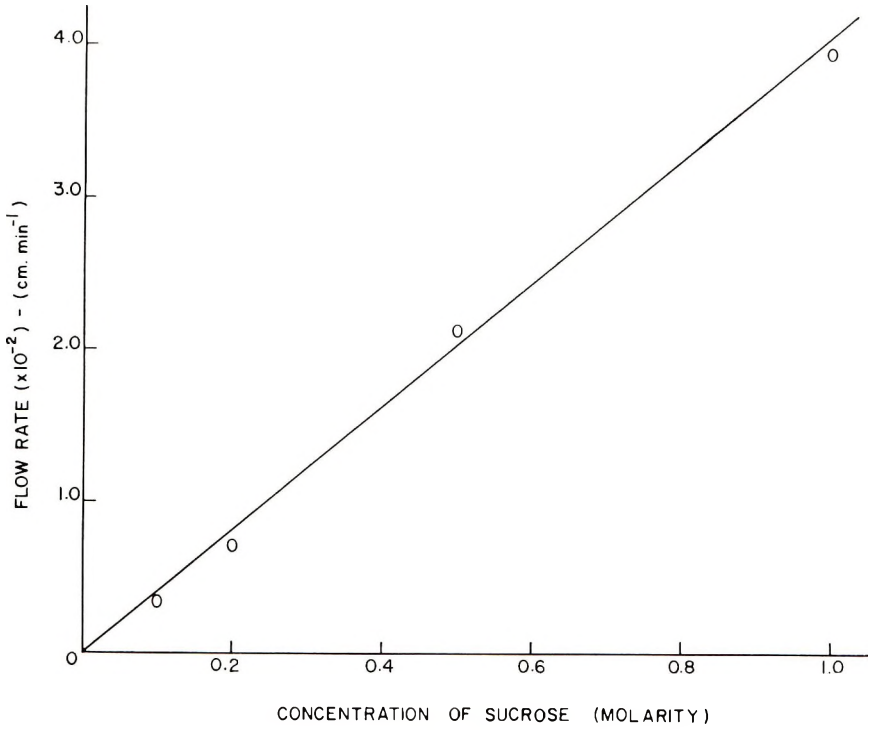


Fig. 2. Water (osmotic) flow rate through AMF C-104 membrane plotted as a function of sucrose solution concentration (osmotic force).

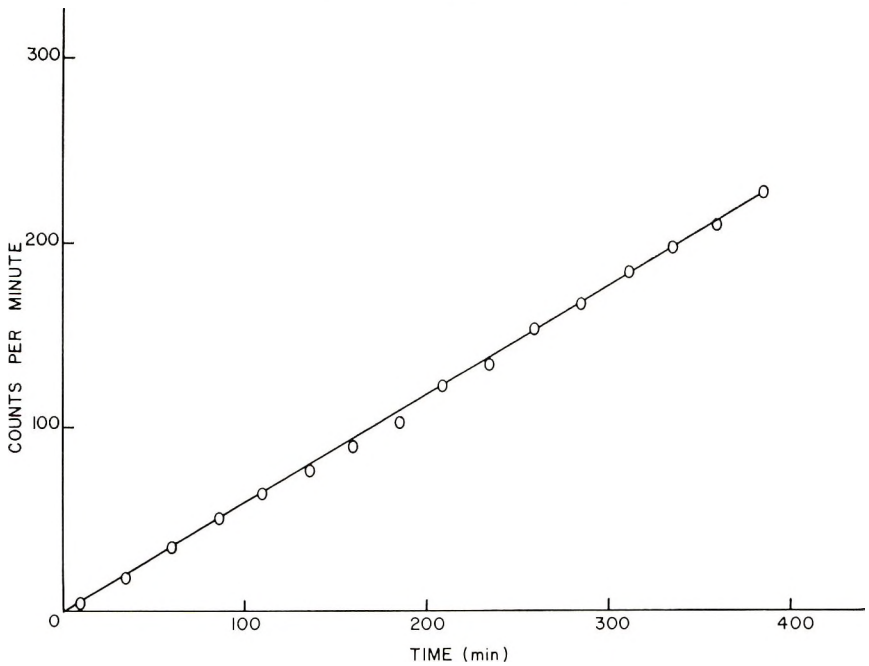


Fig. 3. Tritiated water flow (counts/min) through AMF C-104 membrane plotted as a function of time.

Liquid Membranes

Osmotic and diffusional fluxes are plotted as a function of time and are given in Figures 4 and 5. Experiments involving the flux of THO exhibited a linear increase in counts per minute with time in all cases. The initial curvatures with benzene are attributed to nonequilibrium conditions at the beginning of each experiment. Benzene and water were kept saturated with each other at the desired temperature prior to the experiment but it is presumed that in the transfer of liquid to the cell the degree of

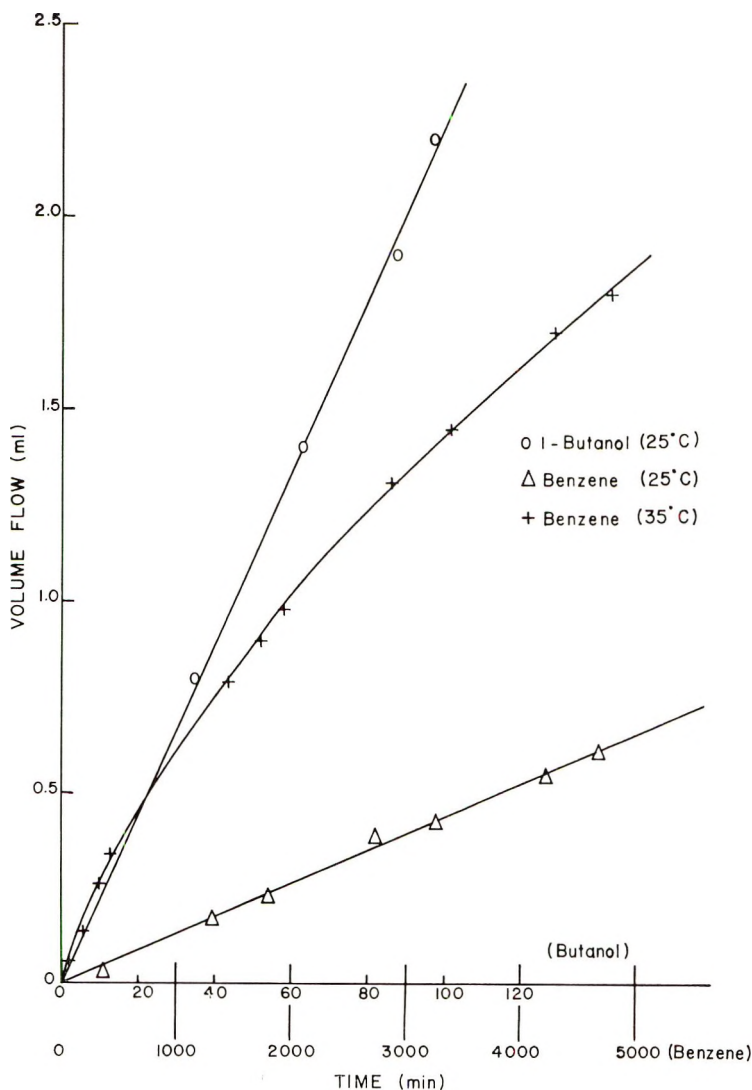


Fig. 4. Volume (osmotic) flow (ml) of water through liquid membranes plotted as a function of time.

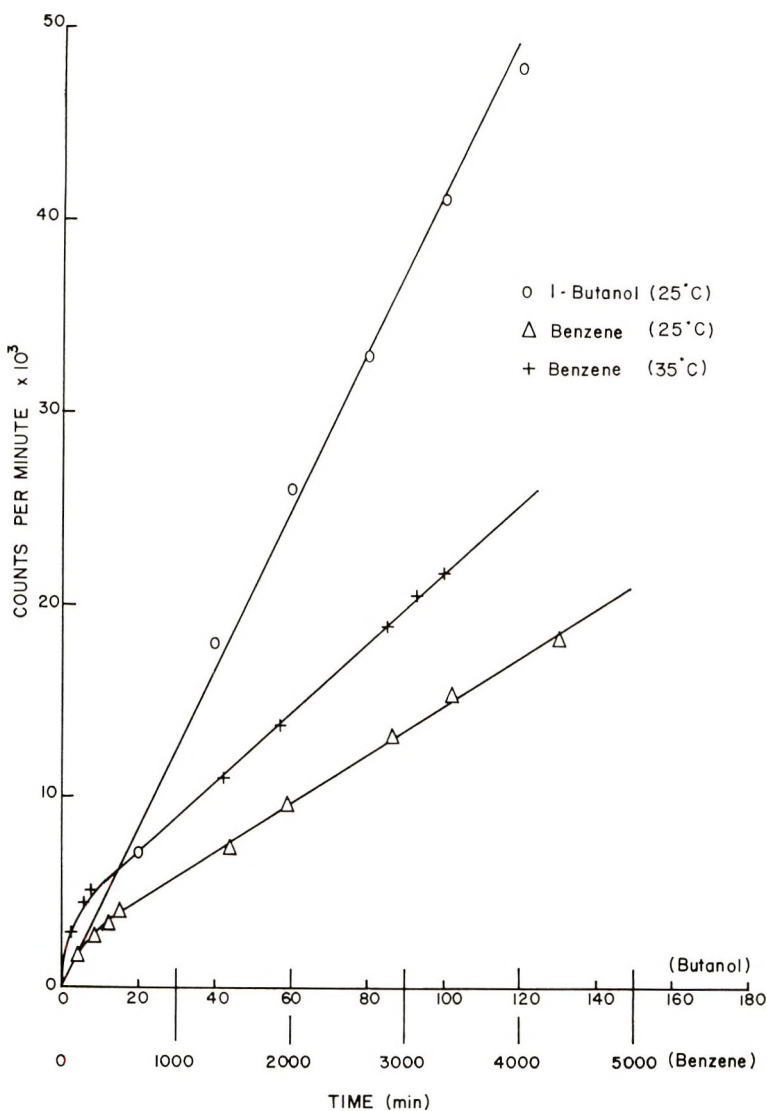


Fig. 5. Tritiated water flow (counts/min) through liquid membranes plotted as a function of time.

saturation was altered. A number of experiments (four) gave different amounts of initial curvature but after approximately 500 min all were linear and with the same gradient ($\pm 5\%$).

Theoretically, experiments involving the volume flow of water will be subjected to a decreasing osmotic force due to the solubility of KCl (and the subsequent transfer of KCl) in the organic medium. Thus the rate of flow of water should decrease with time. The only system where this tendency was observed was water-benzene-KCl at 35°C. However, pro-

vided the experiments were allowed to proceed for a sufficient length of time a similar curvature would occur; thus in a final experiment with 1-butanol at 25°C a curvature was detected after 300 min. The curvature of the plot for water-benzene-KCl at 35°C compared to the linearity at 25°C was attributed to the greater increase in solubility of KCl compared to H₂O in benzene from 25 to 35°C. While no data were available for benzene, an analogy can be drawn from the increased solubility of KCl in 1-butanol (160%) for a temperature rise from 0 to 60°C¹⁶ compared to a 14% increase in water solubility from 5 to 50°C.¹⁷ Values for the osmotic flux of water in the system water-benzene-KCl at 35°C were taken from the slope at 4000 min. where the rate of change of slope was a minimum.

The values of Table I were calculated with the assumption that eqs. (1)–(3) which were derived for the rigid membranes were applicable to the dynamic liquid pores of the liquid membranes. Each value is the average of at least four experiments with an average deviation of $\pm 5\%$.

In the evaluation of the quantity (A_w/d) for the liquid membranes, an uncertainty is introduced by reason of the value of D_w chosen which is the same as in the rigid membranes. The diffusion coefficients of water in various organic liquids have been correlated by Sitaraman et al.,¹⁸ who found D_w for water in 1-butanol and in benzene to be 0.57×10^{-5} and 2.33×10^{-5} cm²/sec, respectively. These values are the same as the self-diffusion coefficients of the individual solvents themselves,^{19,20} but unfortunately little reliance can be placed on the results because of large deviations encountered for 1-butanol. Since, as in the rigid membranes, the total flow is predominantly of a viscous nature (see Table I) it is probably more pertinent to assign D_w the value for the self diffusion coefficient of water. On this basis the values for (A_w/d) given in Table I have been computed.

Rosano,⁷ assuming the applicability of the diffusion theory of gases to liquid systems,²¹ has calculated d for the system water-1-butanol-KCl using the expression

$$J = AD(W_1 - W_2)/d \quad (4)$$

where A is the area of the interface, D is the diffusion coefficient of water $(W_1 - W_2)$ is the respective concentration difference of water at the two interfaces (estimated from the work of Rosano,⁷ this for the present system is $\sim 7 \times 10^{-2}$ g), and J is the mass of water in grams migrated per second. Equation (4) gives an estimate for d of 550μ for our system. In the case of benzene, eq. (4) cannot be used, as no data for $(W_1 - W_2)$ are available. However, an estimate of d for benzene relative to d of 1-butanol can be obtained from the work of Schulman and Teorell²² involving the migration of water with a monolayer moving at constant velocity. They found that the thickness of the rigid structure exhibited a three-fold increase for a corresponding fourfold increase in the ratio (η_{na}/η_a) , where η_{na} and η_a are the viscosities of the nonaqueous and aqueous components respectively. Thus for the systems, water-1-butanol-KCl and water-benzene-KCl one

obtained $(\eta_{\text{butanol}}/\eta_{\text{H}_2\text{O}}):(\eta_{\text{benzene}}/\eta_{\text{H}_2\text{O}})$ as 4.3:1. The value for d in the case of benzene would be approximately $1/3$ of that for 1-butanol. So for the present system the value for d for the benzene/water membrane would be $\sim 180 \mu$. The greater value for d for 1-butanol is not unreasonable, in view of the fact that 1-butanol-water interface is more rigid than benzene-water interface due to alignment of alcohol molecules at the interface. This alignment is reflected in the values of the interfacial tension given in Table II for both 1-butanol and benzene. The other data pertaining to the liquid membranes are presented in Table I.

TABLE II
Interfacial Tension at 25°C^a

System	Interfacial tension, dyne/cm
1-Butanol-air	24
Benzene-air	28.2
1-Butanol-water	1.8
Benzene-water	34.7

^a Data of Davies and Rideal.²³

DISCUSSION

The phenomenon of water transport through rigid membranes differs physically from that through liquid membranes. In the first place, water moves relative to the walls of the fixed pore membranes and the type of flow will vary from hydrodynamic to diffusional as the pore radius decreased.²⁴ Also when the radius of the diffusing molecule is comparable to r , the diffusional flow will be influenced not only by the viscous drag on the walls but also by the steric hindrance at the pore opening. In the case of the "dynamic pore" encountered in liquid membranes, where water channel through an organic phase cannot be defined because of the kinetic motion of all the molecules, a different mechanism must be postulated. Diffusion in liquids can be described as the motion of a species by means of kinetic jumps into neighboring vacancies (of molecular or ionic size). However in the present liquid systems where diffusional flux is only a fraction of the total flow, an alternative mechanism for bulk flow of water must be formulated.

As suggested by Thau et al.,²⁵ the movement of water in a liquid membrane may take place by adsorption at the interface followed by migration of the oil/water associate and subsequent desorption at the other interface. It is possible that bulk flow could occur by means of migration of multi-hydrated organic molecules with associated adsorption-desorption at the corresponding interfaces. Olander²⁶ suggested that water in organic solvents migrated as the species $(\text{H}_2\text{O})_4$, but the more recent findings of Johnson et al.²⁷ have shown that in benzene water is monomeric. Nevertheless, in order to be consistent with the experimental results, a bulk flow of water under the influence of an osmotic gradient is necessary; whether

such flow consists of clusters of water molecules or multihydrated organic phase molecules cannot be determined.

A calculation of the activation energies for water movement in benzene at 25 and 35°C gives values of 9.6 and 12.2 kcal/mole for diffusional and osmotic flows, respectively. These values may be compared with the values derived from viscosity and diffusion data for pure components. Calculations from available data for viscosity²⁸ and diffusion²⁰ in benzene gave values for the activation energies of 2.5 and 2.3 kcal/mole, respectively. On the other hand, for water Miller²⁹ found an activation energy for viscous flow of 1.02 kcal/mole and Gurikov³⁰ for self-diffusion found a value of 4.6 kcal/mole. These values are low compared to the values derived for their mixtures. The higher activation energies for both diffusional and osmotic flows probably indicate extra energy necessary for overcoming the frictional interactions between water molecules moving past benzene molecules. Higher activation energy for osmotic flow compared to diffusional flow seems to reflect presence of aggregates of molecules taking part in that type of flow, greater energy being required to move heavier particles.

The similarities and differences of the two types of membranes can be seen from the data of Table I by comparing the equivalent pore radii and the fractional pore area. It is interesting to note that for each membrane type (i.e., rigid or liquid) the fractional pore area is proportional to the water content of the membrane. No value was calculated for benzene at 35°C, but a similar trend for this liquid can be seen by comparing (A_w/d) for benzene at 25 and 35°C. Even without involving such quantities as D_w and d , the flows themselves (for each membrane type) can be related to water content in a qualitative way.

Calculation of pore radius r by using eq. (3) does not take into account either the steric hindrance at the pore entrance or the frictional resistance with the pores felt by the permeating molecules. Paganelli and Solomon,³¹ taking these factors into account, have given a simple equation

$$r = -a + \sqrt{2a^2 + [8\eta_w L_p / (A_w/d)]} \quad (5)$$

where a is the radius of the permeating molecule. By using $a = 1.97 \text{ \AA}$ in eq. (5), values of 8.6, 6.4, 9.0, and 7.4 \AA were obtained for AMF C-103, C-104, 1-butanol, and benzene, respectively, as their equivalent pore radii r . On taking these values of r , the number of pores in 1 cm² membrane area may be calculated. These values are 15×10^{11} , 20×10^{11} , 90×10^{11} and 4×10^{10} .

Although there are no pores in liquid membranes in the sense in which they are considered to exist in rigid membranes, it turns out that the calculations usually applied to rigid membranes, if applied to liquid membranes, give for the number of pores in 1 cm² surface a value greater in the case of 1-butanol and a value lower in the case of benzene than the value found in rigid membranes.

Another very important point of interest emerging from these studies is the fact that in the case of the two liquid membranes having widely differing

values for water solubility in them (20% and 0.07%) have pores almost of the same dimension, although the number of pores are small in the case of benzene in which water has low solubility. In the case of rigid membranes, such a phenomenon would never occur. For example, phenolsulfonate membranes⁸ having about 59% water have pores of average radius 33 Å. This large according to expectation compared to 8.6 and 6.4 Å obtained for AMF C-103 and C-104 membranes whose water contents are 21% and 16%, respectively. In the case of liquid membranes, water contents change by a factor of nearly 250, and r changes little in comparison. This is probably how it should be for liquids in view of the fact that intermolecular distance (i.e., space vacancy) is determined by their thermal energy which is given by kT (k = Boltzmann constant and T = absolute temperature). So, the value of r is determined by temperature. Values of r at 35 and 25°C (Table I) are in accordance with this concept, i.e., the value at 35°C is greater than the value at 25°C.

References

1. K. Sollner, *J. Electrochem. Soc.*, **97**, 139C (1950).
2. N. Lakshminarayanaiah, *Chem. Rev.*, **65**, 539 (1965).
3. A. M. Shanes, *Pharmacol. Rev.*, **10**, 88 (1958).
4. A. Mauro, *Science*, **126**, 252 (1957); *Circulation*, **21**, 845 (1960).
5. E. Robbins and A. Mauro, *J. Gen. Physiol.*, **43**, 523 (1960).
6. H. L. Rosano, P. Duby, and J. H. Schulman, *J. Phys. Chem.*, **65**, 1704 (1961).
7. H. L. Rosano, *J. Colloid Interface Sci.*, **23**, 73 (1967).
8. N. Lakshminarayanaiah, *Biophys. J.*, **7**, 511 (1967).
9. G. A. Bray, *Anal. Biochem.*, **1**, 279 (1960).
10. N. Lakshminarayanaiah, *J. Appl. Polym. Sci.*, **11**, 1737 (1967).
11. H. C. Longuet-Higgins and G. Austin, *Biophys. J.*, **6**, 217 (1966).
12. J. H. Wang, *J. Phys. Chem.*, **69**, 4412 (1965).
13. B. Z. Ginzburg and A. Katchalsky, *J. Gen. Physiol.*, **47**, 403 (1963).
14. M. A. Peterson and H. P. Gregor, *J. Electrochem. Soc.*, **106**, 1051 (1959).
15. N. Lakshminarayanaiah and S. P. Mouluk, unpublished data.
16. H. Stephen and T. Stephen, *Solubilities of Inorganic and Organic Compounds*, Macmillan, New York, 1963.
17. V. E. Plyushev, I. V. Shakhno, L. N. Komissarova, and G. N. Nadezhkina, *Nauch. Doklady Vysshev Shkoly. Khim. i Khim. Tekhnol.* **1958**, 279.
18. R. Sitaraman, S. H. Ibrahim, and N. R. Kuloor, *AIChE J.*, **8**, 277 (1962).
19. J. R. Partington, R. F. Hudson, and K. W. Bagnall, *Nature*, **169**, 583 (1952).
20. R. E. Rathbun and A. L. Babb, *J. Phys. Chem.*, **65**, 1072 (1961).
21. H. L. Rosano and V. K. La Mer, *J. Phys. Chem.*, **60**, 348 (1966).
22. J. H. Schulman and T. Teorell, *Trans. Faraday Soc.*, **34**, 1337 (1938).
23. J. T. Davies and E. K. Rideal, *Interfacial Phenomena*, Academic Press, New York, 1963, p. 17.
24. J. R. Pappenheimer, *Physiol. Rev.*, **33**, 387 (1953).
25. G. Thau, R. Bloch, and O. Kedem, *Desalination*, **1**, 129 (1966).
26. D. R. Olander, *AIChE J.*, **7**, 175 (1961).
27. J. R. Johnson, S. D. Christian, and H. E. Affsprung, *J. Chem. Soc.*, **1966**, 77.
28. N. A. Lange, *Hand-Book of Chemistry*, McGraw-Hill, New York, 1961.
29. A. A. Miller, *J. Chem. Phys.*, **38**, 1568 (1963).
30. Yu. V. Gurikov, *Zh. Strukt. Khim.*, **5**, 188 (1964).
31. C. V. Paganelli and A. K. Solomon, *J. Gen. Physiol.*, **41**, 259 (1958).

Received January 23, 1969

Termination Rate Constant in Radical Polymerization

KATSUKIYO ITO, *Government Industrial Research Institute, Nagoya,
Kita-ku, Nagoya, Japan*

Synopsis

On the basis of the assumption that the primary radical immerses into a polymeric radical, the rate constant of primary radical termination was derived. By applying and developing further the same treatment, the rate constant of chain termination was derived. This rate constant was experimentally confirmed. It was found that the rate constant of chain termination for the polymerization of some methacrylates depends on the distance of translation of radical chain end per collision, solvent viscosity, and the Taft polar constant for ester group.

INTRODUCTION

It has been recognized experimentally, on the basis of the fact that the rate constant for the bimolecular termination between polymeric radicals is in inverse proportion to solvent viscosity, that this rate constant is diffusion-controlled.¹⁻³ A diffusion-controlled rate constant of chain termination for explaining the experimental facts was theoretically derived.⁴ However, it is impossible that this rate constant applied to bimolecular termination between polymeric radicals, with the different radius because it is derived for bimolecular termination between two polymeric radicals with the same radius. This fact is typically illustrated for the bimolecular termination between a large polymeric radical and a primary radical, that is, it is reasonable in a collision between a large polymeric radical and a primary radical that they do not overlap, but that the primary radical is immersed into the polymer radical.

In this paper, on the basis of the assumption that the primary radical is immersed into the polymeric radical, the rate constant for primary radical termination was derived. On the development of this treatment, a rate constant for chain termination was derived. This rate constant is a greater generality than a rate constant for chain termination given in a previous paper.⁴ By using the results of Yokota et al.⁵ for the polymerization of some methacrylates, this rate constant for chain termination was confirmed.

Rate Constant of Primary Radical Termination

According to Lewis,⁶ the collision number Z_{ni} between a polymeric radical with radius r_n and a primary radical with radius r_i is given by:

$$Z_{ni} = \pi r_{ni}^2 (u_n^2 + u_i^2)^{1/2} N_L^2 [N_n] [N_i] \times 10^{-6} \text{ numbers/(mole-l.)} \quad (1)$$

where r_{ni} is the average distance to which polymeric radical and primary radical approach during a collision, u_n and u_i are the mean velocities of translation of the polymeric radical and primary radical, respectively, N_L is Avogadro's number, and $[N_n]$ and $[N_i]$ are the concentrations of polymeric radical and primary radical respectively. Assuming that the primary radical is immersed by the length L_i and $u_n \ll u_i$, eq. (1) becomes:

$$Z_{ni} = \pi r_n^2 (1 - \mu_i)^2 u_i N_L^2 [N_n] [N_i] \times 10^{-6} \quad (2)$$

where:

$$\mu_i = L_i / r_n$$

We set for convenience that the number of primary radicals reacting with radical chain ends is dc per distance dx of which the primary radical translates in the polymeric radical; then eq. (3) is taken into consideration:

$$dc = -\gamma_i {}^*C_n dx \quad (3)$$

Here γ_i is a reactivity constant, within units of square centimeter per mole, between primary radical and radical chain end, *C_n is the concentration of radical chain ends in the polymeric radical. This notation is equivalent to Beer-Lambert's law for light absorption.

On the assumption that *C_n is constant, *C_n is:

$${}^*C_n = (3/4\pi r_n^3 N_L) \times 10^3 \text{ mole/l.} \quad (4)$$

and the solution of eq. (3) is:

$$c = c_0 \exp\{-\gamma_i {}^*C_n x\} \quad (c = c_0 \text{ at } x = 0) \quad (5)$$

Accordingly, a change Δc for primary radicals during a collision is given by:

$$\Delta c = c_0 \exp\{-2\gamma_i {}^*C_n \alpha L_i\} \quad (6)$$

where the factor 2 *means* indicates distance to a place and back; α is a constant for the distance $x = \alpha L_i$ for the primary radical immersed in the polymeric radical by L_i . On using an approximation:

$$\exp\{-2\alpha\gamma_i {}^*C_n L_i\} = 1 - 2\alpha\gamma_i {}^*C_n L_i$$

under the condition $2\alpha\gamma_i {}^*C_n L_i \ll 1$, a bimolecular combination probability p_{ti} per collision between primary radical and polymeric radical is given by:

$$p_{ti} = (c_0 - \Delta c) / C_0 = 2\alpha\gamma_i {}^*C_n L_i \quad (7)$$

According to eqs. (2) and (7), the rate for primary radical termination is given by:

$$-d[N_i]/dt = Z_{ni} p_{ti} / 10^{-3} N_L = 3/2 \alpha \gamma_i \mu_i (1 - \mu_i)^2 u_i [N_i] [N_n] \quad (8)$$

and the rate constant of primary radical termination k_{ti} is given by:

$$k_{ti} = 3/2\alpha\mu_i u_i (1 - \mu_i)^2 u_i \text{ l./mole-sec} \quad (9)$$

On introduction of Einstein's equation:

$$D_i = h_i u_i / 6$$

where D_i is the diffusion constant of the primary radical in square centimeters per second and h_i is the distance of translation of primary radical per collision, into equation (9), k_{ti} becomes:

$$k_{ti} = 9\alpha\gamma\mu_i (1 - \mu_i)^2 (D_i/h_i) \text{ l./mole-sec} \quad (10)$$

Rate Constant of Chain Termination

In the case that a polymeric radical is completely immersed into another polymeric radical on collision, the rate constant of chain termination can be derived by the same treatment to rate constant of primary radical termination. In this section, the case that two polymeric radicals overlap each other is treated.

An overlap on a collision between polymeric radical with radius r_m and volume V_m and polymeric radical with radius r_n and volume V_n means that a point P_j in the latter immerses into the former by a length L_j . Assuming that the number of radical chain ends on P_j decreases in Δc_j during a collision, according to eq. (5) under the condition $2\gamma^* C_m x_j \ll 1$, Δc_j is given by:

$$\Delta c_j = c_j (1 - 2\gamma^* C_m x_j) \quad (11)$$

where γ is a reactivity constant between radical chain ends in the overlap volume ΔV . The distance of translation of the radical chain end in V_n during a collision is $[u_s / (u_m + u_n)] L_j$, where u_s is the mean velocity of translation of the radical chain end. If it is assumed that the radical chain end is freely diffusing in V_n during a collision, x_j is given by:

$$x_j = [u_s L_j / (u_m + u_n)] \Delta V / V_n \quad (12)$$

If it is assumed that the radical chain end is only diffusing in ΔV , x_j is given by:

$$x_j = u_s L_j / (u_m + u_n) \quad (13)$$

Generally, in this paper, x_j is given by:

$$x_j = \beta u_s L_j / (u_m + u_n) \quad (14)$$

where β is a function which depends on u_s , u_m , u_n , L_j , ΔV , and V_n ; that is, $\beta = \Delta V / V_n$ for the first case above and $\beta = 1$ for the second. By eqs. (11) and (14), a bimolecular combination probability p_t between polymeric radicals is given by:

$$\begin{aligned}
 p_t &= \frac{(c_1 + c_2 + \dots + c_j \dots) - (\Delta c_1 + \Delta c_2 + \dots + \Delta c_j + \dots)}{(c_1 + c_2 + \dots + c_j + \dots)} \\
 &= \frac{2\beta\gamma^* C_m u_s}{(u_n + u_m)} \left(\frac{\Sigma c_j L_j}{\Sigma c_j} \right) \quad (15)
 \end{aligned}$$

According to the same treatment for rate constant of primary radical termination, a rate constant of chain termination is given by:

$$k_t = 2\pi\gamma\beta N_L^* C_m u_s r_{mn}^2 \frac{(u_m^2 + u_n^2)^{1/2}}{(u_n + u_m)} \left(\frac{\Sigma c_j L_j}{\Sigma c_j} \right) \times 10^{-3} \text{ l./mole-sec} \quad (16)$$

DISCUSSION

The calculation of k_t given by eq. (16) in detail is complex and inconvenient. Under the condition: $r_m = r_n = r$ ($V_m = V_n = V$), k_t can be simply calculated by the following treatment.

A set of P_j with the same distance L_j is a part of spherical surface of sphere with radius r and its area is:

$$S = 2\pi r(L - L_j)$$

where L is the maximum value of L_j . Accordingly, $\Sigma c_j L_j / \Sigma c_j$ becomes:

$$\frac{\Sigma c_j L_j}{\Sigma c_j} = \frac{\int_0^L S L_j dL_j}{\int_0^L S dL_j} = \frac{1}{3} L \quad (17)$$

On the introduction of $r_{mn} = 2r(1 - \mu)$ where $\mu = L/2r$ and $u_n = u_m$ and on introducing eq. (17) into eq. (16), k_t becomes:

$$k_t = 8^{1/2} \gamma u_s \beta \mu (1 - \mu)^2 \times 10^3 \text{ l./mole-sec} \quad (18)$$

on taking:

$$\beta = \Delta V/V = 1/2 \mu^2 (3 - \mu) \quad (19)$$

k_t becomes:

$$k_t = 2^{1/2} \gamma u_s \mu^3 (1 - \mu)^2 (3 - \mu) \text{ l./mole-sec} \quad (20)$$

In the previous paper,⁴ k_t was also derived to be:

$$k_t = 96\pi N_L l^2 p_s u_s \mu^3 (1 - \mu)^2 (3 - \mu) \text{ l./mole-sec} \quad (21)$$

where l is the segmental length and p_s is a bimolecular combination probability per collision between radical chain ends. On taking

$$\gamma = 48\sqrt{2}\pi N_L l^2 p_s \times 10^{-3} \text{ cm}^2/\text{mole} \quad (22)$$

eq. (20) is equivalent to eq. (21). When l is evaluated by the length of the C—C bond of unit +CWX—CYZ+_n in the polymer structure, l is 1.55×10^{-8} cm, and the relationship between γ and p_s becomes

$$\gamma = 3.07 p_s \times 10^4 \text{ cm}^2/\text{mole} \quad (23)$$

TABLE I
Values $2k_t$, σ^* , η , and h_s for Ester Groups^a

Ester group	$2k_t \times 10^4$, l./mole-sec.	σ^*	$\frac{[\eta]_{monomer}}{[\eta]_{monomer}^0}$, cP	h_s , 10^{-8} , cm
Isopropyl	4.52	-0.19	0.610	6.22
Ethyl	7.35	-0.10	0.565	5.93
Methyl	11.6	0	0.516	5.63
γ -Phenylpropyl	0.813	0.02	3.42	6.99
β -Phenylethyl	1.88	0.08	2.98	6.77
β -Methoxyethyl	9.30	0.19	1.03	6.24
β -Chloroethyl	6.71	0.385	0.933	6.08
Phenyl	11.9	0.60	3.14	6.35

^a Data of Yokota et al.⁵

In the following discussion, k_t is given by:

$$k_t = 16.9b\gamma_0f(\mu) \frac{\exp\{a_t\sigma^*\}}{h_s\eta} \text{ l./mole-sec} \quad (24)$$

where

$$f(\mu) = \beta\mu(1 - \mu)^2$$

$$D_s\eta = b(\text{constant})$$

$$\gamma = \gamma_0 \exp\{a_t\sigma^*\}$$

and where b , γ_0 , and a_t are constants; σ^* is the Taft polar constant for the ester group,⁷ h_s is the distance of translation of radical chain end, and η is solvent viscosity. The results of Yokota et al. for the polymerization of some methacrylates are given in Table I. h_s was calculated for monomer by using:

$$h_s = (10^{-20}V_s/6.02)^{1/3} \text{ cm}$$

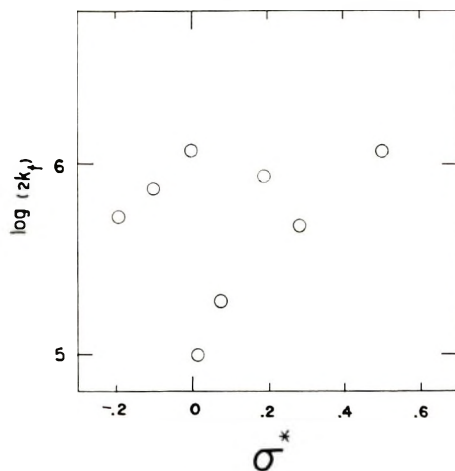


Fig. 1. Taft correlation between $\log(2k_t)$ and σ^* for ester group.

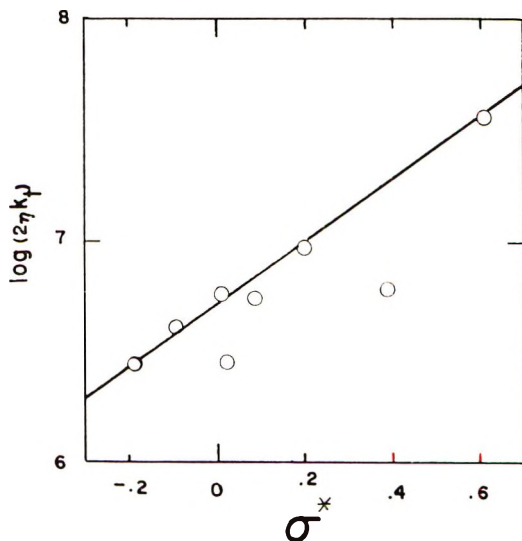


Fig. 2. Taft correlation between $\log(2\eta k_t)$ and σ^* for ester group.

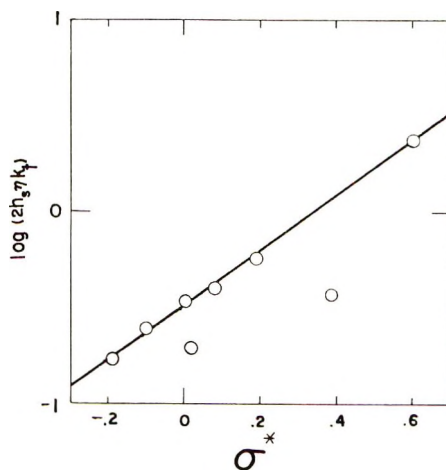


Fig. 3. Taft correlation between $\log(2h_s\eta k_t)$ and σ^* for ester group.

where V_s is the molar volume of solvent.⁴ The Taft correlation between $\log(2k_t)$ and σ^* , shown in Figure 1, is not linear. Taft correlations between $\log(2\eta k_t)$ and σ^* and $\log(2h_s\eta k_t)$ and σ^* are shown in Figures 2 and 3, respectively. The latter is more linear than the former. It thus appears that k_t evaluated by eq. (24) is reasonable for the polymerization of some methacrylates and is calculated to be

$$2k_t = (0.32/h_s\eta) \times 10^{-1.4\sigma^*} \text{ l./mole-sec} \quad (25)$$

at 30°C in the monomer solution.

Full data for the discussion of rate constant for primary radical termination are not available at present. A relationship may exist between μ_t or μ and the shielding length of Debye and Bueche.⁷ This relationship will be experimentally examined in the future.

The author thanks Dr. T. Matsuda for the treatment of polymerization reaction.

References

1. S. W. Benson and A. M. North, *J. Amer. Chem. Soc.*, **81**, 1339 (1959).
2. A. M. North and G. A. Reed, *Trans. Faraday Soc.*, **57**, 859 (1961).
3. A. M. North and G. A. Reed, *J. Polym. Sci. A*, **1**, 1311 (1963).
4. K. Ito, *J. Polym. Sci.*, in press.
5. K. Yokota, M. Kani, and Y. Ishii, *J. Polym. Sci. A-1*, **6**, 1325 (1968).
6. W. C. Wac. Lewis, *J. Chem. Soc.*, **1918**, 471.
7. P. Debye and A. M. Bueche, *J. Chem. Phys.*, **16**, 573 (1948).

Received January 27, 1969

Revised January 28, 1969

Low-Temperature Polymerization of Lactams by Using as Catalyst the Salt Derived from NaAlEt_4 and Monomer and with Several Compounds as Initiator

T. KONOMI* and H. TANI, *Department of Polymer Science, Faculty of Science, Osaka University, Toyonaka, Osaka, Japan*

Synopsis

Low-temperature polymerization of α -pyrrolidone, α -piperidone, and ϵ -caprolactam was examined by using the salts derived from NaAlEt_4 and monomer, sodium lactamates, or the salt derived from AlEt_3 and monomer as catalyst and with *N*-acetyl lactams, ethyl acetate, or lactones as initiator. Sodium lactamate catalyst gave unsatisfactory results in the cases of ethyl acetate or lactones initiators, and gave the following order for the relative efficiency of initiators: *N*-acetyl lactam $>$ ϵ -caprolactone \geq ethyl acetate $>$ β -propiolactone. The polymerization results obtained by the salt from NaAlEt_4 catalyst-ethyl acetate initiator system were nearly the same as those with *N*-acetyl lactam. The increases in the degree of polymerization and in the yield of polymer were observed in case of the salt from NaAlEt_4 catalyst-lactone initiator system, particularly in the cases of α -piperidone and ϵ -caprolactam. Also an incorporation of initiator into polymer chain was observed.

INTRODUCTION

Esters¹ or carbonates^{2,3} such as esters of aliphatic or aromatic mono- or dicarboxylic acid, Et_2CO_3 , ethyl chloroformate, propylene glycol carbonate, or glycerol tris(ethyl carbonate), had been reported to be useful as an initiators for anionic polymerization of ϵ -caprolactam. However, since the polymerization temperature used in these experiments (about 170°C) is one at which alkali metal caprolactamate catalyst itself has a polymerization activity, the real effect of an initiator is not clear.

Moreover, Sebenda et al.⁴ investigated the polymerization of ϵ -caprolactam by using several esters, lactones such as γ -butyrolactone or anhydrides as initiator and sodium salt of ϵ -caprolactam as catalyst at 170 and 80°C. They reported that initiation activity of ester initiator partly depended on its structure, but the relative order of activities is not obvious.

We investigated the apparent initiation effects of some ester compounds by varying the molar ratio of catalyst to initiator at low temperatures. The effect of the acidity of lactam on the polymerization efficiency was examined in the case of ester initiators.

* Present address: Katata Research Institute, Toyo Spinning Co., Ltd., Katata, Shiga, Japan.

EXPERIMENTAL

Monomer

α -Pyrrolidone and ϵ -caprolactam were commercial materials, and α -piperidone was synthesized from cyclopentanone oxime by Beckmann rearrangement. These monomers were purified in the same manner as described in the previous paper.⁵ The boiling points of monomers were 111.1°C/8 mm Hg for α -pyrrolidone, 112.4°C/5 mm Hg for α -piperidone, and 122.5°C/4 mm Hg for ϵ -caprolactam.

Ethyl acetate, a commercial material, was purified by distilling over P_2O_5 .

ϵ -Caprolactone and β -propiolactone were purified by fractional distillation over CaH_2 . Boiling points of caprolactone and β -propiolactone were 85°C/2.5 mm Hg and 90°C/16 mm Hg, respectively.

Preparation of Catalysts

NaAlEt₄. NaAlEt₄ was synthesized in the same manner as described in the preceding paper.⁵

NaAlEt₄ was recrystallized three times from toluene; its melting point (125°C by capillary method in dry nitrogen) is in accordance with that previously reported.⁶

NaOEt. Sodium ethoxide was prepared from metallic sodium and magnesium-treated ethyl alcohol. The excess of ethyl alcohol was removed at 120°C under a reduced pressure (3 mm Hg) after completion of reaction.

Preparation of the Solution of Catalysts in Lactams

NaAlEt₄. A definite amount of a solution of NaAlEt₄ in tetrahydrofuran was added to the molten lactam at a temperature slightly higher than the melting point of the lactam with stirring in a stream of nitrogen. After addition of the catalyst, the reaction mixture was heated at 85–90°C. under 4 mm Hg pressure until the evolution of ethane gas was completed. In this procedure, tetrahydrofuran in the mixture was removed almost completely.

AlEt₃. A solution (25 vol-%) of triethylaluminum in tetrahydrofuran was used for the reaction with lactam. The reaction procedure used was the same as that described in the case of NaAlEt₄.

Metallic Sodium and Sodium Ethoxide. A calculated amount of metallic sodium was added to lactam at a temperature of about the melting point of the lactam with stirring in a dry nitrogen atmosphere.

A solution of sodium ethoxide in lactam was prepared by adding a lactam to sodium ethoxide soon after the isolation of the latter from an ethanol solution.

Polymerization of Lactam

Polymerizations were carried out in the same manner as described in the previous paper.⁵ The polymerization was terminated by adding a mixture of 5.0 wt-% aqueous hydrochloric acid and methanol (1:1, v/v).

The reduced viscosity of the polymer solution was measured in a concentration of 0.5 g of polymer per 100 ml of *m*-cresol at 30°C.

Differential Thermal Analysis

Differential thermal analysis (DTA) was carried out in a stream of dry nitrogen with the use of a Shimadzu DT 10 instrument. A "sandwich" technique was used in which 0.200 g of sample was placed between two layers of alumina. The sample was heated at a constant rate of 8°C/min.

RESULTS

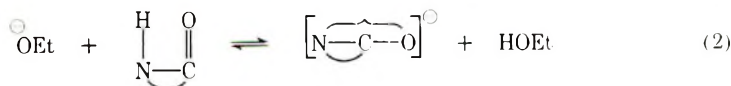
Low-Temperature Polymerization of Lactams by Use of Sodium Lactamate as Catalyst

Initiation efficiencies of some esters and lactones were studied for sodium lactamate-catalyzed polymerization of α -pyrrolidone, α -piperidone, and ϵ -caprolactam. Initiators used were *N*-acetyl lactams, ethyl acetate, ϵ -caprolactone, and β -propiolactone.

Results shown in Table I indicate that relative efficiency of the initiators the three lactams is as follows: *N*-acetyl lactam > ϵ -caprolactone > ethyl acetate > β -propiolactone.

Taking into account the polymerization time used for each, the relative polymerizability of lactam by using an ester or *N*-acetyl lactams as an initiator follows the order: α -pyrrolidone > α -piperidone.

The relative efficiency of the initiators and monomers can be accounted for by assuming the presence of an equilibrium reaction [eq. (2)] between the lactam anion and the alkoxy anion which is derived from another equilibrium reaction of the ester and the lactam anion [eq. (1)].



In addition to these reactions, the attack of the alkoxy anion on the *N*-acetyl lactam moiety of propagating polymer end also must be taken into account.

The equilibrium position of eq. (2) depends on the acidity of the lactam. pK_a values of α -pyrrolidone, α -piperidone, and ϵ -caprolactam estimated potentiometrically by Huisgen⁷ are -0.03 , 0.75 , and 0.36 , respectively.

It is considered from these values that the concentration of *N*-acetyl lactam and lactam anion required for propagation reaction is higher for the *N*-acetyl lactam initiator system than for ester initiator system, and also higher for α -pyrrolidone, which is the most acidic of the three lactams, than for the other two lactams.

To determine the effect of acidity of lactam on the initiation efficiency of an ester, for example ethyl acetate, the apparent number of polymer molecules was estimated by the ratio of yield of polymer to η_{sp}/c . As shown in Figure 1, these values parallel the pK_a values of the three lactams.

To get information on the reaction mechanism, the infrared spectra of

TABLE I
Low-Temperature Polymerization of α -Pyrrolidone, α -Piperidone,
and ϵ -Caprolactam by Using Sodium Lactamate as Catalyst and
Several Compounds as Initiator^a

Monomer	Initiator		Yield of polymer, wt-%	η_{sp}/c
	Compound ^b	Concn, mole-%		
α -Pyrrolidone	Ac-Pyr	0.5	17.5	0.41
		1.0	67.5	1.50
		2.0	91.7	0.89
		4.0	88.2	0.32
	Et-Ac	0.5	12.7	0.31
		1.0	28.9	0.38
		2.0	37.4	0.34
		4.0	76.1	0.29
	ϵ -CLN	0.5	14.1	0.38
		1.0	41.7	0.53
		2.0	80.1	0.50
		4.0	99.4	0.31
	β -PL	0.5	4.3	0.33
		1.0	8.7	0.28
		2.0	3.8	0.23
		4.0	0	—
α -Piperidone	Ac-Pip	0.5	1.2	—
		1.0	7.2	0.20
		2.0	15.4	0.11
		4.0	18.3	0.13
	Et-Ac	0.5	0.3	—
		1.0	0.9	—
		2.0	2.2	0.08
		4.0	6.9	0.08
	ϵ -CLN	0.5	4.0	0.11
		1.0	1.0	—
		2.0	2.2	0.11
		4.0	0	—
	β -PL	0.5	0	—
		1.0	0	—
		2.0	0	—
		4.0	0	—

ϵ -Caprolactam	Ac-cap	0.5	1.0	1.26
		1.0	21.2	1.13
		2.0	65.4	0.78
		4.0	94.1	0.42
	Et-Ac	0.5	0.4	—
		1.0	3.3	—
		2.0	10.0	0.14
		4.0	24.3	0.14
	ϵ -CLN	0.5	2.6	0.22
		1.0	6.3	0.22
		2.0	13.8	0.29
		4.0	25.8	0.14
	β -PL	0.5	0	—
		1.0	0	—
		2.0	0	—
		4.0	0	—

^a Polymerization temperature, 45°C for α -pyrrolidone and α -piperidone, 75°C for ϵ -caprolactam; polymerization time, 20 hr for α -pyrrolidone and ϵ -caprolactam, 3 days for α -piperidone. Catalyst, 2.0 mole-%.

^b Ac-pyr, *N*-acetyl- α -pyrrolidone; Ac-pip, *N*-acetyl- α -piperidone; Ac-cap, *N*-acetyl- ϵ -caprolactam; Et-Ac, ethyl acetate; ϵ -CLN, ϵ -caprolactone; β -PL, β -propiolactone.

the reaction mixtures of MgBr caprolactamate and lactone were examined (Fig. 2). MgBr lactamate has catalytic activity for polymerization of lactam, although less active than alkali metal, and is soluble in THF,⁸ in contrast to the insoluble alkali metal salts.

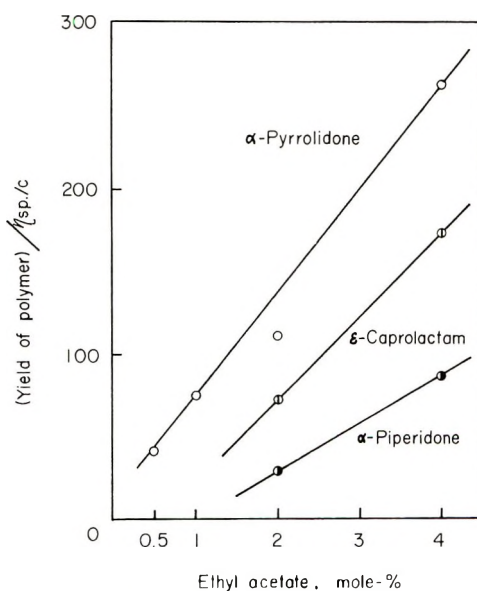


Fig. 1. Comparison of initiation efficacy of ethyl acetate in the polymerization of lactams. Sodium lactamate, 2.0 mole-%; polymerization temperature, 45°C for α -pyrrolidone and α -piperidone, 75°C for ϵ -caprolactam; polymerization time, 20 hr for α -pyrrolidone and ϵ -caprolactam, 3 days for α -piperidone.

The characteristic absorption band of MgBr lactamate in THF is at 1600 cm^{-1} , for α -pyrrolidone, 1623 cm^{-1} for α -piperidone, and 1620 cm^{-1} for ϵ -caprolactam.

Rates of disappearance of the carbonyl absorption bands of lactones in the reactions with MgBr lactamate indicate that the rate of reaction of β -propiolactone with MgBr lactamate is higher than that of ϵ -caprolactone. Also, the characteristic absorption band of MgBr lactamate decreases with

TABLE II
Low-Temperature Polymerization of α -Pyrrolidone, α -Piperidone,
and ϵ -Caprolactam by Using the Salt of NaAlEt₄ as Catalyst
and Several Compounds as Initiator^a

Monomer	Initiator		Yield of polymer, wt.-%	η_{sp}/c
	Compound	Concn, mole-%		
α -Pyrrolidone	Ac-pyr	0.5	25.8	0.743
		1.0	32.3	0.653
		2.0	42.6	0.640
		4.0	39.7	0.224
	Et-Ac	0.5	27.0	0.745
		1.0	44.5	0.549
		2.0	64.4	0.361
		4.0	75.0	0.248
	ϵ -CLN	0.5	47.8	0.669
		1.0	67.0	0.593
		2.0	82.4	0.438
		4.0	85.5	0.270
	β -PL	0.5	37.3	0.639
		1.0	65.4	0.745
		2.0	53.8	0.273
		4.0	28.8	0.208
α -Piperidone	Ac-pip	0.5	10.6	0.321
		1.0	20.0	0.316
		2.0	25.5	0.345
		3.0	34.6	0.296
	Et-Ac	4.0	39.2	0.262
		0.5	9.7	0.296
		1.0	15.9	0.296
		2.0	25.7	0.243
	ϵ -CLN	3.0	31.7	0.197
		4.0	37.5	0.156
		0.5	14.3	0.459
		1.0	21.8	0.414
	β -PL	2.0	30.7	0.319
		3.0	37.4	0.256
		4.0	40.0	0.220
		0.5	12.5	0.447
	1.0	18.5	0.339	
	2.0	16.0	0.209	
	3.0	13.4	0.178	
	4.0	4.7	0.145	

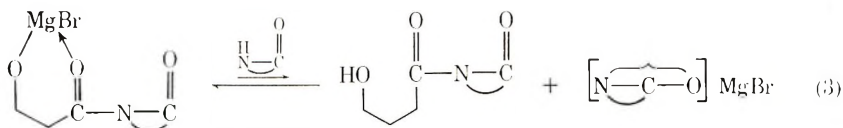
ε-Caprolactam	Ac-cap	0.5	25.3	0.885
		1.0	38.5	0.745
		2.0	58.7	0.493
		4.0	96.4	0.463
	Et-Ac	0.5	13.4	1.09
		1.0	39.6	0.784
		2.0	53.2	0.706
		4.0	93.3	0.460
	ε-CLN	0.5	42.3	1.427
		1.0	65.1	1.169
		2.0	93.6	0.935
		4.0	^b	0.664
	β-PL	0.5	33.6	1.318
		1.0	65.0	1.655
		2.0	74.2	0.803
		4.0	88.1	0.550

^a Polymerization conditions as in Table I.

^b Correct value unobtainable because resulting polymer was a very hard block, from which residual monomer could not be removed.

increasing reaction time. However, the characteristic absorption band of the *N*-acyl lactam, which should be expected to form as an intermediate, could not be observed, similarly to the cases of the reaction mixtures of *N*-acetyl lactams with MgBr lactamates. The new absorption, which is not assignable at present, appears at 1663 cm^{-1} in both reaction mixtures. Some complicated reactions may occur under these conditions between reactive carbonyls of diacylimide and MgBr lactamate or MgBr-OR (where R is propionyl or caproyl lactam).

β-Propiolactone has a low initiation efficiency while it is consumed rapidly in the reaction with catalyst, as mentioned above. This unique behavior may be due to the high stability of the intermediate which suppresses the re-formation of lactam anion by shifting the equilibrium position in eq. (3) to the unfavorable direction.



Low-Temperature Polymerization of Lactams by Use of NaAlEt(Lac)₃ or AlEt(Lac)₂ as Catalyst

NaAlEt₄ acts as a catalyst in the form of NaAlEt(Lac)₃.⁵ In the case of this catalyst, the lactone is equal to or even superior to *N*-acetyl lactam as an initiator (see Table II). This relative efficiency of initiators is contrast to the case of Na lactamate. The relative efficiency of initiators for the polymerization of α-pyrrolidone and ε-caprolactam is in the order: ε-caprolactone > β-propiolactone > *N*-acetyl lactam ≡ ethyl acetate; that for

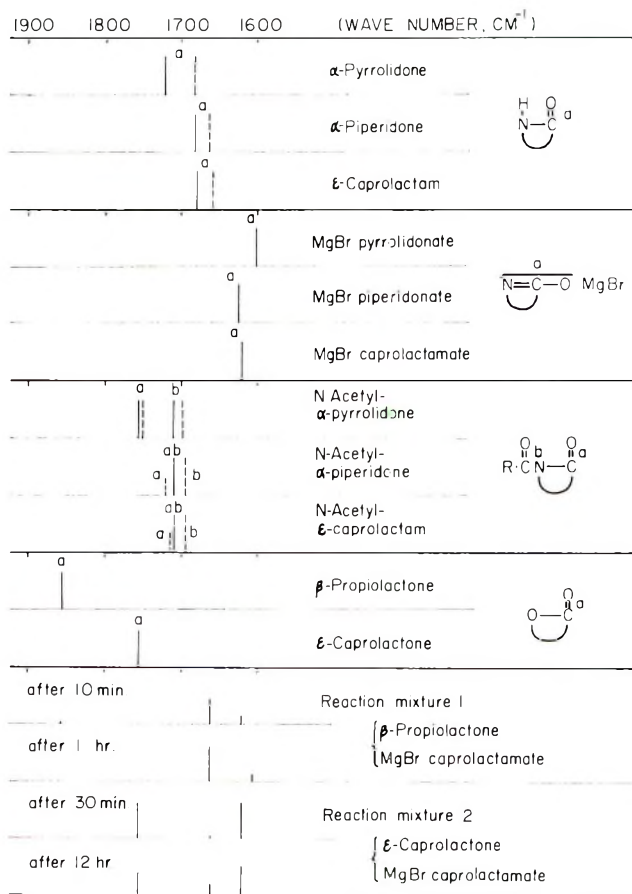


Fig. 2. Infrared spectra of the reaction mixtures of lactones and MgBr caprolactamate and related compounds (characteristic absorption, 1900–1500 cm^{-1}): (—) in THF solution 0.40 mole/l.; (---) no solvent.

polymerization of α -piperidone is ϵ -caprolactone $>$ N -acetyl piperidone \approx ethyl acetate $>$ β -propiolactone.

$\text{AlEt}(\text{Lac})_2$ is inferior to NaLac in catalytic activity for all three lactams (Table III). This is ascribed to the difference in the ionic character of the metal. The N -acetyl lactam is superior to the ester as are initiator, and this relative efficiency of the initiators is same as in the case of NaLac .

A seemingly singular result observed only in the $\text{NaAlEt}(\text{Lac})_3$ -lactone or -ethyl acetate systems cannot be explained by the independent action of NaLac and $\text{AlEt}(\text{Lac})_2$, and must be ascribed to their cooperative action. One possible explanation is the specific action of the complex derived from NaAlEt_4 and the lactam. Alkali metal salt and $\text{AlEt}(\text{Lac})_2$ have been known to interact with each other as revealed by gasometry of the reaction of AlEt_3 or NaAlEt_4 with lactams and by polymerization results with $\text{MAlEt}_{4-n}(\text{Lac})_n$ (when M is alkali metal and $n = 1, 2, \text{ or } 3$) or alkali metal

TABLE III
 Low-Temperature Polymerization of α -Pyrrolidone, α -Piperidone,
 and ϵ -Caprolactam by Using the Salt of Triethylaluminum with
 Monomer as Catalyst and Several Compounds as Initiator^a

Monomer	Initiator		Yield of polymer, wt-%	η_{sp}/c
	Compound	Concn, mole-%		
α -Pyrrolidone	Ac-pyr	1.0	5.4	0.135
		2.0	17.8	0.160
	Et-Ac	1.0	7.3	0.097
		2.0	19.8	0.304
	ϵ -CLN	1.0	18.8	0.233
		2.0	36.8	0.240
	β -PL	1.0	19.2	0.243
		2.0	5.3	0.168
α -Piperidone	Ac-pip	1.0	1.2	—
		2.0	1.5	—
	Et-Ac	1.0	0	—
		2.0	0	—
	ϵ -CLN	1.0	0	—
		2.0	0	—
	β -PL	1.0	0	—
		2.0	0	—
ϵ -Caprolactam	Ac-cap	1.0	36.1	0.246
		2.0	50.3	0.248
	Et-Ac	1.0	24.6	0.245
		2.0	40.7	0.250
	ϵ -CLN	1.0	50.3	0.254
		2.0	57.3	0.248
	β -PL	1.0	0	—
		2.0	trace	—

^a Polymerization conditions as in Table I.

piperidonate-AlEt(piperidone)₂ catalyst systems.^{5,9} The catalytic activity of alkali metal lactamate is somewhat lowered by the interaction, since the alkali metal lactamate is stabilized by complex formation with Al lactamate. This phenomenon is made clear by comparing the results of polymerization of α -pyrrolidone by sodium with that by NaAlEt(Lac)₃. At low temperatures α -pyrrolidone has the highest reactivity towards alkali metal and the highest polymerizability among these lactams. The effect of alkoxy anion formed in the reaction of ester or lactone with the salt on the polymerization efficiency therefore may vary in the presence of AlEt(Lac)₂.

Infrared and elemental analyses indicate that the polymers obtained by using 4 mole-% ϵ -caprolactone or β -propiolactone as an initiator contain the —COO— unit in the polymer chain (see Fig. 3 and Table IV). Infrared spectra of the polymers obtained with ϵ -caprolactone have a shoulder band at 1735 cm⁻¹ which is assignable to a characteristic absorption band of a saturated linear ester.¹⁰ The band at 1715 cm⁻¹ observed in the

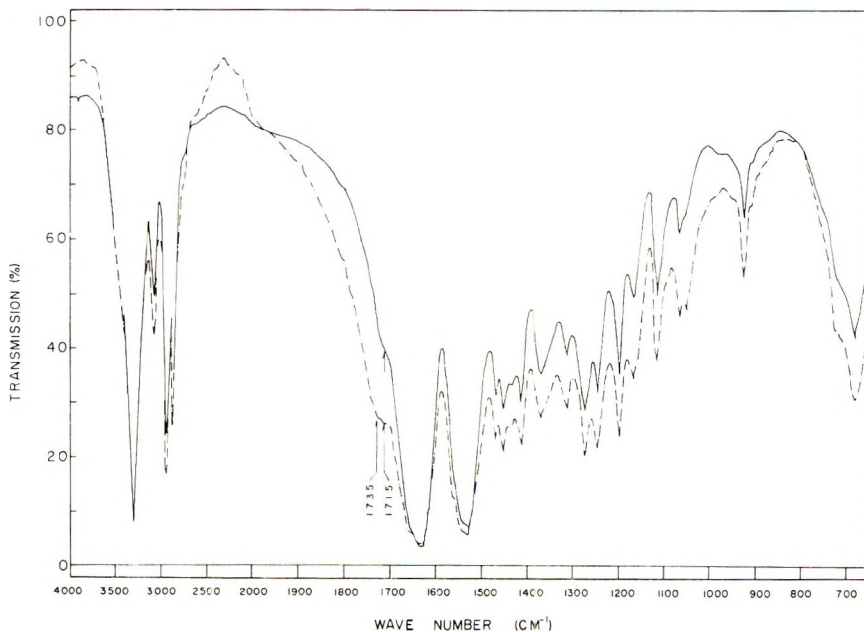
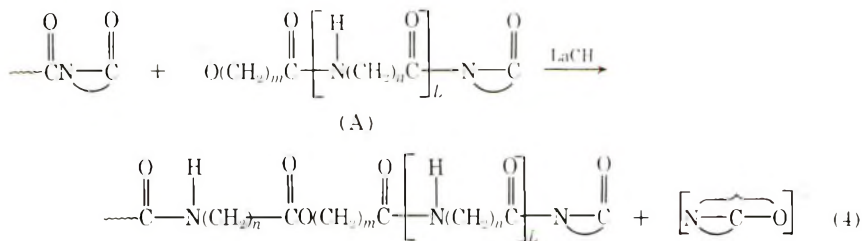


Fig. 3. Infrared spectra (KBr disk) of poly- α -piperidone prepared by use of *N*-acetyl- α -piperidone or ϵ -caprolactone as initiator under various polymerization conditions: (—) $\text{NaAlEt}_4 = 2.0$ mole-%, *N*-acetyl- α piperidone = 4.0 mole-%, $\eta_{sp}/c = 0.31$; (---) $\text{NaAlEt}_4 = 2.0$ mole-%, caprolactone = 4.0 mole-%, $\eta_{sp}/c = 0.28$. Polymerization temperature, 45°C; polymerization time, 3 days.

polymer obtained with *N*-acetyl lactam or ϵ -caprolactone initiator is due to the CO vibration of the carboxylic acid group in the polymer chain end.

The results above imply that the attack of (A) [eq. (4), $L \geq 0$], which is formed by the reaction of the lactone with a lactam anion or its propagating polymer anion at the diacylimide moiety, on the *N*-acyl lactam of polymer end, actually results in the increase of the polymer chain length.



Stability of NaAlEt_4 in THF Solution in the Presence of Ethyl Acetate or ϵ -Caprolactone

Results obtained in the determination of the stability of NaAlEt_4 determined by gasometry in THF solution in the presence of ethyl acetate or

TABLE IV
Some Properties of Polymers Obtained by
Using Several Compounds as Initiator^a

Polymer	Nitrogen content, wt-%	η_{sp}/c	Initiator		Melting point, °C	
			Com- pound	Concn, mole- %	Meiho ^b	DTA ^c
Poly- α -pyrrolidone	16.47(16.46) ^d	0.224	Ac-pyr	4.0	257	258
	16.27	0.248	Et-Ac	4.0	254	—
	15.18	0.270	ϵ -CLN	4.0	251	254
Poly- α -piperidone	15.58	0.208	β -PL	4.0	249	—
	14.13(14.15) ^d	0.262	Ac-pip	4.0	261	261
	14.12	0.197	Et-Ac	3.0	258	—
Poly- ϵ -caprolactam	13.82	0.220	ϵ -CLN	4.0	258.5	259
	13.54	0.209	β -PL	2.0	260	—
	12.79(12.38) ^d	0.607	Ac-cap	1.0	210	—
	12.36	0.651	Et-Ac	1.0	209	—
Poly- ϵ -caprolactam	10.46	0.604	ϵ -CLN	4.0	212	214
	12.13	0.803	β -PL	2.0	209	—

^a Polymerization conditions as in Table I.

^b Measured by using MEIHO SHARP MELTING POINT APPARATUS.

^c Differential thermal analysis, SHIMAZU DT-10, Heating rate, 6°C./min. in N₂.

^d The values in parentheses are calculated nitrogen contents.

ϵ -caprolactone are shown in Tables V and VI. In the presence of ethyl acetate or ethyl benzoate, the concentration of NaAlEt₄ decreased slightly at first, and then remained constant even after 2–3 hr. Although in these systems the formation of ketone from ester may be possible, the absence of

TABLE V
Stability of Sodium Tetraethylaluminate in Ethyl Acetate or Ethyl Benzoate

	Time of treatment hr ^a	Unreacted NaAlEt ₄ , mole $\times 10^3$ ^b
Blank (in THF)	1.0	2.81
	2.0	2.81
	3.0	2.83
In ethyl acetate	1.0	2.73
	2.0	2.57
	3.0	2.60
In ethyl benzoate	0.02	2.73
	1.0	2.79
	2.0	2.51
	3.0	2.54

^a Treatment was carried out at 70°C with 2.0 ml of a solution of NaAlEt₄ (0.141 mole/l) in THF and 2.0 ml of ethyl acetate (water content in ethyl acetate, 0.134 mg/1.0 ml by Karl Fisher Method); 2.0 ml. of a solution of 5 wt-% aqueous HCl, CH₃OH, and THF (50:25:25, by volume) was used for the hydrolysis of pretreated NaAlEt₄.

^b Unreacted NaAlEt₄ calculated by gasometry.

TABLE VI
Stability of Sodium Tetraethylaluminumate in ϵ -Caprolactone

	Time of treatment, hr ^a	Remaining NaAlEt ₄ , mole $\times 10^{11}$ ^b	Poly- ϵ -caprolactone formed, g ^c
Blank (in THF)	0	3.72	
	1	3.58	
	2	3.58	
In ϵ -caprolactone	0	3.63	0.298
	1	3.34	0.258
	2	3.31	0.327

^a Treatment was carried out at 75°C with 0.150 ml. of a solution of NaAlEt₄ (2.48 mole/l) in THF and 1.0 ml of ϵ -caprolactone; 2.0 ml. of a solution of 5 wt-% aqueous HCl, CH₃OH, and THF (25:25:50, by volume) was used for the hydrolysis of pre-treated NaAlEt₄.

^b Unreacted NaAlEt₄ was calculated by gasometry.

^c Poly- ϵ -caprolactone was detected by infrared spectroscopy, melting point, and elementary analysis.

evolution of ethane gas denies this possibility, because ethane should be evolved from methyl ethyl ketone in the reaction with NaAlEt₄ or AlEt₃ at 20 and 70°C, respectively. The observed exothermicity in these systems suggests that a ligand exchange reaction of ester and THF around NaAlEt₄ occurs to some extent. These results strongly suggest that THF solution of NaAlEt₄ and ethyl acetate contains both the components and has the polymerization activity equal to the most ideal system, such as the *N*-acyl system.

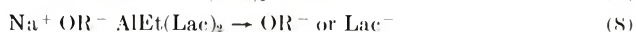
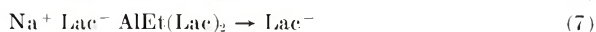
On the other hand, in caprolactone, the concentration of NaAlEt₄ decreased somewhat more at first, and formation of poly- ϵ -caprolactone (about 40% of ϵ -caprolactone) was observed simultaneously.

DISCUSSION

In the case of low-temperature polymerization of lactams with ester as an initiator, the equilibrium reactions (1) and (2) should be taken into consideration. These equilibria affect the polymerization, particularly in the case of α -piperidone, which is the most basic of the three lactams.

The sodium lactamate catalyst-ester initiator systems give unsatisfactory results because of the presence of reactions (1) and (2). A complex, NaAlEt(Lac)₃, promotes both the formation of *N*-acyl lactam and the propagation reaction by depressing the attack of the alkoxy anion on the *N*-acyl lactam moiety of the initiator or of the propagating polymer end.

The anions produced from the various metal salts are listed in eqs. (5)–(8).



Incorporation of an ester group into the polymer chain by the attack of an alkoxyl anion on the propagating polymer end was observed in the case of ϵ -caprolactone or β -propiolactone initiator. This implies that the increase in polymerization efficiency (yield of polymer and degree of polymerization) observed when ϵ -caprolactone or β -propiolactone is used as an initiator is due to the higher concentration of *N*-acyl lactam throughout the polymerization process and to the increase of polymer chain length caused by the attack of alkoxyl anion on propagating polymer end, as shown in eq. (4).

References

1. Ger. (East) 19,839 (1960). A. Matthes, K. Zimmerman, and R. Glasmann, *Chem. Abstr.*, **55**, 22914 (1961).
2. Brit. 945,218 (1963). Farbenfabriken Bayer A.-G., *Chem. Abstr.*, **60**, 14636 (1963).
3. Brit. 931,013 (1963). Imperial Chemical Industries, *Chem. Abstr.*, **59**, 10262 (1963).
4. J. Stehlicek, J. Sebenda, and O. Wichterle, *Collection Czech. Chem. Commun.*, **29**, (1964).
5. H. Tani and T. Konomi, *J. Polym. Sci.*, Part A, **4**, 301 (1966).
6. L. I. Zakharkin and V. V. Gavrilenko, *J. Gen. Chem. USSR*, **32**, 688 (1962).
7. R. Huisgen and H. Walz, *Chem. Ber.*, **86**, 2616 (1956); R. Huisgen, R. and H. Brade, H. Walz, and I. Glogger, *Ber.*, **90**, 1437 (1957).
8. S. Barzakay, M. Levy, and D. Vofsi, *J. Polym. Sci.*, Part A, **4**, 2211 (1966).
9. T. Konomi and H. Tani, *J. Polym. Sci.*, Part A, **6**, 2295 (1968).
10. L. J. Bellamy, *Infra-red Spectra of Complex Molecules*, Wiley, New York, 1958, pp. 161, 178.

Received December 16, 1968

Revised February 10, 1969

High-Temperature Polymerization of ϵ -Caprolactam by Using as Catalyst the Li, Na, or K Salts Derived from $\text{MAI}Et_4$ or $\text{MOAI}Et_2 \cdot \text{Al}Et_3$ and Monomer

T. KONOMI* and H. TANI, *Department of Polymer Science, Faculty of Science, Osaka University, Toyonaka, Osaka, Japan*

Synopsis

High-temperature polymerization of ϵ -caprolactam by using the salts derived from $\text{MAI}Et_4$ (where M is Li, Na, and K) and monomer as catalyst was carried out. Polymerization occurs at 140–170°C, a temperature at which alkali metal caprolactamate has almost no catalytic activity for initiation. *m*-Cresol-insoluble polymer was obtained at temperatures lower than 231°C. Formation of a *m*-cresol-insoluble polymer depends on the polymerization temperature and time, and was observed under conditions where $\text{Al}(\text{Lac})_3$ has no catalytic activity. All the polymers obtained by $\text{NaAl}(\text{Lac})_{4-n}(\text{NHBu})_n$ ($n = 1$ or 2) at 202°C were soluble in *m*-cresol. These trends observed in the case of $\text{MAI}(\text{Lac})_4$ are considered to be due to initiation by $\text{Al}(\text{Lac})_3$, which is a component of the catalyst used.

INTRODUCTION

Various compounds have been reported as catalysts for polymerization of ϵ -caprolactam. For example, alkali metal,¹ alkali metal salts of carboxylic acids,² alkali metal cyanide or azide,² alkali metal hydroxide,³ Grignard reagent⁴ or aluminum trialkyls^{5,6} have been known to be useful.

We have reported the low-temperature polymerization of five-, six-, and seven-membered ring lactams by using the Na piperidonate– $\text{Al}Et$ (piperidone)₂ system⁷ or the salt of $\text{MAI}Et_4$ (where M may be Li, Na, or K) with monomer as catalyst.⁸

In this paper, the high-temperature polymerization of ϵ -caprolactam by using as catalyst the salts derived from the reaction of $\text{MAI}Et_4$ or $\text{MOAI}Et_2 \cdot \text{Al}Et_3$ with monomer is reported.

EXPERIMENTAL

Preparation of Catalyst

$\text{MAI}Et_4$. $\text{NaAl}Et_4$ was synthesized from the mixture of metallic sodium and triethylaluminum in a small amount of toluene under reflux in a dry nitrogen atmosphere with vigorous stirring.^{7,8} Pure crystalline $\text{NaAl}Et_4$, obtained after three recrystallization from toluene, had a melting point of

* Present address: Katata Research Institute, Toyo Spinning Co., Ltd., Katata, Shiga, Japan.

125°C (in dry N₂ atmosphere, capillary method); this value is in accordance with that reported⁹ in the literature.

LiAlEt₄ was synthesized in the same manner as described for NaAlEt₄ from metal and triethylaluminum; the crystals obtained were sublimed at 165°C.

KAlEt₄ was prepared from metallic potassium and triethylaluminum in tetrahydrofuran. Crystalline KAlEt₄ melts at 78°C after removal of tetrahydrofuran at 65–75°C under a pressure of 10⁻² mm Hg.

NaOAlEt₂·AlEt₃.^{10,11} To a suspension of powdery NaOH (2.00 g, 0.050 mole) in 25 ml. of dry benzene, a solution of AlEt₃ (11.14 g, 0.10 mole) in 15 ml. of benzene was added dropwisely with stirring in a stream of dry nitrogen. The reaction temperature was maintained at about the boiling temperature of benzene by controlling the addition rate of a solution of AlEt₃ in benzene. In this reaction, half a mole of ethane gas per mole of AlEt₃ was evolved. After completion of gas evolution, the reaction mixture was heated for 30 min. White crystals separated out from the concentrate obtained by removing about 20 ml of benzene under reduced pressure (40 mm Hg) from the reaction mixture. The crystals were filtered off after adding 40 ml of dry *n*-hexane under vigorous stirring. Dissolution in benzene, crystallization, and washing with *n*-hexane were repeated twice. The crystalline compound had a melting point of 168–173°C (in dry N₂ atmosphere, capillary method).

KOAlEt₂·AlEt₃. KOAlEt₂·AlEt₃ were prepared, in the same manner as described for NaOAlEt₂·AlEt₃, starting from 1.5 g of KOH (0.0268 mole) and 6.12 g of AlEt₃ (0.0536 mole). Crystalline KOAlEt₂·AlEt₃ separated from the viscous liquid obtained by removing benzene at 100–103°C had a melting point of 158–164°C.

NaAlEt₃(OEt). The monoethanolate of NaAlEt₄ was prepared by vigorously stirring an equimolar mixture of NaAlEt₄ and ethanol in benzene at room temperature. Solvent and remaining ethanol were removed as completely as possible after completion of the reaction.

Monomer

ε-Caprolactam was a commercial material purified by fractional distillation in a stream of dry nitrogen. The water content in the monomer used for polymerization was 0.006–0.007 wt-% (Karl Fisher method).

Preparation of Solution of Catalyst in ε-Caprolactam

The catalyst was dissolved in tetrahydrofuran, and its concentration was determined by back-titration and gasometry.

A definite amount of a tetrahydrofuran solution of catalyst was added with stirring to liquid ε-caprolactam maintained at a temperature slightly higher than the melting point. Ethane gas was evolved. The system was heated at 110–120°C under reduced pressure in order to remove tetrahydrofuran in the system as completely as possible. In this procedure, about three-fourths of the ethyl groups in NaAlEt₄ reacted with ε-caprolactam.⁸

In the preparation of the solution of a definite concentration of $\text{Al}(\text{Iac})_3$ in monomer, a solution of AlEt_3 in THF [$\text{AlEt}_3:\text{THF} = 1:4(\text{v/v})$], the concentration of which had been previously determined by gasometry and back-titration, was added stepwise to molten ϵ -caprolactam at $70\text{--}75^\circ\text{C}$ with stirring in a stream of dry nitrogen, and then tetrahydrofuran was removed under a reduced pressure of $5\text{--}10$ mm Hg. The reaction between AlEt_3 and ϵ -caprolactam was completed by maintaining the system at $110\text{--}120^\circ\text{C}$ under about 10 mm Hg for 30 min.

Preparation of Sodium Caprolactamate

About 2.76 g (ca. 30 mole-% based on ϵ -caprolactam) of a freshly cut sodium metal ($1.5 \times 1.5 \times 2.0$ mm³) was mixed with solution consisting of 45.2 g of ϵ -caprolactam and 20 ml of toluene with stirring in a dry nitrogen atmosphere at such a rate that the temperature of the reaction mixture from which hydrogen gas evolved was not elevated above $85\text{--}90^\circ\text{C}$. As the reaction proceeds, the rate of reaction decreased; therefore after addition of about three fourths the calculated amount of sodium metal, the reaction system was heated to $90\text{--}100^\circ\text{C}$. White crystalline of sodium caprolactamate was precipitated by adding a 1:1 solution (v/v) of hexane and toluene. Sodium caprolactamate was isolated by filtration, washed five times with dry benzene in a dry nitrogen atmosphere, and dried at $120\text{--}140^\circ\text{C}$ under reduced pressure (10^{-4} mm Hg) for 2 hr.

Polymerization

A solution having a known catalyst concentration in ϵ -caprolactam was divided into ampoules previously flushed with dry nitrogen, and the ampoules were sealed and allowed to stand in a constant temperature vapor bath for a given time. (*n*-Decyl alcohol, *m*-cresol, and diphenyl were used for vapor bath.) The polymerization mixture was quenched and polymerization was terminated with methanol. The solid product (thickness, 0.1–0.2 mm.; width, 0.5–1.0 mm., and length, 2–30 mm) of polymer was extracted with methanol or water for 6 hr. In the case of low polymer yield, the powderlike polymer was washed with methanol and water. The amount of soluble material in the polymerization system, i.e., monomer and oligomer, was calculated from the weight loss after the extraction. The insoluble polymer fraction was dried at 68°C under reduced pressure (10–20 mm Hg) for 5 days.

The viscosity of polymer was measured in a solution of 0.5 g polymer in 100 ml *m*-cresol at 30°C .

RESULTS

Reaction between $\text{NaOAlEt}_2 \cdot \text{AlEt}_3$ or $\text{KOAlEt}_2 \cdot \text{AlEt}_3$ and ϵ -Caprolactam at Various Temperatures

The number of reactable ethyl groups in $\text{MOAlEt}_2 \cdot \text{AlEt}_3$ with ϵ -caprolactam was examined (Table I). Similar experiments with NaAlEt_4 were reported in a preceding paper.⁸

TABLE I
Ethyl Groups in $\text{MOAlEt}_2 \cdot \text{AlEt}_3$ Reacting with ϵ -Caprolactam^a

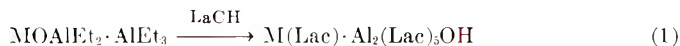
Catalysts	Molar ratio of ethane evolved to catalyst at various reaction temperatures ^b			
	17–20°C ^c	80°C	120°C	160°C
$\text{KOAlEt}_2 \cdot \text{AlEt}_3$	0	1.09	4.29	4.87
$\text{NaOAlEt}_2 \cdot \text{AlEt}_3$	0.25	1.49	4.51–4.63	—

^a 0.50 ml of a solution of catalyst in tetrahydrofuran and 2.0 ml of caprolactam were used. Tetrahydrofuran was removed as well as possible at 60°C under the reduced pressure (4 mm Hg) before mixing the reactants. $\text{KOAlEt}_2 \cdot \text{AlEt}_3$, 0.988 mole/l.; $\text{NaOAlEt}_2 \cdot \text{AlEt}_3$, 1.22 mole/l.; reaction time, 20 min.

^b Blank value of ethane gas evolved obtained by hydrolysis of catalyst with a solution of 5 wt-% aqueous HCl in methanol and tetrahydrofuran (50:25:25, by volume).

^c 4.0 ml. of tetrahydrofuran was added to the system to dissolve ϵ -caprolactam.

The gas evolved in this reaction was proved by gas chromatography and infrared analysis to be ethane. At a temperature of about 120°C, almost all of the ethyl groups in $\text{MOAlEt}_2 \cdot \text{AlEt}_3$ reacted with ϵ -caprolactam.



Since $\text{MAI}(\text{Et})_4$ and $\text{MOAlEt}_2 \cdot \text{AlEt}_3$ show polymerization activity for ϵ -caprolactam at about 140°C, a similar experiment to determine gas evolution at about 120°C was practically impossible, particularly in the case of a high concentration of catalyst. If the polymerization was begun before completion of gas evolution, the polymerization system contained numerous small bubbles of gas.

The temperature dependence of reactivity of $\text{MOAlEt}_2 \cdot \text{AlEt}_3$ was almost same as that of $\text{MAI}(\text{Et})_4$. At low temperatures, $\text{MAI}(\text{Et})_4$ forms the complex $\text{MAI}(\text{Et})_{4-n}(\text{Lac})_n$ ($n = 1, 2$ or 3) in lactam, and the reactivity of ethyl groups in $\text{MAI}(\text{Et})_4$ towards the lactam depends on the nature of alkali metal.* At temperatures higher than 120°C, all of the ethyl groups in $\text{MAI}(\text{Et})_4$ react with ϵ -caprolactam, and at 255°C the complex $\text{MAI}(\text{Lac})_4$ is considered to dissociate into each metal salts. The dissociation of $\text{MAI}(\text{Lac})_4$ at 255°C is deduced from the interpretation of the relationship between concentration of lactam anion and degree of polymerization of the resulting polymers; this subject will be described in a subsequent paper.

Polymerization Behavior of ϵ -Caprolactam

Results of the polymerization of ϵ -caprolactam with the use of $\text{NaAl}(\text{Lac})_4$ as catalyst are shown in Table II.

Polymerization occurs at 170°C at a comparatively rapid rate; this fact is contrast to the case of Na caprolactamate, which shows a low catalytic activity at this temperature.^{12,13} The temperature dependence of the polymerizability of ϵ -caprolactam with the use of the isolated sodium

* Here of M(Lac) , MAI(Lac) , etc. refer to the metal salt of ϵ -caprolactam.

TABLE II
 High-Temperature Polymerization of ϵ -Caprolactam by use of
 the Salt Derived from NaAlEt₄ with ϵ -Caprolactam^a

Polymerization temperature, °C	Polymerization time, min	Methanol-soluble material, ^b wt-%	η_{sp}/c^e
140	20	98.63 ^c	—
	30	98.41 ^c	—
	60	96.25 ^c	—
	120	91.85 ^c	3.53
	180	85.75 ^c	6.36
170	10	98.85 ^c	2.02
	20	79.50 ^c	5.13
	30	65.00	5.77
	60	35.9	14.79
	90	13.2	Insoluble ^d
	120	8.07	Insoluble ^d
202	180	8.05	Insoluble ^d
	10	37.0	Insoluble ^d
	20	13.6	Insoluble ^d
	30	13.1	Insoluble ^d
	60	11.5	Insoluble ^d
	120	9.48	Insoluble ^d
231	180	10.65	Insoluble ^d
	10	11.9	Insoluble ^d
	20	11.2	Insoluble ^d
	30	11.4	Insoluble ^d
	60	11.5	10.1
	120	12.1	3.92
255	180	11.4	3.27
	10	13.1	5.57
	20	12.6	3.61
	30	12.6	3.21
	60	13.3	2.47
	120	12.5	1.72
	180	12.4	1.48

^a Catalyst concentration, 0.25 mole-% (as NaAlEt₄).

^b Weight loss in the polymerized ϵ -caprolactam after extraction with methanol for 6 hr.

^c Calculated from the weight of resulting polymer.

^d Insoluble in *m*-cresol.

^e Reduced viscosity of the solution of methanol-soluble part (polymer) in *m*-cresol.

caprolactamate as a catalyst was examined, and results are shown in Table III.

The polymerization results at the temperatures lower than 230°C were not reproducible because of the extreme sensitivity of the nonactivated polymerization system to impurities. The polymerizability data for ϵ -caprolactam are sufficient to compare efficacy of various catalysts, although the data are somewhat inferior to those obtained with sodium lactamate prepared from sodium methoxide and monomer.¹⁴

TABLE III
Sodium Caprolactamate-Catalyzed Polymerization of ϵ -Caprolactam^a

Polymerization temperature, °C	Polymerization time, min	Methanol soluble ^b wt-%	η_{sp}/c
202	20	99.30	—
	40	98.57	—
	60	90.79	—
230	20	11.56	3.19
	40	11.26	2.90
	60	11.38	2.14
250	20	11.83	1.51
	40	13.50	1.29
	60	12.06	0.977

^a Catalyst concentration: Na(Lac)/Na(Lac) + LacH = 1/100 (mole/mole).

^b Extracted with methanol for 6 hr.

TABLE IV
Polymerization of ϵ -Caprolactam by Use of Aluminum Caprolactamate Al(Lac)₃ as Catalyst^a

Polymerization temperature, °C	Polymerization time, min	Yield of polymer, wt-% ^b	η_{sp}/c
170	60	0	—
	120	0	—
202	10	0	—
	20	0	—
	30	0	—
	60	7.2	0.432
	120	57.3	1.75
231	10	0	—
	20	0	—
	30	14.2	0.732
	60	35.1	0.841
	120	57.3	1.75
255	10	13.5	0.831
	20	46.8	1.69
	30	65.9	1.54
	60	72.1	1.37
	120	54.2	1.26

^a Catalyst concentration [as Al(Lac)₃], 0.50 mole-%.

^b Based on the ϵ -caprolactam charged.

Formation of *m*-cresol-insoluble polymer is observed under certain polymerization conditions. This feature is remarkably different from that observed in the case of Na lactamate. The insoluble polymer is one which swells and does not dissolve in *m*-cresol at temperatures between 20 and 100°C.

In the polymerization initiated by a metal salt of lactam without other initiator, the catalyst should be regarded to participate in initiation, propagation, and depolymerization process. This expectation will be

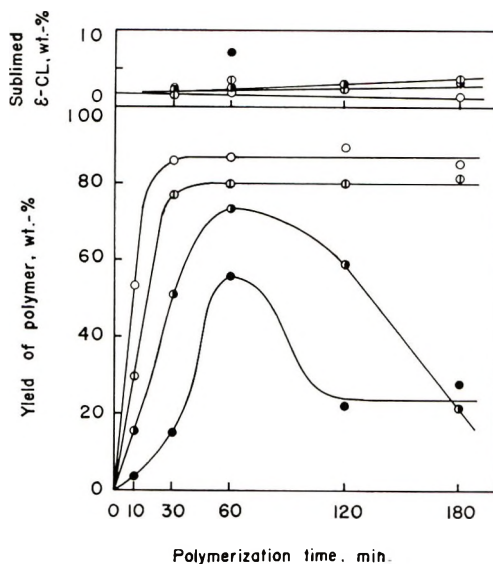


Fig. 1. Yield of polymer and sublimed monomer in polymerization of ϵ -caprolactam by use of the salt derived from AlEt_3 with monomer as catalyst at 255°C at various catalyst concentrations: (O) 1.0 mole-%; (\square) 0.75 mole-%; (\bullet) 0.50 mole-%; (\bullet) 0.25 mole-%.

particularly true in the case of catalyst composed of two different metal salts of lactam, both of which have catalytic activities. In this connection, the catalytic activity of $\text{Al}(\text{Lac})_3$ was investigated and compared to that of $\text{NaAl}(\text{Lac})_4$, because $\text{Al}(\text{Lac})_3$ is a component of $\text{NaAl}(\text{Lac})_4$ never previously investigated in detail¹⁵ (Table IV, Figs. 1 and 2).

$\text{Al}(\text{Lac})_3$ has a low catalytic activity and its activity is evident only at temperatures higher than 231°C . The concentration of $\text{Al}(\text{Lac})_3$ necessary for completing polymerization is somewhat higher than that of Na caprolactamate. This is in accordance with the results in the literature.¹⁵

The relation between formation of insoluble polymer by $\text{NaAl}(\text{Lac})_4$ and catalytic activity of $\text{Al}(\text{Lac})_3$ was studied. On reaction at 255°C for 3 hr, $\text{NaAl}(\text{Lac})_4$ produces *n*-cresol-insoluble polymer and $\text{Al}(\text{Lac})_3$ shows initiation activity. At 231°C , $\text{NaAl}(\text{Lac})_4$ produces polymer: with reaction times less than 30 min and insoluble polymer was obtained; after 30 min, a soluble polymer was obtained. At the threshold condition, 231°C for 30 min, $\text{Al}(\text{Lac})_3$ gradually begins to exhibit its characteristic activity. At 202°C , all of the polymers obtained with $\text{NaAl}(\text{Lac})_4$ are insoluble, and $\text{Al}(\text{Lac})_3$ has almost no catalytic activity. At 170°C , in the polymerization by $\text{NaAl}(\text{Lac})_4$ the amount of *m*-cresol-insoluble material increases with increasing polymerization time, and $\text{Al}(\text{Lac})_3$ has no activity. All of the polymers obtained by $\text{Al}(\text{Lac})_3$ are soluble in *m*-cresol. This result is sharply contrast with results with $\text{NaAl}(\text{Lac})_4$. The peculiar phenomena observed in the case of $\text{NaAl}(\text{Lac})_4$ can be concluded to occur only in the presence of both $\text{Al}(\text{Lac})_3$ and $\text{Na}(\text{Lac})$.

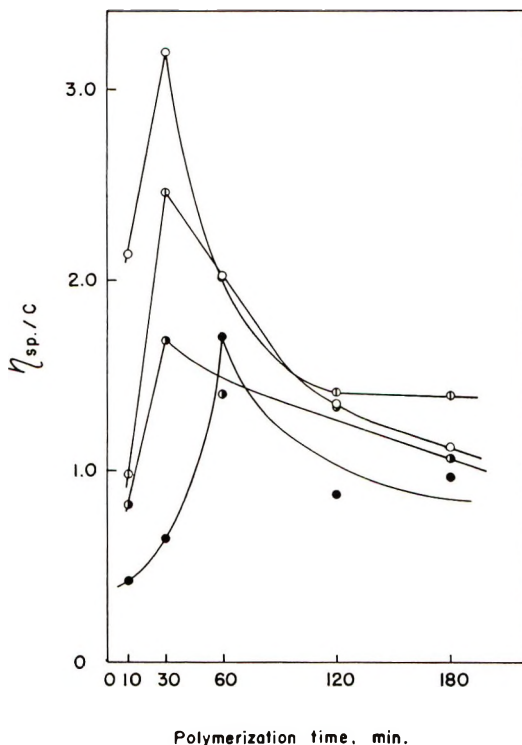


Fig. 2. Reduced viscosity of polymer obtained in polymerization of ϵ -caprolactam by use of the salt derived from $AlEt_3$ with monomer as catalyst at $255^\circ C$. Symbols as in Fig. 1.

Effect of Polymerization Temperature on Solubility of Polymer

The solubility and reduced viscosity of the polymer obtained with $NaAl(Lac)_4$ under different polymerization conditions was studied (Table V).

The polymer, which was polymerized first at $255^\circ C$ for 30 min and then at $202^\circ C$ for 2 hr, was completely soluble in *m*-cresol. The solution viscosity of polymers obtained at various polymerization times at a temperature of $202^\circ C$ was almost the same value. Since $Al(Lac)_3$ has almost no polymerization activity at $202^\circ C$ for less than 3 hr, $Al(Lac)_3$ is considered to take little part in the degradation reaction at this temperature due to low dissociation of $Al(Lac)$. In fact, Sekiguchi¹⁶ reported that, in the case of sodium lactamate, the initiation reaction requires somewhat more severe conditions, that its activation energy estimated from the temperature dependence of conductivity of sodium lactamate is 56 ± 3 kcal/mole and that the polymer obtained in the presence of both $NaLac$ and $Al(Lac)_3$ was thermally stable.

The effect of the polymerization time on the solubility of polymer was studied at $202^\circ C$ (Table VI). Even at this temperature, the resulting

TABLE V
Effect of Polymerization Temperature on Solubility of Polymer^a

Polymerization conditions	η_{sp}/c
255°C, 30 min	2.786
255°C, 150 min	1.289
255°C, 30 min; 200°C, 30 min	2.614
255°C, 30 min; 200°C, 60 min	2.286
255°C, 30 min; 200°C, 120 min	2.339

^a NaAl(Lac)₄, 0.50 mole-%.

polymer was a soluble one if the polymerization time was increased from 6 to 12 hr. Therefore the insolubility of polymer depends on both polymerization temperature and time, which in turn is closely related to the catalytic activity of Al(Lac)₃. This also suggests that the change from an insoluble polymer to a soluble one is due to a splitting off of an Al compound from the polymer by slow dissociation.

TABLE VI
Effect of Polymerization Time on the Solubility of
Polymer Obtained at 202°C^a

Polymerization time, hr.	η_{sp}/c
1.5	Insoluble
3.0	Insoluble
6.0	Insoluble
12	3.395

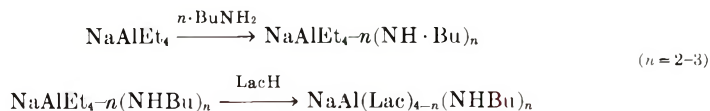
^a NaAl(Lac)₄, 0.50 mole-%.

Polymerization of ϵ -Caprolactam by Using the Lactamate Derived from NaAlEt₄-*n*-BuNH₂ System as Catalyst

It seems reasonable to consider that insoluble polymer has a network structure originating from the growing of three polymer chains from an Al atom. If this speculation is correct, the formation of insoluble polymer should be prevented by blocking at least one of the three groups attached to Al atom by a stable group. To investigate this further, the lactamate derived from NaAlEt₄-*n*-BuNH₂ system was used as a catalyst. The Al-NH bond in Al(Lac)₃-*n*(NHBu)_{*n*} may be considered to be more stable to the attack by a lactam anion than the Al-N bond in Al(Lac) or the Al-O bond in Al(Lac)₂OEt, because an electron deficiency of Al and the electron-donating tendency of the -NHBu group act reciprocally.

The polymerization activity of this catalyst was somewhat lower than that of NaAlEt₄, and an equilibrium between monomer and polymer was attained within 1 hr.

In the reaction of NaAlEt₄ with *n*-BuNH₂ at 150–200°C, 2–3 moles of ethane per NaAlEt₄ was reacted.



All of the polymers obtained at a polymerization temperature of 200°C with $\text{NaAl}(\text{Lac})_{4-n}(\text{NHBu})_n$ were soluble in *m*-cresol, despite the fact that $\text{NaAl}(\text{Lac})_4$ forms an insoluble polymer for polymerization times shorter than 6 hr (Table VII).

TABLE VII
Polymerization of ϵ -Caprolactam by Use of the Salt Derived from the $\text{NaAlEt}_{4-n}\text{BuNH}_2$ System as Catalyst at 202°C^a

$n\text{-BuNH}_2/\text{NaAlEt}_3$ molar ratio	Polymerization time, min	Yield of polymer, wt-% ^b	η_{sp}/c
1.0	5	2.84	0.496
	10	15.6	1.489
	30	88.9	3.850
	60	—	—
	120	91.0	4.153
2.0	5	0	—
	10	4.91	0.363
	30	88.9	2.005
	60	87.5	2.315
	120	90.5	2.402
3.0	5	0	—
	10	0	—
	30	73.0	1.591
	60	90.8	2.083
	120	91.2	1.918
4.0	5	0	—
	10	8.36	0.371
	30	52.6	0.950
	60	89.8	1.469
	120	90.1	1.848

^a Catalyst concentration (as NaAlEt_4), 0.50 mole-%.

^b The polymerized systems were extracted with water for 6 hr. The yield of polymer is based on the polymerized ϵ -caprolactam.

Polymerization Results with Complex Catalysts Containing Alkali Metal and Aluminum

Catalytic activities of some complex catalysts were compared at a polymerization temperature of 170°C (Table VIII). The order of catalytic activity is: $\text{KAl}(\text{Lac})_4 > \text{NaAl}(\text{Lac})_4 > \text{LiAl}(\text{Lac})_4$; $\text{KAl}_2(\text{Lac})_5(\text{OH}) > \text{NaAl}_2(\text{Lac})_5(\text{OH})$.

This tendency is same as that in the low-temperature polymerization of α -piperidone with the use of the salt derived from $\text{MAlEt}_{4-n}(\text{pip})_n$ as catalyst and *N*-acetyl- α -piperidone as initiator.⁷

TABLE VIII
Comparison of Catalytic Activities of the Catalysts Containing
Alkali Metal and Aluminum at 170 and 255°C^a

Polymerization temperature, °C	Catalyst	Polymerization time, 30 min		Polymerization time 2 hr	
		Methanol-soluble		Methanol-soluble	
		part, wt-%	η_{sp}/c	part, wt-%	η_{sp}/c
170	KAlEt ₄	56.25	8.12	6.92	Insoluble
	NaAlEt ₄	61.32	6.28	7.81	Insoluble
	LiAlEt ₄	72.41	3.12	10.75	Insoluble
	KOAlEt ₂ ·AlEt ₃	90.12	5.12	19.41	Insoluble
	NaOAlEt ₂ ·AlEt ₃	94.81	3.38	23.52	Insoluble
255	KAlEt ₄	12.43	2.79	12.61	1.32
	NaAlEt ₄	12.42	3.11	12.62	1.58
	LiAlEt ₄	12.58	3.18	12.75	1.61
	KOAlEt ₂ ·AlEt ₃	13.62	3.16	13.52	1.34
	NaOAlEt ₂ ·AlEt ₃	13.52	3.34	13.72	1.58

^a Catalyst concentration (as MAlEt₄ or MOAlEt₂·AlEt₃), 0.25 mole-%.

All of the catalysts described above produced *m*-cresol-insoluble polymer in the same temperature range as the case of NaAl(Lac)₄.

DISCUSSION

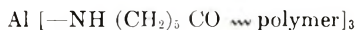
MAlEt₄ forms a complex of the type MAlEt_{4-n}(Lac)_n in lactam monomer at room temperature, and the value of *n* depends on the reaction temperature and increases with the rise in temperature. At a sufficiently high temperature, MAl(Lac)₄ in turn dissociates into two metal salts M(Lac) and Al(Lac)₃.

With regard to the catalytic activities of alkali metal caprolactamates, it has been reported that the degree of dissociation of salt varies with the nature of metal and temperature.¹⁷ The dissociation of Al(Lac)₃, on the other hand, is considered to be small as deduced from the catalytic activity and the character of Al metal.

The formation of *N*-acyl lactam in the reaction of the alkali metal salt of lactam with lactam is crucial, and appreciable polymerization activity of alkali metal salt begins to appear only at a temperature of about 200° C.^{12,13,17}

The fact that the polymerization reaction proceeds implies that the metal used as a catalyst is able to transfer back and forth between monomer and polymer. On the other hand, in the polymerization catalyzed by Al(Lac)₃, the polymerization occurs only at temperatures higher than 230°C. Therefore, the ability of MAl(Lac)₄ catalyst to initiate the polymerization reaction at lower temperatures such as 140°C and the formation of *m*-cresol-insoluble polymer at temperatures at which Al(Lac)₃ has no catalytic activity are considered to be due to the positive participation of Al(Lac)₃

as an initiator. The fact that the formation of an insoluble polymer depends on the concentration of $\text{MAl}(\text{Lac})_4$ at a given temperature also supports the role of $\text{Al}(\text{Lac})_3$, which will be a subject of a subsequent paper. The insolubility of the polymer is considered to be due to the formation of the polymer having a structure such as



This type of structure may be considered to be derived from the attack of a highly dissociated alkali metal salt on the Al salt of ϵ -caprolactam. In addition, an amide group in the polymer chain may act as a ligand for the Al atom. In this connection, the reaction¹⁸ of the trimethylaluminum-trimethylamine complex with 1,2-dimethylhydrazine to form the completely crosslinked polymer $[\text{Al}(\text{MeNNMe})_{1.5}]_n$ is cited.

MAlEt_4 reacts with n -butylamine to form $\text{MAlEt}_{4-n}(\text{NHBu})_n$ where $n = 1$ or 2 . At a temperature of 200°C , the exchange between the $-\text{NHBu}$ group attached to the Al atom and free lactam is believed to be slow because of the electron deficiency of Al atom and the electron-donating properties of the $-\text{NHBu}$ group. As a result, a soluble polymer is produced by $\text{NaAl}(\text{Lac})_{4-n}(\text{NHBu})_n$ catalyst at 202°C .

References

1. W. E. Hanford and R. M. Joyce, *J. Polym. Sci.*, **3**, 167 (1948).
2. O. Wichterle, J. Kralicek, and J. Sebenda, *Collection Czech. Chem. Commun.*, **24**, 755 (1959).
3. W. Voss, *Chem. Technik*, **1**, 111 (1949); Brit. Pat. 538,619 (1941).
4. W. Griehl, *Faserforsch. Textiltech.*, **6**, 260 (1955); *ibid.*, **7**, 207 (1956).
5. M. Ito (Toyo Rayon Co. Ltd.), Jap. Pat. 18590 (1969).
6. O. Fujimoto (Toyo Rayon Co. Ltd.), Japanese Pat. 13794 (1962).
7. H. Tani and T. Konomi, *J. Polym. Sci., Part A*, **4**, 301 (1966).
8. T. Konomi and H. Tani, *J. Polym. Sci., Part A*, **6**, 2295 (1968).
9. L. I. Zakharkin and V. V. Gavrilenko, *J. Gen. Chem. USSR*, **32**, 688 (1962).
10. W. R. Kroll, cited in K. Ziegler's chapter "Organometallic Chemistry," H. Zeiss, Ed., Reinhold, 1960, pp 206.
11. H. Tani, T. Aoyagi, and T. Araki, *J. Polym. Sci., B*, **4**, 97 (1966).
12. J. Stehlicek, J. Sebenda, and O. Wichterle, *Collection Czech. Chem. Commun.*, **29**, 1236 (1964).
13. E. H. Mottus, R. H. Hedrick, and J. M. Butler, Polymer preprint, **9** (1), p. 390. April (1968), San Francisco Meeting.
14. E. Sittler and J. Sebenda, *Collection Czech. Chem. Commun.*, **33**, 3182 (1968).
15. O. Fukumoto (Toyo Rayon Co., Ltd.), Jap. Pat. 10540 (1960).
16. H. Sekiguchi, *J. Chem. Soc. Japan*, **88**, 577 (1967).
17. E. Sittler and J. Sebenda, *J. Polym. Sci., Part C*, No. 16, 67 (1967).
18. N. R. Fetter and B. Bartocha, *Can. J. Chem.*, **39**, 2001 (1961).

Received December 16, 1968

Revised February 10, 1969

Chain Transfer in Anionic Polymerization. Determination of Chain-Transfer Constants by Using Carbon-14-Labeled Chain Transfer Agents

ARNOLD L. GATZKE, *Physical Research Laboratory, The Dow Chemical Company, Midland, Michigan 48460*

Synopsis

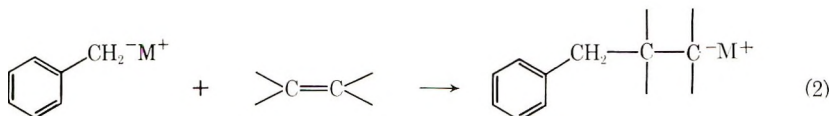
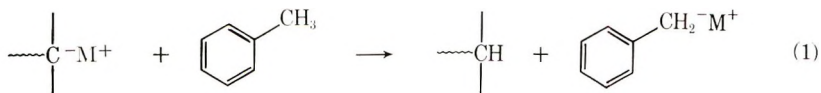
A method is described in which ^{14}C -labeled chain-transfer agents are employed to measure chain-transfer constants in anionic polymerization as low as 10^{-6} . Each chain-transfer step incorporates one molecule of the chain-transfer agent into the polymer so that measurement of the activity and conversion allows evaluation of the chain-transfer constant. This method is independent of the initiator concentration and efficiency, making the technique especially useful when problems with the initiator are encountered. The experimental procedure is described in detail for the case of chain transfer to toluene in the *n*-butyllithium-initiated polymerization of styrene, where C_{RH} was found to be 5×10^{-6} . A mathematical treatment is given showing the relationship between the degree of polymerization (\overline{DP}_n) and chain transfer.

INTRODUCTION

A number of anionic polymerizations of vinyl monomers are known to proceed without any readily detectable chain termination or transfer, hence the origin of the term "living" polymers.¹ Because the chain ends remain active for long periods of time, these polymers are of great utility in the preparation of monodisperse and functionally terminated polymers and block and graft copolymers. If chain transfer occurs, it can have a profound effect on these preparations.

It has been recognized over the past few years that chain transfer can occur in some anionic polymerization systems even though hydrocarbon solvents are used. For example, Brower and McCormick² and later Brooks³ observed molecular weights lower than calculated from the monomer: initiator ratio in organosodium-initiated polymerization of styrene in toluene solution. In more extreme cases, telemerization was found to occur in the polymerization of ethylene initiated with *n*-butyllithium-tetramethylethylenediamine (TMEDA) in benzene solution⁴ and of 1,4-butadiene initiated with organosodium compounds in toluene-tetrahydrofuran (THF) solution.⁵ For the latter two examples, telomers could be isolated containing phenyl and benzyl groups, respectively, on one end of the chain, thus establishing the chain-transfer agents as benzene in the one

case and toluene in the other. The chain-transfer reaction involving toluene can be written as a hydrogen-metal exchange followed by initiation of new chain by the carbanion formed.



Mathematical treatment of the data has been presented^{4,5} which allows evaluation of the chain-transfer constants and prediction of the number-average degree of polymerization ($\overline{\text{DP}}_n$) for the special case where chain transfer constants are large (near unity) and each active center undergoes many transfers.

The effects of small chain transfer constants (10^{-3} – 10^{-6}) on the behavior of an anionic polymerization have not been explored nor have adequate means of their detection and measurement been developed. In this paper a method is developed which employs radioactive (¹⁴C) chain-transfer agents to detect and measure low levels of chain transfer.

Previous use of radioactive chain-transfer agents has been limited to free-radical polymerizations, where their greatest utility is in the measurement of chain-transfer constants larger than unity.⁶

EXPERIMENTAL

The experimental procedure is described for the *n*-butyllithium-initiated polymerization of styrene in toluene-¹⁴C. The method is quite general and can be adapted to a number of other systems.

Materials

Styrene was a Dow polymerization-grade material obtained inhibitor-free directly from the plant stills. The monomer was collected under dry nitrogen and stored at -20°C . *n*-Butyllithium, 1.6*M* in hexane, from Foote Mineral was diluted to 0.5*M* with benzene distilled from sodium and stored at 0°C . Concentrations were obtained by single titration with standard hydrochloric acid after experience showed that Gilman's double-titration technique⁷ indicated negligible quantities of noncarbon-bound lithium. Toluene-¹⁴C, both ring- and methyl-labeled, obtained from New England Nuclear and Nuclear Research Chemicals, was diluted with reagent-grade toluene to the desired activity (2.01×10^6 dpm/ml), and distilled from sodium under nitrogen through a 30-in. fractionating column. In one series of experiments the labeled toluene was diluted with purified

toluene and used directly. In this case, the polymers obtained by the evaporation of the solvent had an activity much higher than expected, suggesting the presence of an involatile radioactive impurity.

Polymerization Procedure

Polymerizations were carried out in a 250-ml three-necked glass flask equipped with recording thermocouple, stirrer, a stopcock near the top of the flask for admitting initiator, and a second stopcock at the bottom for emptying the reactor. A positive pressure was maintained in the reactor with highly purified nitrogen admitted through copper lines. After a preliminary polymerization to flush out the lines and condition the reactor, 100 ml of 10% w/v styrene in labeled toluene contained in a nitrogen-pressurized addition funnel was passed through about 10 g of freshly activated alumina into the reactor. The solution was warmed to 54°C with a hot air gun, then *n*-butyl-lithium was added dropwise from a 500 μ l syringe until the first trace of a permanent yellow color (typically 40 μ l were required), followed by the rapid addition of 200 μ l more. The polymerization was terminated after 10 min by the addition of a few drops of acetic acid. The temperature gradually rose during the polymerization to a maximum of 60°C. The conversion was determined by vapor phase chromatographic analysis for residual styrene with toluene as the internal standard. The radioactive toluene was vacuum-evaporated and collected for repeated use.

Radioactive Counting Procedure

The last traces of radioactive solvent were removed from the polymer by several cycles of redissolving the polymer in xylene and evaporating to dryness under vacuum. The activity of the polymer was monitored after each cycle. A constant level of activity was achieved after four evaporations. The preferred method of removing the last traces of unbound radioactive chain transfer agent is now by repeated precipitation of polymer in methanol, for which three precipitations is usually sufficient. The radioactive solvent should be flashed off and the polymer redissolved in a suitable solvent before precipitation in order to avoid problems with azeotropes in the recovery of the radioactive solvent. Initially this method of achieving constant activity was not favored because of possible fractional precipitation. This could cause an error since the low molecular weight material will be more radioactive than the high molecular weight material. However, it was found that good agreement between the two techniques was achieved, and the latter is preferred because it is more rapid, particularly if the chain-transfer agent has low volatility.

For measuring activity, 1.00 g of the polystyrene sample was weighed into a 20-ml crystallite vial and dissolved in 20 ml of a standard scintillation solution (4 g PPO, 50 mg POPOP per liter of toluene, Liquifluor, Pilot Chemicals, Inc.). The solutions were counted with a Nuclear Chicago liquid

scintillation counter using the two-channel technique for obtaining counting efficiencies.

In a blank experiment polystyrene was dissolved in the radioactive solvent, then precipitated twice in methanol. A 1 g sample of the polymer had an activity of 3 cpm, which is zero within experimental error.

Calculation of the Chain-Transfer Constant

The following results were obtained from the polymerization of styrene.

Conversion = 0.861

Specific activity of toluene = 2.01×10^6 dpm/ml

Specific activity of polystyrene:

1st evaporation = not counted

2nd evaporation = 278 dpm/g

3rd evaporation = 218 dpm/g

4th evaporation = 217 dpm/g

Then the chain-transfer constant C_{RH} is given as*

$$\begin{aligned} C_{RH} &= \frac{-[RH]_p}{[RH]_i \ln(1-x)} \\ &= \frac{217 \text{ (dpm/g)} \times 9.2 \text{ (g)} \times 0.861}{2.06 \times 10^6 \text{ (dpm/ml)} \times 89.9 \text{ (ml)} \times 1.97} \\ &= 5.0 \times 10^{-6} \end{aligned}$$

where $[RH]_p$ = concentration of chain transfer agent in polymer

$[RH]$ = concentration of chain transfer agent in solution

X = degree of conversion

Molecular Weight Distributions

Molecular weight distributions were measured either by ultracentrifugation (Beckman), the data being treated according to the method outlined by McCormick,⁹ or by gel-permeation chromatography (Waters).

Rate of Metalation of Toluene by *n*-Butyllithium

To 200 ml of toluene containing 8.05×10^{-4} mole of dissolved propane in a 250-ml bottle closed with a serum cap was added, from a syringe, 1.5×10^{-2} mole of *n*-butyllithium in 10 ml of hexane. A gas sampling valve of a vapor-phase chromatograph was connected to the bottle by means of narrow-gauge tubing and a syringe needle. After flushing several times, vapor was admitted into the evacuated sampling valve and then chromato-

* The values of the chain-transfer constant for polystyryllithium-toluene reported in a preliminary communication⁸ are now known to be too large as a result of some 30 dpm/g extra activity in the polystyrene samples. Elimination of this extra activity by careful fractionation of the toluene-¹⁴C reveals a temperature dependence of C_{RH} of ~ 6 kcal/mole.

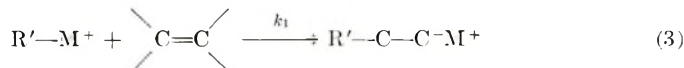
graphed on a column of 30% dimethylsulfolane on 40-60 mesh Chromosorb P at room temperature. Baseline separations of propane, *n*-butane, and 1-butene were achieved. After several hours at 50°C, it was found that the rate of *n*-butane evolution was too small to be measured. The temperature was then rapidly raised to $90 \pm 1^\circ\text{C}$ and the concentrations of *n*-butane and 1-butene were measured relative to propane (taking into account the vapor pressures) until 20% of the theoretical amount of *n*-butane was evolved (50 min). During this period 3% of the *n*-butyllithium had undergone thermal decomposition to give 1-butene. The initial rate of butane evolution obtained from a plot of the butane concentration versus time was 4.7×10^{-7} mole/l. sec. By using the rate equation of Hsieh¹⁰ and an activation of 18 kcal/mole reported by Worsfold and Bywater,¹¹ the initial rate of addition of *n*-butyllithium to 10% styrene under comparable conditions was approximately 6×10^{-4} mole/l. sec.

RESULTS AND DISCUSSION

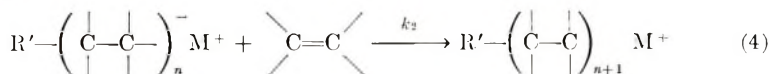
The Chain-Transfer Process

The relevant features of the mechanism of an anionic polymerization incorporating chain transfer can be represented by eqs. (3)–(6).

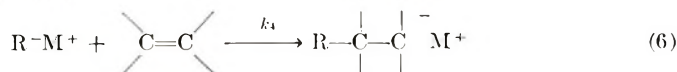
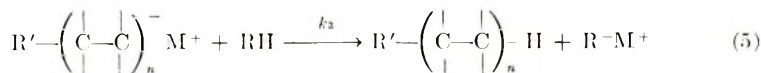
Initiation:



Propagation:



Chain Transfer:



If the carbanion, R^- , formed on chain transfer is sufficiently reactive to add to the vinyl monomer, then it will initiate a new chain and be incorporated into the polymer. Further, if R^- is radioactive (^{14}C in this case), then measurement of the specific activity of the polymer could be related to the value of the chain-transfer constant.

Evaluation of the Chain-Transfer Constant

The chain-transfer constant is a proportionality constant between the rates of chain transfer and chain propagation. From the mechanism indicated earlier, the ratio of these rates is given by:

$$\frac{d[RH]_P/dt}{d[M]/dt} = \frac{k_3 \left[R - \left(\begin{array}{c} | \\ C - C \\ | \quad | \\ n \end{array} \right)^- M^+ \right] [RH]}{k_2 \left[R - \left(\begin{array}{c} | \\ C - C \\ | \quad | \\ n \end{array} \right)^- M^+ \right] [M]} \quad (7)$$

which simplifies to:

$$dRH_P/dM = C_{RH} [RH]/M \quad (8)$$

where $[RH]_P$ is the amount of chain transfer agent incorporated into the polymer, M denotes the vinyl monomer, and C_{RH} is the chain transfer constant which is the ratio k_3/k_2 .

In order for eq. (8) to be valid, the following conditions must be met: (a) the initiator, during its lifetime in the polymerization, must not react with the chain-transfer agent to any appreciable extent; and (b) the kinetic order in growing chains must be the same for both chain transfer and for chain propagation.

The rate of metalation of toluene by *n*-butyllithium was found to be 10^3 times slower than the rate of *n*-butyllithium addition to styrene. As a result, a negligible portion of the initiator will react with toluene in the presence of styrene and the condition (a) is met. Kinetic studies on olefin addition and hydrocarbon metallation by organometallics indicate the kinetic order in organometallic is the same for both reactions if the same solvent is used.^{12,13} Therefore the assumption that the condition (b) is met is probably valid.

If the polymerization is conducted in the presence of a large excess of chain-transfer agent so that its concentration can be regarded as constant, then eq. (8) can be integrated to give the following result:

$$[RH]_P = -C_{RH} [RH] \ln(1 - x) \quad (9)$$

The monomer concentration in eq. (9) has been replaced by the degree of conversion x by using the relation:

$$[M] = [M]_i(1 - x) \quad (10)$$

Equation (9) is used to calculate the chain-transfer constant from the experimental data (see Experimental section).

Dependence of the Degree of Polymerization on the Chain-Transfer Constant

It is of general interest to establish quantitatively the relationship between the degree of polymerization (or molecular weight) and the chain-transfer constant. In particular, since chain transfer can frequently be detected by molecular weight methods, it is of interest to compare the scope and limitations of this method to that of the radioactive tracer method.

For an ideal anionic polymerization, the number-average degree of polymerization (\overline{DP}_n) can be determined from the monomer: initiator ratio and the degree of conversion.

$$\overline{DP}_n = [M]/[I] x \quad (11)$$

If chain transfer occurs, a reduction in \overline{DP}_n will result so that the observed DP_n is given by:

$$DP_n = [M]x/[I] + N \quad (12)$$

where N is the number of transfers and is given by eq. (9).

Substituting eq. 9 in eq. (12) gives:

$$\overline{DP}_n = \frac{[M] x}{[I] - C_{RH} [RH] \ln(1-x)} \quad (13)$$

Figure 1 shows the \overline{DP}_n calculated from eq. (13) as the initiator concentration is decreased while the other variables are held constant. At low

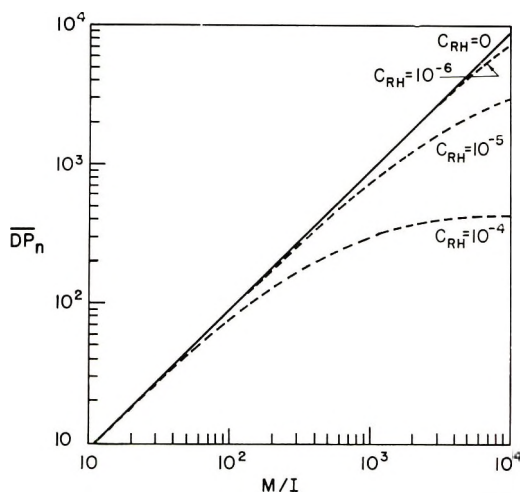


Fig. 1. Predicted number-average degree of polymerization as a function of the monomer/initiator ratio for various values of the chain transfer constant; $[M] = 1.0M$, $x = 0.9$, $[RH] = 10M$.

values of the monomer/initiator ratio, there is very little difference between the \overline{DP}_n predicted with and without chain transfer, but as the monomer to initiator ratio is increased this difference becomes more and more pronounced. Either eq. (13) or the curves in Figure 1 can be used to help interpret molecular weight data reported in the literature.

Using sodium α -methylstyrene tetramer as initiator for the polymerization of styrene in toluene solution, Brooks³ was able to detect chain transfer by observing molecular weights of one-third that calculated from the monomer/initiator ratio when this ratio was 1000. No significant difference was observed at a monomer/initiator ratio of 200. These results would be expected from Figure 1 if $C_{RH} \sim 1 \times 10^{-4}$ (by radioactive tracer technique $C_{RH} = 1.3 \times 10^{-4}$). When a lithium initiator was used, no significant difference could be detected at a ratio of 1000, the highest used, nor would one be expected according to Figure 1 for C_{RH} of 5×10^{-6} .

The radioactive tracer technique is independent of the initiator concentration at constant monomer concentration and can be used to measure chain transfer at all monomer to initiator ratios with equal accuracy. The results in Table I show the specific activity remains constant at constant conversion for a threefold change in initiator concentration. This substantiates the initial assumption that the kinetic order in active chains is the same for both chain transfer and chain propagation.

In order to utilize the molecular weight determination method for the determination of very low chain-transfer constants, it can be argued that differences between the theoretical (no chain transfer) and the observed \overline{DP}_n will eventually be measurable if the monomer/initiator ratio is made very large. Unfortunately the experimental error associated with measuring the very low initiator concentrations becomes very large, rendering the

TABLE I
Effect of *n*-Butyllithium Concentration on the
Activity of Polystyrene Polymerized in Benzene
Containing 5% Diphenylmethane-¹⁴C^a

<i>n</i> -BuLi, mole/l.	Conver- sion <i>x</i>	\overline{DP}_n		Activity/ at <i>x</i> = 0.908, dpm/g	
		Theory	Obs. ^b	Activity, dpm/g	dpm/g
15.9×10^{-4}	0.9083	820	830 ± 30	486	486
5.3×10^{-4}	0.8551	2320	1900 ± 50	416	487

^a Styrene = 150 g/l., 50°C, (C₆H₅)₂CH₂-¹⁴C = 1.52×10^6 dpm/g.

^b Determined by gel permeation chromatography.

method valueless. Figure 2 illustrates this point by showing a series of polystyrenes polymerized in toluene with the use of *n*-butyllithium as initiator where $C_{RII} = 5 \times 10^{-6}$. The expected decrease in the observed \overline{M}_n relative to the theoretical \overline{M}_n is believed masked by errors in measuring the lower initiator concentrations. On the basis of molecular weight determinations alone, no conclusions regarding chain transfer can be made. On the other hand, the molecular weight distributions show a gradual broadening as the monomer to initiator ratio is increased. This is in agreement with the occurrence of chain transfer. For comparison, the calculated distributions are shown.*

* The distributions in molecular weight were calculated by numerical integration of the rate equations derived from the mechanism of anionic polymerization shown in eqs. (3)–(6). The computer program, written by J. E. Huff on the Physical Research Laboratory, The Dow Chemical Company, Midland, Michigan, allows complete simulation of the laboratory experiment. Inputs include rate constants, reaction order and concentrations. The outputs are initiator and monomer conversions, number and weight average molecular weights and the number of transfers per active chain as a function of time. In addition, the complete number and weight average distributions can be obtained at specified conversions.

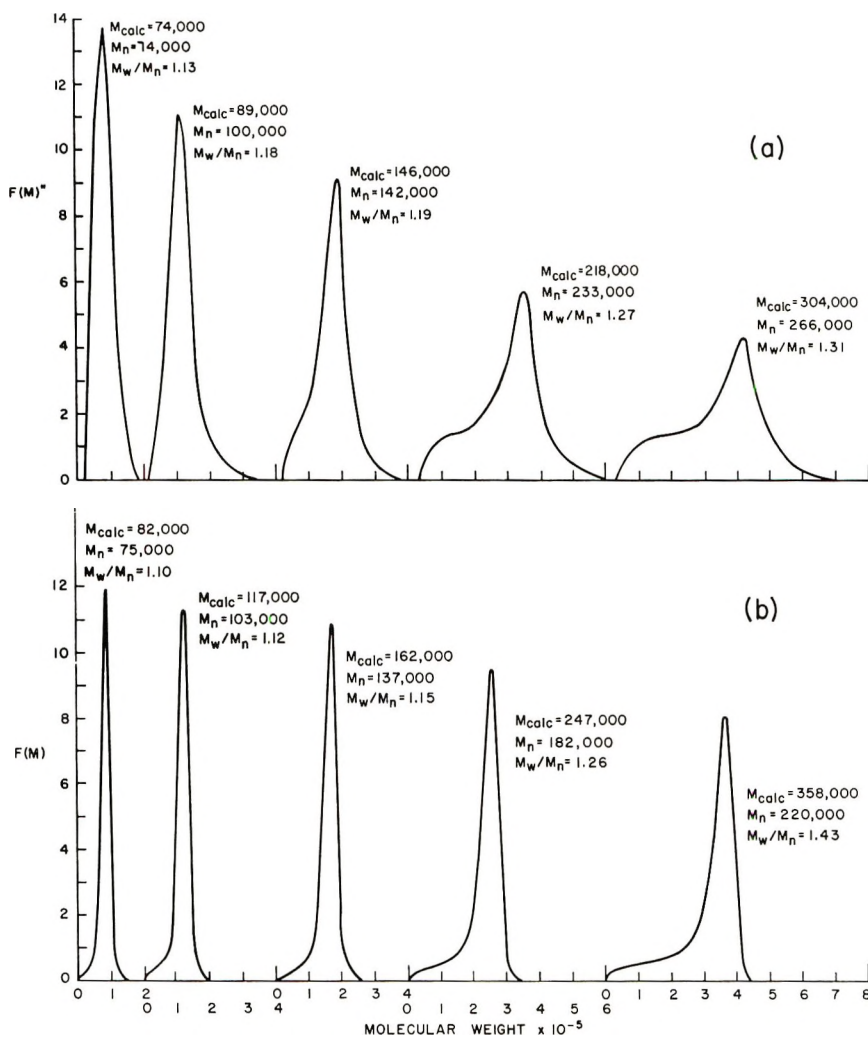


Fig. 2. Molecular weights and molecular weight distributions of polystyrenes at various monomer/initiator ratios for the *n*-butyllithium-initiated polymerization of styrene in toluene: (a) ultracentrifuge determination; (b) computer-calculated distributions.

Effect of Conversion on Chain Transfer

If only a small fraction of the available chain-transfer agent is consumed during the polymerization, then the rate of chain transfer remains essentially constant throughout the polymerization, while the rate of chain propagation decreases due to depletion of the monomer. This has the effect of causing an exponential increase in the number of chain transfer steps with increasing conversion, as illustrated by the lower curve in Figure 3. The sharp increase in the number of transfer steps at high conversion has a pronounced effect on the accuracy in measuring the chain transfer by

the radioactive tracer technique. At very high conversion, small errors in its measurement result in much larger errors in the chain transfer constant. For this reason, conversions should be kept below 95%.

Figure 3 shows various calculated polymerization parameters as a function of conversion. Worth noting is the increase in the difference between \bar{M}_n and \bar{M}_w with increasing conversion which is a measure of the broadness of the distribution.

The exponential increase in the number of transfer steps with conversion can play an important role in macromolecular synthesis involving "living" polymers. In systems where chain transfer can occur, improvement in product purity by attempting to achieve 100% conversion can be offset by chain termination through transfer.

Chain Transfer and Inefficient Initiation

In actual practice an anionic polymerization can be complicated both by inefficient utilization of initiator, typically as a result of slow initiation or reaction with impurities, and by chain transfer. Since the radioactive

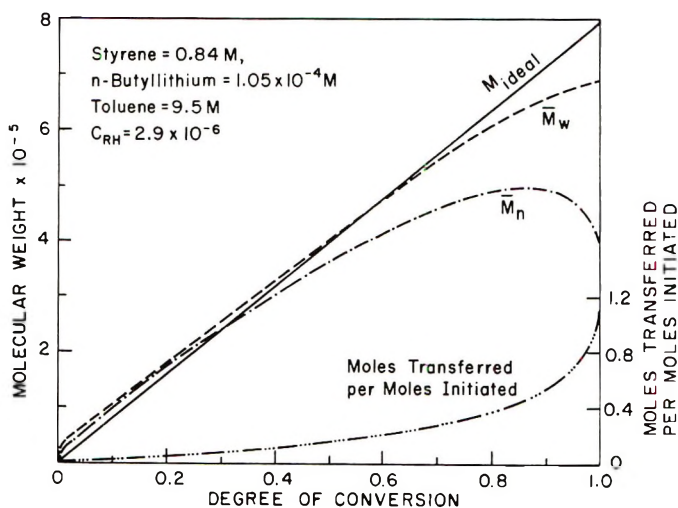


Fig. 3. Various computed polymerization parameters as a function of conversion for the *n*-butyllithium-initiated polymerization of styrene in toluene.

tracer method allows measurement of the number of transfer steps independently of the initiator, both the chain transfer constant [eq. (9)] and the effective initiator concentration [eq. (12)] can be evaluated.

Rearrangement of eq. (12) gives:

$$[I]_{\text{eff}} = (Mx/\overline{DP}_n) - N$$

where all the terms on the right can be experimentally determined. The ratio of the effective concentration $[I]_{\text{eff}}$ to the actual concentration $[I]_{\text{act}}$ is the initiator efficiency. The results in Table II for the phenyl-sodium

TABLE II
Determination of Initiator Efficiency for the Phenylsodium-Initiated
Polymerization of Styrene in Toluene

Activity	
Polymer, dpm/g	1.460×10^3
Toluene, dpm/mole	3.50×10^7
N , mole	4.08×10^{-4}
($[M] = 0.0961$ mole, $x = 0.978$, $\overline{DP}_n = 206$)	
$[I]_{\text{eff}}$, mole	0.58×10^{-4}
$[I]_{\text{act}}$, mole	0.95×10^{-4}
Efficiency	0.61

(added as a slurry in ethylbenzene)-initiated polymerization of styrene in toluene- ^{14}C at 90°C are given as an example. The chain transfer constant was found to be 1.28×10^{-4} . The major cause of the low efficiency of phenylsodium as an initiator is probably a result of its low solubility in the reaction medium.

SUMMARY AND CONCLUSIONS

The radioactive tracer technique is a general method for measuring chain transfer in anionic polymerization, provided it can be established that the initiator does not undergo any appreciable reaction with the chain transfer agent during the polymerization. The main advantages of the technique are: (a) high sensitivity, which allows evaluation of chain transfer constants down to 10^{-6} ; and (b) independence of initiator, which allows evaluation of the chain transfer constant at any initiator concentration and efficiency. The method suffers from the disadvantages that the radioactive chain transfer agents are often costly or require synthesis and the work-up of the polymer is tedious.

In cases where the chain-transfer constant is greater than 10^{-4} and initiator concentrations and efficiencies are known, then determination of the number-average molecular weight is usually a more rapid and convenient method of measuring chain transfer.

I wish to thank J. Ludwick for technical assistance, L. H. Tung and J. R. Runyon for the Ultracentrifuge and Gel Permeation Chromatography measurements, and L. H. Tung and E. F. Gurnee for helpful discussion.

References

1. M. Szwarc, *Nature*, **178**, 1168 (1956).
2. F. M. Brower and H. W. McCormick, *J. Polym. Sci., Part A*, **1**, 1749 (1963).
3. B. W. Brooks, *Chem. Commun.*, **1967**, 68.
4. G. G. Eberhardt and W. A. Butte, *J. Org. Chem.*, **29**, 2928 (1964).
5. S. Kume, A. Takahashi, G. Nishikawa, M. Hatano, and S. Kambara, *Makromol. Chem.*, **84**, 137 (1965); **84**, 147 (1965); **98**, 109 (1966).
6. C. Walling, *J. Am. Chem. Soc.*, **70**, 2561 (1948).
7. H. Gilman and A. H. Haubein, *J. Am. Chem. Soc.*, **66**, 1515 (1944).
8. A. L. Gatzke and Ed Vanzo, *Chem. Commun.*, **1967**, 1180.

9. H. W. McCormick, *J. Polym. Sci.*, **36**, 341 (1959).
10. H. L. Hsieh, *J. Polym. Sci., Part A*, **3**, 163 (1965).
11. D. S. Worsfold and S. Bywater, *Can. J. Chem.*, **38**, 1891 (1960).
12. A. G. Evans, C. R. Gore, and N. H. Rees, *J. Chem. Soc.*, **1965**, 5110.
13. R. Waack, P. West, and M. A. Doran, Preprints, Amer. Chem. Soc., Division of Petroleum Chemistry, Vol. 11, No. 4, 1966.

Received January 13, 1969

Revised February 12, 1969

Self-Condensation Reaction of Aromatic Tetraamines in Polyphosphoric Acid

A. BANIHASHEMI,* D. FABBRO, and C. S. MARVEL, *Department of Chemistry, University of Arizona, Tucson, Arizona 85721*

Synopsis

Ladder and partial ladder polymers have been obtained by self-condensation reactions of 1,2,4,5-tetraaminobenzene, 3,3',4,4'-tetraaminodiphenyl ether, 3,3'-diaminobenzidine and 3,3',4,4'-tetraaminodiphenyl sulfone in polyphosphoric acid. The products thus obtained are highly colored compounds with good thermal stability. They seem to be made up of polyquinoxaline or dihydrophenazine or a mixture of these two recurring units. They are slightly soluble in methanesulfonic acid and concentrated sulfuric acid and have inherent viscosities in the 0.2 to 0.4 range.

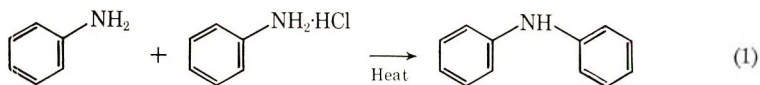
INTRODUCTION

Recent advances in thermostable polymers have shown that aromatic heterocyclic polymers have good thermal stability. Also it has been established that aromatic ladder structures seem to offer further improvement in thermal properties over other polyaromatic types. Polymers of excellent thermal stability have been reported which contain heterocyclic units such as: benzimidazole,¹⁻⁵ 1,3,4-oxadiazole,⁶ imide,^{7,8} quinoxaline,⁹⁻¹¹ benzothiazine,¹² benzoxazine,¹³ and benzoxazoles.¹⁴

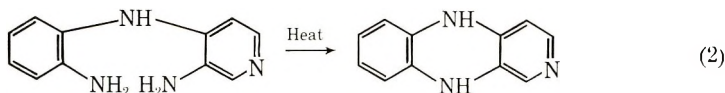
This paper describes the preparation and properties of some new polyamines which contain either quinoxaline or dihydrophenazine recurring units.

RESULTS AND DISCUSSION

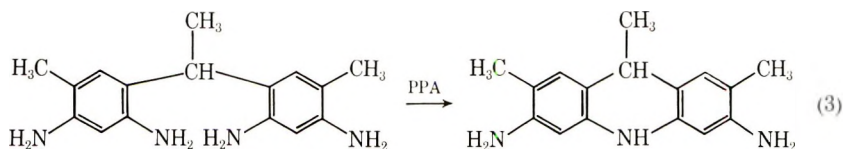
The reaction between aniline and aniline hydrochloride is well known [eq. (1)],



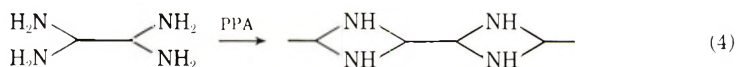
and the reactions (2) and (3) are reported in the literature.^{15,16}



* Present address: Chemistry Department, Pahlavi University, Shiraz, Iran.

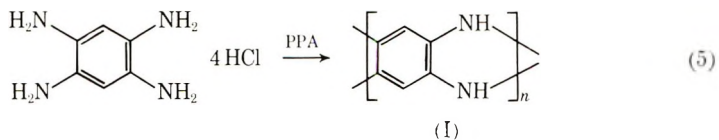


These reactions proceed smoothly and with high yields when the two amino groups are in a position favorable for the ring closure. We have tried to extend these reactions to the preparation of polymers with complete or partial ladder structures by use of appropriate tetrafunctional intermediates.



Polyphosphoric acid (PPA) was chosen as the reaction medium and as the condensing agent. The utility of polyphosphoric acid as a remarkably effective condensing agent in synthetic organic chemistry has been extensively demonstrated in recent years.¹⁵

The first polymerization experiments were carried out with the 1,2,4,5-tetraaminobenzene tetrahydrochloride. The anticipated reaction is shown in eq. (5).



Poly(benzene,-1,2:4,5-tetrayl-1,2-diimino)

The 1,2,4,5-tetraaminobenzene tetrahydrochloride was mixed with polyphosphoric acid and heated at elevated temperature under inert atmosphere. The reaction yielded a polymer (I) of poly (benzene-1,2:4,5-tetrayl-1,2-diimino) in a yield of 84%. It is probable that the polymer was partly oxidized to yield some quinoxaline units (see Table I). The polymer was a blue-black material which was slightly soluble in methanesulfonic acid and concentrated sulfuric acid (about 30%) with an $\eta_{inh} = 0.42$ for the part soluble in sulfuric acid.

Thermogravimetric analysis of polymer I, (Fig. 1) showed that it gradually lost 10% of its weight up to 600°C and about 30% of its weight up to 900°C.

Similarly a polymeric amine has been obtained [eq. (6)] from 3,3',4,4'-tetraaminodiphenyl ether tetrahydrochloride and also from the free base.

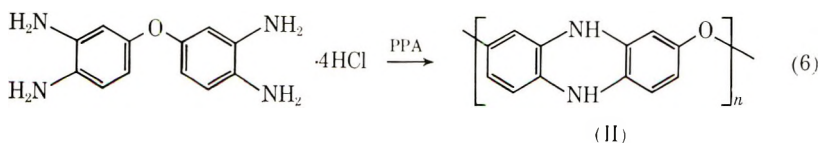
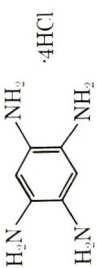
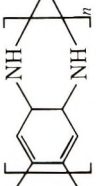
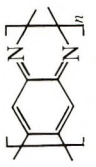
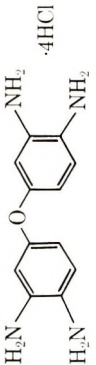
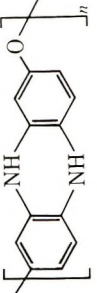
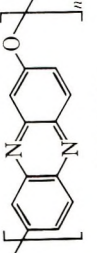


TABLE I
Polymers from Aromatic Tetraamines in PPA

Monomer	Proposed polymer unit	Polymer-ization conditions	Yield, %	Elemental analysis		η_{inh} (H ₂ SO ₄ , 30°C)	λ_{max} , m μ^a
				Calcd, %	Found, %		
	 (C ₆ H ₄ N ₂) _n or  (C ₆ H ₂ N ₂) _n	250°C, 5 hr	84.5	C, 69.2 H, 3.85 N, 26.95	C, 69.15	0.42	320, 340
				C, 70.5 H, 1.97 N, 27.43	H, 3.38 N, 23.63 Res, 0.1		
	 (C ₁₂ H ₈ N ₂ O) _n or  (C ₁₂ H ₆ N ₂ O) _n	330°C, 4 hr	67.3	C, 73.5 H, 4.08 N, 14.3	C, 74.95 ^b H, 3.22 ^b	0.19	314
				C, 74.21 H, 3.11 N, 14.42	N, 13.91 ^b		

^a Ultraviolet spectra were taken in sulfuric acid.

^b The calculation has been made considering the residue (2.05%) as unburnt silica.

The elemental analysis was consistent with the proposed structure (II) of poly(9,10*H*-phenazine-2,7-diyl-2-oxy). This polymer was a blue-black powder. The yield was 67.3%, and the part soluble in concentrated sulfuric acid had $\eta_{inh} = 0.19$. It may also be partly oxidized to a quinoxaline structure.

The thermogravimetric analysis (Fig. 2) of this polymer showed that it lost only 14% of its weight up to 900°C. This polymer showed the best thermal stability of any in this type of polymer.

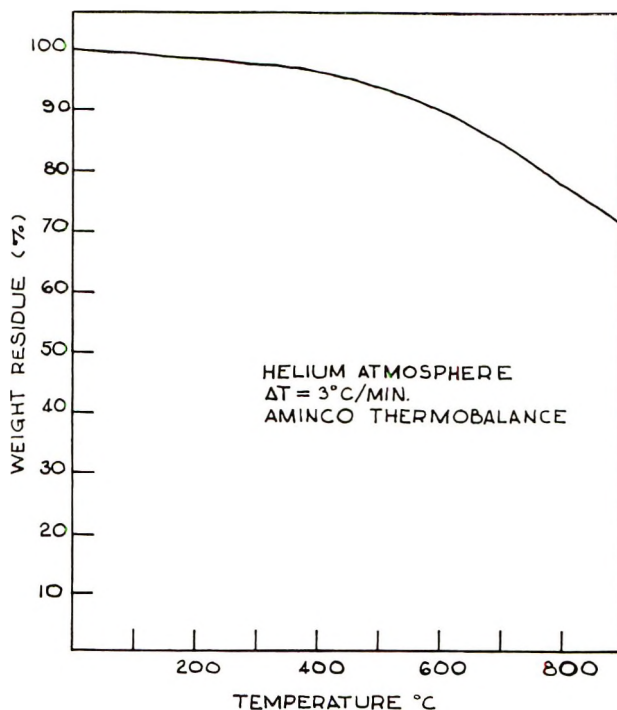


Fig. 1. TGA curve of polyamine I from tetraaminobenzene tetrahydrochloride.

When 3,3'-diaminobenzidine was heated in polyphosphoric acid at 280°C for 9 hr, no polymerization or decomposition occurred. The product was identified by melting point and infrared analysis. When the reaction temperature was raised to 300°C polymerization occurred, but corrosion of the glass vessel by the polyphosphoric acid took place, causing contamination of the product with silica which was impossible to remove completely. The elemental analysis was satisfactory, if the unburned residue was considered as silica. The yield was 57% with $\eta_{inh} = 0.43$ for the part soluble in concentrated sulfuric acid. The thermogravimetric analysis of the polymer showed that it gradually lost 20% of its weight up to 900°C (Fig. 3).

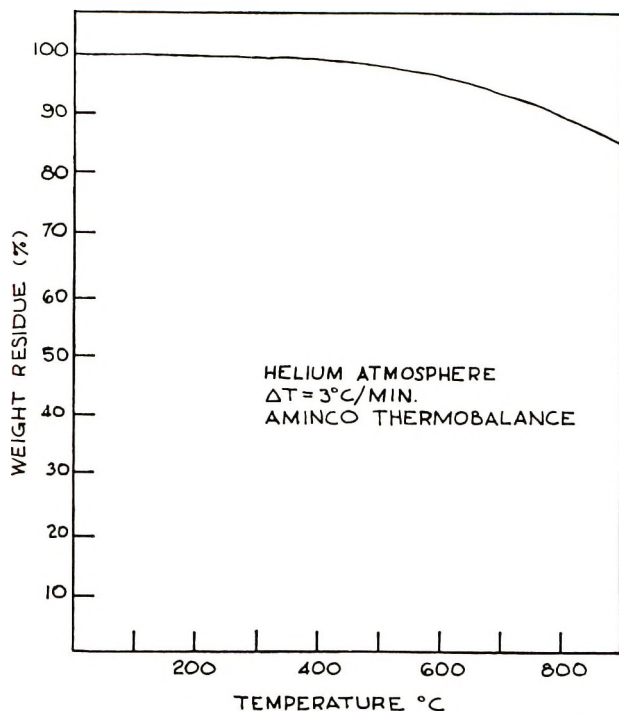


Fig. 2. TGA curve of polyamine II from tetraaminodiphenyl ether.

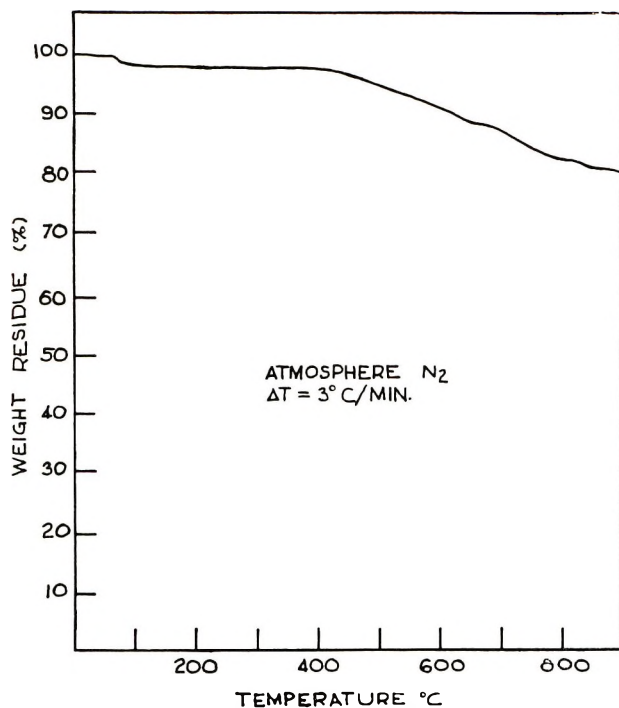
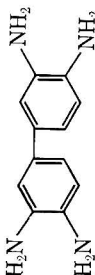
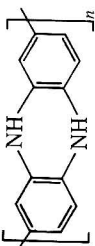
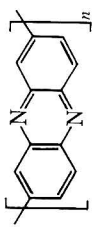
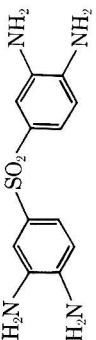
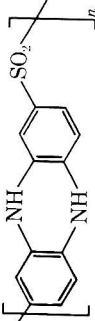
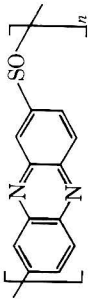


Fig. 3. TGA curve of polyamine III from 3,3'-diaminobenzidine.

TABLE II
 Polymers from Aromatic Tetraamines in PPA

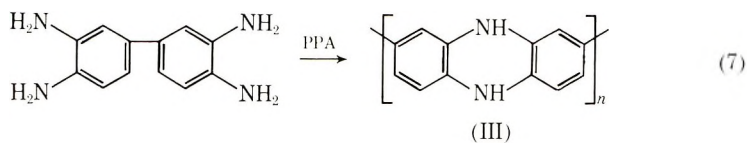
Monomer	Proposed Polymer Unit	Polymerization conditions	Yield, %	Elemental analysis		λ_{\max} $\mu\mu$
				Calcd, %	Found, %	
	 $(C_{12}H_{18}N_2)_n$ or  $(C_{12}H_{18}N_2)_n$	340°C, 9 hr	57.0	C, 80.0 H, 4.45 N, 15.55	C, 79.65 ^b H, 4.76 ^b N, 15.59 ^b	0.43 ^c 297, 320
	 $(C_{12}H_{14}N_2O_2S)_n$ or  $(C_{12}H_{14}N_2OS)_n$	250°C, 9 hr	82	C, 59.00 H, 3.28 N, 11.44 S, 13.15 O, 13.10	C, 62.05 H, 2.71 N, 11.56 S, 14.09	0.35 ^d 238
				C, 63.7 H, 2.56 N, 12.4 S, 14.15 O, 7.19	O, 6.86 Residue 1.1	

^a Ultraviolet spectra were taken in sulfuric acid.

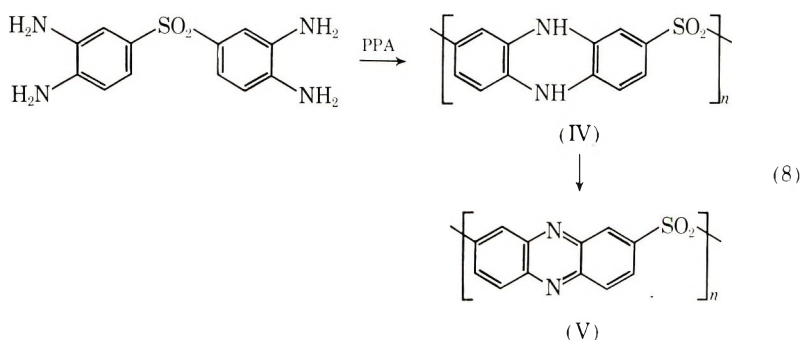
^b The calculation has been made considering the residue (7.09%) as unburnt silica.

^c Measured in sulfuric acid at 30°C.

^d Measured in methanesulfuric acid at 30°C.



3,3',4,4'-Tetraaminodiphenylsulfone has been heated in polyphosphoric acid at 250°C for 4 hr to give a yield of 82% of black polymeric material with low solubility. Hydrogen and oxygen analyses were too low for the expected product. The exact nature of the polymer is uncertain, but it seems likely that the hydrogen of the NH groups in the middle ring reacted with oxygen of the SO₂ group (IV) to yield the quinoxaline and a sulfoxide (V) (Table II).



The resulting polymeric material was slightly soluble in methanesulfonic acid, and the soluble part showed an inherent viscosity of 0.35.

The thermogravimetric analysis showed a good stability for the product (Fig. 4.)

All of these polymeric materials were deeply colored powders which contained some silica and very small amounts of phosphorus. They were insoluble in common organic solvents but did show some solubility in concentrated sulfuric acid and methanesulfonic acid. They colored such solvents as hexamethylphosphoramide, dimethylformamide, and dimethylsulfoxide, but only trace amounts really seemed to dissolve. The visible and the ultraviolet absorption, as well as the analytical results, indicate the presence in these polymers of the oxidized structure (quinoxaline units) as recurring units.

It should be noted that *o*-phenylenediamine did not undergo this type of condensation under the experimental conditions which gave polymers from the tetraamines.

The polyphosphoric acid used in these experiments was prepared from analytical grade phosphorus pentoxide and distilled water to avoid metal contaminants.

The 3,3',4,4'-tetraaminodiphenylsulfone was prepared by the method of Stille and Arnold.¹⁶ Some minor variations in the procedures and melting points of intermediates are recorded in the experimental part.

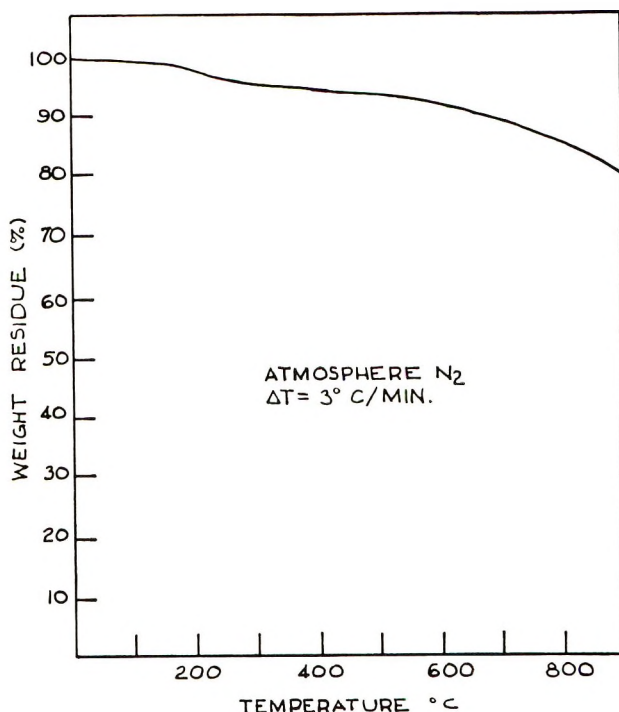


Fig. 4. TGA curve of polyamine IV from tetraaminodiphenylsulfone.

EXPERIMENTAL

Polyphosphoric Acid

In a 500-ml three-necked round-bottomed flask fitted with a mechanical stirrer, inlet tube for nitrogen, and dropping funnel, was placed 100 g of analytical grade phosphorus pentoxide. The flask was cooled with an ice bath, and a slow current of nitrogen was maintained while very slowly 40 ml. of distilled water was added. At the end of the period the temperature was slowly raised to 120°C, and the heating was continued under a slow current of nitrogen for 24 hr. The viscous product so obtained was almost colorless.

Polymerization of 1,2,4,5-tetraaminobenzene Tetrahydrochloride

1,2,4,5-Tetraaminobenzene tetrahydrochloride (7.1 g, 0.025 mole) was mixed with 120 g of polyphosphoric acid, prepared as above, in a 500-ml three-necked round-bottomed flask and the apparatus was repeatedly evacuated and filled with nitrogen. The mixture was then heated carefully at 100°C with stirring in a nitrogen atmosphere until the end of the foaming due to the evolution of hydrogen chloride. The mixture was then heated at 180°C overnight and at 250°C for 5 hr. The reaction mixture was cooled under nitrogen and ammonium carbonate and a little ion-free

water was added. The mixture was poured in a blender containing 1½ l. of saturated ammonium carbonate solution, centrifuged, extracted with water for 2 weeks, and dried. It was next extracted with 95% ethyl alcohol until the extraction liquor, initially pink, became colorless. After drying under reduced pressure, the yield of black polymer was 2.2 g (84.5%). $\eta_{inh} = 0.42$ (0.2% concentrated H₂SO₄, 30°C) $\lambda_{max} = 320, 340$ (H₂SO₄) m μ ; mp >360°C. The elemental analysis is given in Table I.

Polymerization of 3,3',4,4'-Tetraaminodiphenyl Ether Tetrahydrochloride

To 120 g of polyphosphoric acid was added 5.75 g (0.0156 mole) of 3,3',4,4'-tetraaminodiphenyl ether tetrahydrochloride in a 500-ml three-necked round-bottomed flask. The flask was evacuated and filled with nitrogen repeatedly. The mixture was heated at 330°C for 4 hr and then cooled to 100°C. A few grams of ammonium carbonate and 50 ml of distilled water were added and the mixture was carefully poured into two liters of distilled water. After filtration, the precipitate was extracted with water for 5 days and with 95% ethyl alcohol for 10 days. After drying under reduced pressure, the yield of black powdery material was 2.0 g (67.3%), $\eta_{inh} = 0.19$ (0.2% concentrated H₂SO₄, 30°C) $\lambda_{max} = 314$ m μ (H₂SO₄), mp >360°C. Analyses are reported in Table I.

Polymerization of 3,3'-Diaminobenzidine

3,3'-Diaminobenzidine (5 g, 0.0234 mole) was mixed with 120 g of PPA in a 200-ml three-necked flask. The apparatus was evacuated three times and refilled with nitrogen, then heated in nitrogen atmosphere to 340°C during ½ hr and then held at this temperature under stirring for 9 hr. The dark mixture so obtained was cooled to 100°C, carefully poured into 2 l. of well stirred distilled water, and heated for 6 hr. The product was decanted and washed by heating two more times with 2 l. of distilled water, then dried and extracted in a Soxhlet with 95% ethyl alcohol for 90 hr., and then dried again under vacuum. The yield of black powdery material was 2.4 g (57%), $\eta_{inh} = 0.43$ (0.2% concentrated H₂SO₄), $\lambda_{max} = 297; 320$ m μ (H₂SO₄) mp >360°C. The analyses are reported in Table II. The mother liquor of extraction was concentrated to dryness and the solid residue appeared to be unreacted tetraamine.

Polymerization of 3,3',4,4'-Tetraaminodiphenylsulfone

A mixture of 3.2 g (0.0115 mole) of 3,3',4,4'-tetraaminodiphenylsulfone and 120 g. of polyphosphoric acid was placed in a three-necked 200-ml flask. The flask was repeatedly evacuated and filled with dry nitrogen, then heated at 250°C for 9 hr. The color of the mixture changed rapidly to purple and then deep blue. At the end of the reaction, the mixture was cooled to 100°C, and ammonium carbonate and a little ion-free water was added as the whole mixture was poured into 1500 ml of distilled water saturated with ammonium carbonate. The suspension was centrifuged,

dried and the solid mixture was extracted with water for a week, then with 95% ethyl alcohol for 10 days. The black polymer thus obtained had a very low solubility in acids. The yield was 2.56 g (82%), $\lambda_{\max} = 238 \text{ m}\mu$, mp $>360^\circ\text{C}$. The analyses are reported in Table II.

4,4'-Diacetamidodiphenyl Sulfone

This material was prepared in 95% yield as described previously.¹⁶ It was recrystallized from acetic acid and melted at $291\text{--}292^\circ\text{C}$ (lit.¹⁶ mp, $275\text{--}278^\circ\text{C}$).

ANAL. Calcd for $\text{C}_{16}\text{H}_{16}\text{N}_2\text{O}_4\text{S}$: C, 57.83%; H, 4.82%; N, 8.43%. Found: C, 57.95%; H, 4.92%; N, 8.31%.

3,3'-Dinitro-4,4'-Diacetamidodiphenyl Sulfone

The nitration of the diacetamido compound was carried out as previously described to give a yield of 66.6%, mp $247\text{--}248^\circ\text{C}$ (lit.¹⁶ mp $247\text{--}248^\circ\text{C}$).

ANAL. Calcd for $\text{C}_{16}\text{H}_{14}\text{N}_4\text{O}_8\text{S}$: C, 45.5%; H, 3.32%; N, 13.27%. Found: C, 45.10%; H, 3.42%; N, 12.75%.

3,3'-Dinitro-4,4'-Diaminodiphenyl Sulfone Hydrochloride

This compound was prepared as previously described.¹⁶ Our yield was 61%, mp $305\text{--}306^\circ\text{C}$ (lit.¹⁶ mp, $307\text{--}308^\circ\text{C}$).

3,3'-4,4'-Tetraaminodiphenyl Sulfone

This material was prepared as previously described,¹⁶ except the crude solution of the hydrochloride obtained on evaporation of the solvent was filtered before it was diluted and neutralized. Our yield was 58% of a product melting at $176.5\text{--}177.5^\circ\text{C}$ (lit.¹⁶ mp $174\text{--}175^\circ\text{C}$).

ANAL. Calcd for $\text{C}_{16}\text{H}_{14}\text{N}_4\text{O}_2\text{S}$: C, 51.8%; H, 5.04%; N, 19.40%. Found: C, 51.66%; H, 5.08%; N, 19.8%.

We are indebted to Dr. G. F. L. Ehlers of the Materials Laboratory WPAFB for the TGA analyses. Microanalyses were done by Micro-Tech Laboratories, Skokie, Illinois.

This work was supported by the Air Force Materials Laboratory, Air Force Systems Command, Wright-Patterson Air Force Base, Ohio.

References

1. H. Vogel and C. S. Marvel, *J. Polym. Sci.*, **50**, 511 (1961); *J. Polym. Sci. A*, **1**, 1531 (1963).
2. L. Plummer and C. S. Marvel, *J. Polym. Sci. A*, **2**, 2559 (1964).
3. R. T. Foster and C. S. Marvel, *J. Polym. Sci. A*, **3**, 417 (1965).
4. T. V. Lakshmi Narayan and C. S. Marvel, *J. Polym. Sci. A-1*, **5**, 1113 (1967).
5. J. Preston and W. B. Black, *J. Polym. Sci. A-1*, **5**, 2429 (1967).
6. A. H. Frazer, W. Sweeny, and F. T. Wallenberger, *J. Polym. Sci. A*, **2**, 1157 (1964).
7. G. M. Bower and L. W. Frost, *J. Polym. Sci. A*, **1**, 3135 (1963).
8. C. E. Sroog, A. L. Endrey, S. V. Abramo, C. E. Berr, W. M. Edwards, and K. L. Olivier, *J. Polym. Sci., A* **3**, 1373 (1965).
9. J. K. Stille, J. R. Williamson, and F. E. Arnold, *J. Polym. Sci. A*, **3**, 1013 (1965).

10. H. Jadamus, F. DeSchryver, W. DeWinter, and C. S. Marvel, *J. Polym. Sci. A-1*, **4**, 2831 (1966).
11. F. DeSchryver and C. S. Marvel, *J. Polym. Sci. A-1*, **5**, 545 (1967).
12. R. Wolf, M. Okada, and C. S. Marvel, *J. Polym. Sci. A-1*, **6**, 1503 (1968).
13. M. Okada and C. S. Marvel, *J. Polym. Sci. A-1*, **6**, 1259 (1968).
14. T. Kubota and R. Nakanishi, *J. Polym. Sci. B*, **2**, 655 (1964).
15. F. D. Popp and W. E. McEwen, *Chem. Rev.*, **58**, 321 (1958).
16. J. K. Stille and F. E. Arnold, *J. Polym. Sci. A-1*, **4**, 551 (1966).

Received February 12, 1969

Synthesis and Polymerization of 1- and 2-Cyano-1,3-Butadienes

PETER E. WEI* and GEORGE E. MILLIMAN, *Esso Research and
Engineering Company, Linden, New Jersey*

Synopsis

1-Cyano-1,3-butadiene and 2-cyano-1,3-butadiene were prepared and designated 1-cyanoprene and 2-cyanoprene, respectively. These compounds, and their intermediates, were characterized by their infrared and proton magnetic resonance spectra. Their polymerizations with lithium or aluminum alkyl catalysts are described. The synthesis of these monomers involves a thermal cracking process (400–500°C). The yield of monomer by this process depends on the positions of the cyano and acetoxy groups in the butene intermediate; if the cyano and the acetoxy groups are attached to the same allylic carbon, a low monomer yield is obtained. The polymers of 1-cyanoprene are the results of 1,4-enchainment (*cis* and *trans*) and are amorphous; the polymers of 2-cyanoprene may involve 1,4-enchainment but are partially crystalline. Both of these polymers are thermoplastic.

INTRODUCTION

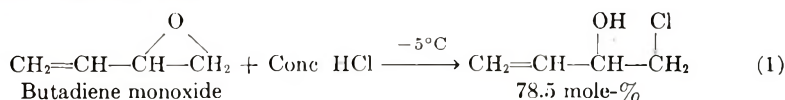
Cyanoprenes bear a resemblance to chloroprenes (monomers used for neoprene rubbers), and polycyanoprenes prepared by emulsion polymerization are known to have better oil-resistant properties than polychloroprene.¹ These polymers have not been extensively investigated primarily because the monomers are not readily available and dimerize on storage. Tanaka² reported the polymerization of 2-cyanoprene with benzoyl peroxide in 1958. Natta and co-workers³ have noted that polymers of 1-cyanoprene can be obtained using lithium alkyl catalysts. The polymerization of these monomers with other organometallic catalysts is now reported.

EXPERIMENTAL

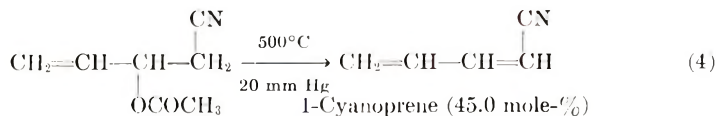
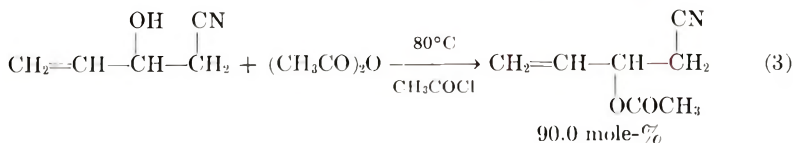
Monomer Preparation

1-Cyanoprene and 2-cyanoprene were prepared by two different routes.

1-Cyanoprene was first obtained by Coffman⁴ and was prepared by us as indicated in eqs. (1)–(4).

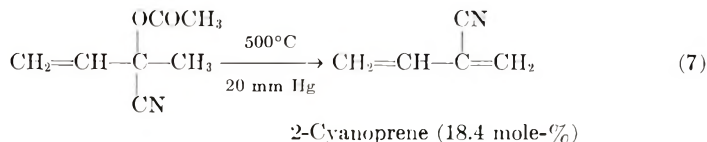
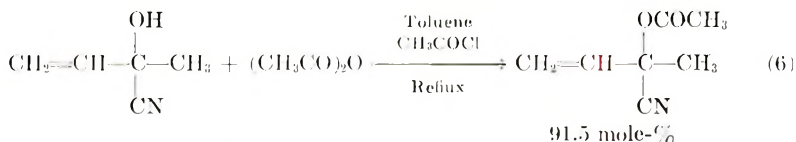
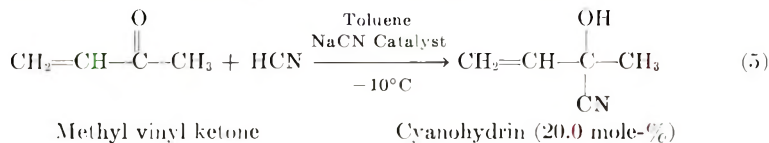


* Present address: Globe Manufacturing Company, Fall River, Massachusetts 02720.



This reaction sequence has been used by other workers⁵⁻⁷ to prepare 1-cyanoprene.

2-Cyanoprene was first prepared by Carter and Johnson in 1940.⁸ We followed their method which is summarized in eqs. (5)–(7).



The yield of the cyanohydrin from methyl vinyl ketone and HCN with the use of base catalysis is dependent upon the reaction temperature and catalyst concentration. If the temperature is lower than -20°C , no reaction or very slow reaction occurs. At temperatures greater than 5°C , the major product is levulinonitrile ($\text{CH}_2\text{COCH}_2\text{CH}_2\text{CN}$). At room temperature, the cyanohydrin prepared from methyl vinyl ketone readily loses HCN, and therefore, must be stabilized by the acetylation of the hydroxyl group. The other reactions are straightforward.

Polymerization Studies

The cyanoprene monomers used for the polymerization studies were freshly prepared; their physical properties are summarized in Table I.

Polymerization reactions were performed in a nitrogen drybox in small flasks equipped with magnetic stirrers. For reactions at -50°C , an isopentane bath cooled with liquid nitrogen was used; the temperature was controlled to $\pm 1^\circ\text{C}$. The flasks were charged with the solvent, the mono-

TABLE I

	1-Cyanoprene	2-Cyanoprene
Boiling point, °C/mm Hg	38-40/12	30/28
n_D	1.4848 (22°C)	1.4468 (18°C)

mer and the catalyst in that order. Polymers were isolated by filtration and washed with isopropanol.

RESULTS AND DISCUSSION

Monomer Preparation

1-Cyanoprene can be separated into its *cis* and *trans* isomers⁹ and was obtained by us as a mixture of these isomers as indicated by its PMR spectrum.

The monomer syntheses involves a thermal cracking process (400-500°C), and the yield of monomer is dependent upon the positions of cyano and acetoxy groups of the butene intermediates (Table II).

In the course of thermal cracking an allylic rearrangement occurs involving the acetoxy group; the ease of rearrangement is II > I >> III. If the cyano group is attached to the same allylic carbon as the acetoxy group (II), the rearrangement is promoted. Intermediate III is thermally stable and does not rearrange to II or crack to yield cyanoprene upon heating to 600°C. The results we have obtained confirm the observations of Marvel.¹⁰ Structural identifications have been made by PMR and infrared spectroscopy on neat samples.

TABLE II

Intermediate	Monomer yield, mole-%
$\text{I } \text{CH}_2=\text{CH}-\underset{\text{OCOCH}_3}{\text{CH}}-\overset{\text{CN}}{\text{CH}_2}$	45.0
$\text{II } \text{CH}_2=\text{CH}-\overset{\text{CN}}{\underset{\text{OCOCH}_3}{\text{C}}}-\text{CH}_3$	18.4
$\text{III } \text{CH}_2-\underset{\text{OCOCH}_3}{\text{CH}}=\overset{\text{CN}}{\text{C}}-\text{CH}_3$	0.0

Characterization of Intermediates and Monomers by 60MHz PMR and Infrared Spectroscopy

3-Acetoxy-4-cyano-1-butene. The PMR spectrum of this compound (Fig. 1) is extremely complex between δ 5.0 and 6.5. This region is attrib-

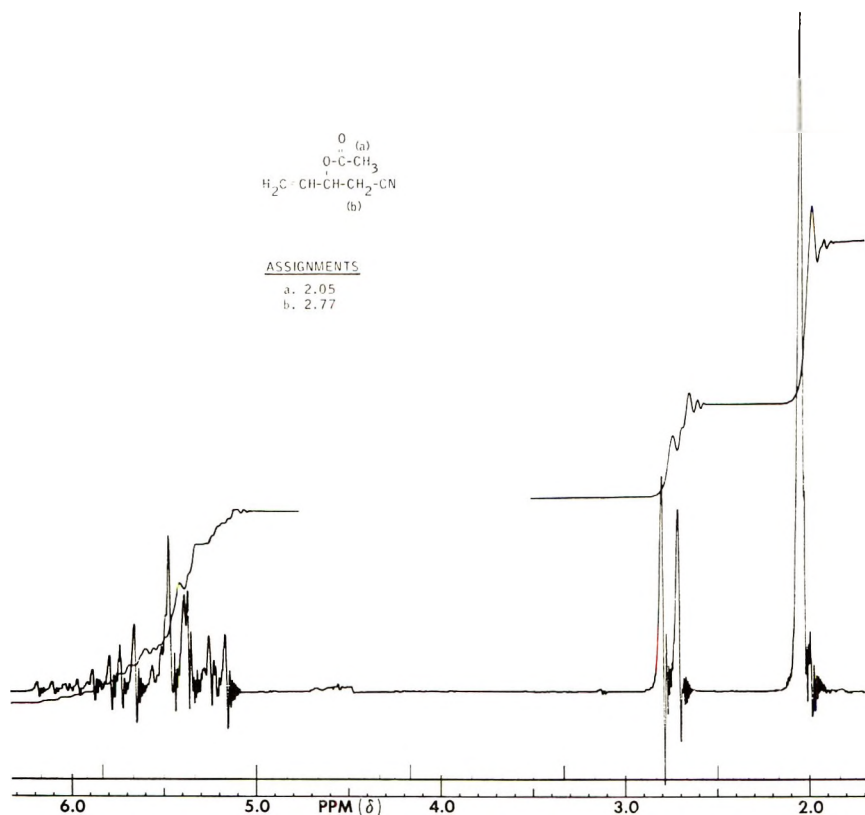


Fig. 1. PMR spectrum of 3-acetoxy-4-cyano-1-butene.

uted to the protons of the vinyl group and the methine proton. The methylene protons next to the cyano group give rise to a doublet at δ 2.77 and the acetoxy methyl protons give rise to a singlet at δ 2.05.

TABLE III
1-Cyanoprene Polymerization

	Expt 1	Expt 2	Expt 3
Solvent	Benzene	Benzene	Toluene
1-Cyanoprene, mmole	43	43	22
1M <i>n</i> -BuLi in <i>n</i> -C ₇ H ₁₆ , cc	5	—	—
1M Et ₂ AlCl, cc	—	5	—
Co(AcAc) ₂ , mmole	—	0.8	—
Li (dispersion), mmole	—	—	3.3 ^a
Catalyst concn, mole/l.	28×10^{-2}	28×10^{-2}	18×10^{-2}
Monomer concn, mole/l.	2.4	2.4	1.2
Catalyst/monomer, mole-%	11.6	11.6	15.0
Polymerization time (at room temp), hr	72	72	1
Conversion, wt-%	19.2	63.0	93.0

^a In conjunction with LiCl (3.3 mmole) and LiOBu (3.3 mmole).

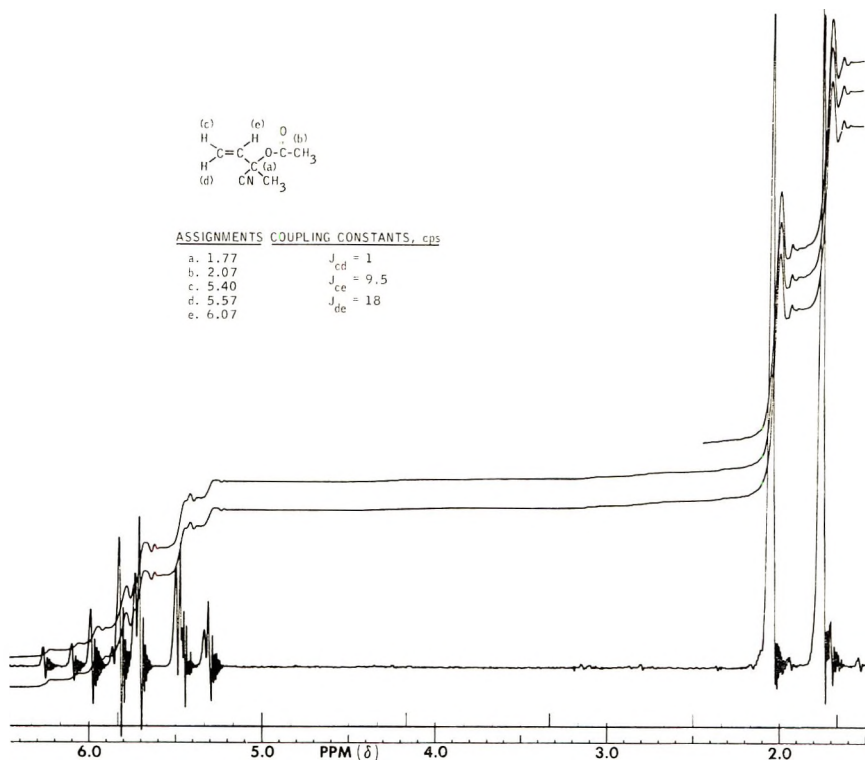


Fig. 2. PMR spectrum of 3-acetoxy-3-cyano-1-butene.

3-Acetoxy-3-cyano-1-butene. In contrast to the compound above, the PMR spectrum of this intermediate (Fig. 2) lends itself to complete assignment; chemical shifts and coupling constants are displayed on the spectrum.

1-Acetoxy-3-cyano-2-butene. The PMR spectrum (Fig. 3) of this compound is consistent with its structure and indicates much long-range

TABLE IV
2-Cyanoprene Polymerization

	Expt 1	Expt 2	Expt 3	Expt 4	Expt 5
Solvent	<i>n</i> -Heptane	EtCl	Toluene	CH ₂ Cl ₂	EtCl
2-Cyanoprene, mmole	44	22	22	16.5	22
1 <i>M</i> <i>n</i> -Buli in <i>n</i> -C ₇ H ₁₆ , cc	2	—	—	—	—
1 <i>M</i> Et ₂ AlCl in <i>n</i> -C ₆ H ₁₄ , cc	—	2	2	0.5	—
0.9 <i>M</i> Et ₃ Al (in <i>n</i> -C ₇ H ₁₆ , cc	—	—	—	—	1.8
Monomer concn, mole/l.	5.5	1.0	1.0	8.3	2.8
Catalyst concn, mole/l.	25 × 10 ⁻²	9 × 10 ⁻²	9 × 10 ⁻²	25 × 10 ⁻²	23 × 10 ⁻²
Catalyst/monomer, mole-%	4.5	9.1	9.1	3.0	8.2
Polymerization conditions, °C(hr)	RT(16)	-50(3)	-50(3)	RT(16)	RT(16)
Conversion, wt-%	11.6	6.0	20.8	6.2	88.5

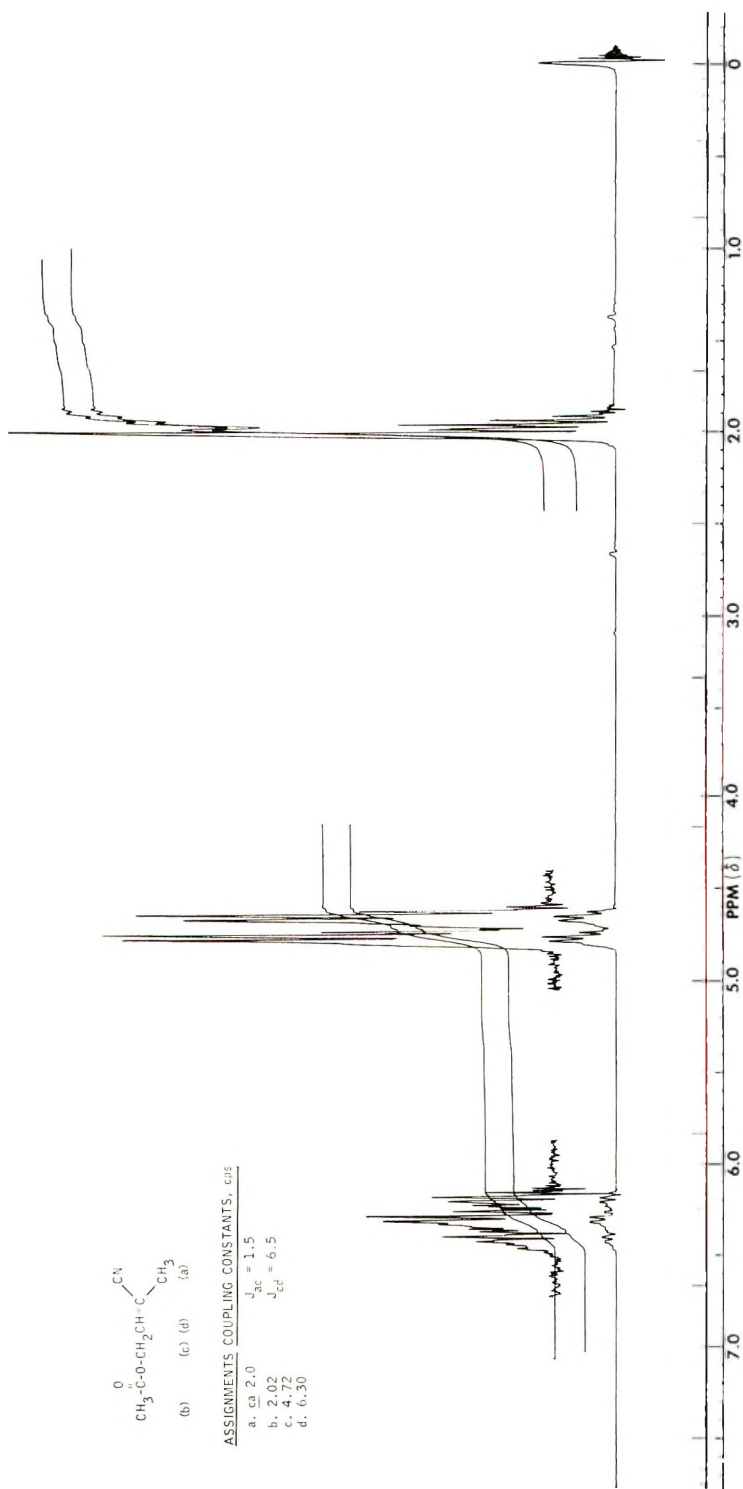


Fig. 3. PMR spectrum of 1-acetoxy-3-cyano-2-butene.

coupling giving rise to many lines for all of the protons except the acetoxy methyl protons; a singlet. Chemical shifts and coupling constants are given in Figure 3.

2-Cyano-1,3-butadiene. All the chemical shifts and coupling constants of this cyanoprene are illustrated on its PMR spectrum (Fig. 4). Its infrared spectrum is given in Figure 5.

1-Cyano-1,3-butadiene. The sample of this compound whose PMR spectrum is given in Figure 6 is evidently a mixture of *cis* and *trans* isomers. No attempt has been made to assign this spectrum due to its complexity. Its infrared spectrum is given in Figure 7.

Polymerization

1-Cyanoprene was polymerized in aromatic solvents at room temperature with the use of butyllithium, diethylaluminum chloride, and a lithium

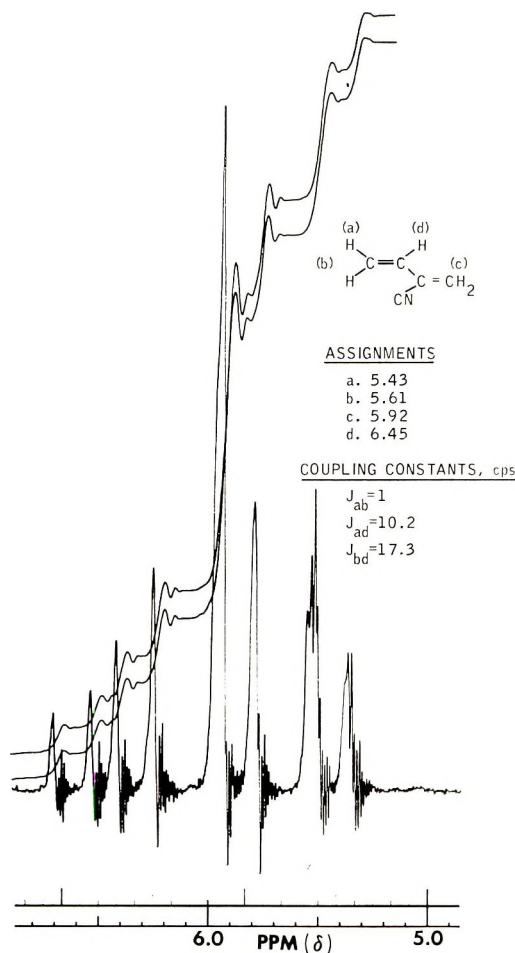


Fig. 4. PMR spectrum of 2-cyano-1,3-butadiene.

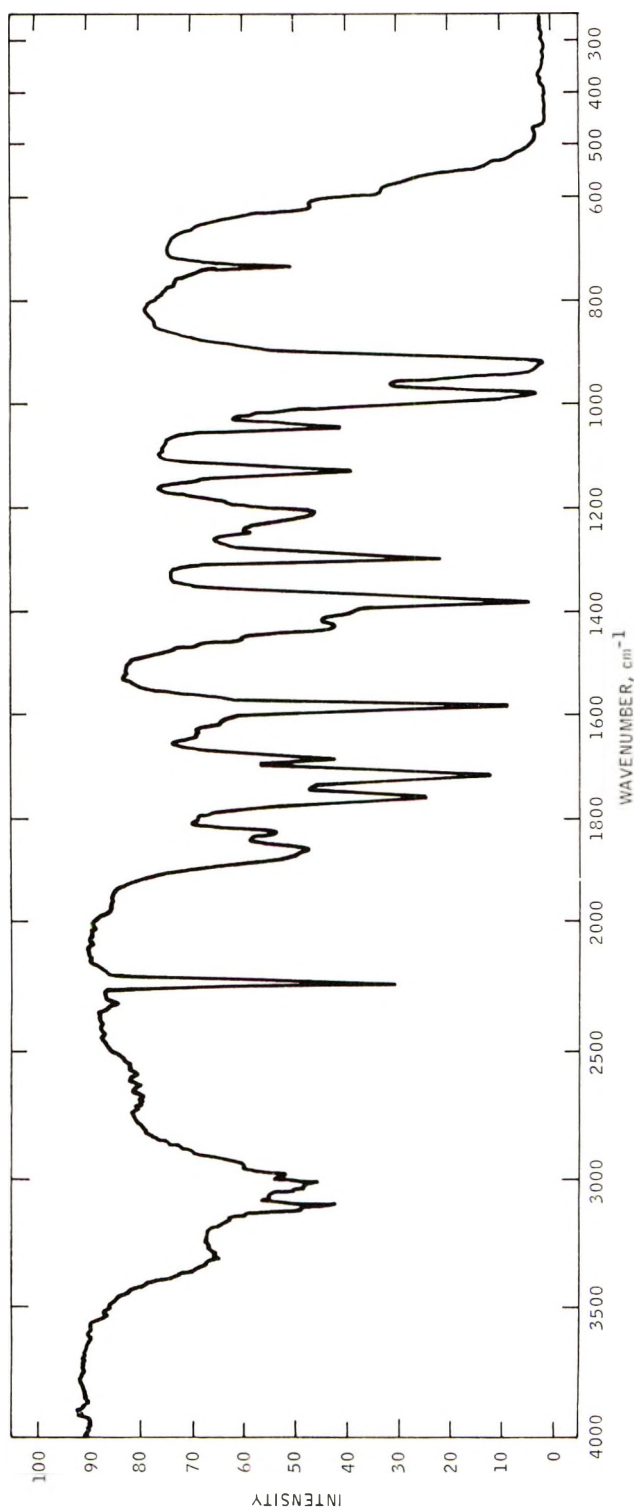


Fig. 5. Infrared spectrum of 2-cyano-1,3-butadiene.

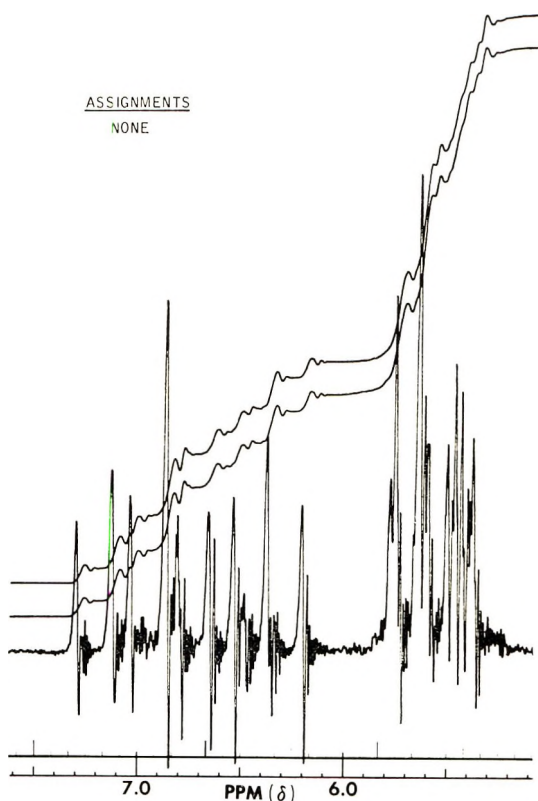


Fig. 6. PMR spectrum of *cis*- and *trans*-1-cyano-1,3-butadiene.

dispersion as catalysts. The conversion data (Table III) show that diethylaluminum chloride and lithium dispersion are more effective than butyllithium in polymerizing 1-cyanoprene. The polymers obtained with these different catalysts have similar infrared spectra by a film technique (Fig. 8). These spectra are poor but do show absorptions at 755 and 965 cm^{-1} , indicating predominant *cis*- and *trans*-1,4-enchainment. This 1,4-polymerization yields amorphous polymers and the polymers appear to be plastic at room temperature. Differential thermal analysis of these polymers indicates an exothermal chemical reaction beginning at 250°C followed by an endothermic decomposition at 317°C.

2-Cyanoprene was polymerized at room temperature and at -50°C with the use of butyllithium, diethylaluminum chloride, or triethylaluminum catalysts (Table IV). Toluene is preferred over ethyl chloride as a solvent for the diethylaluminum chloride catalyst because of higher polymer yields. Triethylaluminum gives the highest yield of polymer. All polymers of 2-cyanoprene have similar infrared spectra by a film technique (Fig. 9) and show absorptions at 745 cm^{-1} (medium) and 863 cm^{-1} (intense) which may indicate 1,4-enchainment. These polymers are partially crystalline as shown by the x-ray diffraction pattern (Fig. 10) and melt

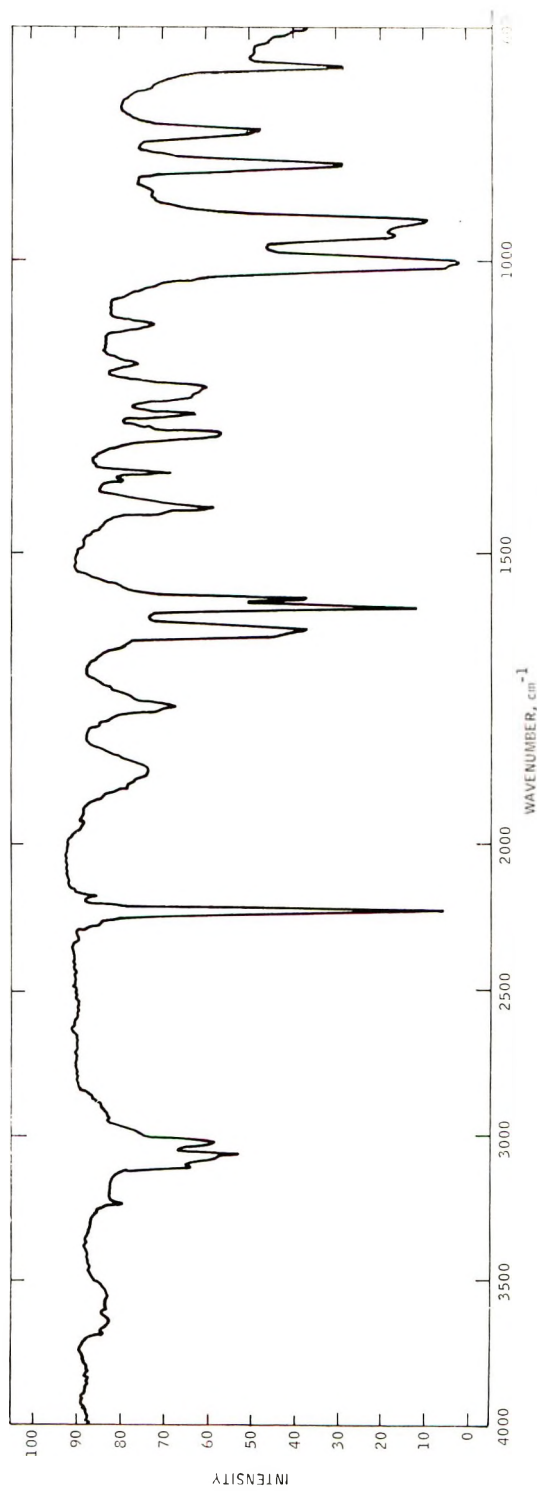


Fig. 7. Infrared spectrum of *cis*- and *trans*-1-cyano-1,3-butadiene.

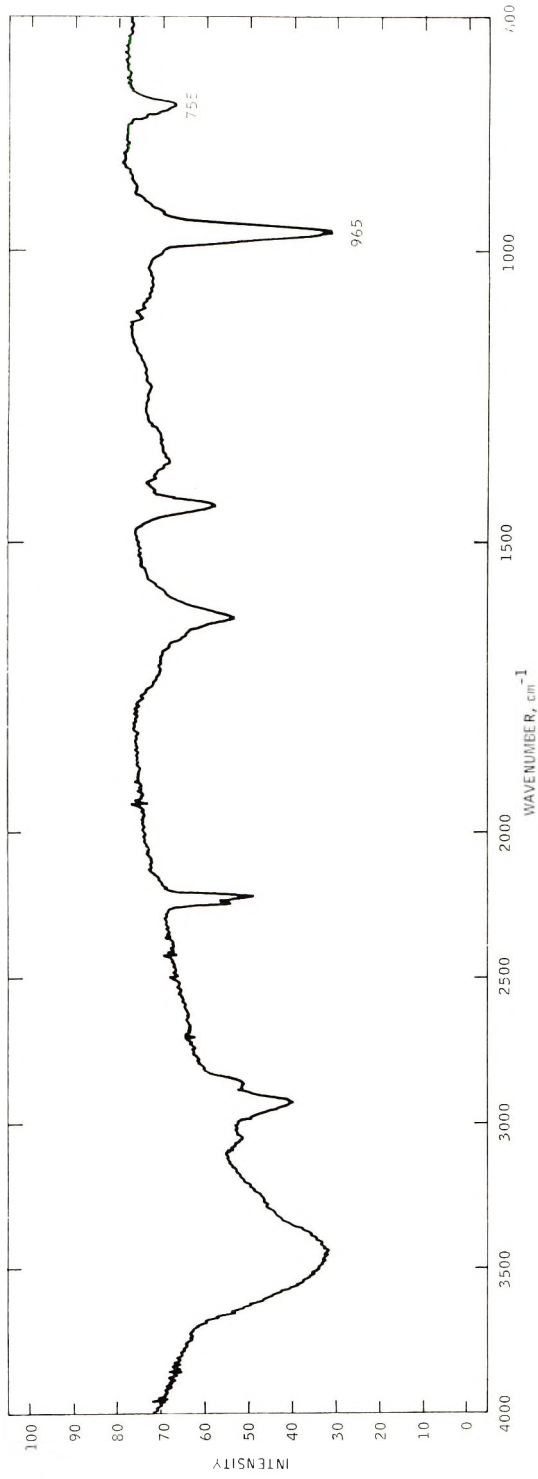


Fig. 8. Infrared spectrum of poly-1-cyano-1,3-butadiene.

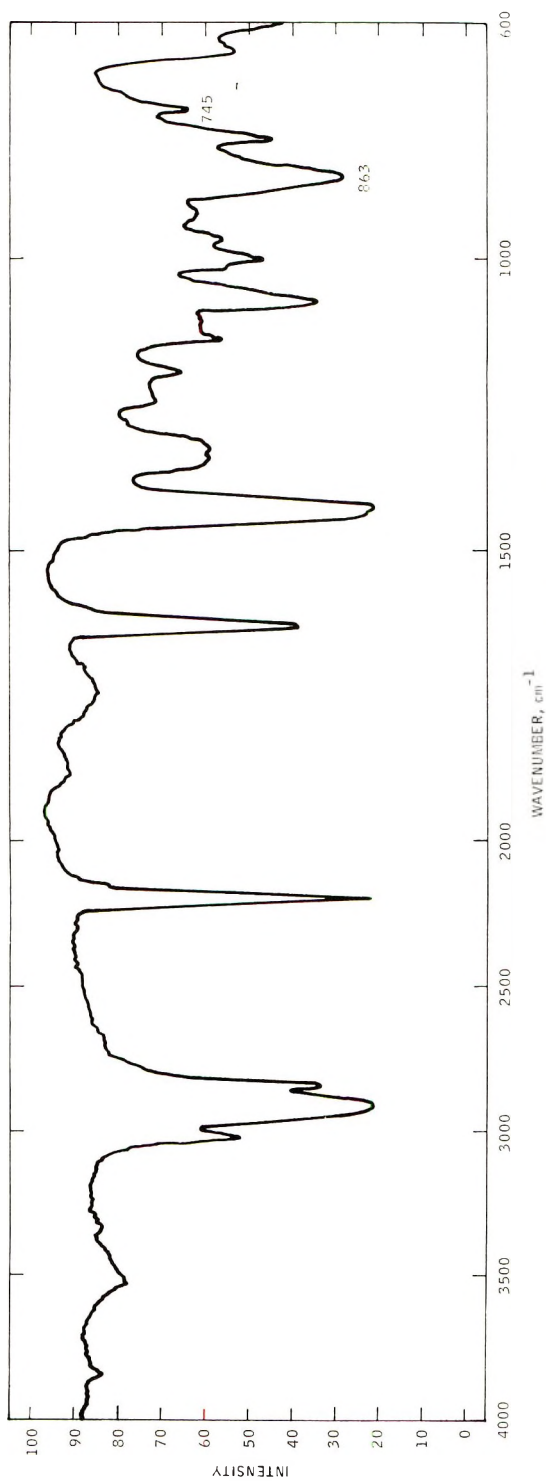


Fig. 9. Infrared spectrum of poly-2-cyano-1,3-butadiene.

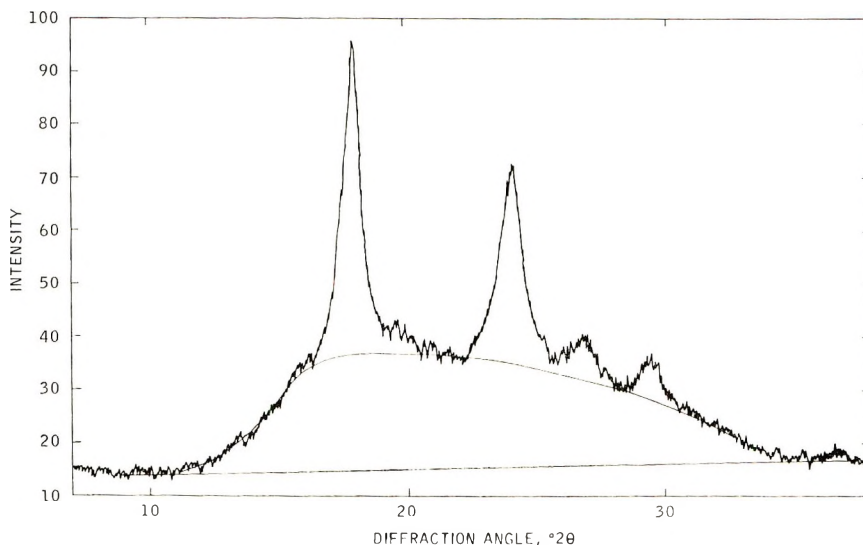


Fig. 10. X-Ray diffractometer pattern of poly-2-cyano-1,3-butadiene.

between 157 and 219°C. Decomposition occurs at 336°C, as indicated by differential thermal analysis.

In conclusion, cyanoprenes can be polymerized in high conversions by organometallic catalysts, and the resulting polymers are thermoplastic.

References

1. G. S. Whitby, *Synthetic Rubber*, Wiley, New York, 1954, p 962.
2. S. Tanaka, *Kogyo Kagaku Zasshi*, **61**, 1367 (1958).
3. G. Natta, U. Giannini, and A. Cassata, U. S. Pat. 3,257,365 (June 21, 1966).
4. D. D. Coffman, *J. Amer. Chem. Soc.*, **57**, 1981 (1935).
5. R. G. Kodesch, *J. Amer. Chem. Soc.*, **68**, 41 (1946).
6. P. H. Wise, U. S. Pat. 2,473,486 (1947).
7. H. Gudgeon, R. Hill, and E. Isaacs, *J. Chem. Soc.*, **1951**, 1926.
8. A. S. Carter and F. W. Johnson, U. S. Pat. 2,205,239 (1940).
9. J. G. Grasselli, B. L. Ross, H. F. Huber, and J. M. Augl, *Chem. Ind. (London)*, **1963**, 162.
10. C. S. Marvel and N. O. Bruce, *J. Amer. Chem. Soc.*, **70**, 1775 (1948).

Received December 23, 1968

Revised February 17, 1969

Four-Center Type Photopolymerization in the Solid State. III. Polymerization of Phenylene Diacrylic Acid and its Derivatives

FUSAE SUZUKI, YASUZO SUZUKI, HACHIRO NAKANISHI,
and MASAKI HASEGAWA, *The Textile Research Institute of
Japanese Government, Yokohama, Japan*

Synopsis

The solid-state photopolymerization of phenylene diacrylic acid (PDA) and its derivatives was studied as an application of solid-state photodimerization of cinnamic acid to photopolymerization of corresponding bifunctional molecule which has two cinnamic units in a single molecule. *p*- and *m*-PDA, and their esters and amides were prepared and investigated with respect to their photopolymerizability. Many of them have been found to polymerize into linear high polymers with the cyclobutane rings in the main chain on irradiation by ultraviolet or visible light. The polymerization process, the structure of the polymers, and their general properties were investigated in several ways. All the polymers are very similar to poly-2,5-distyrylpyrazine and poly-1,4-bis(β -pyridyl-2-vinyl) benzene with respect to their polymerization behavior, polymer structure, and some polymer properties: these polymers are soluble in a limited number of solvents, they have a high melting point and an extremely high crystallinity. On the basis of chemical behavior of poly-PDA and its phenyl ester the possible steric configurations of these polymers are discussed. It is demonstrated for the PDA series that solid-state dimerization can be generally extended to solid-state photopolymerization of the compound having two dimerizable units in a single molecule, although the crystal structure renders polymerization impossible in certain cases.

INTRODUCTION

We have reported on four-center type photopolymerization in the solid state of 2,5-distyrylpyrazine (DSP) and its related compounds in previous papers.¹⁻⁵ The results prompted us to extend the study to other types of compounds in order to assess the generality of this new type of polymerization. So far no papers have dealt with topochemical photopolymerization in detail. At this stage there is no way to predict polymerizable monomers by this type of polymerization. To explore further monomers for the polymerization we have assumed the simple rule that the photodimerization can be generally extended to photopolymerization with the same relation as shown in photodimerization of stilbazole⁶ and photopolymerization of 1,4-bis(β -pyridyl-2-vinyl)benzene (P2VB). Thus, following the DSP series, we have studied the photopolymerization of phenylene diacrylic acid (PDA) and its derivatives which have two cinnamic units

in a single molecule. Among many photodimerizations reported, one of the well known is that of cinnamic acid derivatives, crystallographic studies of which by Schmidt and co-workers⁷ have revealed the correlation between its crystal structure and photochemical behavior. We have prepared several derivatives of PDA which include *p*- and *m*-PDA, their esters and amides and surveyed the photopolymerizability of these compounds. It was found that many of them photopolymerize to linear high polymers. The polymerization rate or polymer yield vary with the different monomers, while the kinetic polymerization behavior and polymer structure are quite similar to those of the DSP series. All the polymers thus obtained are soluble in a limited number of solvents; they are highly crystalline and have a high melting point (e.g., 415°C for the polymer of *p*-PDA methyl ester, 420°C for the polymer of *p*-PDA phenyl ester). In this paper, the preparation of the monomers, the photopolymerization procedure of these compounds, and the study of their structure and general properties are described. In addition, a study of the pyrolysis and anhydride formation from poly-*p*-PDA and its phenyl ester was carried out in order to obtain some information on the possible steric configuration of these polymers.

This is the first demonstration in the field of solid-state polymerization of polymerizability governed by steric factors and of a simple correlation between dimerizable and polymerizable compounds.

EXPERIMENTAL

Preparation of Monomers

The monomers examined were *p*- and *m*-PDA, their esters, and *p*-PDA amides (Tables I-III). *p*-PDA⁸ was prepared by condensation of terephthalaldehyde and malonic acid in the presence of piperidine. *m*-PDA⁹ was prepared in a similar way by using isophthalaldehyde. *p*- and *m*-PDA chloride were prepared by reaction of *p*- and *m*-PDA and thionyl chloride. All esters were prepared in quantitative yield by refluxing *p*- and *m*-PDA chloride with the corresponding alcohol. *p*-PDA amides were prepared from *p*-PDA chloride and aqueous ammonia or the corresponding amine. 1,4-Bis(β -benzoylvinyl)benzene was prepared by aldol condensation of terephthalaldehyde with acetophenone.

Polymerization

In order to check the photopolymerizability of the monomers, each monomer (250 mg) was dispersed as a solid in a suitable inert solvent such as water or water-ethanol (50 ml) in a quartz flask and irradiated with a 500 W xenon lamp for 50 hr at room temperature with stirring. After irradiation the product was washed with the solvent such as acetone which dissolves the monomer and dried *in vacuo* at room temperature. One of the two following light sources was employed for polymerization: (A) a 450-W high-pressure mercury lamp or (B) an immersion-type 100-W high-pressure mercury lamp. The irradiation time required to completion

TABLE I
 Polymerizable Monomers and Their Polymerization

Compound ROCH=CH— Ar—CH=CHCOR	Mp, °C	λ_{\max} , $\mu\mu^a$ (ϵ)	Elementary analysis			Reference	Light source ^b	Reac- tion time, hr	Reaction tempera- ture, °C	Polymer		
			C, %	H, %	N, %					Yield, %	Mp, °C	η_{red}^c
Ar: <i>p</i> -C ₆ H ₄ R: OH	360	363 (55 500)	66.05 ^d 63.47 ^e	4.62 4.80	— —	8	A	27	Room	Quantitative	290	0.12
Ar: <i>p</i> -C ₆ H ₄ R: OCH ₃	171	320 (49 900)	68.28 ^d 68.10 ^f	5.73 5.80	— —	New compound	B A	1.5 1.5	Room Room	Quantitative 55	415 —	25.00 8.95
Ar: <i>p</i> -C ₆ H ₄ R: OC ₂ H ₅	94	320 (44 700)	70.05 ^d 69.79 ^f	6.61 6.56	— —	New compound	B C	1.5 50	—25 Room	Quantitative Quantitative	347 —	1.41 0.16
Ar: <i>p</i> -C ₆ H ₄ R: <i>n</i> -OC ₃ H ₇	73	321 (49 700)	71.50 ^d 71.39 ^f	7.34 7.40	— —	New compound	B	50	0-5	42	360	0.26
Ar: <i>p</i> -C ₆ H ₄ R: iso-OC ₃ H ₇	84	321 (50 500)	70.34 ^e 71.50 ^d	7.35 7.34	— —	New compound	A	49	Room	65	320	0.45
Ar: <i>p</i> -C ₆ H ₄ R: OC ₃ H ₅	165	328 (51 900)	69.23 ^e 77.82 ^d	7.23 4.90	— —	New compound	B B	10 10	Room Room	85	420	0.90
Ar: <i>p</i> -C ₆ H ₄ R: NH ₂	320	353 (52 600)	77.76 ^f 76.13 ^e	4.97 4.84	— —	8	B	10	Room	Quantitative	405	1.50

^a Measured in dioxane except for *p*-PDA and *p*-PDA amide, which were measured in concentrated H₂SO₄.

^b (A) 450-W high-pressure mercury lamp; (B) 100-W high-pressure mercury lamp; (C) 500-W xenon lamp.

^c Reduced viscosity (0.36 g/100 ml in concentrated H₂SO₄ at 30°C. Aqueous sodium hydroxide was used for poly-*p*-PDA phenyl ester).

^d Calculated.

^e Found for irradiated product.

^f Found for monomer.

TABLE II
 Monomers Changed Chemically or Spectrally on Irradiation

Compound ROCC=CH— Ar—CH=CHCOR	Mp °C	λ_{\max} (ϵ) ^a	Elementary analysis			Reference	Light source ^b	Reac- tion time, hr	Reaction tempera- ture	Polymer	
			C, %	H, %	N, %					Yield, %	MP, °C
Ar: <i>p</i> -C ₆ H ₄	273	329 (37 000)	62.61 ^c	3.51	6.09	New compound	B	50	Room	89	310–320
R: OC ₆ H ₄ NO ₂			61.74 ^d	3.85	5.83						
			62.46 ^e	3.32	5.97						
Ar: <i>m</i> -C ₆ H ₄	295	272 (54 500)	66.05 ^c	4.62	—	9	A	72	Room	Quantitative	230–260
R: OH			67.62 ^e	5.33	—						
Ar: <i>m</i> -C ₆ H ₄	134	274 (51 400)	68.28 ^c	5.73	—						
R: OCH ₃	94	323 (52 100)	67.40 ^c	5.68	—	New compound	B	30	Room	Quantitative	85–95
Ar: <i>p</i> -C ₆ H ₄ ^f			78.37 ^c	5.57	—						
R: OCH ₂ C ₆ H ₅	188	320 (73 800)	78.47 ^d	5.54	—						
Ar: <i>p</i> -C ₆ H ₄ ^f			78.37 ^c	5.57	—	New compound					
R: OC ₆ H ₄ CH ₃	74	320 (49 900)	77.61 ^d	5.61	—						
Ar: <i>p</i> -C ₆ H ₄ ^f			72.70 ^e	7.93	—						
R: OC ₄ H ₉	292	320 (45 200)	73.21 ^d	8.20	—	New compound					
Ar: <i>p</i> -CH ^f			73.14 ^c	8.59	8.53						
R: NHC ₄ H ₉	133	277 (50 400)	73.00 ^d	8.73	8.44						
Ar: <i>m</i> -C ₆ H ₄ ^f						9					
R: OC ₆ H ₅											

^a Measured in dioxane.^b (A) 450-W high-pressure mercury lamp; (B) 500-W xenon lamp.^c Calculated.^d Found for monomer.^e Found for irradiated product.^f Spectral change of these monomers was checked by potassium bromide pellet method.

TABLE III
 Nonpolymerizable Monomers

Compound	Mp, °C	λ_{\max} , $m\mu$ (ϵ) ^a	Elementary analysis			Reference
			C, %	H, %	N, %	
$\text{ROCCH}=\text{CH}-\text{Ar}-\text{CH}=\text{CHCOR}$ Ar: $p\text{-C}_6\text{H}_4$ R: OC_{10}H_7 Ar: $p\text{-C}_6\text{H}_4$ R: C_6H_5	188	328 (60 000)	81.68 ^b 81.41 ^c 85.18 ^b 85.07 ^c	4.72 4.79 5.36 5.30	— — — —	New compound New compound
$\text{C}_6\text{H}_5\text{CH}=\text{CHC}(\text{O})\text{O}-\text{CCH}=\text{CHC}_6\text{H}_5$	134	259 (49 100)				11

^a Measured in dioxane.^b Calculated.^c Found for monomer.

of polymerization varied greatly with the type of light sources and the temperature.

Polymerization at low temperature was carried out by using an immersion-type vessel which was cooled from outside by a Dry Ice-acetone mixture. Aqueous ethanol (5–40%) was used as dispersant.

A few milligrams of monomer in a potassium bromide pellet was irradiated with a 450-W high-pressure mercury lamp. The polymerization was followed by infrared spectroscopic analysis.

Attempted Photopolymerization of *p*-PDA Ethyl Ester in Solution

p-PDA ethyl ester (242 mg) was dissolved in ethanol (60 ml) in a quartz flask and irradiated with a 500-W xenon lamp for 18 hr at room temperature. After removing solvent under reduced pressure a slightly yellowish residue was obtained. It was identified as *p*-PDA ethyl ester by melting temperature and infrared spectrum.

Attempted Photopolymerization of Molten *p*-PDA Ethyl Ester

p-PDA ethyl ester (518 mg) was placed in a Pyrex flask and irradiated with a 450-W high-pressure mercury lamp for 6 hr at 100–110°C under nitrogen. *p*-PDA ethyl ester remained almost unchanged.

Chemical Reaction of Polymers

Hydrolysis of Poly-*p*-PDA Phenyl Ester. The polymer (216 mg) gradually dissolved when stirred with 1.7*N* aqueous sodium hydroxide at 70–80°C for 24 hr. After cooling, the product was precipitated by hydrochloric acid, collected by filtration and dried *in vacuo* over phosphorous pentoxide.

The infrared spectrum showed an absorption peak of the carboxylic acid group and agreed with that of poly-*p*-PDA.

Poly-*p*-PDA ethyl ester and methyl ester could not be hydrolyzed by this procedure.

Formation of Anhydride from Poly-*p*-PDA. A mixture of poly-*p*-PDA (72 mg) and acetic anhydride (6 ml) containing a small amount of *p*-toluenesulfonic acid was refluxed for 6 hr. Removal of the solvent under reduced pressure left a brown residue. The infrared spectrum showed new bands at 1860 and 1780 cm^{-1} which indicate a five-membered anhydride ring.

The hydrolyzed polymer (70 mg) from poly-*p*-PDA phenyl ester was also treated in the same way as described above. The product showed weak infrared absorption bands corresponding to a six membered anhydride ring at 1765 and 1820 cm^{-1} .

Thermal Decomposition of Polymers

Poly-*p*-PDA Ethyl Ester. The polymer (117 mg) was placed in a sublimation apparatus and heated under reduced pressure (1–2 mm Hg) at

320–350°C. A small amount of *p*-PDA ethyl ester sublimed, but the most of the polymer changed into undefined brown tar within 2–3 hr.

Poly-*p*-PDA Methyl Ester. The polymer (170 mg) was subjected to thermal decomposition at 340–360°C. A slightly yellowish white powder sublimed gradually, consisting mainly of *p*-PDA methyl ester and other unidentified low molecular weight products. Its yield was 103 mg.

RESULTS AND DISCUSSION

Polymerization

All the monomers examined are shown in Tables I–III with melting points, maximum absorption bands, and the results of elementary analysis. All monomers were confirmed to have the *trans, trans* orientation by infrared or NMR spectroscopy. The NMR doublets with a coupling constant of 18 cps and the infrared absorption peak at 1000–970 cm^{-1} indicate *trans* CH=CH bonding. The monomers were classified into three groups with regard to photopolymerizability. The first group, which includes photopolymerizable monomers, is listed in Table I with the polymerization conditions and the properties of the resulting polymers. Though the rate and the degree of polymerization varied considerably, these monomers polymerize into linear high polymers in essentially the same way as DSP. For example, *p*-PDA methyl ester polymerizes most rapidly, yielding a linear polymer of surprisingly high molecular weight. Other monomers

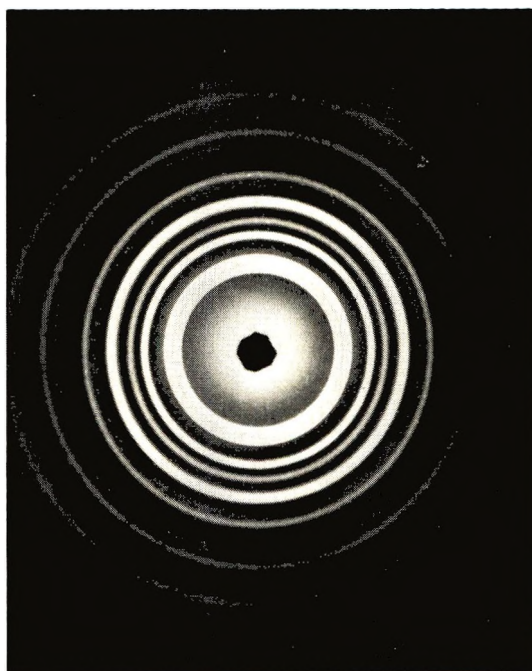


Fig. 1. X-ray diffraction pattern of poly-*p*-PDA amide.

which polymerize into high molecular weight polymers are the ethyl ester, phenyl ester, and amide of *p*-PDA. It should be emphasized that the polymers from these monomers have extremely high crystallinity (Fig. 1). Figure 2 shows a polarizing micrograph of a single crystal of *p*-PDA phenyl ester and its polymer. It shows a clear birefringence. According to x-ray powder analysis the degree of crystallinity of these polymers is comparable with that of the monomers (Fig. 3). It should be noted that



(a)



(b)

Fig. 2. Polarizing micrograph of (a) *p*-PDA phenyl ester and (b) its polymer.

polymerization of *p*-PDA ethyl ester at 30°C gave an amorphous polymer with a low molecular weight, while the polymer obtained at -25°C was highly crystalline with high molecular weight (Fig. 3). The same tendency was observed in the *p*-PDA *n*-propyl and isopropyl esters, which have relatively low melting points (73 and 84°C, respectively) similar to that of the *p*-PDA ethyl ester (94°C). From these observations it appears that temperature is a critical factor in determining the crystallinity and molecular weight of the polymer.

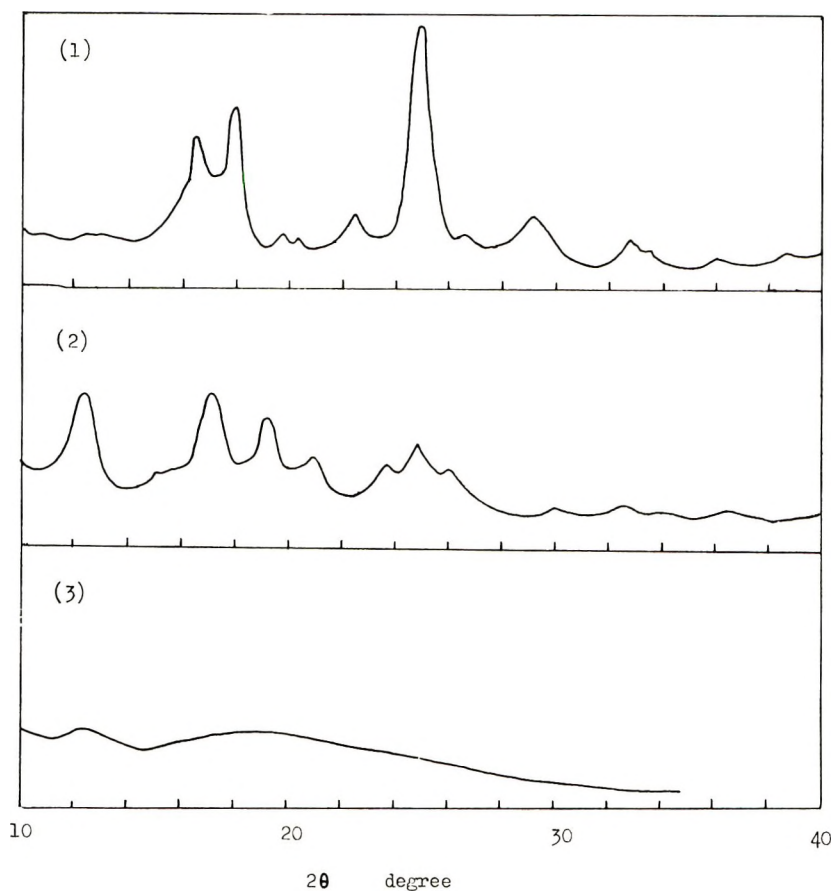


Fig. 3. X-ray diffraction diagrams of *p*-PDA ethyl ester and its polymers: (1) *p*-PDA ethyl ester; (2) poly-*p*-PDA ethyl ester obtained at 0–5°C; (3) poly-*p*-PDA ethyl ester obtained at 30°C.

Attempts to photopolymerize *p*-PDA ethyl ester in the melt or solution were unsuccessful, which implies that four-center type photopolymerization proceeds only in the solid state.

The second group monomers which were changed chemically or spectrally on irradiation are shown in Table II. The infrared spectra of these monomers changed on irradiation in a similar manner as the polymerizable monomers, but the products were amorphous and solution viscosity measurements did not indicate a high polymer. Among these, further characterization was carried out on the product from *m*-PDA methyl ester. Based on the results such as a peak at $\delta = 4.5$ in the NMR spectrum and the molecular weight estimated by means of vapor-pressure osmometry (MW = 1,040), it seems reasonable to conclude that the product is oligomeric. The other monomers listed in Table II are considered on similar evidence to be changed to oligomers.

Some monomers react very slowly on irradiation and it is difficult to obtain enough of the product under the described conditions. As previously suggested,¹⁰ the potassium bromide pellet method provides a very convenient way to detect polymerizability on irradiation. For example, *p*-PDA methyl ester showed an infrared spectrum typical of a polymer after irradiation for 10 min. *p*-PDA benzyl ester showed an analogous change of the infrared spectrum after 10 hr. The monomers behaving like *p*-PDA benzyl ester are listed in Table II. They are considered to be slightly photopolymerizable.

The third group, which is insensitive to light, is listed in Table III. Stobbe¹¹ reported briefly that cinnamic acid anhydride gave insoluble polymeric material on ultraviolet irradiation. We considered it might be the same type of polymer, and it is of interest from the viewpoint of structure elucidation and we reinvestigated the photopolymerization of this monomer, but so far no polymeric material has been obtained, to judge from spectral or melting point changes.

There is a report¹² on the solid-state photodimerization of chalcone. This led us to check the photopolymerizability of the corresponding bifunctional compound 1,4-bis(β -benzoyl vinyl)benzene. It was insensitive on irradiation.

From the results shown in Table I and II, it is concluded that photodimerization in the solid state can be extended to solid-state photopolymerization of the corresponding bifunctional compounds as is common in the case of liquid-phase polymerization where the monofunctional reaction is generally applicable to the corresponding bifunctional reagents.

It was demonstrated in the photodimerization of substituted cinnamic acids that the steric relation between the double bonds in the monomer crystal is of crucial importance. It may be said that in both the cinnamic acid and PDA series of compounds, olefinic double bonds have a strong tendency to be placed close to each other.

Polymer Structure

The structure of polymers was studied by ordinary methods including infrared and NMR spectroscopy and chemical means. The results of elementary analysis are shown in Tables I and II. The compositions of polymers were nearly the same as those of the monomers. All polymers exhibited the same type of infrared spectra. Some of them are shown in Figure 4 with that of monomer for comparison. It can be seen in Figure 4 that the absorption peak at 1640 cm^{-1} corresponding to C=C double bond and absorption peak at $1000\text{--}970\text{ cm}^{-1}$ disappeared in the spectra of the polymers and also the absorption peak of carbonyl group shifted to higher frequency. These data prove the disappearance of the olefinic double bonds in the polymers.

The NMR spectra of the polymers and the assignment of each peak are summarized in Table IV. New peaks between $\delta = 4$ and $\delta = 5$ are considered to be cyclobutane ring protons by analogy with those of poly-DSI⁹

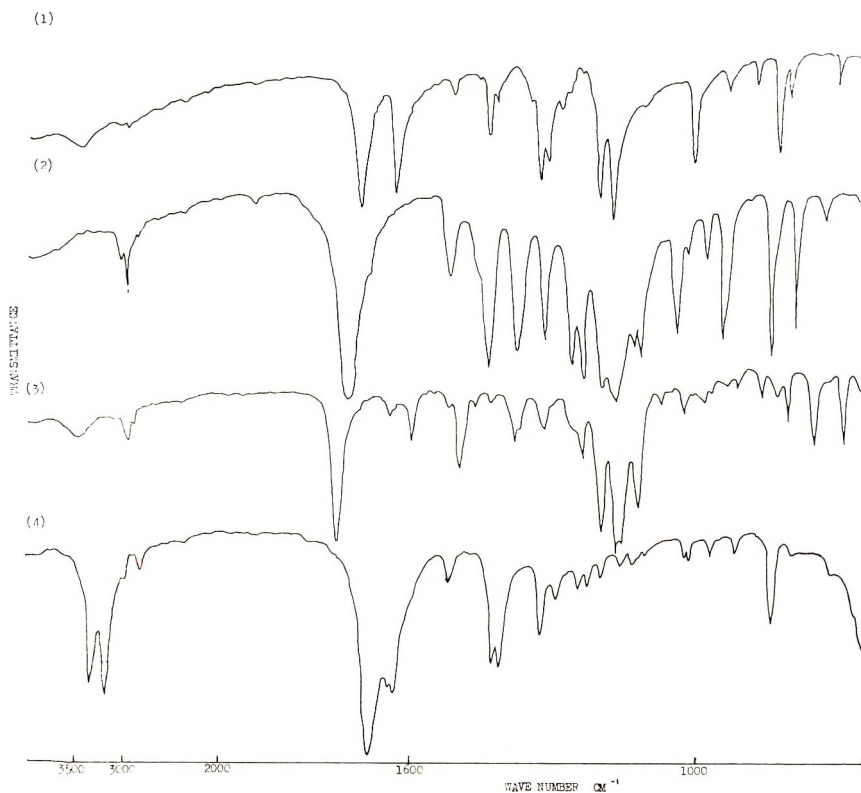
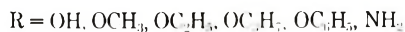
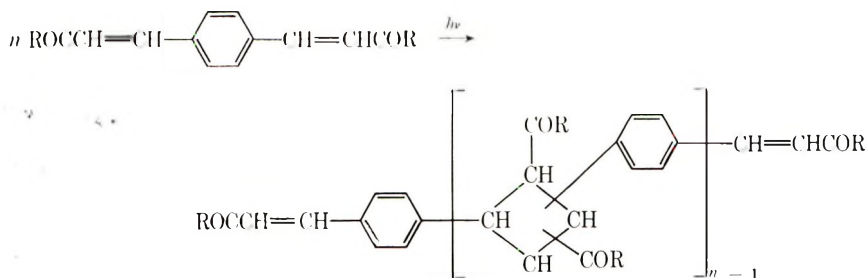


Fig. 4. Infrared spectra of monomer and polymers: (1) *p*-PDA methyl ester; (2) poly-*p*-PDA methyl ester; (3) poly-*p*-PDA phenyl ester; (4) poly-*p*-PDA amide.

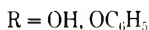
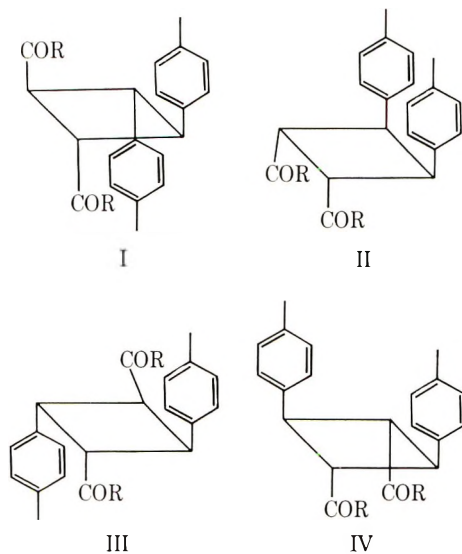
and poly-P2VB. All these results indicate that the polymerization proceeds through cycloaddition between double bonds resulting in cyclobutane rings in the main chain.

TABLE IV
NMR Spectra of Polymers

Polymer	Peak δ				Conditions (solvent, temperature, frequency)
	Aromatic protons (4H)	Cyclo- butane protons (4H)	Methyl protons (6H)	Methy- lene protons (4H)	
Poly- <i>p</i> -PDA methyl ester	7.0	4.2	3.6		Conc. H ₂ SO ₄ , 100°C, 60 Mcps
Poly- <i>p</i> -PDA ethyl ester	7.4	4.4	1.1	4.05	CF ₃ COOH, room temp, 100 Mcps
Poly- <i>p</i> -PDA amide	7.9	5.1			Conc. H ₂ SO ₄ , room temp, 60 Mcps



Regarding the configuration of substituents on the cyclobutane ring, there are eleven possible structures, five for head-to-tail, six for head-to-head. Supposing that the polymerization of the *trans, trans* monomer proceeds with a minimum of atomic or molecular movement, the *trans, trans* orientation must be kept in the polymer and we can eliminate seven of the eleven structures. Therefore, four structures, I–IV, are considered for the polymer.



The symmetric nature of the NMR spectrum of poly-*p*-PDA ethyl ester suggests that its steric configuration is one of these. However it is difficult to establish further detail of structure from that spectrum⁵ because of poor resolution.

For certain polymers, formation of a five- or six-membered cyclic anhydride provides useful information to determine steric configuration provided this reaction is intramolecular. For example, the anhydride ob-

tained from poly-*p*-PDA suggests the five-membered cyclic anhydride like that of β -truxinic acid. Therefore the head-to-head structure II is probable for poly-*p*-PDA. The acid-type polymer from poly-*p*-PDA phenyl ester seems to give a polymer with a six-membered cyclic anhydride, suggesting that the head-to-tail structure IV is likely for the poly-*p*-PDA phenyl ester.

Polymer Properties

One of the features of this type of polymerization is that a linear high polymer with high crystallinity can be synthesized easily. The crystalline polymers have high melting points and they decompose on heating near their melting point. The difference in the thermal decomposition of poly-*p*-PDA methyl ester and poly-*p*-PDA ethyl ester should be noted. The former decomposed mainly into monomer, while the latter decomposed into a tarlike material. This may reflect their structural difference. As expected from their high crystallinity, the solubility of the crystalline polymers is very limited. They do not dissolve in common organic solvents. Poly-*p*-PDA alkyl ester and amide are soluble in concentrated sulfuric acid, whereas poly-*p*-PDA phenyl ester dissolves only in aqueous sodium hydroxide after hydrolysis. Some amorphous polymers are soluble in organic solvents such as *m*-cresol, trifluoroacetic acid. *p*-PDA alkyl esters are very stable toward alkali. Neither ester hydrolysis nor chain scission were observed in these polymers. It is presumable that the extremely high crystallinity of these polymers governs the observed hydrolytic behavior.

References

1. M. Hasegawa and Y. Suzuki, *J. Polym. Sci. B*, **5**, 813 (1967).
2. M. Iguchi, H. Nakanishi, and M. Hasegawa, *J. Polym. Sci. A-1*, **6**, 1055 (1968).
3. M. Hasegawa, Y. Suzuki, F. Suzuki, and H. Nakanishi, *J. Polym. Sci. A-1*, **7**, 743-752 (1969).
4. H. Nakanishi, Y. Suzuki, F. Suzuki, and M. Hasegawa, *J. Polym. Sci. A-1*, **7**, 753-760 (1969).
5. M. Hasegawa, F. Suzuki, H. Nakanishi, and Y. Suzuki, *J. Polym. Sci. B*, **6**, 293 (1968).
6. J. L. R. Williams, *J. Org. Chem.*, **25**, 1839 (1960).
7. M. D. Cohen and G. M. J. Schmidt, *J. Chem. Soc.*, **1964**, 1996.
8. P. Ruggli and W. Theilheimer, *Helv. Chim. Acta*, **24**, 899 (1941).
9. P. Ruggli and A. Staub, *Helv. Chim. Acta*, **17**, 1523 (1934).
10. M. Miura, T. Kitami, and K. Nagakubo, *J. Polym. Sci. B*, **6**, 463 (1968).
11. H. Stobbe, *Ber.*, **25**, 2859 (1925).
12. H. Stobbe and A. Hensel, *Ber.*, **59**, 2260 (1926).

Received January 20, 1969

Revised February 18, 1969

Polyperfluorobutadiene. II. Fractionation and Crosslinking*

MADELINE S. TOY and J. MELFORD NEWMAN,
*Astropower Laboratory, McDonnell Douglas Astronautics Company,
Newport Beach, California 92660*

Synopsis

Perfluorobutadiene was polymerized in bulk under low pressure and temperature in the presence of diisopropyl peroxydicarbonate, bis(trifluoromethyl) peroxide, and benzoyl peroxide. Fractional solvent extraction of polyperfluorobutadiene by *n*-hexane and hexafluorobenzene into three polymeric fractions was described. The hexafluorobenzene-soluble fraction was used for crosslinking studies. Direct fluorination of solid polyperfluorobutadiene required no catalyst. The fluorine-polyperfluoropolyene reactions furnished a mechanism for crosslinking the unsaturated chains. Fluorination by gaseous fluorine formed free radical sites on the polymer chains besides saturation reactions. The presence of excess monomer in contact with these partially fluorinated solid polyperfluorobutadienes under controlled conditions were capable of crosslinking and grafting to the linear chains. Direct fluorination of solid polyperfluorobutadiene tends to involve reaction with the internal double bonds rather than the pendant perfluorovinyl group; the converse is true for crosslinking with hexamethylenediamine. The mechanisms are discussed.

INTRODUCTION

Rubbery perfluoropolymers were obtained from polymerization of perfluoro-1,4-pentadiene under high pressure and γ -irradiation. The product is actually a copolymer of the 1,4- and 1,3-pentadiene due to migration of double bonds during the polymerization reaction.¹ Perfluorobutadiene was reported to polymerize under high pressure with oxygen and peroxide promotion to high polymer. By fluorination of the homopolymer its olefinic bonds were saturated and crosslinked.²

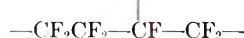
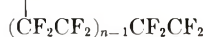
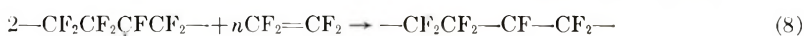
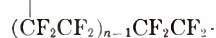
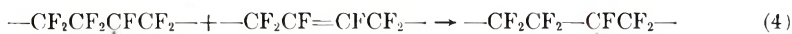
In a previous paper,³ we reported the free-radical bulk polymerization of perfluorobutadiene under low pressure and temperature to involve one or both double bonds to give a copolymer of the 1,2- and 1,4-butadiene. In view of the low yields, other free-radical catalysts are explored. Fractional extractions of the homopolymer and crosslinking by direct fluorination and diamine are described.

*This paper was presented in part at the 155th American Chemical Society Meeting, San Francisco, California, April 1968.

RESULTS AND DISCUSSION

Bulk polymerization of perfluorobutadiene takes place in the presence of free radical catalysts under autogenous pressure (i.e., about 2 atm) at ambient or slightly elevated temperature. The purpose of lower temperatures is to minimize chain transfer reactions and possibly ring formations⁴ leading to low molecular weight polymers. Under the polymerization conditions, free radical catalysts, which are readily soluble in the monomer, such as (i-PrOCO₂)₂ and CF₃OOCF₃ gave better yields of the white solid resin (40% to quantitative yield under ultraviolet irradiation) than bulk polymerization in the presence of insoluble catalysts such as benzoyl peroxide (only 15–18% conversion).³

Direct fluorination of polyperfluorobutadiene was studied in the absence of catalysts, the series of reactions described in eqs. (1)–(8) is proposed:



The reaction of fluorine molecules with olefinic bonds was reported by Miller and Koch⁵ to produce a fluorinated free radical and a fluorine atom. The advantage of solid polyperfluorobutadiene is that the fluorocarbon radicals thus produced should be fairly stable [eq. (1)]. The high stability of fluorocarbon radicals has been reported by other workers.^{6,7} The fluorine atom and fluorocarbon radicals of step (1) can serve as free-radical initiators [steps (2)–(4)], dimerize [step (5)], saturate [step (6)], or graft [step (7)] and crosslink [step (8)] in the presence of excess monomer.

The purpose of low concentration vapor fluorination of the solid homopolymer is to favor formation of radical sites on the polymer chain than saturation reaction. The electron spin resonance (ESR) spectra of polyperfluorobutadiene (curves 1 and 2 of Fig. 1) show the dependence of radical concentrations to the fluorine pressure after identical length of evacuation. The difference of radical concentrations between curves 2 and 3 of Figure 1 may be explained by possible crosslinking [step (8)] besides graft copolymerization [step (7)].

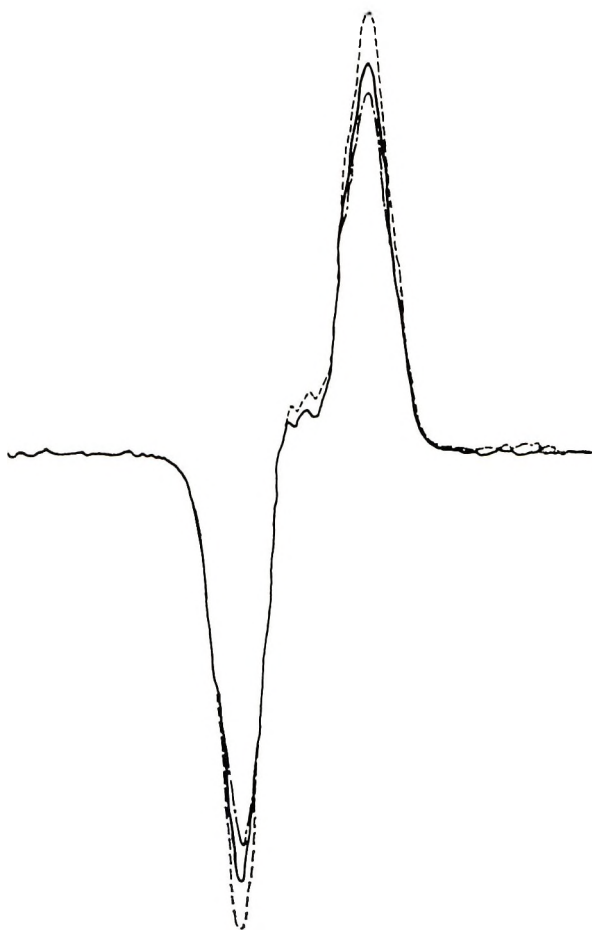


Fig. 1. ESR spectra of fluorine-treated polyperfluorobutadienes (PPFB) and poly tetrafluoroethylene (PTFE) grafted PPFB at ambient temperature: (1) — — —, PPFB treated at $2/3$ atm F_2 ; (2) — — —, PPFB treated at $1/6$ atm F_2 ; (3) - - -, PTFE grafted at $1^{1/3}$ atm TFE pressure onto PPFB pretreated at $1/6$ atm F_2 .

The bulk polymers initiated by $(i\text{-PrOCO}_2)_2$ catalyst could be fluorinated without prior solvent extraction. This was not feasible for the bulk polymers initiated by benzoyl peroxide catalyst due to inflammation during fluorination. Table I describes the fractional solvent extraction of polymer initiated by benzoyl peroxide. The difference is probably because $(i\text{-PrOCO}_2)_2$ is unstable at ambient temperature.⁸ Its volatile decomposition products can easily be removed by evacuation; while excess benzoyl peroxide and its decomposition products remain in the bulk polymer to react vigorously with fluorine. Fluorination reactions also showed that the bulk polymer initiated by CF_3OOCF_3 catalyst could be fluorinated not only without solvent extraction but also at ambient temperature with a higher initial fluorine pressure without burning than $(i\text{-PrOCO}_2)_2$ -initiated

TABLE I
Fractional Extraction of Polyperfluorobutadiene by *n*-Hexane
and Hexafluorobenzene^a

Fraction	Condition of extraction	Method of recovery and drying	Nature of product	T_m , °C ^b	Per cent by weight
<i>n</i> -Hexane-soluble fraction (fraction I _A)	Soxhlet extraction for 4 hr	Precipitation after cooling in refrigerator overnight and drying the solid at 50°C under evacuation	White crystals	105–106	27.6
<i>n</i> -Hexane-soluble fraction (fraction I)		Evaporation of filtrate of fraction I _A to dryness under reduced pressure	White wax	95–98	29.5
Hexafluorobenzene-soluble fraction (fraction II) ^c	Soxhlet extraction for 2 days	Freeze-drying	White powder	138–141	32.6
Hexafluorobenzene-insoluble fraction (fraction III)		Evacuation at 50°C	White solid	159–163	10.1

^a Benzoyl peroxide as initiator.

^b In sealed capillary tube.

^c $[\eta] = 0.018$ in hexafluorobenzene at 30.1°C and molecular weight 3 530 (Rast Method-22 repeating units).

bulk polymers. This suggests that fluorination reactions are very sensitive to impurities in the polymers and to the terminal groups of the polymer chains. The ease of flammability of the bulk polymer during fluorination is dependent upon the initiator used. The flammability of the catalysts decreases in the order: $(C_6H_5COO)_2 > (i\text{-PrOCO}_2)_2 > CF_3OOCF_3$.

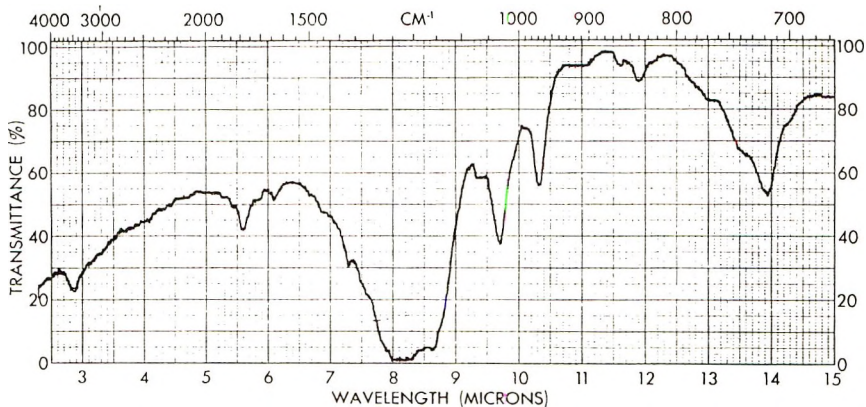
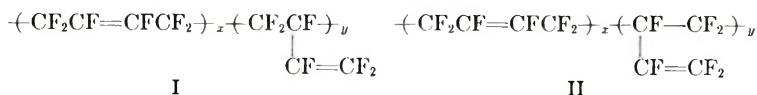


Fig. 2. Infrared spectrum of fluorine-treated polyperfluorobutadiene.

Polyperfluorobutadiene initiated by free radical catalysts is a copolymer of perfluoro-1,2- and -1,4-butadiene as a result of 1,2- and 1,4-addition polymerization.³ The structures are probably atactic mixtures of structures I and II,



with possible head-to-tail and head-to-head arrangements for the 1,2-polymer.

The infrared spectra of the copolymers show very strong broad band between 7.5 and 9.1 μ region for C—F absorption.⁹ The two other characteristic absorption bands at 5.6 μ , indicating perfluorovinyl groups, and at 5.8 μ , indicating —CF=CF— groups,¹ are also present. The 5.8 μ peak disappears before 5.6 μ after fluorination of polyperfluorobutadiene as shown in Figure 2, while the reverse occurs after crosslinking with hexamethylenediamine. This means that the internal double bonds of polyperfluorobutadiene are more susceptible to direct fluorination reaction than its pendant perfluorovinyl groups and *visa versa* for crosslinking with hexamethylenediamine.

The two crosslinking agents, fluorine and hexamethylenediamine, involve different mechanisms. The former, being free-radical type, favors the vinylene bonds (—CF=CF—) while the latter, being ionic type, favors the pendant vinyl bonds (—CF=CF₂) due to increased polarity of the double bonds; that hexamethylenediamine is a more sterically hindered molecule is also a factor.

EXPERIMENTAL

Starting Materials

Perfluorobutadiene was obtained from Peninsular ChemResearch Co. and was shown by Mitsch and Neuvar to be 98–99% pure by vapor-phase chromatography.¹⁰ The commercial monomer showed three groups of lines for its F¹⁹ NMR spectrum as reported by Toy and Lawson,³ and identical vapor infrared spectrum as reported by Weiblen.¹¹

Diisopropyl peroxydicarbonate (mp 8–10°C) was obtained from Pittsburgh Plate Glass Co., and bis(trifluoromethyl)peroxide was obtained from Peninsular ChemResearch Co. The latter showed a vapor infrared spectrum identical to that reported by Porter and Cady.¹² Benzoyl peroxide was obtained from Lucidol. The catalysts and the monomer were used directly without further purification.

Polymer Preparation

The polymerizations of perfluorobutadiene were carried out in bulk under autogenous pressure (i.e., about 1.5 atm) and vigorous magnetic stirring in sealed Pyrex or quartz tubes or pressure bottles (Fischer Porter Aerosol

Compatibility Tube). The catalysts, CF_3OOCF_3 and $(i\text{-PrOCO}_2)_2$, are readily soluble in the monomer, while benzoyl peroxide is insoluble. The yields ranged from 40% to almost quantitative when the polymerization was carried out in the quartz pressure bottle under ultraviolet irradiation with CF_3OOCF_3 catalyst (3–5% catalyst concentration) at ambient temperature for one month. The yields were 40–70% with $(i\text{-PrOCO}_2)_2$ and 20% with benzoyl peroxide (without irradiation). The white resins were dried at 50°C under reduced pressure for 24 hr.

Compatibility of Bulk Polymers with Fluorine

The bulk polymers, 0.5 g, prepared by $(i\text{-PrOCO}_2)_2$, CF_3OOCF_3 , and $(\text{C}_6\text{H}_5\text{COO})_2$ as catalysts were partially dissolved and partially suspended in hexafluorobenzene and freeze-dried separately in borosilicate glass tubes with $1/4$ -in. necks, which were connected to a stainless-steel vacuum line by a Swagelok fitting. The stainless-steel manifold for handling fluorine was similar to the one previously described.^{13,14} The freeze-dried bulk polymer was evacuated at 50–60°C for 1 hr and cooled to –80°C. Gaseous fluorine, which was passed through a sodium fluoride scrubber to remove the trace amount of hydrogen fluoride impurity, was introduced slowly into the reaction tube to $1/3$ atm at –80°C and warmed gradually to ambient temperature. The benzoyl peroxide-initiated bulk polymer was burnt. When gaseous fluorine was initially introduced at 1 atm and ambient temperature, $(i\text{-PrOCO}_2)_2$ -initiated bulk polymer, which survived the previous initial fluorination temperature and pressure treatment, was burnt. Only CF_3OOCF_3 -initiated bulk polymer was compatible to initial fluorination at 1 atm fluorine pressure and ambient temperature.

Polyperfluorobutadiene Radicals

Polyperfluorobutadiene radicals were measured by freeze-drying a series of four ESR tubes containing the same suspension of CF_3OOCF_3 -initiated bulk polymer in hexafluorobenzene. The freeze-dried bulk polymers in ESR tubes were evacuated at 50–60°C for 1 hr and vacuum sealed; the first tube of starting material gave no signals. Figure 1 shows the ESR spectra of polyperfluorobutadienes which were exposed to $2/3$ and $1/6$ atm of fluorine pressures at ambient temperature for 5 min, evacuated for $1/2$ hr, and vacuum sealed. Another ESR tube of polyperfluorobutadiene identically fluorinated at $1/6$ atm and evacuated was exposed to $1 1/3$ atm of tetrafluoroethylene (Thiokol Chemical; a silica gel column was used to remove terpene inhibitor) monomer pressure for 20 min at ambient temperature and was then evacuated for $1/2$ hr and vacuum-sealed (Fig. 1, curve 3).

Polymer Fractionation

Fractionation into three polymeric fractions (see Table I) was carried out for polyperfluorobutadiene initiated by benzoyl peroxide. The sol-

vents employed for fractional extractions were *n*-hexane and hexafluorobenzene. The bulk polymer (8.6 g) was extracted first by 50 ml of *n*-hexane in a Soxhlet apparatus for 4 hr. The *n*-hexane-soluble fraction was cooled in the refrigerator overnight. The white crystalline precipitate was filtered and dried and weighed 2.38 g, mp 105–106°C (fraction I_A in Table I). The filtrate of Fraction I_A was evacuated to dryness to give 2.54 g of white wax, mp 95–98°C (fraction I in Table I). The *n*-hexane-insoluble residue was extracted by hexafluorobenzene in a Soxhlet apparatus for 4 days and freeze-dried to give 2.81 g of white powder, mp 138–141°C (fraction II in Table I). The hexafluorobenzene-insoluble residue was dried at 50°C under reduced pressure to 0.87 g of white solid, mp 159–163°C (fraction III in Table I).

Crosslinking by Direct Fluorination

The polyperfluorobutadiene used for this study was the hexafluorobenzene-soluble fraction (fraction II of Table I). The homopolymer (0.10 g, $[\eta] = 0.018$ dl/g in hexafluorobenzene at 30.1°C, molecular weight 3530) was weighed into a Pyrex reaction tube (3¹/₂ in. × 1/2 in. OD with a 1/4 in. OD neck), and connected to a stainless steel vacuum manifold by a Swagelok fitting. The sample was evacuated at 65°C for 1 hr and was cooled to –80°C. Gaseous fluorine, which had been passed through a sodium fluoride scrubber to remove the trace amount of hydrogen fluoride impurity, was introduced slowly into the reaction tube to 1/3 atm at –80°C and evacuated at –20°C for 10 min, before warming to ambient temperature. The monomer (0.91 g) was then condensed into the partially fluorinated polyperfluorobutadiene tube and sealed under vacuum. The sealed polymerization tube was placed in a 60°C bath for three weeks. The unpolymerized monomer was transferred to another tube. The residue was evacuated at ambient temperature for 1 hr to give 0.18 g of white resin; it was insoluble in hexafluorobenzene, concentrated sulfuric acid, concentrated ammonium hydroxide, dimethyl sulfoxide, dimethylformamide, and 3 M Brand Fluorochemicals FC-43 and FC-75. These solvents were tested at both ambient and boiling temperatures.

The above procedure was followed for another sample of the hexafluorobenzene-soluble fraction, except that gaseous fluorine was not evacuated at 1/3 atm but gradually increased to 1 atm for 1 day at ambient temperature, and 2 atm of fluorine at 125°C for 1 day, and, finally, 2 atm of fluorine at 150°C for 4 hr. The gaseous phase was evacuated at room temperature. The white resin was washed with water and hexafluorobenzene and dried. It is insoluble in concentrated sulfuric acid, concentrated ammonium hydroxide, dimethyl sulfoxide, hexafluorobenzene, dimethylformamide, and chloroform at ambient and boiling temperatures. The infrared spectrum shows the disappearance of the 5.8 μ peak (Fig. 2).

ANAL. Calcd. for $(C_4F_6)_n$: C, 29.63%; F, 60.37%; calcd. for $(C_4F_8)_n$: C, 24.00%; F, 76.00%. Found: C, 24.37%; F, 74.98%.

Crosslinking by Diamine

Polyperfluorobutadiene (fraction II of Table I; 0.50 g) was dissolved in 7.0 ml of hexafluorobenzene. Hexamethylenediamine (0.18 g) was added slowly with stirring. The solid was collected, washed with distilled water and dried at 50°C under reduced pressure to give 0.56 g of yellow resin, mp > 310°C (dec).

ANAL. Calcd for $C_{30}F_{36}H_{16}N_2$: C, 33.11%; F, 62.84%; H, 1.48%; N, 2.57%. Found: C, 34.36%; F, 61.89%; H, 1.18%; N, 2.03%. (This corresponds to six repeating units of polyperfluorobutadiene per one mole of hexamethylenediamine.)

The yellow resin was insoluble in hexafluorobenzene, concentrated sulfuric acid, concentrated ammonium hydroxide, dimethyl sulfoxide and 3M Brand Fluorochemicals FC-43 and FC-75 at ambient and boiling temperatures. The infrared spectrum of the yellow resin shows the disappearance of the peak at 5.6 μ .

The authors gratefully acknowledge the support of NASA-Jet Propulsion Laboratory and Mr. J. D. Ingham as technical monitor. We are indebted to Mr. D. D. Lawson for helpful suggestions and to Dr. D. Stamirus for electron spin resonance spectra.

References

1. J. E. Fearn, D. W. Brown, and L. A. Wall, *J. Polym. Sci.*, **4**, 131 (1966).
2. W. T. Miller, *Preparation, Properties and Technology of Fluorine and Organic Fluoro Compounds*, ed. by C. Slesser and S. R. Schram, McGraw-Hill, N.Y., 1951, pp. 624-626 and p. 587.
3. M. S. Toy and D. D. Lawson, *J. Polym. Sci., Part B*, **6**, 639 (1968).
4. H. C. Brown, *J. Org. Chem.*, **22**, 1256 (1957).
5. W. T. Miller and S. D. Koch, *J. Am. Chem. Soc.*, **79**, 3084 (1957).
6. L. A. Wall and R. E. Florin, *J. Appl. Polym. Sci.*, **2**, 251 (1959).
7. M. S. Toy, *J. Electrochem. Soc.*, **114**, 1042 (1967).
8. F. Strain, U.S. Patent 2,464,062, March, 1949.
9. L. J. Bellamy, *The Infrared Spectra of Complex Molecules*, 2nd ed., John Wiley, N.Y., 1958, p. 30.
10. R. A. Mitsch and E. W. Neuvar, *J. Phys. Chem.*, **70**, 546 (1966).
11. D. G. Weiblen, *Fluorine Chemistry*, Vol. 2, ed. by J. H. Simons, Academic Press, N.Y., 1954, p. 478.
12. R. S. Porter and G. H. Cady, *J. Am. Chem. Soc.*, **79**, 5628 (1957).
13. M. S. Toy and W. A. Cannon, *J. Electrochem. Soc.*, **114**, 940 (1967).
14. M. S. Toy and W. A. Cannon, *J. Phys. Chem.*, **70**, 2241 (1966).

Received February 18, 1969

Revised February 18, 1969

Methyl Methacrylate Polymerization Initiated by Triethylborane-Peroxide Mixtures

I. CONTRERAS, J. GROTEWOLD, E. A. LISSI, and R. ROZAS,
*Laboratorio Central de Quimica, Universidad Tecnica del Estado,
Santiago, Chile*

Synopsis

The polymerization of methyl methacrylate initiated by triethylborane or triethylborane-peroxide mixtures was studied. The rate of initiation by a mixture of triethylborane and *tert*-butyl peroxide was found to be first-order in peroxide. The order in triethylborane changes from one at low triethylborane/peroxide to nearly zero at high triethylborane/peroxide. The possibility of a mechanism involving a fast reaction followed by a slow reaction that would initiate the polymerization is discussed.

In spite of the great number of investigations in which alkylboron compounds were used as initiators of vinyl polymerization,¹⁻⁷ most of the main features of the mechanism involved have not yet been solved.

Among the points not completely elucidated can be mentioned: (a) the mechanism of the polymerization by alkyl boron compounds in the absence of air (if polymerization under these conditions does occur at all^{1,2,5,8-12}); (b) the mechanism of the polymerization by alkyl boron compounds in the presence of oxygen;^{1,2,13} and, related to this point, (c) the polymerization by mixtures of peroxides or hydroperoxides and trialkyl boron compounds.¹⁴⁻¹⁶

The present work was aimed towards gathering information about points (a) and (c) of the foregoing discussion.

EXPERIMENTAL

Experimental conditions were similar to those described in a previous paper.¹⁷ Commercial methyl methacrylate (99.8% pure) was washed with sodium hydroxide and distilled water. After being dried with calcium chloride, 4 cc monomer was thoroughly degassed and then vacuum-distilled into a container attached to a conventional high-vacuum apparatus.

Triethylborane (an Ethyl Corporation product), stored under high vacuum conditions, was added to the monomer after having been measured by vaporizing a certain amount into a known volume and reading the corresponding pressure.

Benzoyl peroxide was weighed and introduced into the reaction tube prior to its being joined to the vacuum line.

tert-Butyl peroxide was mixed with the monomer prior to its degassing.

The reaction tubes, about 7 cc in volume, were then sealed under high vacuum and placed in a thermostat. After the reaction had taken place, the reaction tubes were cooled down, broken off, and the mixture poured into a beaker containing 45 cc of methanol. The solid precipitate was filtered, washed, and dried to constant weight.

The ultraviolet analyses were carried out with a Hilger-Watts spectrometer; the cells were charged and sealed under high vacuum conditions.

RESULTS AND DISCUSSION

Initiation by Triethylborane in the Absence of Oxygen

Some results obtained with mixtures of triethylborane and methyl methacrylate are presented in Table I.

Several features of this table can be pointed out: (1) a small amount of polymerization at zero time, $t = 0$; (2) the small dependence of $(\%)_t - (\%)_{t=0}/t$ on the triethylborane concentration; (3) the high dispersion of the data; and (4) a noticeable increase in conversion with temperature.

The polymerization at zero time, $(\%)_{t=0}$, was not observed by Hansen¹ and can be due to several factors (residual air, impurities in the monomer or polymerization in the quenching mixture). The obtained results do not

TABLE I

Temp. °C	[TEB] × 10 ² , mole/l.	Time, min.	Conversion, %	v , (%c)/hr ^a
0	3.09	5	0.23	—
0	3.09	2730	0.82	0.015
0	6.29	2680	0.59	0.01
19	0	13080	4.03	0.02
19	1.82	60	0.42	—
19	2.12	30	0.40	—
19	2.12	60	0.42	—
19	6.17	5	0.52	—
19	6.17	5	0.44	—
19	6.17	780	0.85	0.03
35	3.27	40	0.28	—
35	3.39	120	1.19	0.44
35	6.35	120	0.63	0.17
50	0	120	0.90	0.45
50	0	120	0.96	0.48
50	3.03	5	0.49	—
50	3.03	5	0.23	—
50	3.03	60	1.32	0.97
50	3.03	120	2.13	0.89
50	6.17	5	0.59	—
50	6.17	30	1.07	0.96
50	6.17	120	4.04	1.72

^a Rate of polymerization obtained from $v = (\%)_c/t$, where $(\%)_c = (\%)_t - (\%)_{t=0}$ where $(\%)_t$ represents conversion at time t .

allow a differentiation of these effects, but the important point is that this amount of polymerization is small and fairly reproducible, allowing us to apply a correction to the following results.

The high dispersion of the data can be related to the small amounts measured, to traces of residual air, or to traces of peroxides in the monomer. The increase in conversion with temperature rules out that all the polymerization is arising from residual air or impurities in the quenching mixture.

At a given triethylborane concentration, plots of percentage of polymerization against time gave very small slopes, with no clear trend with triethylborane concentration. It is then very difficult to try to interpret the polymerization mechanism that is operative under these conditions, and even to establish conclusively if the triethylborane has any influence at all. Nevertheless, it must be noted that blank runs without triethylborane gave the smallest amounts of polymer (see Table I). We can thus conclude that the polymerization by triethylborane in the absence of oxygen is a very slow process, and that for all practical purposes it can be disregarded. This is in agreement with recent work in similar systems.¹²

Initiation by Triethylborane-Peroxide Mixtures

Results obtained when methyl methacrylate was polymerized in the presence of mixtures of triethylborane and peroxides are given in Figures 1-3 and in Table II.

Figure 1 shows the percentage of polymerization plotted against time for mixtures of peroxides and triethylborane.

TABLE II

Temperature, °C	Peroxide		[TEB], mole/l.	Time, min	Con- version (%) _c , %	<i>v</i> (P + TEB), %/hr
	Type	Concn., mole/l.				
20	Benzoyl peroxide	0.050	0.066	15	0.8	1.68
				15	0.6	0.93
				40	1.3	1.28
				60	1.94	1.45
				60	2.35	1.90
				95	1.66	0.54
				100	2.19	0.89
				135	2.88	0.94
				360	13.4	2.08
50	<i>tert</i> -Butyl peroxide	0.062	0.034	60	3.2	3.08
				60	4.1	4.02
				135	9.7	4.35
				60	6.0	5.73
		0.063	60	5.5	5.18	
			100	10.3	5.95	
			120	10.9	5.10	

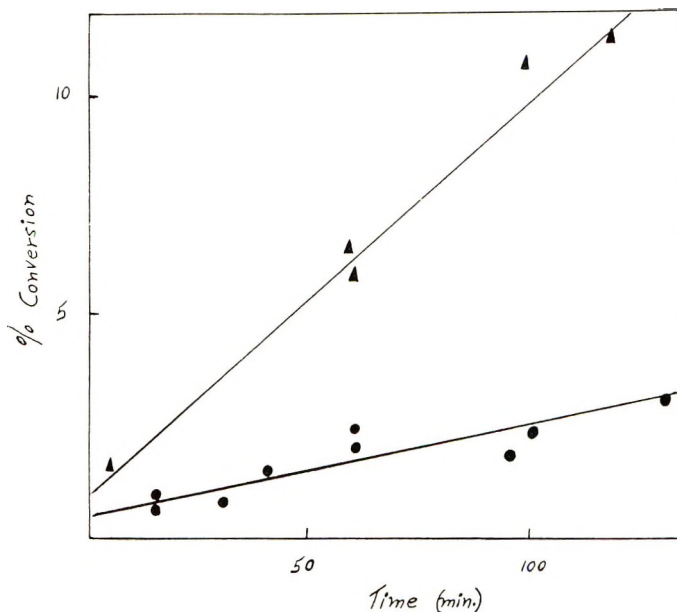


Fig. 1. Plot of percentage conversion against time in minutes for mixtures of triethylborane and peroxides: (▲) [TEB] = 0.063 mole/l., [*tert*-butyl peroxide] = 0.062 mole/l. 50°C; (●) [TEB] = 0.066 mole/l., [benzoyl peroxide] = 0.050 mole/l. 20°C.

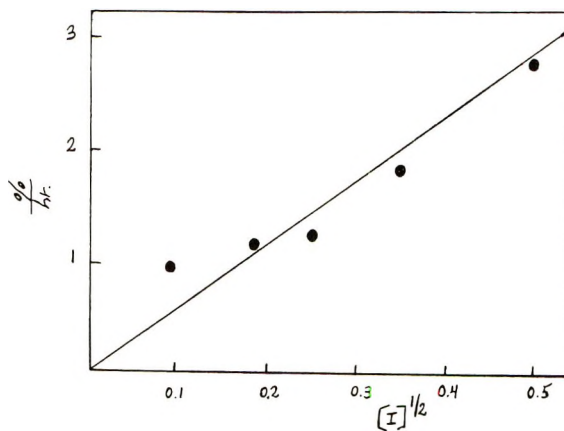


Fig. 2. Dependence of $v_{(P+TEB)}$ on *tert*-butyl peroxide concentration. [TEB] = 0.063 mole/l., 35°C.

Table II shows values of $v(P + TEB)$ at several reaction times. In Table II, $v(P + TEB)$ is the rate of polymerization that can be attributed to an initiation that involves both initiators, the peroxide (P) and the triethylborane (TEB). The values of $v(P + TEB)$ were deduced as follows: the rate of polymerization v can be obtained from

$$v = (\%_0)_c/t$$

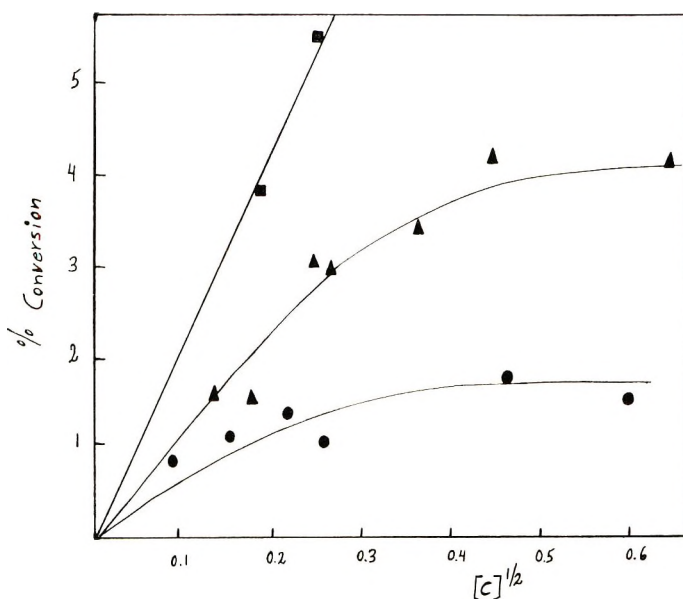
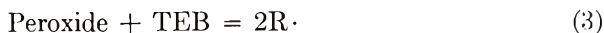


Fig. 3. Dependence of $v_{(P+TEB)}$ on TEB concentration: (■) [*tert*-butyl peroxide] = 0.062 mole/l., 50°C; (▲) [*tert*-butyl peroxide] = 0.062 mole/l., 35°C, (●) [benzoyl peroxide] = 0.050 mole/l., 20°C.

where

$$(\%)_c = (\%)_t - (\%)_{t=0}$$

In mixtures of peroxide and triethylborane, and if a free radical polymerization is assumed in every case, the following initiations can be postulated:



where reaction (1) is the well known decomposition of the peroxide and reaction (2) comprises all the initiations operative when only TEB is employed. Reaction (3) can be assumed to be of the form

$$v_3 = k_3 [\text{TEB}]^x [\text{P}]^y \quad (4)$$

With these initiations

$$v = k_1[\text{P}] + v_2 + k_3[\text{TEB}]^x[\text{P}]^y \quad (5)$$

where

$$A = 100(k_p/k_t^{1/2}) \quad (6)$$

and k_p and k_t are the rate constants for propagation and termination, respectively.

Then

$$v(\text{P}+\text{TEB}) = k_3^{1/2} A [\text{TEB}]^{x/2} [\text{P}]^{y/2} \quad (7)$$

can be obtained from eq. (8)

$$v(\text{P}+\text{TEB}) = (v^2 - v_P^2 - v_2^2)^{1/2} \quad (8)$$

where v_P is the rate of polymerization when only peroxide and monomer are present. From 12 runs carried out at 20°, a mean value of $v_P = 0.63\%$ /hr was obtained for benzoyl peroxide (peroxide concentration = 0.05 mole/l.). For *tert*-butyl peroxide, v_P was practically zero over the entire temperature range investigated (0–50°C).

Values of v_2 were obtained from the slopes of plots of percentage polymerization against time when only triethylborane was employed. This correction, a minor one, amounts to no more than 15% under the most critical conditions.

In Table II, typical values of $v(\text{P}+\text{TEB})$ are given. From then it can be concluded that, in spite of the high dispersion, they show no time dependency. This finding is in disagreement with previous results^{2,13} obtained with mixtures of trialkyl boranes and boron peroxides. The discrepancy can probably be related to the better definition of the reactants under our present conditions.

Order of Reaction (3)

Figure 2 shows a plot of $v(\text{P}+\text{TEB})$ against $[\text{P}]^{1/2}$ for runs employing *tert*-butyl peroxide. It can be seen from this plot that a reasonably straight line can be drawn through the experimental points. This implies that $y = 1$, in agreement with previous results.^{1, 14}

Figure 3 shows the dependence of $v(\text{P}+\text{TEB})$ with $[\text{TEB}]^{1/2}$. It can be observed that results with both peroxides show a similar pattern: a linear dependence with $[\text{TEB}]^{1/2}$ might be assumed at low $[\text{TEB}]$, but a clear curvature is observed at higher concentrations. This unexpected result is in line with Hansen's findings¹ and results obtained in similar systems.^{13,15,16} No clear explanation for this curvature has yet been given, and the effect is being further investigated in this laboratory.

Dependence of k_3 with Temperature

From the previous discussion it can be concluded that at low TEB/P, v_3 can be represented by eq. (9)

$$v_3 = k_3[\text{TEB}][\text{P}] \quad (9)$$

in agreement with results obtained¹⁴ in the polymerization of methyl methacrylate initiated by mixtures of Bu_3B and Bu_2BOOBu .

Values of $k_{(\text{P}+\text{TEB})}$ for *tert*-butyl peroxide were obtained at several temperatures from average values of $v(\text{P} + \text{TEB})$ for at least two triethylborane concentrations and at low TEB/P. These values were plotted in

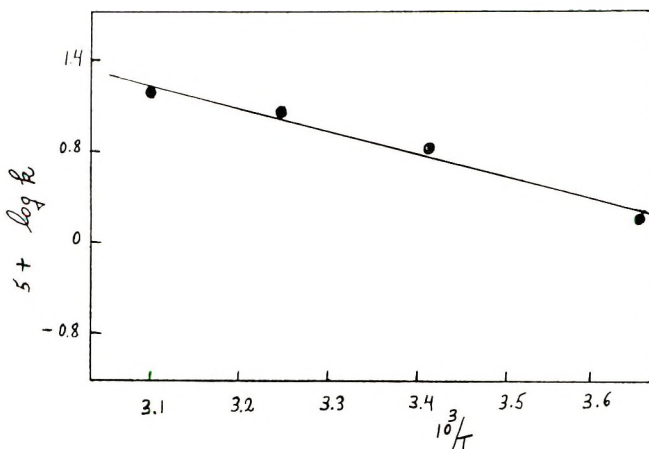


Fig. 4. Arrhenius plot for $k_{(P+TEB)}$ for runs with *tert*-butyl peroxide.

Arrhenius' plots. From this plot (shown in Figure 4), an activation energy of 10.0 kcal/mole can be obtained.

A summary of the experimental data found in the present work is given in Table III, together with previous results obtained in similar systems.

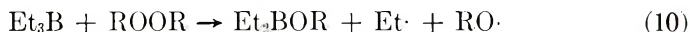
TABLE III^a

Peroxide	$k_{(P+TEB)} \times 10^5$, l./mole-sec	$E_{\text{activation}}$, kcal/mole	Solvent	Ref.
Benzoyl	8.0	—	None	This work
<i>tert</i> -Butyl	5.8	10.0	None	This work
Bu ₂ BOOBu	72	12.9	Benzene	14

^a Temperature: 20°C.

Mechanism of Reaction (3)

From the foregoing discussion, reaction (3) could be replaced by reaction (10)



where Et_3B can be stabilized by association with molecules of the monomer. This reaction is similar to that proposed¹⁸ for the reaction of triethylborane with Et_2BOOEt .

The low values of $k_{(P+TEB)}$ found in the present work mean either that (a) reaction (10), which would produce the free radicals, is very slow, or (b) there is a fast reaction between the peroxide and the triethylborane (that does not produce high molecular weight polymer), and afterwards the product of this reaction is able to initiate a very slow polymerization.

Previous work in which a fast reaction between R_3B and peroxides or hydroperoxides has been mentioned^{16,18-20} can be considered to lend support

to the second mechanism. We tried to follow the reaction between the triethylborane and benzoyl peroxide spectroscopically with the use of chloroform as solvent. Even with excess triethylborane, the absorption band of benzoyl peroxide at about 2850 \AA was observed after more than 6 weeks. This supports mechanism (a) (unless a new substance with an absorption band in the same region were being formed).

We tried to follow the reaction between *tert*-butyl peroxide and triethylborane in the gas phase and in cyclohexane solution. In the first case, *tert*-butyl peroxide and triethylborane were mixed in an infrared cell. After 3 hr at room temperature, the spectrum was identical to that of a mixture of triethylborane and peroxide. No new peaks were registered and no change in the reactant peaks could be detected. Furthermore, after more than 24 hr at room temperature, no change in pressure could be detected.

When TEB and *tert*-butyl peroxide were mixed in cyclohexane in the presence of iodine under high vacuum conditions, no iodine consumption could be detected after more than two weeks at room temperature. This indicates that no ethyl radicals are produced in the system.

The lack of reactivity of *tert*-butyl peroxide towards trialkyl boron compounds is further confirmed by the work of Davies and co-workers,²¹ who found that the peroxide stabilizes tributylborane.

We consider then that, with the available information, the initiation of methyl methacrylate polymerization by mixtures of TEB and organic peroxides can be ascribed to a reaction that can be represented by eq. (10). Nevertheless, the low value of the energy of activation given in Table III cannot easily be related to a slow bimolecular initiation. Furthermore, no satisfactory explanation can be given for the quasi-independence of the rate on triethylborane concentration found in this and previous work when the TEB/peroxide ratio is higher than 1.

Thanks are given to Forge for financial support.

References

1. R. L. Hansen, *J. Polym. Sci. A*, **2**, 4215 (1964).
2. F. J. Welch, *J. Polym. Sci.*, **61**, 243 (1962).
3. J. Furakawa, T. Tsuruta, and S. Inone, *J. Polym. Sci.*, **26**, 234 (1957).
4. N. Ashikari, *J. Polym. Sci.*, **28**, 641 (1958).
5. J. Furakawa and T. Tsuruta, *J. Polym. Sci.*, **28**, 227 (1958).
6. J. W. Fordham and C. L. Sturm, *J. Polym. Sci.*, **33**, 504 (1958).
7. N. L. Zutty and F. J. Welch, *J. Polym. Sci.*, **43**, 445 (1960).
8. R. D. Burkhalt and N. L. Zutty, *J. Polym. Sci. A*, **1**, 1137 (1963).
9. F. S. Arimoto, *J. Polym. Sci. A-1*, **4**, 275 (1966).
10. G. S. Lolesnikow and N. V. Klimentova, *J. Polym. Sci.*, **39**, 560 (1959).
11. S. Inone, T. Tsuruta, and J. Furakawa, *Makromol. Chem.*, **40**, 13 (1961).
12. M. Bednarek, M. Kolinsky, and D. Lim, *Czechoslovak. Chem. Comm.*, **32**, 1575 (1967).
13. G. Borsini and M. Cipolla, *J. Polym. Sci. B*, **2**, 291 (1964).
14. C. E. H. Bawn, D. Margerison, and N. M. Richardson, *Proc. Chem. Soc.*, **1959**, 397.

15. A. Misono, Y. Uchida, and K. Yamada, *Bull. Chem. Soc. Japan*, **39**, 2458 (1966).
16. K. Noro, H. Kawazura, and E. Uemura, *Kogyo Kagaku Zasshi*, **65**, 973 (1962).
17. J. Grotewold, E. A. Lissi, and A. Villa, *J. Polym. Sci. A-1*, **6**, 3157 (1968).
18. R. L. Hansen and R. R. Hamann, *J. Phys. Chem.*, **67**, 2868 (1963).
19. J. R. Johnson and M. G. Van Campen, *J. Amer. Chem. Soc.*, **60**, 121 (1938).
20. J. Furakawa, T. Tsuruta, and S. Shiotani, *J. Polym. Sci.*, **40**, 237 (1959).
21. A. G. Davies, D. G. Hare, and O. R. Khan, *J. Chem. Soc.*, **1963**, 1125.

Received October 30, 1968

Revised February 19, 1969

Production of Organometallic Polymers by the Interfacial Technique. I. Interfacial Production of Polyalkyloxysilanes and a Study of Some Reaction Variables

CHARLES E. CARRAHER, JR., *Chemistry Department, University of South Dakota, Vermillion, South Dakota 57069*

Synopsis

The first interfacial synthesis of polyalkyloxysilanes of the form —O—Si—O—R'—

$$\begin{array}{c} \text{R} \\ | \\ \text{—O—Si—O—R'—} \\ | \\ \text{R''} \end{array}$$

where R' = alkylene, and R'' , R = alkyl or aryl is reported. It is found, in the range studied for the stirred systems, that as organic solvent viscosity and organic phase volume are increased, rate of polymer formation is decreased. Little difference in polymer formation rate is observed when the nature of the diol is varied, but considerable difference is noted when the nature of the organosilane is varied such that the most electropositive silane has the highest rate of polymer formation. Molecular weight is approximately constant as diol is changed but varies markedly when the silane is changed, so that the silane with the most bulky substance will give polymer with the lowest molecular weight.

INTRODUCTION

Little work has been reported on the production of organometallic polymers by the interfacial technique. Iskenderov et al. in 1965 reported¹ the first interfacial production of silicon-containing polymers by reacting sodium terephthalate in water with diethyldichlorosilane in benzene at room temperature. Migdal et al.²⁻⁴ in 1968 reported the production of low molecular weight tin polyesters from the reaction of dialkyl(aryl)dichlorotin or tetraalkyl(aryl) dichlorotin in an organic solvent with the sodium salt of bis[*o*-(carboxymethyl)phenyl]- or bis[*p*-(carboxymethyl)phenyl]dimethylsilanes.

Only recently has much work been done on the production of polyaryl-

(alkyl)oxysilanes of the general formula —Si—O—R'—O— , where R , R'' ,

$$\begin{array}{c} \text{R} \\ | \\ \text{—Si—O—R'—O—} \\ | \\ \text{R''} \end{array}$$

are alkyl or aryl groups and R' is an alkylene group.

Krimm and Schnell⁵ prepared a resin with the above repeating structure, using the solution technique by combining equivalents of 2,2-bis(4-hydroxyphenyl)propane and dimethyldichlorosilane in a benzene-pyridine solution. In pyridine alone Goldberg and Powers⁶ obtained only oligomeric material.

Morgunova et al.⁷ prepared such structures by the reaction of cyclosilazanes with diols. For example, polymer was obtained when hexamethylcyclotrisilazane or octamethylcyclotetrasilazane was treated with ethylene glycol. Similar ring-opening processes are believed to occur with aromatic diols.⁸ Andrianov et al.,⁹ in the attempted solution polymerization of diphenyldichlorosilane and resorcinol, obtained only cyclic dimers and trimers.

MacFarland and Yankura¹⁰ reported the preparation of a polymer with the above structure by two methods. One was by an alcoholysis-type condensation of $R_2Si(OC_2H_5)_2$ with aromatic diols. The second was the condensation of dialkyl(aryl)dichlorosilanes with aromatic diols.^{10,11}

Curry, Byrd, and co-workers¹²⁻¹⁵ reported the preparation of polymers with the above structure from the melt condensation of diols with bis-(anilino)diaryl(alkyl)silanes. They reported the production of high molecular weight products, some being stable to 600°C for short periods of time.¹² Polymers with such a structure may present an alternative to the synthesis of thermally stable ladder, ring, and network polymers with backbones which are largely or wholly carbon. Also fibers may be drawn directly and continuously from some polymer melts; some polymers form a hard protective coating on metals¹² while others form films.¹³ Thus polymers with the above structure possess potentially usable properties.

There has been no reported polymer synthesis of polymers with the above structure by the interfacial technique.

EXPERIMENTAL

Unstirred Interfacial Systems

Unstirred polymerizations were carried out by adding a known amount of diol, and (where used) base to a 150-ml beaker. The organic phase, containing organic solvent and a given amount of the organosilicon reactant, was added to the beaker. A watch glass was placed over the beaker and the beaker set aside for the reaction time.

Stirred Interfacial Systems

Stirred polymerizations were carried out in a 1-pt Kimax emulsifying mill jar which was placed on a Waring Blendor (Model 1001 Series 724) with a listed rotor speed of 15000 rpm. The jar was vented by placing a glass tube, inserted in a cork, in the jar cap. A known amount of diol and (where used) base was added to the reaction jar. The organic phase, containing a known amount of organosilicon reactant, was added to the jar. The lid was screwed on and the blender motor run for a specified time.

Polymer Recovery

Polymer separates from the liquid phases as a tacky, coherent mass, and was separated from the liquid phase by use of suction filtration. The polymer is white to yellow-tan and can be drawn to give fibers. The polymer was washed with ice water and the solid dissolved in acetone. The acetone solution was filtered by means of gravity onto a preweighted watch glass. The acetone was evaporated off by means of a steam bath and the solid residue weighed. The recovered polymer was clear to brown and was a highly viscous liquid to a glassy solid.

Physical Determinations

Infrared spectra were obtained on KBr pellets by use of a Beckman IR-10 instrument. The spectra were consistent with a polyalkyloxysilane repeating unit. Viscometry was carried out in acetone at 30°C by use of a Cannon-Ubbelohde 50 viscometer. Melting ranges obtained on a Fisher-Johns melting point apparatus at a heating rate of 2°C/min were taken to be the range between the beginning of melting to the point at which melting was complete.

RESULTS

It is found that as the volume of the organic phase is increased, rate of polymer formation (yield at constant time) decreases and polymer viscosity remains constant (Table I).

In the stirred systems, as organic solvent viscosity decreases, the rate of polymer production increases and molecular weight remains approximately constant (Table II), while in the unstirred systems there is no direct relationship between rate and solvent viscosity or organic solvent dielectric constant. Polymer viscosity remains essentially constant (Table II).

In the stirred interfacial systems no polymer was formed in the absence of base (Table III). In the stirred systems employing carbon tetrachloride as the organic solvent polymer was formed, whereas in cyclohexane no polymer was formed (Table III). It is further noted that the material

TABLE I
Variation of Polymer Yield and Molecular Weight
with Variation of Volume of the Organic Phase (*n*-Pentane)^a

Volume <i>n</i> -pentane, ml	Yield, %	Limiting viscosity number (LVN), ml/g
20	69	6
50	46	6
100	40	6
150	35	6

^a At 25°C, 0.018*M* diphenyldichlorosilane, 0.030*M* sodium hydroxide, 0.090*M* ethylene glycol, 3 min stirring time.

TABLE II
Variation of Polymer Yield and Molecular Weight with Variation of the Nature of the Organic Phase^a

Organic solvent	Viscosity (100) at 20 ± °C ^b	Dielectric constant (20°C) ^c	Unstirred		Stirred		Solubility of ethylene glycol in organic solvent, g/100 ml
			Yield, %	LVN, ml/g	Yield, %	LVN, ml/g	
Cyclohexane	0.960	2.05	96	6	5	9	0.7
Carbon tetrachloride	0.952	2.24	61	7	8	8	0.0
Toluene	0.590	2.39	13	7	13	9	0.0
<i>n</i> -Heptane	0.403	1.97	80	5	41	41	0.0
<i>n</i> -Pentane	0.235	1.83			46	6	0.0

^a At 25°C, 0.018*M* diphenyldichlorosilane, 0.030*M* sodium hydroxide, 0.090*M* ethylene glycol, 50 ml organic solvent, and 3 min stirring time for stirred systems and 1 week setting period for unstirred systems.

^b Data of *International Critical Tables*.^{16a}

^c Data of *International Critical Tables*.^{16b}

TABLE III
Variation of Polymer Yield and Viscosity with and without Added Base^a

NaOH, <i>M</i>	Reaction time	Organic solvent	Yield, %	LVN, ml/g	System type
0.030	1 week	Cyclohexane	96	6	Unstirred
0.000	1 week	Cyclohexane	96	3	Unstirred
0.030	1 week	CCl ₄	61	7	Unstirred
0.000	1 week	CCl ₄	0		Unstirred
0.030	3 min	Cyclohexane	5	9	Stirred
0.000	3 min	Cyclohexane	0		Stirred
0.000	7 min	Cyclohexane	0		Stirred
0.000	15 min	Cyclohexane	0		Stirred
0.030	3 min	CCl ₄	8	8	Stirred
0.000	3 min	CCl ₄	0		Stirred

^a At 25°C, 0.018*M* diphenyldichlorosilane, 0.090*M* ethylene glycol, and 50 ml organic solvent.

obtained in the absence of base is of relatively lower molecular weight than that produced in systems where base is present.

Table IV shows the yield and viscometry results when the nature of the two reactants is varied. Both yield and molecular weight remain essentially constant as the diol is changed but vary markedly when the nature of the silane is changed.

TABLE IV
Variation of Polymer Yield and Viscosity with Varying Reactants^a

Organosilane	Diol	% Yield	LVN, ml/g	Melting range °C
Diphenyldichlorosilane	Ethylene glycol	46	6	71-93
Diphenyldichlorosilane	2-Butene-1,4-diol	54	7	175-193
Diphenyldichlorosilane	1,3-Propanediol	51	7	67-75
Dimethyldichlorosilane	Ethylene glycol	10	20	291-312
Methylphenyldichlorosilane	Ethylene glycol	15	12	214-235

^a At 25°C, 0.018*M* organosilane, 0.030*M* sodium hydroxide, 0.090*M* diol, 50 ml *n*-pentane, and 3 min stirring time.

DISCUSSION

Interfacial systems generally consist of an organic phase with a water-sensitive reactant such as an acid chloride and an aqueous phase with a reactant such as a diol. In the presence of water, competition is such that inclusion of diol is not accomplished, resulting in a polymer containing a repeating backbone unit of (—Si—O—) but not the desired product. Thus a nonwater system was used where diol acted not only as a reactant but also as an "aqueous solvent" in forming an interface with the organic solvent permitting polymer formation at the interface.

The interfacial method, compared to previous methods employed in the synthesis of polyalkyl(aryl)oxysilanes, offers in general the following advantages: (a) use of commercially available reactants, (b) possible use of or production of thermally unstable compounds, since interfacial synthesis can take place at or below room temperature and (c) rapid production of polymer by use of simple equipment and procedure. The major disadvantage with the modified interfacial system used in this study is that it is limited to using diols which are liquid or which have low enough melting points so that the temperature of the interfacial system can be raised above the melting point of the diol.

In the stirred interfacial systems, over the range studied, the polymerization rate increases as the viscosity of the organic solvent decreases. Also, for the experimental range, as volume of organic solvent increased, polymerization rate decreased. These trends could be expected in diffusion-controlled reactions, but as shown by Carraher,¹⁷ the rate constant for the reaction in cyclohexane is of the order of 10^{-4} l.^{2/3}/mole^{2/3}-sec or about a power of 10^{10} smaller than normally found for diffusion-controlled reactions. A possible answer may be that the reaction occurs in certain steps with initial migration of reactants to the reaction zone followed by migration back to the reaction zone for further reaction with complementary reactants; migration occurring back and forward until polymer is formed. By using common values for the diffusion of macromolecules, it can be shown that the diffusion of large molecules compared to small molecules such as carbon tetrachloride and benzene is only a factor of 10^1 to 10^3 slower¹⁸ and thus does not account for the factor of 10^{10} difference observed in the rate constant observed for the reactions presented in this work compared to usual diffusion controlled rate constants. Other diffusion arguments can be given. None of these account for the difference of 10^{10} found. A definitive description as to why reaction rate follows such a solvent viscosity and solvent volume trend cannot be given now; but as already noted, a simple diffusion to the reaction zone with immediate reaction upon contact of reactants is not the answer.

No observable trend is noted for the unstirred systems with regards to yield and such physical properties as organic solvent viscosity or dielectric constant of organic solvent. This is not unexpected, since no attempt has been made to regulate polymer removal from the interface.

The exact identity of the active diol species is unknown but it is not the protonated diol species since polymerization does not occur under acid conditions. Thus base reacts with formed hydrogen chloride to prevent protonation of the diol.

For systems in which no base was added and the organic solvent was cyclohexane, polymer was formed under unstirred conditions, but no polymer was formed under stirred conditions (Table III). For similar systems but with carbon tetrachloride as solvent no polymer was formed whether the systems were stirred or unstirred (Table III). These observations can be explained in the following manner. In the carbon tetrachloride systems,

the organic phase is heavier than the diol phase. When oligomers are formed at the interface of unstirred systems, hydrogen chloride is given off. The hydrogen chloride rises and protonates diols entering the reaction zone, and other diols making up the lighter upper phase, rendering the diols inactive. In the unstirred system with cyclohexane, the organic phase is lighter than the diol phase and thus resides over the diol phase. As hydrogen chloride is formed, it escapes through the organic phase and does not protonate diol which is residing in the lower phase.

In the stirred systems any hydrogen chloride that is formed will come into contact with and protonate diol, regardless of the nature of the organic phase, since the system is homogeneous in content (on a macroscopic scale) with regard to the organic and diol phases.

Carraher¹⁷ has shown that the reaction between diphenyldichlorosilane (DPDS) and ethylene glycol (EG) follows the following rate expression:

$$\text{Rate} = k[\text{DPDS}] [\text{EG}]^{2/3}$$

It is noted that varying the nature of the diol has little influence on rate, whereas when the nature of the organosilane is changed there is a marked change in rate (Table IV). This might be interpreted to mean that the electron-withdrawing power of the phenyl groups (Hammett $\sigma(\widehat{meta}) = 0.22$,¹⁹ Taft $\sigma^* = 0.60$,²⁰ compared to the methyl groups ($\sigma(\widehat{meta}) = -0.07$,¹⁹ $\sigma^* = 0.00$ ²⁰) is important, resulting in an increased rate of polymer formation for the diphenylsilane system over the dimethylsilane system. This would further suggest that steric considerations about the silicon atom are minimal in determination of rate since the phenyl groups offer more bulk than do the methyl groups.

It is further noted that changing the diol results in little change in the molecular weight of the product, but changing the nature of the silane greatly influences the molecular weight of the product (Table IV). Whereas electronic arguments were used to explain the rate observations concerning change in the nature of the silane so that faster rates were found for systems containing diphenylsilane than dimethylsilane, just the opposite is observed for molecular weight. The dimethylsilane gives product with higher molecular weight than does diphenylsilane. An explanation is that the greater steric hindrance of the bulky phenyl groups in diphenyldichlorosilane, while tending not to block the entrance of monomers and oligomeric material, tend to block the approach of larger reactive molecules resulting in generally stepwise growth. The dimethylsilane, by comparison, does not block the approach of larger molecules making it possible for larger molecules to add, greatly increasing the molecular weight of the product.

If the conclusions drawn concerning steric and electronic effects of the organosilane on the rate of polymer formation and polymer molecular weight are correct, then an intermediate yield and molecular weight response should be observed for methylphenyldichlorosilane which is intermediate in steric and electronic character between diphenyldichlorosilane

and dimethyldichlorosilane. Such is experimentally observed to be the case (Table IV).

The kinetic evidence and rate trends are consistent with a S_N2 mechanism with the silicon atom of the silane or silane derivative being the electrophilic site of attack by the diol or diol derivative. This is in agreement with a number of kinetic studies of reactions of compounds of silicon (IV) which are interpreted as proceeding by an S_N2 mechanism.^{21,22}

More study is needed to discern more exactly the influence of steric and electronic effects on the production of polyalkyloxysilanes.

The author wishes to thank General Aniline and Film Corporation, New York, N.Y. for a sample of butenediol (2 butene-1,4-diol).

References

1. M. Iskenderov, K. Plekhanova, and N. Adigezalova, *Uch. Zap. Azerb. Gos. Univ., Ser. Khim. Nauk*, **4**, 71 (1965).
2. S. Migdal, D. Gerther, and A. Zilkha, *J. Organometal. Chem.*, **11**, 441 (1968).
3. M. Frankel, G. Gerther, D. Wagner, and A. Zilkha, *J. Organometal. Chem.*, **9**, 83 (1967).
4. M. Frankel, D. Gerther, D. Wagner, and A. Zilkha, *J. Appl. Polym. Sci.*, **9**, 3383 (1965).
5. H. Krimm and H. Schnell, German Pat. 1,082,057 (1962).
6. E. Goldberg and E. Powers, *J. Polym. Sci.*, **B2**, 835 (1964).
7. M. Morgunava, D. Zhinkin, and M. Sobolevskii, *Plasticheskie Massy*, **3**, 26 (1963).
8. V. Losev and V. Astakhin, *Plasticheskie Massy*, **4**, 26 (1964).
9. K. Andrianov, A. Varlamov, L. Khanashvili, N. Gashmidova, and M. Strashnykh, *Izv. Akad. Nauk. SSSR, Ser. Khim.* **1967**, 909.
10. R. MacFarlane and E. Yankura, Quarterly Report No. 7, Naugatuck Division of United States Rubber Company, Contract No. DA-19-020-ORD-5507.
11. H. Hopf and R. Egli, *Kunststoffe-Plastics*, **6**, 433 (1959).
12. J. Curry and J. Byrd, *J. Appl. Polym. Sci.*, **9**, 295 (1959).
13. W. Dunnivant, R. Markle, P. Stickney, J. Curry, and J. Byrd, *J. Polym. Sci. A-1*, **5**, 707 (1967).
14. W. Dunnivant, R. Markle, R. Sinclair, P. Stickney, J. Curry, and J. Byrd, *Polymer Preprints*, **8**, 1163 (1967).
15. W. Dunnivant, R. Markle, R. Sinclair, P. Stickney, J. Curry, and J. Byrd, *Macromolecules*, **1**, 249 (1968).
16. *International Critical Tables*, Vol. 5, (a) pp. 10-12, 211-214; (b) *ibid.*, pp. 83-98.
17. C. Carraher, *J. Polym. Sci. A-1*, in press.
18. C. Tanford, *Physical Chemistry of Macromolecules*, Wiley, New York, 1961.
19. H. H. Jaffe, *Chem. Revs.*, **53**, 191 (1953).
20. R. Taft, *J. Amer. Chem. Soc.*, **75**, 4231 (1953).
21. F. Basolo and R. G. Pearson, *Mechanism of Inorganic Reactions*, Wiley, New York, 1958, p. 210.
22. L. Kaplan and K. E. Wilzbach, *J. Amer. Chem. Soc.*, **77**, 1298 (1955).

Received October 22, 1968

Revised February 19, 1969

Production of Organometallic Polymers by the Interfacial Technique. II. Kinetic Study of the Production of Polyoxyethyleneoxy(diphenylsilylene) by the Interfacial Technique

CHARLES E. CARRAHER, JR., *Chemistry Department, University of South Dakota, Vermillion, South Dakota 57069*

Synopsis

The stirred interfacial production of polyoxyethyleneoxy(diphenylsilylene) was found to be five-thirds order and dependent on the concentrations of both ethylene glycol and diphenyldichlorosilane, indicating that the character of the rate-determining step involves reaction of the ethylene glycol or ethylene glycol derivative and diphenyldichlorosilane or diphenyldichlorosilane derivative. A model consisting of ethylene glycol droplets residing in the organic phase is proposed which follows the rate expression:

$$\begin{aligned} \text{Rate} &= k (\text{spherical area of ethylene glycol})[\text{silane}] \\ &= k [\text{ethylene glycol}]^{2/3}[\text{silane}] \end{aligned}$$

This is in agreement with experimental findings. A rate constant of $1.4 \times 10^{-4} \text{ c.}^{2/3} \text{ m}^{2/3} \text{ sec}$ is found. The rates in unstirred interfacial systems are found to be slower than in the stirred systems.

INTRODUCTION

In a paper by Carraher¹ the first interfacial polymerization of dihalosilane compounds with diols was reported.

Rate studies of interfacial polymerization systems are not numerous. One reason is the difficulty of removing polymer from the reaction zone at a constant or known rate. A second difficulty is the theoretical treatment of concentrations of the reactants present in the two immiscible phases. A third difficulty is that the interfacial system by its very nature is heterogeneous in nature, which complicates the gathering and interpretation of data.

In stirred interfacial systems, the rate of removal of polymer from the interface and rate of production of new interfacial area can be assumed to be approximately constant where stirring rate, polymerizing vessel, volumes of immiscible phases, and temperature are held constant.

EXPERIMENTAL AND RESULTS

Experimental procedure as reported by Carraher¹ was followed. Polymer yield and viscometry results appear in Table I. It is noted that in both

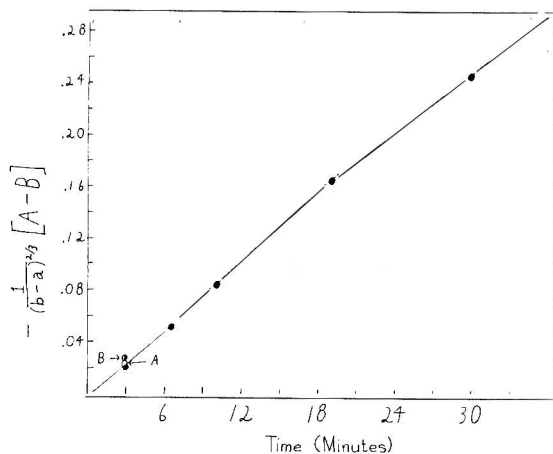


Fig. 1. Polymer yield results for stirred reaction systems plotted for a reaction of five-thirds order as a function of time at $25 \pm 1^\circ\text{C}$. a = concentration of ethylene glycol = 1.50 mole/l., b = concentration of diphenyldichlorosilane = 0.30 mole/l. Concentration of glycol and silane reacted to form polymer at time $t = x$; total volume = 60 ml. At point A , $a = 2.25$ mole/l., at point B , $b = 0.45$ mole/l. Results from Table I.

the stirred and unstirred systems yield increases with time and molecular weight remains approximately constant. It is further noted that an increase in the glycol concentration increases the rate of polymer formation

TABLE I
Yield and Viscosity for Systems Consisting of Diphenyldichlorosilane,
Ethylene Glycol, Sodium Hydroxide, and Cyclohexane at $25 \pm 1^\circ\text{C}$ ^a

Type of system	Reaction time	Polymer yield, %	Concn of comer used to form polymer mole/l.	Limiting viscosity number, LVN (in acetone, 30°C), ml/g
Stirred	3.0 min	4.8	0.014	9
	6.5 min	9.1	0.027	10
	10. min	13.	0.039	9
	17. min	19.	0.057	10
	30. min	30.	0.090	9
	3.0 min ^b	6.9	0.031	18
	3.0 min ^c	7.8	0.024	8
Unstirred	1 day	18.	0.055	7
	4 days	31.	0.094	7
	7 days	96.	0.29	6
	14 days	99.	0.30	6

^a Diphenyldichlorosilane, 0.30 mole/l.; ethylene glycol, 1.50 mole/l.; NaOH, 0.030 mole/l.; 60 ml. total volume.

^b Diphenyldichlorosilane = 0.45 mole/l.

^c Ethylene glycol = 2.25 mole/l.

but influences molecular weight little, while an increase in the silane concentration increases the rate of polymer formation and molecular weight (cf. also Fig. 1).

Let us assume the rate expression for the reaction is of the form

$$\text{Rate} = k(a - x)^{2/3}(b - x) \quad (1)$$

where k is the rate constant, a is the initial concentration of ethylene glycol, b is the initial concentration of diphenyldichlorosilane, and x concentration of ethylene glycol and silane reacted to form polymer at time t .

By appropriate changes of variables and appropriate integration, eq. (2) is derived from eq. (1) for the $a - x$ and $b - x$ greater than zero, where a is not necessarily equal to b .

$$\begin{aligned} -1/(b - a)^{2/3} \left(\left\{ \frac{1}{2} \ln \frac{[(b - a)^{1/3} + (a - x)^{1/3}]^2}{(b - a)^{2/3} - (b - a)^{1/3}(a - x)^{1/3} + (a - x)^{2/3}} \right. \right. \\ \left. \left. + (3)^{1/2} \tan^{-1} \frac{2(a - x)^{1/3} - (b - a)^{1/3}}{(b - a)^{1/3}(3)^{1/2}} \right\} \right. \\ \left. - \left\{ \frac{1}{2} \ln \frac{[(b - a)^{1/3} + a^{1/3}]^2}{(b - a)^{2/3} - (b - a)^{1/3}a^{1/3} + a^{2/3}} \right. \right. \\ \left. \left. + (3)^{1/2} \tan^{-1} \frac{2a^{1/3} - (b - a)^{1/3}}{(b - a)^{1/3}(3)^{1/2}} \right\} \right) = kt \quad (2) \end{aligned}$$

For simplicity let us represent eq. (2) as $-[1/(b - a)^{2/3}][A - B]$ where A represents the first term in braces and B represents the second set of terms in braces for $x = 0$ at $t = 0$. Figure 1 contains a plot of the data in Table I for stirred systems as a function of time according to eq. (2). A straight line is obtained.

DISCUSSION

In this study, one phase is pure ethylene glycol; since in rapidly stirred systems ethylene glycol can be assumed to be randomly dispersed throughout the reaction system, it was assumed that the ethylene glycol concentration could be expressed as concentration of glycol in the whole reaction system.

It is found that a straight line was obtained when the data for stirred systems from Table I, treated as indicated in eq. (2), was plotted as a function of time. Point A (Fig. 1) is for a system where only the initial concentration of ethylene glycol was changed from 1.50 mole/l. to 2.25 mole/l. Point B is for a system where the initial concentration of diphenyldichlorosilane was changed from 0.30 mole/l. to 0.45 mole/l. It is seen that both points fall on the line for $a = 1.50$ mole/l. and $b = 0.30$ mole/l. and that both systems (represented by points A and B , Fig. 1, Table I) have increased rates of polymer formation compared to systems where $a = 1.50$ mole/l. and $b = 0.30$ mole/l. This indicates that the rate of polymer

formation is dependent on both ethylene glycol and diphenyldichlorosilane concentration and that the experimental data are consistent with a reaction whose rate can be expressed as shown in eq. (1).

It is known that the number of moles n of a compound can be expressed as a function of volume V as shown in eq. (3)

$$n = \rho V/M \quad (3)$$

where ρ is density and M is molecular weight. It can be shown that the area of a sphere, A , is proportional to $V^{2/3}$

$$\begin{aligned} A &= 4\pi r^2 \\ &= 4\pi(9V^2/A^3) \\ &= 36\pi V^2/A^3 \end{aligned} \quad (4)$$

Then

$$A^3 = 36\pi V^2 \quad (5)$$

$$A = (36\pi V^2)^{1/3} \cong 4.7V^{2/3} \quad (6)$$

Hence

$$A \propto n^{2/3} \quad (6)$$

Morgan^{2a} notes that polymerization in interfacial systems takes place near or at the interface. It is not unexpected that the reaction should be dependent on the concentration of the silane and the spherical area for ethylene glycol. The following expression, eq. (7) can be written to describe this dependency:

$$\text{Rate} = k(\text{spherical area of ethylene glycol})[\text{silane}] = k[\text{ethylene glycol}]^{2/3}[\text{silane}] \quad (7)$$

Equation (7) is the same as eq. (1) and is in agreement with the experimental findings and the model of spheres of ethylene glycol contained in an organic phase. The model is further based on the assumptions that polymer is removed from the reaction zone (via precipitation, removal by the blender stirring blade, etc.) away from the glycol droplets, in a random manner, throughout the reaction such that polymer-free interfacial area will be proportional to the surface area of the glycol droplets, and that the number of droplets in a given system will remain approximately constant throughout the observation period (reaction time).

More work is needed in the area of defining such interfacial systems. The system used in this study is a limiting case where the organic phase is in great excess and aqueous phase is neat. It is noted that while the above explanation is consistent with experimental observation, some other artifact may account for such findings.

The rate constant for the reaction is $1.4 \times 10^{-4} \text{ l.}^{2/3}/\text{mole}^{2/3}\text{-sec.}$ (When data are plotted for a second-order reaction an approximately straight line is found for systems where $a = 1.50 \text{ mole/l.}$ and $b = 0.30 \text{ mole/l.}$ where $k =$

1.8×10^{-4} l./mole-sec, but points *A* and *B* do not fall on the line.) It is noted that the rate constant is for polymer production, not necessarily for reaction by one or both comers. In general, stirred interfacial reactions have faster rates,^{2b} although rates of the order as reported here have been reported for some interfacial reactions. Hodnett and Holmer³ report that the interfacial production of poly(phthaloylpiperazine) required 150 min for 80% conversion.

No noticeable variation of polymer viscosity with time was noted for the stirred and unstirred systems. This is in accord with a chain-type mechanism proposed for interfacial polymerizations^{2c} as well as being in agreement with experimental findings of others.³

There was no attempt to correlate yield data for the unstirred systems with rate parameters, since no attempt was made to regulate polymer removal from the interface. It is found that yield increases with time and that the rate of polymer formation is less in the unstirred systems, compared with the stirred systems. This is expected, since in the stirred systems a larger interfacial area will be available for polymer formation at any given time.

In stirred systems it has been shown that reaction rates are dependent on such physical variables as shape and size of the reaction vessel and stirring rate;^{2c} consequently reaction rates and reaction rate constants must be viewed as approximate values relative to such above mentioned variables. The reaction order results should be independent of such physical variables at high stirring rates.

The author wishes to thank Professors E. Howard Coker and Clyde A. Wiles for suggestions in preparing the paper.

References

1. C. Carraher, *J. Polym. Sci. A-1*, this issue.
2. P. W. Morgan, *Condensation Polymers, by Interfacial and Solution Methods*, Wiley, New York, 1965, (a) p. 22; (b) p. 66; (c) pp. 20-30, 65, 68-75.
3. E. M. Hodnett and D. A. Holmer, *J. Polym. Sci.*, **58**, 1415 (1962).

Received October 22, 1968

Revised February 19, 1969

Polymers from 12-Hydroxymethyltetrahydroabietic Acid and Its Vinyl and Acrylate Esters

MOTOO SAGA and C. S. MARVEL, *Department of Chemistry,
The University of Arizona, Tucson, Arizona 85721*

Synopsis

12-Hydroxymethyltetrahydroabietic acid has been homopolymerized by melt condensation and homopolyester has been obtained. Vinyl 12-hydroxymethyltetrahydroabietate has been prepared from 12-hydroxymethyltetrahydroabietic acid by vinyl interchange procedure with vinyl acetate, and has been homopolymerized, copolymerized with vinyl chloride, vinyl acetate, and terpolymerized with styrene and acrylonitrile. The acrylate ester of 12-hydroxymethyltetrahydroabietic acid also has been prepared from 12-hydroxymethyltetrahydroabietic acid and acrylyl chloride. The acrylate thus obtained has been homopolymerized and copolymerized with vinyl chloride and vinyl acetate. Polymers thus obtained have been characterized.

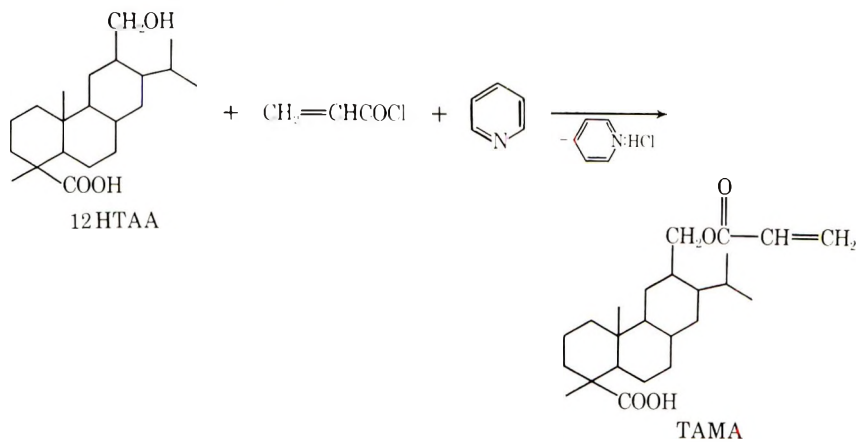
INTRODUCTION

In continuation of the studies on the preparation of polymers containing abietic acid derivatives,¹⁻⁶ this present paper deals with the preparation and polymerization of 12-hydroxymethyltetrahydroabietic acid (12-HTAA) and its vinyl and acrylyl derivatives. 12-HTAA which was derived from 12-hydroxymethyldihydroabietic acid by catalytic hydrogenation was provided by Dr. Glen Hedrick of the Naval Stores Research Laboratory, Olustee, Florida, one of the laboratories in the Southern Utilization Research and Development Divisions of USDA.

We have already reported⁶ on the polymerization of 12-hydroxymethylabiet-7,8-enoic acid (12-HMAA) but 12-HTAA seemed to be more promising for polymerization work because there is no unsaturation in the ring system which might retard polymerization. 12-HTAA was provided as a white fine powder which had a melting point of 239-240°C, and the elemental analysis showed it to be pure.

Vinyl 12-hydroxymethyltetrahydroabietate has been prepared from 12-HTAA by the usual vinyl interchange procedure with vinyl acetate in the presence of mercuric acetate and sulfuric acid. 12-HTAA has both hydroxyl and carboxyl groups in the same molecule, and there is a possibility that several undesirable side reactions with vinyl acetate may occur as has been reported.^{7,8} To avoid any undesirable reaction, the material obtained was treated with acid washed activated alumina or washed with diluted hydrochloric acid solution at room temperature. A colorless vis-

ous liquid which had a high boiling point was obtained. The infrared spectrum of this compound showed characteristic vinyl ester absorption band at 1745 cm^{-1} , —C=C— stretching frequency at 1650 cm^{-1} , and —OH at 3430 cm^{-1} . The vinyl ester obtained was very soluble in common organic solvents and the elemental analysis indicated it was the expected vinyl 12-hydroxymethyltetrahydroabietate (VTMA). The acrylate (TAMA) was made from 12-HTAA and acrylyl chloride with pyridine as an acid acceptor in tetrahydrofuran solution at low temperature.



A colorless viscous oily liquid was obtained. The boiling point of this material is too high to distill ($>270^\circ\text{C}/0.1\text{ mm Hg}$). For use in polymerization, the acrylate obtained was purified by chromatography on silica gel. The infrared spectrum of this material exhibited —C=C— stretching frequency at 1630 cm^{-1} (w) and 1640 cm^{-1} (M). It also exhibited strong absorption bands at about 1750 cm^{-1} which were assigned to carboxyl and ester carbonyl groups.

TAMA thus obtained as a viscous material is insoluble in benzene, ethyl acetate, acetone, *n*-hexane, and *n*-heptane, but slightly soluble in toluene and soluble in tetrahydrofuran.

POLYMERIZATION

The self condensation of 12-HTAA has been conducted by melt polymerization methods with the use of a small amount of antimony trioxide⁹ or no catalyst. The experimental data are given in Table I. All of the polymers were obtained as pale yellow to pale brown clear glassy materials which gave white powders on reprecipitation from a tetrahydrofuran or dimethylformamide solution by pouring into methanol. It was not a film forming polymer.

The infrared spectrum of the polyester obtained showed an ester carbonyl absorption band at 1730 cm^{-1} , whereas starting material, 12-HTAA, showed acid carbonyl absorption at 1700 cm^{-1} . 12-HTAA exhibited a very strong OH stretching frequency at 3440 cm^{-1} , but no hydroxyl bands

TABLE I
 Self-Condensation of 12-HTAA^a

Run no.	Catalyst		Temp, °C	Time, hr	Conversion, %	Softening range, °C	η_{inh}^b
	Type	%					
I-1	—		265	24	71.6	230	0.135
I-2	—		265	48	74.3	230	0.146
I-3	Sb ₂ O ₃	0.25	265	24	73.7	230	0.183
I-4	Sb ₂ O ₃	0.5	265	48	69.5	230	0.246

^a All of the self condensations were conducted in a Pyrex test tube in a metal bath.

^b Determined on the solution of ca. 0.25 g/100 ml of dimethylformamide at 30°C.

were indicated in the polyester. Compared with the homopolyesters obtained from 12-hydroxymethyl-abiet-7,8-enoic acid⁶ the polymers were a bit higher in molecular weight but the other polymer properties were almost the same.

Free-radical homopolymerization of VTMA has been conducted in emulsion, in solution, and in bulk. The experimental data are given in Table II.

 TABLE II
 Homopolymerization of VTMA^a

Run no.	System	Catalyst		Time, hr	Conversion, %	Softening range, °C	η_{inh}^c
		Type ^b	%				
II-1	Bulk	AIBN	5	24	42.3	230–235	0.083
II-2	Bulk	AIBN	5	48	44.5	240	0.115
II-3	Emulsion	K ₂ S ₂ O ₈	5	24	10.6	240	0.093
II-4	Emulsion	K ₂ S ₂ O ₈	5	48	12.8	240	0.133
II-5	Solution ^d	AIBN	5	48	40.5	238–242	0.136
II-6	Solution ^d	DEABIB	5	48	38.7	235–239	0.127

^a All of the polymerizations were conducted at 60 ± 2°C by tumbling in water bath.

^b AIBN = azobisisobutyronitrile; DEABIB = diethyl azobisisobutyrate.

^c Determined on a solution of ca 0.3 g/100 ml of THF at 30°C.

^d *n*-Heptane was used as a solvent.

The polymers were obtained as white powders soluble in tetrahydrofuran and having rather high softening points. The results were slightly different according to the method and catalyst used. The infrared spectrum of homopolymer exhibited a clear —OH stretching frequency at 3430 cm⁻¹, but no —C=C— stretching frequency, which is a characteristic band for VTMA, is observed.

Copolymers of VTMA and vinyl chloride have been prepared with different charged compositions by means of a free radical initiator. The experimental data are given in Table III.

TABLE III
 Copolymerization of VTMA and VCl (in Emulsion)^a

Run no.	Charged composition		Conversion, %	Analyses			Incorporated ratio ^b VTMA, %	VCl, %	η_{inh}^c
	VTMA, wt-%	VCl, wt-%		C, %	H, %	Cl, %			
III-1	10	90	78.6	40.92	5.11	53.42	6.7	93.3	0.81
III-2	20	80	73.2	43.94	5.50	58.81	14.6	85.4	0.86
III-3	30	70	75.5	47.18	5.63	43.62	23.5	76.5	0.66
III-4	40	60	68.7	49.31	5.82	40.28	29.0	71.0	0.57

^a All of the polymerizations were conducted at $60 \pm 2^\circ\text{C}$ by tumbling the tubes end over end for 24 hr, using 5 g of total monomers, 0.1 g of $\text{K}_2\text{S}_2\text{O}_8$ as an initiator, and 15 ml of air-free distilled water; 0.1 g of DS-10 was used as an emulsifier.

^b Based on analyses for C, H and Cl in the copolymer.

^c Determined on the solution of ca 0.25 g./100 ml. of THF at 30°C .

The per cent of VTMA incorporated was calculated from the percent of carbon, hydrogen and chlorine in the copolymer. Copolymers were obtained as white or pale tan powders. All were soluble in tetrahydrofuran and could be molded into transparent tough films. The inherent viscosities of these copolymers were, in general, higher than those from vinyl 12-hydroxymethylabiet-7,8-enoate.⁶

Four different vinyl acetate copolymers have been prepared by using potassium persulfate as initiators. The experimental data are given in Table IV.

TABLE IV
Copolymerization of VTMA and VAc (in emulsion)^a

Run	Charged composition		Conversion %	Analysis		Incorporated ratio ^b		η_{inh}^c
	VT- MA, %	VAc, %		C, %	H, %	VTMA, %	VAc, %	
IV-1	10	90	73.6	58.24	7.59	12.2	87.8	0.66
IV-2	20	80	75.7	60.38	7.89	22.6	77.4	0.58
IV-3	30	70	58.3	61.87	8.01	30.1	69.9	0.52
IV-4	40	60	60.3	63.21	8.22	36.7	63.3	0.31

^a All of the polymerizations were conducted at $60 \pm 2^\circ\text{C}$ by tumbling the tubed end over end for 33 hr; 5 g of total monomers was used, 0.1 g of $\text{K}_2\text{S}_2\text{O}_8$ as an initiator and 15 ml of air-free distilled water; 0.1 g of DS-10 was used as an emulsifier.

^b Based on analyses for C and H in the copolymer.

^c Determined on solutions of ca. 0.3 g/100 ml of THF at 30°C .

All of these copolymers were obtained as pale yellow to pale brown powders according to the charged composition, and were soluble in tetrahydrofuran. The copolymers could be molded into water-clear but rather brittle films. These results indicated that VTMA could be incorporated into the polymer composition up to 36.7% when 40% was charged. The inherent viscosities of copolymers were higher than those of VHMA copolymer,⁶ but were not high enough to show good mechanical properties.

Another combination of monomers which might give some useful polymer is the VTMA, styrene and acrylonitrile. Four different terpolymers of varying compositions were prepared. The experimental data are given in Table V. All of the terpolymers were obtained as white powder which could be molded into clear tough films. The terpolymers obtained were soluble in dimethylformamide and dimethylacetamide, but were only slightly soluble in tetrahydrofuran. The infrared spectra of polymers obtained exhibits ester carbonyl absorption around 1720 cm^{-1} and $-\text{CN}$ at 2250 cm^{-1} and $-\text{OH}$ at 3430 cm^{-1} . These results and elemental analyses support the formation of copolymers as products.

Polymerization studies on the acrylate of 12-hydroxymethyltetrahydroabietic acid (TAMA) also have been conducted.

TABLE V
 Terpolymerization of VTMA, St, and AN^a

Run no.	Charged composition			Conversion, %	Elemental analyses			Incorporated ratio ^b			η_{inh}^c
	VTMA, wt-%	St, wt-%	AN, wt-%		C, %	H, %	N, %	VTMA, %	St, %	AN, %	
V-1	10	60	30	88.9	83.87	7.23	8.08	6.0	63.4	30.6	2.31
V-2	20	50	30	79.5	82.54	7.18	8.55	11.5	56.1	32.4	3.47
V-3	30	40	30	72.1	80.66	7.14	9.32	19.0	45.7	35.3	4.12
V-4	40	30	30	67.5	78.59	7.21	10.12	27.2	34.4	38.4	3.16

^a All of the terpolymerizations were conducted at $60 \pm 2^\circ\text{C}$ by tumbling the tubes end over end for 48 hr with the use of 5.0 g of total monomers Siponate DS10 (0.1 g) as emulsifier, $\text{K}_2\text{S}_2\text{O}_8$ (0.1 g) as initiator, and 15 ml of air-free distilled water.

^b Per cent by weight, based on analysis for C, H and N in the copolymers.

^c Determined on solution containing ca. 0.25 g/100 ml of dimethylformamide at 30°C .

TABLE VI
 Homopolymerization of TAMA

Run no.	System	Initiator		Temp, °C	Time, hr	Conversion, %	Softening range, °C	Analyses ^b		η_{inh}^c
		Type ^a	%					C, %	H, %	
VI-1	Solution ^d	AIBN	3	70	24	62.1	195-200			0.13
VI-2	Solution ^d	AIBN	5	70	24	60.1	195-200			0.15
VI-3	Solution ^d	AIBN	5	70	48	61.5	196-202			0.19
VI-4	Bulk	AIBN	5	60	5	77.0	220	73.55	9.67	0.24
VI-5	Bulk	AIBN	3	60	3	62.7	220	73.42	9.58	0.22
VI-6	Bulk	DEABIB	5	60	5	76.5	220	72.99	9.70	0.24
VI-7	Bulk	DEABIB	3	60	3	63.7	220			0.21

^a AIBN = azobisisobutyronitrile; DEABIB = diethyl azobisisobutyrate.

^b Calcd for TAMA monomer, $C_{23}H_{34}O_4$: C, 73.84%; H, 9.74%; O, 13.85%. Found: C, 73.85%; H, 9.58%; O, 13.33%.

^c VI-1, 2, 3 were determined on the solution of ca. 0.3 g/100 ml of THF at 30°C. VI-4, 5, 6 were determined on the solution of ca. 0.3 g/100 ml of dimethylformamide at 30°C.

^d Benzene-tetrahydrofuran (1:1) mixed solution was used as solvent.

TABLE VII
Copolymerization of TAMA and VCl^a

Run no.	Charged composition		Temp, °C	Time, hr	Conversion, %	Analyses			Incorporated ratio ^b		η_{inh}^c
	TAMA, wt-%	VCl, wt-%				C, %	H, %	Cl, %	TAMA, %	VCl, %	
VII-1	10	90	70	3	Gel						Insoluble
VII-2	10	90	50	6	Gel						Insoluble
VII-3	10	90	50	3	64.5	44.14	5.84	47.38	16.4	83.6	0.63
VII-4	20	80	50	3	63.3	46.57	6.15	43.62	23.3	76.7	0.49
VII-5	30	70	50	3	58.6	47.86	6.23	40.82	27.0	73.0	0.40

^a All of the copolymerizations were conducted in bulk, with the use of 5.0 g of total monomers and 2% (0.1 g) of AIBN as an initiator.

^b Based on analyses for C, H and Cl in the copolymer.

^c Determined on solutions of ca. 0.25 g/100 ml of THF at 30°C.

TABLE VIII
 Copolymerization of TAMA and VAc^a

Run no.	Charged composition		Temp, °C	Time, hr	Conversion, %	Analyses		Incorporated ratio ^b		η_{inh}^c
	TAMA, wt-%	VAc, wt-%				C, %	H, %	TAMA, %	VAc, %	
VIII-1	10	90	60	24	gel					Insoluble
VIII-2	10	90	60	10	gel					Insoluble
VIII-3	10	90	50	15	68.9	56.99	7.24	7.0	93.0	0.49
VIII-4	20	80	50	15	71.1	58.10	7.48	13.3	86.7	0.28
VIII-5	30	70	50	15	67.7	59.74	7.89	22.6	77.7	0.26

^a All of the copolymerizations were conducted in bulk, using 5 g. of total monomers and 2% (0.1 g) of AIBN as an initiator.

^b Per cent by weight, based on analysis for C and H in the copolymers.

^c Determined on solutions of ca. 0.3 g/100 ml of THF at 30°C.

TAMA have been homopolymerized in solution and in bulk using AIBN or DEABIB as an initiator. The experimental data are given in Table VI. Due to the poor solubility of TAMA in common organic solvents, solution polymerizations were conducted in benzene-THF (1:1) mixed solvent. The polymers obtained in solution showed lower inherent viscosities than those obtained in bulk. All of the polymers were obtained as white, fine powders having a high softening point. Of the two initiators, almost no differences were observed in conversions and viscosities. The polymers obtained in bulk did not melt even up to 220°C, but solubilities in THF were less. The infrared spectra of these polymers showed no —C=C— stretching frequencies which are characteristic bands for the monomer. The other absorption bands for the polymers were almost the same as those of the monomer.

Copolymers of TAMA and vinyl chloride have been prepared with different compositions and conditions in order to see whether some useful polymers could be prepared. The experimental data are given in Table VII.

All of the copolymerizations were conducted in bulk with the use of AIBN as a catalyst. The copolymers were obtained as white powders which formed transparent tough films and were soluble in THF. The copolymer contained up to 27% of TAMA when 30% of TAMA was charged. The infrared spectra of the copolymers obtained have no absorption bands for unsaturation. The copolymers became insoluble in the usual organic solvents when higher temperature ($>50^\circ\text{C}$) or prolonged time were used in the polymerization conditions.

A set of bulk TAMA and vinyl acetate copolymers also have been prepared. The experimental data are given in Table VIII.

All of these copolymerizations were conducted with the use of free-radical initiator. The copolymers were obtained as pale yellowish powders and could be molded into transparent films. All of the copolymers obtained were soluble in THF. About 70% of charged TAMA was incorporated in each copolymer. The infrared spectra of these copolymers showed characteristic bands for both monomers, but no —C=C— stretching frequencies were observed.

The solution copolymerization of TAMA and vinyl acetate also have been conducted in benzene-THF (1:1) mixed solvent. The copolymers obtained showed lower conversions and viscosities than those from bulk polymerization.

EXPERIMENTAL

Preparation of VTMA

In a one-liter three-necked round-bottomed flask equipped with a magnetic stirrer and a condenser protected with a drying tube, 30 g (0.89 mole) of 12-HTAA, 2 g of mercuric acetate, 0.1 g of copper resinate, and 700 ml of freshly distilled vinyl acetate was added. The mixture was stirred vigor-

ously, then 0.3 ml of sulfuric acid was added at 0–5°C. The reaction was allowed to continue for 72 hr at room temperature (25–30°C). The pale green reaction mixture was heterogeneous in the beginning and became homogeneous as the reaction proceeded. At the end of the reaction, 2.0 g of sodium acetate was added to stop the reaction. At room temperature, the excess of vinyl acetate was distilled under reduced pressure. The residue was dissolved in 5 ml of ether and was washed with 1 liter of 2% sodium bicarbonate solution and finally with water. The ether solution was decolorized by activated charcoal, then 100 g of acid-washed activated alumina (Merck and Co., Inc.) was added and stirred for 10 hr. The filtrate was dried over anhydrous sodium sulfate and chromatogrammed on silica gel. The ether was removed under reduced pressure. A colorless, oily liquid was obtained. The yield was 27.6 g (85.4%).

ANAL. Calcd for $C_{23}H_{38}O_3$: C, 76.19%; H, 10.56%; O, 13.24%. Found: C, 76.22%; H, 10.16%; O, 13.53%.

Preparation of TAMA

In a one-liter three-necked round-bottomed flask equipped with a magnetic stirrer and an additional dropping funnel were placed 33.6 g (0.1 mole) of 12-HTAA, 9.05 g (0.1 mole) of acrylyl chloride, 0.05 g of copper resinate, and 400 ml of freshly distilled tetrahydrofuran. To this was added a solution of 8.0 g (0.1 mole) of pyridine in 30 ml of anhydrous tetrahydrofuran over a period of 30 min. During the addition of pyridine solution, the reaction mixture was stirred vigorously and cooled to below 0°C. After stirring for 48 hr at room temperature, precipitated pyridine hydrochloride was removed by filtration. Then 300 ml of ether was added to the filtrate which was washed with 500 ml of 1*N* hydrochloric acid, 500 ml of 2% sodium bicarbonate solution, and finally with water. After drying over anhydrous sodium sulfate, the solution was chromatogrammed on silica gel. The solvent was evaporated on a Rotovap to leave behind a colorless oily liquid. The yield was 28.5 g (73.1%) of TAMA; the boiling point of this product was over 270°C at 0.1 mm Hg; $n_D^{25} = 1.5033$. Results of analysis are given in Table VI.

Homo-, Co-, and Terpolymerization of VTMA

Conditions used for homo-, co- and terpolymerization of VTMA were the same as those used in the work on vinyl 12-hydroxymethylabiet-7,8-enoate.⁶

Homopolymerization of TAMA

Solution. In a Pyrex test tube was placed 5 ml of benzene-THF mixed solution containing 1 g of TAMA. To this was added 0.03 g of AIBN and cooled to Dry Ice-acetone temperature, evacuated, and filled with nitrogen three times before sealing. The polymerization tube was put in an oil bath

and heated at $70 \pm 1^\circ\text{C}$ for 24 hr. After this period, the polymer solution was poured into 100 ml of *n*-hexane. The polymer isolated was reprecipitated from THF with *n*-hexane. The yield was 0.62 g (62%) of vacuum oven-dried ($50^\circ\text{C}/24$ hr) white powder (run no. VI-1, Table VI). The procedure for the other solution homopolymerizations was similar to the one described.

Bulk. TAMA (2.0 g) and DEABIB (0.1 g) were charged in a pressure tube (1×5 in.), evacuated under 0.1 mm Hg, and flushed with nitrogen three times before capping, then was allowed to stand at 60°C for 5 hr. After this period, the contents were dissolved in 20 ml of dimethylformamide and poured into 100 ml of methanol. The yield was 1.53 g (76.5%) of vacuum oven-dried ($50^\circ\text{C}/24$ hr) white powder. (run no. VI-6, Table VI). The procedure for the other free-radical polymerizations in bulk were similar to the one described.

Copolymerization of TAMA

TAMA/VCl Copolymer. TAMA (0.5 g) and AIBN (0.1 g) were charged in a pressure tube (1×5 in.), which was evacuated under 0.1 mm Hg and flushed with nitrogen three times at Dry Ice-acetone temperature. Then VCl was charged in excess and was allowed to boil down to 4.5 g. After capping the tube, the contents were shaken vigorously to form a homogeneous solution, then polymerized at $50 \pm 1^\circ\text{C}$ by tumbling end over end for 3 hr. The reaction mixture was dissolved in 50 ml of THF and reprecipitated in 300 ml of methanol. This procedure was repeated again. The yield was 3.23 g (64.5%) of vacuum oven-dried ($50^\circ\text{C}/24$ hr) white powder (run no. VIII-3, Table VIII). The procedure for the other polymers given in Table VIII was similar.

TAMA/VAc Copolymer. TAMA (0.5 g), VAc (4.5 g), and AIBN (0.1 g) were charged in a pressure tube (1×5 in.), cooled to Dry Ice-acetone temperature, evacuated under 0.1 mm Hg, and flushed with nitrogen three times before capping. The content was shaken vigorously for 30 min at room temperature, then polymerized at $50 \pm 1^\circ\text{C}$ by tumbling end over end for 15 hr. The reaction contents were dissolved in 50 ml of THF and reprecipitated in 300 ml of *n*-hexane. This procedure was repeated again to purify the polymer. The yield was 3.45 g (68.9%) of vacuum oven-dried ($50^\circ\text{C}/24$ hr) pale yellowish powder (run no. VIII-3, Table VIII). The procedure for the other polymers given in Table VIII was similar to the one described.

We are indebted to Dr. Glen Hedrick of the Naval Stores Research Laboratory, Southern Utilization Research and Development Division, USDA for the starting monomer used in this work.

This is a partial report of work done under contract with the Southern and Western Utilization Research and Development Divisions, Agricultural Research Service, U. S. Department of Agriculture, and authorized by the Research and Marketing Act of 1946. The contract was supervised by Dr. Glenn Fuller of the Western Division.

References

1. J. R. Sowa and C. S. Marvel, *J. Polym. Sci. B*, **4**, 431 (1966).
2. R. Liepins and C. S. Marvel, *J. Polym. Sci. A-1*, **4**, 2003 (1966).
3. W. Fukuda and C. S. Marvel, *J. Polym. Sci. A-1*, **6**, 1050 (1968).
4. W. Fukuda and C. S. Marvel, *J. Polym. Sci. A-1*, **6**, 1281 (1968).
5. W. Fukuda, M. Saga, and C. S. Marvel, *J. Polym. Sci. A-1*, **6**, 1523 (1968).
6. M. Saga and C. S. Marvel, *J. Polym. Sci.*, in press.
7. R. L. Adelman, *J. Amer. Chem. Soc.*, **75**, 2689 (1953).
8. T. Shono and C. S. Marvel, *J. Polym. Sci. A*, **1**, 2067 (1963).
9. N. A. Higgins, U. S. Pat. 2,676,945 (April 27, 1954).

Received February 24, 1969

Studies on the Polymerization of Ethyl Acrylate. II. Chain Transfer Studies

P. V. T. RAGHURAM and U. S. NANDI, *Indian Association for the Cultivation of Science, Calcutta, India*

Synopsis

Transfer constants for different solvents representing hydrocarbons, halogenated compounds, alcohols, ketones, acids, and esters were determined in the thermal polymerization of ethyl acrylate at 80°C and they are compared with the available data on methyl acrylate and ethyl methacrylate. It was observed from the values of transfer constants that ethyl acrylate radicals are a little more effective than methyl acrylate or ethyl methacrylate in abstracting hydrogen atom from hydrocarbons and alcohols. In acetic and *n*-butyric acid media, it has been found, by the aid of endgroup analysis, that the derived solvent radicals from transfer reactions are not too efficient to start a new chain.

In our earlier paper¹ we reported the results on kinetic studies on the AIBN-initiated solution polymerization of ethyl acrylate, and in this present communication transfer constants for nineteen selective solvents are reported in the thermal polymerization of ethyl acrylate at 80°C.

EXPERIMENTAL

Monomer and Solvents

Monomer was purified in a similar way as that described in our earlier paper.¹ Solvents used were mostly of analytical reagent (B.D.H.) or G.R. quality (E. Merck) and were further purified by the usual methods.²

Polymerization Experiments

Polymerization was carried out in sealed Pyrex glass ampoules.¹ As mentioned earlier, the use of initiator was avoided. Conversions were kept sufficiently low to permit the assumption of constancy in the value of $[S]/[M]$. The polymer was precipitated three times from benzene solution by petroleum ether, and the samples were dried by the usual procedure.

Degree of Polymerization (\bar{P}_n)

Intrinsic viscosities of the polymer samples were determined in an Ubbelohde viscometer at 30°C in benzene solutions, and the number-average degrees of polymerization were calculated from the equation:

$$\bar{P}_n = K[\eta]^a;$$

the values of K and α used in the present work are 2.03×10^3 and 1.492, respectively.³

Endgroup Estimation

The dye-interaction technique⁴ was employed in benzene solution to estimate the number of COOH endgroups in poly(ethyl acrylate) samples. The basic dye used in the present case was a benzene extract of Rhodamine 6 GX. Equal volumes of dye-reagent and polymer solution of known concentration in benzene were added together in cleaned test tubes and thoroughly mixed. After allowing sufficient time for interaction, optical densities of the solutions were measured at $515 \text{ m}\mu$ in a Hilger spectrophotometer. From the value of optical density the number of endgroups per chain could be calculated by the relationship.

$$\text{No. of COOH endgroups per chain} = \frac{\text{Normality of formic acid} \times \text{molecular weight of the polymer}}{\text{Concentration of the polymer (in g/l. solvent)}}$$

Formic acid was used as reference acid for standardization and has been discussed in detail in an earlier publication.⁴

RESULTS AND DISCUSSION

In thermal polymerization at 80°C the values of $R_p\delta^2/[\text{M}]^2$ have been found to be negligible in comparison to $1/\bar{P}_n$ values, and hence the transfer constant C_s has been computed from the slope of the conventional plot of $1/\bar{P}_n$ against $[\text{S}]/[\text{M}]$;⁵ results are shown in Table I and Figures 1 and 2.

In the hydrocarbon series the transfer constants for benzene, toluene, ethylbenzene, and isopropylbenzene are in the ratio of 1:5.5:32:42, respectively, and evidently one can expect that the benzylic hydrogen atoms are the most susceptible to transfer. This is in accordance with the suggestion of Basu et al.⁸ that the enhanced activity in the above order is due to increased substitution at the α -carbon atom and the consequent effect on C—H bond due to substitution.⁹ On similar arguments, one can explain the low C_s values for benzene and cyclohexane.

Although bromobenzene seems to be comparatively more reactive than chlorobenzene, their C_s values are comparable to that of benzene. Chloroform and carbon tetrachloride have almost identical values, although in the polymerization of methyl acrylate chloroform had a higher value. It would be rather hasty to comment on this unless the activation parameters are known.

In isomeric butyl alcohols, the transfer activity is in the order of *sec*-butyl > *n*-butyl > *isobutyl* > *tert*-butyl and is in general agreement with the α -hydrogen concept.¹⁶ The concept of the reactive hydrogen under-

going transfer and of the nontransfer of hydroxylic hydrogen from free-radical attack is certainly evident from this order, and this receives further confirmation from the results of Kharasch et al.¹⁰

In ketonic compounds the activity increases from acetone to methyl ethyl ketone, and the reactive hydrogens at α, α' positions to the carbonyl group probably take part in transfer reaction.¹¹ In the light of evidence of Evans and Gordon,¹² the higher activity of methyl ethyl ketone probably suggests that transfer takes place with the keto form rather than the enol form.

TABLE I
Comparison of Transfer Constants for Various Solvents
with Methyl Acrylate, Ethyl Acrylate, and Ethyl Methacrylate at 80°C

Solvent	$C_s \times 10^6$		
	Ethyl acrylate ^a	Methyl acrylate ^b	Ethyl methacrylate ^c
Benzene	5.25(3)	3.26	0.81
Toluene	26.00(4)	17.75	4.36
Ethylbenzene	168.00(4)	60.56	14.28
Isopropylbenzene	222.00(4)	69.66	20.67
<i>n</i> -Hexane	9.70(3)	11.32	—
Cyclohexane	12.20(3)	0.27	9.28
Chlorobenzene	3.70(4)	9.86	4.36
Bromobenzene	6.85(3)	—	—
Chloroform	14.89(4)	21.44	7.03
Carbon tetrachloride	15.50(4)	13.23	9.01
<i>n</i> -Butyl alcohol	58.50(3)	27.47	4.54
<i>sec</i> -Butyl alcohol	222.00(4)	141.40	16.04
<i>tert</i> -Butyl alcohol	7.12(3)	3.89	4.17
Isobutyl alcohol	46.50(4)	24.96	4.45
Acetone	11.00(3)	6.22	1.02
Methyl ethyl ketone	32.90(3)	32.38	2.52
Ethyl acetate	8.90(3)	—	9.19
Acetic acid	5.37(3)	—	0.95
Formic acid	0.46(4)	—	—
<i>n</i> -Butyric acid	8.55(4)	—	—
Acetonitrile	5.50(3)	—	—

^a The figures given in parentheses refer to the number of sets of experiments from which the C_s value is evaluated.

^b Data of Sen et al.⁶

^c Data of Chatterjee et al.⁷

In the acid series the order of chain transfer was found to be formic < acetic < *n*-butyric, an order expected from the theory of Basu et al.⁸ The transfer value for ethyl acetate is slightly higher than that for acetic acid. Another interesting observation is that in the thermal polymerization of ethyl acrylate in acetic acid R_p is found to be very low, and endgroup studies were undertaken to elucidate the reasons.

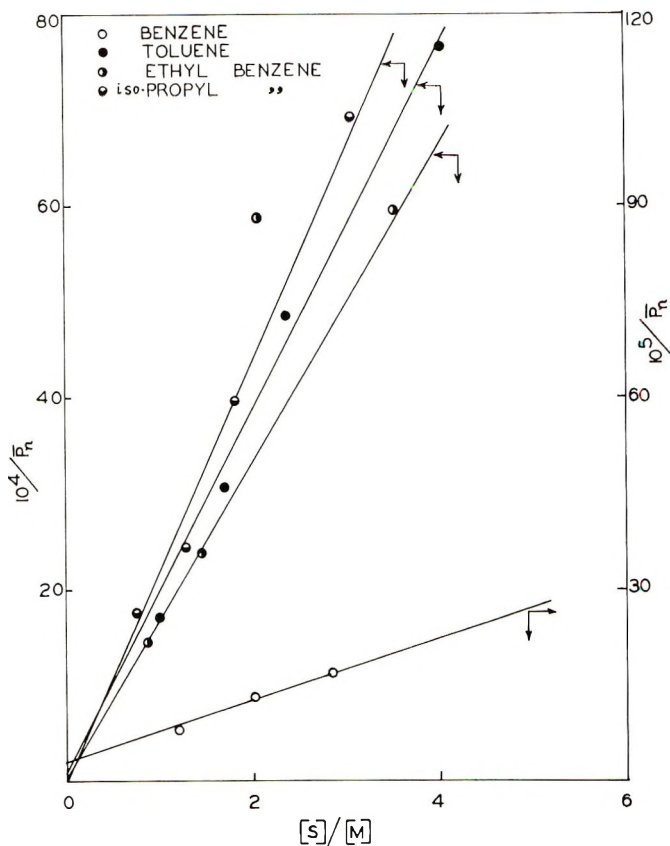


Fig. 1. Effects of hydrocarbons on the degree of polymerization of ethyl acrylate at 80°C: (O) benzene; (●) toluene; (◐) ethylbenzene; (◑) isopropylbenzene.

Endgroup Studies on Polymers Obtained in the Presence of Acids

In the present work, we have determined the number of COOH endgroups in polymers obtained by polymerizing ethyl acrylate in presence of acids by the sensitive dye-interaction techniques recently introduced.^{17,18} The abstraction of the hydrogen atom from the rupture of C—H bond would produce a derived radical of the type $R\dot{C}HOOH$. This radical is expected to initiate a new chain by adding monomer molecules successively. In this case, one COOH endgroup would be incorporated in each polymer chain assuming that polymer radicals are terminated only by transfer reactions. We have subjected poly(ethyl acrylate) samples obtained in different concentrations of acids to endgroup analysis by the dye interaction technique,⁴ and the results are given in Table II.

It is observed from Table II that one endgroup on the average was obtained for the samples in formic acid medium. For acetic and *n*-butyric acid media, very low —COOH contents were detected, the relative COOH content decreased with increasing solvent concentration. It has been

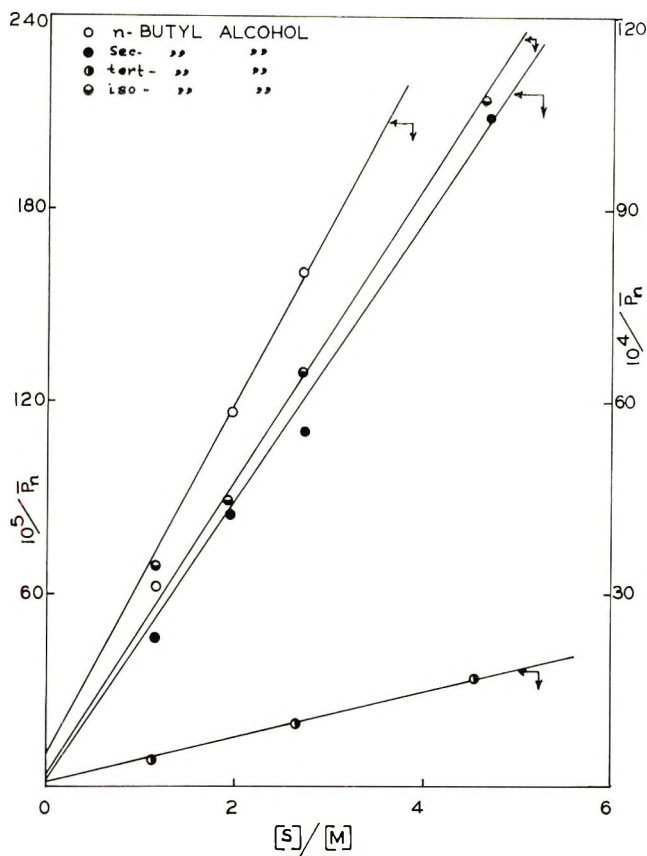


Fig. 2. Effects of alcohols on the degrees of polymerization of ethyl acrylate at 80°C: (○) *n*-butyl alcohol; (●) *sec*-butyl alcohol; (◐) *tert*-butyl alcohol; (◑) isobutyl alcohol.

established that in carboxylic acids, the free-radical attack will be on the hydrogen of the alkyl group to give rise to succinic acid derivatives,¹³ which was confirmed by the work of Fry et al.¹⁴ on ¹⁴C acetic acid.

Considering the success in the applicability of the α -hydrogen theory and the above facts, it is quite clear that polymer radical attacks the hydrogen atom attached to the alkyl group and not the hydrogen atom of the —COOH group. Even on structural considerations, the hydrogen atom of COOH group is comparatively difficult to be abstracted in view of higher bond energy.

From the fact that the polymer samples obtained from the experiments with acetic and *n*-butyric acids showed only moderate response for the dye test, it is quite likely that derived free radicals of the solvent molecules from transfer reactions are resonance-stabilized and are destroyed by mutual interaction or dimerization before they initiate a new chain. This argument appears to be in line with the results obtained in which —COOH content was found to be decreasing with increasing concentrations of the

TABLE II
Determination of Number of COOH Endgroups in the Polymerization
of Ethyl Acrylate with Formic, Acetic and *n*-Butyric Acids

Acid	Optical density at 515 m μ ^a	Corresponding formic acid concentration (10 ⁻⁶ N)	Molecular wt. of the polymer (10 ⁶)	End- groups/chain
Formic acid	0.581	0.34	4.76	1.90
	0.556	0.30	3.20	0.91
	0.662	0.51	2.13	1.03
	0.869	0.93	1.71	1.43
Acetic acid	0.632	0.45	0.96	0.51
	0.665	0.51	0.79	0.32
	0.887	0.96	0.52	0.43
	0.590	0.36	0.36	0.12
<i>n</i> -Butyric acid	0.520	0.25	0.83	0.16
	0.488	0.15	0.62	0.08
	0.655	0.50	0.40	0.12
	0.584	0.35	0.32	0.07

^a Blank (optical density for polymer obtained in the absence of acid) 0.406.

solvent and might be due to increased participation of solvent molecules in transfer reactions at higher concentrations. The inability of derived solvent radicals to initiate a new chain and their subsequent destruction resulting in low overall rates of polymerization (R_p) may account for the low R_p values obtained in acetic acid medium which were reported a little earlier. In order to check up the effect of poor reinitiating capacity of the derived radicals from acetic acid on transfer as calculated from the conventional method, a set of experiments was carried out with 2,2'-azobisisobutyronitrile as an initiator at 80°C. The rates of polymerization were, more or less, identical with those obtained in other solvents. Compared to methyl acrylate radical, ethyl acrylate radical due to its bulky ester group is expected to be more stabilized but compared to ethyl methacrylate radical it is less so. Values of solvent transfer constants in ethyl acrylate should, therefore, be in between methyl acrylate and ethyl methacrylate. Experimental values of transfer constants for solvents in ethyl acrylate, as seen from Table I, are invariably higher than those of methyl acrylate or ethyl methacrylate. The high C_s value for ethyl acrylate compared to that of ethyl methacrylate may be due to higher resonance stabilization in the latter case, an effect from hyperconjugation with the CH₃ group at the α -carbon atom on the ethylene double bond in conjunction with C=O bonds. This obviously cannot be a complete picture, since styrene, which is heavily stabilized by resonance, has high transfer constants. Apart from the steric factor and bond strength, the propagation rate constant does influence the C_s value to a great extent. It is quite probable that the propagation rate constant for ethyl acrylate is rather low compared to methyl acrylate or ethyl methacrylate. In fact, we can arrive at the same conclusion from a comparison of δ values for these monomers.¹ At 50°C, ethyl

methacrylate has a δ value of 9.43,¹⁵ whereas methyl and ethyl acrylates have δ values of 2.49⁶ and 2.13,¹ respectively and the only logical explanation, therefore, appears to be a low value of k_p for ethyl acrylate compared to the other two monomers. This point can be clarified only by measurement of absolute propagation rate constant which, unfortunately, we are unable to determine.

The authors acknowledge their gratitude to Prof. Santi R. Palit for helpful discussions and encouragement. One of the authors (P. V. T. R.) is grateful to the Council of Scientific and Industrial Research, New Delhi for their financial help. Thanks are due to Mr. Sailes Mukhopadhyay for his assistance in endgroup studies.

References

1. P. V. T. Raghuram and U. S. Nandi, *J. Polym. Sci. A-1*, **5**, 2005 (1967).
2. A. Weissberger and E. S. Proskauer, Eds., *Organic Solvents*, Interscience, New York, 1955.
3. Y. Hachihama and H. Sumitomo, *Technol. Repts. Osaka Univ.*, **5**, 485 (1956).
4. S. R. Palit and P. Ghosh, *J. Polym. Sci.*, **58**, 1225 (1962).
5. S. R. Palit, U. S. Nandi, and N. G. Saha, *J. Polym. Sci.*, **14**, 295 (1954).
6. J. N. Sen, U. S. Nandi, and S. R. Palit, *J. Indian Chem. Soc.*, **40**, 729 (1963).
7. S. R. Chatterjee, S. N. Khanna, and S. R. Palit, *J. Indian Chem. Soc.*, **41**, 622 (1964).
8. S. Basu, J. N. Sen, and S. R. Palit, *Proc. Roy. Soc. (London)*, **A202**, 485 (1950).
9. R. A. Gregg and F. R. Mayo, *Disc. Faraday Soc.*, **2**, 328 (1947).
10. M. S. Kharasch, J. L. Rowe, and W. H. Urry, *J. Org. Chem.*, **16**, 905 (1951).
11. W. G. Moore and H. S. Taylor, *J. Chem. Phys.*, **8**, 466 (1940).
12. D. P. Evans and J. J. Gordon, *J. Chem. Soc.*, **1938**, 1434.
13. M. S. Kharasch and M. T. Gladstone, *J. Amer. Chem. Soc.*, **65**, 15, (1943).
14. A. Fry, B. M. Tolbert, and M. Calvin, *Trans. Faraday Soc.*, **49**, 1944 (1953).
15. S. N. Khanna, S. R. Chatterjee, U. S. Nandi, and S. R. Palit, *Trans. Faraday Soc.*, **58**, 1827 (1962).
16. D. H. Hey and W. A. Waters, *Chem. Rev.*, **21**, 179, (1937).
17. S. R. Palit, *Makromol. Chem.*, **36**, 89 (1959); **38**, 96 (1960).
18. S. R. Palit, *Chem. and Ind. (London)* 1531 (1960).

Received September 6, 1958

Revised February 25, 1969

Block Polymers of Isocyanates and Vinyl Monomers by Homogeneous Anionic Polymerization

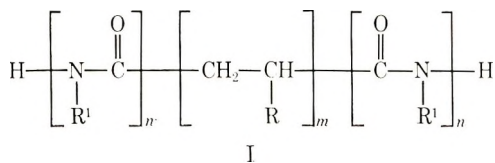
R. A. GODFREY and G. W. MILLER, *Mobay Chemical Company,
Pittsburgh, Pennsylvania 15205*

Synopsis

The "living" polymer method was used to prepare block polymers of vinyl monomers and isocyanates at low temperatures in toluene-tetrahydrofuran mixtures. Vinyl monomers and diisocyanates, which have one hindered isocyanate group, as in 2,4-toluene diisocyanate, form block polymers which contain pendant reactive isocyanate groups. These block polymers can be crosslinked with water, diols, diamines, etc. The polymerization is apparently limited to block polymer formation, since the polyisocyanate anion is incapable of initiating the polymerization of common vinyl monomers.

INTRODUCTION

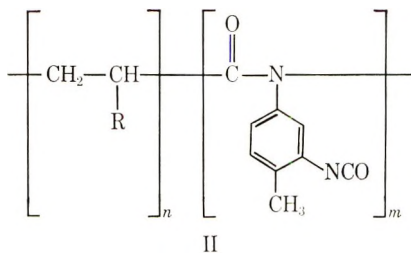
An investigation by Shashoua and co-workers¹ first revealed that monoisocyanates could be homopolymerized by an anionic mechanism at low temperatures to form *N*-substituted 1-nylons. Natta et al. have prepared crystalline 1-nylons of phenyl and *n*-butyl isocyanates.² The first attempts to copolymerize isocyanates with vinyl monomers were the subjects of patent applications. The first, by Furukawa and co-workers,³ alleged copolymerization by addition of various initiators to mixtures of vinyl monomers and diisocyanates in the temperature range of -78 to 60°C and reported obtaining insoluble, infusible products. The initiators used included triethylamine, phenylmagnesium bromide, and *n*-butyllithium. The second application was issued to Baker⁴ and involved the formation of block polymers of vinyl monomers and monoisocyanates. These block polymers have the structure BAB, where B is the *N*-substituted 1-nylon block and A is the polyolefin block (I)



These were prepared by initiation of the vinyl monomer with an electron-transfer type catalyst, such as sodium naphthalene, with formation of

propagating dicarbanions as taught by Szwarc et al.,⁵ there was subsequent addition of the isocyanate to the preformed "living" polymer.

The present investigation involved reactions between monoterminally living polymers and isocyanates to form AB block polymers. In extending these reactions to diisocyanates in which one isocyanate group was sterically hindered, as in 2,4-toluene diisocyanate, we obtained block polymers having pendant reactive isocyanate groups (II).



In contrast to electron-transfer type living polymer reactions, these reactions may be carried out in aromatic hydrocarbons as well as ethereal solvents or mixtures thereof.

Certain organolithium catalysts, such as *n*-butyllithium, have been shown to induce the formation of polymeric monocarbanions⁶⁻¹⁸ of vinyl monomers, such as styrene, isoprene, butadiene, and methyl methacrylate, which remain "living" in the absence of reactive impurities.

In the presence of even small quantities of polar solvents, especially ethers and tertiary amines, the rate of initiation is several orders of magnitude faster than the rate of propagation, and the initiation reaction is virtually complete before any measurable polymerization occurs.¹⁶⁻¹⁸ Therefore, after consumption of the original monomer, initiation of additional monomer or a second monomer is caused only by active polymeric chain ends.^{12,13}

This paper presents the synthesis, proof of block polymer formation, and some physical properties of these A-B block polymers of vinyl monomers and isocyanates. In addition, an attempt has been made to examine the scope and limitations of this reaction of isocyanate as well as to propose a probable mechanism for the polymerization.

EXPERIMENTAL

Purification of Reagents

Reagent grade toluene and tetrahydrofuran (THF) were refluxed over sodium for 4 hr, distilled under nitrogen, and stored over molecular sieve type 5-A. Methyl methacrylate (MMA) was washed once with a 5% aqueous NaOH solution and three times with distilled water. It was then allowed to stand over molecular sieve for at least 24 hr before distillation under vacuum immediately prior to the polymerization. Isoprene, styrene, butyl isocyanate, 2,4-toluene diisocyanate (TDI), and 1-methyl-2,4-

TABLE I
 Sources of Reagents

Reagent	Source
Styrene	Eastman Organic Chemicals
Isoprene	" " "
Methyl methacrylate	Matheson Scientific
<i>n</i> -Butyl isocyanate	" "
<i>n</i> -Butyllithium	" "
2,4-Toluene diisocyanate	Mobay Chemical Company
1-Methyl-2,4-diisocyanato cyclohexane	" " "

diisocyanato cyclohexane (HTDI) were fractionally distilled under nitrogen, and only the middle constant-boiling fraction of each was used. *n*-Butyllithium was obtained as a 15% solution in hexane and was used without further purification. Table I shows the sources of the reagents that were used.

Preparation of the Homopolymers

Polystyrene (PS), poly(methyl methacrylate) (PMMA), polyisoprene (PI), and the *N*-substituted I-nylon homopolymers were prepared by using *n*-butyllithium in a toluene-tetrahydrofuran mixture.

Preparation of the Block Polymers

Table II shows representative reaction conditions for each of the block polymerization systems. In a typical polymerization procedure, a 500-ml, three-necked flask was equipped with a stirrer, a vacuum outlet, an injection port, and a low-temperature thermometer for insertion in the reaction medium. The injection port consisted of a tube sealed with a rubber septum and inserted through a Teflon adapter having an O-ring seal. The flask was flamed while being evacuated to approximately 10^{-1} mm Hg and thereafter cooled in a Dry Ice-acetone bath. Toluene (70 ml), tetrahydrofuran (40 ml), and styrene (50 ml) were added by syringe and cooled with rapid stirring to about -50°C . *n*-Butyllithium (0.0063 mole) was added, and the solution assumed the characteristic red color of the styryl anion.⁴ The polymerization was carried to essentially 100% conversion and butyl isocyanate (50 ml) was added. The red color rapidly disappeared, and a marked increase in viscosity was observed over the next 2 hr. Methanol was then added, and the block polymer precipitated. It was filtered, washed twice with methanol (350 ml), and dried at 40°C in a vacuum oven.

In the polymerizations involving diisocyanates, the block polymers were precipitated and washed with hexane instead of methanol to avoid reaction with free isocyanate. Only those products which were insoluble in methanol or hexane were recovered, so that no attempt was made to recover cyclic trimer or unreacted isocyanate in this investigation.

TABLE II
 Block Polymerization Systems

Expt no	Vinyl Monomer		Isocyanate ^a			Solvent(s) ^b		Initiator	
	Type	Amt, ml	Type	Amt, ml	Temp, °C	Type	Amt, ml	Type	Amt, mole
1	Styrene	50	<i>n</i> -Butyl	50	-50	Toluene	50	<i>n</i> -BuLi	0.0063
						THF	50		
2	Styrene	70	<i>n</i> -Butyl	50	-50	Toluene	70	<i>n</i> -BuLi	0.0019
						THF	40		
3	Styrene	50	TDI	20	-60	Toluene	70	<i>n</i> -BuLi	0.0013
						THF	40		
4	Styrene	50	HTDI	30	-50	Toluene	100	<i>n</i> -BuLi	0.0025
						THF	50		
5	MMA	50	TDI	40	-50	Toluene	90	<i>n</i> -BuLi	0.0025
						THF	50		
6	Isoprene	40	TDI	30	-50	Toluene	75	<i>n</i> -BuLi	0.0025
						THF	65		

^a TDI = 2,4-toluene diisocyanate; HTDI = hydrogenated TDI.

^b THF = tetrahydrofuran.

Characterization of the Products

Block polymer compositions were determined by elemental analysis and products were identified on the basis of their infrared and solubility data. Infrared spectra were obtained from solution-cast films and KBr dispersion pellets on a Beckman IR-4 spectrophotometer. Apparent molecular weights and molecular weight distribution curves were obtained by using a Water's gel permeation chromatograph.

The solubility tests were made by placing 0.1 g of polymer in 4 ml of the desired solvent and stirring for several hours or until all the polymer had gone into solution. The solution was then filtered through a fritted glass filter under pressure and evaporated to dryness on a salt plate. An infrared spectrum was taken and compared to that of the original polymer. The polymer was termed soluble if no particles were observed upon passing a light beam through the solution before filtering and was said to be insoluble if the infrared spectrum of the filtrate (after evaporation of solvent) showed no absorption bands. The term slightly soluble indicates that a thin film was formed on the salt plate (0.01–0.03 g), and relatively soluble denotes about 50% dissolution of the polymer (0.04–0.06 g).

RESULTS AND DISCUSSION

In order to prove the formation of a block polymer of a vinyl monomer and an isocyanate we must show two things: that initiation of the isocyanate by the polymeric anion occurs, i.e., that both polymeric segments are present, and secondly, that the two polymeric segments are joined by a primary valence bond, i.e., that the product is indeed a block polymer and

not a mixture of homopolymers. The first of these requisites is satisfied by infrared absorption and elemental analysis data. The second is proven by solubility data.

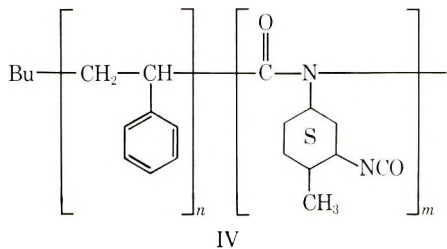
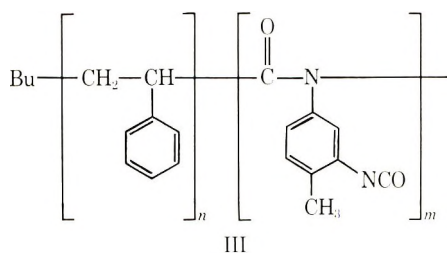
Infrared Analysis

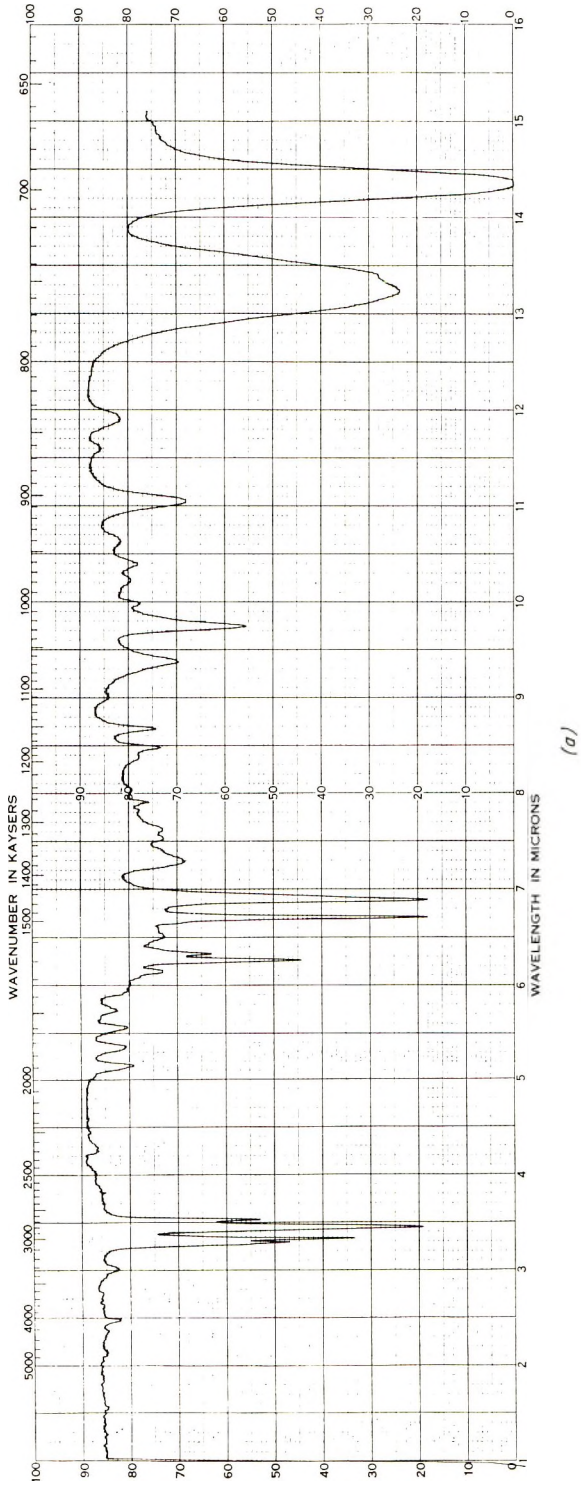
For most cases, the infrared spectrum of a block polymer does not differ from that of a mixture of homopolymers of the same composition,¹⁹ except in isolated cases, where absorption bands due to crystalline regions are observed.²⁰ However, if the infrared spectrum of the product is identical to that of a mixture of the two corresponding homopolymers, we can conclude, at least, that both polymeric segments are present.

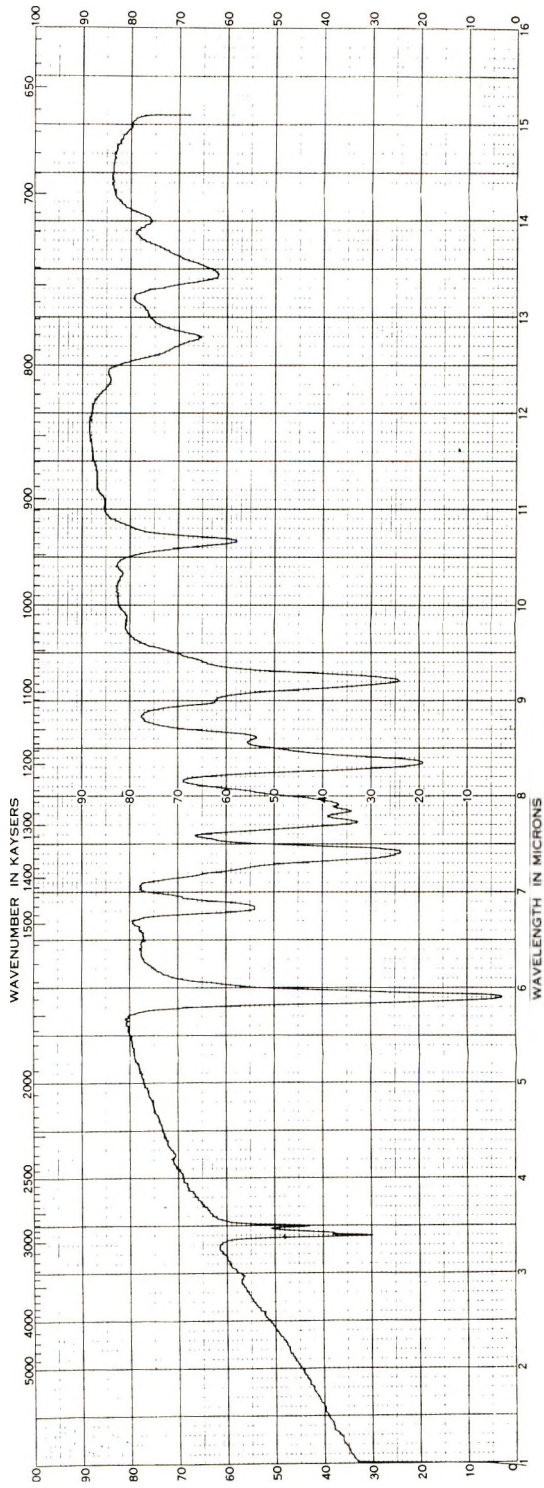
Figure 1 shows the infrared spectra for two representative systems. Here the infrared spectra of polystyrene and *N*-butyl 1-nylon are compared to that of poly(styrene-*b*-butyl isocyanate), and the infrared spectra of polystyrene and poly(TDI) are compared to that of poly(styrene-*b*-TDI). Table III summarizes the spectral data used to confirm the presence of both corresponding polymeric segments of each system. In every case, the block polymer contains the major absorption bands of each homopolymer.

In the systems styrene-RNCO, initiation of the isocyanate was evidenced also by the rapid disappearance of the characteristic red color of the polystyryl anion. Further polymerization was observed by a sharp increase in viscosity of the solution on addition of the isocyanate monomer to the polymeric anion.

The infrared spectra of block polymers of vinyl monomers and diisocyanates, such as TDI and HTDI, which have one hindered isocyanate group, indicated that they contain pendant isocyanate groups in the polymer side chain as shown in structures III and IV,

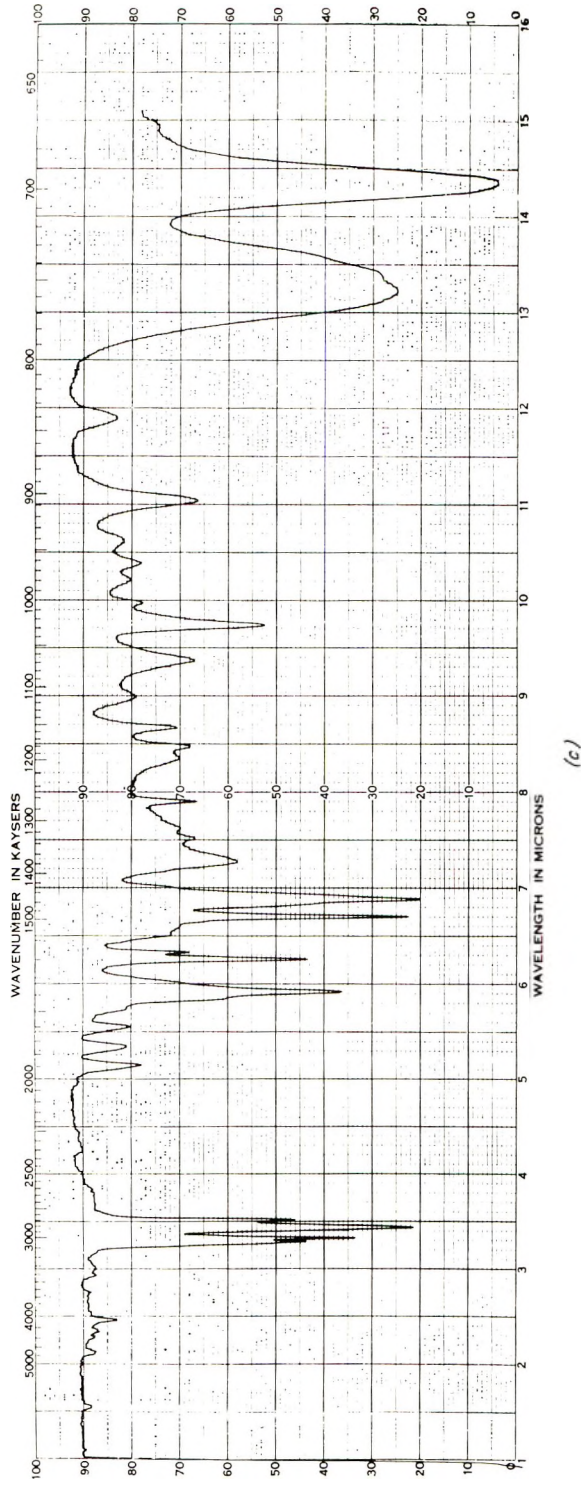




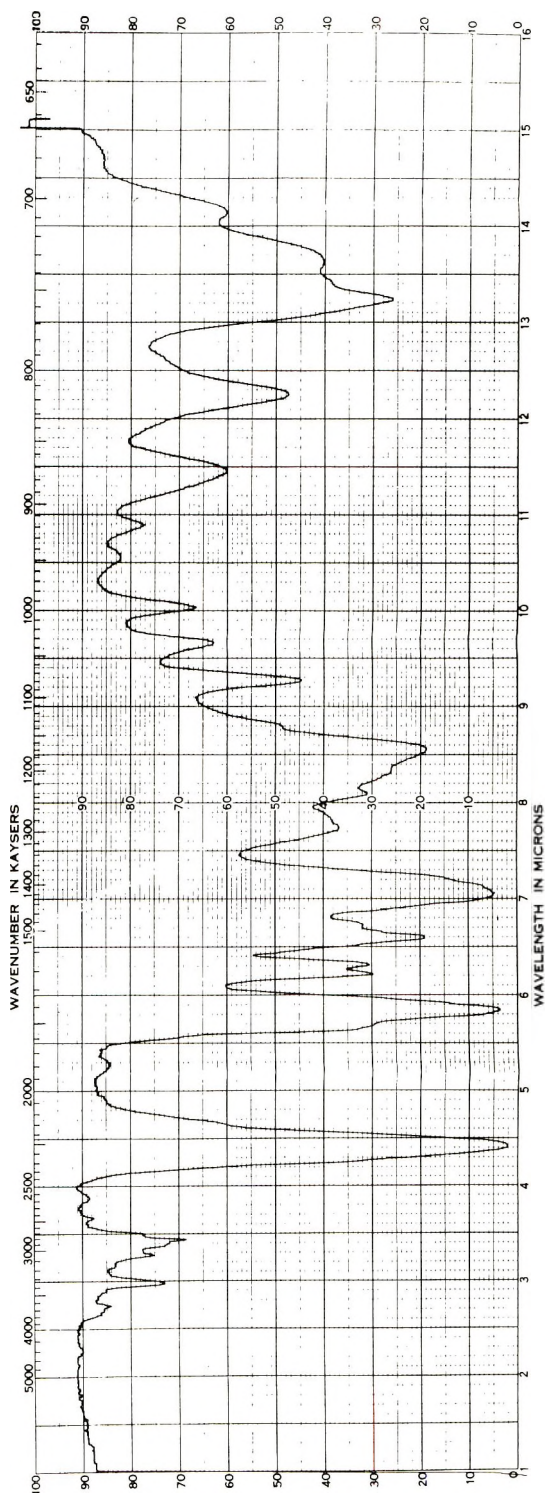


(b)

Figure 1 (continued)



(c)



(d)

Fig. 1 (continued)

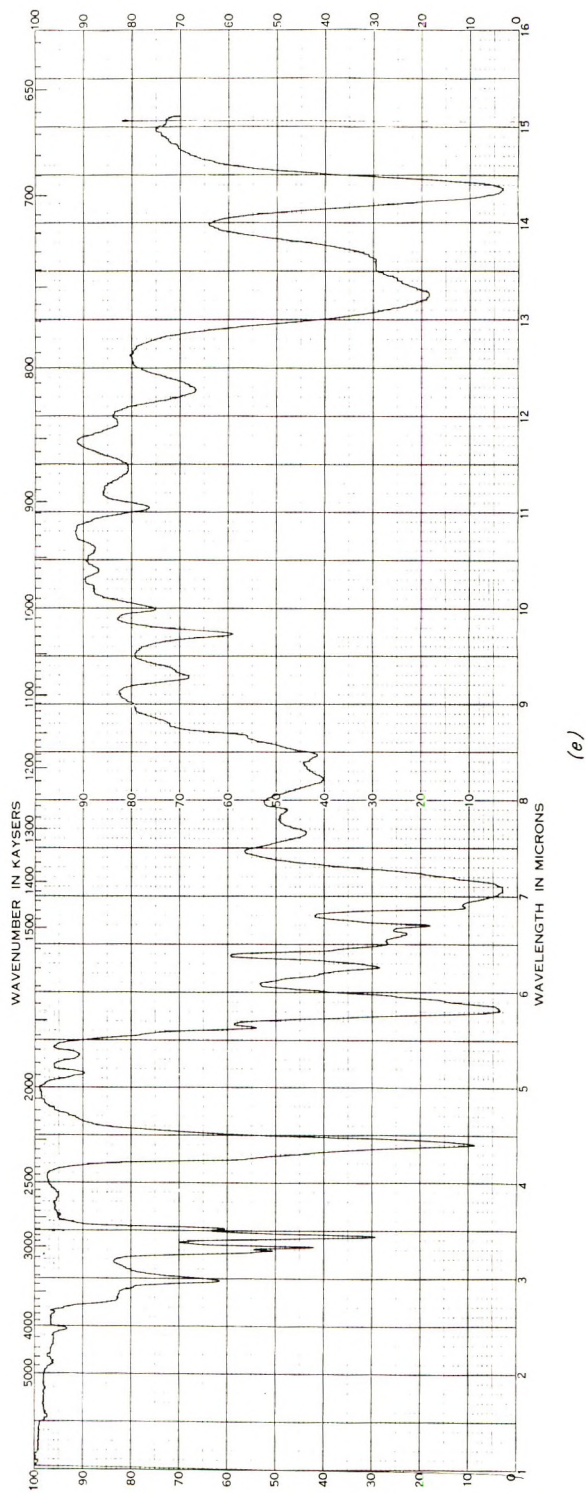


Fig. 1. Infrared spectra: (A) polystyrene, (B) poly(butyl isocyanate); (C) poly(styrene-b-butyl isocyanate); (D) poly(TDI); (E) poly(styrene-b-TDI).

TABLE IV
Elemental Analysis of the Block Polymers

Expt no	System	Composition mole ratio vinyl monomer to isocyanate	Calculated			Found		
			C, %	H, %	N, %	C, %	H, %	N, %
1	Styrene-BuNCO	13.6/1	90.17	7.84	0.92	89.83	7.88	0.92
2	Styrene-BuNCO	4/1	86.21	8.03	2.72	86.14	7.87	2.73
3	Styrene-TDI	4.15/1	83.35	6.49	4.74	83.21	6.14	4.73
4	Styrene-HTDI	5.2/1	84.92	6.69	3.92	83.88	6.85	3.85
5	MMA-TDI	0.17/1	61.84	3.89	14.89	61.20	4.08	14.15
6	Isoprene-TDI	0.036/1	62.41	3.59	15.87	61.64	4.01	15.74

whereas crosslinking occurred with diisocyanates such as 4,4'-diisocyanatodiphenylmethane, 4,4'-diisocyanatodicyclohexylmethane, and hexamethylene diisocyanate.

Furthermore, solubility characteristics of the block polymers with pendant —NCO groups indicated that they were not crosslinked. However, they were readily crosslinked with diols to form hard, tough, infusible, insoluble polymers.

Elemental Analysis

Overall compositions of the block polymers were determined by elemental analysis and were useful in proving the presence of both monomers. Table IV shows results obtained for the block polymers.

Solubility Properties

Positive differentiation between block polymer formation and a physical mixture of homopolymers was provided by an evaluation of the solubility characteristics of the polymers. Table V summarizes the experimentally determined solubility behavior of the block polymers and the corresponding homopolymers. Results for the vinyl homopolymers are substantiated in the literature.²¹

TABLE V
Solubility Properties of the Copolymers

Polymer	Solubility ^a							
	Acetone	Ethyl acetate	THF	DMF	MeCl ₂	Benzene	Toluene	Methyl ethyl ketone
Polystyrene	Ins	S	S	S	S	S	S	S
Polyisoprene	Ins	Ins			RS	RS	RS	Ins
<i>N</i> -Butyl 1-nylon	Ins	Ins	∓	Ins	RS	S	S	Ins
Poly(methyl Methacrylate)	S	S	∓		S	∓	S	S
TDI homopolymer	Ins	Ins	∓		S	SS	SS	Ins
HTDI homopolymer	Ins	Ins	∓	Ins	∓	∓	S	Ins
Styrene-BuNCO copolymer	Ins	∓	∓		∓	∓	S	S
Styrene-TDI	Ins	SS	∓		∓	RS	RS	SS
MMA-TDI	S	S	∓		∓	∓	S	S
Isoprene-TDI	Ins	Ins	SS		RS	SS	SS	Ins
Styrene-HTDI			∓	∓	S	∓	S	S

^a S = soluble, RS = relatively soluble, SS = slightly soluble, Ins = Insoluble

Styrene-Butyl Isocyanate. Polystyrene is soluble in *N,N*-dimethylformamide, ethyl acetate, and methyl ethyl ketone. *N*-Butyl 1-nylon is insoluble in each of these three solvents. The block polymer of styrene and butyl isocyanate, however, is soluble in each of these solvents, and yields clear, transparent films when these solutions are evaporated to dryness. Infrared analysis confirmed the presence of the 1-nylon segment.

Styrene-TDI. As seen in Table V, the solubility characteristics of the styrene-TDI block polymers are intermediate between those of the corresponding homopolymers, i. e., the block polymers showed partial insolubility in solvents in which polystyrene is soluble, and the homopolymer of TDI shows little, if any, solubility, (see ethyl acetate, benzene, toluene, and methyl ethyl ketone). The infrared spectra of the soluble portions, however, were identical to those of the insoluble products.

Styrene-HTDI. The block polymer of styrene and 1-methyl-2,4-diisocyanatocyclohexane is soluble in *N,N*-dimethylformamide, ethyl acetate, and methyl ethyl ketone, whereas the homopolymer of HTDI is insoluble in each of these three solvents.

MMA-TDI. The block polymer of MMA and TDI is soluble in ethyl acetate and methyl ethyl ketone, whereas the homopolymer of TDI is insoluble in each of these solvents.

Isoprene-TDI. The solubility behavior of the block polymer is intermediate between that of the corresponding homopolymers, but the infrared spectra of the soluble and insoluble fractions are identical.

In every case, repeated reprecipitation of the products did not alter their infrared spectra.

Solution-cast films of the block polymers differed considerably in appearance and properties from those of physical mixtures of the two corresponding homopolymers. More noticeable differences were apparent with melt-cast films. Whereas inhomogeneities and areas of opacity were characteristic of films of the physical mixtures, films of the block polymers were homogeneous and in most cases transparent.

Molecular Weight Distribution

Generally, the block polymers displayed narrow molecular weight distributions typical of anionic polymerizations in which the initiation step is rapid.¹⁶⁻¹⁸ Wider distributions were observed for those which began to precipitate towards the end of the polymerization. In Figure 2 are the gel permeation chromatograms of a styrene-butyl isocyanate block polymer and a styrene-TDI block polymer both prepared using *n*-butyllithium. The styrene-butyl isocyanate block polymer had a polydispersity of 1.14 (Fig. 2A) while that of the styrene-TDI block polymer was 1.55 (Fig. 2B). The higher value for the styrene-TDI system can be attributed to precipitation of the block polymer formed after addition of TDI. Table VI illustrates experimental values for molecular weights and polydispersities of the block polymers. These were estimated from gel permeation chromatograms in the following manner. Scale models of the block polymers were constructed from the compositions determined by elemental analysis, and, from these models, average *Q* values were determined. The factor *Q* represents the number of molecular weight units equivalent to one angstrom of effective molecular size. Calculations for \bar{M}_w and \bar{M}_n were then made from a calibration curve based on GPC standards. These calculations

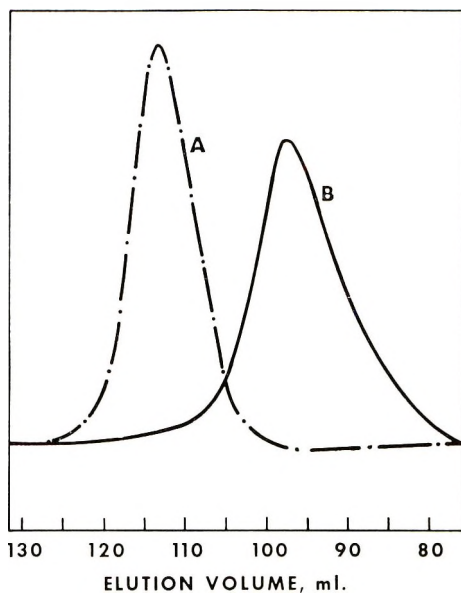


Fig. 2. Gel-permeation chromatograms of (A) poly(styrene-*b*-butyl isocyanate) and (B) poly(styrene-*b*-TDI).

and the basic principles of gel-permeation chromatography are described in several sources.²²⁻²⁵

The following example illustrates a recheck on the reliability of these results. A styrene-TDI block polymer was shown by elemental analysis to have a composition of 4.15 styrene monomers per TDI monomer, giving a calculated 7.10% isocyanate and an equivalent weight of 592. Its molec-

TABLE VI
Molecular Weight Distribution of the Block Polymers

System	\bar{M}_w	\bar{M}_n	\bar{M}_w/\bar{M}_n
Styrene-BuNCO	8 529	7 481	1.14
Styrene-BuNCO	48 200	41 100	1.17
Styrene-TDI	48 945	31 629	1.55
Styrene-HTDI	48 900	40 700	1.20
MMA-TDI	25 100	16 900	1.49
Isoprene-TDI	22 700	14 100	1.61

TABLE VII

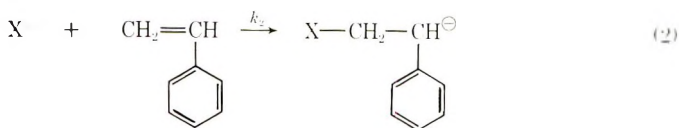
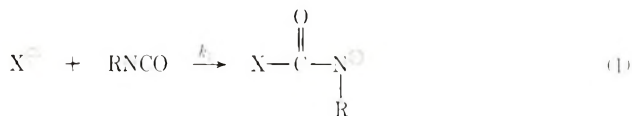
Method	NCO, %	Equivalent weight	Functionality
Elemental analysis	7.10	592	—
Calculation from molecular weight	6.92	602	80.7
Dibutylamine titration	7.4	567	—

ular weight (\bar{M}_n) was estimated to be 48945. The number of TDI monomers per chain calculated from the molecular weight, and number of moles of *n*-butyllithium (0.0013), assuming all of the styrene had been consumed, was 80.7, giving a per cent isocyanate of 6.92% and an equivalent weight of 607. Dibutylamine titration of the free NCO gave values of per cent isocyanate and equivalent weight in good agreement of 7.4% NCO and 567. These results are summarized in Table VII.

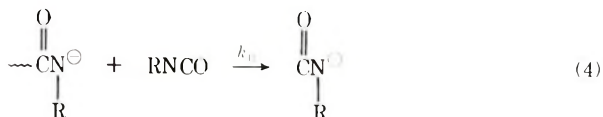
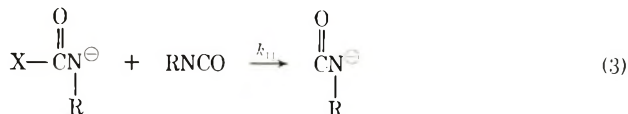
Mechanism of the Copolymerization

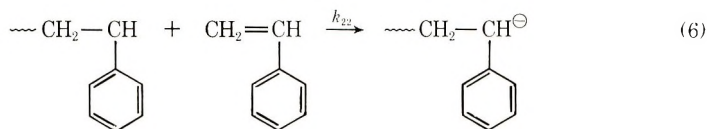
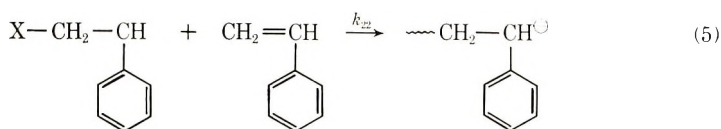
In an anionic copolymerization system, the types of structures possible (random, block, etc.) depend on the relative tendency of the monomers to undergo anionic polymerization. As the reactivity of the monomer increases, however, the reactivity or basicity of the resulting anion decreases, i.e., the more easily polymerizable monomers such as acrylonitrile and methyl methacrylate form weaker polymeric anions than the less easily polymerized monomers, such as styrene and butadiene. Observations during this study suggest that isocyanates are considerably more anionically polymerizable than most common vinyl monomers, and form correspondingly weaker anions, i.e., copolymerizations with simultaneous addition of both monomers yielded products which contained very little, if any, vinyl monomer. This is not surprising when we consider that isocyanates can be homopolymerized easily with bases which are ineffective for most common vinyl monomers¹ and that isocyanates are highly susceptible to other modes of nucleophilic attack. Therefore, we would expect that once a chain is terminated by the anion of an isocyanate, monomers such as styrene and MMA will no longer add. The reaction scheme shown in eqs. (1)–(9) is probable.

Initiation:

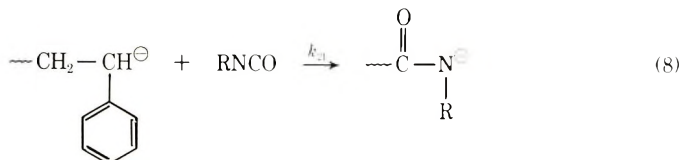
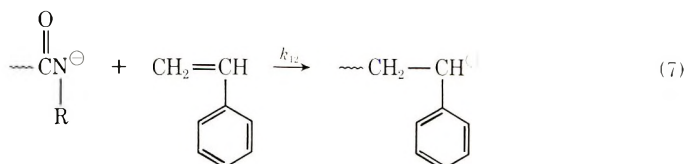


Propagation:

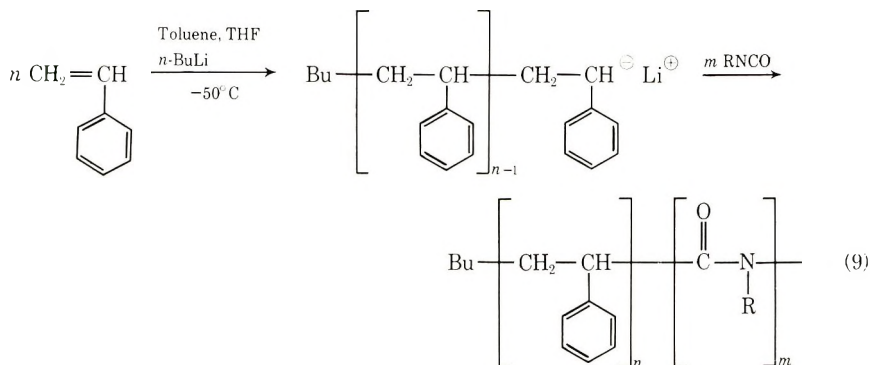




Crossover:

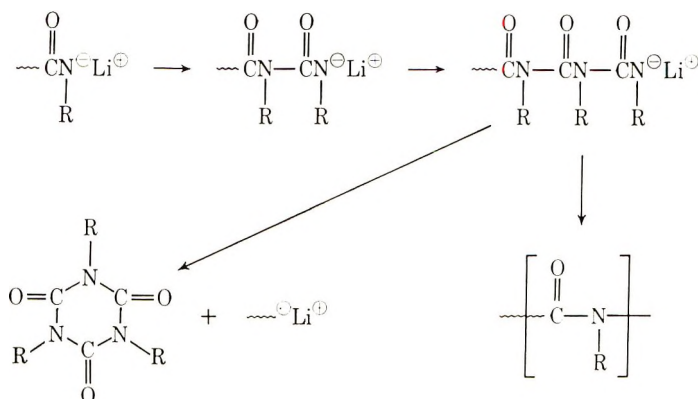


Here $k_{12} = 0$, as previously suggested. However, if we first initiate the vinyl monomer and carry it to a desired molecular weight, and if the chain ends remain active, addition of an isocyanate yields a block polymer of the structure A-B [eq. (9)].



Thus, the block polymerization of isocyanates and vinyl compounds can be viewed as an isocyanate homopolymerization with a polymeric anion as initiator.

Once the isocyanate anion is formed, the propagation step is believed to be continued until the linear trimer stage.¹ Then, there are two paths for reaction open: (a) cyclization with the release of the initiating anion to give trimer, or (b) reaction with more monomer to give linear polymer.



Polymer formation is favored at low temperatures ($< -20^{\circ}\text{C}$), while isocyanurate formation is favored at high temperatures.

The authors wish to thank Messrs. O. L. Sheaffer, R. L. Haradzin, P. L. Bonnaure, and C. Crookshanks for their assistance in obtaining the necessary data for this publication. We also thank Mobay Chemical Company for permission to publish this work.

References

1. V. E. Shashona, W. Sweeny, and R. F. Tietz, *J. Am. Chem. Soc.*, **82**, 866 (1960).
2. G. Natta, J. D. Pietro, and M. Cambini, *Makromol. Chem.*, **56**, 200 (1962).
3. J. Furukawa, S. Yamashita, and H. Okamoto, Japan Patent 7146/63 (1963).
4. W. P. Baker, Jr., U.S. Patent 3,225,119 (1965).
5. M. Szwarc, M. Levy, and R. Milkovich, *J. Am. Chem. Soc.*, **78**, 2656 (1956).
6. A. V. Tobolsky and C. E. Rogers, *J. Polym. Sci.*, **38**, 205 (1959).
7. *Ibid.*, **40**, 73 (1959).
8. R. S. Stearns and L. E. Forman, *J. Polym. Sci.*, **41**, 381 (1959).
9. F. J. Welch, *J. Am. Chem. Soc.*, **81**, 1345 (1959).
10. *Ibid.*, **82**, 6000 (1960).
11. R. K. Graham, D. L. Dunkelberger, and W. E. Goode, *J. Am. Chem. Soc.*, **82**, 400 (1960).
12. R. K. Graham, D. L. Dunkelberger, and E. S. Cohn, *J. Polym. Sci.*, **42**, 501 (1960).
13. C. Geacintov, J. Smid, and M. Szwarc, *J. Am. Chem. Soc.*, **83**, 1253 (1961).
14. D. L. Glusker, E. Stiles, and B. Yoncoskie, *J. Polym. Sci.*, **49**, 297 (1961).
15. D. M. Wiles and S. Bywater, *Polymer*, **3**, 175 (1962).
16. M. Morton, E. E. Bostick, R. A. Livigni, and L. J. Fetters, *J. Polym. Sci.*, **A1**, 1735 (1963).
17. M. Morton and L. J. Fetters, *J. Polym. Sci.*, **A2**, 3311 (1964).
18. M. Morton, L. J. Fetters, and E. E. Bostick, *J. Polym. Sci.*, **C1**, 311 (1963).
19. G. Guiochon and J. Hennicker, *British Plastics*, February, 1964.
20. G. E. Ham, Ed., "Copolymerization," Interscience Publishers, New York, N. Y., 1964, pp. 231-232.
21. J. Brandrup and E. H. Immergut, "Polymer Handbook," Interscience Publishers, New York, N. Y., 1966, pp. 189-202.
22. J. Cazes, *J. Chem. Ed.*, **43**, (7) A 567 (1966).
23. L. E. Maley, *J. Polym. Sci.*, **C8**, 253 (1968).
24. Bulletin No. 2-2064, Waters Associates, Inc., 61 Fountain Street, Framingham, Mass.
25. J. C. Moore, *J. Polym. Sci.*, **A2**, 1835 (1964).

Received December 31, 1968

Cationic Polymerization Behavior of Hydroxystyrenes

MASAO KATO, *The Textile Research Institute of the Japanese Government, Yokohama, Japan*

Synopsis

Solution polymerizations of *o*-, *m*- and *p*-hydroxystyrene with boron trifluoride etherate were investigated. The results of infrared and ultraviolet spectroscopic investigations of the polymers thus obtained indicate that *p*-hydroxystyrene polymer consisted mainly of the structure formed through the normal vinyl polymerization mechanism, whereas *o*- and *m*-hydroxystyrene polymers contained considerable portions of the structures due to the reaction of the vinyl group with the phenol nucleus. The rate of polymerization and the intrinsic viscosity of the polymer decreased in the order *p*-hydroxystyrene \gg *o*-hydroxystyrene $>$ *m*-hydroxystyrene. It was of interest that on the cationic polymerization only *p*-hydroxystyrene gave polymer of high molecular weight. Plausible polymerization mechanisms were considered. Solid-state polymerization of *p*-hydroxystyrene at solid carbon dioxide temperature with the use of boron trifluoride etherate was also investigated. Appreciable polymerization occurred only at fairly high catalyst concentrations.

INTRODUCTION

The present investigation was undertaken in order to study the polymerization of *o*-, *m*-, and *p*-hydroxystyrene initiated by cationic catalyst (boron trifluoride etherate).

In the previous paper,¹ it was suggested that in the radical polymerization with azobisisobutyronitrile these hydroxystyrene monomers polymerized through almost the normal vinyl polymerization mechanism, although a somewhat anomalous reaction mechanism was noted for *o*-hydroxystyrene. On the other hand, in the case of cationic polymerization it was found that the polymerization of *o*- and *m*-hydroxystyrene proceeded not only through the normal polymerization reaction but also to a considerable extent through reaction between the vinyl group and the phenol nucleus; however *p*-hydroxystyrene followed only the normal vinyl polymerization mechanism and gave polymer with very high intrinsic viscosity which could not be reached by the radical polymerization.

EXPERIMENTAL

Materials

o-Hydroxystyrene (OHS), *m*-hydroxystyrene (MHS) and *p*-hydroxystyrene (PHS) were synthesized according to the methods described in the previous papers.^{1,2} These monomers were purified just before use.

Ethylene chloride and methylene chloride (the solvents for solution polymerization) and *n*-hexane (dispersant for solid-state polymerization of PHS) were distilled over phosphorus pentoxide.

Boron trifluoride etherate (BTE) catalyst was purified by distillation, bp 126°C.

OHS, MHS, and PHS model polymers^{1,2} were used as control samples.

Polymerization

Solution Polymerization. Solvent and monomer were measured into a flask, which was then sealed with a serum stopper. The flask was immersed in a thermostatted bath. Catalyst solution prepared by dilution of BTE with the same solvent was injected through the stopper into the flask. Mild intermittent shaking was given during the course of polymerization.

After the polymerization, the catalyst was neutralized by adding a small amount of methanolic ammonia. Solvent was removed under reduced pressure, and the residue was dissolved in methanol. Isolation of OHS and PHS polymers was carried out by pouring the polymer solutions into vigorously stirred water in the case of high conversion. When the conversion was low, the solution was treated by the procedure described in the previous paper.² Polymers thus precipitated were filtered and rinsed with water followed by drying *in vacuo* at 50°C. In the case of MHS polymer, the solution was poured into a large excess of petroleum ether, and oily product thus isolated was separated by centrifugation. The product was washed twice with hot water, and then dried *in vacuo* at 50°C. (Therefore, it was inevitable that this product contained some impurities.) Slightly tacky polymers were obtained.

Solid-State Polymerization. *n*-Hexane and vacuum-dried PHS crystals were measured into a flask which was sealed with a serum stopper. The flask was cooled to -78°C in a bath of methanol and solid carbon dioxide, and the contents were stirred with a magnetic stirrer. BTE was introduced, and stirring was continued at this temperature for 8 hr, after which the flask was stored in a jar with solid carbon dioxide. After the polymerization, a small amount of methanolic ammonia was added to the flask with stirring. The contents was filtered, and the filtrate was extracted three times with chloroform. The residue was filtered, rinsed with chloroform and then with water and subsequently dried at 50°C.

Characterization of Polymer

Measurements of viscosity and infrared and ultraviolet spectra of the polymers were carried out by the methods used in the previous work.¹ Molecular weight determinations were made by using a Mechrolab vapor-pressure osmometer. Tetrahydrofuran was used as solvent. The x-ray diffraction spectra of the powdered polymers were measured by means of a Rigaku Denki Co. Ltd. Model D-3F x-ray diffraction apparatus.

RESULTS AND DISCUSSION

Solution Polymerization

Polymerization conditions and the results of the polymerizations are listed in Table I. Most of the polymers were isolated from solution after polymerization, except when conversion was low (all MHS polymers and an OHS polymer). The polymerizations of PHS went to completion very rapidly. The rate of polymerization for OHS appeared to be significantly slower than that for PHS but considerably faster than that for MHS. Dependence of the molecular weight was independent on the polymerization conditions in the case of OHS and MHS. The molecular weight for the MHS polymers seems to be relatively lower. This may be due to the purification method used for the polymer. It is remarkable that only PHS gave a polymer with a very high intrinsic viscosity which could not be reached by the radical polymerization.¹ Furthermore, Table I shows that only PHS follows the normal vinyl polymerization mechanism. If polymerization of PHS was to be conducted in suitable solvents capable of dissolving the resulting polymers, polymers of higher molecular weight might be produced. The x-ray diffraction profile of the PHS polymer did not show any crystalline peaks.

The infrared spectra of MHS and PHS polymers and the corresponding model polymers were compared. The spectrum of OHS polymer has been discussed in a previous paper.² The infrared spectrum of PHS polymer corresponded perfectly with that of the PHS model polymer and indicated that the polymerization of PHS by the cationic mechanism as well as the radical one gives polymer consisting mainly of normal vinyl-type polymer. On the contrary, some differences were observed between the spectra of

TABLE I
Cationic Polymerizations of *o*-, *m*-, and *p*-Hydroxystyrene

Monomer	Sol-vent ^a	Monomer concn, %	BTE, % based on monomer	Temp, °C	Time, min	Conversion, %	$[\eta]$, dl/g	MW
OHS	EC	33.3	2.9	-30	120	98	0.061	—
OHS	MC	33.3	8.5	-15	900	94	0.066	3900
OHS	MC	22.2	0.2	-22	120	29	0.043	—
MHS	MC	20.0	3.0	-20	120	20	—	—
MHS	MC	20.0	3.0	-20	1140	54	0.040	—
MHS	MC	20.0	3.0	3	120	18	0.037	710
MHS	MC	20.0	0.3	-40	120	trace	—	—
PHS	MC	25.0	3.0	10	10	96	0.345	—
PHS	MC	20.0	3.0	12	5	93	0.330	—
PHS	MC	16.7	0.2	12	5	95	0.505	—
PHS	MC	3.2	0.2	-22	60	93	0.545	—

^a EC = ethylene chloride; MC = methylene chloride.

MHS polymer and the MHS model polymer. Two absorption bands with medium intensity at 820 and 1110 cm^{-1} , which are absent in the model polymer and the monomer, might be attributable to the 1,2,4-trisubstituted aromatics. In the case of OHS polymer prepared by the polymerization with BTE, an absorption possibly due to the 1,2,4-trisubstituted aromatics was noted at 890 cm^{-1} as a weak band.²

Ultraviolet spectra of OHS, MHS, and PHS polymer and the model polymers were also compared. Again, the spectrum of PHS polymer corresponded perfectly with that of the PHS model polymer. On the other hand, the spectra of OHS and MHS polymer were considerably different from those of the corresponding model polymers: the absorption maxima of these cationically obtained polymers were shifted toward higher wavelength as shown in Table II; in addition, shapes of the absorption curves of the polymers changed considerably. With reference to the previously established ultraviolet spectra,¹ these results appear to suggest that OHS and MHS polymers contain considerable portions of structures caused by the substitution of phenol nucleus, especially by the substitution of the *para* position with respect to the hydroxyl group.

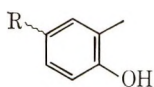
TABLE II
Absorption Maxima of Ultraviolet Spectra for Cationically
Obtained *o*-, *m*-,
and *p*-Hydroxystyrene Polymers and Model Polymers in Absolute Ethanol

	$\lambda_{\text{max}}, \text{m}\mu$	
	Model polymer	Polymer
OHS	275	280
MHS	274	281
PHS	279	279

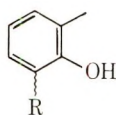
These infrared and ultraviolet spectroscopic investigations indicate that the polymerization of PHS takes place almost exclusively through the normal vinyl polymerization mechanism. On the other hand, the polymerization of OHS and MHS proceeds through the reaction between the vinyl group and the phenol nucleus, in addition to the one between the vinyl groups.

The structures due to the substitution of phenol nucleus in OHS and MHS polymers obtained by the cationic polymerization with BTE are shown as I-V.

OHS polymer:

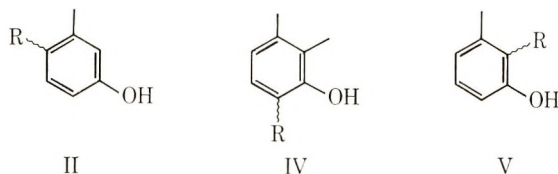


I

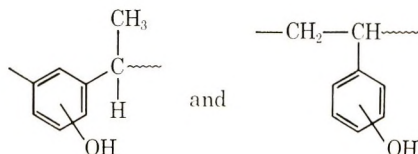


II

MHS polymer:



where *R* may be



Owing to steric hindrance, contributions of the structure V for MHS polymer might be few, if any. It might be presumed that these structures cause formation of highly branched polymers.

The vinyl groups in OHS and PHS are more negative than that in MHS, since the hydroxyl group can exert an influence to the vinyl group by conjugation only when it is in the *ortho* or *para* position. Hence, OHS and PHS should be more susceptible to cationic catalyst than MHS. In the case of OHS, some steric hindrance may be induced because the hydroxyl group is located adjacent to the vinyl group. Accordingly, the reactivity between the vinyl groups decreases in the order PHS > OHS > MHS. On the other hand, the phenol nucleus itself is also susceptible toward electrophilic reagents. Such reactivity might decrease in the order MHS > OHS > PHS, because of the number of reaction sites and the fact that the reactivity of the *para* position with respect to the hydroxyl group is stronger than the *ortho* position. Thus competition between the reactions of two vinyl groups and the vinyl versus the nucleus may be induced, namely, the lower the reactivity, for the vinyl, the more the structure caused by the latter reaction increases. Thus, it is anticipated that the rate of polymerization, the degree of polymerization, and the contribution of structures formed through the vinyl polymerization mechanism decrease in the order PHS > OHS > MHS (actually, PHS \gg OHS > MHS). This agrees well with the experimental evidence.

Because of the uncertainty of the mechanism of catalytic action in these systems, no detailed explanation of the polymerization mechanism has been offered.

It has been reported³ that the cationic copolymerization of OHS with ethyl vinyl ether with the use of BTE proceeds smoothly but the results in a polymer of low molecular weight. However, copolymerization of PHS with ethyl vinyl ether with the use of BTE appears to give polymer of relatively higher molecular weight. For example, an equimolar copolymerization conducted in methylene chloride at -22°C with the use of 0.2% of BTE gave a 95% yield of a polymer having an intrinsic viscosity of 0.384 dl/g.

Solid-State Polymerization of PHS

Brief experiments on solid-state polymerization of PHS with the use of BTE as catalyst were carried out at solid carbon dioxide temperature. The polymerization conditions and the results of polymerization are given in Table III. The polymerization was successfully effected at high catalyst concentration but little reaction occurred at lower catalyst concentrations. The infrared spectrum of the polymer thus produced showed the same pattern with as that of the polymer obtained by the solution polymerization. The x-ray diffraction profile of the polymer did not show any crystalline peaks.

TABLE III
Cationic Solid-State Polymerization of *p*-Hydroxystyrene

Weight ratio, monomer/dispersant ^a	BTE, % based on monomer	Temp, °C	Time, hr	Conversion, %	[η], dl/g
1/20	5.0	-78	24	43	0.157
1/20	0.3	-78	66	trace	—

^a *n*-Hexane.

Grateful acknowledgement is made to Prof. S. Okajima of Tokyo Metropolitan University and Dr. M. Hasegawa of our laboratory for kind advice.

References

1. M. Kato, *J. Polym. Sci. A-1*, in press.
2. M. Kato and H. Kamogawa, *J. Polym. Sci. A-1*, **4**, 1773 (1966).
3. M. Kato and H. Kamogawa, *Kogyo Kagaku Zasshi*, **71**, 587 (1968).

Received November 15, 1968

Revised January 20, 1969

NOTES

Copolymerization of Acrylonitrile or Other Polar Monomer Complexes with Olefins or Other Vinyl Monomer

Iirooma et al.¹ obtained alternating copolymers of acrylonitrile and ethylene, propylene, and other olefins in the presence of various alkylaluminum compounds.

The purpose of the present paper is to study complex copolymerization of acrylonitrile, methyl methacrylate, or other polar monomers with olefins or other vinyl monomers.

The yield of the acrylonitrile-propylene copolymer was studied in relation to mole ratio of ethylaluminum dichloride to acrylonitrile. The polymerization experiments were carried out in a toluene at -78°C and at room temperature (for the copolymerization of pure acrylonitrile-ethylaluminum dichloride complex). After the reaction had been completed (60 min), a large amount of methanol was added, the polymer was filtered off, washed with methanol, and dried *in vacuo* at 30°C .

As demonstrated by elemental analysis data, equimolecular copolymers were formed at all mole ratios investigated. Infrared spectra of these copolymers are very similar. No homopolymers of either acrylonitrile or propylene were obtained.

The data show that it is a pure complex of acrylonitrile with ethylaluminum dichloride that copolymerizes with propylene, i.e., no initiator is involved. Free uncomplexed acrylonitrile distinctly decreases the yield of copolymerization. With the acrylonitrile completely complexed by ethylaluminum dichloride (mole ratio 1:1), the copolymer is obtained in the maximum yield. An excess of dichloride does not enhance the copolymer yield.

The acrylonitrile-ethylaluminum dichloride complex was also found to copolymerize with vinyl chloride (Table I). Elemental analyses showed the copolymers obtained to be composed of equimolecular quantities of acrylonitrile and vinyl chloride. Their infrared spectra are very similar. Neither acrylonitrile nor vinyl chloride was found to homopolymerize in the prevailing conditions. Earlier we established that with aromatic hydrocarbons as solvents, vinyl chloride reacts with methylaluminum dichloride (a Friedel-Crafts reaction) at -78°C to yield aliphatic and aromatic hydrocarbons and aluminum chloride.² Ethylaluminum dichloride reacts with vinyl chloride in a similar manner. If the dichloride is complexed by benzonitrile, such a reaction fails to proceed. During the copolymerization in a toluene solution, vinyl chloride was found not to react with the acrylonitrile-complexed ethylaluminum dichloride, and thus formation of the copolymer is possible.

The present studies showed that in the presence of organoaluminum compounds methyl methacrylate does not copolymerize with ethylene, propylene, isobutylene, and vinyl chloride. The polymerization experiments were carried out in toluene at -35°C and -78°C . As organoaluminum compound ethylaluminum dichloride, diethylaluminum chloride, and triethylaluminum were examined. The mole ratio of these compounds to methyl methacrylate was equal to 1 or 2, and an excess of the olefin or vinyl chloride in relation to methyl methacrylate was used. None of these monomers was found to homopolymerize under the conditions used. With no methyl methacrylate present in the reaction mixture, isobutylene and propylene polymerized under the action of ethylaluminum dichloride. With the methacrylate present in a toluene solution, vinyl chloride did not react with ethylaluminum dichloride.

The above data indicate that copolymerization of complexed acrylonitrile and propylene or vinyl chloride proceeds by a specific mechanism which provides for selectivity

TABLE I
 Polymerization of Acrylonitrile and Vinyl Chloride^a

Monomers, g (mmole)		C ₆ H ₅ CN, g (mmole)	Toluene, ml.	Polymer, % ^b	Friedel-Crafts products, % ^c
Acrylonitrile	Vinyl chloride				
0.77 (12.7)	—	—	25.0	— ^d	—
—	45	—	2.5	—	100
—	45	1.31 (12.7)	2.5	—	Trace
0.77 (12.7)	45	—	2.5	82.5 ^e	Trace
0.77 (12.7)	15	—	—	32.0 ^f	—

^a Polymerization conditions: temperature, -78°C .; EtAlCl_2 , 1.78 g (14 mmole); reaction time, 60 min; reactor, a 100-ml four-necked stirred flask; nitrogen atmosphere. To a solution of EtAlCl_2 in toluene, acrylonitrile or benzonitrile was added and then vinyl chloride. After the reaction had been completed, 50 ml of methanol was added, the polymer was filtered, washed with methanol, and dried *in vacuo* at 60°C . for 24 hr.

^b Copolymer composition 1:1. The yield based on the acrylonitrile added.

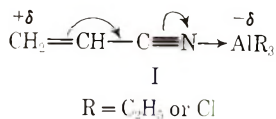
^c The yield based on the EtAlCl_2 added.

^d At temperatures higher than 100°C , reactions of trimerization of the complex take place accompanied by elimination of ethane and reduction accompanied by liberation of ethylene.³

^e The copolymer is soluble in the cold in dimethylformamide and in boiling acetone. In cold acetone it is only partially soluble.

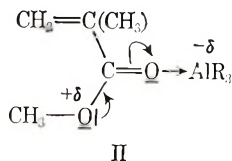
^f The copolymer is completely soluble in cold acetone.

of polymerization and for spontaneous initiation. The electron density on the vinyl group in the complex molecule I is lower than that in the free acrylonitrile molecule. This fact results from both the electron-accepting properties of the aluminum atom and the coupling of π -electrons of the triple and double bonds.



The decrease in the electron density, and thus an increase in the electron-accepting properties of the vinyl group has presumably the decisive effect on the course of the copolymerization reaction. The electron-accepting properties of the vinyl group in the complex I are related to the acid strength of the given organoaluminum compound and increase in the order: $\text{R}_3\text{Al} < \text{R}_2\text{AlCl} < \text{RAlCl}_2$. Experiments confirmed that the copolymer yield is related to the nature of the organoaluminum compound in the acrylonitrile complex. Ethylaluminum dichloride is the best complexing agent and with it the copolymer yield attains a maximum; with diethylaluminum chloride the yields are lower, and with triethylaluminum no copolymer is formed at all.¹

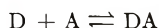
As already indicated, complexes of methyl methacrylate with organoaluminum compounds produce no copolymers with ethylene, propylene, isobutylene, and vinyl chloride. Presumably the methoxy group in complex II depresses the electron-accepting properties of the vinyl group enough to prevent copolymerization.



The nature of the uncomplexed monomer, particularly its donating properties, are important in the copolymerization investigated. The experimental data show the yield of copolymerization of complex I and isobutylene to be greater than that obtained with propylene or ethylene. A comparison of the above monomers in terms of the electron-donating properties proves isobutylene to be the strongest electron donor.

In the copolymerization investigated, complex I is an electron-accepting A monomer, whereas the olefin or the vinyl chloride molecule is an electron-donating D monomer.

The experimental evidence suggests that the first stage of the reaction involves formation of a transitory charge-transfer complex DA



The stronger the monomer A as acceptor and the stronger monomer D as donor, the greater is the case with which the complex DA is formed.

The complex DA can polymerize only after the reaction has been initiated by the ethyl group combined with the aluminum atom (although aluminum chloride is a strong Lewis-type acid, the acrylonitrile-aluminum chloride complex does not copolymerize with the above-mentioned monomers). In the complex DA the ethyl group is more readily abstracted as anion than it is in a pure organoaluminum compound or in complex I.³ Owing to the fact that in this type of copolymerization the complex DA undergoes polymerization, only the alternating copolymer is formed.

References

1. M. Hirooka, H. Yabuuchi, S. Morita, S. Kawasumi, and K. Nakaguchi, *J. Polym. Sci. B*, **5**, 47 (1967).
2. S. Pasynkiewicz and W. Kuran, *J. Organometal. Chem.*, **15**, 307 (1968).
3. S. Pasynkiewicz and W. Kuran, *J. Organometal. Chem.*, **10**, 23 (1967); *ibid.*, in press.

STANISŁAW PASYNKIEWICZ
WITOLD KURAN
TADEUSZ DIEM

Department of Organic Technology I
Institute of Technology (Politechnika)
Warsaw, Poland

Received June 24, 1968

Revised November 11, 1968

Preparation and Copolymerization of p-Vinylphenylalkylcarbinol

It may be of interest to examine the chemical reactions, copolymerizations, and polymer reactions of styrene derivatives having reactive hydroxy groups. However, there are very few reports of such monomers and polymers have appeared in the literature. It was previously reported that *p*-vinyl-benzylmethylcarbinol¹ (*p*-VBMC) and *p*-vinyl-benzylethylcarbinol² (*p*-VBEC) react with phenyl isocyanate to yield urethane compounds which gave homopolymers soluble in ethanol, tetrahydrofuran, and dioxane and insoluble in toluene, petroleum ether, and carbon tetrachloride. And it was found that the both monomers could be well copolymerized with acrylonitrile (AN). This work was carried out to study some characteristics of the polymerizations of *p*-vinylphenyldimethylcarbinol (*p*-VPhDMC), *p*-vinylphenylmethylethylcarbinol (*p*-VPhMEC), and *p*-vinylphenyldiethylcarbinol (*p*-VPhDEC).

EXPERIMENTAL

Monomers

p-VPhDMC was prepared by the same method described in the literature.³ The clear white crystal after several recrystallizations had a melting point of 42.9°C. The NMR spectra showed for *p*-VPhDMC: phenyl H, τ 2.76; $-\text{CH}=\text{CH}_2$, τ 3.14-4.96; $-\text{OH}$, τ 7.68; $-\text{CH}_3$, τ 8.52. *p*-VPhMEC was prepared by hydrolysis after the reaction of *p*-vinylphenylmagnesium chloride and methyl ethyl ketone in THF at 60°C. The appearance of this monomer obtained by several vacuum distillations was a transparent, viscous liquid having bp 90.5-91.5°C/2.2 mm Hg, n_D^{20} 1.5494.

ANAL. Calcd: C, 81.77%; H, 9.15%. Found: C, 81.43%; H, 9.02%.

TABLE I
Infrared Spectra of Monomers

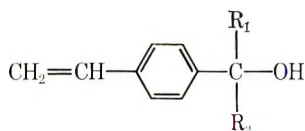
<i>p</i> -VPhDMC		<i>p</i> -VPhMEC		<i>p</i> -VPhDEC	
Assignment	Ab- sorp- tion band, μ	Assignment	Ab- sorp- tion band, μ	Assignment	Ab- sorp- tion band, μ
ν_{OH}	3.00	ν_{OH}	2.92	ν_{OH}	2.89
$\nu_{\text{C}=\text{C}}$	6.12	$\nu_{\text{C}=\text{C}}$	6.13	$\nu_{\text{C}=\text{C}}$	6.13
$\delta_{\text{C}-\text{H}} (-\text{CH}=\text{CH}_2)$	10.06	$\delta_{\text{C}-\text{H}} (-\text{CH}=\text{CH}_2)$	10.10	$\delta_{\text{C}-\text{H}} (-\text{CH}=\text{CH}_2)$	10.10
$\delta_{\text{C}-\text{H}} (-\text{CH}=\text{CH}_2)$	11.00	$\delta_{\text{C}-\text{H}} (-\text{CH}=\text{CH}_2)$	11.00	$\delta_{\text{C}-\text{H}} (-\text{CH}=\text{CH}_2)$	11.07
$\delta_{\text{C}-\text{H}} (p\text{-subst.})$	11.82	$\delta_{\text{C}-\text{H}} (p\text{-subst.})$	11.88	$\delta_{\text{C}-\text{H}} (p\text{-subst.})$	11.90

The NMR spectra showed for *p*-VPhMEC: phenyl H, τ 2.79; $-\text{CH}=\text{CH}_2$, τ 3.15-4.96; $-\text{OH}$, τ 6.97; $-\text{CH}_2-\text{CH}_3$, τ 8.10-8.48; $-\text{CH}_3$, τ 8.58; $-\text{CH}_2-\text{CH}_3$, τ 9.16-9.40. *p*-VPhDEC was prepared by the same method as above described, except that diethyl ketone was used in place of methyl ethyl ketone.

ANAL. Calcd: C, 82.06%; H, 9.54%. Found: C, 82.26%; H, 9.72%.

The product was a clear, viscous liquid, bp 93.5-94.0°C/2.0 mm Hg and n_D^{20} 1.5432. The NMR spectra showed for *p*-VPhDEC: phenyl H, τ 2.75; $-\text{CH}=\text{CH}_2$, τ 3.23-4.92; $-\text{OH}$, τ 7.63; $-\text{CH}_2-\text{CH}_3$, τ 8.22-8.35; $-\text{CH}_2-\text{CH}_3$, τ 9.20-9.35. *p*-Chlorostyrene (*p*-ClSt) was prepared by the Walling method:⁴ It had bp 62.0-62.5°C/6.0

mm Hg and n_D^{20} 1.5646. Styrene (n_D^{20} 1.5468) was purified by vacuum distillation after washing with 10% KOH solution and water and drying over anhydrous calcium chloride.



- I: $R_1, R_2 = -CH_3$
 II: $R_1 = -CH_3, R_2 = -C_2H_5$
 III: $R_1, R_2 = -C_2H_5$

AN (n_D^{20} 1.3912) was used after several vacuum distillations. Infrared spectra for *p*-VPhDMC, *p*-VPhMEC, and *p*-VPhDEC are summarized in Table I.

Solvent

Dioxane was dried with solid KOH and metal sodium after washing with concentrated HCl and was purified by distillation (bp 100.5–100.6°C, n_D^{20} 1.4223) after treatment with Al_2O_3 . THF was purified by distillation after the dehydration with metallic sodium; bp 65.5–66.0°C, n_D^{20} 1.4065. Azobisisobutyronitrile (AIBN) was purified by recrystallization from ethanol.

Polymerization

All polymerizations and copolymerizations were carried out in 50 wt-% dioxane at 60°C under nitrogen in a sealed tube with addition of 0.2 wt-% AIBN for 1–5 hr. Polymers were purified by the reprecipitation method by using THF as solvent and petroleum ether as nonsolvent. In the case of copolymerization, before the polymerization conversion reached 10%, polymerization mixture was poured into petroleum ether; and precipitation was repeated several times. The polymers were then dried under reduced pressure to reach to constant weight at room temperature.

RESULTS AND DISCUSSION

It has been pointed out that secondary alcohols such as *p*-VBMC and *p*-VBEC give the urethane compounds on reaction with phenyl isocyanate at room temperature without any catalyst. However, no change occurred when the mixture of *p*-VPhDMC and phenyl isocyanate allowed to stand at room temperature for 24 hr. On warming the mixture at 40°C for 1.5 hr on a water bath, white crystals precipitated, which on recrystallization yielded white needles, mp 236°C. The white crystals were identified as 1,1-diphenylurea by means of elemental analysis and infrared spectroscopy. In this reaction we did not investigate further, but it was presumed that 1,1-diphenylurea and *p*-vinyl- α -methylstyrene were produced by dehydration.

Conversions of *p*-VPhDMC, *p*-VPhMEC, and *p*-VPhDEC were 32.9, 20.6, and 25.0%, respectively, for 5 hr homopolymerization. All the polymerization products were white powders, soluble in methanol, THF, and dioxane but insoluble in benzene, petroleum ether, and carbon tetrachloride. When the polymers were dissolved in THF and spread on glass plates and THF was removed by heating in an oven at 60°C for 5 hr, hard, clear films were formed. NMR spectra showed for poly(*p*-VPhDMC): phenyl H, τ 2.75–3.42; —OH, τ 6.30; —CH—CH₂, τ 7.20; —CH—CH₂, τ 8.20; —CH₃, τ 8.48; and for poly(*p*-VPhMEC): phenyl H, τ 2.80–3.46; —OH, τ 6.22; —CH—CH₂, τ 7.20; —CH—CH₂, —CH₂—CH₃, τ 8.30; τ —CH₃; τ 8.53, —CH₂—CH₃; τ 9.14–9.20. $(CD_3)_2CO$ was used as the solvent for NMR spectral measurements. The absorptions in the infrared spectra which indicate $\nu_{C=C}$ disappeared after polymerization of the all monomers. It is apparent that the monomers were polymerized by a radical mechanism. The monomer reactivity ratios of *p*-VPhDMC(M_2), *p*-VPhMEC(M_2), and *p*-

VPhDEC(M₂) were calculated by graphically solving the Fineman-Ross equation,⁵ and Q and e values were estimated by the Alfrey-Price equation.⁶ r_1 , r_2 , Q , and e values are shown in Table II.

TABLE II
 r_1 , r_2 , Q , and e values

	r_1	r_2	r_1r_2	e	Q
AN- <i>p</i> -VPhDMC	0.05	0.41	0.02	-0.8	0.80
AN- <i>p</i> -VPhMEC	0.06	0.39	0.02	-0.8	0.67
AN- <i>p</i> -VPhDEC	0.04	0.38	0.02	-0.8	0.97
<i>p</i> -ClSt- <i>p</i> -VPhDMC	1.24	0.53	0.66	-0.9	0.85
<i>p</i> -ClSt- <i>p</i> -VPhMEC	1.43	0.33	0.47	-1.2	0.97
St- <i>p</i> -VPhMEC	0.79	1.25	0.99	-0.7	1.17

The three monomers have similar copolymerizabilities, with AN, despite the differences of the substituents, as can be seen in Table II. The e values indicate the substituents donate electrons to the vinyl groups.

References

1. K. Anda and S. Iwai, *Kogyo Kagaku Zasshi*, **70**, 557 (1967).
2. K. Anda and S. Iwai, unpublished results.
3. T. Kunitomo, S. Tanimoto, and R. Oda, *Kogyo Kagaku Zasshi*, **68**, 1967 (1965).
4. C. Walling and B. Woltstirn, *J. Amer. Chem. Soc.*, **69**, 852 (1947).
5. M. Fineman and S. D. Ross, *J. Polym. Sci.*, **5**, 259 (1950).
6. T. Alfrey and C. Price, *J. Polym. Sci.*, **2**, 101 (1947).

KINJI ANDA
SHINJI IWAI*

Tokyo Metropolitan Industrial Research Institute
Tokyo, Japan

Received December 9, 1968

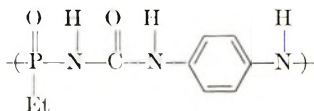
Revised February 27, 1969

* Present address: Faculty of Industrial Engineering, Nihon University, Narashino, Chiba, Japan

Interfacial Synthesis of Polyiminocarbonylimino(phenylphosphinylidene) and Polyiminocarbonylmethylenecarbonylimino(phenylphosphinylidene)

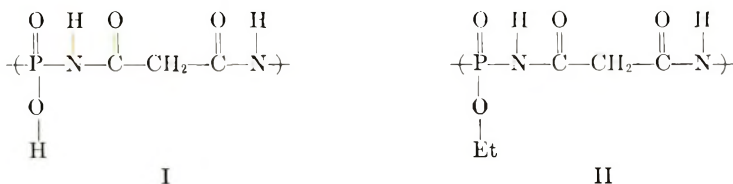
INTRODUCTION

Polyphosphonylureas have been prepared by the high melt condensation of phosphonyl chlorides and urea¹ and the condensation of phosphonic amides and urea.^{2,3} Haven⁴ reports the production of polymeric material with the structure



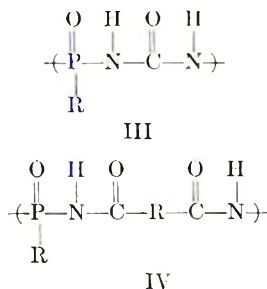
from the condensation of ethylphosphonic diisocyanate and *p*-phenylenediamine, on heating the reaction mixture at 70–90°C for 1.5 hr. Popoff and King⁵ report the production of the same product from the reaction of the diisocyanate and diamine in acetone with the mixture refluxed one hour. In the latter case the products are rather ill defined due to a side reaction involving homopolymerization of the isocyanate to phosphonyl-triazines, which in turn are able to react with diamines.⁵ The reaction of phosphoric or phosphonic diamides with organic diisocyanates gives products of a similar undefined structure.⁶

Devillers et al.⁷ report the synthesis of a polymer from the condensation of dichloroethylphosphonate and malonamide which is agitated at 65°C with increasing vacuum to a final vacuum of 2–3 mm. Elemental analysis indicated a repeating structure consisting of both units I and II:



In none of the above studies were molecular weights or spectra presented.

Sander and Steininger⁸ have recently reviewed the production of phosphorus polymers containing P–N bonding in the backbone. The production of such polymers (such as the polyphosphonamides) by the interfacial method is well known.^{9–16} There have been no reported interfacial synthesis of polymers with the general formula III or IV:



It is the purpose of this paper to report such synthesis by the interfacial technique.

EXPERIMENTAL and RESULTS

Polymerizations were conducted in a 1-pt Kimax milling jar with the use of a Waring Blender (No. 700-S) stirrer. The jar cap was fitted with two steel pipes (1 in. in diameter, 6 in. in length with a shoulder 1 in. from the base). One pipe was used as a vent for escaping gases. The second pipe was fitted with a 500-ml separatory funnel.

A 75-ml portion of the aqueous phase, containing 0.021 mole of urea or malonamide with 0.060 mole of sodium hydroxide, was added to the jar. The jar cap, equipped with pipes and funnel, was screwed onto the jar and the jar placed on the blender motor. Then 75 ml of carbon tetrachloride containing 0.021 mole of phenylphosphonic dichloride was added to the closed separatory funnel. The blender motor was started and the separatory funnel was opened, allowing the organic phase to flow freely into the jar. The blender was turned off after 10 min. A white to light brown solid was recovered by centrifugation from the reaction mixture. The solid was washed repeatedly with portions of water and dried over a water bath. The product forms a brown, brittle film.

Infrared studies were conducted on potassium bromide pellets on a Beckman IR-10. Representative spectra appear in Figures 1 and 2.

Melting ranges were determined on a Fisher-Johns melting point apparatus at a heating rate of 2C°/5 min. No melting was observed to a temperature of 325°C for either of the two polymer types.

Viscometry was conducted at 30°C in *m*-cresol with the use of a semi-micro dilution Cannon-Ubbelohde (75) viscometer.

Light scattering was conducted at 25°C in *m*-cresol with a Brice-Phoenix light-scattering photometer, Model 2000, by using the P_c dissymmetry factor method, assuming a random coil chain.

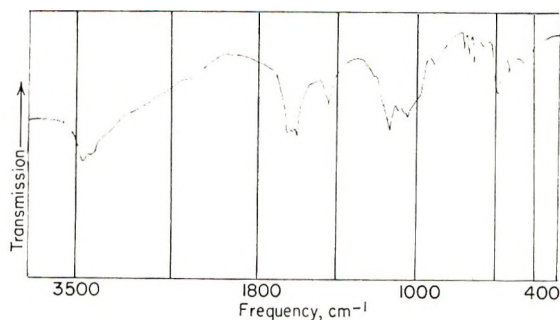


Fig. 1. Infrared spectrum of polyiminocarbonylimino(phenylphosphinylidene).

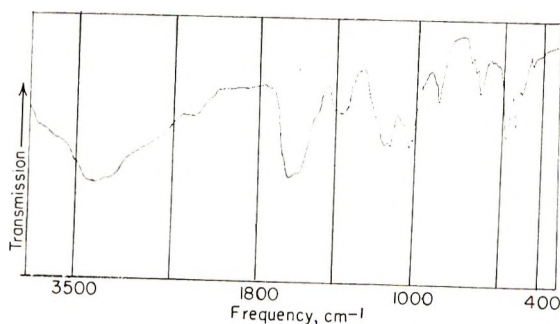


Fig. 2. Infrared spectrum of polyiminocarbonylmethylenecarbonylimino(phenylphosphinylidene).

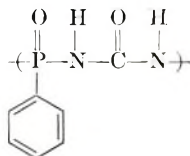
TABLE I
Physical Values of Polymers

Properties	Polyiminocarbonylimino(phenylphosphinylidene)	Polyiminocarbonylmethylenecarbonylimino(phenylphosphinylidene)
Limiting viscosity number, ml/g	18	39
Weight-average mol. wt.		1.8×10^6
Polymer soluble in:	dimethylsulfoxide, <i>m</i> -cresol	dimethylsulfoxide, <i>m</i> -cresol, formic acid
Polymer insoluble in:	water, chloroform, benzene, formic acid, methanol, carbon tetrachloride, ether	water, chloroform, benzene, methanol, ethanol, ether, carbon tetrachloride, acetone, dimethylformamide

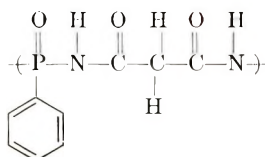
DISCUSSION

The polymers produced in this study are of high molecular weight and show solubilities, melting points, and general physical appearances generally the same as those reported in other syntheses.^{1-3,7}

The spectra are consistent for the structure of the repeating unit of the urea-phenylphosphonic dichloride polymer to be



and for the structure of the repeating unit of the malonamide-phenylphosphonic dichloride polymer to be



Products of the above general form can be used as textile flameproofing agents.^{1,6,8} They have generally high melting points (> 300°C) and thus may be a useful alternative to the general approach for producing polymers with high thermal stability which utilize generally wholly or mainly carbon backboned ladder, network and ring polymers.

The interfacial technique is, in general, a simpler, faster way of obtaining polymers with the above general type of bonding in the backbone than the methods employed previously. It can be used for systems employing or producing temperature sensitive compounds, since the reaction can be conducted at or below room temperature. It also employs comers which are commercially available.

This report was abstracted from the MA thesis of D. Winthers.

References

1. A. C. Haven, U.S. Pat. 2,716,639 (1955).
2. H. W. Coover, U.S. Pat. 2,642,413 (1953).
3. H. W. Coover, R. L. McConnell, and N. H. Shearer, *Ind. Eng. Chem.*, **52**, 412 (1960).
4. A. C. Haven, U.S. Pat. 2,835,652 (1958).
5. I. C. Popoff and J. P. King, *J. Polym. Sci. B*, **1**, 247 (1963).
6. J. R. Caldwell, U.S. Pat. 3,041,207 (1962).
7. J. Devillers, A. Munoz, J. Navech, and J. P. Vives, *Compt. Rend.*, **261**, 15-17 (1965).
8. M. Sander and E. Steininger, *J. Macromol. Sci. Revs.*, **C**, **1**, 91 (1967).
9. S. Hashimoto, I. Furukawa, and S. Tamibuchi, *Kobunshi Kagaku*, **23**, 877 (1966).
10. M. Nielsen and G. Deebel, U.S. Pat. 3,227,685 (1966).
11. T. Ogawa, T. Nishimatsu, and Y. Minoura, *Makromol. Chem.*, **114**, 275 (1968).
12. J. Farago, U.S. Pat. 3,116,268 (1963).
13. L. A. Rodivilova, M. S. Akutne, K. P. Baebakov, and L. P. Nekrasova, USSR Pat. 125,566 (1960).
14. M. Nielsen and D. Harris, U.S. Pat. 3,290,258 (1966).
15. D. Harris, R. Jenkins, and M. Nielsen, *J. Polym. Sci.*, **35**, 540 (1959).

CHARLES E. CARRAHER, JR.
D'ORSAY WINTHERS

University of South Dakota
Chemistry Department
Vermillion, South Dakota 57069

Received July 29, 1968
Revised August 26, 1968

Cationic Polymerization of Styrene in the Presence of π -Electron Acceptors

Ionic processes are strongly affected by the nature of the solvent, i.e., its ionizing and solvating ability. It is known that ionic polymerization proceeds more rapidly in solvents with high dielectric constants. Ion solvation in anionic polymerization seems to have been investigated to a great extent.¹⁻⁴ Little is known, however, of the solvation of the growing ion pair in cationic polymerization. Solvents capable of solvating the counterion of the carbonium macroion would be electron acceptors, such as nitrobenzene and nitromethane. These are also highly polar, and the solvation effect could hardly be distinguished from ionization. On the other hand, the effect of strong electron acceptors could show itself even in small quantities, as the ion concentration is fairly low during polymerization. Furthermore, a pure solvation effect should be best observed in low concentration of solvating agent, for some side reactions are likely to occur with excess solvating agent.

In cationic polymerization π -electron acceptors could probably act as counterion (anion) solvating agent, for it is known that they are capable of complex formation with anions.⁵ In the present work the effect of some strong π -electron acceptors on the cationic polymerization of styrene in quantities which are commensurate with the catalyst concentration ($\text{BF}_3 \cdot \text{Et}_2\text{O}$) is reported.

EXPERIMENTAL

Materials

Styrene was washed with 5% NaOH and kept for 24 hr over anhydrous Na_2SO_4 and then distilled *in vacuo* under a nitrogen atmosphere. The middle fraction, amounting to about 60%, was collected, stored over CaH_2 , and redistilled immediately before use.

Benzene (BZ), free from thiophene, was dried over CaCl_2 , distilled, and stored in a nitrogen atmosphere over sodium wire. Nitrobenzene (NBZ) was dried over CaCl_2 and fractionated, the fraction with bp $211^\circ\text{C}/760$ mm being collected and stored over molecular sieve 4A in a nitrogen atmosphere. Chlorinated hydrocarbons were fractionated, dried for 24 hr over P_2O_5 , then distilled *in vacuo* in a nitrogen atmosphere. The dielectric constants of the solvents used (literature data) are: tetrachloromethane (TCM), 2.28/ 20°C ; tetrachloroethane (TCE), 8.08/ 20°C ; dichloroethane (DCE), 9.80/ 20°C ; benzene, 2.24/ 25°C ; nitrobenzene, 34.75/ 25°C .

Boron trifluoride diethyl etherate (The British Drug Houses Ltd.) was distilled *in vacuo* in a nitrogen atmosphere. Freshly distilled product was used.

Tetracyanoethylene (TCNE) (Eastman) was recrystallized from dichloroethane, mp 139 – 140°C . Chloranil (CA) (Th. Schuchardt) was recrystallized from toluene, mp 290°C . 1,3,5-Trinitrobenzene (TNB) (Eastman), mp 112 – 113°C , was used without further purification. The electron acceptors were kept in a desiccator over P_2O_5 .

Polymerization Technique

Polymerization was carried out in glass vessels equipped with magnetic stirrer and serum cap in an atmosphere of pure nitrogen under isothermal conditions. Moisture was removed by heating the vessels *in vacuo* and cooling in a nitrogen atmosphere. Solvent, monomer, and electron acceptor were mixed in a nitrogen atmosphere, then catalyst was introduced by means of an automatic micropipet. In the course of the polymerization, samples were withdrawn with a hypodermic syringe. The polymer was isolated by precipitation in ethanol and centrifugation. Conversions were estimated from the weight of the polymer isolated. In some runs conversion was checked by gas chromatography.

RESULTS

All other conditions being equal the rate of the styrene polymerization in the absence of electron acceptors in chlorinated hydrocarbons depends on the dielectric constants of the solvents used. In the same solvents small amounts of electron acceptor have a clear effect on the polymerization rate (Fig. 1). However little or no effect was observed in BZ (Fig. 2) and in NBZ (Fig. 3).

The electron acceptors used have different electron acceptor activities; these are:⁵ TCNE, 1.6 eV; CA, 1.35 eV; TNB, 0.6 eV. As seen from Figure 4, the increase of the

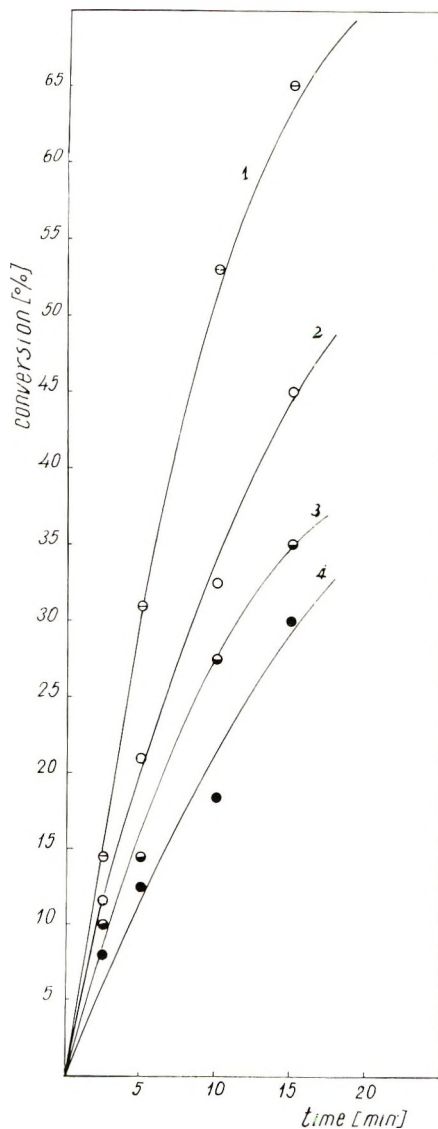


Fig. 1. Polymerization in DCE and TCE: (1) in DCE, with TCNE; (2) in DCE, no electron acceptor; (3) in TCE, with TCNE; (4) in TCE, no electron acceptor. $[TCNE]/[BF_3 \cdot Et_2O] = 2$; styrene, 1 mole/l.; $BF_3 \cdot Et_2O$, 10^{-2} mole/l.; $20^\circ C$.

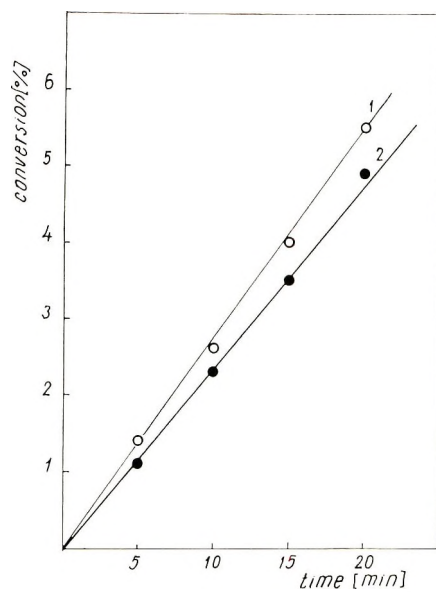


Fig. 2. Polymerization in BZ: (1) no electron acceptor; (2) with TCNE. Other conditions as in Fig. 1.

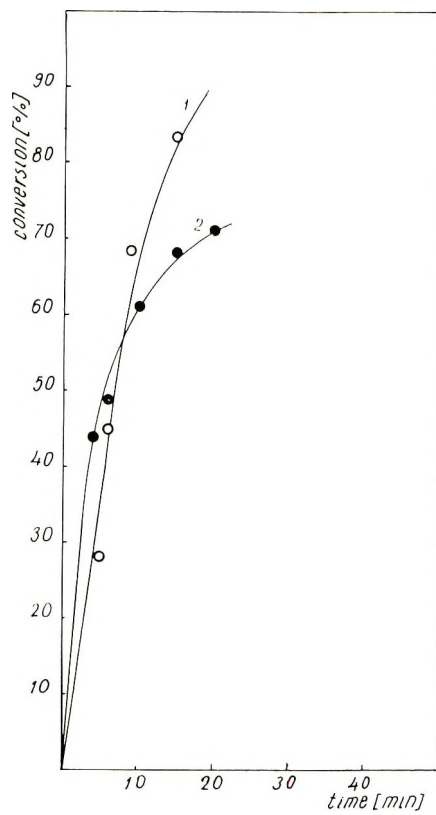


Fig. 3. Polymerization in NBZ: (1) no electron acceptor; (2) with TCNE. Other conditions as in Fig. 1.

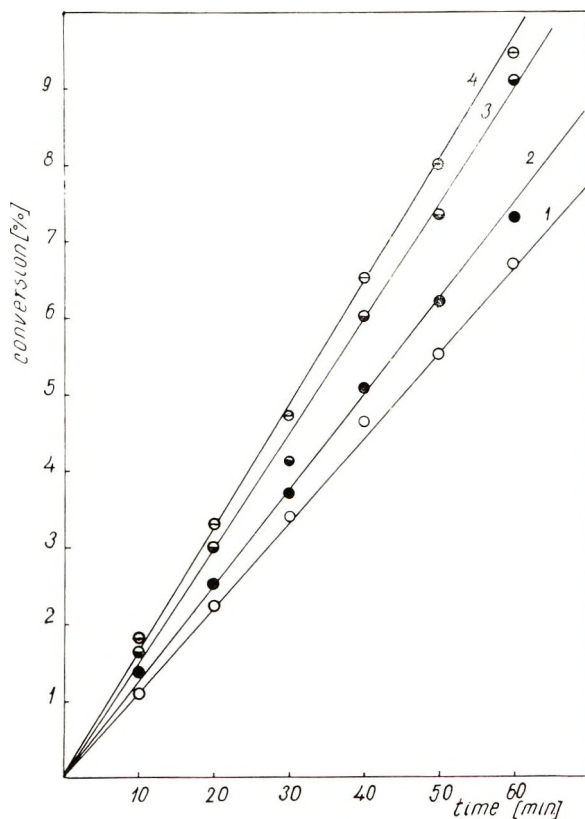


Fig. 4. Polymerization in the presence of different electron acceptors: (1) no electron acceptor; (2) with TNB; (3) with CA; (4) with TCNE. $[EA], 2 \times 10^{-2}$ mole/l.; solvent, TCM. Other conditions as in Fig. 1.

polymerization rate in the presence of an electron acceptor is proportional to their electron acceptor activities.

The rate of polymerization increases on increasing the concentration of electron acceptor, and this dependence goes through a maximum (Fig. 5).

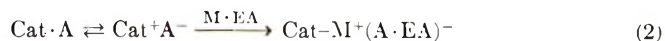
DISCUSSION

In the system consisting initially of monomer and solvent, then of monomer, solvent, and catalyst, different interactions with an electron acceptor should be considered.

If the solvent has no electron donor properties, a complex is formed between monomer and electron acceptor (EA), as shown by appearance of color:



On addition of catalyst, destruction of the monomer-EA complex occurs, as shown by decoloration of the solution with disappearance of the absorption maximum of the monomer-EA complex (Fig. 6). Complex formation between EA and negatively charged counterion of the catalyst is likely to follow:



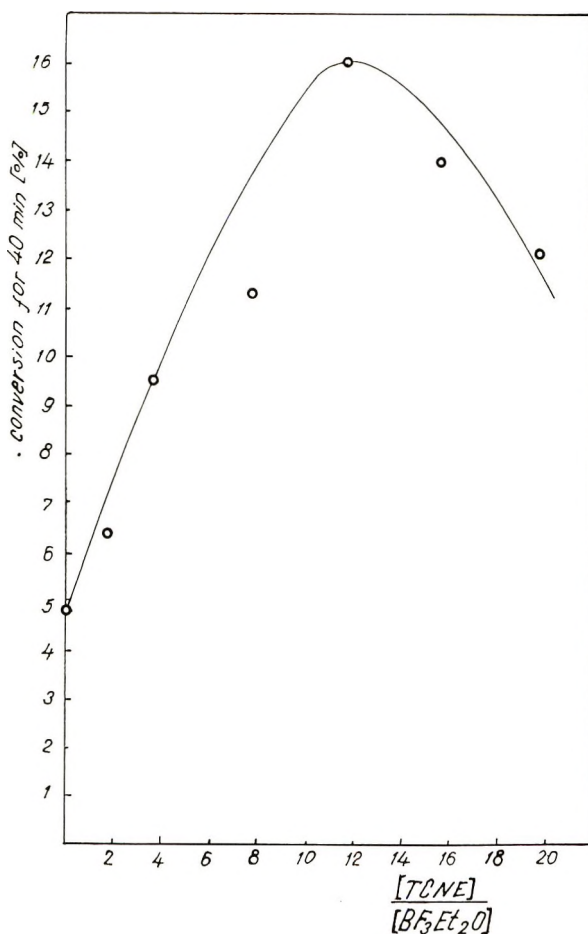


Fig. 5. Polymerization in the presence of different amounts of TCNE. Time 40 min; other conditions as in Fig. 1.

Polymerization will proceed at a higher rate owing to the growing ion-counterion separation.

The effect of the electron acceptor is shown to a much smaller extent (if at all) in solvents with electron-donating properties such as BZ (Fig. 2), as well as in solvents of an electron-acceptor nature, especially those with high polarity (Fig. 3). In the latter case solvation and ionization will operate in the same direction.

It should be expected that on increasing the amount of electron acceptor the effect will increase to a certain extent, i.e., until the saturation of the solvation layer of the counterion. Further increase of the electron acceptor concentration could not influence the polymerization rate, which should remain constant. However, this will be the case only if the excess electron acceptor does not interact with other components of the system. In our case, electron acceptor in excess will react with the monomer [reaction (1)]. The resulting complex will polymerize reluctantly. Reaction (2) could not proceed, as counterion is already bound with electron acceptor, and thus the effective monomer concentration would be reduced. This results in a decrease of the polymerization rate (Fig. 5).

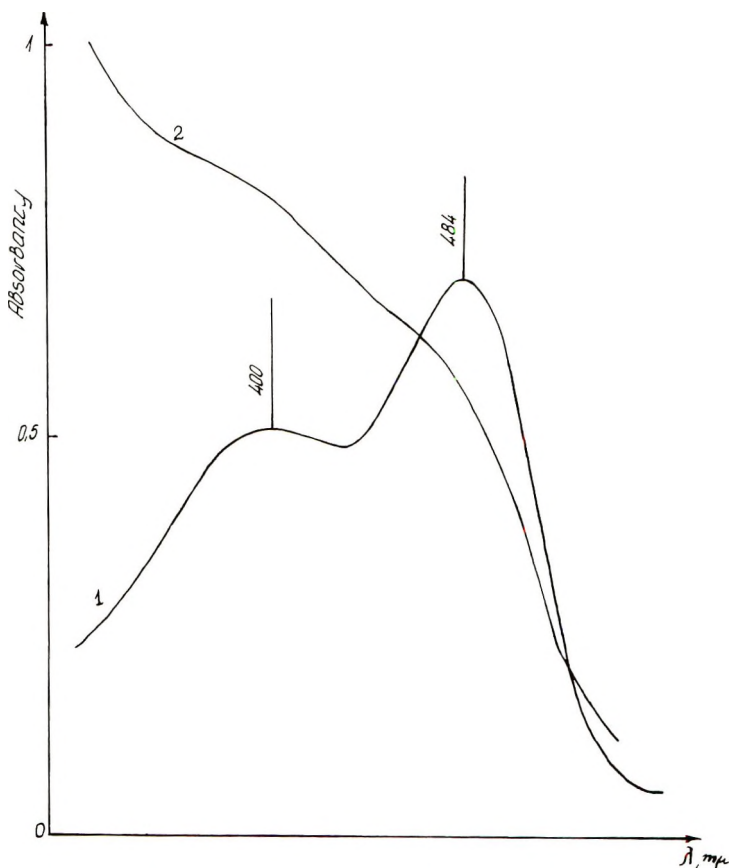


Fig. 6. Visible spectra of the styrene-TCNE complex in TCM at 20°C: (1) styrene-TCNE complex; (2) styrene-TCNE complex after addition of $\text{BF}_3 \cdot \text{Et}_2\text{O}$. Styrene, 1 mole/l.; TCNE, 2×10^{-2} mole/l.; $\text{BF}_3 \cdot \text{Et}_2\text{O}$, 2×10^{-1} mole/l.

Further work on polymerization in the presence of electron acceptors is in progress and will be reported later.

References

1. F. J. Welch, *J. Amer. Chem. Soc.*, **82**, 6000 (1960).
2. S. Bywater, D. J. Worsfold, *Can. J. Chem.*, **40**, 1564 (1962).
3. K. O'Driscoll and R. Patsiga, *J. Poly. Sci., A*, **3**, 1037 (1965).
4. C. G. Overberger, T. M. Chapman, and T. Wojnarowski, *J. Polym. Sci., A*, **3**, 2865 (1965).
5. I. B. Ainscough and E. F. Caldin, *J. Chem. Soc.*, **1956**, 2528, 2540, 2546.
6. G. Briegleb, *Elektronen-Donator-Acceptor-Komplexe*, Springer, Berlin-Göttingen-Heidelberg, 1961, p. 183.

IVAN M. PANAYOTOV
 IVAN K. DIMITROV
 IVAN E. BAKERDJEV

Institute of Organic Chemistry
 Bulgarian Academy of Sciences
 Sofia, Bulgaria

Received September 4, 1968

Revised October 28, 1968

Effect of Previous History on Kinetics of Sorption by Wood Cell Walls

This paper reports observations which show that the rate of sorption of water vapor by wood and perhaps other swelling polymers depends strongly on the length of time for which they have been held at the preceding "equilibrium" condition.

It has long been known that wood, wool, and other swelling polymers do not behave reversibly during adsorption and desorption of vapors. One example of this is sorption hysteresis. It has also been shown¹⁻³ that, even if sorption equilibrium at a given vapor pressure is approached in one direction only (e.g., by adsorption) and from a reproducible starting point (e.g., zero moisture content), the equilibrium moisture content may differ according to the number and size of the intermediate equilibrium steps by which it is reached. Another manifestation of dependence on sorption history has been observed during experiments on vacuum drying.^{4,5} It was found that after vacuum drying at room temperature, a quantity of water was retained which varied according to the period of previous exposure to vapor.

When the kinetics of sorption of water vapor or of swelling of wood cell walls in water were studied, new phenomena which did not conform to any simple pattern of dependence on external conditions were revealed.⁶ These included findings such as (1) the time required to reach equilibrium at a given vapor pressure increased greatly as the commencing moisture content was increased; (2) these times were inordinately long, amounting to days or sometimes weeks, even though the wood cell walls were only a few microns thick; (3) although the rate of swelling of wood cell walls in water was many times faster than in water vapor, there was a similar strong dependence on the initial moisture content.

The difficulty of interpreting these findings in terms of concentration-dependent diffusion stimulated a search for an alternative explanation.⁶ This appeared to require that the course of the prolonged swelling was determined by processes which had occurred earlier at the surface of the cell wall and occupied a much shorter period of time.

It was also found that repeated tests on the same or on similar fresh material, sometimes yielded varying results: the nonreproducibility could be tolerated only because of the large effects produced by the test parameters. The erratic behavior suggested either unexpected sensitivity to one or more of the "constant" experimental conditions, or variability arising from differing histories of the material.

In earlier sorption studies,³ the uptake of vapor by dry wood had been found virtually to cease after a few hours. Unpublished measurements have shown that swelling also ceased within this period. It had therefore been assumed that after 24 hr the wood was in equilibrium. Evidence that this assumption might not be true had come first from the drying experiments.⁵ These showed that the amount of water retained by the wood after vacuum drying increased with the time of exposure to water vapor before drying was commenced up to at least 900 hr. It was also shown however that if wood containing such "retained" water was wetted and then re-evacuated, all the water could be removed easily.

The question thus arose as to whether the slow changes occurring after sorption was apparently complete were having any other effects on the wood properties. For example, would samples of initially dry wood, brought to a constant moisture content at a relative vapor pressure p_1 , but for different periods of time, behave similarly when exposed to a higher vapor pressure p_2 ?

To answer this question, two 60 μ thick microtomed sections of wood (klinki pine, *Araucaria hunsteinii* K. Schum.) were so cut that all their cell walls were directly accessible to water vapor. After repeated extraction with benzene-alcohol and distilled water, each section was dried under vacuum in a sorption apparatus (a calibrated quartz helix in a vacuum chamber) and exposed to water vapor at $p_1 = 0.53$, equivalent to a moisture content of approximately 10% of the dry weight. At a selected time (2, 4, 24,

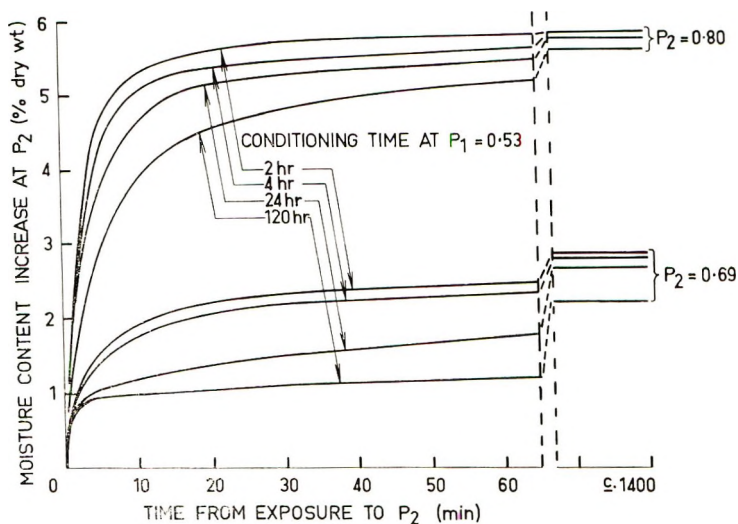


Fig. 1. Effect of conditioning period at p_1 on course of sorption at p_2 .

or 120 hr) after exposure, the vapor pressure was quickly changed to one of two higher values, p_2 (corresponding to either 13 or 16% moisture content at equilibrium), and the second sorption step was plotted. This procedure was repeated a number of times, the specimens being given an intermediate wetting *in situ* followed by redrying to restore them as nearly as possible to a reproducible starting condition.⁵ The results are presented in Figure 1. It should be recorded that there was little change in moisture content at p_1 between 2 and 120 hr, so that all the second steps started from approximately the same moisture content (between 10.1 and 10.3%); the variations which did occur were not related to the length of the conditioning period.

The short answer to the question asked above is immediately clear. The course of the second sorption step was markedly dependent on the period of conditioning at p_1 . Before discussing this further, however, some additional points need to be noted. The first is that if the curves for the two different increments after the same conditioning period (say, 24 hr) are compared, the 10–16% moisture change is faster, confirming the behavior observed previously.³

The second point concerns the shape of the sorption curves, particularly for the 10–13% change. Despite the effect of conditioning time apparent in the later part of these curves, the moisture increments during the first minute were almost identical in all four cases, namely 0.70, 0.77, 0.70, and 0.69%. This is supporting evidence for the existence of at least two stages in the sorption process, a phenomenon frequently observed but variously interpreted in the history of sorption kinetics research. It is sufficient to note here that the first stage, constituting approximately a quarter of the total moisture increment, appears to be little dependent on sorption history.

For the 10–16% step, the separation into two stages was not as clear because the second stage was so much faster. In order to make quantitative comparisons, however, it was assumed that both stages were again present, and also that the first stage constituted the same fraction (approximately a quarter) of the total moisture change as it did in the 10–13% step.

For a quantitative comparison of the effect of different conditioning times on sorption during the second step, an effect which now appears to be confined to the second stage of that step, the times taken to reach half of the second stage were determined and plotted against the initial conditioning period in Figure 2. This shows that there is a strong interaction between the period of conditioning and the size of the second step. More

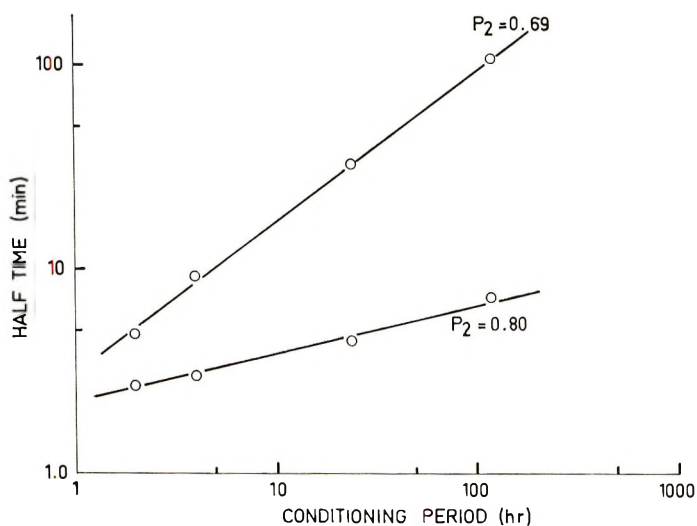


Fig. 2. Dependence of sorption half time at p_2 (second stage only) on conditioning period at p_1 .

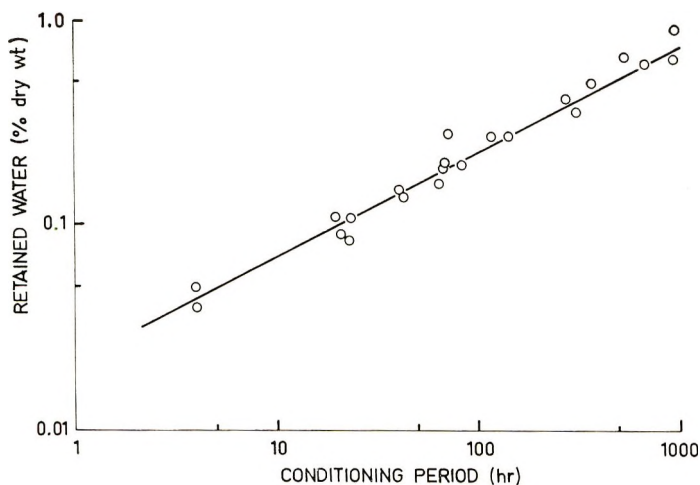


Fig. 3. Retention of water on vacuum drying after conditioning for different periods.

specifically, the conditioning period has a much larger effect on the sorption rate for the 10–13% increment (half times of 6–230 min) than for the 10–16% increment (half times of 3–8 min).

The linearity apparent in Figure 2 also indicates that the changes taking place during conditioning at p_1 had not ceased by the longest time allowed, i.e. 120 hr. A similar presentation of the published data on the effect of the conditioning period on the retention of water after vacuum drying,⁵ as replotted in Figure 3, shows a linearity persisting up to 1000 hr. Thus, when a dry wood cell wall is exposed to water vapor at constant pressure, its attainment of constant moisture content within a few hours does not mean that complete equilibrium has been reached. Clearly, significant internal changes (and perhaps barely detectable moisture changes⁵) continue for a long time and have profound effects on its subsequent behavior. These changes are being studied further.

At this stage it appears that the slow changes are accompanied by increasing stability of the system and that binding of water into the structure is probably involved. Both effects can be reversed however by first saturating and then redrying the wood. Concentration gradients associated with the initial transport of water within a swelling gel may be expected to generate stresses between the swollen and unswollen regions of the material. In a complex structure such as a wood cell wall, swelling stresses may occur also between regions of differing composition or molecular orientation, even with uniform moisture distribution. It has already been proposed that these swelling stresses may determine the speed of the sorption process.^{3,6}

It is now suggested that some of the energy derived from water uptake is temporarily stored and only slowly released by the complex molecular rearrangements which lead ultimately to the most stable state. The present results can be explained if, following the second vapor pressure increment, the residual energy from the first step becomes available to augment that from the second. The stored energy would have a proportionately greater effect in accelerating sorption when the second pressure change and hence the new sorption energy available, is small. The slow molecular changes and the gradual reduction of stored energy may be considered as analogous to stress relaxation in the rheological sense, a process known from experiments involving the use of external stresses to continue for a considerable time.⁷

One implication of these results is that it may be a relatively rare occurrence for wood, and perhaps other swelling gels, to be in a state of complete equilibrium. It also follows that to obtain experimental results of a meaningful and reproducible character on such materials, much greater attention must be paid to their sorption and stress histories than is commonly the case.

References

1. G. N. Christensen and K. E. Kelsey, *Austral. J. Appl. Sci.*, **9**, 265 (1958).
2. J. G. Downes and B. H. Mackay, *J. Polym. Sci.*, **28**, 45 (1958).
3. G. N. Christensen and K. E. Kelsey, *Holz Roh-Werkst.*, **17**, 178 (1959).
4. I. C. Watt and R. H. Kennett, *Text. Res. J.*, **39**, 489 (1960).
5. H. F. A. Hergt and G. N. Christensen, *J. Appl. Polym. Sci.*, **9**, 2345 (1965).
6. G. N. Christensen, *Nature*, **213**, 782 (1967).
7. P. U. A. Grossman and R. S. T. Kingston, *Austral. J. Appl. Sci.*, **5**, 403 (1954).

G. N. CHRISTENSEN
H. F. A. HERGT

Division of Forest Products,
Commonwealth Scientific and Industrial Research Organization,
South Melbourne, Australia.

Received November 6, 1968

Analysis of Heterodisperse Copolymerization

Several years ago one of us observed very unusual physical properties in a 1:1 copolymer of octyl acrylate and methacrylic acid, batch-polymerized with radical initiators. The modulus-temperature curve of the copolymer is shown in Figure 1, where it

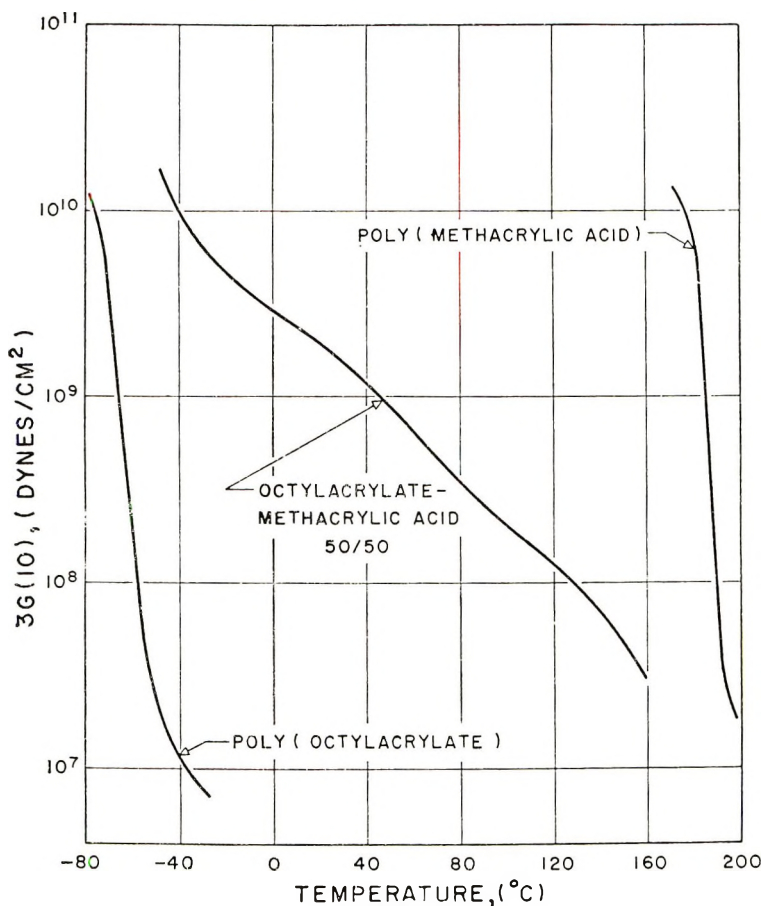


Figure 1.

is compared with the modulus-temperature curves of the homopolymers. The very shallow slope of the modulus-temperature curve of the copolymer is an indication of compositional heterogeneity. The copolymer films, although translucent, would whiten upon stretching, and were also very tough. These also are indicators of compositional heterogeneity and partial phase separation.

It was considered that a mathematical analysis of the distribution of sequence lengths might be illuminating. A computer program equipped to treat this aspect of the copolymer equation was devised. The values of r_1 and r_2 for these monomers (computed from the Q, e values listed by Ham¹) are $r_1 = 0.0954$ and $r_2 = 8.78$.

The specific answer sought was: what is the weight fraction of the already polymerized monomers that exists in sequences of four or greater? This quantity was calculated as a function of the overall conversion. The results are shown in Table I.

TABLE I

Composition of Copolymer of Octyl Acrylate and Methacrylic Acid as a Function of overall Conversion at Initial Feed Ratio = 1.

Overall conversion, %	Conversion of octyl acrylate, %	Conversion of methacrylic acid, %	Wt. fraction of octyl acrylate in sequences of 4 or greater, %	Wt. fraction of methacrylic acid in sequences of 4 or greater, %
0.	0.	0.	0.3	94.6
10.	2.2	17.8	0.3	93.7
20.	4.7	35.3	0.4	92.6
30.	7.9	52.1	0.6	91.0
40.	11.9	68.1	1.1	88.7
50.	17.5	82.5	2.6	85.0
60.	26.1	93.9	8.6	79.6
70.	40.7	99.3	30.6	75.8
80.	60.0	100.	56.6	75.2
90.	80.0	100.	64.5	75.2
100.	100.	100.	71.6	75.2

The degree of compositional heterogeneity in these two monomers is impressive.

Reference

1. G. E. Ham, *Copolymerization*, Interscience, New York, 1964, pp. 859-860.

A. V. TOBOLSKY

Department of Chemistry
Princeton University
Princeton, New Jersey 08540

I. L. HOPKINS

Bell Telephone Laboratories, Inc.
Murray Hill, New Jersey 07974

Received November 13, 1968

Structure and Reactivity of α,β -Unsaturated Ethers. VI. Cationic Copolymerization of β -Chlorovinyl Ethyl Ether

It has been known that various β -substituted vinyl ethers are easily polymerized by cationic mechanism. Most previous investigations have been concerned with alkenyl alkyl ethers.¹⁻⁷ Thus, it has been shown that their reactivities are comparable to those of vinyl ethers in homogeneous polymerizations⁵⁻⁷ and that *cis*-alkenyl alkyl ethers, less stable isomers,⁸ are several times more reactive than the corresponding *trans* isomers.⁵⁻⁷

Few investigations have so far been reported on the polymerization of β -halogenovinyl ethers. In an early report, van Dorp *et al.*⁹ noted that pure β -chlorovinyl ethyl ether spontaneously polymerizes to give a glassy solid. Natta *et al.*¹⁰ carried out detailed investigations on the structure of the stereoregular polymers formed from both *cis*- and *trans*- β -chlorovinyl alkyl ethers with boron trifluoride etherate or ethylaluminum chlorides as catalyst and thereby deduced the important steric courses involved in these polymerizations. However, the kinetic phase of the polymerizations does not appear to have attracted interests of these previous investigators.

Isomerization equilibrium experiments conducted by us⁸ have shown that, in the liquid phase, β -chlorovinyl ethyl ether (CVE) is thermochemically more stable in the *cis* form than in the *trans* form, in contrast to alkenyl alkyl ethers where the *trans* isomers are generally the more stable. Our interests in the relative reactivities of *cis*- to *trans*-unsaturated ethers have thus urged us to investigate the *cis-trans* copolymerization of CVE.

In the present communication, results of both the mutual copolymerization of the isomeric CVE pair and the copolymerization of *cis*-CVE with vinyl isobutyl ether (VIBE) will be presented. On the basis of the results obtained, the effects of the β -chloro substitution on the vinyl ether polymerizability will be discussed.

EXPERIMENTAL

Materials

CVE was prepared from ethyl alcohol and gaseous chlorine by the method of van Dorp *et al.*⁹ The *cis* and *trans* isomers were separated by fractional distillation through a column packed with Raschig rings; *cis* (isomeric purity 99.2%), bp 62–63°C/90 mm Hg (lit.⁹ 59–62°C/79 mm Hg), n_D^{20} 1.4355 (lit.⁹ 1.4365); *trans* (isomeric purity 98.5%), bp 45–46°C/80 mm Hg (lit.⁹ 45–47°C/79 mm Hg), n_D^{20} 1.4257 (lit.⁹ 1.4270). VIBE, methylene chloride, toluene, and boron trifluoride etherate ($\text{BF}_3 \cdot \text{OEt}_2$) were purified as described previously.⁶

Procedure

Both the polymerization procedure and the method of calculation of the monomer reactivity ratios were the same as have been described previously.⁶ Monomer concentrations were determined by use of a Shimadzu gas chromatograph Model GC-2C with a Disc chart integrator Model 239. A 3 mm \times 3 m column packed with 25% Apiezon grease L-dioctyl phthalate mixture (3:1) on Shimallite (60–80 mesh) was operated at 105°C with hydrogen as carrier gas.

RESULTS AND DISCUSSION

Polymerization was carried out in methylene chloride at -78°C by use of $\text{BF}_3 \cdot \text{OEt}_2$ as catalyst. During the homopolymerization of either one of the CVE isomers, no formation of the other isomer was observed in the reaction mixture. This observation indicates that neither isomer suffers geometrical isomerization during polymerization, a situation which is like that found for the case of alkenyl alkyl ethers.⁷

Mixtures of *cis*- and *trans*-CVE's of varying isomeric ratios were copolymerized in methylene chloride at -78°C with $\text{BF}_3 \cdot \text{OEt}_2$. The polymers obtained were white powders and insoluble in methanol. Variations of the monomer concentrations due to copolymerization were as given in Table I. Treatments of these data by the aid of the

TABLE I
cis-trans Copolymerization of CVE^a

Polymerization time, min	Monomer feed ^b		Residual monomer ^c	
	$[\text{M}_c^0]$	$[\text{M}_t^0]$	$[\text{M}_c]$	$[\text{M}_t]$
3	0.336	0.664	0.288	0.616
4	0.528	0.472	0.378	0.399
6	0.487	0.513	0.354	0.441
3	0.528	0.472	0.407	0.409
3	0.716	0.284	0.502	0.228
4	0.716	0.284	0.471	0.219

^a Monomer and catalyst concentrations were 7 vol-% and 0.02 mole/l, respectively. Toluene was used as an internal standard (3 vol-%).

^b Initial molar compositions of the monomer mixture.

^c Molar fractions of the residual monomers with respect to the total monomer feeds.

TABLE II
Copolymerization between *cis*-CVE (M_c) and VIBE (M_V)^a

Polymer- ization time, min	Monomer feed		Residual monomer		r_V^b
	$[\text{M}_c^0]$	$[\text{M}_V^0]$	$[\text{M}_c]$	$[\text{M}_V]$	
16	0.367	0.633	0.362	0.236	26.0
20	0.562	0.438	0.534	0.110	26.8
28	0.562	0.438	0.522	0.071 ₆	24.6
40	0.721	0.279	0.679	0.058 ₅	25.8

^a Polymerization conditions were the same as is shown in foot note a of Table I except that catalyst concentration was 5 mmoles/l.

^b Relative polymerizability, $r_V = \log([\text{M}_V^0]/[\text{M}_V])/\log([\text{M}_c^0]/[\text{M}_c])$.

integral form of the Mayo-Lewis copolymerization equation gave the monomer reactivity ratios, $r_{cis} = 1.39 \pm 0.04$ and $r_{trans} = 0.28 \pm 0.04$. It may be noted that the *cis* isomer is the more reactive and that the product, $r_{cV} = 0.39$, is considerably smaller than unity.

Next, VIBE was copolymerized with *cis*-CVE in order to compare their reactivities. The results are given in Table II, where it may readily be seen that there is a large difference in reactivity between the two ethers.

In a special case, in which the monomer reactivity ratios are such that $r_1 \gg 1 \gg r_2$, the usual differential form of binary copolymerization equation simplifies to

$$dM_1/dM_2 = r_1[M_1]/[M_2] \quad (1)$$

provided the monomer concentration ratio $[\text{M}_1]/[\text{M}_2]$ is not greatly different from unity. Integration of eq. (1) gives

$$r_1 = \log([\text{M}_1^0]/[\text{M}_1])/\log([\text{M}_2^0]/[\text{M}_2]) \quad (2)$$

where $[\text{M}_1^0]$ and $[\text{M}_2^0]$ are the respective initial concentrations of the two monomers.

Equation (2) permits the evaluation of r_1 from the variations in the monomer concentrations. The values appearing in the final column of Table II are such monomer re-

activity ratios calculated by taking VIBE and *cis*-CVE as M_1 and M_2 , respectively. The values of r_V thus obtained were nearly constant for various runs started with different monomer feeds, the average value being about 26.

cis-CVE has thus proved to be less reactive than VIBE by a factor of about 26 under the present experimental conditions. *trans*-CVE should be still less reactive. These low reactivities of CVE in cationic polymerization could be explained primarily from an inductive effect of the β -chloro group acting to reduce the electron density on the β -carbon atom.

The finding that the monomer reactivity ratio product $r_c r_t$ for the *cis-trans* copolymerization of CVE was not equal to unity indicates that the polymer chain ends formed from the respective isomeric monomers are different in structure. This conclusion is in agreement with that reached previously for the case of alkenyl alkyl ethers.⁷

The average relative *cis-trans* polymerizability, $(r_c/r_t)^{1/2} = 2.23$, is of the same order of magnitude as that found for alkenyl alkyl ethers.⁵⁻⁷ However, alkenyl alkyl ethers are generally more stable in the *trans* form, while CVE has been found to be more stable in the *cis* form.⁸ Thus, the relative polymerizabilities of isomeric CVE's are opposite to those to be expected from their thermochemical stabilities in the ground state. No doubt, the polymerization must have proceeded through a special mechanism which favored the reaction of the *cis* isomer, the more stable form. Natta et al.¹⁰ ascribed the stereospecificity of the polymers obtained from β -chlorovinyl alkyl ethers to the basic character of the monomers which allows a direct coordination with catalysts. One possible interpretation of the higher reactivity of *cis*-CVE might then be that the *cis* isomer, which is more polar than the *trans* isomer, is more amenable to the coordination with the catalytic species.

References

1. R. F. Heck and D. S. Breslow, *J. Polym. Sci.*, **41**, 520 (1959).
2. G. Natta, M. Farina, M. Peraldo, P. Corradini, G. Bressan, and P. Ganis, *Atti accad. nazl. Lincei, Rend., Classe Sci. fis. mat. nat.*, **28**, 422 (1960).
3. G. Natta, M. Farina, and M. Peraldo, *J. Polym. Sci.*, **43**, 289 (1960).
4. G. Natta, *J. Polym. Sci.*, **48**, 219 (1960).
5. A. Mizote, S. Kusudo, T. Higashimura, and S. Okamura, *J. Polym. Sci. A-1*, **5**, 1727 (1967).
6. T. Okuyama, T. Fueno, and J. Furukawa, *J. Polym. Sci. A-1*, **6**, 993 (1968).
7. T. Okuyama, T. Fueno, J. Furukawa, and K. Uyeo, *J. Polym. Sci. A-1*, **6**, 1001 (1968).
8. T. Okuyama, T. Fueno, J. Furukawa, and Y. Yonezawa, to be published.
9. D. A. van Dorp, J. F. Arens, and O. Stephenson, *Rec. Trav. Chim.*, **60**, 289 (1950).
10. G. Natta, M. Peraldo, M. Farina, and G. Bressan, *Makromol. Chem.*, **55**, 139 (1962).

T. OKUYAMA
T. FUENO

Faculty of Engineering Science
Osaka University
Toyonaka, Osaka, Japan

J. FURUKAWA

Department of Synthetic Chemistry
Kyoto University
Yoshida, Kyoto, Japan

Received December 3, 1968

Condensation of Thiourea with Phosphorus-Containing Reactants

INTRODUCTION

We have been interested in producing inexpensive phosphorus containing polymers from readily available reactants. There has been little reported work on the condensation of thiourea with phosphorus containing reactants.

Polyphosphonylureas have been prepared by the high melt condensation of phosphonyl chlorides and urea^{1,2} and the condensation of phosphonic amides and urea.^{2,3} Devillers et al.⁴ reported the synthesis of a polymer from the condensation of dichloroethylphosphonate and malonamide. Elemental analysis indicated a repeating structure consisting of two types of units:



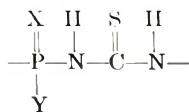
Coover et al.² reported the melt condensation of phenylphosphonic dichloride and thiourea. Hydrogen chloride was evolved copiously when the reaction temperature reached approximately 140°C. Coover³ reported the formation of a polymer of unknown structure from the condensation of 50–95 mole-% organosphosphonic acid diamide with 50–5 mole-% thiourea.

Sander and Steininger⁵ have recently reviewed the production of phosphorus polymers containing P—N bonding in the backbone. The production of such polymers (as the polyphosphonamides) by the interfacial method is well known.^{6–16} Carraher and Winthers¹⁴ recently reported the condensation of phosphonic dichlorides with urea and malonamide by the interfacial technique.

There have been no reported interfacial condensation of thiourea with phosphorus-containing reactants. It is the purpose of this paper to report such synthesis.

EXPERIMENTAL AND RESULTS

Interfacial stirred polymerization procedure as described by Carraher and Winthers¹⁴ was followed, a 1-pt Kimax milling jar being used on a Waring Blendor (NO 7700-S, approximate stirring speed 15000 rpm). The thiourea was recrystallized from hot water (mp 179–180°C). The acid chlorides were used without purification. All acid chlorides were received from the Aldrich Chemical Company except chloromethylphosphonic dichloride which was a gift from the Stauffer Chemical Company. Infrared spectra were obtained with a Beckman IR-10 instrument with potassium bromide pellets. The spectra are in agreement with a repeating unit exemplified by I, where X is O or S and Y is alkyl, aryl, alkoxy, or aryloxy. Viscometry was carried out in formic



acid at 25°C with the use of a Cannon-Ubbelohde (75) viscometer. Melting ranges were taken on a Fisher-Johns melting point apparatus at a heating rate of 2°C/min and were taken to be the temperature at which melting initially began to where melting was complete. Melting ranges obtained in this manner are given without claim to being a measure of the glass transition temperature or the crystalline melting point. A listing of some physical properties of the polymers appear in Table I. Representative infrared spectra appear in Figures 1 and 2. All products were soluble in *m*-cresol and formic acid and insoluble in water, carbon tetrachloride, methanol, dimethyl sulfoxide, benzene, acetone, and chloroform.

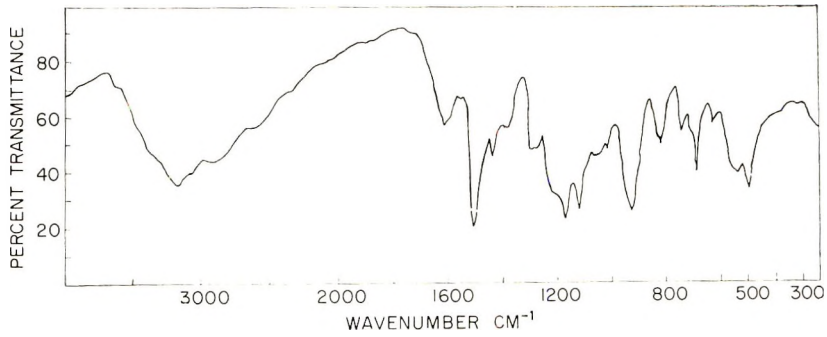


Fig. 1. Infrared spectrum of the product of phenylphosphonic dichloride and thiourea.

TABLE I
Physical Properties of Polymers Made from Urea and
Phosphorus-Containing Dichlorides*

Acid chloride	LVN, ml/g	Melting range, °C	Physical appearance	Color
Phenylphosphonothioic dichloride	51	203-225	Glassy	Dark brown
Phenylphosphonic dichloride	28	210-239	Powdery	Brown
Chloromethyl phosphorodichloridate	32	200-220	Powdery	Light brown
Phenyl phosphorodichloridate		208-230	Powdery	Brown
Ethyl phosphorodichloridate		203-234	Glassy	Dark brown
Ethyl phosphorodichloridothionate	12	200-225	Powdery	Dark brown

*0.021 mole acid chloride, 0.021 mole of thiourea, 50 ml carbon tetrachloride, 50 ml water, 0.048 mole sodium hydroxide, 1 min stirring time.

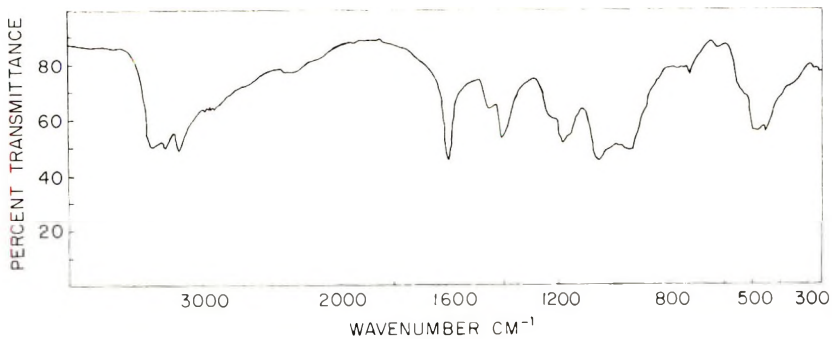


Fig. 2. Infrared spectrum of the product of ethyl phosphorodichloridate and thiourea.

DISCUSSION

The products may possess interesting properties due to the high polar nature of the chains and possibility of existence of resonance forms, which could result in a chain stiffening to take advantage of the various resonance forms. We plan further characterization of the products.



The interfacial technique is, in general, a simpler, faster way of obtaining products of the above general form than methods previously employed. It can be used for systems employing or producing temperature sensitive compounds, since the reaction can be conducted at or below room temperature. It also employs reactants which are commercially available.

References

1. Haven, A. C., U. S. Pat. 2,716,639 (1955).
2. Coover, H. W., R. L. McConnell, and N. H. Shearer, *Ind. Eng. Chem.*, **52**, 412 (1960).
3. Coover, H. W., U. S. Pat. 2,642,413 (1953).
4. Devillers, J., A. Munoz, J. Navech, and J. P. Vives, *Compt. Rend.*, **261**, 1547 (1965).
5. Sander, M., and E. Steininger, *J. Macromol. Sci. Revs.*, **C1**, 91 (1967).
6. Hashimoto, S., I. Furukawa, and S. Tamibuchi, *Kobunshi Kagaku*, **23**, 877 (1966).
7. Nielsen, M., and G. Deebel, U. S. Pat. 3,227,685 (1966).
8. Harris, D., R. Jenkins, and M. Nielsen, *J. Polym. Sci.*, **35**, 540 (1959).
9. Nielsen, M., and D. Harris, U. S. Pat. 3,290,258 (1966).
10. Rodivilova, L. A., M. S. Akutne, K. P. Baebakov, and L. P. Nekrasova, U.S.S.R. Pat. 125,566 (1960).
11. Farago, J., U. S. Pat. 3,116,268 (1963).
12. Ogawa, T., T. Nishimatsu, and Y. Minoura, *Makromol. Chem.*, **114**, 275 (1968).
13. Carraher, C., D. Winthers and F. Millich, *J. Polym. Sci.*, in press.
14. Carraher, C., and D. Winthers, *J. Polym. Sci.*, in press.
15. Carraher, C., and T. Brandt, *Makromol. Chem.*, **123**, 144 (1969).
16. Carraher, C., G. Klimiuk, and T. Brandt, *Macromolecules*, in preparation.

CHARLES E. CARRAHER, JR.
DAVID M. POSEY

Chemistry Department
University of South Dakota
Vermillion, South Dakota 57069

Received December 18, 1968

***Effect of Substituents on Copolymerization Reactivities of
1,1-Disubstituted Ethylenic Monomers***

Many attempts to clarify the correlation between the structure and the reactivity of a series of monosubstituted ethylenic monomers in their radical copolymerizations have been made by comparing the effect of substituents. However, the substituent effect on the copolymerization reactivity of 1,1-disubstituted ethylenic monomers has not been adequately studied. The effects of α -alkyl groups in methyl α -alkylacrylates^{1,2} and of nuclear substituents in ethyl α -benzylacrylates³ have recently been investigated in detail.

In the original discussions of the Alfrey-Price Q - e scheme,^{4,5} it was suggested that the values of $\log Q$ and e of 1,1-disubstituted ethylenic monomers would be expected from those of the unsubstituted monomers by using the additivity of the polar and resonance contributions of the substituents. Since the accurate copolymerization data on 1,1-disubstituted ethylenic monomers were not available, the validity of this expectation has not been proved.

TABLE I
Copolymerization Parameters of 1,1-Disubstituted Ethylenic Monomers ($\text{CH}_2 = \text{CXY}$)
in their Radical Copolymerizations with Styrene (M_2) at 60°C.

X	Y	r_1	r_2	e_1	Q_1	Reference
CN	OCH ₃	0.35	0.35	0.40	0.72	6
CN	CH ₃	0.16	0.30	0.81	1.12	8
CN	C ₆ H ₅	0.7	0.02	1.26	9.60	8
CN	H	0.04	0.40	1.20	0.60	8
CN	Cl	0.13	0.06	1.40	2.83	7
CN	OCOCH ₃	0.20	0.16	1.06	1.17	9
CN	COOCH ₃	0.03	0.01	2.1	11.6	8
CN	CN	0.001	0.005	2.85	20.1	8
COOCH ₃	OCH ₃	0.51	1.10	0.04	0.47	6
COOCH ₃	CH ₃	0.50	0.50	0.40	0.74	8
COOCH ₃	C ₆ H ₅	0.19	0.04	1.41	4.28	8
COOCH ₃	H	0.18	0.75	0.60	0.42	8
COOC ₂ H ₅	Cl	0.30	0.08	1.13	2.65	7
COOC ₂ H ₅	Br	0.50	0.06	1.07	3.70	7
COOC ₂ H ₅	OCOCH ₃	0.20	0.57	0.67	0.54	8
COOC ₂ H ₅	COOC ₂ H ₅	0.08	0.03	1.66	4.78	7
COOCH ₃	CN	0.03	0.01	2.1	12.6	8

Recently, we carried out the radical copolymerizations of methyl α -methoxyacrylate, ethyl α -chloroacrylate, ethyl α -bromoacrylate, diethyl methylenemalonate, α -methoxyacrylonitrile and α -chloroacrylonitrile with styrene at 60°C, and the copolymerization parameters were determined. On the basis of these data^{6,7} and the reported data,^{8,9} the effects of α -substituents on the relative reactivities of α -substituted acrylic esters and acrylonitriles toward a polystyryl radical were discussed.

In Table I the copolymerization parameters of $\text{CH}_2 = \text{CXY}$ monomers (M_1), in which X is CN or COOR, and Y is OCH₃, CH₃, C₆H₅, H, Cl, Br, OCOCH₃, COOR, or CN with styrene (M_2) are summarized. The values of e_1 and Q_1 were calculated from the monomer reactivity ratios (r_1 and r_2) by assuming that the e_2 and Q_2 for styrene are -0.80 and 1.0, respectively.

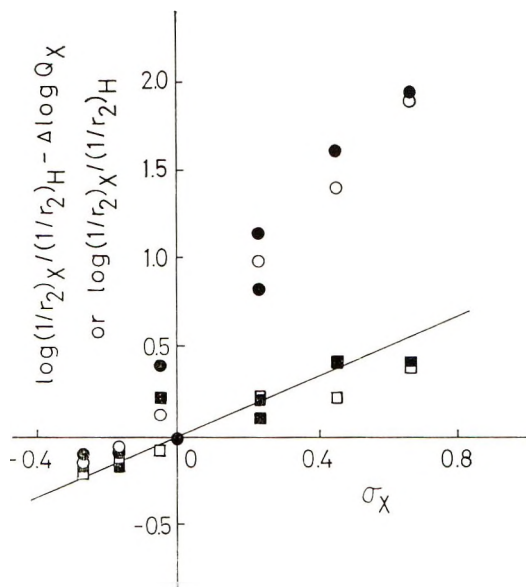


Fig. 1. Plots by eq. (4): (●) $\log(1/r_2)_X/(1/r_2)_H - \Delta \log Q_X$ vs. σ_X ; (■) $\log(1/r_2)_X/(1/r_2)_H$ vs. σ_X for α -substituted acrylonitriles, respectively; (○), (□) respective plots for α -substituted acrylic esters.

Since the reactivities for acrylic methyl and ethyl esters were almost the same as shown in the previous papers,^{10,11} the correlations given in eqs. (1)–(5) were found to be established satisfactorily.

$$\begin{aligned} e_{\text{CH}_2=\text{CXY}} &= e_{\text{CH}_2=\text{CHY}} + 2.4\sigma_X \\ &= e_{\text{CH}_2=\text{CXH}} + 2.4\sigma_Y \end{aligned} \quad (1)$$

$$\begin{aligned} \log Q_{\text{CH}_2=\text{CXY}} &= \log Q_{\text{CH}_2=\text{CHY}} + (\log Q_{\text{CH}_2=\text{CXH}} - \log Q_{\text{CH}_2=\text{CH}_2}) \\ &= \log Q_{\text{CH}_2=\text{CHY}} + \Delta \log Q_X \end{aligned} \quad (2)$$

or

$$\begin{aligned} \log Q_{\text{CH}_2=\text{CXY}} &= \log Q_{\text{CH}_2=\text{CXH}} + (\log Q_{\text{CH}_2=\text{CHY}} - \log Q_{\text{CH}_2=\text{CH}_2}) \\ &= \log Q_{\text{CH}_2=\text{CXH}} + \Delta \log Q_Y \end{aligned} \quad (3)$$

$$\log(1/r_2)_{\text{X}}/(1/r_2)_{\text{H}} = 0.83\sigma_X + \Delta \log Q_X \quad (4)$$

or

$$\log(1/r_2)_{\text{Y}}/(1/r_2)_{\text{H}} = 0.83\sigma_Y + \Delta \log Q_Y \quad (5)$$

Here σ_X and σ_Y are the Hammett polar substituent constants, and $\Delta \log Q_X$ or $\Delta \log Q_Y$ are the resonance substituent constant which was determined from $\log Q_{\text{CH}_2=\text{CXY}} - \log Q_{\text{CH}_2=\text{CHY}}$. The mean values of $\Delta \log Q$ for CH_3O , CH_3 , H , Cl , Br , OCOCH_3 , COOCH_3 , and CN substituents were evaluated as 0.06, 0.26, 0, 0.74, 0.95, 0.20, 1.19, and 1.50, respectively.

Figure 1 shows the plots by eq. (4) or (5). Since $\log(1/r_2)_Y/(1/r_2)_H$ represents the reactivities of α -substituted acrylic esters and acrylonitriles relative to unsubstituted ones, the establishment of eqs. (4) or (5) might strongly indicate that the two substituents contribute additively to the reactivities of α -substituted acrylic esters and acrylonitriles. These correlations [eqs. (1)–(5)] must also be applicable to the

copolymerization reactivities of the monosubstituted ethylenic monomer series other than acrylic ester and acrylonitrile. However, these correlations failed to the reported reactivities for α -substituted styrenes, probably because of the low ceiling temperatures.¹²

Correlations similar to eqs. (4) or (5) were also found in radical polymerization, and the resonance substituent constants, E_R and R , were determined on the basis of hydrogen abstraction from nuclear-substituted cumenes by a polystyryl radical¹³ and of mutual copolymerizations of nuclear-substituted styrenes,¹⁴ respectively. The resulting $\Delta \log Q$ values were closely related to those in E_R and R , except for CH_3O substituent.

From these observations, it might be concluded that the steric effect of the α -substituents in these 1,1-disubstituted ethylenic monomers was not significant compared with the polar and resonance effects.

References

1. K. Chikanishi and T. Tsuruta, *Makromol. Chem.*, **73**, 231 (1964).
2. G. G. Cameron and G. P. Kerr, *European Polymer J.*, **3**, 1 (1967).
3. B. Yamada, T. Hayashi, and T. Otsu, *Kogyo Kagaku Zasshi*, **71**, 2045 (1968).
4. T. Alfrey, Jr., J. J. Bohrer, and H. Mark, *Copolymerization*, Interscience Pub., Inc., New York (1952) p. 81.
5. T. Alfrey, Jr., and L. J. Young, in *Copolymerization*, G. E. Ham, Ed., Interscience Pub. Inc., New York (1964) p. 73.
6. T. Otsu, B. Yamada, and H. Yoneno, *Bull. Chem. Soc. Japan*, in press.
7. B. Yamada and T. Otsu, in preparation.
8. H. Mark, B. Immergut, E. H. Immergut, L. J. Young and K. I. Benyon, in *Polymer Handbook*, J. Brandrup and E. H. Immergut, Eds., Interscience Pub. Inc., New York (1966) p. II-141.
9. T. Oota, M. Kobayashi, and H. Ogawa, *Kogyo Kagaku Zasshi*, **71**, 1542 (1968).
10. T. Otsu, T. Ito, T. Fukumizu, and M. Imoto, *Bull. Chem. Soc. Japan*, **39**, 2206 (1966).
11. T. Otsu, T. Ito, and M. Imoto, *J. Polym. Sci. C* **16**, 2121 (1967).
12. H. Lüssi, *Chimia*, **20**, 379 (1966).
13. T. Yamamoto and T. Otsu, *Chem. Ind.*, **1967**, 787.
14. M. Imoto, M. Kinoshita, and M. Nishigaki, *Makromol. Chem.*, **94**, 238 (1966).

BUNICHIRO YAMADA
TAKAYUKI OTSU

Department of Applied Chemistry
Faculty of Engineering
Osaka City University
Osaka, Japan

Received October 29, 1968

Revised January 6, 1969

Determination of Carboxyl Groups in Water-Soluble Copolymers by a Reverse Dye Partition Method and Calculation of r_1

A reverse dye-partition technique¹ has been developed for the estimation of acid groups in water-soluble polymers. Copolymers of acrylamide and other carboxyl-bearing monomers such as acrylic acid have been prepared, and the monomer reactivity ratio r_1 has been determined by measuring the carboxyl group content in those copolymers by using eq. (1):^{2,3}

$$\lim_{(M_2/M_1)_f \rightarrow 0} \frac{(M_2/M_1)_f}{(M_2/M_1)_p} = r_1 \quad (1)$$

where $(M_2/M_1)_f$ and $(M_2/M_1)_p$ represent the molar ratio of the component monomers M_1 and M_2 in the feed and the copolymer, respectively.

The copolymers of acrylamide and acrylic acid were prepared in an aqueous medium as well as in a mixture of methanol and water (80:20). The first reaction in aqueous media used was H_2O_2 -ultraviolet light to initiate polymerization; the polymerization in methanol-water was carried out at 60°C with benzoyl peroxide as initiator. Copolymers of acrylamide and methacrylic acid were prepared very similarly. A solution of acrylic acid neutralized to pH 7 was used as a solution of sodium acrylate⁴ and polymerized along with acrylamide to copolymers of acrylamide and sodium acrylate. The

TABLE I
Copolymer Composition and Monomer Reactivity Ratio as Determined by Reverse Dye-Partition Method

Copolymer	Conditions of polymerization	$(M_2/M_1)_f$	$(M_2/M_1)_p$	r_1	
				Experimental	Literature
Acrylamide (M_1)- acrylic acid (M_2)	60°C,	0.0150	16.52	1.40	1.38
	Methanol (80%),	0.0125	14.85		
	Bz_2O_2 ,	0.0100	12.29		
	$2 \times 10^{-2} M$	0.0050	9.04		
Acrylamide (M_1)- acrylic acid (M_2)	25°C, aqueous,	0.0200	12.45	0.62	0.60 ± 0.02
	H_2O_2 ,	0.0150	9.67		
	$2 \times 10^{-2} M$,	0.0100	7.04		
	UV	0.0075	5.89		
Acrylamide (M_1)- sodium acrylate (M_2)	60°C	0.0200	9.40	1.00	1.10 ± 0.05
	Methanol (80%),	0.0125	6.15		
	Bz_2O_2	0.0075	4.30		
Acrylamide (M_1)- methacrylic acid (M_2)	25°C,	0.0175	5.13	0.50 ± 0.01	—
	Aqueous,	0.0150	4.38		
	H_2O_2	0.0125	3.49		
	$2 \times 10^{-2} M$, UV	0.0100	2.91		
Acrylamide (M_1)- methacrylic acid (M_2)	60°C,	0.0150	3.70	1.00	—
	Methanol (80%),	0.0125	3.00		
	Bz_2O_2 ,	0.0100	2.78		
Acrylamide (M_1)- crotonic acid (M_2)	$2 \times 10^{-2} M$	0.0075	2.32	54 ± 2	—
	30°C,	0.3000	220		
	Aqueous, H_2O_2 ,	0.2500	205		
	$2 \times 10^{-2} M$,	0.1500	150		
	UV	0.1000	105		

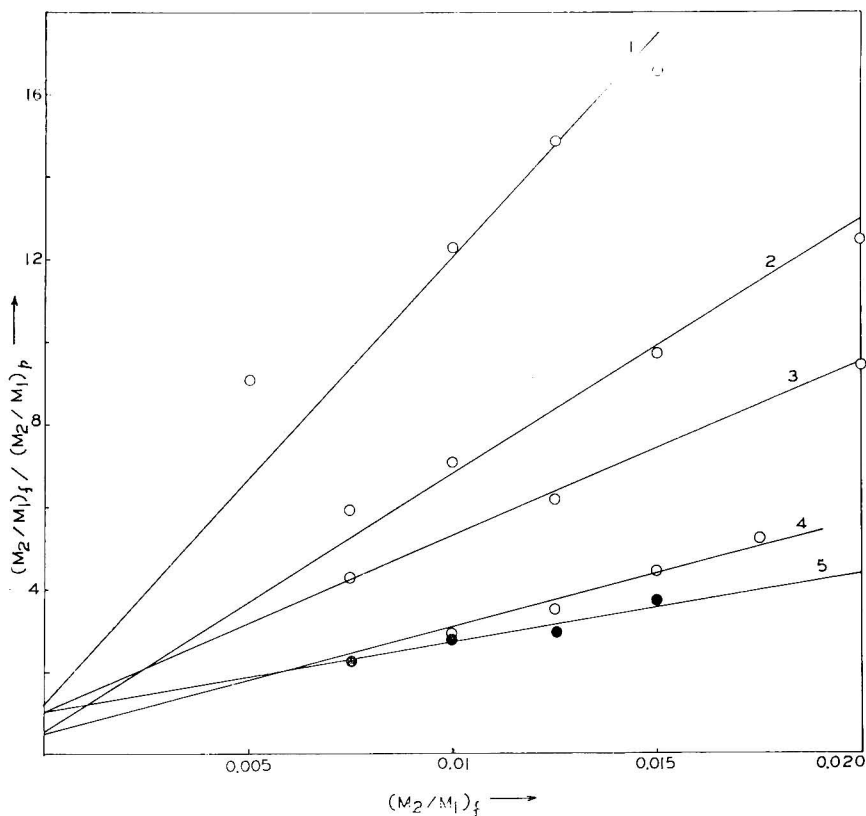


Fig. 1. Plot of $(M_2/M_1)_f / (M_2/M_1)_p$ vs. $(M_2/M_1)_f$ for copolymers: (1) acrylamide-acrylic acid, 60°C; (2) acrylamide-acrylic acid, 25°C; (3) acrylamide-sodium acrylate, 60°C; (4) acrylamide-methacrylic acid, 25°C; (5) acrylamide-methacrylic acid, 60°C.

acid comonomers were generally used in very small proportions in comparison to the other monomer, e.g., acrylamide; however, to get a copolymer of acrylamide and crotonic acid, crotonic acid had to be used in a larger proportion since it has a lower reactivity. The conversion of monomers in all cases was limited to 15–20%. The copolymers were rigorously purified by reprecipitation with methanol from aqueous solution.

The carboxyl contents of the purified copolymers were determined by the reverse dye-partition method. The results of copolymerization are shown in Table I and Figure 1. The monomer reactivity ratio was obtained with help of eq. (1). For each copolymer $(M_2/M_1)_f / (M_2/M_1)_p$ values were plotted against $(M_2/M_1)_f$ values. The plots follow a straight line. The intercept obtained by extrapolating to zero $(M_2/M_1)_f$ value, gives the r_1 value for the copolymer (Fig. 1). The copolymer composition in the polymer $(M_2/M_1)_p$ was obtained by the dye-partition method by comparison against sodium lauryl sulfate.

It may be seen from Table I that for the acrylamide-acrylic acid (at 25°C and 60°C) and acrylamide-sodium acrylate (60°C), the experimental r_1 values are almost identical with the literature values; this gives an idea of the order of accuracy attainable by the present method.

Since the copolymer of acrylamide and methacrylic acid becomes insoluble when the proportion of methacrylic acid in the copolymer is more than 10%, the reactivity ratio r_1 of this copolymer cannot be determined by any common method. But the application of eq. (1) requires the $M_1:M_2$ ratios in the neighborhood of 100:1. At this composition the copolymer is soluble in water and the dye partition technique can be used successfully to determine the r_1 values given in Table I.

Thanks are due to National Bureau of Standards (U.S.A.) for financial assistance to B.C.M. and S.M. in the form of PL-480 Scheme.

References

1. S. Mukhopadhyay, B. C. Mitra, and S. R. Palit., *J. Polym. Sci. A-1*, this issue.
2. S. R. Palit and P. Ghosh, *J. Polym. Sci.*, **58**, 1225 (1962).
3. M. K. Saha, P. Ghosh, and S. R. Palit, *J. Polym. Sci. A*, **2**, 1365 (1964).
4. J. Bourdais, *Bull. Chim. Soc. France*, **1955**, 485.

SAILES MUKHOPADHYAY
BHAIKAB CHANDRA MITRA
SANTI R. PALIT

Department of Physical Chemistry,
Indian Association for the
Cultivation of Science, Jadavpur,
Calcutta, India

Received June 19, 1968

Revised January 8, 1969

A Novel Method of Metal Ion Removal and Recovery from Water by Complex Formation with Polyelectrolytes

It is well known that polyelectrolytes form complexes with metal cations and also with a number of anions. This is widely utilized in the case of ion-exchange resins. Also, linear polyelectrolytes form complexes;¹ poly(methacrylic acid) and poly(acrylic acid), for instance, combine with heavy metal ions. These complexes are usually water-soluble and stable. Similarly, polyelectrolytes such as proteins can complex with metal ions. These complexes are of great biological significance. The complexation is often a function of the spacing of the reactive groups in the polyelectrolyte. Thus stereospecific isomers of polyelectrolytes show differences in their complexing capacity due to differences in spacing of their side groups.

The metal ion is frequently formulated as belonging to one polymer chain only; alternately, the metal ion is considered to be bound to two chain molecules. Morawetz¹ maintains that, for instance, copper complexes with two poly(methacrylic acid) chains, whereas results obtained by Jellinek and Lipovac² indicate that only one chain is involved. The latter authors worked with lower concentrations than Morawetz; thus it may be possible that the type of complex is dependent on the polymer and metal ion concentrations, respectively.

PRINCIPLE OF METHOD OF METAL REMOVAL AND RECOVERY

The principle of the new method is based on the observation that heavy metal ions (e.g. Cu^{2+} ions) form water soluble complexes with poly-acids, e.g. poly-(acrylic acid) and atactic and isotactic poly(methacrylic acid), over a wide range of pH values. Addition of a polybase to a complex such as poly(ethylene imine) produces immediately an insoluble complex, consisting of metal-polyacid-polybase, which precipitates. The precipitate can be filtered and decomposed with small amounts of mineral acid. The polyacid-polybase compound remains insoluble, while the metal is leached out and goes into the filtrate forming a highly concentrated solution. The "insoluble" polyacid-polybase compound can be used again for further metal complexation. Thus the loss in polymer is quite small.

EXPERIMENTAL RESULTS

Various Ions

Experiments were carried out with a number of ions. It was ascertained that the following ions are "completely" precipitated within the sensitivity of the analytical method by this procedure. (Only one ion was contained in each solution): Zn^{2+} , Cd^{2+} , Ni^{2+} , Co^{2+} , $\text{Cr}_2\text{O}_7^{2-}$, Cu^{2+} , Fe^{3+} , and CN^- . Mg^{2+} and Pb^{2+} ions are removed only to the extent of 70% by one precipitation. The concentration of each solution was $10^{-2}M$ with respect to each ion. Higher concentrations have to be treated with proportionately larger amounts of polyelectrolyte. CN^- ions form a white precipitate with the polyelectrolytes, when the pH is below 10; they do not precipitate above this pH value. The iron (III) complex (orange color) is hardly decomposed by mineral acid (pH = 1). Thus, iron cannot be easily recovered from the complex.

Some experiments were performed with solutions containing a number of ions. For instance, 10 mg of poly(methacrylic acid) and 10 mg of poly(ethylene imine) were added to 40 ml (pH ~ 10) of a solution $10^{-4}M$ with respect to Zn^{2+} , Cu^{2+} , Pb^{2+} , Mg^{2+} , Ni^{2+} , Fe^{3+} , Cr^{6+} , Cd^{2+} , Co^{2+} , and CN^- ions. A precipitate was formed at once. The remaining solution was filtered. The filtrate contained very small amounts of a Mg^{2+} ion complex and some metal cyanide complexes.

Metal cyanide complexes cannot be precipitated because of their extremely small instability constants. Whether Cd^{2+} ions can be precipitated in the presence of CN^-

ions by polyelectrolytes remains to be seen; however, there is a possibility that this may be the case, as the instability constant for this cyanide complex is about 10^{11} times that for the copper cyanide complex.

Detailed Experiments with Cu^{2+} and Co^{2+} Ions

Cu^{2+} Ions. CuCl_2 was a purified product (Fisher Scientific Company, Inc.); 25% (w/v) aqueous poly(acrylic acid) (PAA, I) was obtained from Rohm and Haas Company; 5% (w/v) aqueous atactic poly(methacrylic acid) (PMAA-A, II) and 50% (w/v) aqueous poly(ethylene imine) (PEI, IV) were supplied by Borden Chemical Company; isotactic poly(methyl methacrylate) was prepared by Grignard reagent.³ Its viscosity-average chain length and intrinsic viscosity in benzene solution were 1.43×10^4 and 2.72 dl/g, respectively.^{4,5} Chain scission does not take place during acid hydrolysis of the ester with concentrated sulfuric acid;² the viscosity-average molecular weight of the isotactic poly(methacrylic acid) (PMMA-I, III) calculated on this basis was 1.23×10^6 .

Complex formation of I, II, III, and IV with copper(II) ions has been reported repeatedly in the literature.⁶⁻¹⁰ I, II, and IV are soluble in water over the whole range of pH values, except that I and II are not soluble at very low pH values and IV is not soluble at very high pH values.

Initially, experiments were carried out on precipitation of the copper complex with I, II, III, and IV from aqueous solutions by sodium chloride. The initial copper concentration was $1 \times 10^{-4}M$ in each case. The amounts of sodium chloride sufficient for the precipitation of the copper complex were determined. pH values were adjusted by 0.1N NaOH or HCl, respectively; borax and phosphate buffers were avoided, as these are partly precipitated under the relevant conditions. Copper concentrations were determined colorimetrically with $\text{K}_4[\text{Fe}(\text{CN})_6]$;¹¹ 0.4 ppm copper in water can be detected in this way.* The solutions containing the complexes with I and II had practically to be saturated with sodium chloride before some precipitation of the complex took place; however, appreciable amounts of the complex remained in solution. In the case of IV, even saturation with sodium chloride was not sufficient. The complex with III can be precipitated with moderate amounts of sodium chloride, but a fairly large excess of III is needed (ca. 12×10^{-4} monomeric unit mole/l.) for an initial copper concentration of $1 \times 10^{-4}M$.

The complex with III can be precipitated by lowering the pH value of the solution to about 4; but only about 50% of the copper complex (initial Cu^{2+} concentration $1 \times 10^{-4}M$) is precipitated and a large excess of III has to be taken (ca. 14×10^{-4} monomeric unit moles). All of the copper can be removed in this way by successive complexation. However, this procedure is quite laborious and not efficient.

Successful and efficient precipitation was effected by adding a polybase, such as IV, to the copper complex formed with one of the polyacids. The results are shown in Figure 1, for pH 7.0 and 4.5, respectively. Here the copper (II) ion concentration in the filtrates, after filtering the insoluble complexes, (with the use of glass crucibles, "fine"), obtained with different ratios of polyacid and polybase (see Fig. 1) is plotted against the Cu^{2+} concentration in the initial solutions. The maxima and the subsequent decrease in the curves at pH 7 are due to hydrolysis of copper (II) ions. A straight line is obtained at pH 4.5, where hydrolysis is negligible. Table I shows the maximum initial Cu^{2+} concentration, which can be taken for complete removal of the copper by complexation (i.e., all copper bound in the respective complex) by definite monomeric unit molar ratios of polymer.

* The legal limit of Cu^{2+} in water was 1.6×10^{-3} mole/l. in 1962. We have assumed that, generally, not more than about 1.5×10^{-4} mole/l. of Cu^{2+} is present in the water. About 7×10^{-6} mole/l. can be detected with $\text{K}_4[\text{Fe}(\text{CN})_6]$; there is almost certainly less than this amount left in the solution after precipitation. Larger amounts of the Cu^{2+} can be removed by increasing the polyelectrolyte concentrations correspondingly.

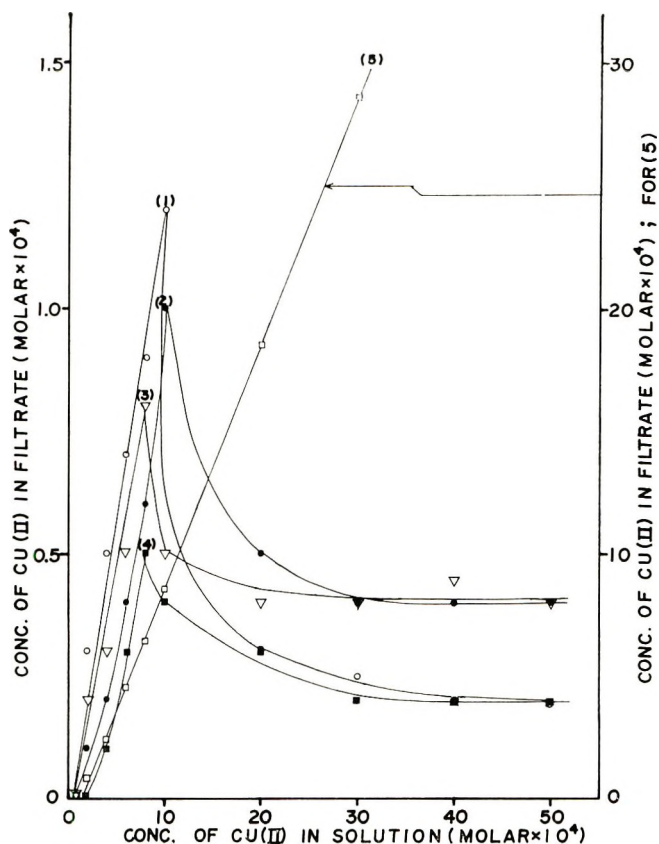


Fig. 1. Copper (II) concentration in filtrate vs. initial Cu (II) concentration in solution. Numbers on curves refer to Table I for various monomeric unit molar ratios of polyacid and polybase.

The efficiency of II and III is similar; it appears to increase with decreasing pH value. Small variations in the amounts of polybase do not have a great influence on the maximum initial Cu^{2+} concentration.

Copper (II) ions may be obtained from the precipitated complex as follows. The complex with I, II, and III precipitated with IV is destroyed by washing it with acid of approximately pH 3 (in case of III, the pH can be appreciable lower than 3). The complex is destroyed and Cu^{2+} ions go into the filtrate while the polymer remains as precipitate. Very small amounts of liquid are needed for this purpose, so that the Cu^{2+} concentrations are appreciably higher than those in the initial solutions. The polymer acid-base compound is only very slightly soluble at these pH values. It can be used again for complex formation by introducing it into a copper solution (pH 4.5), stirring and filtering the formed complex. The procedure from there on is then the same as described above.

For example, equal volumes of solutions of 25 mg/l. each of II and IV, respectively, were combined. Precipitation took place (pH 5). A solution of cupric chloride was added with stirring and the resulting mixture adjusted to pH 4.5. The precipitated complex and solution were $1 \times 10^{-4}M$ in Cu^{2+} , $2.90 \times 10^{-4}M$ (monomeric unit) with respect to II and $5.80 \times 10^{-4}M$ (monomeric unit) with respect to IV. The experiments were carried out in duplicate; one of the mixtures was stirred for 1 hr and the other for

TABLE I
Maximum Initial Concentration of Cu^{2+} for Complete Complexation as a
Function of Monomeric Unit Molar Ratios of Polymers

pH	Polymer, monomeric unit molar ratio	Maximum initial Cu^{2+} concentration for practically 100% complexation, M	Fig. 1 curve
7	IV/III-isotactic, 2.10 (25 mg/l. each)	1.0×10^{-4}	1
7	IV/III-isotactic, 1.50 (18.75 mg/l. IV; 25 mg/l. III).	1.0×10^{-4}	2
7	IV/III-isotactic, 1.00 (12.5 mg/l. IV, 25 mg/l. III).	1.0×10^{-4}	3
7	IV/III-isotactic, 0.50 (12.5 mg/l. IV; 50 mg/l. III).	2.0×10^{-4}	4
4.5	IV/II atactic = 2.00 (25 mg/l. each)	1.5×10^{-4}	5

15 min. The precipitates were filtered; copper could not be detected in the filtrate in either case, indicating that under these conditions, all copper was in complex form in the precipitate.

Co²⁺ Ions. Co²⁺ ions are very strongly bound to isotactic PMA.¹² Our experiments showed that Co²⁺ ions form water-soluble complexes with II and III and also with IV alone in solution at very low Co²⁺ concentrations (ca. $3 \times 10^{-6}M$). The polyacid-(or polybase-) Co-complex can be precipitated by adding polybase (or polyacid). The experimental procedure is the same as that described for copper.

After precipitation, cobalt was determined spectrophotometrically in the filtrate with the use of Nitroso-R salt reagent. For instance, when 1 mg of IV and 1 mg of III (molar ratio 2.09) were added to 40 ml of a $1 \times 10^{-4}M$ Co²⁺ solution, the filtrate was $1.26 \times 10^{-3}M$ with respect to Co²⁺ ions. However, when the polyelectrolyte amounts were doubled (2 mg each, molar ratio 2.09), Co²⁺ ions could no longer be detected in the filtrate. Thus 2.36×10^{-4} g of Co can be removed completely from 40 ml of an $1 \times 10^{-4}M$ Co²⁺ solution by adding 2 mg each of the respective polyelectrolytes; 90% can be removed by adding 1 mg of each electrolyte.

The procedure for cobalt recovery from the precipitated complex is as follows. The precipitate is washed with acidic water (pH < 3). Cobalt goes into solution, while the polyelectrolyte compound remains on the filter.

SUMMARY

A novel method of metal removal and recovery is described. This method may be useful in connection with various types of water pollution. It is based on the fact that metal ions form water-soluble complexes with water-soluble polyelectrolytes, such as polyacids. These complexes can be precipitated with polybases and the metal can be recovered by treating the precipitate with mineral acid. The remaining polymer complex can be used again for further precipitation. Experiments with Cu^{2+} and Co^{2+} ions are given in some detail; general observations concerning other cases are included.

References

1. H. Morawetz, *Macromolecules in Solution*, High Polymers, Vol. XXI, Interscience, New York, 1965.
2. H. H. G. Jellinek and S. N. Lipovac, *J. Macromol. Chem.* **1**, 773 (1966); H. H. G. Jellinek and S. N. Lipovac, *J. Polym. Sci. C*, in press.

3. W. E. Goode, F. H. Owens, R. P. Fellmann, W. H. Snyder, and J. E. Moore, *J. Polym. Sci.*, **46**, 317 (1960).
4. E. M. Loebel and J. J. O'Neill, *J. Polym. Sci.*, **45**, 538 (1960).
5. S. Krause and E. Cohn-Ginsberg, *J. Phys. Chem.*, **67**, 1479 (1963).
6. E. M. Loebel, L. B. Luttinger, and H. P. Gregor, *J. Phys. Chem.*, **59**, 559 (1955).
7. H. P. Gregor, L. B. Luttinger, and E. M. Loebel, *J. Phys. Chem.*, **59**, 34 (1955).
8. F. T. Wall and S. T. Gill, *J. Phys. Chem.*, **58**, 1128 (1954).
9. A. M. Kotliar and H. Morawetz, *J. Phys. Chem.*, **77**, 3692 (1955).
10. T. D. Perrine and W. R. Landis, *J. Polym. Sci. A-1*, **5**, 1993 (1967).
11. A. Vogel, *A Textbook of Quantitative Inorganic Analysis*, Longmans, Green, New York, 1948, p. 727.
12. L. Constantine, V. Crescenti, L. Quadrifoglio, and J. Vitaglione, *J. Polym. Sci. A-2*, **5**, 771 (1967).

H. H. G. JELLINEK
MING DEAN LUH

Department of Chemistry
Clarkson College of Technology
Potsdam, New York 13676

Received January 13, 1969

Kinetics of Acyl Chloride Reactions with Diols

The publication of some rate constants for hydroxyl-acyl chloride reactions in dioxane solution by Tiger, Yevreinov, and Entelis¹ prompts us to report similar results previously available only in thesis form.²

EXPERIMENTAL

Solvent and reactants were carefully purified by standard procedures. The acyl chloride was contained in an ampoule of thin-walled glass and reaction was started by breaking the ampoule under the dioxane solution of the appropriate alcohol. Portions of the reaction system were removed by hypodermic syringe via a rubber serum cap and quenched in a water-dioxane-butanone mixture. After quenching, the reaction samples, of measured weight, were titrated against nonaqueous (benzene-ethanol 50/50) sodium hydroxide to a phenolphthalein endpoint. Following acidimetry, the chloride ion content was found by titration of the solution (brought to apparent pH 5-6) against aqueous silver nitrate, using dichlorofluorescein as indicator. A slight loss of HCl from the system occurred during reaction and the necessary correction was made in calculation of the extent of reaction.

RESULTS

The data are summarized in Table I. In all cases, second-order kinetics were followed to ca. 70% conversion, after which a slight decrease in slope of the second-order plot was detected.

Most attention was paid to the decan-1,10-diol-hexadioic acid dichloride reaction. The rate constant is not affected by a change in the ratio of reactant concentrations and increases slightly with diol concentration. Tiger et al.¹ also find, for the propan-1,3-diol-decandioic acid dichloride reaction, a drift of the second-order rate constant with hydroxyl concentration and were able, by the use of supplementary dielectric constant data, to show that their results were consistent with the Kirkwood equation. Only minor changes in the experimentally observed rate constant occur on changing reactant structure.

The activation energy is estimated to be 10.8 ± 1.0 kcal/mole (expts E1, E2, and A4) whereas Tiger et al.¹ report 8.8 kcal/mole (for the reaction of propan-1,3-diol with decandioic acid dichloride). For this reaction, the rate constant at 30°C is ca. 13.5×10^{-4} l./mole-sec compared to our value of ca. 6.4×10^{-4} l./mole-sec with the longer diol molecule.

It is perhaps a little surprising that in both the Russian work and our own studies, simple second-order kinetics are well obeyed in view of the known complexity and strong solvent dependence of acylation reactions.³ Although early work reported acylations in various solvents to be third-order⁴ and second-order,⁵ more recent work has shown that the rate of ethanolsis of *p*-nitrobenzoyl chloride in dioxane⁶ is proportional to the concentration of self-associated alcohol. However, Price et al.⁷ found second-order behavior between hexandioic acid dichloride and 2,2-dimethylpropan-1,3-diol in tetrachlorethane solution and suggest that solvation of the transition complex is provided by solvent rather than by further alcohol molecules. A similar situation appears to exist in the polycondensations reported here and by Tiger.¹

References

1. R. P. Tiger, V. V. Yevreinov, and S. G. Entelis. *Polym. Sci. USSR*, **8**, 2209 (1966.)
2. P. V. Wright, M.Sc. Thesis, University of Manchester, 1964.
3. R. F. Hudson, *Chimica*, **15**, 394 (1961).

TABLE I
Second-Order Rate Constants in Acylation

Expt	Temperature, °C	Hydroxy compound	[OH] ₀ , mole/l.	AcyI chloride	[COCl] ₀ , mole/l.	$k \times 10^4$, l./mole-sec
A1	30	Decan-1,10-diol	0.095	Hexandioic acid dichloride	0.095	6.07
A2	"	"	0.180	"	0.180	6.31
A3	"	"	0.294	"	0.294	6.85
A4	"	"	0.379	"	0.379	7.25
A5	"	"	0.423	"	0.423	7.47
B1	"	"	0.384	"	0.767	7.29
B2	"	"	0.392	"	0.196	7.31
C1	"	"	0.186	Decandioic acid dichloride	0.186	5.68
C2	"	"	0.393	"	0.393	6.52
C3	"	Hexan-1,6-diol	0.229	Hexandioic acid dichloride	0.229	6.38
C4	"	"	0.376	"	0.376	6.84
D1	"	Decan-1,10-diol	0.381	Hexanoic acid chloride	0.381	6.18
D2	"	Decan-1-ol	0.454	Hexandioic acid dichloride	0.454	7.06
E1	40	Decan-1,10-diol	0.367	"	0.367	13.61
E2	20	"	0.381	"	0.381	4.08
F1	30	"	0.418	"	0.418	7.71 ^a

^a In presence of excess HCl and ester (dibutyl adipate).

4. A. A. Ashdown, *J. Amer. Chem. Soc.*, **52**, 268 (1930).
5. J. F. Norris and E. C. Haines, *J. Amer. Chem. Soc.*, **57**, 1425 (1935).
6. R. F. Hudson and I. Stelzer, *Trans. Faraday Soc.*, **54**, 213 (1958).
7. F. P. Price, J. M. Gibbs, and B. H. Zimm, *J. Phys. Chem.*, **62**, 972 (1958).

G. J. HOWARD
P. V. WRIGHT*

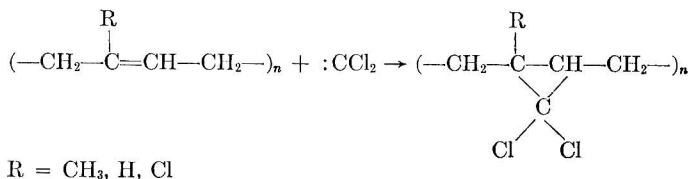
Department of Polymer and Fibre Science
University of Manchester Institute of Science and Technology
Manchester, England

* Present address: Department of Chemistry, University of York, England.
Received January 23, 1969

Preparation and Properties of Polyisoprene-Dichlorocarbene Adduct

INTRODUCTION

The reaction of dichlorocarbene with polyenes to give polymers with backbones containing cyclopropane rings has been the subject of several recent publications.¹⁻⁴ As a result of these studies, it is known that the addition of



dichlorocarbene to a polyene will result in an increase in T_g of the polymer and that the greater the percentage conversion of olefin to cyclopropane ring for a given polyene, the higher the rise in T_g . The present study was undertaken in an attempt to determine the highest rise in T_g possible, that is, with quantitative carbenylation, and to determine the mechanical properties of such a material.

It has been established that the most reactive common polyene towards dichlorocarbene is polyisoprene¹ (R = CH₃) and thus *cis*-1,4-polyisoprene (Shell IR-350) was chosen for this study. The following procedure was developed for large-scale preparation of nearly quantitatively dichlorocarbenylated polyisoprene.

EXPERIMENTAL

Dry powdered sodium methoxide (1430 g) was added with stirring to 300 g of polyisoprene dissolved in 6 l. of tetrahydrofuran (Matheson Coleman and Bell) in a 12-l., three-necked, round-bottomed flask equipped with stirrer, nitrogen inlet, reflux condenser topped by a Dry Ice condenser, thermometer, and a pressure-equalizing addition funnel. Stirring was continued until the powder was dispersed.

With the mixture under positive nitrogen pressure, 150 g of chloroform was added; and with the aid of an acetone-ice bath, the resultant exotherm was controlled at a maximum temperature of 60°C. The temperature was maintained above 35°C by the dropwise addition of 1200 g of chloroform and the slurry stirred for 16 hr. Next, a slurry of 456 g of sodium methoxide in tetrahydrofuran was added followed by dropwise addition of 1530 g of chloroform. Again the reaction was allowed to stir for 16 hr. In general, heating was not necessary to keep the temperature above 35°C. Finally, slurries of sodium methoxide in tetrahydrofuran were added until no further exotherm was observed.

The product was precipitated and powdered by pouring the reaction mixture into methanol in a Waring Blender. After filtration and more methanol washes, the product was stirred overnight as a slurry in methanol. The polymer was washed with water until the wash water was neutral to litmus paper. The polymer was dried under vacuum at 50°C. The material had a hot-stage softening point of 80-85°C, yield 561 g.

The entire sample was dissolved in 11.2 l. of ethylene dichloride in a 22-l. flask. Chloroform (1500 g) was added followed by 50 g. portions of sodium methoxide every 20 min as slurries in ethylene dichloride. (Ethylene dichloride reacts with base much slower than does chloroform under these conditions⁵ and does not give a carbene.⁶ The walls of the flask were rinsed with excess ethylene dichloride after each addition to prevent the buildup of high methoxide concentrations. The temperature was maintained between 35-45°C. with the aid of an ice bath. A total of 670 g of sodium methoxide

was added. Finally, addition of 100 g of chloroform gave no temperature increase. After stirring for 16 hr, the above procedure was repeated with 1400 g of chloroform and portionwise addition of 830 g of sodium methoxide.

The material was isolated as before to yield 554 g. of product. A compression-molded sample softened at 115–120°C.

ANAL. Calcd. for $(C_6H_8Cl_2)_n$: C, 47.71%; H, 5.34%; Cl, 46.95%. Found: C, 49.51%; H, 5.54%; Cl, 44.83, 44.76%; Na, 0.046%.

POLYMER CHARACTERIZATION and DISCUSSION

The NMR spectrum substantiated the proposed structure. The methyl group showed as an absorption at $\tau = 8.6$, the methylene groups at $\tau = 8.33$, and the ring proton in a broad band centered near $\tau = 9$. There was no evidence of an olefinic proton. Two minor peaks were found at $\tau = 7.9$ and 6.4. No absorption characteristic of an insertion reaction was detected. Such a reaction, as shown below, would give rise to an absorption of $\tau = 4-5$ for the $-CCl_2H$ group.⁷

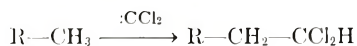


Table I compares the NMR spectrum of the adduct with that of the starting polyisoprene. It can be seen that the effect of dichlorocarbene addition on the chemical shift of the methyl and methylene groups is minor. On the other hand, conversion of the olefinic proton to a ring hydrogen causes a significant change in chemical shift.

The extent of olefin conversion was estimated from the chlorine analysis. The level of chlorine corresponds to 95.5% conversion of olefin to cyclopropane ring, assuming that the carbene insertion reaction is negligible. As a cross check, the iodine number was

TABLE I


	τ	
	τ , Polyisoprene	CCl_2 adduct
$-CH_3$	8.4	8.6
$-CH_2-$	8.01, 8.02	8.33
$=C$	5.1	—
	—	~ 9 (broad)

TABLE II

Property	
T_g (by strain gauge measurement), °C	82–83
60-cycle dissipation factor, α -peak, °C	108
Deflection temperature under load (DTUL) at 264 psi, °C	86.7
Impact strength, ft-lb/in.	
Izod notched ft-lb/in.	0.3
Tensile ft-lb/in. ²	16
Tensile properties	
Elongation at maximum stress, %	1.97
Maximum stress, psi	5897
Modulus, psi	428,000

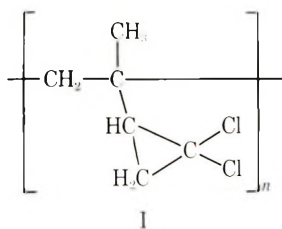
determined to be 10.0 and 10.1 which corresponds to a 94.3% conversion for a polymer with the determined percentage of chlorine.

The limited thermal stability¹ of this compound necessitated changes in the conventional methods of processing for thermoplastic materials. Samples were milled on a mill roll at room temperature for 15 sec and granulated with a Cumberland cutter. The flakes were compression molded into sheets $\frac{1}{8}$ in. thick. The sheets were dark brown and opaque although thin films were transparent.

The mechanical properties of the material are listed in Table II.

It can be seen from the strain gauge T_g measurement that nearly quantitative addition of dichlorocarbene to the polyisoprene backbone causes a sharp increase in glass temperature (polyisoprene $T_g = -73^\circ\text{C}^8$). Values of 108°C for the α -peak and 86.7°C for the DTUL at 264 psi substantiate this higher glass transition temperature.

A small amount (4-5%) of the isoprene in the starting polymer is incorporated by a 1,2 addition rather than the predominant 1,4 addition. This results in a small amount of olefin on the side chain which reacts to give the structure I.



The addition of this bulky group to the side chain should also serve to increase the T_g , but the relative effect would be minor compared to that of adding dichlorocarbene to the polymer backbone.

We would like to acknowledge the assistance of Dr. S. Havriliak and co-workers during the processing and testing programs, of Mrs. Naomi Steck and co-workers for determination of the 60-cycle dissipation factor, and of Dr. A. R. Weiss, Mrs. E. C. Ginsberg, and co-workers for the determination of T_g .

References

1. C. Pimazzi and G. Levesque, *C. R. Acad. Sci., Paris*, **260**, Groupe 7, 3393 (1965).
2. I. S. Lishanskii, V. A. Tsitskhtsev, and N. D. Vinogradova, *Vysokomolekul. Soedin.*, **8**, 186 (1966).
3. J. Lal and W. M. Saltman, *J. Polym. Sci., Pt. A-1*, **4**, 1637 (1966).
4. C. Pimazzi and G. Levesque, *C.R. Acad. Sci., Paris, C*, **264**, 228 (1967).
5. P. Petrenko-Kritschenko and V. Opotsky, *Ber.*, **59B**, 2131 (1926).
6. R. J. Koll, U.S. Patent 2,539,307 (1951).
7. NMR Spectra Catalog, Varian Associates, Volume 1, 1962, Spectra Numbers N149, N218, 2.
8. J. Brandrup and E. H. Immergut, Eds., "Polymer Handbook," Interscience Publishers, New York, 1966, p. III-73.

W. G. DEWITT III
M. J. HURWITZ
F. ALBRIGHT

Research Laboratories
Rohm and Haas Company
Bristol, Pennsylvania 19007

Received February 18, 1969

A Novel Determination of the Molecular Weight of Nylon 66

The number-average molecular weight of nylon 66 has been measured many times by titration of the acidic and basic endgroups.¹ The results obtained are comparable with those determined by Staudinger's viscometric method and vary from about 10000 to 20000. In the present work nylon 66 has been methylated with ethereal diazomethane and the molecular weight calculated from the methoxyl content of the product assumed to contain one methyl ester endgroup per chain molecule.

Preliminary experiments showed that the degree of methylation of nylon, unlike that of cotton cellulose,² is very little, if at all, increased by the presence of water in the ethereal diazomethane. Portions of nylon were methylated once and twice respectively with a large excess of reagent and the methoxyl contents of the products and of the original nylon were determined twelve times. The results were as shown in Table I. These figures indicate a molecular weight of about 13000-14000, which is within the usual range found by other methods.

TABLE I

	Methoxyl content (mean), %	Standard error of estimate
Nylon	0.005	±0.00074
Nylon methylated once	0.226 ^a	±0.0044
Nylon methylated twice	0.246	±0.0038

^a Mean of 11 determinations.

Materials

Nylon 66 filament (45 den) was boiled for 1 hr in a solution containing 0.5% soap and 1% sodium hydroxide. Before methylation it was steeped in 10% acetic acid, freed from acid by washing with ammonia-free distilled water, dried over phosphorus pentoxide and exposed to moist air for 0.5 hr in a closed vessel.

Diazomethane was prepared by distilling a mixture of nitrosomethylurea ether and 50% aqueous potassium hydroxide,³ and the concentration of the distillate was determined by adding a portion to an excess of benzoic acid dissolved in ether and back-titrating the excess.³ It was diluted with ether to give a 0.5M solution. Immediately before use water was added (10 g/l.).

Methylation Procedure

Nylon was steeped in moist 0.5M diazomethane (50 cc/g) for 24 hr at 0°C, filtered, washed with ether, steeped in 10% acetic acid, washed with ammonia-free distilled water, and dried as already described. A portion was methylated a second time. There was no appreciable increase in weight on methylation.

Determination of Methoxyl Content

The modified procedure of Samsel and McHard⁴ was used but with the time of heating extended to 1 hr.² Nylon samples (0.1 g) were dried to constant weight *in vacuo* over phosphorus pentoxide. Determinations were carried out in sets of four: (a) reagent blank, (b) original nylon, (c) once-methylated nylon, and (d) twice-methylated nylon. Results for runs b, c, and d were corrected for the blank titer. Freshly standardized 0.01N sodium thiosulfate was used for each set of determinations.

References

1. H. F. Mark, S. M. Atlas, and E. Cernia, *Man-made Fibers*, Vol. 2, Interscience, New York, 1968.
2. F. S. H. Head, *J. Text. Inst.*, **43**, T1 (1952) and references therein.
3. F. Arndt, in *Organic Syntheses*, Coll. Vol. II, A. H. Blatt, Ed., Wiley, New York, 1943, p. 165.
4. E. P. Samsel and J. A. McHard, *Ind. Eng. Chem. Anal. Ed.*, **14**, 750 (1942).

FRANK S. H. HEAD

Cotton Silk and Man-made Fibres Research Association
Shirley Institute
Manchester 20, England

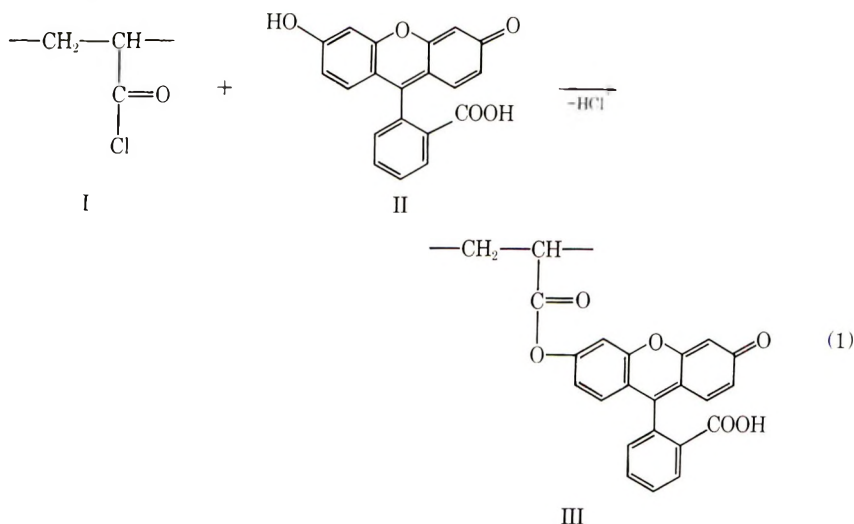
Received March 4, 1969

Preparation and Property of Acrylyl Fluorescein Polymer

In a previous paper,¹ the author reported the synthesis of a redox polymer containing the isalloxazine side chains which also emits a strong fluorescence in aqueous solutions.

In this report the synthesis of vinyl polymers containing fluorescein as side chains and the properties of the resulting polymers will be described.

The fluorescein polymers were prepared by the reactions of acrylyl chloride polymers with the phenolic hydroxyl of fluorescein as shown in eq. (1):



The polymer thus produced emit an extremely light-sensitive fluorescence in the presence of water or alcohols, accompanied with small shifts of absorption peak in the visible region towards lower wavelengths, thereby leading to the change in color from orange red to greenish yellow with moisture ($-\text{COOK}$ or $-\text{COONa}$ type).

Poly(acrylyl fluorescein)

A 10-g portion of purified acrylyl chloride was dissolved in 10 g of anhydrous dioxane. The resulting solution was subjected to 48 hr polymerization at 50°C under nitrogen, with the use of 0.15 g of azobisisobutyronitrile as initiator.

The resulting viscous solution ($[\eta]$ in dioxane at 20°C = 0.24) was added dropwise to a suspension of 50 g of fluorescein in 500 ml of anhydrous dioxane under vigorous agitation. The red mixture soon turned yellow, and gel formation of the whole mass was observed subsequently. Stirring was continued for an additional 5 hr and the reaction mixture was extracted with tetrahydrofuran containing a small portion of water until color was no longer discernible in the extract. The polymer was then extracted with water several times to destroy the most of the anhydride linkages formed and dried to yield a yellow mass (polymer A).

The infrared spectrum of the product indicates a strong ester carbonyl absorption around 1750 cm^{-1} which is unexpected for a mixture, but (on the basis of the absorption of acetyl fluorescein, the model compound, at 1770 cm^{-1}) is expected for the reaction product. Polymer A is partly soluble in aqueous alkali due to the conversion into its alkali salt and the cleavage of some of the remaining anhydride crosslinks to emit a strong fluorescence (emission peak, 520–530 $m\mu$). There were observed no changes in absorption peaks of polymer A in infrared spectrum on alkali treatment and subsequent isolation of free carboxylic groups for the soluble portion. The extent of reaction of the

soluble portion of polymer A, as determined by spectroscopy with the absorbance of the potassium salt at 500 m μ in ethanol-water (1:1 volume ratio) against acetyl fluorescein potassium salt as standard, was 92%.

Conductometric titration of ca. 0.01 *N* solutions of the potassium salt of the soluble portion of polymer A in aqueous solutions with 0.531 *N* hydrochloric acid afforded the total free carboxylic group content (recognized in infrared spectrum as 1700 cm⁻¹ band) of 0.00284 mole/g polymer, which corresponds to 89% of units of structure III and the remaining 11% in acrylic acid unit.

ANAL. Calcd. for the above composition: C, 71.22%; H, 3.68%. Found: C, 70.56%; H, 3.61%.

Acrylyl Fluorescein Copolymer

In a typical preparation of alcohol-soluble but water-insoluble fluorescein polymers, 1 g of purified acrylyl chloride, 5 g of styrene, and 5 g of butyl acrylate were dissolved in 20 ml of benzene; the solution thus formed was subjected to polymerization for 5 hr at 80°C under nitrogen, 0.1 g of azobisisobutyronitrile being used as initiator. A 0.7-g portion of the resulting viscous polymer solution ($[\eta]$ in tetrahydrofuran at 20°C = 0.32) was added dropwise to a suspension of 1 g of fluorescein in 10 ml of anhydrous dioxane at ambient temperature under vigorous agitations. Stirring was continued for an additional 5 hr at ambient temperature, and the unreacted fluorescein was removed by filtration, followed by the pouring of the filtrate into water to isolate a light yellow precipitate. The precipitate was then dissolved in ethanol, potassium hydroxide was added to convert the carboxyl groups in polymer to their potassium salt, and the resulting solution was precipitated into water to obtain a purified product (polymer B).

The purified product in the form of the potassium salt, when subjected to drying under reduced pressure, assumes the form of an orange mass, is soluble in alcohol and alcohol-water mixtures, and emits a strong fluorescence 520–530 m μ in peak wavelength in the presence of water or alcohol even under room lights. The infrared spectrum indicates a strong ester carbonyl absorption around 1750 cm⁻¹ as in the case of polymer A. The extent of reaction determined by spectroscopy was 88% against the acrylyl chloride component in polymer.

The free carboxylic acid content determined as above in ethanol-water (1:1 volume ratio) was 0.000268 mole/g polymer, which corresponds to 9.7% of units having structure III, 1.7% of acrylic acid units, 48.8% of styrene units, and 39.8% of butyl acrylate units.

ANAL. Calcd. for the above composition: C, 77.15%; H, 6.36%. Found: C, 78.90%; H, 7.01%.

The use of conventional basic acceptors of hydrogen chloride produced as the result of the Schotten-Baumann reaction, such as pyridine and aqueous alkali, is also possible but inferior to the above procedure in yield. The fluorescent polymers, when they are water-soluble in the form of alkali salts or in the form of copolymers with water-soluble components such as sodium acrylate, can be purified by dialysis through cellophane membrane against water.

Polarographic Reduction Wave with the Dropping Mercury Electrode

Figure 1 indicates a typical polarographic reduction wave of the polymers in contrast with acetyl fluorescein. These waves possibly indicate the first step of the reductions, i.e., to the fluorescein component and figures in the diagram denote the half-wave potentials.

Determination of Fluorescence

Figure 2 indicates the fluorescences emitted from a fluorescein copolymer (polymer B) in ethanol and an ethanol-water mixture. For excitations, the wavelengths inducing the maximum emission intensities were employed (maximum excitation wavelength).

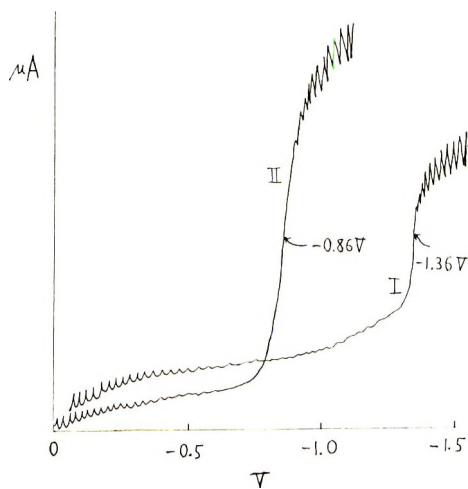


Fig. 1. Polarographic reduction wave for acrylyl fluorescein polymer and model compound with the dropping mercury electrode: (I) Polymer B; (II) acetyl fluorescein. An equivolume mixture of ethanol and water containing 0.1*N* sodium acetate was employed for solvent.

It can be determined from this that the addition of water to alcohol considerably increases the emission intensity at peak wavelengths, since the concentration of the polymer in ethanol is exactly twice as high as that in the ethanol-water mixture.

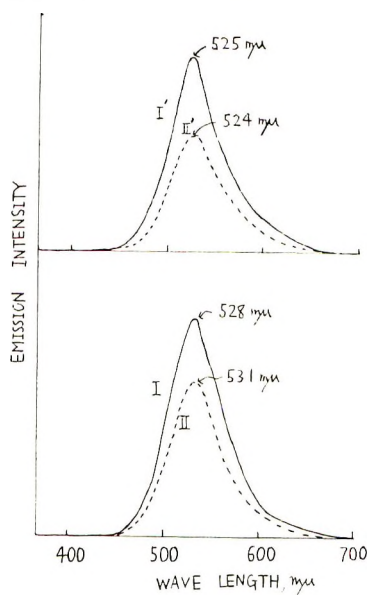


Fig. 2. Fluorescences emitted from acrylyl fluorescein polymer and model compound: (I) (polymer B), potassium salt in ethanol; (I') polymer B, potassium salt, in ethanol-water (1:1 volume ratio); (II) for acetyl fluorescein potassium salt, in ethanol; (II') acetyl fluorescein, potassium salt, in ethanol-water (1:1). The excitation wavelengths are 498 $\mu\mu$ for I and 495 $\mu\mu$ for I', II, and II'. The ordinates represent the emission energy intensity in the same equi-energy scale.

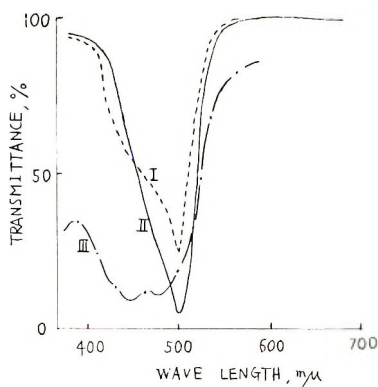


Fig. 3. Visible absorption spectra for acrylyl-fluorescein polymers and related model compound: (I) polymer B (K form); (II) acetyl fluorescein (K form); (III) polymer B in free carboxyl ($-\text{COOH}$) form. The solvent employed was ethanol.

Visible Absorption Spectra

Figure 3 shows the visible absorption spectra of the fluorescein polymer in the carboxylic acid and potassium salt forms. It is seen from this that the absorption peak for the free acid type is somewhat lower than that for the salt type.

All these results indicate that the fluorescein polymers take the structure III, in which the functional portion of fluorescein is kept unchanged by its incorporation to vinyl polymers. The use of *N*-hydroxymethylacrylamide, for example, was found to affect the functional portion, thereby reducing the emission of fluorescence considerably.

As a notable property of this polymer, an apparent color change from orange-red to greenish yellow is observed with the increase in moisture content in polymer. This can be explained as due to the combination of the following two effects: (1) emission of green fluorescence in the presence of moisture; (2) small shifts of the absorption maximum towards lower wavelengths due to the hydrolysis of the alkali salts (potassium or sodium salt type) to free carboxyl group with moisture.

Table I indicates the shifts of the absorption peak for polymer B film (potassium salt).

TABLE I
Dependence of the Absorption Peak of Polymer B Film
on Relative Humidity

RH, %	Absorption peak, $m\mu$
0	508
60	506
80	500

Reference

- H. Kamogawa, *J. Polym. Sci. A-1*, **7**, 409 (1969).

HIROYOSHI KAMOGAWA

Textile Research Institute
4 Sawatari, Kanagawa
Yokohama, Japan

Received December 31, 1968
Revised February 19, 1969

BOOK REVIEWS

Man-Made Fibers

Science and Technology. Volume I. H. F. Mark, S. M. Atlas, and E. Cernia, Eds., Interscience, New York, 1967. xi \$17.50.

My original copy of this book was lost in the mails, so this review is unavoidably late. There is one advantage of the delay, however. I have been able to check my opinion with that of a colleague, who is a spinning expert. He was initially disappointed because he found so few new leads to problems that had been facing him. On reflection, however, he realized that, to quote, "But, to be fair, I think that we must admit that very little is known about the subjects that aren't treated adequately in the book, in spite of the incredible size of the fiber industry and the large expenditure on research and development." This book, then, is not so much for the specialist as it is for those who hope to become specialists, or those like myself, who never expect to spin fibers, but need to know a good deal about the field.

The two chapters by A. Ziabicki, on fundamentals of spinning, were very interesting to me. I particularly liked the discussion of tensile viscosity and of the factors limiting the amount of draw-down during spinning. I wondered whether more emphasis shouldn't be paid to the amount of stored elastic energy in the spinning melt or dope, rather than the main relaxation time, particularly when dealing with fiber breakage and fluctuations of diameter. (My colleague doubts the validity of my contention.)

The chapter on dry-spinning, by J. Corbiere, is more restricted in scope. The emphasis is on practical matters, and primarily on cellulose acetate.

Chapters on transition phenomena, by K. Ueberreiter, and chain folding, by A. Peterlin, are very good. However, so little is known about fiber problems in these fields that much of the treatment applies to polymers in general, rather than specifically to fibers. What I particularly missed throughout the book were thorough discussions of the effects of melt orientation and of solvents on crystallization. I also did not note a complete treatment of the effects of temperature and of solvents on fiber drawing.

The chapter on morphology, by O. and I. Szabolis, is even less definite. Many details are presented, but useful generalizations are rare.

"Conjugate Fibers," by E. M. Hicks, E. A. Tippetts, J. V. Hervett and R. H. Brand differs from the rest of the book, in that a very specialized topic is discussed. The treatment is good.

I must now warn the reader that two of the chapters are very inadequate. The first, by two of the editors, is far too short to serve as a proper introduction to structural principles of fiber-forming polymers. Almost every statement made is subject to so many qualifications that very misleading impressions can be created. For example, it is stated that addition polymerization is more versatile than condensation polymerization because the breadth of the distribution can be varied from very narrow to very wide. In the first place, the statement isn't generally true. Interfacial polymerization leads to a wide distribution and all that limits one with other condensation polymers is the ability to make the high molecular weight component of a blend. It is exceedingly difficult to secure a narrow distribution with Ziegler catalysts, and unusual with other systems. In the second place, there are no hints as to the beneficial or adverse effects of a wide or narrow distribution. This discussion is not given elsewhere in the book, so this would have been an excellent place to round out the picture.

The chapter on wet-spinning is so deficient that the editors recommend other treatments of the subject.

All in all, I feel that the effect of the editors to assemble discussions from European authors has been successful. Only one translation was poor.

A final judgment must await completion of the other two volumes. Also, we must remember that the editors have not attempted to replace the works of Rowland Hill and others, but rather to bring the story up to date. Nevertheless, I am sorry to report that I didn't learn very much about the special problems involved in the development of new polymers for fibers, or about the relative virtues of various methods of spinning, when the polymer is at hand.

H. M. Spurlin

Hercules Inc.
Research Center
Wilmington, Delaware

New Linear Polymers. Henry Lee, Donald Staffey and Kris Neville McGraw-Hill, New York, 1967. x + 374 pp, illus.

The volume is principally concerned with 10 new linear commercially available polymers or polymer classes, namely, the polyimide, polyamide-imides, polyester-imides, aromatic polyamides, polyclamides, polybenzimidazoles, polyphenylene oxides, polysulfones, poly(*p*-xylylenes) and phenoxies. It is organized into an introductory chapter containing a listing of commercially available linear polymers and a discussion of the structural characteristics of these new polymers which lead to their superior properties, eight chapters covering these new linear polymers, and a final chapter surveying the research polymers which are not commercial but under study. The authors consider the eight chapters dealing with these new polymers as complete and self-contained reviews covering history, chemistry, properties, application methods and end-uses. In these chapters which are the most important the coverage is quite comprehensive and authoritative. However, the stress is disproportionately on application and end-uses, with even the discussion of properties couched in terms of applications and end-uses. There is no question as to the importance of the extensive property data quoted, but in terms of producing a more balanced volume, in a scientific sense, less stress in these areas would be in order.

In spite of the comprehensive and authoritative coverage, this volume remains highly specialized and as such must be regarded as a volume suitable for a library but not normally worth a permanent place on the individual scientist's bookshelf.

A. H. Frazer

Pioneering Research Laboratory
E. I. du Pont de Nemours and Co.
Wilmington, Delaware

Chemistry in Nonaqueous Solvents, Vol. III, Part 1, "Chemistry in Liquid Dinitrogen Tetroxide," C. C. Addison, and Part 2, "Chemie in flüssigem Schwefeldioxid," W. Karcher and H. Hecht, Pergamon Press, 1967, 206 pp.

This, the third volume in an excellent series of monographs on nonaqueous ionizing solvents, covers the chemistry of the so-called oxidotropic solvents, N_2O_4 and SO_2 , in which the transfer of oxygen atoms is considered an important process. The first part (on N_2O_4) comprises 78 pages and has 199 references—72 of which were authored or coauthored by Professor Addison himself, and the latest of which is dated 1965. The

second part (on SO_2) comprises 115 pages and has 195 references—the latest of which is dated 1964.

This volume is probably the best available summary of chemistry in liquid dinitrogen tetroxide and liquid sulfur dioxide. Nevertheless there are some obvious shortcomings. Both parts consist mainly of summaries of the physical properties of the solvents and the inorganic reactions which have been carried out in them. This emphasis is understandable in the case of N_2O_4 , in which relatively little organic chemistry has been studied, but it is surprising to find that the reactions of organic compounds in liquid SO_2 are confined to two and a half pages. Both parts could be improved by the inclusion of discussions of the techniques for handling the solvents.

Several omissions were noted in the part on N_2O_4 , by C. C. Addison. Although a postulated chelate structure for the dioxane- N_2O_4 adduct is mentioned on page 26, no mention is made of the x-ray diffraction study¹ which showed the structure to consist of chains of alternating dioxane and N_2O_4 molecules. On page 40, the structures $\text{NO}_2^+[\text{BF}_3\text{NO}_2]^-$ and $\text{NO}_2^+[(\text{OBF}_3)_2]^-$ are given as the products of the reaction of N_2O_4 with BF_3 , even though it has been shown² that NO_2BF_4 and NOBF_4 are the predominant products of this reaction. And surprisingly, no mention is made, on pages 57–58, that the syntheses of the compounds $\text{Na}_2\text{N}_2\text{O}_5$ and $\text{Na}_2\text{N}_2\text{O}_6$ have not been successfully reproduced.³

1. P. Groth and O. Hassel, *Proc. Chem. Soc.*, **1962**, 379.
2. J. C. Evans, H. W. Rinn, S. J. Kuhn and G. A. Olah, *Inorg. Chem.*, **3**, 857 (1964).
3. E. S. Scott, U. S. Dept. Com. Office Tech. Serv., P. B. Rept. 143, 484, 1959; also see A. J. Vosper, *J. Chem. Soc.*, (A), **1968**, 2403.

William L. Jolly

Department of Chemistry
University of California
Berkeley, California 94720

Epoxy Resin Technology, Ed., Paul F. Bruins, Interscience, New York, 1968, 275 pp. \$16.50

The hard cover literature on epoxy resins continues to grow. There are now eight books on epoxy resins, as noted in the bibliography below.

This reviewer is of the opinion that no specialty field, especially one concerned with a resin as versatile as epoxy resins, can suffer from too many text books. Although most of the basic information contained in *Epoxy Resin Technology* is contained in Ref. 6, and much of the chemistry and formulation concepts are contained in Ref. 1, nevertheless it is useful and worthwhile to have these concepts and this information presented by a fresh group of authors who are presenting the data in their own style and with their own personal experiences to give it new vitality.

Epoxy Resin Technology, in surveying epoxy resins from their synthesis, handling, curing, physical properties, and fields of end uses—flooring, adhesives, molding compounds, electrical applications, coatings, and filament reinforced structures, provides a number of interesting discussions and up-to-date concepts useful to both the newcomer to the field and to the expert.

The book is recommended for the library of anyone who is concerned with epoxy resins in any of their applications.

Henry Lee

The EpoxyLite Corp.
South El Monte, Calif.

References and Bibliography of Textbooks on Epoxy Resins

1. Henry Lee & Kris Neville, *Epoxy Resins—Their Applications & Technology*, McGraw-Hill Book Co., New York, New York, 1957, 308 p.
2. Alfred Max Paquin, *Epoxydverbindungen und Epoxydharze*, Springer-Verlag, Heidelberg, 1958, 853 p.
3. Jean Schrade, *Les Resines Epoxy*, Dumod, Paris, 1957, 181 p.
4. Irving Skeist, *Epoxy Resins*, Reinhold, New York, New York, 1958, 308 p.
5. Kurt Weigel, *Epoxydharz-lacke*, Wissenschaftliche Verlagsgesellschaft M.B.H., Stuttgart, 1965, 381 p.
6. Henry Lee and Kris Neville, *Handbook of Epoxy Resins*, McGraw-Hill Book Co., New York, New York, 1967, 899 p.
7. Henry Lee & Kris Neville, *Epoxy Resins*, Encyclopedia of Polymer Science & Technology, Interscience, 1967, Vol. 6.
8. Paul F. Bruins, *Epoxy Resin Technology*, Interscience Publishers, 1968, 275 p.

Physical Properties of Molecular Crystals, Liquids and Glasses. Arnold Bondi, Wiley, New York, 1968, 502 pp. \$18.50

This remarkable book can be highly recommended to all persons interested in correlations between chemical structure and properties of materials in a condensed phase, i.e., crystals, liquids and glasses. The intent of the author has been succinctly stated as follows: "The primary purpose of this book is the development of a methodology that should enable chemists and chemical engineers to relate certain physical properties of condensed phases to molecular structure—the chemist in order to guide the synthesis of compounds with specific physical properties and the chemical engineer in order to estimate property data required for process calculations on new substances."

His general approach is to use the method of reduced variables which permits relating the behavior of a vast range of compounds in very condensed form. For example, in Tables 3.7 and 3.8, the reduced coefficient of cubical expansion at 0.9 T_m is shown to range from 0.53 to 0.25 on going from argon to polyethylene terephthalate, with an average value of 0.31.

Another part of his methodology is to offer tables of procedures for calculating various physical constants. For example, on page 50, six procedures are given for calculating the cubic thermal expansion coefficient of crystals within a certain range, 0.7 to 0.9 of the melting temperature, the specific method varying with the type of molecules, i.e., rigid, nonassociated, flexible nonassociated, hydrogen bonded, etc. The feature could well prove valuable to the professor interested in problems to assign to graduate students.

The reviewer has just spent six months surveying a considerable body of literature relating to polystyrene in the glassy state. He found that Chapter 13 of Bondi on "Physical Properties of Molecular Glasses" had not only covered the key references on polystyrene but had placed polystyrene in perspective with respect to other glassy polymers.

Another interesting aspect of the book is the inclusion of significant unpublished data, such as Figure 13.6 showing a large increase in the elongation of polystyrene at break when under hydrostatic pressure as measured by Holliday and Mann; or Figures 13.24 to 13.5d showing relaxation maps for a variety of polymers prepared by McCall.

In brief, we found this both an exciting and a rewarding book—a book that invites frequent perusal of its many provocative tables and figures, as well as the text.

Raymond F. Boyer

The Don Chemical Co.
Midland, Mich.

ERRATA**Thermally Stable Polymers from 1,4,5,8-Naphthalenetetracarboxylic Acid and Aromatic Tetraamines**

By R. L. VAN DEUSEN, O. K. GOINS, and A. J. SICREE

*Air Force Materials Laboratory, Nonmetallic Materials Laboratory, Polymer Branch,
Wright-Patterson Air Force Base, Ohio 45433*(article in *Journal of Polymer Science A-1*, **6**, 1777, 1968)

The curve shown for Figure 4 on page 1785 should be the curve in Figure 5. The curve shown for Figure 5 should be the curve in Figure 4 on the same page.

Polytriphenodithiazine

By M. OKADA and C. S. MARVEL

*Department of Chemistry, University of Arizona,
Tucson, Arizona 85721*(article in *Journal of Polymer Science A-1*, **6**, 1774, 1968)

Line 15 in text: The weight loss at 900°C in the TGA text should read 13%, not 93%.